The Behaviour of Antioxidants in Automotive Engine Oils

Alfahad Alfadhl

Doctor of Philosophy Thesis

University of York
Department of Chemistry
July 2008

ALL MISSING
PAGES ARE
BLANK
IN
ORIGINAL

ABSTRACT

The behaviours of phenolic and aminic radical scavenging antioxidants in model base fluids (e.g. squalane), semi-, and fully-formulated automotive engine lubricants have been studied, to understand how antioxidants behave at high temperatures, under engine conditions, and also how they interact with other lubricant additives, by oxidation in bench-top reactors and degradation in a research spark-ignition engine. Lubricant samples were collected from bench-top reactors, top ring zone of the piston assembly, and engine sump of a research gasoline engine. The reactants, products, and intermediates were identified and quantified.

The bis-phenolic antioxidant 4,4'-methylenebis[2,6-bis(1,1-dimethylethyl)]phenol (AN2), at a treat rate of 0.5 % w/w, was found to provide a full antioxidative protection to squalane, and squalane would only oxidise when AN2 is totally consumed. In contrast, the diaromatic aminic antioxidant 4-octyl-N-(4-octylphenyl)benzenamine (Amine101), at a treat rate of 0.5 % w/w, was found to provide partial antioxidative protection to squalane at temperatures below 210 °C and a negligible antioxidative protection above 210 °C.

The critical antioxidant concentration of AN2 was found to be 0.22 ± 0.05 mmol dm^{-3} at 220 °C, and that of Amine101 was found to be 5.7 ± 0.5 mmol dm^{-3} at 180 °C. The stoichiometry coefficients of AN2 and BHT at 90 °C were found to be 4.1 ± 0.2 and 4.3 ± 0.2, respectively.

The levels of antioxidants in the top ring zone varied from ~30 to ~95 % and ~60 % when the piston rings were unpinned and pinned, respectively. Pinning the piston rings greatly enhanced the precision of top ring zone data. The oil residence time in the sump was found to be 7.6 ± 1.0 hours and the temperature of the top ring zone was estimated to be ~250 °C as an upper limit.

Sterically-hindered phenols and diaromatic amines were found to interact strongly with each other. In the bench-top reactor, the degree of synergism was found to be ≈0.3. In the top ring zone, ≈10 % of the aminic was regenerated at the expense of 50 % of the phenolic. AN2 was found to interact strongly with the succinimide dispersant; the degree of synergism was found to be 0.5.

LIST OF CONTENTS

LIST OF FIGURES

LIST OF TABLES

AUTHOR, SUPERVISORS, AND EXAMINERS

Author

Alfahad Alfadhl, BSc, MSc (London, 2005)

Academic supervisors

Moray Stark, DPhil (York, 1986), CChem, MRSC
His research is centred on the study of the oxidation mechanisms of hydrocarbon and ester lubricant base fluids, and the effects that oxidation products have on the rheology of lubricants. Doctor Stark is the author or co-author of 17 publications. Contact him on mss1@york.ac.uk

John Lindsay Smith, DPhil (Oxon, 1965), CChem, FRSC
His research is centred on mechanistic studies of organic and bioorganic oxidation reactions. Professor Lindsay Smith is the author or co-author of 179 publications. Contact him on jrls1@york.ac.uk

Industrial supervisors

Robert Ian Taylor, PhD (Durham, 1987), CEng
He is the manager of the Automotive Lubricants Division at Shell Global Solutions (UK). Doctor Taylor is the author or co-author of 45 publications. Contact him on robert.i.taylor@shell.com

Christopher Booth, PhD (Hull, 1993)
He is a technologist in the Components Technology Division at Infineum (UK) Limited. Doctor Booth is the author or co-author of 3 publications. Contact him on chris.booth@infineum.com

External and internal examiners

Malcolm Fox, PhD (London)
He is situated in the School of Mechanical Engineering of the University of Leeds. Professor Fox is the author or co-author of 52 publications. Contact him on m.f.fox@leeds.ac.uk

Adrian Whitwood, PhD (York, 1990)
He is situated in the Department of Chemistry of the University of York. Doctor Whitwood is the author or co-author of 79 publications. Contact him on acw1@york.ac.uk

ACKNOWLEDGEMENTS

The financial support from the Engineering and Physical Sciences Research Council, Shell Global Solutions, and Infineum Limited; student tax exemption by York Council; academic supervision of Moray Stark and John Lindsay Smith; industrial supervision of Robert Ian Taylor and Christopher Booth; various additives provided by Christopher Booth; Shell XHVI 8.2 base fluid provided by Robert Ian Taylor; many helpful comments and suggestions by Adrian Whitwood and Simon Chung; general technical assistance of Julian Wilkinson and Lawrence Abbot; proof-reading of thesis by Yasir Alfadhl; collection of oil samples and operation of Ricardo Hydra engine by Peter Lee; mass spectrometry analysis by Trevor Dransfield and Ben Glennie; nuclear magnetic resonance analysis by Heather Fish; assistance to use differential scanning calorimetry by Paul Elliot; ordering of custom-made 23-gauge needles by Steve Hau; and comments and suggestions on radical clocks from Keith Ingold, Ned Porter, and Martin Newcomb are gratefully acknowledged.

AUTHOR'S DECLARATION

The collection of the majority engine oil samples and operation of Ricardo Hydra engine was by Peter Lee from the Institute of Tribology at the School of Mechanical Engineering of the University of Leeds. The gas and liquid chromatography-mass spectrometry analysis was performed by Trevor Dransfield and Ben Glennie. The nuclear magnetic resonance phosphorus-31 analysis was performed by Heather Fish. The pressurised differential scanning calorimetry analysis was performed by Alex Wang from Infineum Limited.

LIST OF ABBREVIATIONS

A	pre-exponential factor (s^{-1} [unimolecular] and dm^3 mol^{-1} [bimolecular])
Am•	diaromatic aminyl radical
AmH	diaromatic amine
Amine101	4-octyl-N-(4-octylphenyl)benzenamine
Aminic	diaromatic amine
AmO•	diaromatic nitroxyl radical
AmOH	diaromatic hydroxylamine
AN2	4,4'-methylenebis[2,6-bis(1,1-dimethylethyl)]phenol
APCI	atmospheric pressure chemical ionisation
Ar_2O•	sterically-hindered phenoxyl radical
Ar_2OH	sterically-hindered phenol
BDE	bond dissociation energy
BHT	2,6-bis(1,1-dimethylethyl)-4-methylphenol
DSC	differential scanning calorimetry
E	activation energy (kJ mol^{-1})
ECN	effective carbon number
EPR	electron paramagnetic resonance
Formylphenol	3,5-bis(1,1-dimethylethyl)-4-hydroxybenzaldehyde
FTIR	Fourier transform infrared
Galvinol	4-[[3,5-Bis(1,1-dimethylethyl)-4-hydroxyphenyl]methylene]-2,6-bis(1,1-dimethylethyl)- 2,5-cyclohexadien-1-one
Galvinoxyl	4-[[3,5-Bis(1,1-dimethylethyl)-4-oxo-2,5-cyclohexadien-1-ylidene]methyl]-2,6-bis(1,1-dimethylethyl)phenoxyl
GC	gas chromatography
GC-MS	gas chromatography-mass spectrometry
HOO•	hydroperoxyl radical
InH	antioxidant
Irganox L135	3,5-di-tert-butyl-4-hydroxyhydrocinnamate
IT	Reaction time
k	reaction rate constant (s^{-1} [unimolecular] and dm^3 mol^{-1} [bimolecular])
Lauroyl peroxide	bis(1-oxododecyl)peroxide
LC	liquid chromatography
LC-MS	liquid chromatography-mass spectrometry
Me	CH_3
MS-CI	mass spectrometry-chemical ionisation
MS-EI	mass spectrometry-electron impact
n	stoichiometric coefficient
Naugalube 438L	4-nonyl-N-(4-nonylphenyl)benzenamine
NIST	National Institute of Standards and Technology (US)
NMR	nuclear magnetic resonance
PDSC	pressurised differential scanning calorimetry
Phenolic	sterically-hindered phenol
POP	pristane oxidation product
ppm	parts-per-million
PTFE	polytetrafluroethylene
Quinone	2,6-bis(1,1-dimethylethyl)-2,5-cyclohexadiene-1,4-dione
R	universal molar gas constant, R = 8.3145 (J mol^{-1} K^{-1})
R•	alkyl radical
RH	alkane
R_i	rate of initiation

RMM	relative molecular mass
RO•	alkoxyl radical
ROO•	peroxyl radical
ROOH	hydroperoxide
rpm	revolutions-per-minute
SDBS	Spectral Database for Organic Compounds; National Institute of Advanced Industrial Science and Technology (Japan)
Squalane	2,6,10,15,19,23-hexamethyltetracosane
sRH	secondary hydrocarbon
T	absolute temperature (K)
TAN	total acid number
tRH	tertiary hydrocarbon
TRZ	top ring zone
XHVI 8.2	extra high viscosity index
ZDDP	zinc dithiophosphate

1. INTRODUCTION

1.1. INTRODUCTION TO LUBRICATION

The rubbing of two solid surfaces against each other causes friction between the two surfaces. The amount of energy needed to drive the rubbing process is proportional to the extent of the frictional force (Bhushan, 2005); that is to say, low energy is needed for low friction and high energy is needed for high friction. In order to conserve energy, a liquid (e.g. hydrocarbon) or a solid (e.g. graphite) substance is added between the two rubbing surfaces to form a thin layer that reduces or completely prevents the two rubbing surfaces from contact each other. This substance is called a lubricant and the process of preventing friction by a lubricant is known as lubrication.

1.2. LUBRICATION OF AUTOMOTIVE ENGINES

Lubrication of moving parts (e.g. in a piston assembly, Figure 1.1) in automotive engines is absolutely essential; the lubricant reduces friction between moving parts, dissipates heat from hot areas to cooler ones, and prevents metal rust by restricting the oxygen presence on metal surfaces (Daintith, 2000, p.342).

Automotive engines are generally divided into spark-ignition (also called gasoline or petrol) and compression-ignition engines. A schematic diagram of a typical spark-ignition engine is illustrated in Figure 1.1.

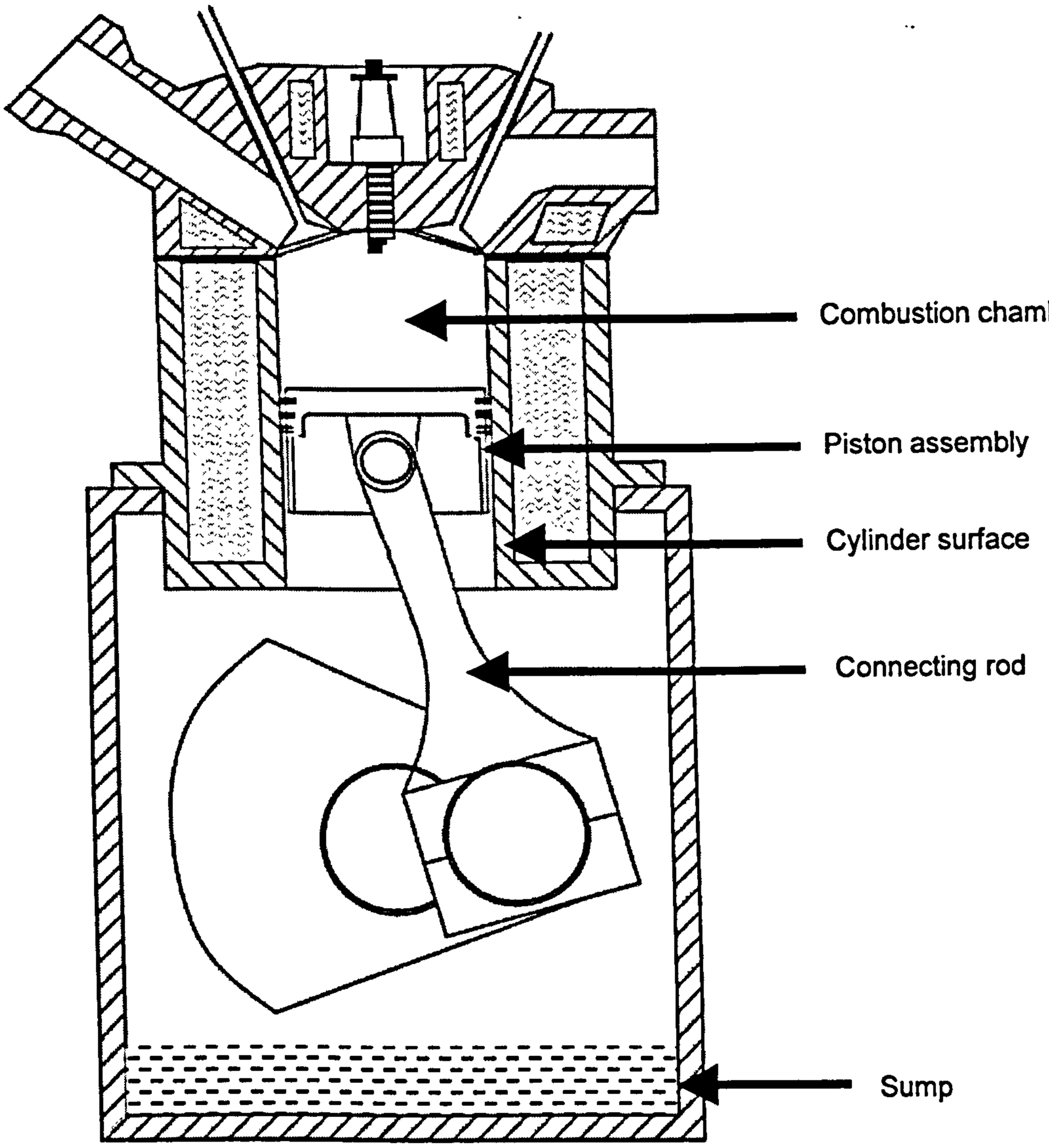

Figure 1.1: A simplified schematic diagram of a typical spark-ignition engine (Lee, 2006)

1.2.1. Lubricant composition

A typical automotive engine lubricant consists of a base fluid (~75-95 % mass) and additives (~25-5 % mass) (Taylor et al, 2005). The base fluids are either mineral (i.e. derived directly from crude oil) or synthetic; which are divided into five standard groups according to the composition (e.g. saturates and sulphur content) and overall chemistry. The standard groups of base fluids are listed in Table 1.1.

Table 1.1: Classification of base fluids (Delaney, 2005)

Group	Saturated (mass %)	Sulphur (mass %)	Viscosity index
I	< 90	> 0.03	≥ 80 and < 120
II	≥ 90	< 0.03	≥ 80 and < 120
III	≥ 90	≤ 0.03	≥ 120
IV	Synthetic, e.g. poly-alpha-olefins		
V	Lubricants not included in Groups I, II, III, or IV; e.g. ester lubricants		

Additives are added to the base fluid to enhance the quality of the base fluid; for instance, antioxidants are added to prevent oxidative degradation. Typical automotive engine lubricant additives are listed in Table 1.2.

Table 1.2: Typical automotive engine lubricant additives and concentrations (Rizvi, 1999)

Additive	% mass	Function	Example
Antioxidants	~3	Prevent base fluid oxidation	Diaromatic amines
Antiwear agents	~2	Form a solid film between metal surfaces	Zinc dithiophosphate
Corrosion inhibitors	~0.5	Form a film between metal surfaces	Sulphonates
Overbase detergents	~2	Neutralise acids and clean surfaces	Natural calcium sulphonate
Dispersants	~3	Suspend oxidation products and particulate contaminants	Succinimides
Foam inhibitors	Parts-per-million	Enhance the separation of air bubbles from the lubricant	Polysiloxanes
Friction modifiers	~1	Form a tenacious lubricant film	Molybdenum dithiocarbamate
Pour point depressants	~0.5	Inhibit wax crystal aggregation to keep the lubricant fluid at low temperatures	Styrene esters
Viscosity modifiers	~20	Minimize viscosity variations with temperature	Olefin copolymers

1.2.2. Engine conditions

The lubricant is carried in the sump, at the bottom of the engine (Figure 1.1). The lubricant flow is forced by a pump through a filter to the main bearings. Oil squirting from a small hole at the top of the connecting rod lubricates the contacting surfaces between the piston rings and interior surfaces of the cylinders. The excess lubricant then drains back to the sump.

The proximity of the piston assembly to the combustion chamber (Figure 1.1) exposes the lubricant to very harsh conditions such as high temperatures[1] and reactive nitrogen oxides (Korcek and Johnson, 1993).

The development of higher performance engines has increased the maximum compression ratio,[2] which is related to engine power, of a spark-ignition engine from 7:1 in the 1940s to about 10:1 (Rose, 1991) and the oil drain intervals has increased from an average of 10000 km in 1995 to an average of 20000 km in

[1] For gasoline engines: 160 °C for piston second land at 3000 rpm / full load (Moritani and Nozawa, 2004) and 280 °C for piston top ring groove at ≈4500 rpm / unknown load (Kim et al, 1998).
[2] Compression ratio is the ratio between the volume of a combustion chamber when the piston is at the bottom of its stroke, and the volume when the piston is at the top of its stroke.

2003 (Lee, 2006, p.2). The increase in engine power while the engine size (i.e. engine displacement)[3] not increasing and the increase in oil drain intervals while the sump volume not increasing led to an increase in the oil stress factor, which can be calculated as:

$$\text{Oil stress factor} = \frac{\text{Engine power}}{\text{Engine displacement}} \times \frac{\text{Oil drain interval}}{\text{Sump volume}}$$

Figure 1.2 shows the increase in the automotive engine oil stress factor over a period of five decades.

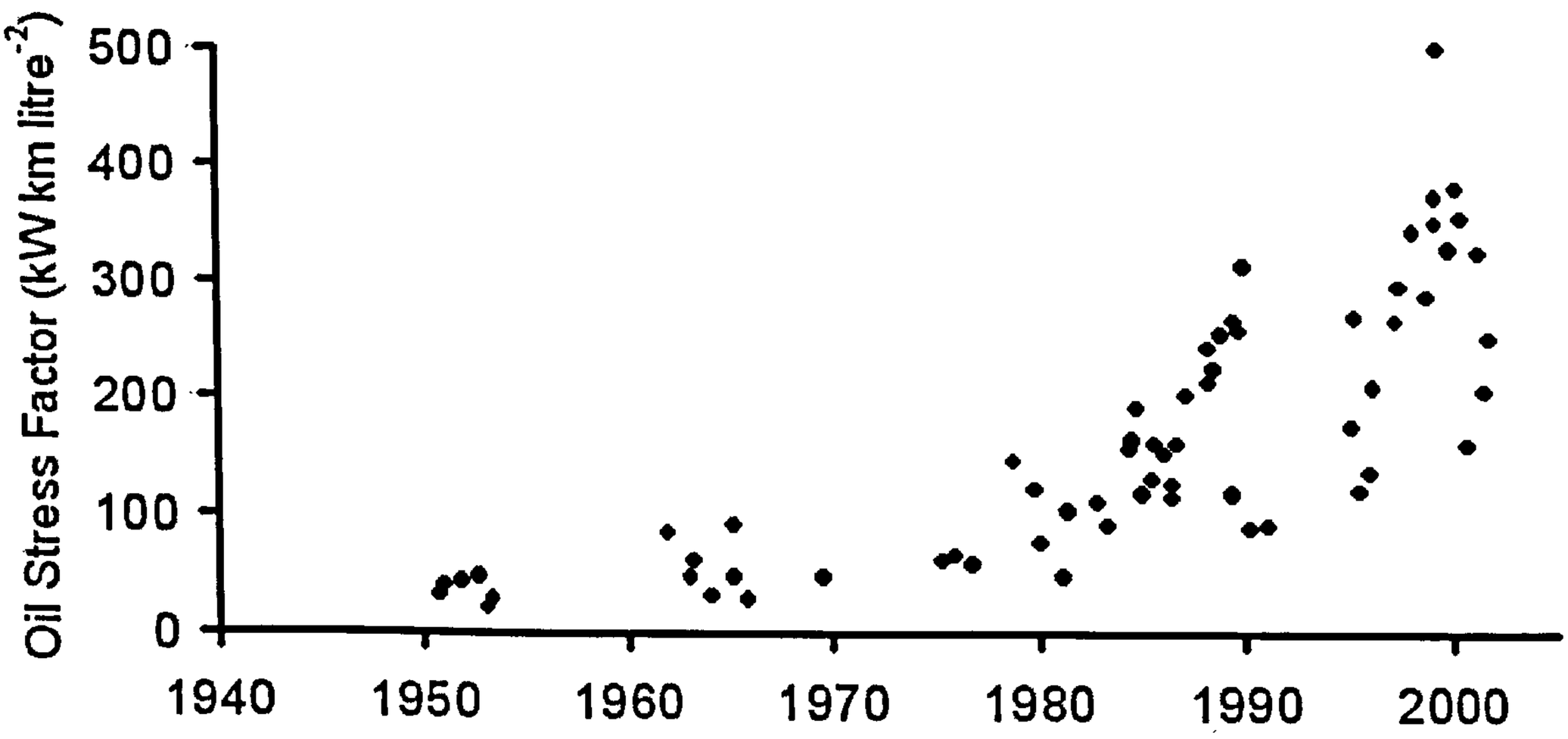

Figure 1.2: Automotive engine oil stress factor versus decade (Taylor et al, 2005)

High oil stress factors can adversely affect the performance of the lubricant (Taylor et al, 2005). Lubricant deterioration includes viscosity increase and soot formation.

There is a link between lubricant deterioration and automotive greenhouse emissions (Bates, 1995); that is to say, extra emissions are produced from the extra combusted fuel that is needed to overcome the extra resistance of a lubricant that is more viscous due to being degraded.

[3] Engine displacement is the total volume of air/fuel mixture an engine can take in during one cycle.

1.2.3. Automotive greenhouse emissions

The obligation to comply with the United Nations Framework Convention on Climate Change Treaty (See, 2001) and the Automotive Greenhouse Emissions Standards of the European Union has led countries to force car manufacturers to reduce automotive greenhouse emissions (European Environment Agency Technical Report).[4] The automotive greenhouse emissions standards of the European Union for gasoline-engine passenger cars are listed in Table 1.3.

Table 1.3: Automotive greenhouse emissions standards of the European Union for gasoline-engine passenger cars (Bosch, 2007)

Year	Carbon monoxide (g/km)	Hydrocarbons (g/km)	Nitrogen oxides (g/km)	Carbon dioxide (g/km) [Voluntary target]
1992	2.72	0.5	0.5	-
1996	2.3	0.25	0.25	190
2000	2.3	0.2	0.15	190
2005	1.0	0.1	0.08	190
2008	-	-	-	140
2012	-	-	-	120

1.3. LUBRICANT DETERIORATION

The causes of lubricant degradation in automotive engines are not well understood (Moritani and Nozawa, 2004). However, it is generally thought that the high temperature of the engine causes the lubricant to oxidise (with oxygen) to give oxidation products that are thought to be responsible for the viscosity increase (Rasberger, 1997).

The basic autoxidation[5] mechanism of base fluids of lubricants that consist of branched alkanes[6] is briefly summarised in Table 1.4.

---

[4] [Unspecified authors]. Success stories within the road transport sector on reducing greenhouse gas emission and producing ancillary benefits. European Environment Agency Technical Report number 2/2008, Copenhagen, 2008.

[5] Autoxidation is generally defined as a spontaneous reaction between oxygen and an organic compound (Pezzuto and Park, 2004).

[6] Only branched alkanes are introduced here because the main base fluids (e.g. Shell XHVI 8.2) and model base fluids (e.g. squalane) used in this project are branched alkanes.

Table 1.4: General phases in the radical chain mechanism in the autoxidation of hydrocarbons (RH: Hydrocarbon; R•: Alkyl radical; HOO•: Hydroperoxyl; ROO•: Alkylperoxyl radical; ROOH: Alkylhydroperoxide; RO•: Alkoxyl radical, and HO•: Hydroxyl radical) (Rasberger, 1997)

Phase	Reaction			Reaction number
Initiation	$RH + O_2$	→	R• + HOO•	R1
Propagation	R• + O_2	→	ROO•	R2
	ROO• + RH	→	ROOH + R•	R3
Branching	ROOH	→	RO• + HO•	R4
	RO• + RH	→	ROH + R•	R5
	HO• + RH	→	H_2O + R•	R6
Termination	R• + R'•	→	RR'	R7
	R• + R'OO•	→	R'OOR	R8
	ROO• + R'OO•	→	Products	R9

The autoxidation of branched alkanes is initiated by the reaction with oxygen to give alkyl and hydroperoxyl radicals (R1). The alkyl radicals react very rapidly with oxygen to give alkylperoxyl radicals (R2), whereas the hydroperoxyl radicals react with the alkane to give further alkyl and hydrogen peroxide. The alkylperoxyl radicals react with the alkane to give alkyl radicals and alkylhydroperoxides (R3). The hydroperoxides readily decompose homolytically to give alkoxyl and hydroxyl radicals (R4). A scheme for the basic hydrocarbon autoxidation chain reaction is shown in Figure 1.3.

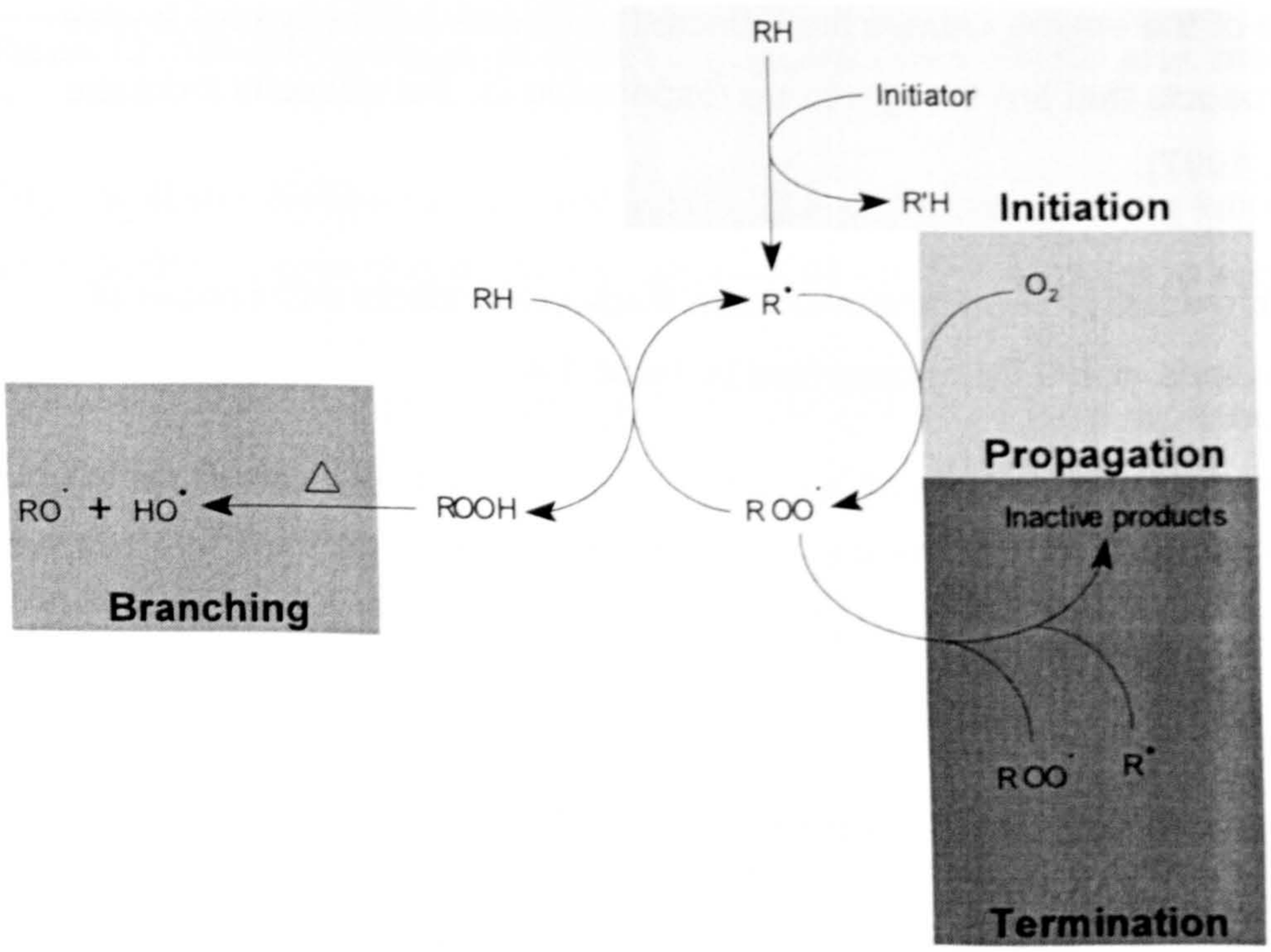

Figure 1.3: Basic hydrocarbon autoxidation chain reaction (Denisov and Afanasev, 2005, p.24)

1.3.1. Previous work on lubricant degradation

Studying lubricant degradation in automotive engines (Saville et al, 1988; Vipper, 1995; Moritani and Nozawa, 2004; Stark et al, 2005, and Wilkinson, 2006) is very expensive and therefore cost-effective laboratory bench-top reactors are used instead to simulate the engine environment. Previous work on lubricant and alkane degradation in bench-top reactors are listed in Table 1.5.

Table 1.5: Previous work on lubricant and alkane degradation in bench-top reactors (references within table)

Technique	Substrate	Temperature (°C)	Reference
Heated glass reactor	Engine lubricant	180	Vipper et al, 2002
Heated glass reactor	Engine lubricant	180	Vipper, 1995
Heated reactor	Engine lubricants	200	Cerny et al, 2001
Heated reactor	Engine lubricants	180	Egharevba and Maduako, 2002
Heated reactor	Engine lubricants	150	Gatto et al, 2007
Heated oven	Engine lubricants	150	Kudynska and Buckmaster, 1997
Heated borosilicate tube	Engine lubricants	550	Owrang et al, 2004
Heated glass reactor	Engine lubricants	171	Roby et al, 2004
Heated flask	Engine lubricants	150-210	Santos et al, 2004
Heated glass and stainless steel reactors	Engine lubricants, base fluids, and hydrocarbons	180-250 and 170-220 (with respect to techniques)	Spiiners and Hedenburg, 1985
Heated tube	Base fluids	150	Adhvaryu et al, 1999
Heated vial	Base fluids	93 and 149	Barman, 2002
Heated reactor	Base fluids	180	Korcek and Jensen, 1976
Heated reactor	Base fluids	180	Zinbo et al, 1987
Heated glass flask	Hexadecane	140-180	Blain et al, 1991
Heated flask	Hexadecane	120-180	Jensen et al, 1974
Heated flask	Hexadecane	120°C, 160, and 180	Jensen et al, 1981
Heated flask	Hexadecane	120-190	Jensen et al, 1990
Heated flask	Hexadecane	120-190	Jensen et al, 1994
Heated flask	Hexadecane	160-190	Korcek et al, 1987
Heated reactor	Hexadecane	150-170	Oganesova et al, 2004
Heated flask	Butane	100 and 125	Mill et al, 1972
Heated glass flask	Pentane and octane	100 and 125 (with respect to substrate)	Sickle et al, 1973
Glass reactor	Octane	135°C, 140, and 145	Garcia-Ochoa et al, 1989
Heated glass-borosilicate flask	Dodecane	165	Boss and Hazlett, 1975
Heated stainless steel reactor	Pristane	170-230	Wilkinson, 2006
Heated Pyrex reactor	Dimethylalkanes	115-120	Rust, 1957

The bench-top reactors are mainly made out of glass to eliminate potential metal catalysis by metal reactors (e.g. stainless steel)[7] and heated to temperatures relevant to those found in automotive engines.

[7] Wilkinson (2006) found that the effect of stainless steel reactors on reactions to be negligible.

Fully-formulated engine lubricants have been investigated but they are complex to investigate due to the presence of many additives, which makes primary chemical analysis very challenging; nevertheless, useful generic data such as total acid content and viscosity increase can be obtained (Cerny et al, 2001 and Roby et al, 2004). Researchers took a step back and investigated base fluids without additives present (Barman, 2002) to minimise the number of chemical reactions taking place at the same time. This proved to be difficult too due to the presence of many structures and isomers of the branched alkane and the difficulty in linking the oxidation products with the starting material. This led researchers to investigate pure alkanes such as hexadecane and octane (Blain et al, 1991 and Sickle et al, 1973) as model base fluids. Some of these pure alkanes are not ideal models for lubricant base fluids; for instance, hexadecane is a linear alkane that only has secondary hydrogen atoms with no tertiary hydrogen atoms. It is well known that alkylperoxyl radicals preferentially abstract tertiary hydrogen atoms (Rasberger, 1997) due to the weak bond dissociation energy (Table 1.6) and secondary alkylhydroperoxides from a linear alkane can decompose directly to ketones whereas tertiary alkylhydroperoxides from a branched alkane cannot because tertiary alkylhydroperoxides have no hydrogen atoms attached to the carbon atom of the C-O group (Stark, 2003, p.33).

Table 1.6 shows that tertiary hydrogen atoms have lower bond dissociation energies than secondary hydrogen atoms; and the lower the bond dissociation energy, the lower the activation energy for abstraction of the hydrogen atom and hence the faster the reaction rate constant.

Table 1.6: Bond dissociation energies (C-H) of alkanes (references within table)

Compound	Hydrogen atom type	Bond dissociation energy (kJ mol^{-1})	k[RH+ROO•] (M^{-1} s^{-1}) at 200 °C for 3-methylpentane + Me_3COO•	Activation energy (kJ mol^{-1})
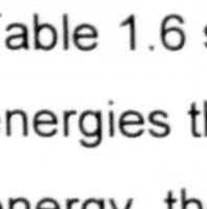	Tertiary	400	93	68.2
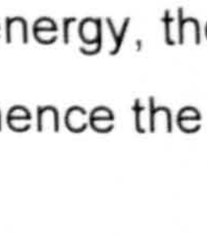	Secondary	412	6.4	73.3
References	-	Denisov and Denisova, 2000, p.21	Howard, 1997, p.291	Howard, 1997, p.291

1.4. INHIBITION OF LUBRICANT DEGRADATION

The key additives that can control the deterioration of lubricants are antioxidants (Muller et al, 1982; and Hamblin and Rohrbach, 2001). Typical commercial antioxidants used in lubricants are listed Table 1.7.

Table 1.7: Examples of commercial lubricant antioxidants (Migdal, 2003)

CAS name	Commercial name	Producer	Structure
4,4'-Methylenebis[2,6-bis(1,1-dimethylethyl)]phenol	Hitec 4702 or AN2	Ethyl	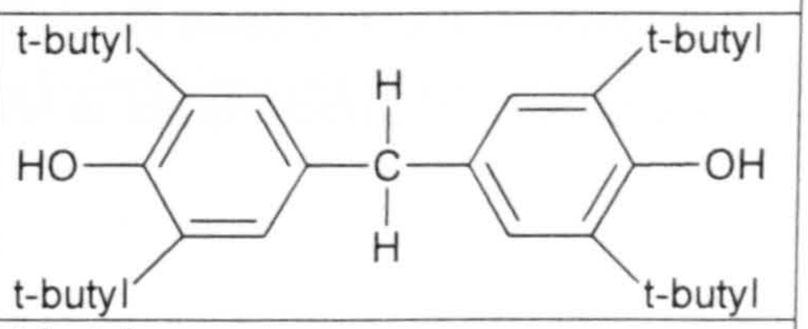
2,6-Bis(1,1-dimethylethyl)-4-methylphenol	Naugard BHT	Crompton	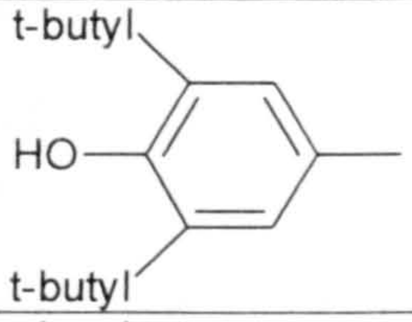
3,5-Di-tert-butyl-4-hydroxyhydrocinnamate	Irganox L135	Ciba	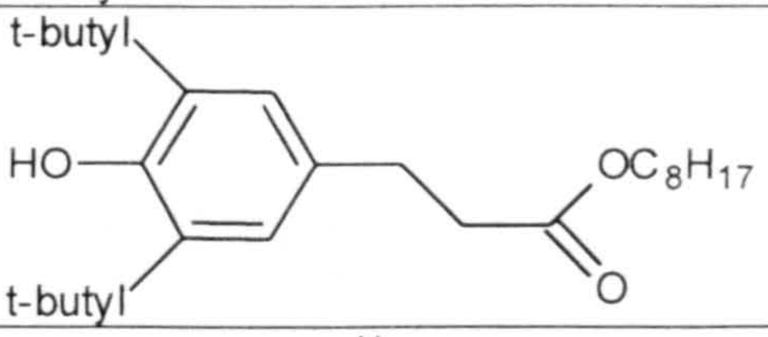
4-Nonyl-N-(4-nonylphenyl)benzenamine	Naugalube 438L	Chemtura	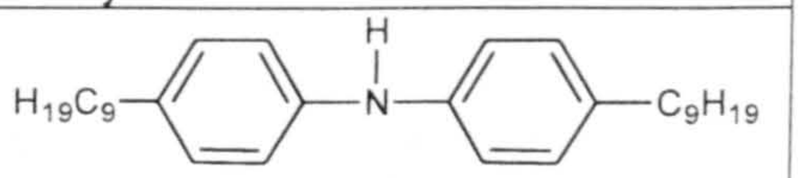

The basic inhibition mechanism of antioxidants is briefly summarised in Table 1.8.

Table 1.8: General phases in the inhibition of radical chain mechanism in the autoxidation of hydrocarbons (RH: Hydrocarbon; R•: Alkyl radical; HOO•: Hydroperoxyl radical; ROO•: Alkylperoxyl radical; InH: Phenolic or aminic antioxidant; and In•: Phenoxyl or aminyl radical) (Rasberger, 1997)

Phase	Reaction			Reaction number
Initiation	$RH + O_2$	→	R• + HOO•	R1
Propagation	R• + O_2	→	ROO•	R2
Inhibition	InH + ROO•	→	In• + ROOH	R10
	In• + ROO•	→	InOOR	R11

Antioxidants function by intercepting alkylperoxyl radicals (R10) and thus preserving the integrity of the base fluid (Rasberger, 1997). Antioxidants have readily abstractable hydrogen atoms and hence are added to base fluids so that alkylperoxyl radicals can abstract hydrogen atoms from the antioxidant instead of the base fluid. The resulting product of the antioxidant is a relatively stable radical that is too unreactive to react with the base fluid but which has the ability to react with and remove further alkylperoxyl radicals (R11). Alkoxyl and hydroxyl radicals are very reactive and as a result, generally, react non-selectively with the antioxidant and the base fluid (Rasberger, 1997). A scheme for the basic inhibition mechanism of antioxidants is shown in Figure 1.4.

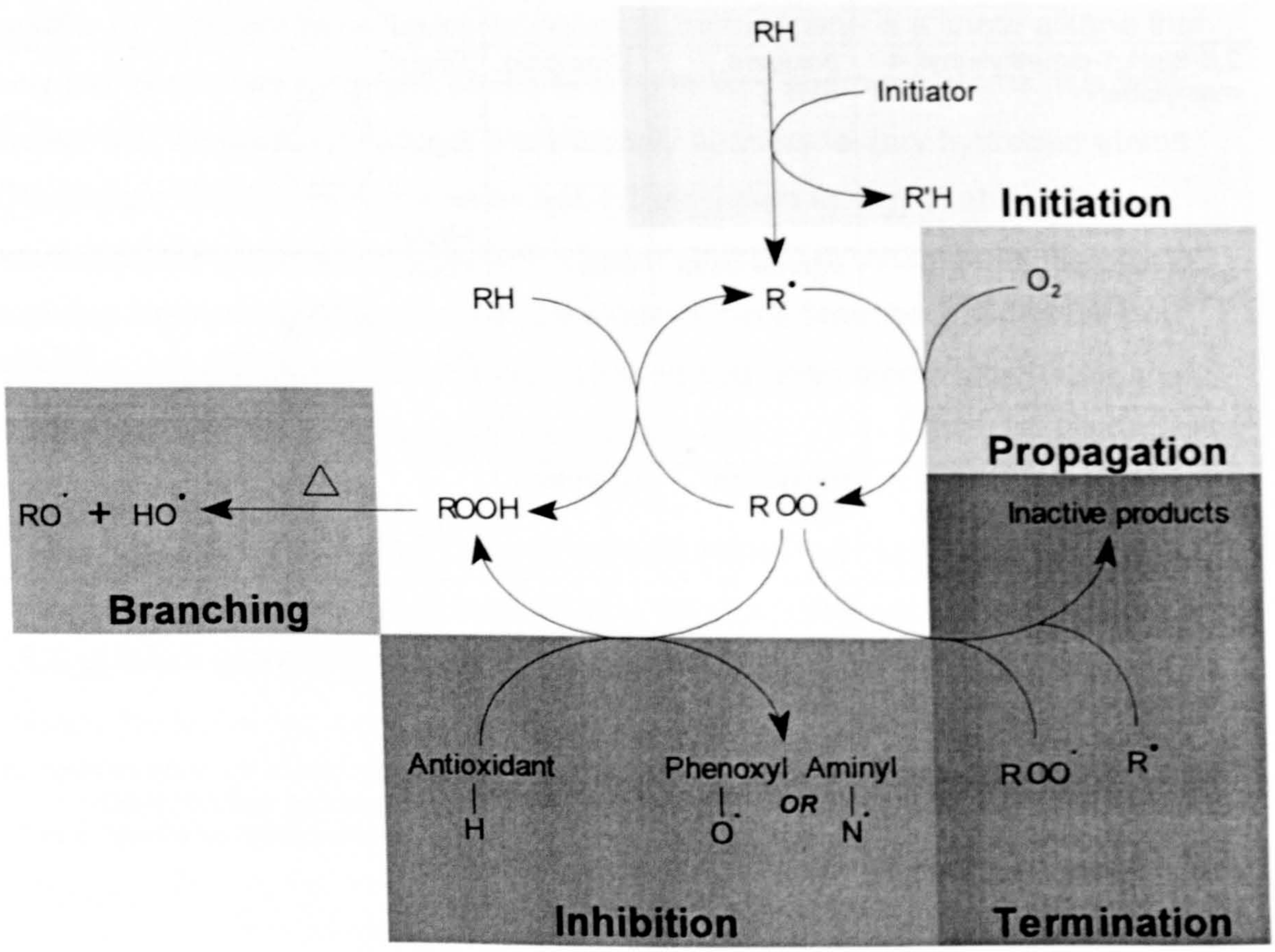

Figure 1.4: Interruption of alkylperoxyl radical chain reaction cycle by an antioxidant (Denisov and Afanasev, 2005, p.24 and Rasberger, 1997)

Antioxidants can be generally divided into phenolics and aminics (Rasberger, 1997). The initial step in the inhibition process for phenolics and aminics is the donation of hydrogen atoms to alkylperoxyl radicals (Rasberger, 1997). The resulting phenoxyl radicals (from phenolics) and aminyl radicals (from aminics) function substantially differently, with the latter being more complex and less understood (Denisov and Afanasev, 2005, p.508-512).

Figure 1.5 and Figure 1.6 show the inhibition mechanisms of typical phenolic and aminic antioxidants, respectively.

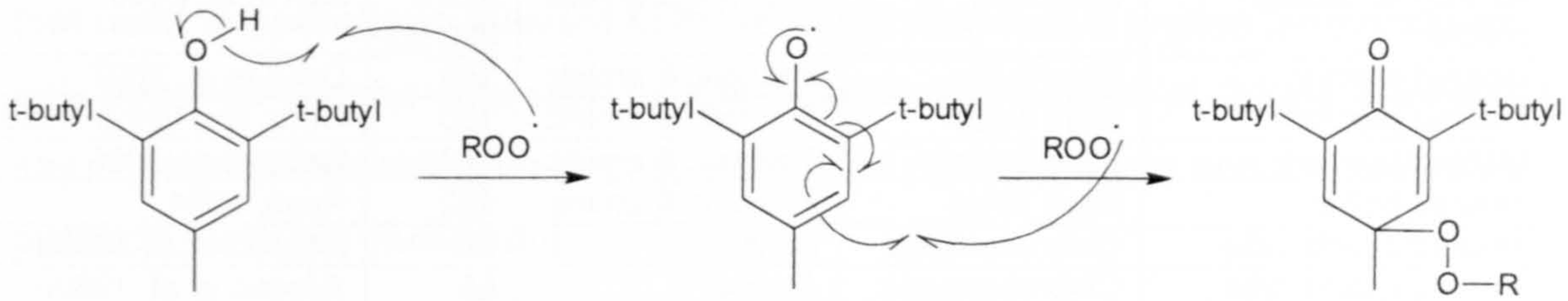

BHT **Phenoxyl radical**

Figure 1.5: Proposed inhibition mechanism of a phenolic antioxidant (Rasberger, 1997)

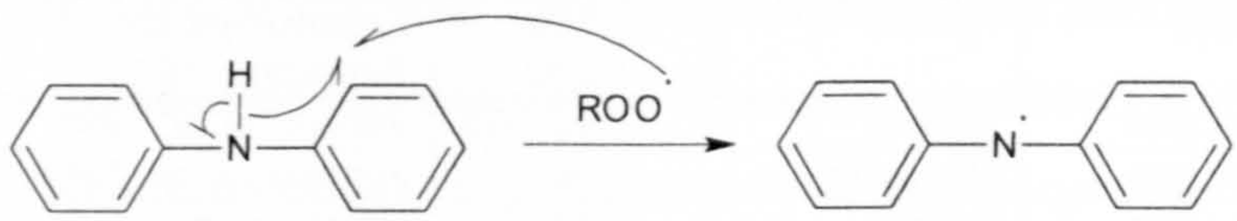

Diphenylamine **Diphenylaminyl**

Figure 1.6: Proposed inhibition mechanism of a diaromatic amine antioxidant (Migdal, 2003)

1.4.1. Previous work on inhibition of lubricant degradation

The behaviour of antioxidants has been studied in automotive engines by Yasutomi et al, 1981, Muller et al, 1982, Bigarre and Legeron, 1987, Inoue and Yamanaka, 1990, and Hamblin and Rohrbach, 2001. However, the major drawback in the above studies is that no oil samples were collected from the piston assembly where the antioxidant decay and lubricant degradation are thought to occur (Bush et al, 1991). Only Bush et al (1991) extracted oil samples from the top ring zone of the piston assembly but indirectly, by using pressurised differential scanning calorimetry, commented on the antioxidant level in the piston assembly by stating that oil samples from the top ring zone have shorter induction times than those of those of the starting material probably due to the oxidation of the antioxidants in the top ring zone.

Studying antioxidants in automotive engines is also very expensive and therefore cost-effective laboratory bench-top reactors are often used instead to simulate the engine environment. Previous work on the oxidation of antioxidants in bench-top reactors are listed in Table 1.9.

Table 1.9: Previous work on the oxidation of antioxidants in bench-top reactors (RPVOT: Rotating pressure vessel oxidation test; Phenolic: Sterically-hindered phenols; Aminic: Diaromatic amines) (references within table)

Technique	Substrate	Antioxidants	T. (°C)	Reference
RPVOT & heated reactor	Base fluid	Phenolic & aminic	225 & 200 (‡)	Jain et al, 2005
Heated reactor	Base fluids	Phenolic & aminic	150	Dong et al, 2007
Heated reactor	Base fluids	Phenolic & aminic	150	Gatto and Grina, 1999
Heated reactor	Base fluids	Phenolic & aminic	150	Gatto et al, 2006
Heated bottle	Base fluids	Phenolic & aminic	152	Rose, 1991
Heated quartz tube	Chlorobenzene	Aminic	65	Adamic et al, 1969a
Heated quartz tube	Chlorobenzene	Aminic	65	Adamic et al, 1969b
Heated reactor	Chlorobenzene	Aminic	57 & 69	Thomas and Tolman, 1962
Heated reactor	Chlorobenzene	Aminic	75	Varlamov and Denisov, 1987
Heated tube	Chlorobenzene & diphenyl ester	Phenolic & aminic	80 & 177 (§)	Low, 1966
Heated Pyrex flask	Dodecane	Aminic	180-230	Ekechukwu and Simmons, 1988
Heated reactor	Hexadecane	Aminic	90-160	Jensen et al, 1995
Heated reactor	Hexadecane	Phenolic	160	Johnson et al, 1983
Oxygen uptake technique	Hexadecane	Aminic	140	Psikha and Kharitonov, 1999
Heated glass reactor	Hexadecane & base fluids	Phenolic	160	Johnson et al, 1987
Heated Pyrex flask	Hexadecane & engine lubricants	Phenolic & aminic	160	Korcek et al, 1986
Heated reactor	Hexadecane & pentaerythrityl tetraheptanoate	Phenolic & aminic	180-220	Mahoney et al, 1979
Heated flask	Hexadecane, paraffinic oil, & hexylbenzene	Aminic	130	Bolsman et al, 1978b
Oxygen uptake technique	Hydraulic oils	Aminic	120	Sheikina et al, 2005
Heated reactor	Lithium grease	Phenolic & aminic	115	Ischuk and Butovets, 1991
Heated reactor	Mineral oils	Phenolic	160	Milton et al, 1987
Heated flask	Paraffinic oil	Aminic	130	Bolsman et al, 1978a
Heated steel chamber	Polyolester	Phenolic & aminic	220	Mousavi et al, 2006
Glass reactor	Propyl alcohol	Phenolic	22	Kharasch and Joshi, 1957
Conductometry	Rapeseed & sunflower oils	Phenolic & aminic	130	Becker and Knorr, 1996
Heated reactor	Soybean oil	Phenolic & aminic	150	Sharma et al, 2007
Heated Pyrex flask	Styrene	Phenolic	65	Howard and Ingold, 1963
Oxygen uptake technique	Styrene & cumene	Phenolic	30	Amorati et al, 2003
Heated Pyrex flask	Tetralin	Phenolic	40	Horswill and Ingold, 1966
Heated Pyrex flask	Tetralin	Phenolic	65	Howard and Ingold, 1964
Oxygen uptake technique	Tetralin	Phenolic & aminic	60	Nishiyama et al, 1994
Oxygen uptake technique	Tetralin	Phenolic	60	Prusikova et al, 1972

(‡): with respect to technique, (§): with respect to substrate

The majority of the temperatures used to study antioxidants in bench-top reactors do not represent those found in automotive engines (Amorati et al, 2003; and Horswill and Ingold, 1966), particularly the piston assembly. The other few studies that used temperatures relevant to those found automotive engine temperatures only obtained generic data such as total acid content (Jain et al, 2005). That is to say, systematic identification and quantification of antioxidants and their oxidation products were not carried out.

1.5. AIMS

The aims of this study are to understand how antioxidants behave at high temperatures representative of engine conditions and how they interact with other lubricant additives, e.g. dispersants and detergents, by oxidation in bench-top reactors and degradation in a research gasoline engine with oil sampling from the piston assembly.

The overall aim of this work is to aid lubricant formulators by extending the understanding of antioxidant behaviour to high temperatures and assessing the compatibility of antioxidants with other lubricant additives.

1.6. REFERENCES

Adamic, K.; Dunn, M.; and Ingold, K. Formation of diphenyl nitroxide in diphenylamine inhibited autoxidations. *Canadian Journal of Chemistry*, 1969a, **47** (2): 287-294.

Adamic, K.; Dunn, M.; and Ingold, K. Formation of radicals in the amine inhibited decomposition of t-butyl hydroperoxide. *Canadian Journal of Chemistry*, 1969b, **47** (2): 295-309.

Adhvaryu, A.; Sharma, Y.; and Singh, I. Studies on the oxidative behaviour of base oils and their chromatographic fractions. *Fuel*, 1999, **78**: 1293-1302.

Amorati, R.; Lucarini, M.; Mugnaini, V.; and Pedulli, G. Antioxidant activity of o-bisphenols the role of intramolecular hydrogen bonding. *Journal of Organic Chemistry*, 2003, **68** (13): 5198-5204.

Barman, B. Behavioral differences between group I and group II base oils during thermo-oxidative degradation. *Tribology International*, 2002, **35**: 15-26.

Bates, T. Effect of automotive technology and environmental factors on lubricant requirements. In: Dowson, D. (editor) Lubricants and lubrication. Elsevier Science B.V., Amsterdam, 1995.

Becker, R. and Knorr, A. An evaluation of antioxidants for vegetable oils at elevated temperatures. *Lubrication Science*, 1996, **8** (2): 95-117.

Bhushan, B. Measurement techniques and applications. In: Bhushan, B. (editor) Nanotribology and nanomechanics an introduction. Springer-Verlag, Berlin, 2005.

Bigarre, I. and Legeron, J. Antioxidant kinetics in synthetic lubricants field testing. *Journal of Synthetic Lubrication*, 1987, **4** (3): 203-218.

Blaine, S. and Savage, P. Reaction pathways in lubricant degradation 2 n-hexadecane autoxidation. *Industrial and Engineering Chemistry Research*, 1991, **30** (9): 2185-2191.

Bolsman, T.; Blok, A.; and Frijns, J. Catalytic inhibition of hydrocarbon autoxidation by secondary amines and nitroxides. *Journal of the Royal Netherlands Chemical Society*, 1978a, **97** (12): 310-312.

Bolsman, T.; Blok, A.; and Frijns, J. Mechanism of the catalytic inhibition of hydrocarbon autoxidation by secondary amines and nitroxides. *Journal of the Royal Netherlands Chemical Society*, 1978b, **97** (12): 313-319.

Bosch, R. Automotive handbook (seventh edition). Robert Bosch GmbH, Plochingen, 2007, p.576-577.

Boss, B. and Hazlett, R. n-Dodecane oxidation elucidation by internal reference techniques. *Industrial and Engineering Chemistry Product Research and Development*, 1975, **14** (2): 135-138.

Bush, G.; Fox, M.; Picken, D.; and Butcher, L. Composition of lubricating oil in the upper ring zone of an internal combustion engine. *Tribology International*, 1991, **24** (4): 231-233.

Cerny, J.; Strnad, Z.; and Sebor, G. Composition and oxidation stability of SAE 15W-40 engine oils. *Tribology International*, 2001, **34**: 127-134.

Daintith, J. (editor) Oxford dictionary of chemistry (fourth edition). Oxford University Press Incorporation, New York, 2000.

Delaney, M. Modeling the chemical degradation of lubricants in advanced engines. PhD thesis, University of Manchester, 2005.

Denisov, E. and Afanasev, I. Oxidation and antioxidants in organic chemistry and biology. CRC Press of Taylor and Francis Group, Florida, 2005.

Denisov, E. and Denisova, T. Handbook of antioxidants bond dissociation energies rate constants activation energies and enthalpies of reactions (second edition). CRC Press LLC, Florida, 2000.

Dong, J.; Mulqueen, G.; Goode, M.; and Holt, A. Stabilizing compositions for lubricants. Chemtura Corporation, 2007, patent WO 2007/100726 A2.

Egharevba, F. and Moduako, A. Assessment of oxidation in automotive crankcase lube oil effects of metal and water activity. *Industrial and Engineering Chemistry Research*, 2002, **41** (14): 3473-3481.

Ekechukwu, A. and Simmons, R. Inhibition of the thin-film oxidation of n-dodecane by diphenylamine. *Journal of the Chemical Society Faraday Transactions* 1, 1988, **84** (6): 1871-1878.

Garcia-Ochoa, F.; Romero, A.; and Querol, J. Modeling of the thermal n-octane oxidation in the liquid phase. *Industrial and Engineering Chemistry Research*, 1989, **28** (1): 43-48.

Gatto, V. and Grina, M. Effects of base oil type oxidation test conditions and phenolic antioxidant structure on the detection and magnitude of hindered phenol/diphenylamine synergism. *Lubrication Engineering*, 1999, **55** (1): 11-20.

Gatto, V.; Elanagar, H.; and Moehle, W. Lubricant oil and lubricating oil additive concentrate compositions. Albemarle Corporation, 2007, patent WO 2007/084854 A1.

Gatto, V.; Moehle, W.; Cobb, T.; and Schneller, E. Oxidation fundamentals and its application to turbine oil testing. *Journal of ASTM International*, 2006, **3** (4): 1-20.

Hamblin, P. and Rohrbach, P. Piston deposit control using metal-free additives. *Lubrication Science*, 2001, **1** (14): 3-23.

Horswill, E. and Ingold, K. The oxidation of phenols I the oxidation of 2,6-di-t-butyl-4-methylphenol 2,6-di-t-butylphenol and 2,6-dimethylphenol with peroxy radicals. *Canadian Journal of Chemistry*, 1966, **44** (3): 263-268.

Howard, J. and Ingold, K. The inhibited autoxidation of styrene part III the relative inhibiting efficiencies of ortho-alkyl phenols. *Canadian Journal of Chemistry*, 1963, **41** (11): 2800-2806.

Howard, J. and Ingold, K. The kinetics of the inhibited autoxidation of tetralin. *Canadian Journal of Chemistry*, 1964, **42** (10): 2324-2333.

Howard, J. Radical reaction rates in liquids, In: Fischer (editor), H. Peroxyl and related radicals. Subvolume D2. Springer, London, 1997.

Inoue, K. and Yamanaka, Y. Change in performance of engine oils with degradation. *SAE Technical Paper*, 1990, paper 902122: 1-10.

Ischuk, Y. and Butovets, V. Estimation of grease oxidation stability under dynamic conditions and antioxidant testing. *NLGI Spokesman*, 1991, **55** (4): 133-138.

Jain, M.; Sawant, R.; Paulmer, R.; Ganguli, D.; and Vasuder, G. Evaluation of thermo-oxidative characteristics of gear oils by different techniques effect of antioxidant chemistry. *Thermochimica*, 2005, **435**: 172-175.

Jensen, R.; Korcek, S.; and Zinbo, M. Liquid-phase autoxidation of organic compounds at elevated temperatures absolute rate constant for intermolecular hydrogen abstraction in hexadecane autoxidation at 120-190°C. *International Journal of Chemical Kinetics*, 1994, **26**: 673-680.

Jensen, R.; Korcek, S.; Mahoney, L.; and Zinbo, M. Liquid-phase autoxidation of organic compounds at elevated temperatures 1 the stirred flow reactor technique and autoxidation at 120-180°C. *Journal of the American Chemical Society*, 1974, **101** (25): 7574-7584.

Jensen, R.; Korcek, S.; Mahoney, L.; and Zinbo, M. Liquid-phase autoxidation of organic compounds at elevated temperatures 2 kinetics and mechanisms of the formation of cleavage products in n-hexadecane autoxidation. *Journal of the American Chemical Society*, 1981, **103** (7): 1742-1749.

Jensen, R.; Korcek, S.; Zinbo, M.; and Gerlock, J. Regeneration of amine in catalytic inhibition of oxidation. *Journal of Organic Chemistry*, 1995, **60** (17): 5396-5400.

Jensen, R.; Korcek, S.; Zinbo, M.; and Johnson, M. Initiation in hydrocarbon autoxidation at elevated temperatures. *International Journal of Chemical Kinetics*, 1990, **22**: 1095-1107.

Johnson, M.; Korcek, S.; and Zinbo, M. High-temperature antioxidant capabilities of base oils and base oil-additive mixtures. *Industrial and Engineering Chemistry Research*, 1987, **26** (9): 1754-1757.

Johnson, M.; Korcek, S.; and Zinbo, M. Inhibition of oxidation by ZDTP and ashless antioxidants in the presence of hydroperoxides at 160°C – part I. *SAE Technical Paper*, 1983, paper 831684: 71-81.

Kharasch, M. and Joshi, B. Reactions of hindered phenols I reactions of 4,4'-dihydroxy-3,5,3',5'-tetra-tert-butyl diphenylmethane. *Journal of Organic Chemistry*, 1957, **22**: 1435-1438.

Korcek, S. and Jensen, R. Relation between base oil composition and oxidation stability at increased temperatures. *ASLE Transactions*, 1976, **19** (2): 83-94.

Korcek, S. and Johnson, M. Effects of NOx on liquid phase oxidation and inhibition of elevated temperatures. In: Bartz, W. (editor). Engine oils and automotive lubrication. Marcel Dekker Incorporation, New York, 1993.

Korcek, S.; Jensen, R.; Zinbo, M.; and Mohoney, L. Effects of oxygen pressure on liquid-phase autoxidation of hexadecane at 160 to 190°C. Symposium on hydrocarbon oxidation, New Orleans, 30 August – 4 September, 1987.

Korcek, S.; Johnson, M.; Jensen, R.; and Zinbo, M. Determination of the high-temperature antioxidant capability of lubricants and lubricant compounds. *Industrial and Engineering Chemistry Product Research and Development*, 1986, **25** (4): 621-627.

Kudynska, J. and Buckmaster, H. Oxidation of motor oils at crankcase temperatures further studies. *Fuel*, 1997, **76** (2): 195-198.

Lee, P. Lubricant degradation transport and the link to piston assembly tribology. PhD Thesis, University of Leeds, 2006.

Low, H. Antioxidants free radical chain terminators. *Industrial and Engineering Chemistry Product Research and Development*, 1966, **5** (1): 80-86.

Mahoney, L.; Korcek, S.; Willermet, P.; Hamilton, E.; Jensen, R.; Zinbo, M.; Kandah, S.; Norbeck, J.; and Scheich, L. Time-temperature studies of high temperature deterioration phenomena in lubricant systems synthetic ester lubricants. Internal Report of Ford Motor Company, 1979.

Migdal, C. Antioxidants. In Rudnic, L. (editor) Lubricant additives chemistry and application. Marcel Dekker, New York, 2003.

Mill, T.; Mayo, F.; Richardson, H.; Irwin, K.; and Allara, D. Gas- and liquid-phase oxidations of n-butane. *Journal of the American Chemical Society*, 1972, **94** (19): 6802-6811.

Milton, J.; Korcek, S.; and Zinbo, M. High-temperature antioxidant capabilities of base oils and base oil-additive mixtures. *Industrial and Engineering Chemistry Research*, 1987, **26**: 1754-1757.

Moritani, H. and Nozawa, Y. Oil degradation in second-land region of gasoline engine pistons. *R&D Review of Toyota CRDL*, 2004, **38** (3): 36-43.

Mousavi, P.; Wang, D.; Grant, C.; Oxenham, W.; and Hauser, P. Effects of antioxidants on the thermal degradation of a polyol ester lubricant using GPC. *Industrial and Engineering Chemistry Research*, 2006, **45** (1): 15-22.

Muller, K.; Kristen, U.; and Hamblin, P. Effectiveness of ashless antioxidants in motor oils. From: Wirksamkeit von aschefreien antioxidantien in motorolen. *Schmiertechnik Tribologie*, 1982, **29** (3): 92-97.

Nishiyama, T.; Kagimasa, T.; and Yamada, F. Comparison of heteroatom-bridged analogues of methylenebisphenols for antioxidant activities. *Canadian Journal of Chemistry*, 1994, **72** (5): 1412-1414.

Oganesova, E.; Bordubanova, E.; Popova, Z.; Bakunin, V.; Kuzmina, G.; and Parenago, O. Influence of the conditions of the liquid-phase oxidation of hexadecane on the reaction mechanism. *Petroleum Chemistry*, 2004, **44** (2): 99-105.

Owrang, F.; Mattsson, H.; Olsson, J.; and Pedersen, J. Investigation of oxidation of a mineral and a synthetic engine oil. *Thermochimica Acta*, 2004, **413**: 241-248.

Pezzuto, J. and Park E. Autoxidation and antioxidants. In: Swarbrick, J. and Boylan, J. (editors) Encyclopedia of pharmaceutical technology (second edition), volume 1, Informa Health Care, 2004, page: 97.

Prusikova, M.; Jirackova, L.; and Pospisil, J. Antioxidants and stabilizers XXXIV antioxidative activity of bisphenols during stabilization of tetralin. *Collection of Czechslovak Chemical Communications*, 1972, **37** (11): 3788-3799.

Psikha, B. and Kharitonov, V. Specific features of inhibition by some aromatic amines I the effect of inhibitors on the initiation properties of dicumyl peroxide. *Kinetic and Catalysis*, 1999, **40** (4): 459-466.

Rasberger, M. Oxidative degradation and stabilisation of mineral oil based lubricants. In: Mortier, R. and Orszulik, S. (editors) Chemistry and technology of lubricants (second edition). Blackie academic and professional, London, 1997.

Rizvi, S. Additives for automotive fuels and lubricants. *Lubrication Engineering*, **55** (4): 33-39, 1999.

Roby, S.; Mayer, R.; Ruelas, S.; Martinez, J.; and Rutherford, J. Development of a bench test to predict oxidative viscosity thickening in the sequence IIIG engine test. *SAE Technical Paper*, 2004, paper 2004-01-2985: 99-104.

Rose, D. Analysis of antioxidant behaviour in lubricating oils. PhD thesis, University of Leeds, 1991.

Rust, F. Intramolecular oxidation the autoxidation of some dimethylalkanes. *Journal of the American Chemical Society*, 1957, **79**: 4000-4003.

Santos, J.; Santos, I.; Souza, A.; Sobrinho, E.; Fernandes, V.; and Silva, Arilson. Thermoanalytical and rheological characterization of automotive mineral lubricants after thermal degradation. *Fuel*, 2004, **83**: 2393-2399.

Saville, S.; Gainey, F.; Cupples, S. Fox, M.; and Picken, D. A study of lubricant condition in the piston ring zone of single cylinder diesel engines under typical operating conditions. *SAE Technical Paper*, 1988, paper 881586.

See, M. Greenhouse gas emissions global business aspects. Springer, Germany, 2001. Page: 7.

Sharma, B.; Perez, J.; and Erhan, S. Soybean oil-based lubricants a search for synergistic antioxidants. *Energy and Fuels*, 2007, **21** (4): 2408-2414.

Sheikina, N.; Petrov, L.; Psikha, B.; Kharitonov, V.; Tyshchenko, V.; and Shabalina, T. Quantitative study of the inhibited oxidation of hydraulic oils. *Petroleum Chemistry*, 2005, **45** (4): 284-288.

Sickle, D.; Mill, T.; Mayo, F.; Richardson, H.; and Gould, C. Intramolecular propagation in the oxidation of n-alkanes autoxidation of n-pentane and n-octane. *Journal of Organic Chemistry*, 1973, **38** (26): 4435-4440.

Spiiners, I. and Hedenburg, J. Chemiluminescence in autoxidation of hydrocarbons a method for fingerprinting and evaluation of oxidative stability. *Industrial and Engineering Chemistry Product Research and Development*, 1985, **24** (3): 442-447.

Stark, M. The oxidation of hydrocarbon base-fluid lubricants in gasoline engines. Internal Report. 2003, Department of Chemistry, University of York.

Stark, M.; Gamble, R.; Hammond, C.; Gillespie, H.; Lindsay Smith, J.; Nagatomi, E.; Priest, M.; Taylor, C.; Taylor, R.; and Waddington, D. Measurement of lubricant flow in a gasoline engine. *Tribology Letters*, 2005, **19** (3): 163-168.

Taylor, R.; Mainwaring, R.; and Mortier, R. Engine lubricant trends since 1990. *Proceedings of the Institution of Mechanical Engineers-part J-Journal of Engineering Tribology*, **219**: 1-16, 2005.

Thomas, J. and Tolman, C. Oxidation inhibited by diphenylamine. *Journal of the American Chemical Society*, 1962, **84**: 2930-2935.

Varlamov, V. and Denisov, E. Kinetic spectrophotometric study of the kinetics of direct and reverse reactions of the peroxide radical with diphenylamine. *Russian Chemical Bulletin*, 1987, **36** (8): 1607-1612.

Vipper, A. Influence of oil-soluble copper salts on catalytic oxidation of lubricating oil in laboratory conditions and in a single-cylinder engine. *Lubricant Science*, 1995, **1** (8): 73-83.

Vipper, A.; Zadko, I.; Ermolaev, M.; and Oleinik, J. Engine oil ageing under laboratory conditions. *Lubrication Science*, 2002, **3** (14): 363-375.

Wilkinson, J. The autoxidation of branched hydrocarbons in the liquid phase as models for understanding lubricant degradation. PhD thesis, University of York, 2006.

Yasutomi, S.; Maeda, Y.; and Maeda, T. Kinetic approach to engine oil 2 antioxidant decay of lubricant in engine system. *Industrial and Engineering Chemistry Product Research and Development*, 1981, **20** (3): 536-540.

Zinbo, M.; Jensen, R.; Johnson, M.; and Korcek, S. Relative inhibiting efficiency of base oils. *Industrial and Engineering Chemistry Research*, 1987, **26** (5): 902-906.

2. EXPERIMENTAL

2.1. BENCH-TOP OXIDATIONS

2.1.1. Bench-top reactors

Oxidations were carried out in three bench-top reactors; described here as micro, intermediate, and large, and which were made in-house at the Department of Chemistry of the University of York. Photographs of the reactors are shown in Figure 2.1, Figure 2.2, and Figure 2.3.

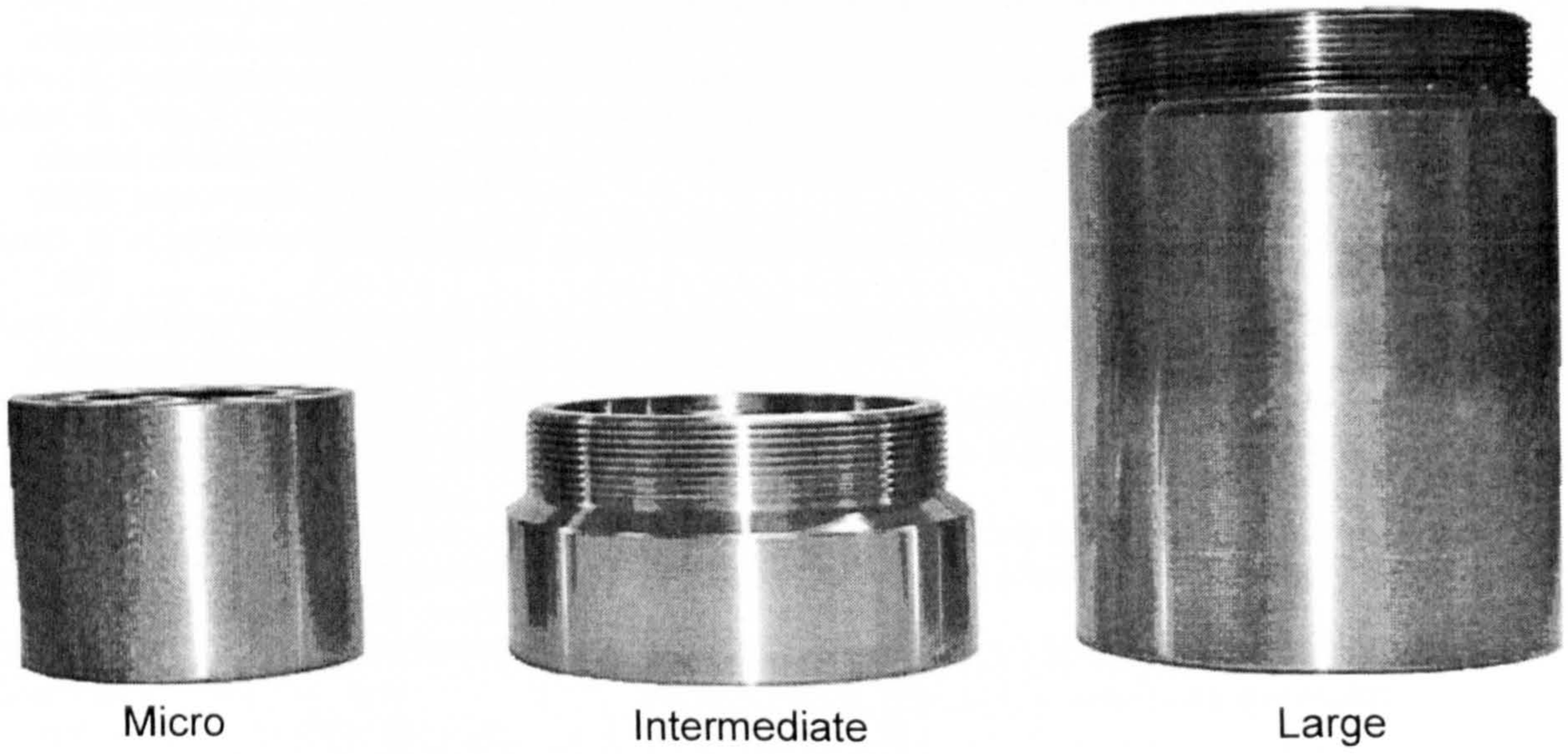

Figure 2.1: A side view of reactors (all three reactors are shown to the same scale)

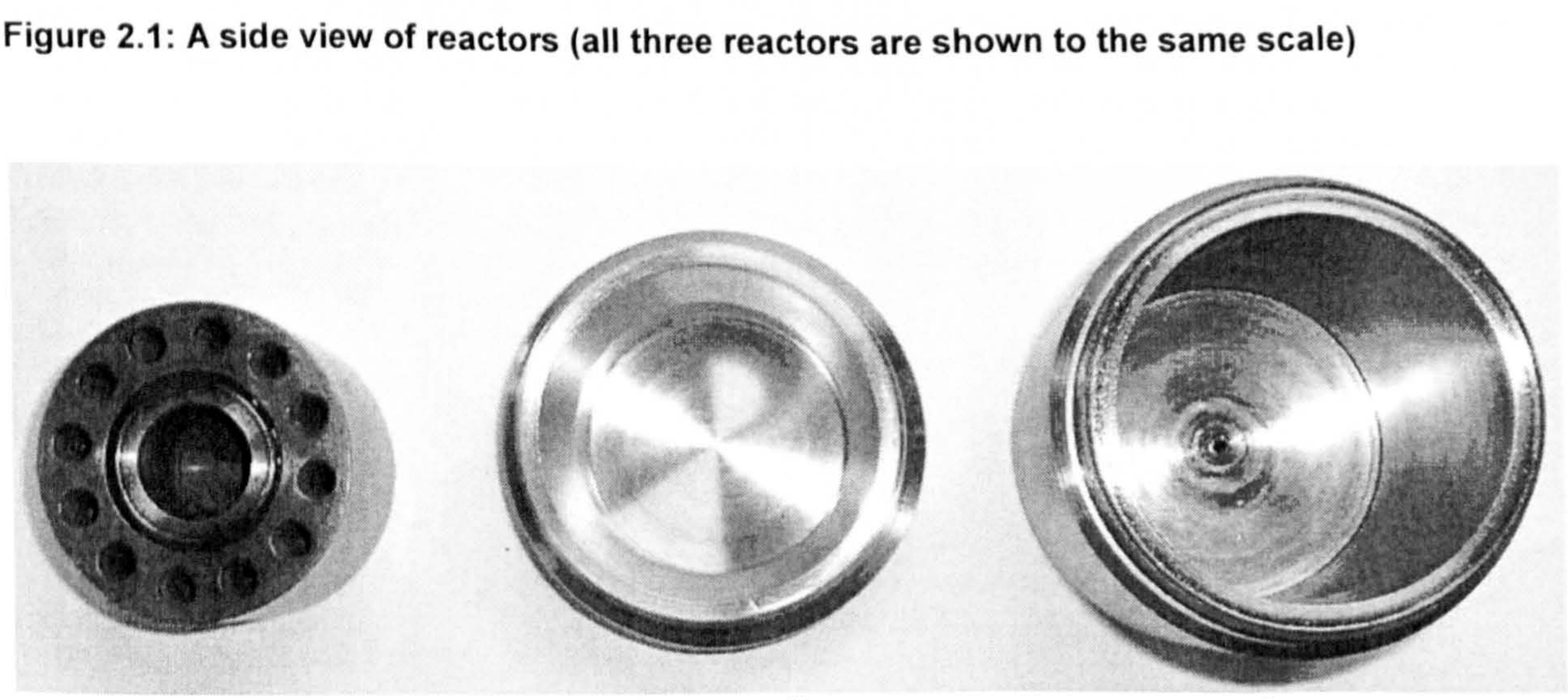

Figure 2.2: A top view of reactors (all three reactors are shown to the same scale)

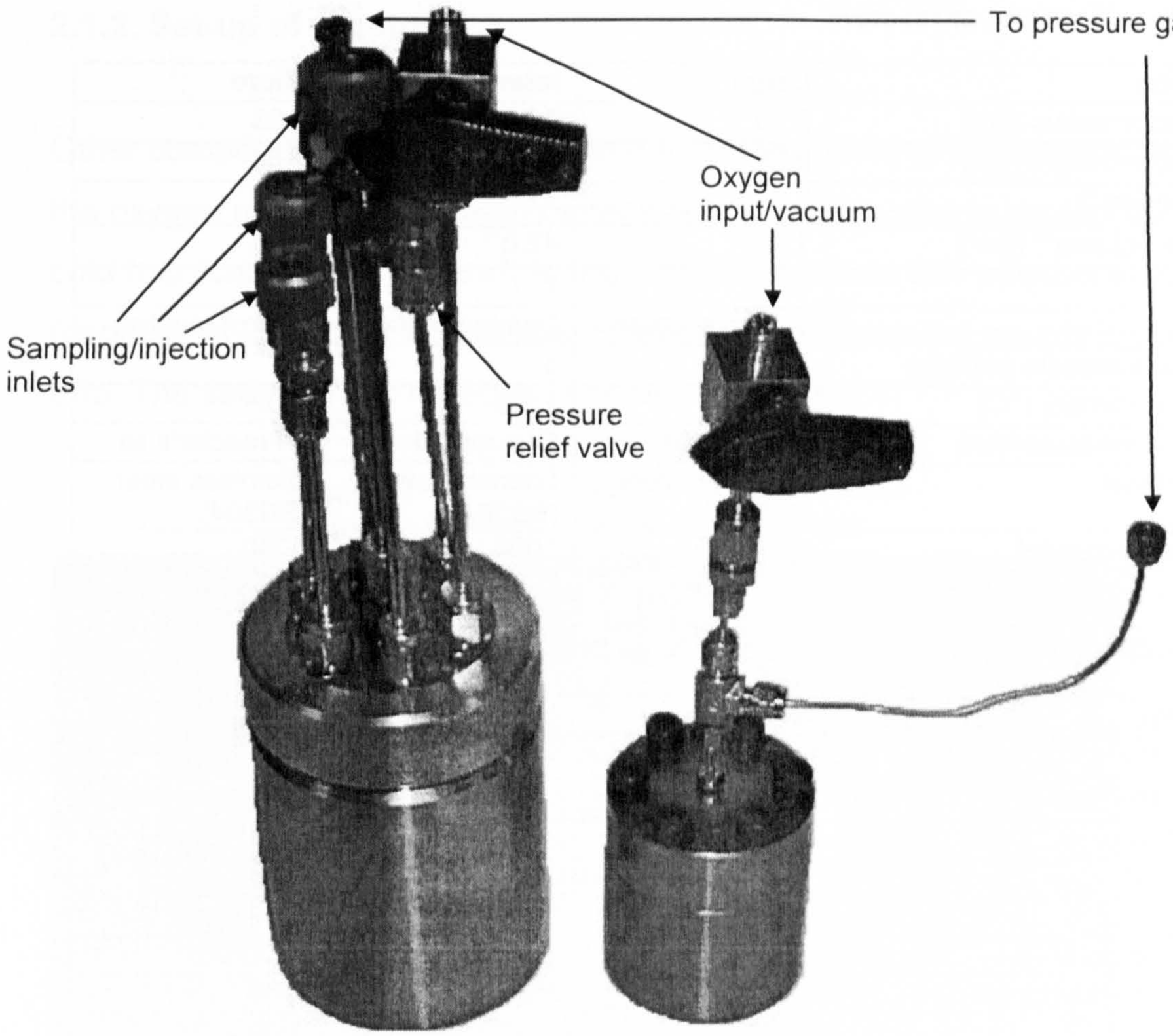

Figure 2.3: Parts of reactors

The same lid and connections used with the large and intermediate reactors.

The specifications of the reactors are listed in Table 2.1; and the substrate parameters inside the reactors are listed in Table 2.2.

Table 2.1: Specifications of reactors

Specification	Large	Intermediate	Micro
Internal reactor radius (cm)	2.70	2.70[8]	0.93
Internal reactor height (cm)	8.22	2.25	1.84
Flea volume (cm^3)	7.0	7.0[9]	0.3
Head space volume[10] (cm^3)	176.7	42.0[11]	3.65
Inlets	7	7	2
Sampling	During reaction	During reaction	End of reaction
Time to heat substrate (minute)	3	3	30
Temperature stability (°C)	± 0.3	± 0.3	± 0.1
Temperature measurement	Of substrate	Of substrate	Of reactor's lid
Surface material	Stainless steel (BS304)	Stainless steel (BS304)	Stainless steel (BS304)
Stirring (cycles/minute)	1000	1000	5000

Table 2.2: Substrate parameters (assuming it to be Shell XHVI 8.2)

Specification	Large	Intermediate	Micro
Typical substrate volume (cm^3)	5.00	5.00	1.00
Substrate density (g/cm^3)	0.834	0.834	0.834
Substrate mass (g)	4.17	4.17	0.83
Substrate RMM ($g\ mol^{-1}$)	522	522	522
Substrate (mol)	7.99×10^{-3}	7.99×10^{-3}	1.60×10^{-3}
Typical temperature (K)	473.15	473.15	473.15
Gas/liquid (v/v) [at 473.15 K]	34.34	7.40	2.65
Pressure (Pa)	1.00×10^5	1.00×10^5	1.00×10^5
O_2 (mol)[12] [at 473.15 K]	4.49×10^{-3}	1.07×10^{-3}	9.27×10^{-5}
O_2:substrate (mol/mol) [at 473 K]	0.56	0.13	0.058
Film thickness (mm)[13]	2.2	2.1	3.7

[8] Radius at the bottom of the reactor.
[9] Volume measured by water displacement.
[10] Calculated from (3.142 x (Radius)^2 x Length) – (Substrate volume + Flea volume).
[11] The intermediate reactor has curved angles, which would make the calculation of the reactor volume difficult. So the volume of the reactor was measured by measuring the volume of water needed to fill the reactor.
[12] Calculated from (Pressure x Reactor volume) / (Universal molar gas constant x Temperature).
[13] Calculated from (Substrate volume) / (3.142 x (Reactor radius)^2).

2.1.2. Set-up of reactors

Other components were attached to the reactors. One of these components was the oxygen meter. The oxygen meter has two accessories to protect its sensor: A cold trap (capacity of 5.6 cm^3) to trap volatile products and a hydrocarbon trap (capacity of 25.0 cm^3) to dissolve volatile hydrocarbons not caught by the cold trap. The setup for the reactors is shown in Figure 2.4.

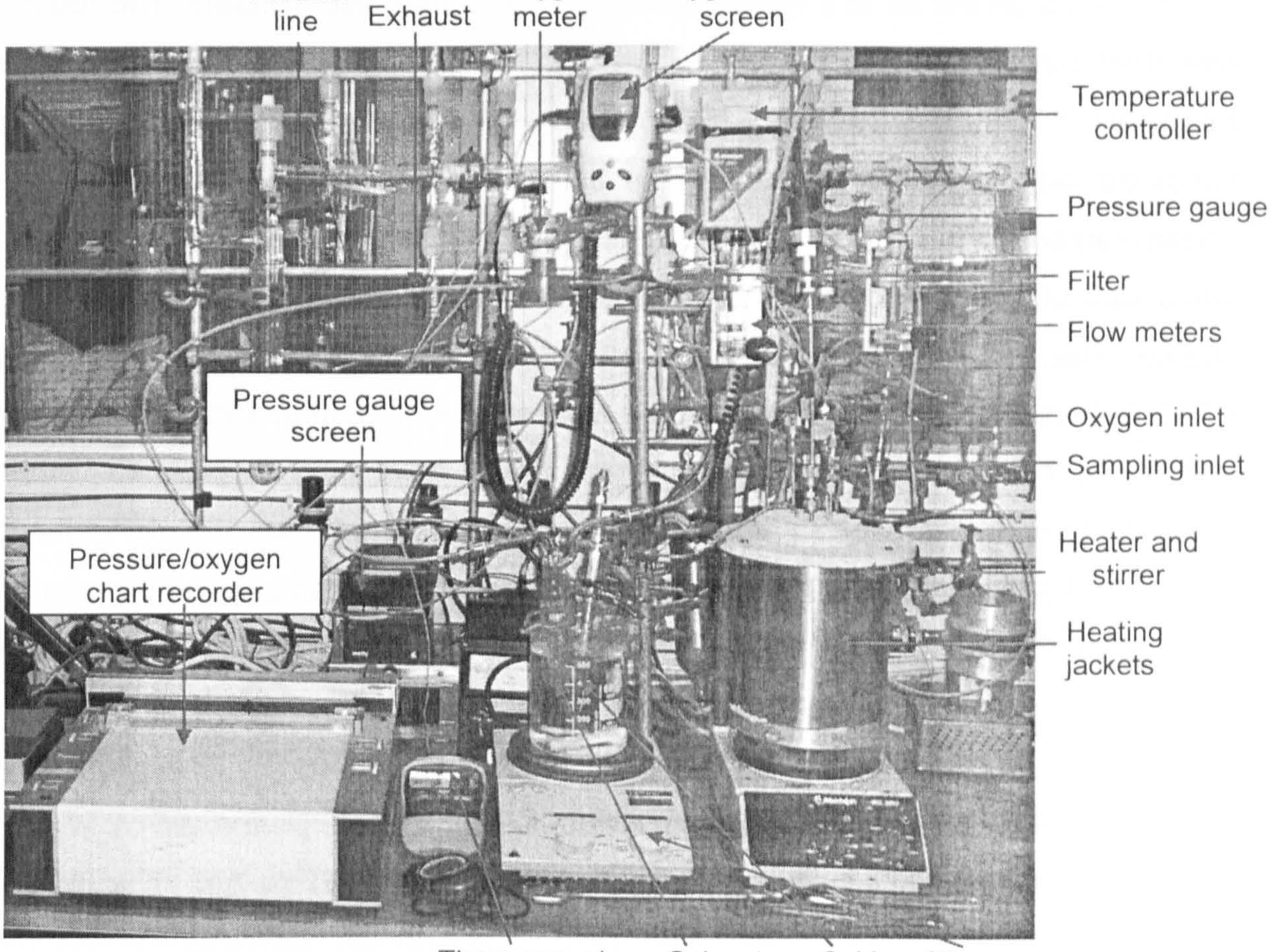

Figure 2.4: Setup of reactors

2.1.3. Static oxidations

Static oxidations, in the micro reactor, were performed by pipetting the substrate and placing a PTFE-coated magnetic flea into the reactor. A PTFE ring was placed between the base of the reactor and the lid to make a gas-tight-seal. The lid was screwed on to the base with six allanbolts. The pressure gauge (specification precision of 0.1 mbar to 2 bars from Transinstruments) and the vacuum lines were then attached to their respective inlets. The vacuum valve was opened to purge the air to a typical pressure of less than five millibars. The reactor was then placed into the preheated oven with the temperature controlled by a heater band (Jencons 230 V / 320 W) fitted with a feedback thermocouple. The substrate was degassed by stirring for a few seconds. When the temperature (measured by a Fluke S1 II thermocouple) reached the desired level, the vacuum valve was closed and one bar of pure oxygen was introduced, which was then sealed. The magnetic stirrer and the pressure chart recorder (Kipp and Zonen BD40 04) were turned on. The pressure minimum was assumed to represent the end of the oxidation; as all of the oxygen would have been consumed. When pressure reached its minimum point, the reactor was immersed in cold water to terminate the oxidation. The lid was then removed and the sample was transferred via a glass Pasteur pipette to a vial to be kept in a fridge or freezer, to stop/slow down reactions including the decomposition of alkylhydroperoxides, until analysis.

Static oxidations in the intermediate and large reactors were performed by sealing the reactor with the lid, which has an embedded O-ring to fill the gap. The reactor was then placed into the preheated oven and the air removed. When the temperature of the reactor reached the desired level, and while under vacuum, the substrate was introduced into the reactor either by injection through the septum (via a 26-gauge needle) or bypassing the septum (via an 18-gauge needle) using a 5 cm^3 plastic syringe. The substrate was then degassed by stirring for a few seconds. The vacuum valve was closed and one bar of oxygen was introduced. The magnetic stirrer and the pressure chart recorder were turned on. Online samples (typically ~50 μm^3) were collected via a 26-gauge needle to monitor the reaction throughout the experiment. A schematic diagram of reactor in the static mode is shown in Figure 2.5.

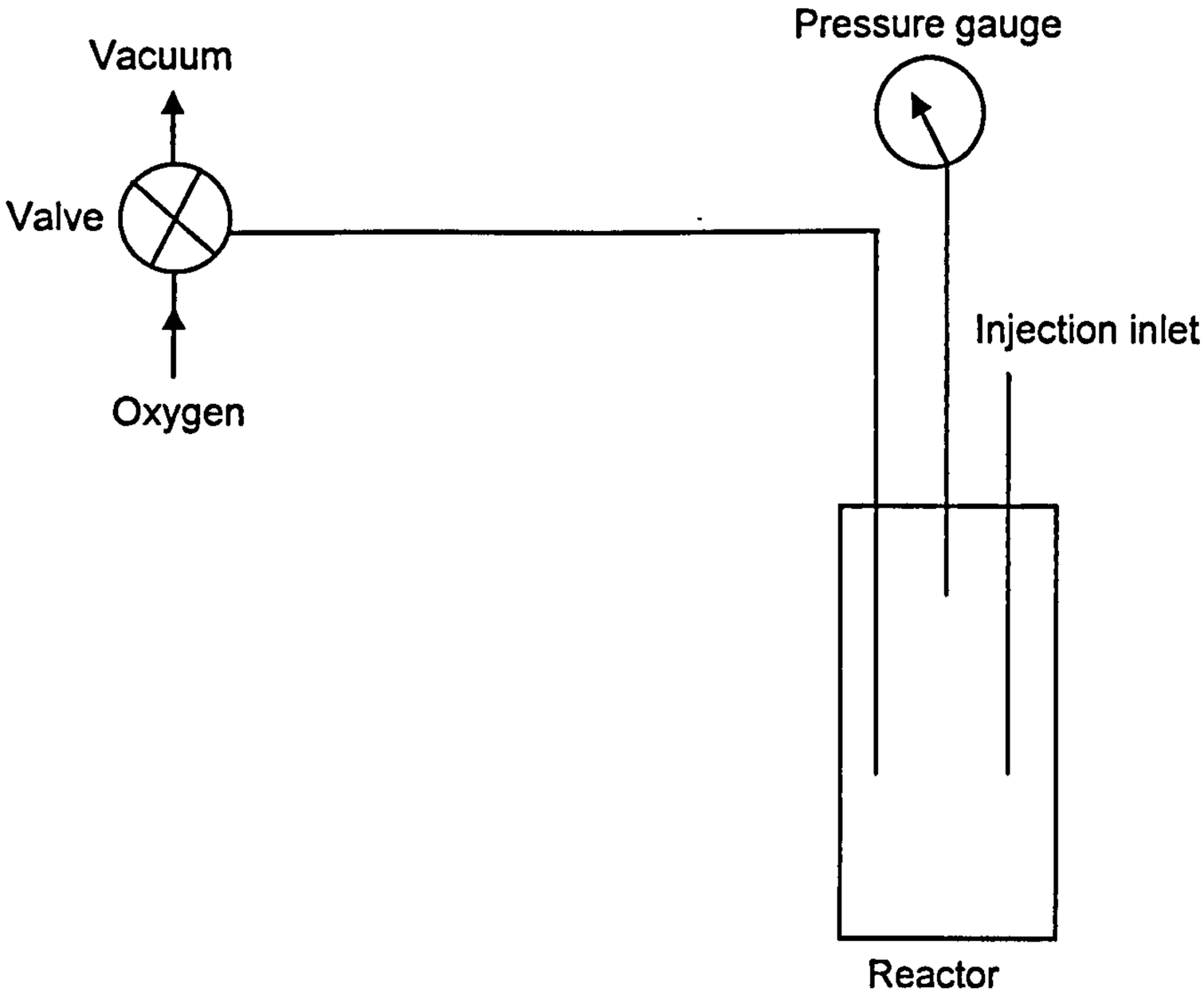

Figure 2.5: Schematic diagram of reactor in static mode

2.1.4. Flow oxidations

Flow oxidations in the intermediate and large reactors were performed in a similar manner to that of the static oxidation. The sealed reactor was placed into the preheated oven and the oxygen valve was turned on with the flow controller adjusted at a flow rate of 0.1 litres per minute; higher flow rates could result in backup pressure. When the temperature of the reactor reached the desired level and the level of oxygen reaches one hundred per cent, the substrate was introduced into the reactor by injection. The magnetic stirrer, and the pressure and oxygen chart recorders were turned on. The oxygen consumption was monitored over time to monitor the oxidation of the substrate. A schematic diagram of reactor in the flow mode is shown in Figure 2.6.

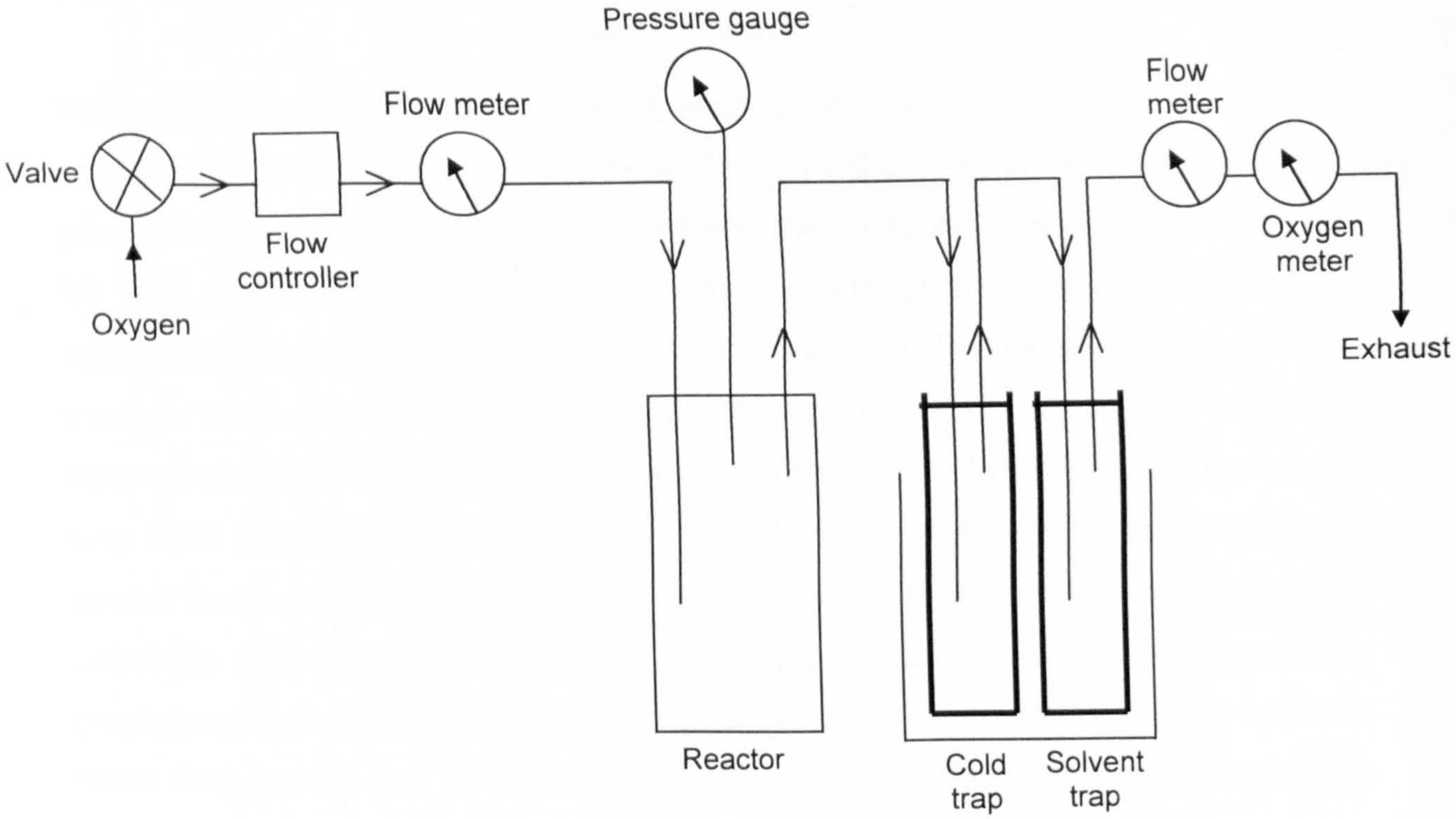

Figure 2.6: Schematic diagram of reactor in flow mode

2.2. ENGINE DEGRADATION

2.2.1. Engine specification

The degradation of engine lubricants was carried in a single cylinder Ricardo Hydra gasoline fuelled research engine (manufactured by Ricardo Consulting Engineers limited), at the School of Mechanical Engineering of the University of Leeds, to complement oil oxidations data from bench-top reactors at the Department of Chemistry of the University of York. The specifications of the Ricardo Hydra engine are listed in Table 2.3 and a photograph of the engine is shown in Figure 2.7.

Table 2.3: Specifications of Ricardo Hydra engine (Lee, 2006, p.206)

Number of cylinders	1
Compression ratio	10.5 : 1
Bore	86 mm
Stroke	86mm
Induction system	Naturally aspirated
Petrol injection	Indirect
Liner material	Cast iron

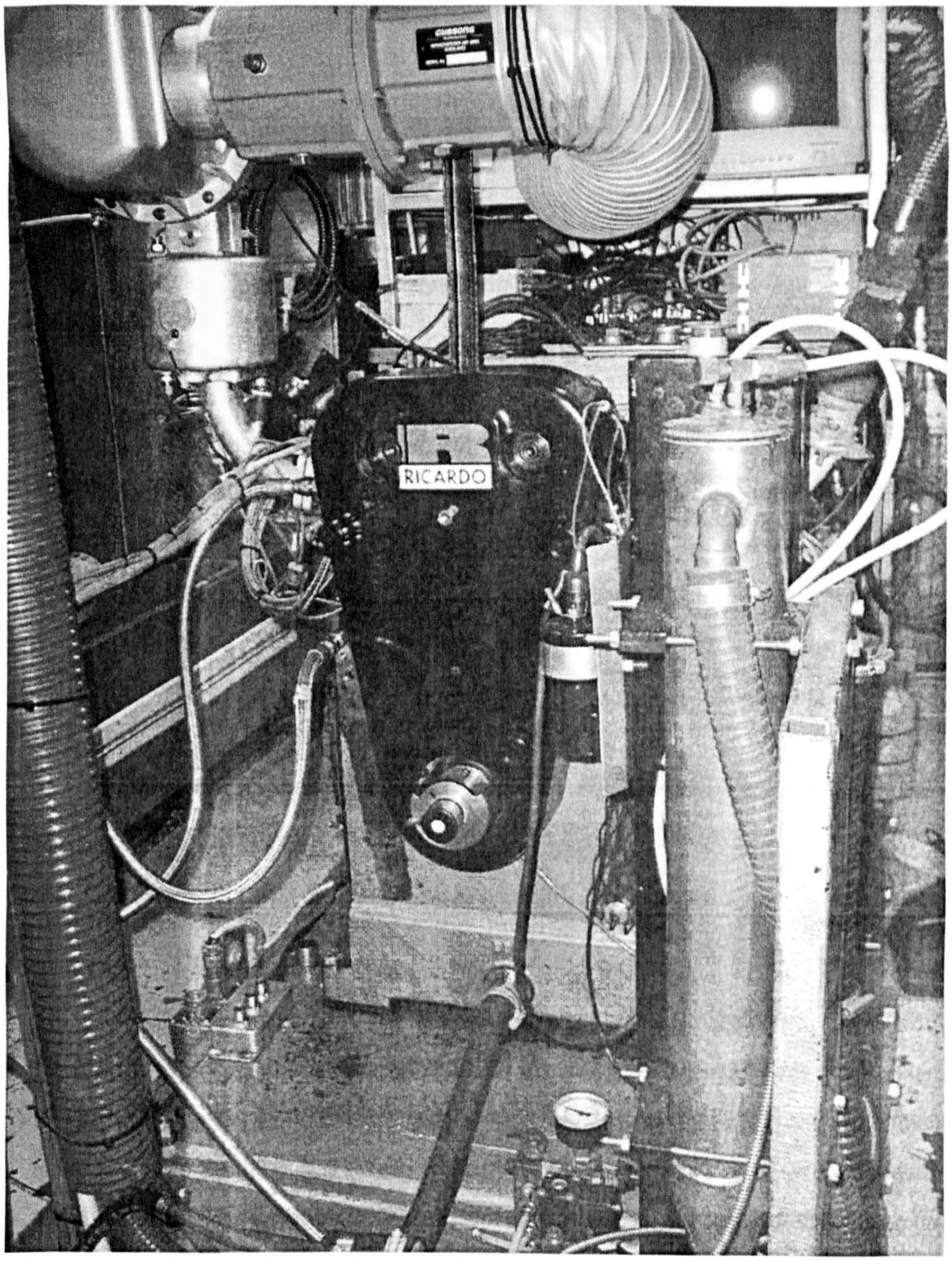

Figure 2.7: Ricardo Hydra gasoline engine

The piston ring pack consists of two compression rings and an oil control ring. A schematic diagram of the piston ring pack assembly and the free volumes available between the different parts of the assembly is shown in Figure 2.8.

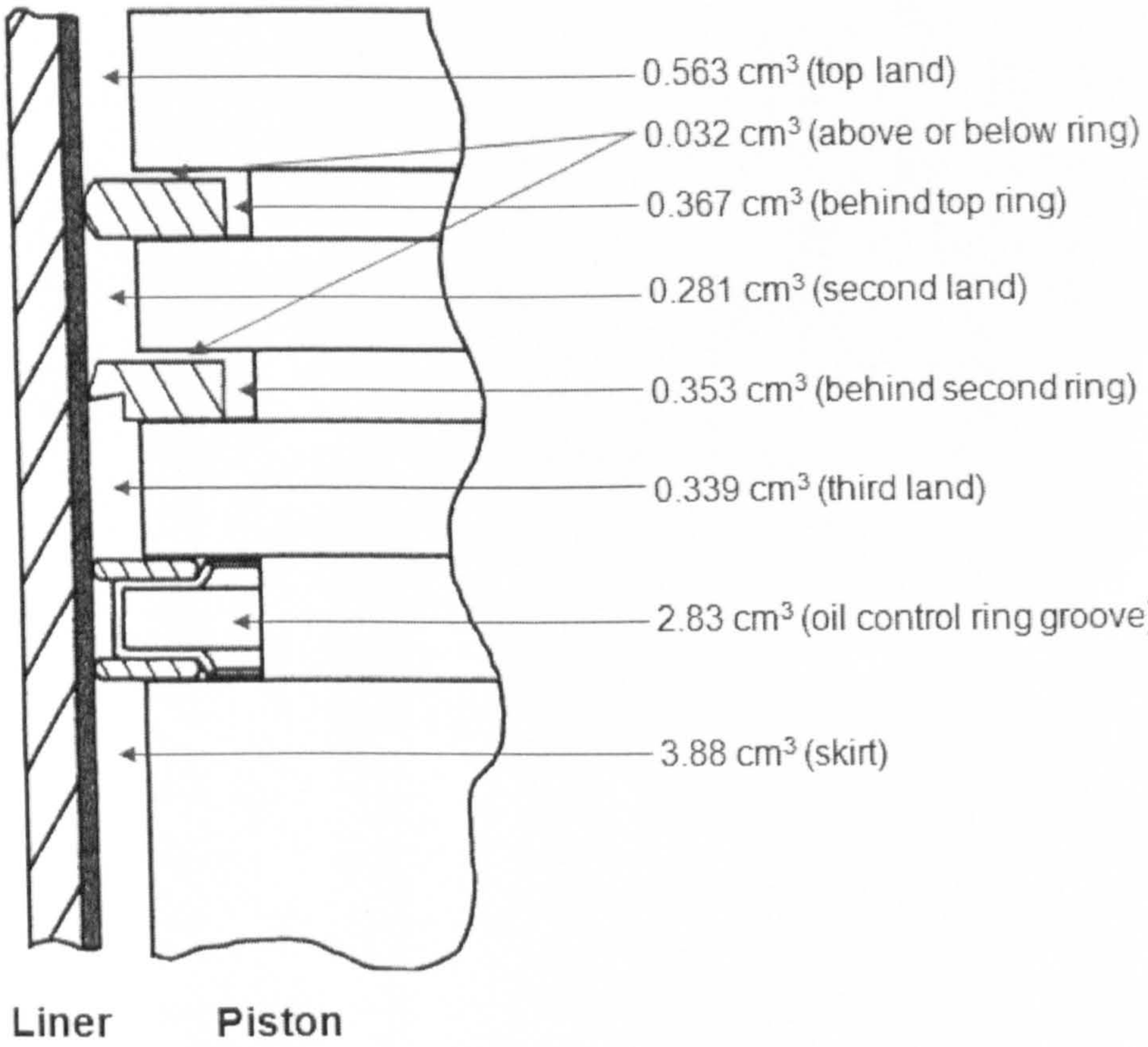

Figure 2.8: Free volume available in piston ring pack assembly (Stark, 2003, p.23)

2.2.2. Oil sampling

Oil samples were collected from the sump and the top ring zone at specific intervals, while the engine was running at 1500 revolutions-per-minute with a 50 % load. Oil samples from the sump (temperature was maintained at ~80 °C to avoid lubricant degradation in the sump) were collected using a 5 cm^3 disposable plastic syringe. Oil samples from the top ring zone were collected via a 1/8" PTFE tube attached to a 0.5 mm hole, drilled behind the top ring zone. The combustion pressure forces the oil droplets from the vicinity of the hole in the piston assembly through the tube to be collected in small sample vials which were kept in a fridge or freezer until analysis. A photograph and a schematic diagram of the modified piston assembly are shown in Figure 2.9 and Figure 2.10, respectively.

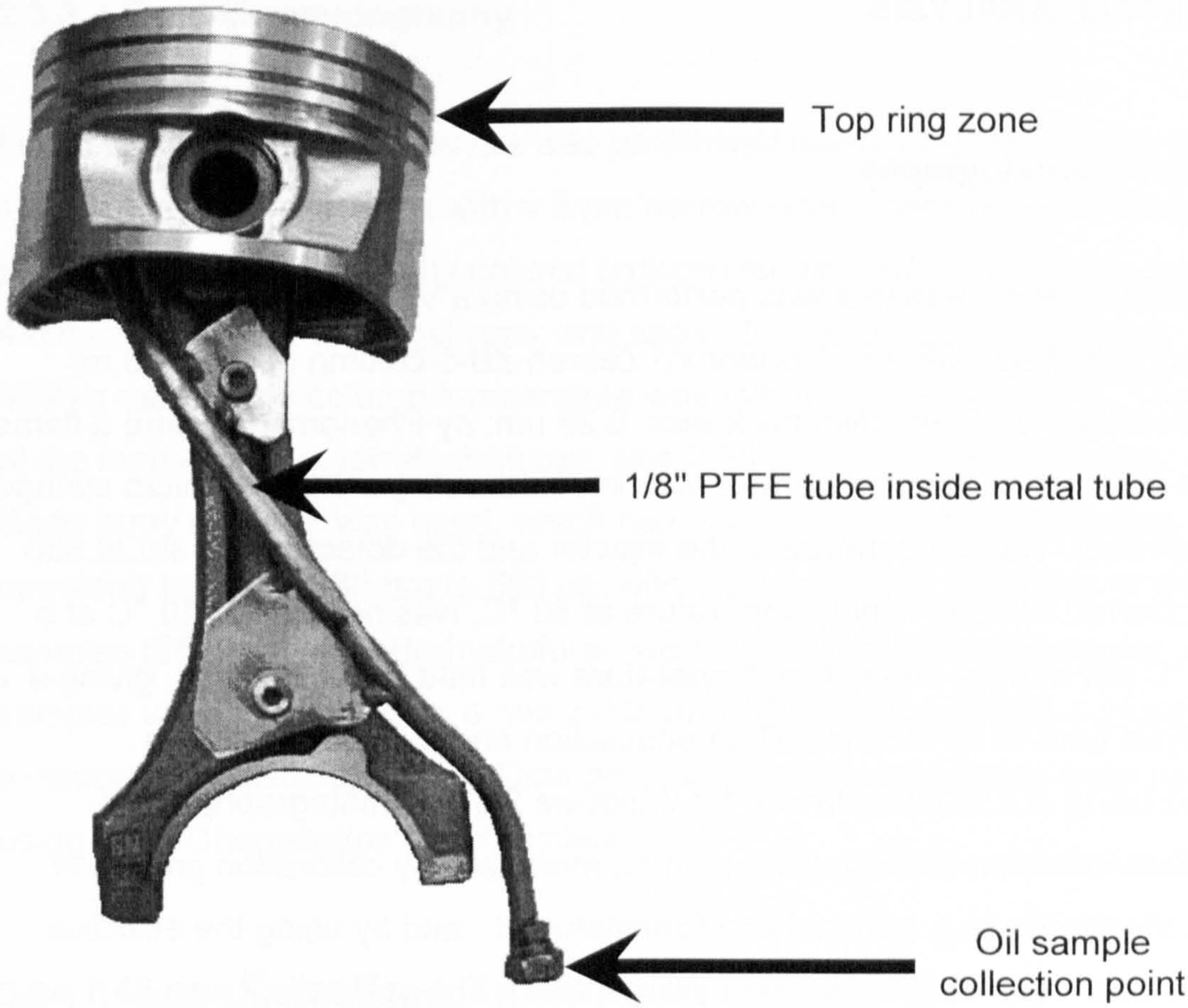

Figure 2.9: Ricardo Hydra piston assembly (Gamble, 2002)

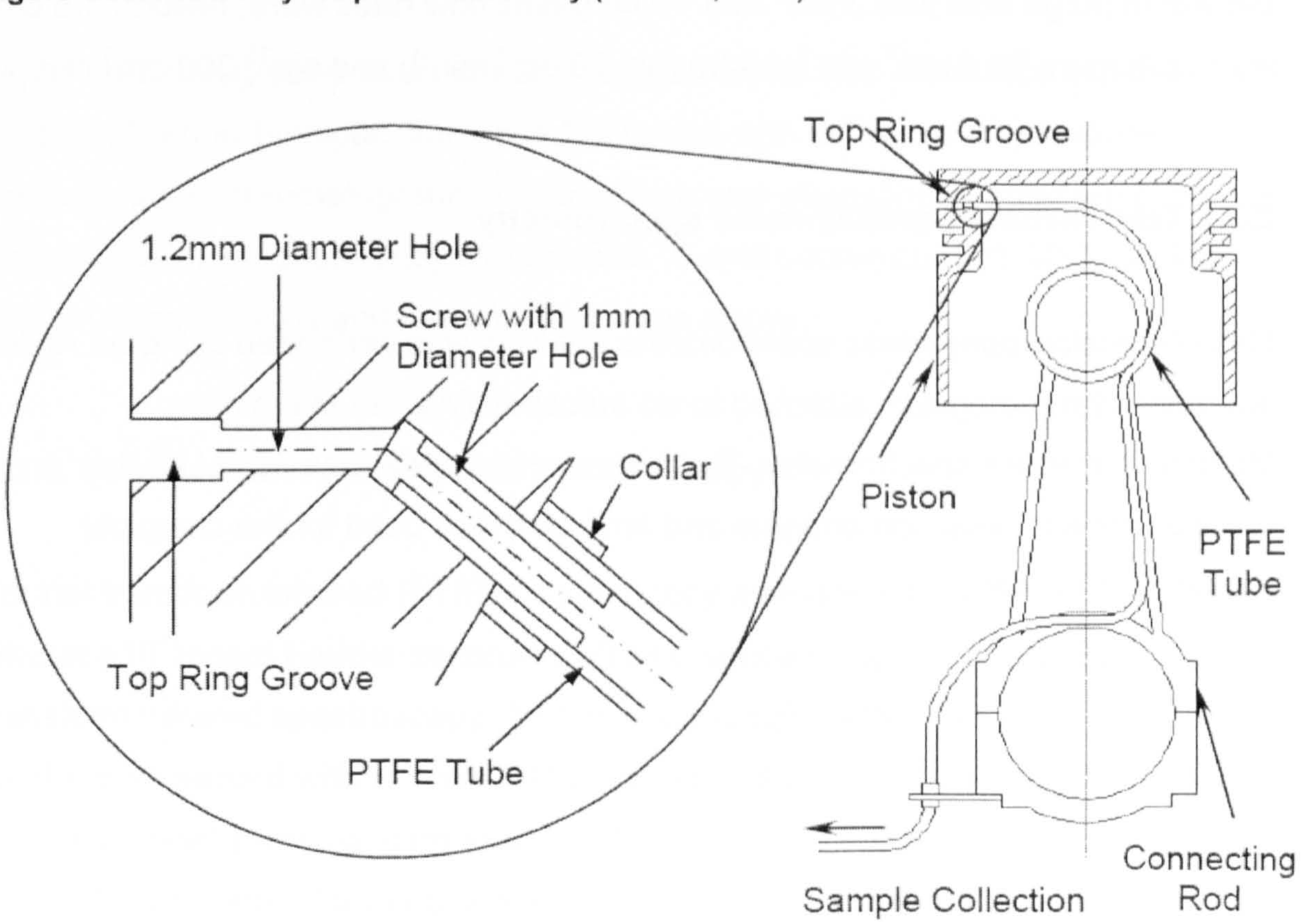

Figure 2.10: Oil sample collection from top ring zone (Gamble, 2002)

2.3. CHEMICAL ANALYSIS

2.3.1. Gas chromatography

Gas chromatographic analysis was performed using a Varian 3380 gas chromatograph fitted with a 5 % phenoxyl Zebron ZB-5 column (length: 30 m; internal diameter: 0.25 mm; film thickness: 0.25 µm; by Phenomenex) and a flame ionisation detector. 0.3 μm^3 of sample was injected, using a 0.5 μm^3 micro syringe (SGE Australia). The temperature of the injector and the detector was set at 350 °C. The column, with the initial temperature at 50 °C, was heated to 340 °C at a rate of 8 °C per minute. Then, the temperature was held for 14 minutes, giving a total analysis time of 50 minutes. Data acquisition and manipulation were performed using JCL 6000 software for Windows 2.0 chromatography data system. Quantification was by using starting materials, by calibration graphs of authentic standards (e.g. galvinol and formylphenol), and by using the effective carbon number method (Scanlon and Willis, 1985). The split ratio[14] was 33:1 and the waste purge flow was 3 cm^3 min^{-1}. The gases flow rates were, helium: 1.5 cm^3 min^{-1}; nitrogen: 28.5 cm^3 min^{-1}; hydrogen: 30 cm^3 min^{-1}; and air:[15] 300 cm^3 min^{-1}.

2.3.2. Gas chromatography-mass spectrometry

Gas chromatography-mass spectrometric analysis was performed using an Agilent 5890 gas chromatograph attached to an autospec (Waters-Micromass; Manchester) mass spectrometer. The ionisation potential was 70 eV for the electron impact ionisation analysis and ammonia was used for the chemical ionisation analysis.

---

[14] Split ratio = Helium split flow to the atmosphere / Helium column flow; where, helium split flow is 50:1 and helium column flow is 1.5 cm^3 min^{-1}.

[15] Air flow was calculated as follows: Air = Hydrogen / 10; Nitrogen + Helium = 5 cm^3 per 10 sec = 1 cm^3 per 2 sec; (1 cm^3 per 2 sec) / 10 = (1 cm^3 in 0.2 sec) x 50 = 50 cm^3 in 10 sec; Helium + Nitrogen + Hydrogen = 10 cm^3 per 10 sec; Air = (50 cm^3 per 10 sec) / (60 cm^3 per 10 sec); 10 sec / 60 cm^3 = 0.167 sec; 50 cm^3 x 0.167 sec = 8.35 sec.

2.3.3. Liquid chromatography

Liquid chromatographic analysis was performed using a Hewlett Packard series 1090 liquid chromatograph with a 5 µm narrow bore Phenomenex Phenogel gel permeation chromatography column (column length: 300 mm; column diameter: 4.6 mm; pore size: 50 Angstroms; and separation molecular mass range: 100-3000 g mol^{-1}). The column temperature was maintained at 35 ± 1 °C. The flow rate of the mobile phase, tetrahydrofuran, was 0.35 cm^3 min^{-1} for 20 minutes. A photo diode array detector was used, which had eight simultaneous acquisition channels operating between 280 nm to 560 nm with a 20 nm width. Undiluted or diluted samples (25 μm^3) with tetrahydrofuran were injected by an autosampler. All the samples were filtered with a 4 mm x 0.2 µm ISO-disc filter (PTFE-4-2) attached to a disposable plastic syringe.[16] Data acquisition and manipulation were performed using a HP Chemstation for LC software.

2.3.4. Liquid chromatography-mass spectrometry

Liquid chromatography-mass spectrometric analysis was performed using an LCQ Classic (Thermo-Finnigan San Jose California) with a Thermo Separations Products liquid chromatograph. The interface was atmospheric pressure chemical ionisation with vaporiser temperature: 500 °C and source current: 10.0 µA. The column specifications and parameters are as above.

2.3.5. Fourier transform infrared spectroscopy

Fourier transform infrared (FTIR) spectroscopy analysis was performed using a Nicolet 410 impact Fourier transform infrared spectroscopy or Avatar 360 Fourier transform infrared spectroscopy. An Omni liquid cell (1800) with calcium fluoride windows separated with a 1 mm PTFE spacer. Undiluted or diluted (20 μm^3 in 0.5 cm^3 dodecane) samples were scanned 128 times at a resolution of 4 cm^{-1} and a total collection time of around two and a half minutes. Data acquisition and manipulation were performed using OMNIC 6.1a software. The infrared functional group frequencies for the analysed samples are listed in Table 2.4.

---

[16] Tetrahydrofuran leached species with chromophores from the plastic syringe. Using a glass syringe would increase the sample preparation time to an impractical level.

Table 2.4: Infrared functional group frequencies

Compound	Group	Wavenumber (cm^{-1})
Phenolic	-OH	3660-3640
Galvinol	-OH	3650-3630
Carbonyl	-C=O	1760-1690
Aminic	-N-H	1529-1508
ZDDP	O-P-O	990-970
Succinimide	-C-N-	1238-1220
Lauroyl peroxide	-O-O-	1830-1805

2.3.6. Differential scanning calorimetry

Differential scanning calorimetry analysis was performed using a STA 625 TG-DSC thermal analyser (Stanton Redcroft). Samples of mass 3 to 6 mg were placed in aluminium crucibles and heated in the oven with air from 25 °C to 600 °C at a rate of 20 °C min^{-1}. Data acquisition and manipulation were performed using Trace 2 706 (version 4.30) software.

2.3.7. Determination of metals content

Five grams of oil were heated in a crucible with a Bunsen burner for five minutes. The oil was ignited, while heating with a Bunsen burner, until the flame ceased. The resulting charred oil was heated in a furnace at 550 °C for one hour. 1.0 cm^3 of concentrated 100 % nitric acid was added to the cooled ash and the solution was diluted with deionised water. The content of the metals in the diluted solution was determined by a Philips PU9200 double beam atomic absorption spectroscopy.

2.3.8. Determination of kinematic viscosity

Kinematic viscosity measurements were made by using a Cannon-Manning micro-viscometer U-tube 300, calibrated with authentic materials. The temperature of the water bath (Towson and Mercer E270 series 4) was maintained at a temperature of 40.0 ± 0.1 °C. To charge the sample into the viscometer (Figure 2.11), the viscometer tube was inverted upside down. Arm N was immersed in the sample and suction was applied to arm L. The sample (~0.3 cm^3) was drawn to mark G. Arm N was wipe cleaned and the viscometer tube was turned to its normal vertical position. The viscometer tube was placed into a holder and inserted into the constant temperature bath. The sample was allowed five to ten minutes to reach the bath temperature. Suction was applied to arm N (or pressure to arm L) and the sample was slightly drawn above mark E. To measure the efflux time, the sample was allowed to flow freely down past mark F, measuring the time for the meniscus to pass from mark E to mark F. The kinematic viscosity, which is proportional to efflux time,[17] of each sample was measured twice.

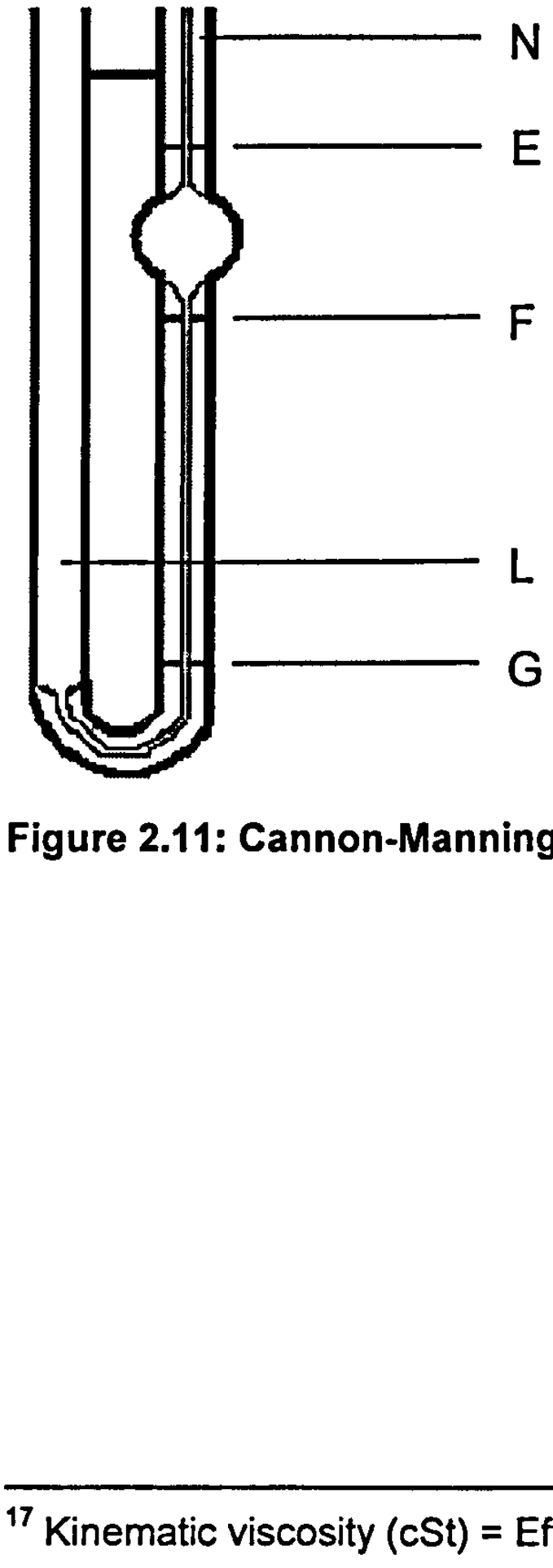

Figure 2.11: Cannon-Manning viscometer

[17] Kinematic viscosity (cSt) = Efflux time (second) x Viscometer tube constant

2.3.9. Determination of oxygen uptake

The oxygen uptake was determined by an AX300 electrochemical medical oxygen sensor (Teledyne analytical instruments) with an accuracy of ± 2 % and a precision of ± 0.1 % at full span, i.e. 1 mbar. Calculations of the oxygen uptake can be found in Appendix A.

2.3.10. Determination of hydroperoxides

The method used for the detection of hydroperoxides was based on previous works (West et al, 2005 and Parker, 2007). 20 μm^3 of the sample was mixed with 10 μm^3 of 250 mmol dm^{-3} of triphenylphosphine in toluene (toluene was purified with aluminium oxide) in a 2 cm^3 glass vial. The mixture was shaken by hand for a few seconds and left to stand at room temperature for five minutes to allow triphenylphosphine to react with the hydroperoxides in the sample. 10 μm^3 of 500 mmol dm^{-3} of sulphur in toluene was then added to the mixture to let the sulphur react with the unreacted triphenylphosphine. The vial was shaken by hand for a few seconds and left at room temperature for five minutes. The mixture was analysed by gas chromatography and the amount of triphenylphosphine oxide was quantified. The amount of triphenylphosphine oxide was found to be equal to the amount of hydroperoxides; this was validated by reaction with tertiary butyl hydroperoxide and tertiary butanol standards. The products of the reaction between hydroperoxides and triphenylphosphine are shown in Figure 2.12.

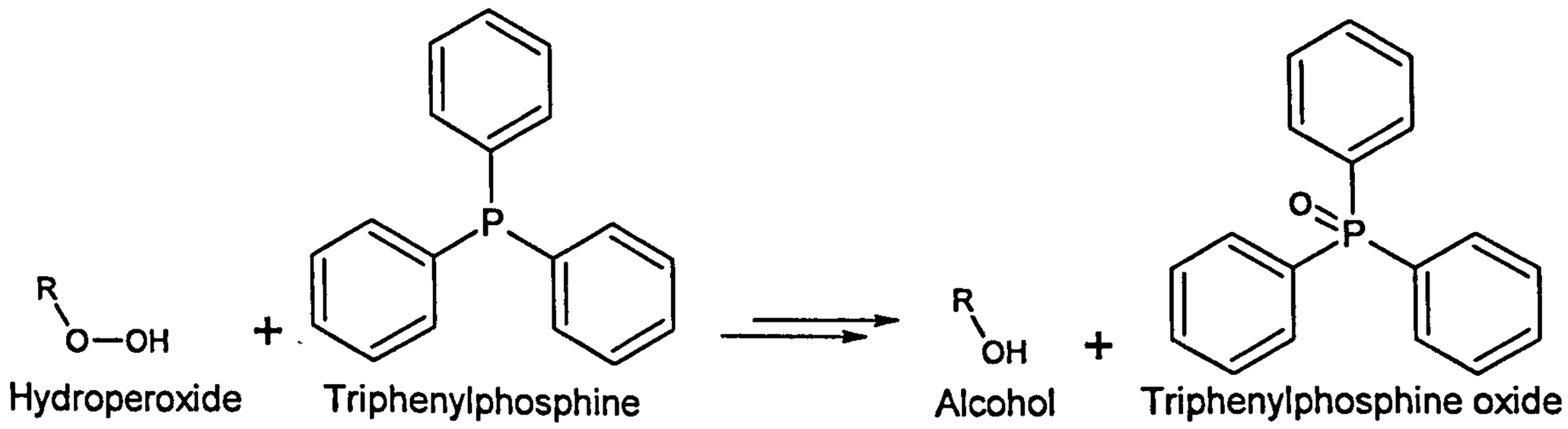

Figure 2.12: Reaction between hydroperoxides and triphenylphosphine (West et al, 2005)

2.4. MATERIALS

Table 2.5: Description of materials

CAS name	Alternative name	CAS number	Purity (%) or grade	Supplier (United Kingdom)
	Calcium alkyl sulphonate	Proprietary		Infineum
	Succinimide dispersant	Proprietary		Infineum
1-Undecanol		112-42-5	99	Aldrich
1-Undecene		821-95-4	>95	Fluka
2,6,10,15,19,23-Hexamethyltetracosane	Squalane	111-01-3	99	Aldrich
2,6-Bis(1,1-dimethylethyl)-2,5-cyclohexadiene-1,4-dione	Quinone	719-22-2	98	Aldrich
2,6-Bis(1,1-dimethylethyl)-4-methylphenol	BHT	128-37-0	99+	Aldrich
3,5-Bis(1,1-dimethylethyl)-4-hydroxybenzaldehyde	Formylphenol	1620-98-0	98+	Alfa Aesar
3,5-Di-tert-butyl-4-hydroxyhydrocinnamate	Irganox L135 (CIBA)	152618-44-5		Infineum
4,4'-Methylenebis[2,6-bis(1,1-dimethylethyl)]phenol	AN2 (Albemarle)	118-82-1	98	Aldrich
4-[[3,5-Bis(1,1-dimethylethyl)-4-hydroxyphenyl]methylene]-2,6-bis(1,1-dimethylethyl)-2,5-cyclohexadien-1-one	Galvinol	4359-97-1		Labotest (Germany)
4-[[3,5-Bis(1,1-dimethylethyl)-4-oxo-2,5-cyclohexadien-1-ylidene]methyl]-2,6-bis(1,1-dimethylethyl)phenoxyl	Galvinoxyl	2370-18-5		Aldrich
4-Nonyl-N-(4-nonylphenyl)benzenamine	Naugalube 438L (Chemtura)	58916-57-7		Infineum
4-Octyl-N-(4-octylphenyl)benzenamine	Amine101	101-67-7		Chem Service (UK) Yasho (India)
Bis(1-oxododecyl)peroxide	Lauroyl peroxide	105-74-8	97	Aldrich
Docosane		629-97-0	99	Alfa Aesar
Dodecane		112-40-3	99+	Alfa Aesar
Dodecanoic acid	Lauric acid	143-07-7	99.5	Alfa Aesar
Hexadecane		544-76-3	99	Alfa Aesar
Hydrotreated slack wax (petroleum)	Shell XHVI 8.2	92062-09-4		Shell Global Solutions
Nitric acid fuming 100%		7697-37-2	100	Fluka
N-phenylbenzenamine	Diphenylamine	122-39-4	99+	Aldrich
Sulphur		7704-34-9	99.998	Sigma-Aldrich
Tetrahydrofuran		109-99-9	HPLC	Fisher Scientific
Toluene			Reagent	Fisher Scientific
Trichloromethane-d	Chloroform-d	865-49-6	99.8	Aldrich
Triphenylphosphine	TPP	603-35-0	99	Aldrich
Triphenylphosphine oxide	TPPO	3878-45-3	99+	Acros Organics
Undecanal		112-44-7	97	Aldrich
Undecane		1120-21-4	99+	Aldrich
Zinc dithiophosphate	ZDDP			Infineum

Purity of Amine101

The purity of Amine101 from Yasho and Chem Service was claimed to be >90 %[18] and 97 %, respectively. The purities of amines were not measured for this work, but Figure 2.13 suggests that Amine101 from Yasho is as pure as that from Chem Service.

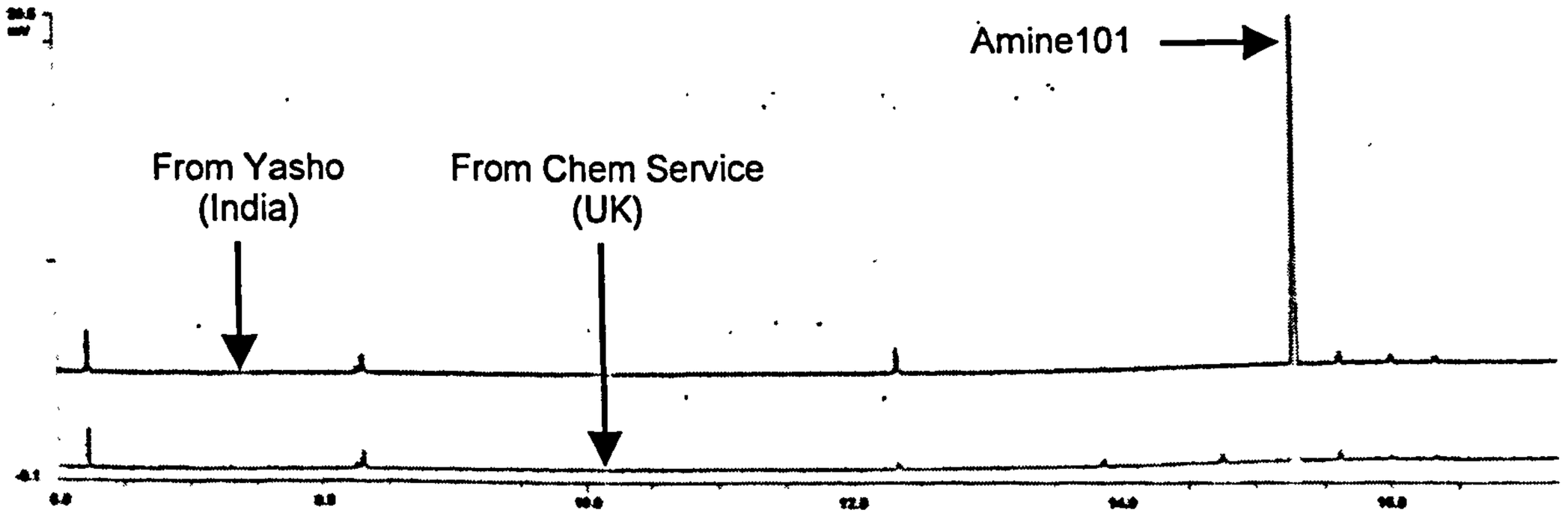

Figure 2.13: GC traces of Amine101 from Yasho (top trace) and Chem Service (bottom trace)

2.5. REFERENCES

Gamble, R. Influence of lubricant degradation on piston assembly tribology. PhD Thesis, University of Leeds, 2002.

Lee, P. Lubricant degradation transport and the link to piston assembly tribology. PhD Thesis, University of Leeds, 2006.

Parker, J. Methyl oleate as a chemical model for the degradation of biodiesel. Masters in Chemistry Dissertation, University of York, 2007.

Scanlon, J. and Willis, D. Calculation of flame ionization detector relative response factors using the effective carbon number concept. *Journal of Chromatographic Science*, 1985, **23**: 333-340.

Stark, M. The oxidation of hydrocarbon base-fluid lubricants in gasoline engines. Internal Report, Department of Chemistry, University of York, June 2003.

West, Z.; Zabarnick, S.; and Striebich, R. Determination of hydroperoxides in jet fuel via reaction with triphenylphosphine. *Industrial and Engineering Chemistry Research*, 2005, **44** (10): 3377-3383.

[18] The remainder of the ~10 % was claimed to be diphenylamine alkylated on one para-position (note that Amine101 is diphenylamine alkylated on two para-positions).

3. BEHAVIOUR OF PHENOLIC ANTIOXIDANTS IN BENCH-TOP REACTORS

3.1. INTRODUCTION

Phenolic antioxidants are widely used to control deterioration of the automotive engine lubricants (Muller et al, 1982; and Hamblin and Rohrbach, 2001). A thorough understanding of the mechanisms by which phenolic antioxidants control lubricant deterioration should enable lubricant formulators to formulate better lubricants.

The study of phenolic antioxidants in bench-top reactors instead of a research automotive engine has two advantages. First, in the bench-top reactors the antioxidants can be studied under controlled conditions; unlike the complex and variable conditions such as temperature in an automotive engine. Second, the cost of operating a bench-top reactor is considerably lower than a research engine; and so initial evaluations of the antioxidants can be carried out in the cost-effective bench-top reactors instead of the research engine.

Previous work on the behaviour of phenolic antioxidants in bench-top reactors suffer from one or more of the following drawbacks:

- Oxidations were carried out at temperatures that do not represent those found in an automotive engine (Howard and Ingold, 1963 and Amorati et al, 2003)
- Oxidations were carried out in model base fluids (Johnson et al, 1983), e.g. hexadecane, that physicochemically do not represent those of automotive engine base fluids
- Oxidations were carried out in base fluids that have complex and varied chemical composition, e.g. sulphur content (Jain et al, 2005; Dong et al, 2007; and Gatto et al, 2006)

- Oxidations were carried out in the presence of many other lubricant additives (Korcek et al, 1986), which would complicate the interpretation of results due to the interactions of various additives
- Only a single reaction parameter was used as a measure of antioxidant efficiency, e.g. reaction time, viscosity increase, and total acid number (Nishiyama et al, 1994 and Prusikova et al, 1972)

Previous work on the behaviour of phenolic antioxidants in polymers were not consulted due to the low diffusion and solubility of oxygen, and the exaggerated cage effect in polymers (Denisov and Afanasev, 2005, p.431), which could give different results from those obtained in liquid hydrocarbons.

A comprehensive list of previous work on the oxidation of phenolic antioxidants in bench-top reactors is shown in Table 3.1.

Table 3.1: Previous work on the oxidation of phenolic antioxidants in bench-top reactors (RPVOT: Rotating pressure vessel oxidation test; Phenolic: Sterically-hindered phenols) (references within table)

Technique	Substrate	T. (°C)	Reference
RPVOT and heated reactor	Base fluid	225 and 200 (‡)	Jain et al, 2005
Heated reactor	Base fluids	150	Dong et al, 2007
Heated reactor	Base fluids	150	Gatto and Grina, 1999
Heated reactor	Base fluids	150	Gatto et al, 2006
Heated bottle	Base fluids	152	Rose, 1991
Heated tube	Chlorobenzene and diphenyl ester	80 and 177 (§)	Low, 1966
Heated reactor	Hexadecane and pentaerythrityl tetraheptanoate	180-220	Jensen et al, 1979
Heated reactor	Hexadecane	160	Johnson et al, 1983
Heated glass reactor	Hexadecane and base fluids	160	Johnson et al, 1987
Heated Pyrex flask	Hexadecane and engine lubricants	160	Korcek et al, 1986
Heated reactor	Lithium grease	115	Ischuk and Butovets, 1991
Heated reactor	Mineral oils	160	Milton et al, 1987
Heated steel chamber	Polyolester	220	Mousavi et al, 2006
Glass reactor	Propyl alcohol	22	Kharasch and Joshi, 1957
Conductometry	Rapeseed and sunflower oils	130	Becker and Knorr, 1996
Heated reactor	Soybean oil	150	Sharma et al, 2007
Heated Pyrex flask	Styrene	65	Howard and Ingold, 1963
Oxygen uptake technique	Styrene and cumene	30	Amorati et al, 2003
Heated Pyrex flask	Tetralin	40	Horswill and Ingold, 1966
Heated Pyrex flask	Tetralin	65	Howard and Ingold, 1964
Oxygen uptake technique	Tetralin	60	Nishiyama et al, 1994
Oxygen uptake technique	Tetralin	60	Prusikova et al, 1972

(‡): with respect to technique, (§): with respect to substrate

The aim of this chapter is to study the behaviour of phenolic antioxidants, AN2 (4,4'-Methylenebis[2,6-bis(1,1-dimethylethyl)]phenol) and Irganox L135 (3,5-Di-tert-butyl-4-hydroxyhydrocinnamate), in squalane (2,6,10,15,19,23-hexamethyltetracosane) and Shell XHVI 8.2 (Group III base fluid, hydrotreated petroleum slack wax), by oxidations at 180 °C to 210 °C and monitoring the concentrations of the starting materials, intermediates, oxygen uptake, and total carbonyl formation during the oxidations; to provide lubricant formulators with a good understanding of the mechanisms by which phenolic antioxidants control lubricant deterioration to enable them to formulate better lubricants. Chemical structures of the investigated compounds are listed in Table 3.2.

3.2. PREVIOUS WORK

AN2 was studied in detail in this work, as will be seen later in the chapter, and so previous work on the oxidation of AN2 will be presented in this section.

There are two proposed inhibition mechanisms for AN2 antioxidant. The first mechanism is by Jensen et al (1979) and the second is by Gatto et al (2006).

Jensen's inhibition mechanism of AN2

Jensen et al (1979) studied AN2 in hexadecane and pentaerythrityl tetraheptanoate in a bench-top reactor at 180 °C to 220 °C. The inhibition times were measured by monitoring total hydroperoxide formation, and the concentrations of AN2 and galvinol were monitored during the reactions. The results were interpreted by using complex kinetic equations; and consequently, an inhibition mechanism was constructed. The main steps of this mechanism are:

- Addition of peroxyl radicals to the para-position of AN2 phenoxyl radicals step was proposed
- Reaction of peroxyl radicals with galvinol to give a galvinoxyl radical step was proposed
- Reaction of peroxyl radicals with AN2 to give a phenoxyl radical was referenced to Mahoney (1969)
- Reaction of two peroxyl radicals together to give galvinol and regenerate the AN2 molecule was referenced to Weiner and Mahoney (1972)

Figure 3.1 shows the proposed inhibition mechanism of AN2 by Jensen et al (1979).

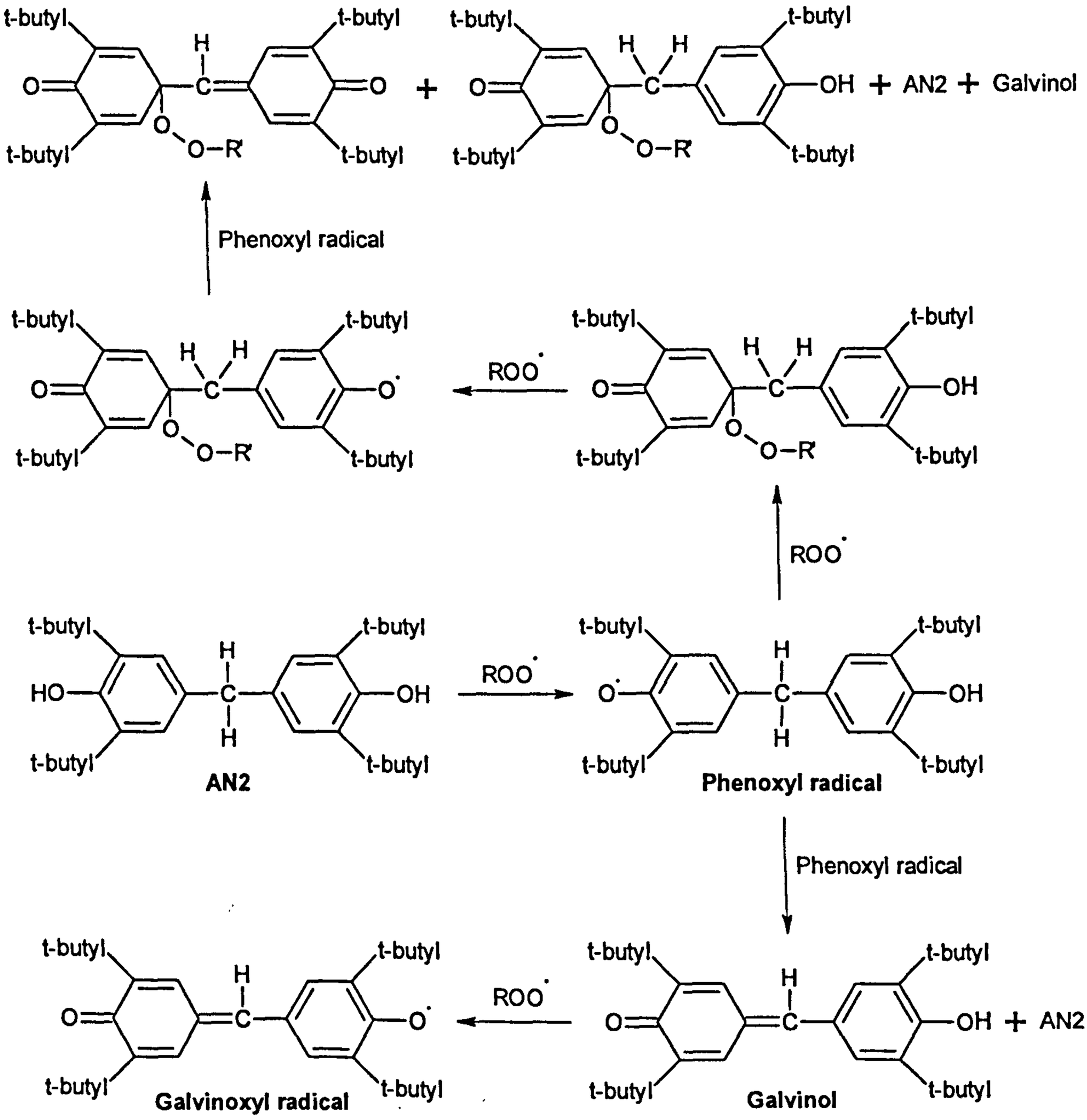

Figure 3.1: Jensen's inhibition mechanism of AN2 (Jensen et al, 1979)

Gatto's inhibition mechanism of AN2

Gatto et al (2006) constructed an inhibition mechanism for AN2. The mechanism was backed up by no experimental data. The main steps of this mechanism are:

- Reaction of peroxyl radicals with hydrogen atoms from the methylene bridge of AN2 phenoxyl radicals to give galvinol
- Reaction of peroxyl radicals with galvinol to give a galvinoxyl radical

• Addition of oxygen to galvinoxyl radical to eventually give quinone and formylphenol step was referenced to Greene and Adam (1963)

Figure 3.2 shows the proposed inhibition mechanism of AN2 by Gatto et al (2006).

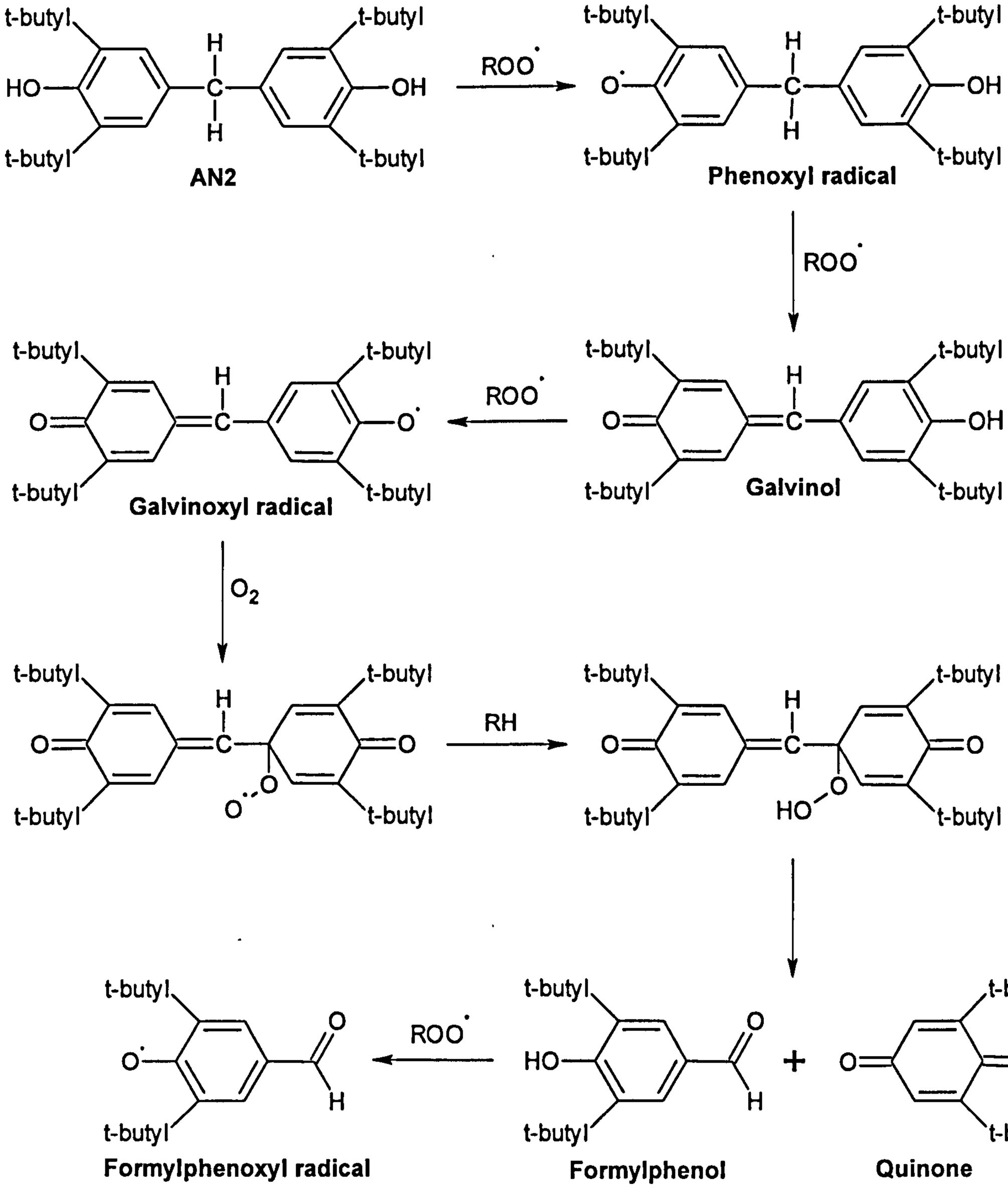

Figure 3.2: Gatto's inhibition mechanism of AN2 (Gatto et al, 2006)

3.3. PRODUCT IDENTIFICATION

Knowledge of the identities and quantities of intermediates and end-of-reaction oxidation products from antioxidants and substrate can aid the understanding of reaction pathways by which antioxidants function.

Antioxidants and base fluids used in engine oils generally consist of a mixture of structures and also their respective oxidation products are commercially unavailable. Therefore, AN2 and squalane have been used here as models for Irganox L135 and Group III lubricant base fluids, respectively.

The chemical structures of the oxidation products of AN2 were identified by comparison with authentic materials and confirmed by GC-MS. The chemical structures of the oxidation products of the model base fluid (i.e. squalane) were identified by GC-MS in electron impact and chemical ionisation modes. GC traces of oxidised squalane and AN2, and the mass spectra of the oxidation products can be found in Appendix B. Examples of the GC traces are shown in Figure 3.3.

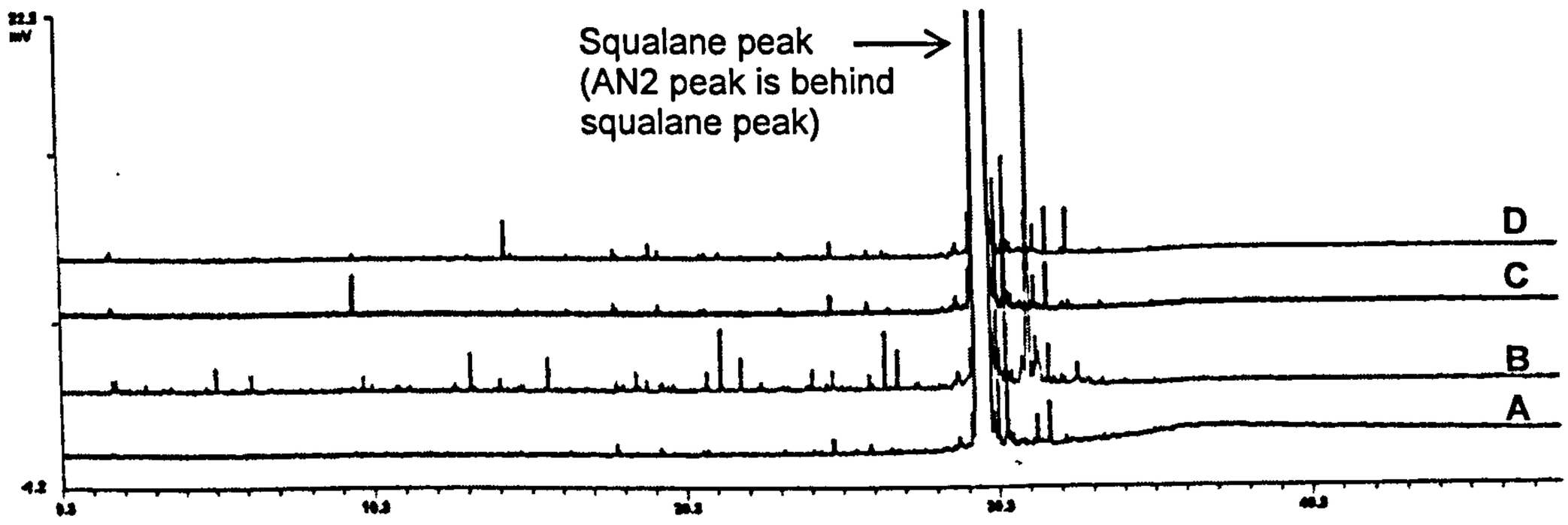

Figure 3.3: GC traces of unoxidised (trace A) and oxidised (trace B) squalane at 200 °C for 9 minutes in static intermediate reactor; and unoxidised (trace C) and oxidised (trace D) 10.0 mmol dm^{-3} AN2 in squalane at 200 °C for 21 minutes in flow intermediate reactor

Chemical structures of starting materials and oxidation products

Table 3.2: Chemical structures and names of starting materials and oxidation products

Structure	CAS name	Abbreviation
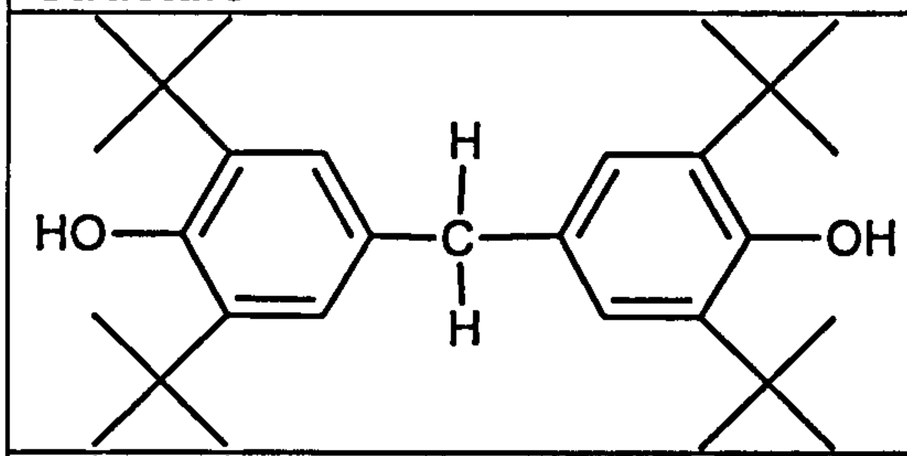	4,4'-Methylenebis[2,6-bis(1,1-dimethylethyl)]phenol	AN2
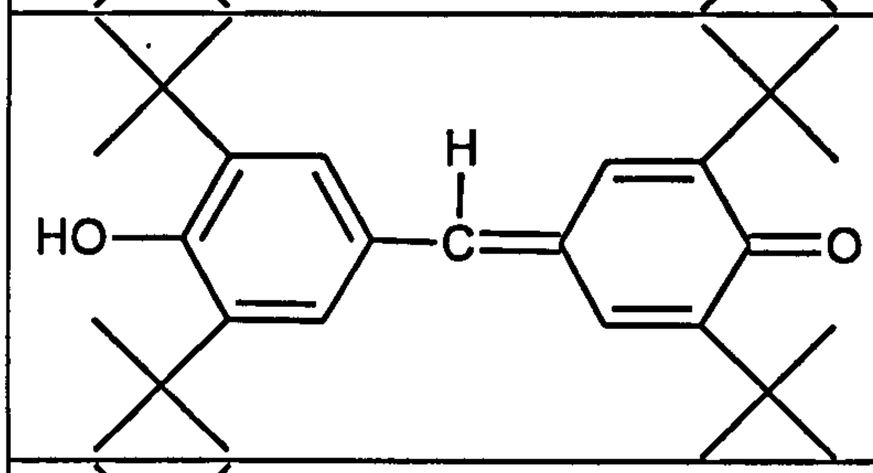	4-[[3,5-Bis(1,1-dimethylethyl)-4-hydroxyphenyl]methylene]-2,6-bis(1,1-dimethylethyl)- 2,5-cyclohexadien-1-one	Galvinol
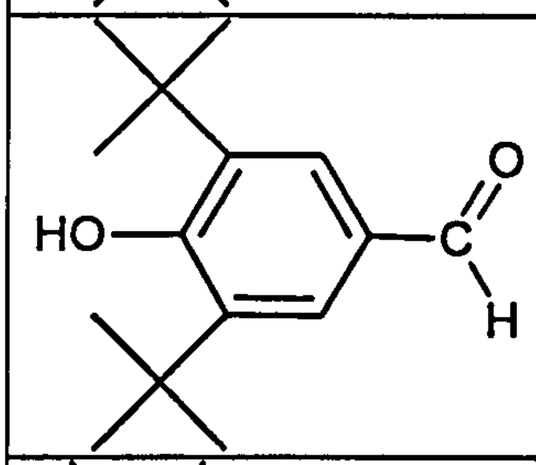	3,5-Bis(1,1-dimethylethyl)-4-hydroxy-benzaldehyde	Formylphenol
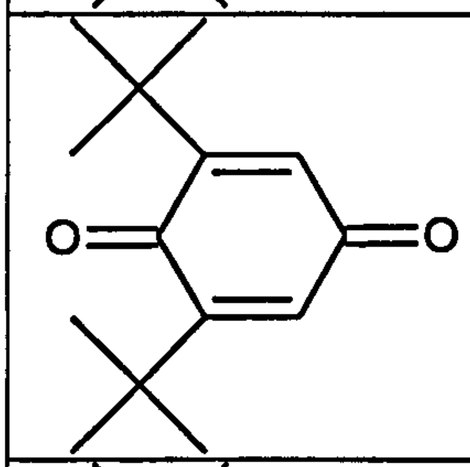	2,6-Bis(1,1-dimethylethyl)-2,5-cyclohexadiene-1,4-dione	Quinone
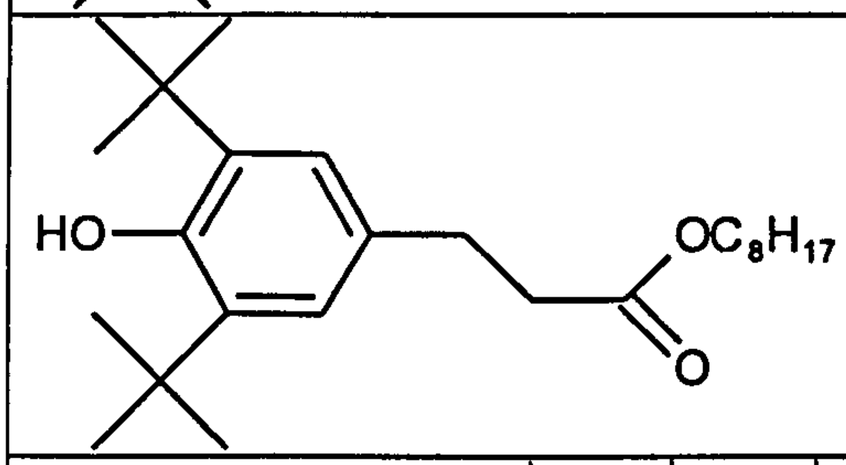	3,5-Di-tert-butyl-4-hydroxyhydrocinnamate	Irganox L135
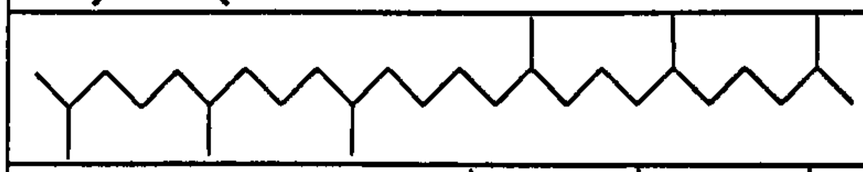	2,6,10,15,19,23-Hexamethyltetracosane	Squalane
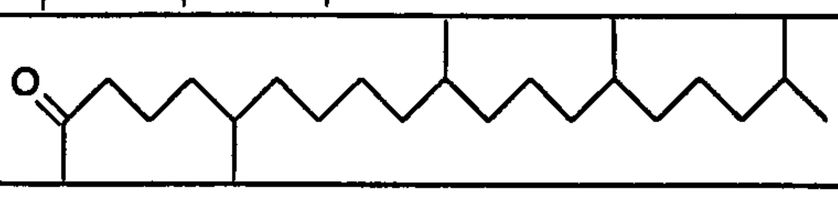	6,11,15,19-Tetramethyl-2-eicosanone	-

3.4. RESULTS

AN2 (10.0 mmol dm^{-3} or 0.5 % w/w) in 5.0 cm^3 of squalane or Shell XHVI 8.2 was oxidised at temperatures between 180 °C to 210 °C in the flow intermediate reactor.

Table 3.4 shows the formation of the total hydroperoxide and 6,11,15,19-tetramethyl-2-eicosanone ketone (from squalane) as oxygen is being consumed.

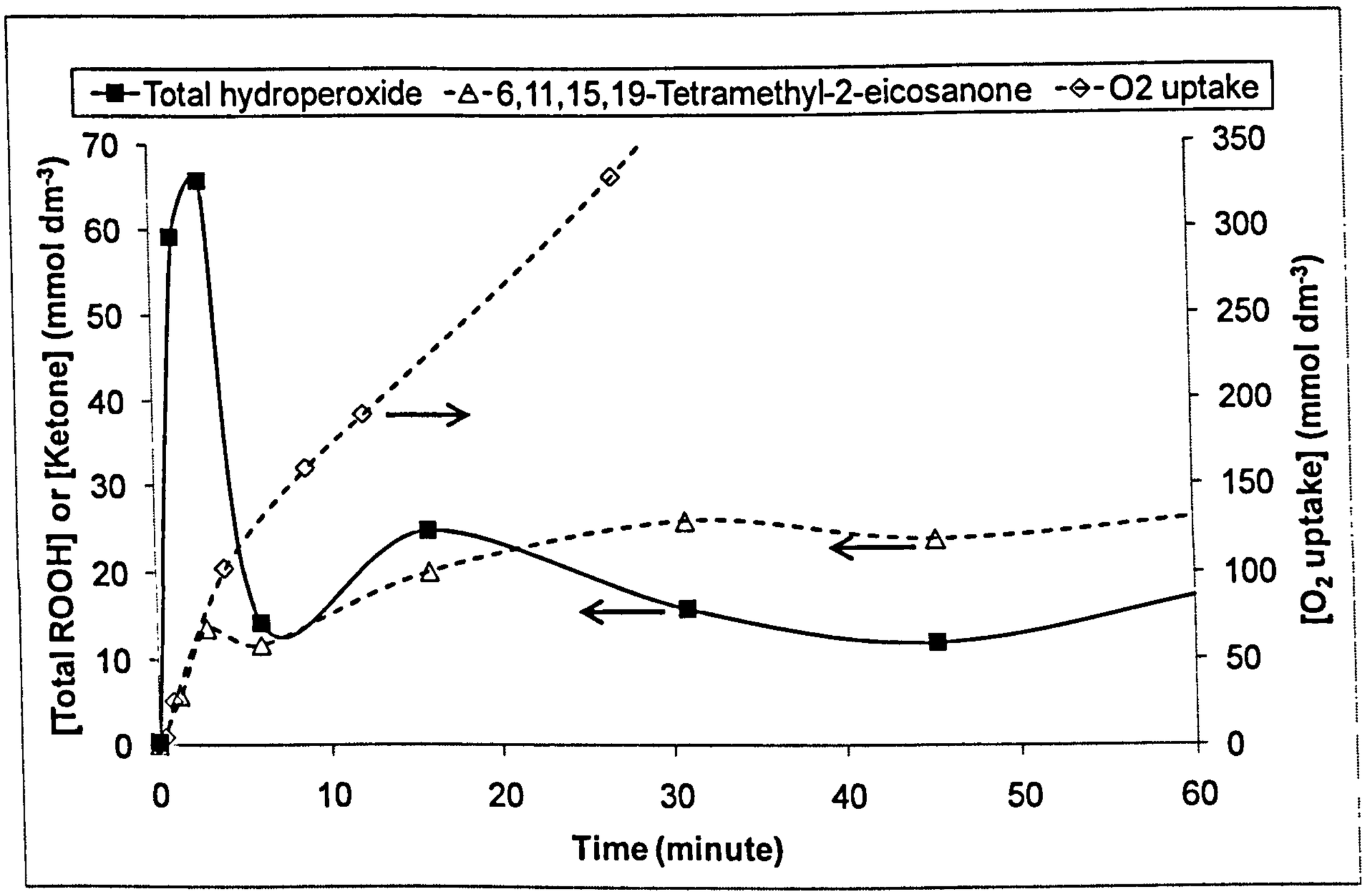

Figure 3.4: Oxygen uptake and formation of total hydroperoxide and 6,11,15,19-tetramethyl-2-eicosanone (by GC) in the oxidation of squalane at 200 °C in flow intermediate reactor

Figure 3.5 shows that the rate of AN2 consumption increases with temperature.

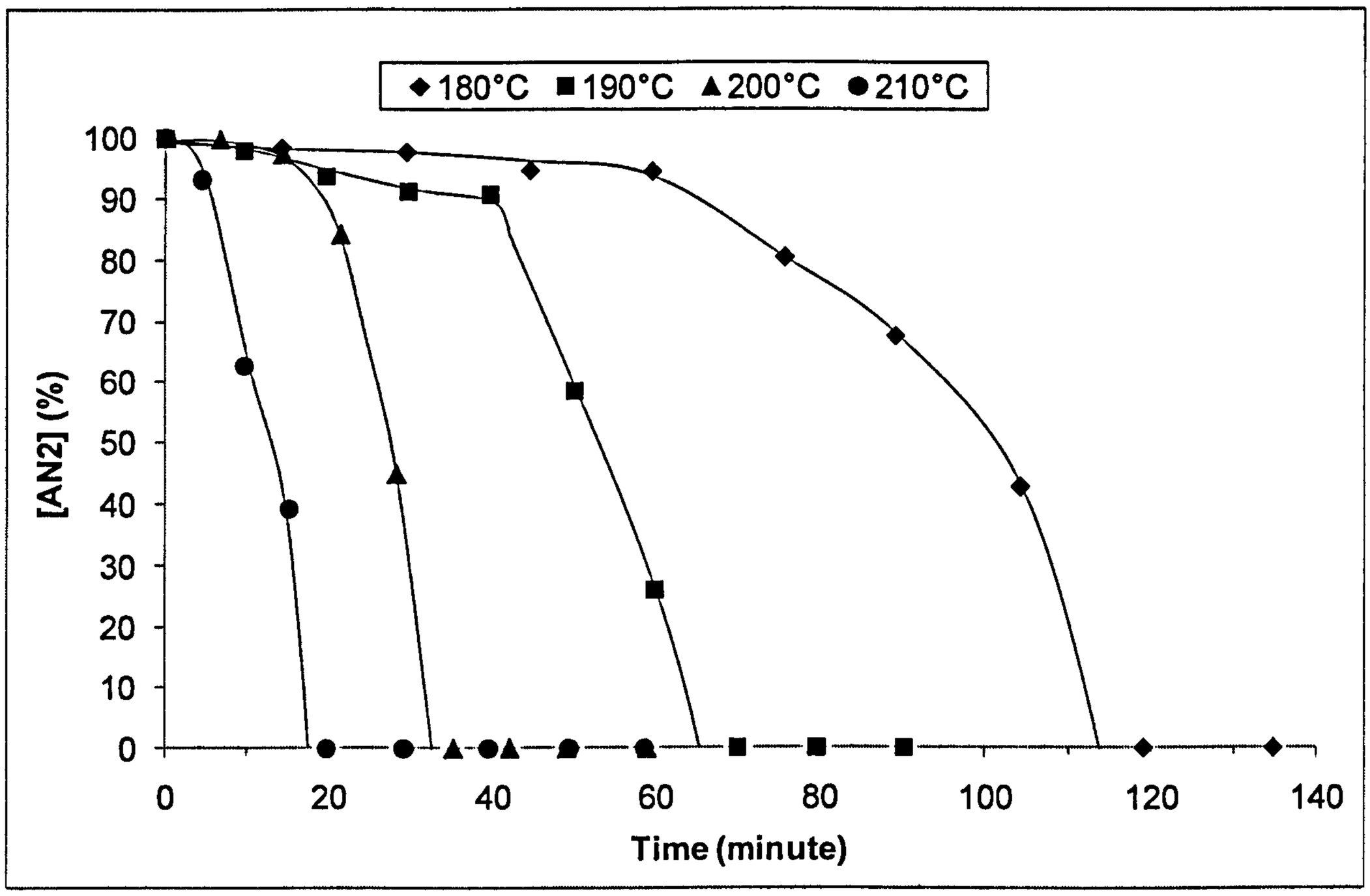

Figure 3.5: AN2 concentration versus time and temperature in the oxidation of 10.0 mmol dm^{-3} AN2 (by FTIR) in squalane between 180 °C to 210 °C in flow intermediate reactor

Figure 3.6 shows that no oxygen appears[19] to be consumed in the presence of the antioxidant and the oxygen uptake only starts after effectively all of the antioxidant has been consumed.

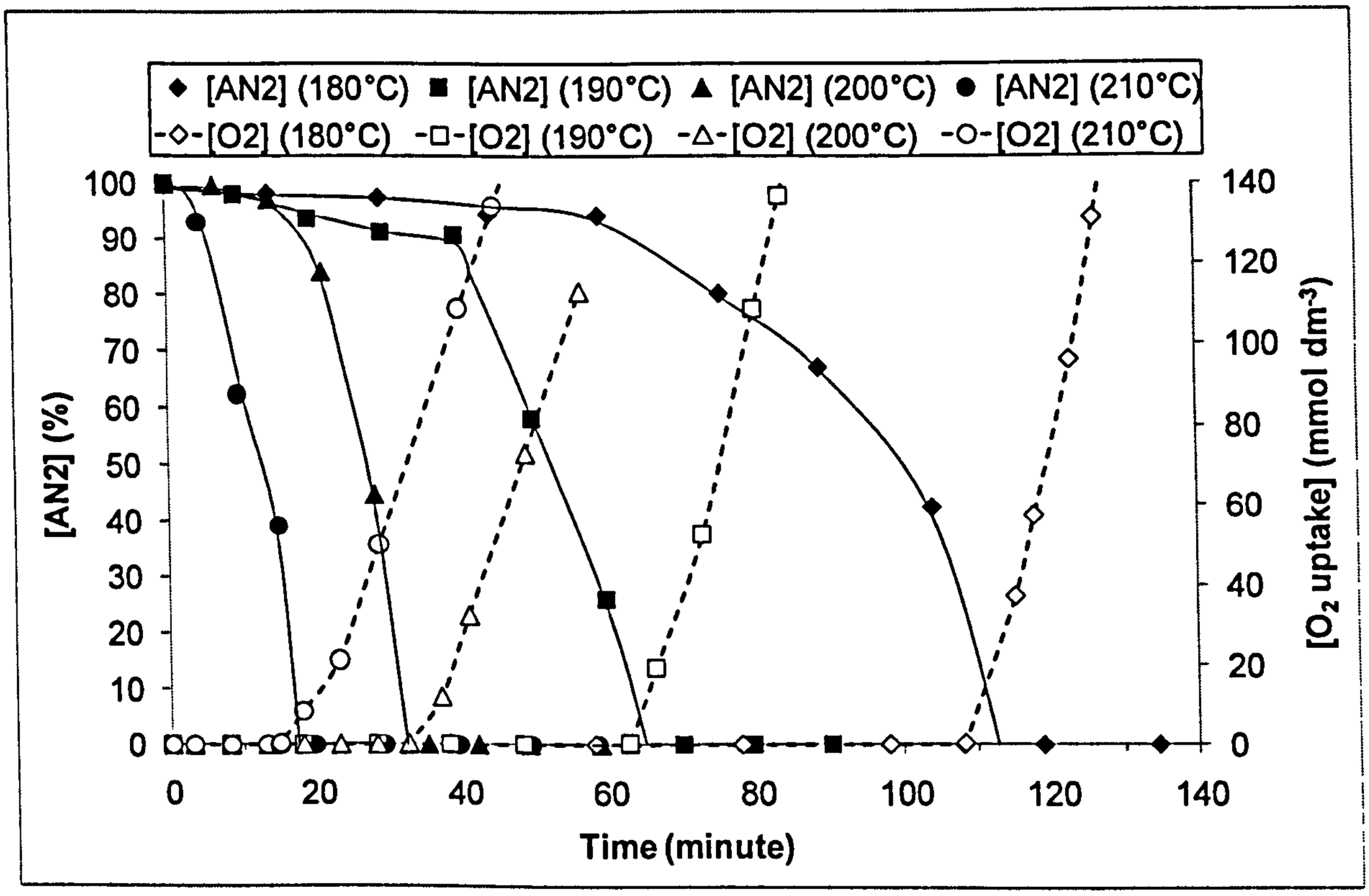

Figure 3.6: Oxygen uptake in the oxidation of 10.0 mmol dm^{-3} AN2 (by FTIR) in squalane between 180 °C to 210 °C in flow intermediate reactor

[19] Actually, the oxygen uptake is not zero but rather negligible. The oxygen uptake was not recorded due to the lack of sensitivity of the oxygen sensor, which is caused by the signal conversion from digital to analogue (Sanders and Maloney, 2002).

Figure 3.7 shows that the model base fluid remained almost intact in the presence of the antioxidant and squalane only degrades to give carbonyl products after effectively[20] all of the antioxidant has been consumed.

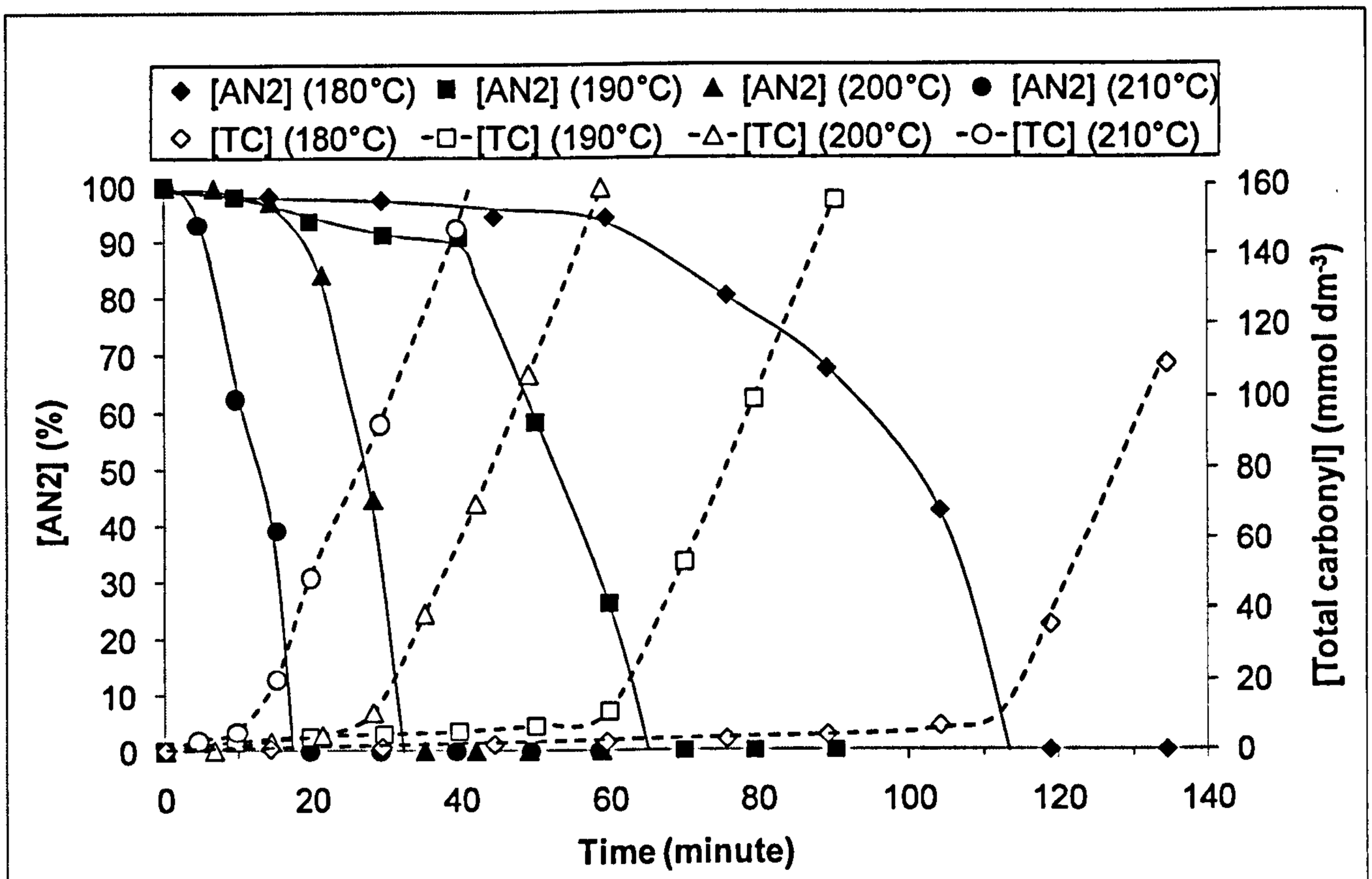

Figure 3.7: Total carbonyl formation (by FTIR) in the oxidation of 10.0 mmol dm^{-3} AN2 (by FTIR) in squalane between 180 °C to 210 °C in flow intermediate reactor. TC: Total carbonyl

[20] The majority of the observed carbonyl formed before the total depletion of the antioxidant is actually originated from the oxidation products of AN2 (see discussion).

Figure 3.8 shows the formation of one of the ketones from the model base fluid after all of the antioxidant has been consumed. Ketone 6,11,15,19- tetramethyl-2-eicosanone was chosen as a representative oxidation product from the model base fluid because it was the biggest observed ketone and hence its quantity is not affected by volatility at high temperatures.

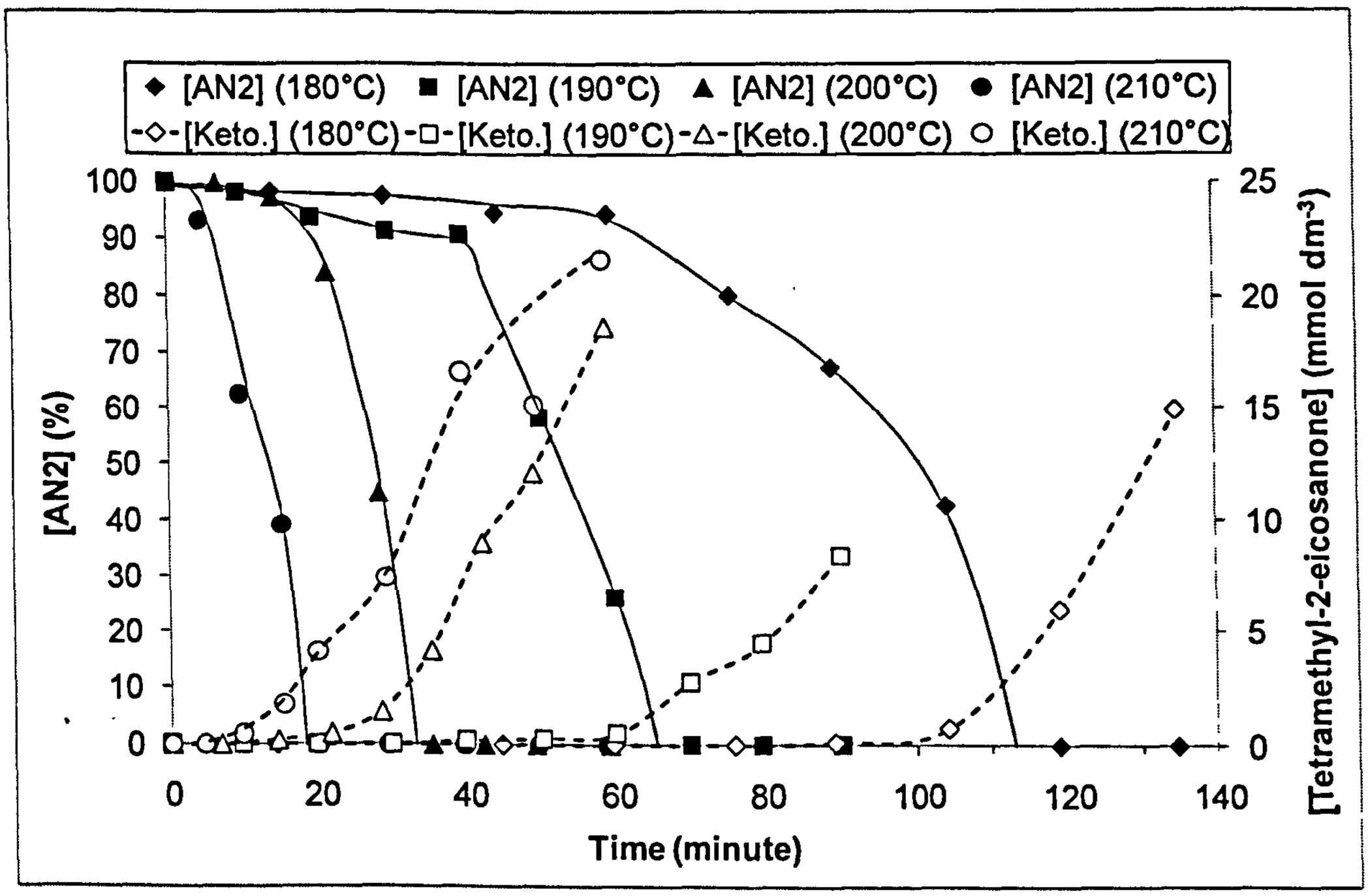

Figure 3.8: 6,11,15,19-tetramethyl-2-eicosanone (from squalane) formation (by GC) in the oxidation of 10.0 mmol dm^{-3} AN2 (by FTIR) in squalane between 180 °C to 210 °C in flow intermediate reactor

Figure 3.9 and Figure 3.10 shows the distribution of oxidation products of AN2 and galvinol, respectively.

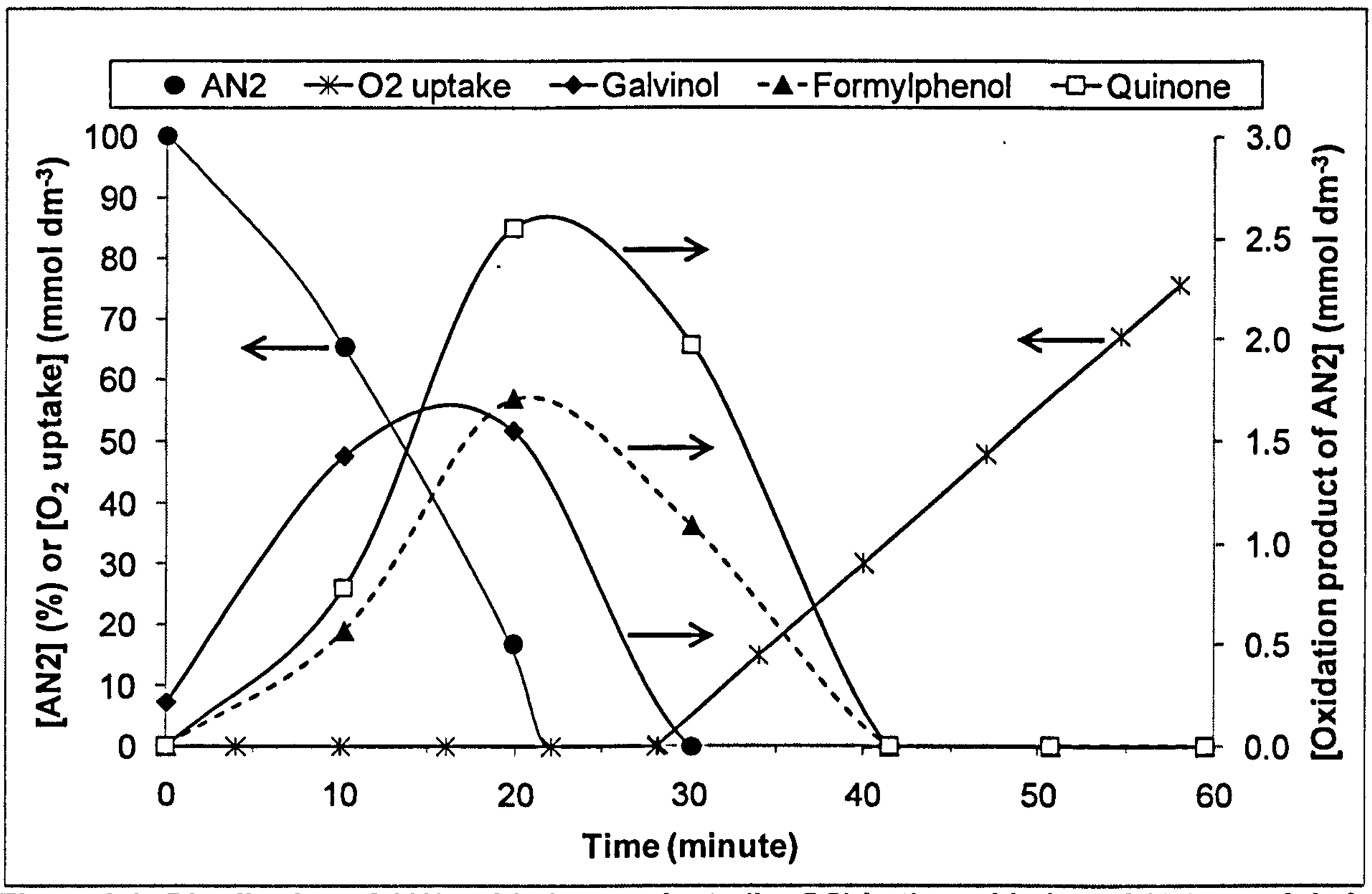

Figure 3.9: Distribution of AN2 oxidation products (by GC) in the oxidation of 10.0 mmol dm^{-3} AN2 (by GC) in Shell XHVI 8.2 at 200 °C in flow intermediate reactor

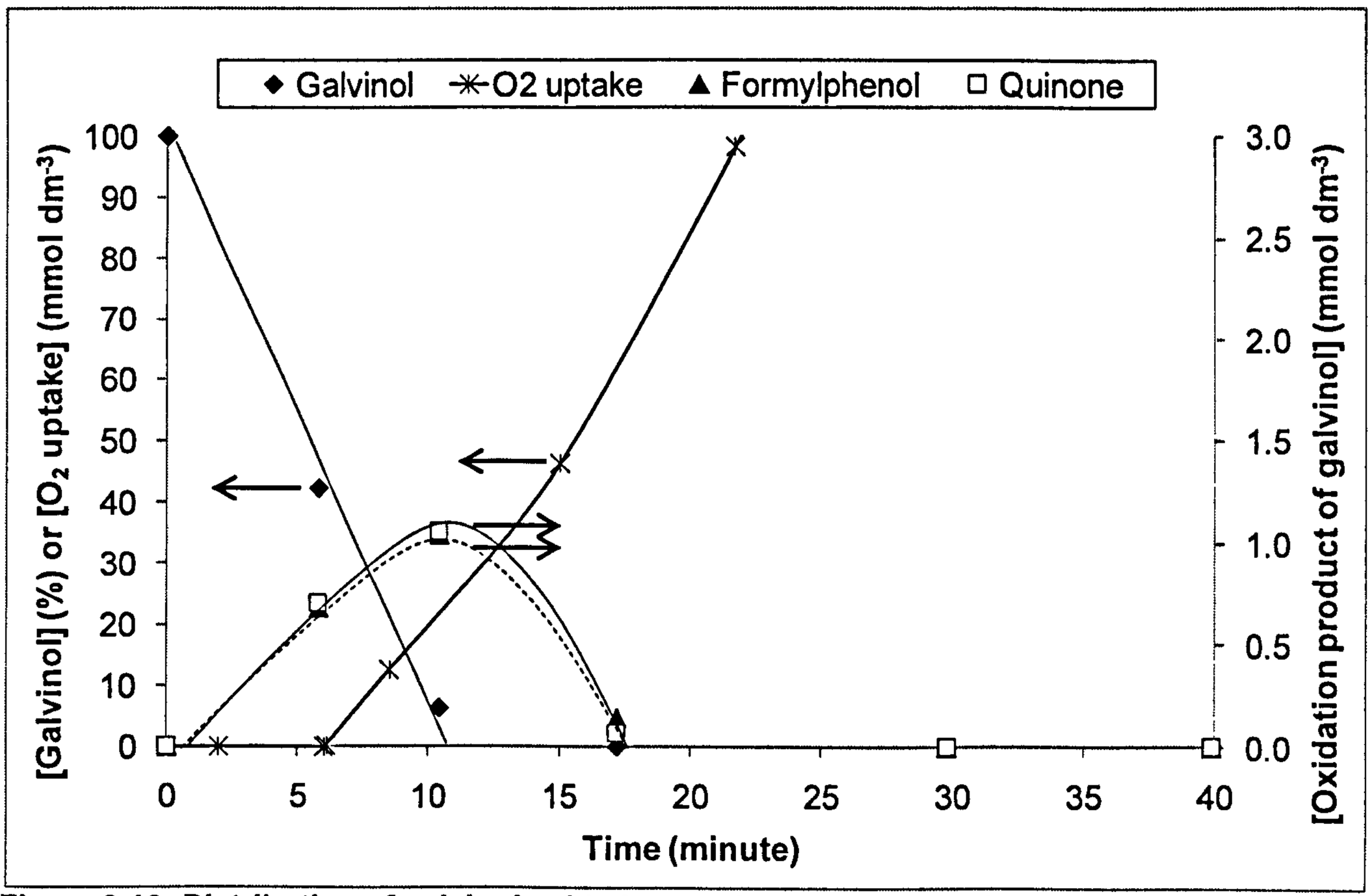

Figure 3.10: Distribution of galvinol oxidation products (by GC) in the oxidation of 5.0 mmol dm^{-3} galvinol (by GC) in Shell XHVI 8.2 at 200 °C in flow intermediate reactor

Figure 3.11 shows that it takes half an hour for Irganox L135 to be consumed and doubling the concentration of Irganox L135 almost doubles the antioxidant consumption time.

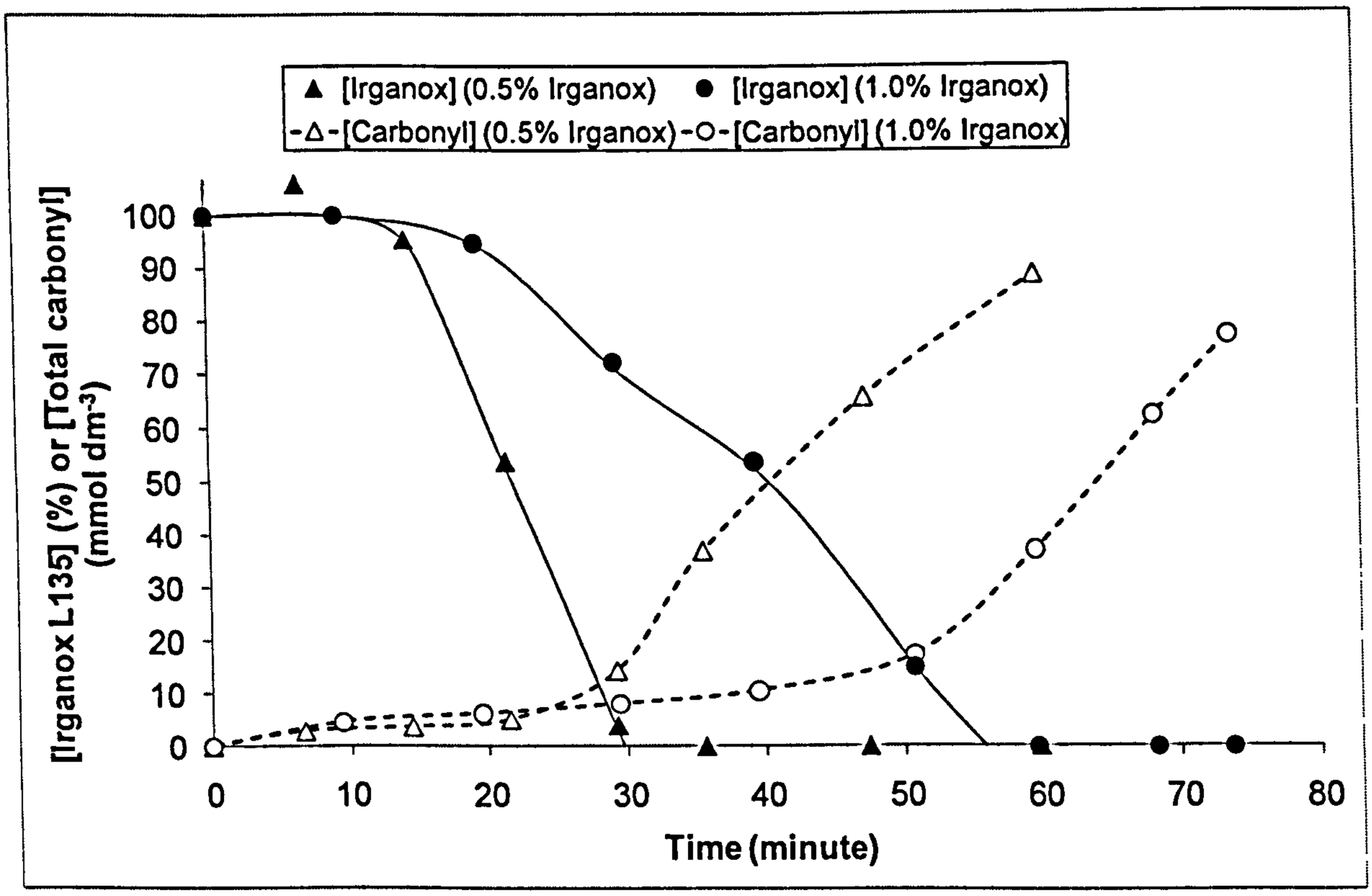

Figure 3.11: Decay of Irganox L135 (by GC) in the oxidation of Shell XHVI 8.2 (+ succinimide dispersant & sulphonate detergent) at 200 °C in static large reactor

3.5. DISCUSSION

3.5.1. Oxidation mechanism of squalane

The process of 6,11,15,19-tetramethyl-2-eicosanone ketone and hydroperoxides formation from the oxidation of squalane (Figure 3.4) begin with the reaction of oxygen with squalane (Denisov and Denisova, 2000, p.52). The initiation step of the autoxidation reaction, i.e. the reaction of oxygen with squalane, requires high activation energy (159.0 kJ mol^{-1}, Denisov and Denisova, 2000, p.52) and so this step becomes marginal once free radicals (e.g. peroxyl radicals) are formed. However, the high activation energy means that this reaction is highly temperature dependent and hence expected to become more significant as the temperature increases. At the temperatures used in this study, the reaction between oxygen and squalane is limited to the initiation step.

The alkyl radicals formed from the reaction between oxygen and squalane react with oxygen at the diffusion level (i.e. rate constant of $\approx 10^9$ M^{-1} s^{-1}) to give peroxyl radicals (Maillard et al, 1983).

The formed peroxyl radicals react preferentially with tertiary C-H bonds (Howard, 1997, p.291) due to their lower bond dissociation energies than the secondary or primary C-H bond of squalane, with the C-H bonds at the terminal being more prone to attack than the internal C-H bonds (McCaffrey and Forbes, 2005). The bond dissociation energies of tertiary and secondary C-H bonds and their consequent effect on activation energy and rate constant of the hydrogen atom abstraction are listed in Table 3.3.

Table 3.3: Bond dissociation energies (C-H) of hydrocarbons (references within table)

Compound	Hydrogen atom type	BDE (kJ mol^{-1})	k[RH+ROO•] (M^{-1} s^{-1}) at 200 °C for 3-methylpentane + Me_3COO•	E (kJ mol^{-1})
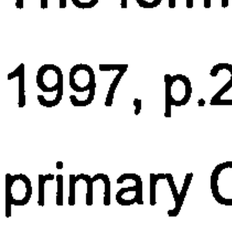	Tertiary	400	93	68.2
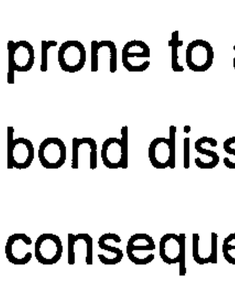	Secondary	412	6.4	73.3
References	-	Denisov and Denisova, 2000, p.21	Howard, 1997, p.291	Howard, 1997, p.291

The base fluid (Shell XHVI 8.2) and model base fluid (squalane) used in this study have comparable concentrations of tertiary and secondary carbon atoms with those used in automotive engine lubricants as base fluids. The concentrations of tertiary and secondary carbon atoms in base fluids are listed Table 3.4.

Table 3.4: Concentrations of tertiary and secondary carbon atoms in base fluids (references within table)

Base fluids	Tertiary carbons (%)	Secondary carbons (%)	Reference
Group I	~17.5-19	~62.5	McKenna et al, 2002
Group II	~19-21.5	~63.5	McKenna et al, 2002
Group III	~14-15.5	~69	McKenna et al, 2002
Poly-α-olfin	~7-10	~73	McKenna et al, 2002
Shell XHVI 8.2	14	74	Stark, 2003, p.107
Squalane	20.0	53.3	Calculated

The hydroperoxides formed from the reaction of peroxyl radicals with squalane, decompose to give alkoxyl and hydroxyl radicals (Jensen et al, 1990). The tertiary alkoxyl radicals either decompose to give ketones or abstract hydrogen atoms to give alkyl radicals and alcohol (Denisov and Afanasev, 2005, p.73-74). Detailed mechanisms in the oxidation of squalane can be found in Appendix C.

3.5.2. Oxidation mechanism of AN2

Squalane was fully protected from oxidation in the presence of AN2 (Figure 3.6, Figure 3.7, and Figure 3.8). By contrasting Figure 3.6 and Figure 3.7, one notices that the oxygen uptake appears to be zero, while the total carbonyl formation appears to begin before total depletion of the antioxidant for the lowest temperature studied. The apparent inconsistency of these results arises from the lack of sensitivity of the oxygen sensor, which is caused by the signal conversion from digital to analogue (Sanders and Maloney, 2002); thus, the oxygen uptake in Figure 3.6 is actually not zero but rather negligible. The majority of the observed carbonyl formed before the total depletion of the antioxidant is actually originated from the oxidation products of AN2, i.e. formylphenol (Figure D.15) and quinone (Figure D.16).

AN2 protected squalane by providing easy-to-abstract hydrogen atoms to free radicals so that free radicals would react with the antioxidant instead of squalane. The reaction between AN2 and peroxyl radicals (Amorati et al, 2003) is expected to be much more dominant than that with alkoxyl (Snelgrove et al, 2001) and alkyl

radicals (Franchi et al, 1999) because peroxyl radicals have long life times (i.e. in the milliseconds range) and high rate of formation (Maillard et al, 1983) and consequently available on abundant quantities, whereas alkoxyl and alkyl radicals have short life times (i.e. in the microseconds range) and low rate of formation (Jensen et al, 1990 and Denisov and Denisova, 2000, p.52) and are expected to be present in low concentrations (Denisov and Afanasev, 2005, p.176; Ingold and MacFaul, 2000; and Wallington et al, 1997). Peroxyl radicals react preferentially with the hydrogen atom of the hydroxyl group due to the weaker phenolic O-H bond strength (Figure 3.12).

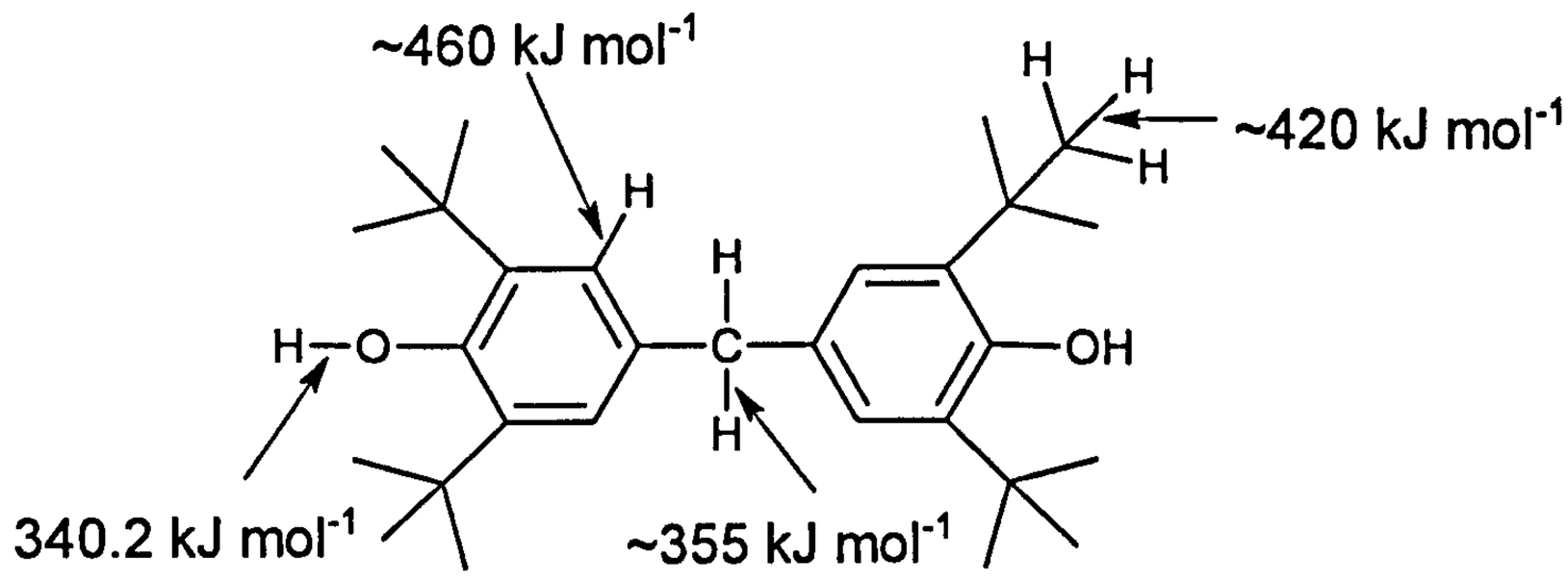

Figure 3.12: Bond strengths of AN2 (Denisov and Denisova, 2000)

The mechanism for the reaction AN2 with peroxyl radicals is shown in Figure 3.13.

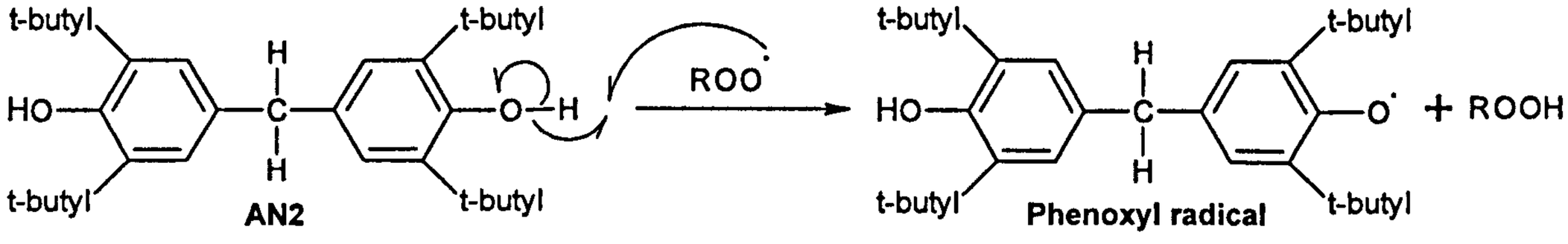

Figure 3.13: Reaction mechanism between AN2 and peroxyl radicals (Amorati et al, 2003)

The only datum on the reaction of a peroxyl radical with AN2, without the usage of a reference compound (e.g. BHT), is at 30 °C (Amorati et al, 2003). The Arrhenius parameters for the reaction of peroxyl radicals with AN2 are not available and so data from other similar sterically-hindered phenols (e.g. BHT and 2,4,6-tri-tert-butylphenol) are given to enable the extrapolation of the temperature of the reaction to the temperatures used in this study (i.e. 180 °C to 210 °C). The Arrhenius parameters for the reaction of sterically-hindered phenols with peroxyl radicals are given in Table 3.5.

Table 3.5: Arrhenius parameters for the reaction of sterically-hindered phenols with peroxyl radicals (a: Amorati et al, 2003; b: Honeywill and Mile, 2002; c: Howard, 1972, p.131)

Reaction	Solvent	A ($M^{-1} s^{-1}$)	E (kJ mol^{-1})	k ($M^{-1} s^{-1}$) at 30 °C	k ($M^{-1} s^{-1}$) at 200 °C	Ref.
AN2 + styrylperoxyl	Chloro-benzene	-	-	7.70×10^{3}	-	a
BHT + tert-BuOO•	2-Methylbutane	2.5×10^{5}	7.2	1.4×10^{4}	4.0×10^{4}	b
BHT + styrylperoxyl	-	7.9×10^{7}	23.5	7.2×10^{3}	2.0×10^{5}	c
BHT + cumylperoxyl	-	6.3×10^{6}	16.8	8.2×10^{3}	8.9×10^{4}	c
BHT + cyclohexylperoxyl	-	1.0×10^{7}	18.8	5.9×10^{3}	8.7×10^{4}	c
BHT + 1-methylcyclohexylperoxyl	-	3.9×10^{7}	20.9	9.6×10^{3}	1.9×10^{5}	c
BHT + 4-methylcyclohexylperoxyl	-	3.6×10^{7}	20.9	8.9×10^{3}	1.8×10^{5}	c
BHT + 4,5-dimethylcyclohexylperoxyl	-	2.0×10^{8}	23.0	2.1×10^{4}	5.7×10^{5}	c

Figure 3.10 shows that galvinol protected the base fluid against oxidation for 6 minutes (or possibly 12 minutes if 10 mmol dm^{-3} of galvinol were used); whereas, Figure 3.9 shows that AN2 protected the base fluid against oxidation for 28 minutes. It is likely that galvinol lagged by 16 minutes (from 28 min of AN2 – 12 min of galvinol = 16 minutes) not because it provides an inferior protection than AN2, but because AN2, galvinol, and formylphenol trap free radicals in the autoxidation of AN2; whereas, only galvinol and formylphenol trap free radicals in the autoxidation of galvinol. The phenolic O-H of galvinol (an oxidation product of AN2) are expected to react with peroxyl radicals because the O-H bond dissociation energy of galvinol is 329.1 kJ mol^{-1} (Denisov and Denisova, 2000, p.89), that is to say, 11 kJ mol^{-1} lower than that of AN2, which in turn means the reaction of peroxyl radicals with galvinol is more favourable than that with AN2. The mechanism for the reaction of galvinol with peroxyl radicals is shown in Figure 3.14.

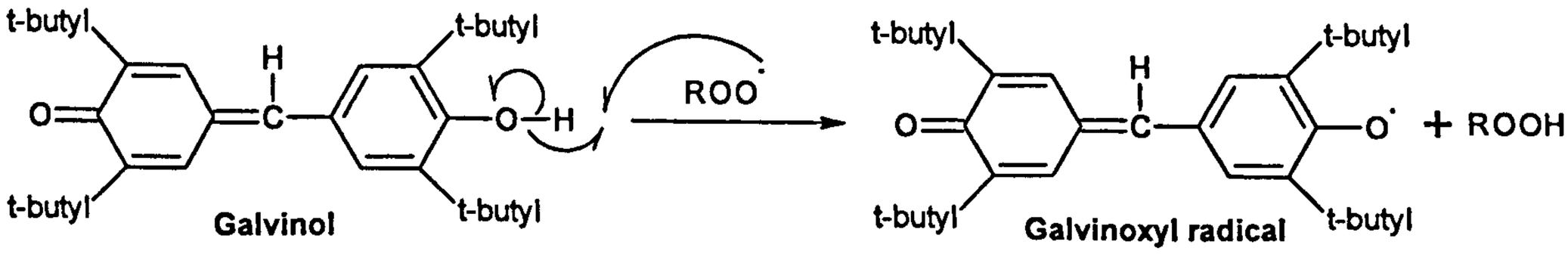

Figure 3.14: Reaction mechanism between AN2 and peroxyl radicals (Jensen et al, 1979)

Identical quantities of formylphenol and quinone were detected in the oxidation of galvinol (Figure 3.10); whereas, in the oxidation of AN2, the concentration of quinone is almost twice that of formylphenol (Figure 3.9). The differences in the ratio of the concentration of formylphenol to that quinone in the oxidation of

galvinol and AN2 are probably due to the reaction of AN2 phenoxyl with formylphenol in the latter reaction. AN2 phenoxyl is after all a radical and so its reaction of formylphenol should not be eliminated; for instance, galvinoxyl reacts with AN2 at a relatively sufficient rate constant (1.1 x 10^3 M^{-1} s^{-1} at 200 °C, Adam and Chin, 1971) in spite of the fact that the galvinoxyl radical is more stable than the AN2 phenoxyl radical.

Critical evaluation of previous work

Jensen et al (1979) proposed that peroxyl radicals add to the para-position of AN2 phenoxyl radicals; whereas, Gatto et al (2006) proposed that peroxyl radicals abstract hydrogen atoms from the methylene bridge of AN2 phenoxyl radicals. The C-H bond dissociation energy of the methylene bridge of AN2 phenoxyl is expected to be too weak[21] and hence readily extractable. The peroxyl radical addition to the para-position is possible (Rubtsov et al, 1979) but readily decomposes back to the original reactants (Denisov and Afanasev, 2005, p.510).

Additional mechanistic clarifications

The phenolic hydrogen atom of AN2 phenoxyl radical has a higher O-H bond dissociation energy (BDE ≈ 344 kJ mol^{-1}, estimated from values in Amorati et al, 2003) than that of the C-H of the methylene bridge. There is no datum about the BDE of C-H of the methylene bridge of AN2 phenoxyl but one can estimate it from available values of AN2. The BDE of C-H of the methylene bridge of AN2 is 352 ± 8 kJ mol^{-1} (McMillen and Golden, 1982); the radical on the oxygen atom of AN2 phenoxyl is expected to substantially weaken the C-H to a value much lower than that of the O-H of the AN2 phenoxyl. Thus, peroxyl radicals should react with the methylenic C-H in preference to the phenolic O-H of the AN2 phenoxyl.

The O-H bond dissociation energies of formylphenol (an oxidation product of AN2) and AN2 are 347.8 ± 0.5 kJ mol^{-1} and 340.2 kJ mol^{-1}, respectively (Denisov and Denisova, 2000); hence, peroxyl radicals react preferentially with AN2. Peroxyl

[21] The BDE of the C-H bond of methylene bridge of AN2 is 352 ± 8 kJ mol^{-1} (McMillen and Golden, 1982) but the BDE of the C-H bond of the methylene bridge of the AN2 phenoxyl is expected to be much lower than 352 kJ mol^{-1} due to the destabilisation by the radical on the oxygen atom.

radicals abstract the acyl and phenolic hydrogen atoms at similar rate constants.[22] However, peroxyl radicals are expected to abstract the latter from formylphenol due to favourable enthalpy:

ΔH = BDE(**C(O)H**) – BDE(ROO-H) in kJ mol^{-1}
= 374[23] – 359[24] = 15 kJ mol^{-1} (endothermic, i.e. reversible)

ΔH = BDE(**ArO-H**) – BDE(ROO-H) in kJ mol^{-1}
= 347.8[25] – 359[26] = -11 kJ mol^{-1} (exothermic, i.e. favourable)

Detailed mechanisms in the oxidation of AN2 can be found in Appendix C.

AN2 oxidation mechanism for this work

The important steps in the oxidation of AN2 for this work are highlighted in Figure 3.15, which are essentially the same as those of Gatto et al, 2006.

[22] For aldehydes: k[$Me(CH_2)_8CHO$+$Me(CH_2)_8C(O)OO\bullet$] = $1.4x10^6$ exp(-17.6 kJ/mol / RT) M^{-1} s^{-1} in decane, i.e. 1.6×10^4 M^{-1} s^{-1} at 200 °C (Denisov and Afanasev, 2005, p.303); for phenolics: k[BHT+styrylperoxyl] = $7.9x10^7$ exp(-23.5 kJ/mol / RT) M^{-1} s^{-1}, i.e. $2.0x10^5$ M^{-1} s^{-1} at 200 °C (Howard, 1972, p.131).
[23] Denisov and Denisova, 2000, p.25.
[24] Denisov and Afanasev, 2005, p.41.
[25] Denisov and Denisova, 2000, p.88.
[26] Denisov and Afanasev, 2005, p.41.

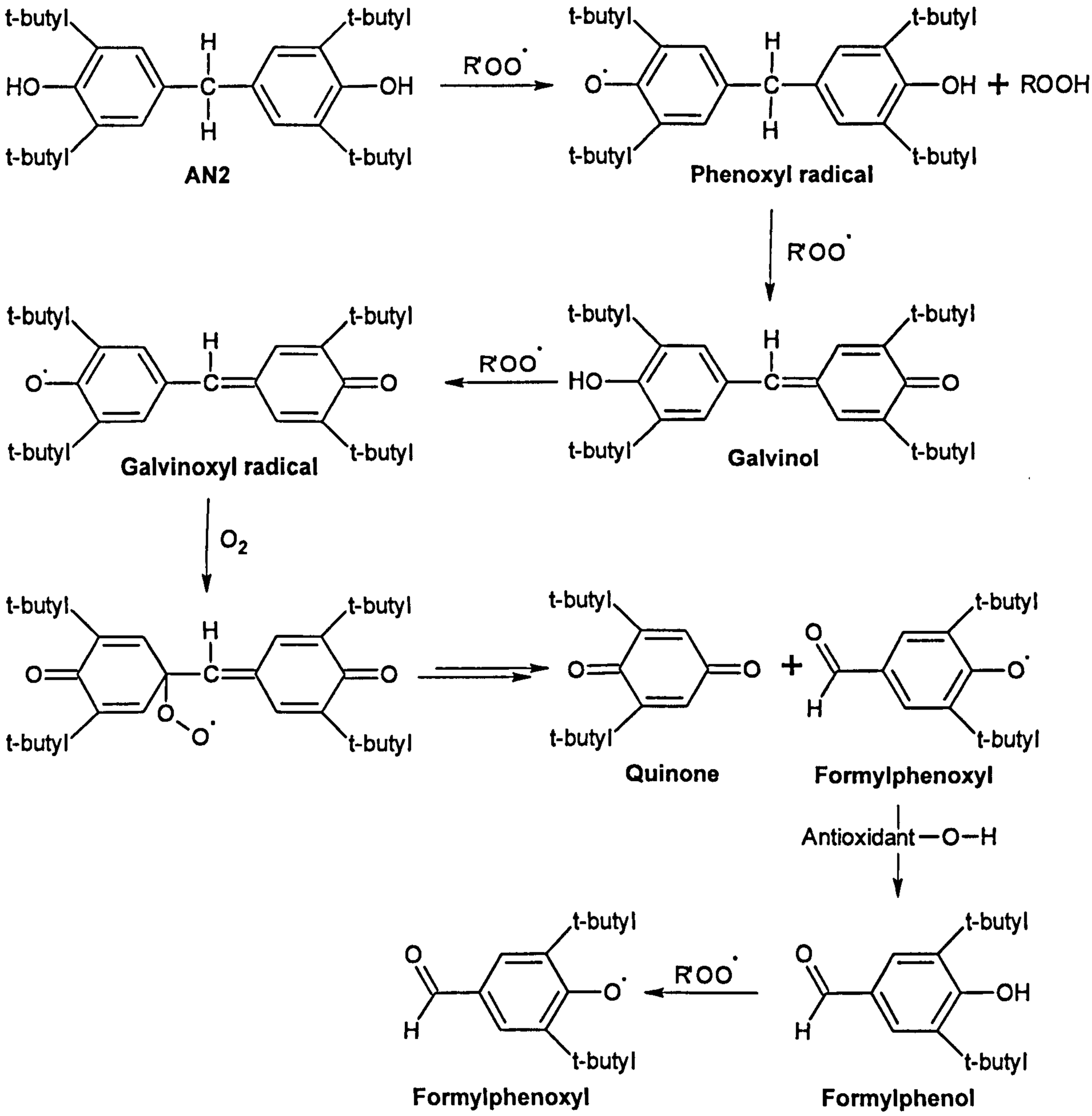

Figure 3.15: Scheme highlighting expected important steps in the oxidation of AN2 for this work

3.5.3. Oxidation of Irganox L135 antioxidant

Results for the oxidation of Irganox L135 show that 1.0 % w/w of Irganox L135 was almost as twice as effective as 0.5 % w/w of Irganox L135 (Figure 3.11) and as effective as 0.5 % w/w of AN2 (Figure 3.7), which was expected, because Irganox L135 has one phenolic group whereas AN2 has two phenolic groups.

3.6. SUMMARY

The behaviour of AN2, at treat rate of 0.5 % w/w, has been studied in squalane in a bench-top reactor by oxidations at 180 °C to 210 °C and monitoring the concentrations of the starting materials, intermediates, oxygen uptake, and total carbonyl formation during the oxidations; to provide lubricant formulators with a good understanding of the mechanisms by which phenolic antioxidants control lubricant deterioration.

AN2 and squalane were chosen as models for commercial phenolics (e.g. Irganox L135) and base fluids (e.g. Shell XHVI 8.2), respectively, because they are made out of single structures and hence easier to analyse; in contrast, commercial phenolics and base fluids are made out of a combination of several structures. Previous work, mainly, investigated over-simplified model structures of antioxidants (e.g. BHT) that have high volatility at high temperatures, in model base fluids that are physiochemically different from those used commercially (see Table 3.1 for references).

The antioxidant concentration, oxygen uptake, carbonyl formation, and oxidation products from both the antioxidant and the model base fluid were directly monitored online to observe how the antioxidant decay and the extent of protection the antioxidant provides to the base fluid. Previous work, usually, monitor the above reaction parameters at the end of the reaction (i.e. when the reaction is terminated) and not throughout the reaction.

AN2, at a treat rate of 0.5 % w/w, in squalane provided the inhibition times of 107, 62, 31, and 14 minutes at 180, 190, 200, and 210 °C, respectively. AN2 was found to provide a full antioxidative protection to squalane, and squalane would only oxidise when AN2 is totally consumed. The high antioxidative efficiency of AN2 was attributed to its ability to provide ready-to-abstract hydrogen atoms to peroxyl radicals.

The most important steps in the inhibition mechanism of AN2 are the abstraction of the easy-to-abstract hydrogen atoms of AN2, AN2 phenoxyl radical, galvinol, and formylphenol by peroxyl radicals.

3.7. REFERENCES

Adam, W. and Chiu, W. The mechanism of a rate-controlled cross-disproportionation between phenoxyl radicals. *Journal of the American Chemical Society*, 1971, **13** (15): 3687-3693.

Amorati, R.; Lucarini, M.; Mugnaini, V.; and Pedulli, G. Antioxidant activity of o-bisphenols the role of intramolecular hydrogen bonding. *Journal of Organic Chemistry*, 2003, **68** (13): 5198-5204.

Becker, R. and Knorr, A. An evaluation of antioxidants for vegetable oils at elevated temperatures. *Lubrication Science*, 1996, **8** (2): 95-117.

Denisov, E. and Afanasev, I. Oxidation and antioxidants in organic chemistry and biology. CRC Press of Taylor and Francis Group, Florida, 2005.

Denisov, E. and Denisova, T. Handbook of antioxidants bond dissociation energies rate constants activation energies and enthalpies of reactions (second edition). CRC Press LLC, Florida, 2000.

Dong, J.; Mulqueen, G.; Goode, M.; and Holt, A. Stabilizing compositions for lubricants. Chemtura Corporation, 2007, patent WO 2007/100726 A2.

Franchi, P.; Lucarini, M.; Pedulli, G.; Valgimigli, L.; and Lunelli, B. Reactivity of substituted phenols toward alkyl radicals. *Journal of the American Chemical Society*, 1999, **121** (3): 507-514.

Gatto, V. and Grina, M. Effects of base oil type oxidation test conditions and phenolic antioxidant structure on the detection and magnitude of hindered phenol/diphenylamine synergism. *Lubrication Engineering*, 1999, **55** (1): 11-20.

Gatto, V.; Moehle, W.; Cobb, T.; and Schneller, E. Oxidation fundamentals and its application to turbine oil testing. *Journal of ASTM International*, 2006, **3** (4): 1-20.

Greene, F. and Adam, W. Autoxidation of galvinoxyl. *Journal of Organic Chemistry*, 1963, **28** (12): 3550-3551.

Hamblin, P. and Rohrbach, P. Piston deposit control using metal-free additives. *Lubrication Science*, 2001, **1** (14): 3-23.

Honeywill, J. and Mile, B. The use of the tertiary alkyl tetraoxide-peroxyl equilibrium ROOOOR ↔ 2 RO2• as a clean source of tertiary alkyl peroxyls. *Journal of the Chemical Society Perkin Transactions 2*, 2002, (3): 569-575.

Horswill, E. and Ingold, K. The oxidation of phenols I the oxidation of 2,6-di-t-butyl-4-methylphenol 2,6-di-t-butylphenol and 2,6-dimethylphenol with peroxy radicals. *Canadian Journal of Chemistry*, 1966, **44** (3): 263-268.

Howard, J. Absolute rate constants for reactions of oxyl radicals. In: Williams, G. (editor). Advances in free-radical chemistry, volume 4. Logos Press Limited, London, 1972.

Howard, J. and Ingold, K. The inhibited autoxidation of styrene part III the relative inhibiting efficiencies of ortho-alkyl phenols. *Canadian Journal of Chemistry*, 1963, **41** (11): 2800-2806.

Howard, J. and Ingold, K. The kinetics of the inhibited autoxidation of tetralin. *Canadian Journal of Chemistry*, 1964, **42** (10): 2324-2333.

Howard, J. Radical reaction rates in liquids, In: Fischer (editor), H. Peroxyl and related radicals. Subvolume D2. Springer, London, 1997.

Ingold, K. and MacFaul, P. Distinguishing biomimetic oxidations from oxidations mediated by freely diffusing radicals. In: Meunier, B. (editor) Biomimetic oxidations catalyzed by transition metal complexes. Imperial College Press, London, 2000, page: 63.

Ischuk, Y. and Butovets, V. Estimation of grease oxidation stability under dynamic conditions and antioxidant testing. *NLGI Spokesman*, 1991, **55** (4): 133-138.

Jain, M.; Sawant, R.; Paulmer, R.; Ganguli, D.; and Vasuder, G. Evaluation of thermo-oxidative characteristics of gear oils by different techniques effect of antioxidant chemistry. *Thermochimica*, 2005, **435**: 172-175.

Jensen, R.; Korcek, S.; Mahoney, L.; and Zinbo, M. Mechanism of 4,4-methylenebis(2,6-di-tert-butylphenol) inhibited autoxidations at 180 to 220°C. In: Mahoney, L.; Korcek, S.; Willermet, P.; Hamilton, E.; Jensen, R.; Zinbo, M.; Kandah, S.; Norbeck, J.; and Scheich, L. Time-temperature studies of high temperature deterioration phenomena in lubricant systems synthetic ester lubricants. Internal Report of Ford Motor Company, 1979, pages: 25-45.

Jensen, R.; Korcek, S.; Zinbo, M.; and Johnson, M. Initiation in hydrocarbon autoxidation at elevated temperatures. *International Journal of Chemical Kinetics*, 1990, **22**: 1095-1107.

Johnson, M.; Korcek, S.; and Zinbo, M. High-temperature antioxidant capabilities of base oils and base oil-additive mixtures. *Industrial and Engineering Chemistry Research*, 1987, **26** (9): 1754-1757.

Johnson, M.; Korcek, S.; and Zinbo, M. Inhibition of oxidation by ZDTP and ashless antioxidants in the presence of hydroperoxides at 160°C – part I. *SAE Technical Paper*, 1983, paper 831684: 71-81.

Kharasch, M. and Joshi, B. Reactions of hindered phenols I reactions of 4,4'-dihydroxy-3,5,3',5'-tetra-tert-butyl diphenylmethane. *Journal of Organic Chemistry*, 1957, **22**: 1435-1438.

Korcek, S.; Johnson, M.; Jensen, R.; and Zinbo, M. Determination of the high-temperature antioxidant capability of lubricants and lubricant compounds. *Industrial and Engineering Chemistry Product Research and Development*, 1986, **25** (4): 621-627.

Low, H. Antioxidants free radical chain terminators. *Industrial and Engineering Chemistry Product Research and Development*, 1966, **5** (1): 80-86.

Mahoney, L. Antioxidants. *Angewandte Chemie International Edition*, 1969, **8** (8): 547-555.

Maillard, B.; Ingold, K.; and Scaiano, J. Rate constants for the reactions of free radicals with oxygen in solution. *Journal of the American Chemical Society*, 1983, **105** (15): 5095-5099.

McCaffrey, V. and Forbes, M. Time-resolved EPR studies of main chain radicals from acrylic polymers structural characterization at high temperatures. *Macromolecules*, 2005, **38** (8): 3334-3341.

McKenna, S.; Casserino, M.; and Ratliff, K. Comparing the tertiary carbon content of PAO's and mineral oils. Society of Tribologists and Lubrication Engineers annual meeting, Houston, 2002.

McMillen, D. and Golden, D. Hydrocarbon bond dissociation energies. *Annual Review of Physical Chemistry*, 1982, **33**: 493-532.

Milton, J.; Korcek, S.; and Zinbo, M. High-temperature antioxidant capabilities of base oils and base oil-additive mixtures. *Industrial and Engineering Chemistry Research*, 1987, **26**: 1754-1757.

Mousavi, P.; Wang, D.; Grant, C.; Oxenham, W.; and Hauser, P. Effects of antioxidants on the thermal degradation of a polyol ester lubricant using GPC. *Industrial and Engineering Chemistry Research*, 2006, **45** (1): 15-22.

Muller, K.; Kristen, U.; and Hamblin, P. Effectiveness of ashless antioxidants in motor oils. From: Wirksamkeit von aschefreien antioxidantien in motorolen. *Schmiertechnik Tribologie*, 1982, **29** (3): 92-97.

Nishiyama, T.; Kagimasa, T.; and Yamada, F. Comparison of heteroatom-bridged analogues of methylenebisphenols for antioxidant activities. *Canadian Journal of Chemistry*, 1994, **72** (5): 1412-1414.

Prusikova, M.; Jirackova, L.; and Pospisil, J. Antioxidants and stabilizers XXXIV antioxidative activity of bisphenols during stabilization of tetralin. *Collection of Czechslovak Chemical Communications*, 1972, **37** (11): 3788-3799.

Rose, D. Analysis of antioxidant behaviour in lubricating oils. PhD thesis, University of Leeds, 1991.

Rubtsov, V.; Roginskii, V.; Dubinskii, V.; and Miller, V. Rate constants for phenoxy radical reactions in hydrocarbon oxidations inhibited by 2,4,6-tri-tert-butylphenol. 1979: 921-925.

Sanders, S. and Maloney, P. Controller for use with wide range oxygen sensor. *US Patent 6497135*, 2002.

Sharma, B.; Perez, J.; and Erhan, S. Soybean oil-based lubricants a search for synergistic antioxidants. *Energy and Fuels*, 2007, **21** (4): 2408-2414.

Snelgrove, D.; Lusztyk, J.; Banks, J.; Mulder, P.; and Ingold, K. Kinetic solvent effects on hydrogen-atom abstractions reliable quantitative predictions via a single empirical equation. *Journal of the American Chemical Society*, 2001, **123** (3): 469-477.

Stark, M. The oxidation of hydrocarbon base-fluid lubricants in gasoline engines. Internal Report. 2003, Department of Chemistry, University of York.

Wallington, T.; Nielsen, O.; and Sehested, J. Reactions of organic peroxy radicals in the gas phase. In: Alfassi, Z. (editor) Peroxyl radicals. John Wiley and Sons Limited, Chichester, 1997.

Weiner, S. and Mahoney, L. Mechanistic study of termination reactions of 2,4,6-trialkylphenoxy radicals. *Journal of the American Chemical Society*, 1972, **94** (14): 5029.

4. BEHAVIOUR OF AMINIC ANTIOXIDANTS IN BENCH-TOP REACTORS

4.1. INTRODUCTION

Aminic antioxidants are widely used to control deterioration of the automotive engine lubricants (Muller et al, 1982; and Hamblin and Rohrbach, 2001). A thorough understanding of the mechanisms by which aminic antioxidants control lubricant deterioration should enable lubricant formulators to formulate better lubricants.

Previous work on the behaviour of aminic antioxidants in bench-top reactors suffer from the same drawbacks as those of phenolic antioxidants (see Section 3.1 for more details). A comprehensive list of previous work on the oxidation of aminic antioxidants in bench-top reactors is shown in Table 4.1.

Table 4.1: Previous work on the oxidation of aminic antioxidants in bench-top reactors (RPVOT: Rotating pressure vessel oxidation test; Aminic: Diaromatic amines) (references within table)

Technique	Substrate	T. (°C)	Reference
RPVOT & heated reactor	Base fluid	225 & 200 (‡)	Jain et al, 2005
Heated reactor	Base fluids	150	Dong et al, 2007
Heated reactor	Base fluids	150	Gatto and Grina, 1999
Heated reactor	Base fluids	150	Gatto et al, 2006
Heated bottle	Base fluids	152	Rose, 1991
Heated quartz tube	Chlorobenzene	65	Adamic et al, 1969a
Heated quartz tube	Chlorobenzene	65	Adamic et al, 1969b
Heated reactor	Chlorobenzene	57 & 69	Thomas and Tolman, 1962
Heated reactor	Chlorobenzene	75	Varlamov and Denisov, 1987
Heated tube	Chlorobenzene & diphenyl ester	80 & 177 (§)	Low, 1966
Heated Pyrex flask	Dodecane	180-230	Ekechukwu and Simmons, 1988
Heated reactor	Hexadecane	90-160	Jensen et al, 1995
Oxygen uptake technique	Hexadecane	140	Psikha and Kharitonov, 1999
Heated Pyrex flask	Hexadecane & engine lubricants	160	Korcek et al, 1986
Heated reactor	Hexadecane & pentaerythrityl tetraheptanoate	180-220	Jensen et al, 1979a
Heated flask	Hexadecane, paraffinic oil, & hexylbenzene	130	Bolsman et al, 1978b
Oxygen uptake technique	Hydraulic oils	120	Sheikina et al, 2005
Heated reactor	Lithium grease	115	Ischuk and Butovets, 1991
Heated flask	Paraffinic oil	130	Bolsman et al, 1978a
Heated steel chamber	Polyolester	220	Mousavi et al, 2006
Conductometry	Rapeseed & sunflower oils	130	Becker and Knorr, 1996
Heated reactor	Soybean oil	150	Sharma et al, 2007
Oxygen uptake technique	Tetralin	60	Nishiyama et al, 1994

(‡): with respect to technique, (§): with respect to substrate

The aim of this chapter is to study the behaviour of aminic antioxidants, Amine101 (4-octyl-N-(4-octylphenyl)benzenamine) and Naugalube 438L (4-nonyl-N-(4-nonylphenyl)benzenamine), in squalane (2,6,10,15,19,23-hexamethyltetracosane) and Shell XHVI 8.2 (Group III base fluid, hydrotreated petroleum slack wax), by oxidations at 180 °C to 210 °C and monitoring the concentrations of the starting materials, oxygen uptake, and total carbonyl formation during the oxidations; to provide lubricant formulators with a good understanding of the mechanisms by which aminic antioxidants control lubricant deterioration to enable them to formulate better lubricants. Chemical structures of the investigated compounds are listed in Table 4.2.

4.2. PREVIOUS WORK

Diaromatic amines were studied in detail in this work, as will be seen later in the chapter, and so previous work on the oxidation of diaromatic amines will be presented in this section.

There are two proposed inhibition mechanisms for diaromatic amines. The first mechanism is by Thomas and Tolman (1962) and the second is by Jensen et al (1995).

Thomas and Tolman's inhibition mechanism of diaromatic amines

Thomas and Tolman (1962) studied diphenylamine in chlorobenzene and cumene in a bench-top reactor at 57 *C and 69 °C. The antioxidant intermediates were monitored by an electron paramagnetic resonance spectrometer, and the antioxidant concentration and oxygen uptake were monitored during the reactions. The detailed results enabled the authors to propose a mechanism for the oxidation of diphenylamine. The main steps of this mechanism are:

- Formation of a complex between peroxyl radicals and diphenylamine step was proposed
- Peroxyl-diphenylamine complex reaction with peroxyl radicals to give a nitroxyl radical, an aminyl radical, a hydroxylamine, or a diphenylamine step was proposed
- Peroxyl radicals' reaction with aminyl radicals to give nitroxyl radicals step was proposed
- Nitroxyl radicals' reactions with alkyl radicals and peroxyl radicals steps were proposed

Figure 4.1 shows the proposed inhibition mechanism of diphenylamine by Thomas and Tolman (1962).

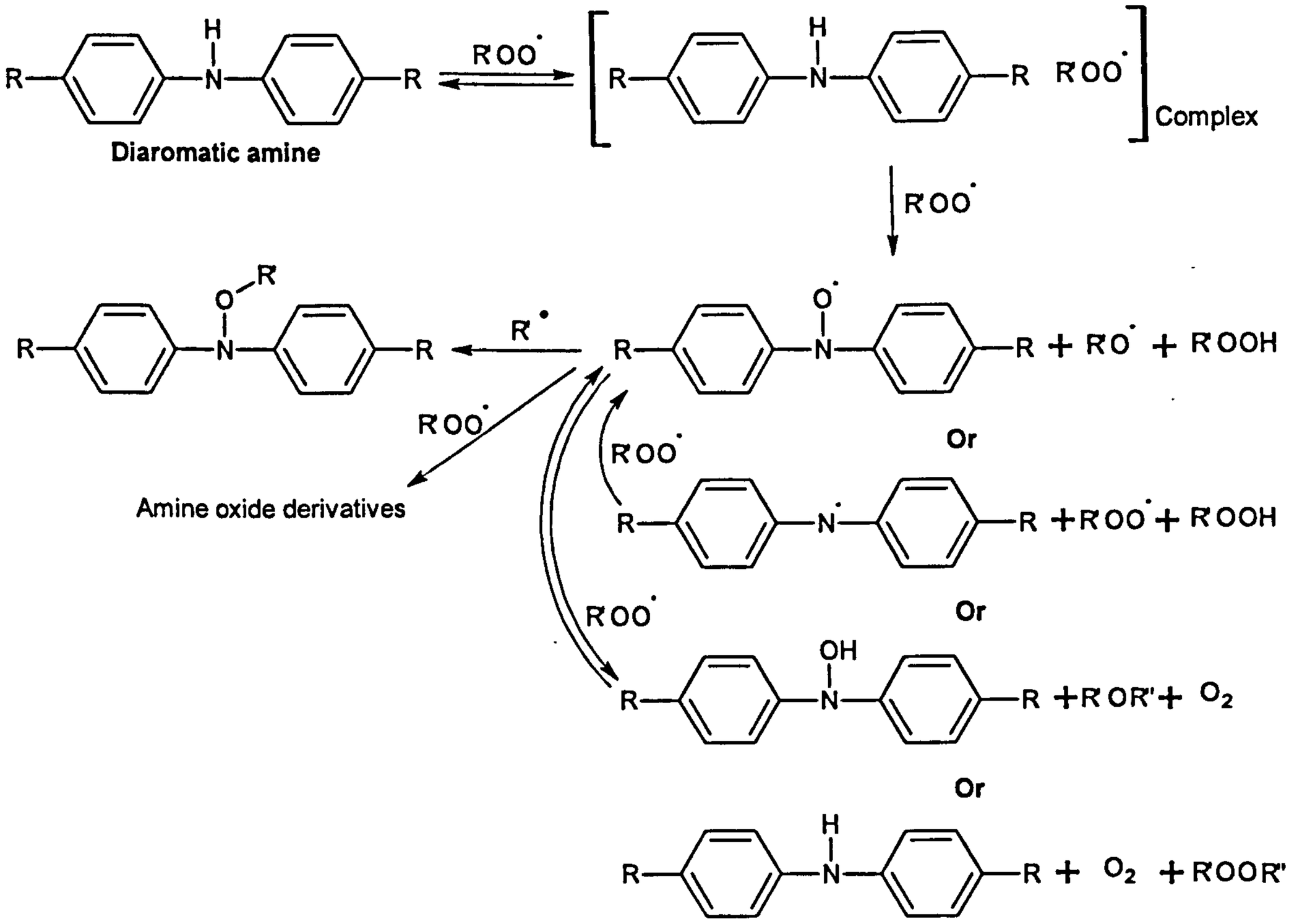

Figure 4.1: Thomas and Tolman's inhibition mechanism of aromatic amines (Thomas and Tolman, 1962)

Jensen's inhibition mechanism of diaromatic amines

Jensen et al (1995) studied Amine101 in hexadecane in a bench-top reactor at 90 °C to 160 °C. The concentrations of the antioxidant and its intermediates were monitored by liquid chromatography. The detailed results enabled the authors to propose a mechanism for the oxidation of Amine101. The main steps of this mechanism are:

- Peroxyl radicals' reaction with Amine101 to give an aminyl radical step was proposed
- Peroxyl radicals and oxygen reaction with aminyl radicals to give nitroxyl radicals step was referenced to Adamic et al (1969a)
- Nitroxyl radicals' reaction with alkyl radicals to give N-alkoxyldiaromatic amine step was proposed
- N-alkoxyldiaromatic amine decomposition to the original Amine101 molecule and/or the hydroxylamine step was proposed
- Peroxyl radicals' reaction with nitroxyl radicals step was proposed

Figure 4.2 shows the proposed inhibition mechanism of Amine101 by Jensen et al (1995).

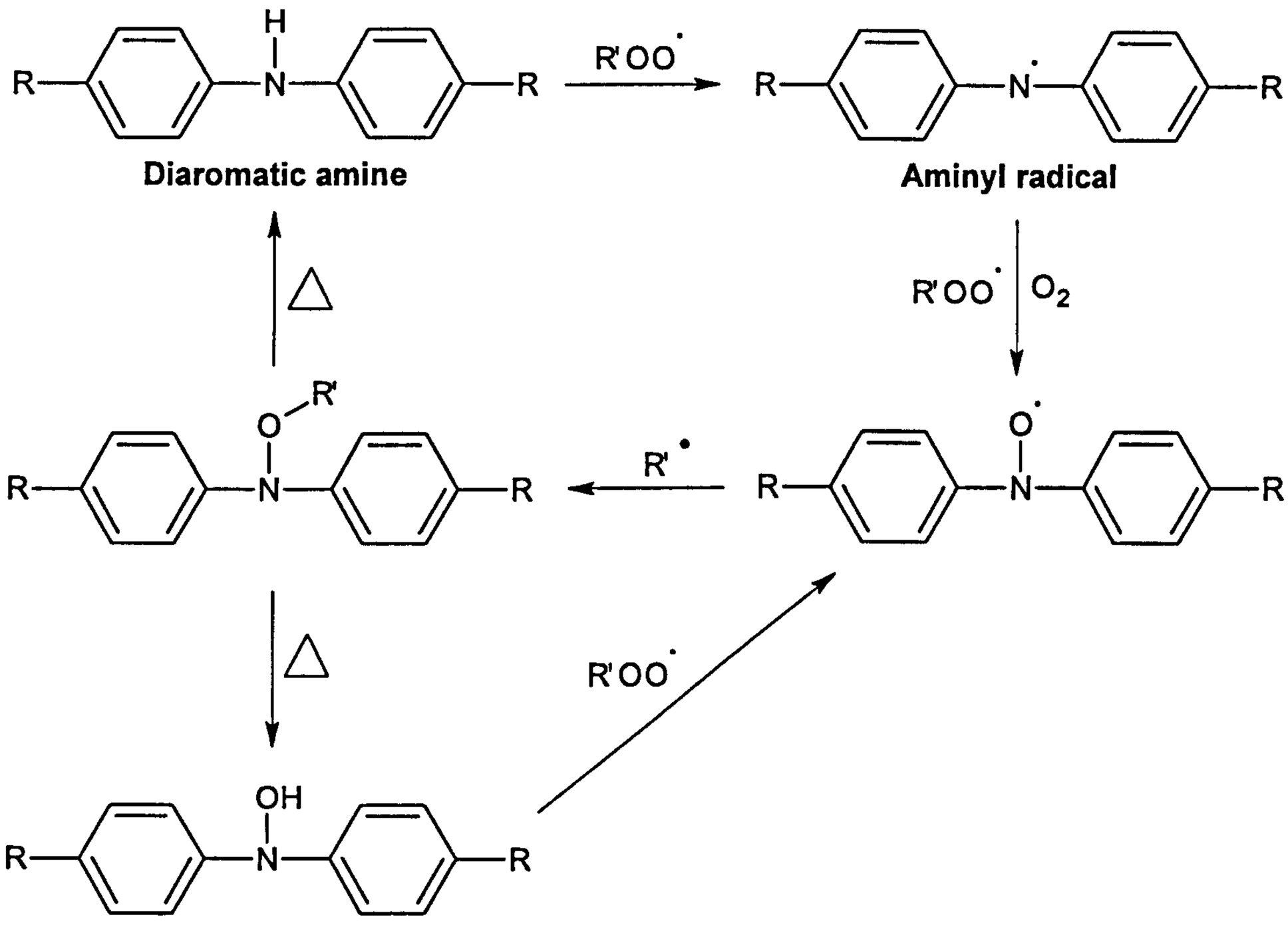

Figure 4.2: Jensen's inhibition mechanism of aromatic amines (Jensen et al, 1995)

4.3. PRODUCT IDENTIFICATION

Amine101 was used as a model antioxidant for Naugalube 438L, because Naugalube 438L consists of a mixture of structures and its oxidation products are commercially unavailable.

No oxidation products of Amine101 were identified. GC traces of oxidised Amine101 can be found in Appendix B. Examples of the GC traces are shown in Figure 4.3.

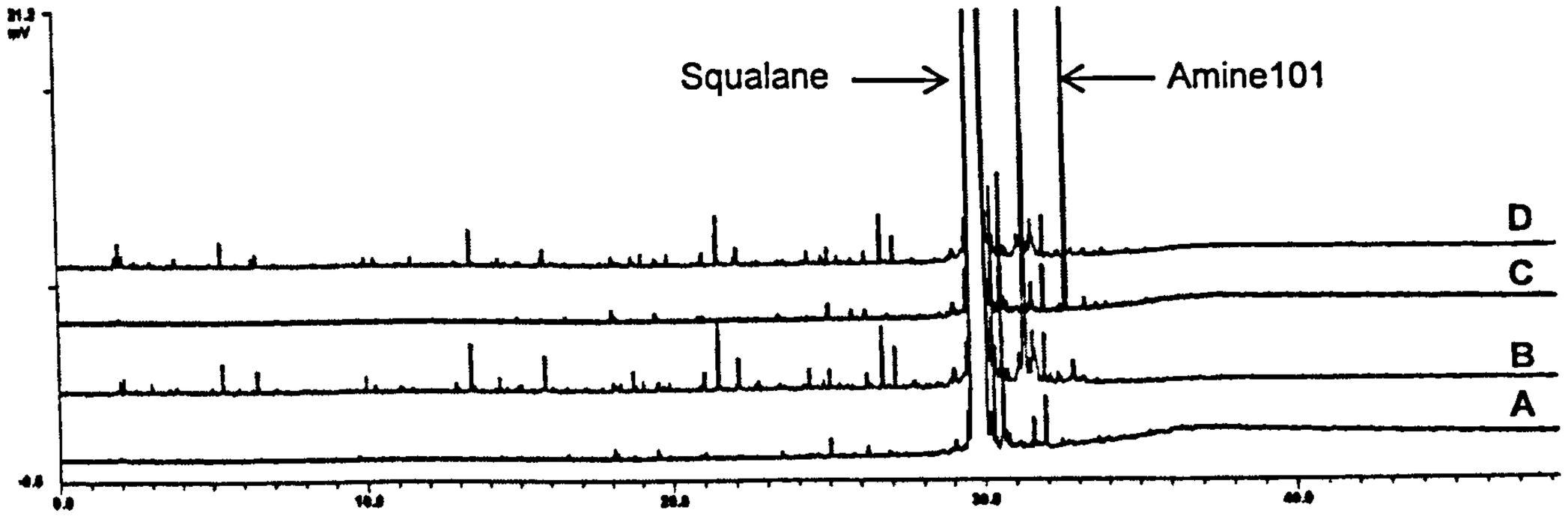

Figure 4.3: GC traces of unoxidised (trace A) and oxidised (trace B) squalane at 200 °C for 9 minutes in static intermediate reactor; and unoxidised (trace C) and oxidised (trace D) 10.0 mmol dm^{-3} Amine101 in squalane at 200 °C for 20 minutes in flow intermediate reactor

Chemical structures of starting materials and oxidation products

Table 4.2: Chemical structures and names of starting materials and oxidation products

Structure	CAS name	Abbreviation
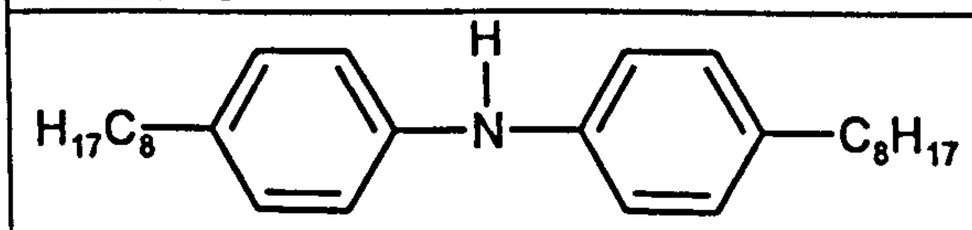	4-Octyl-N-(4-octylphenyl)benzenamine	Amine101
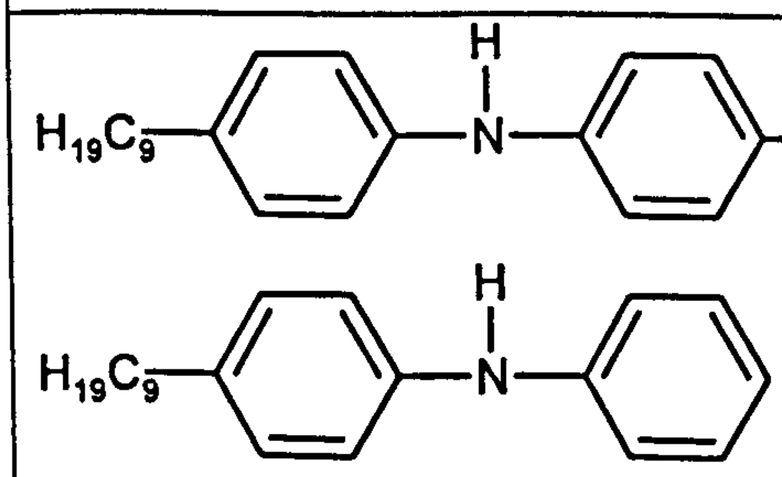 (~75%) (~25%)	4-Nonyl-N-(4-nonylphenyl)benzenamine	Naugalube 438L
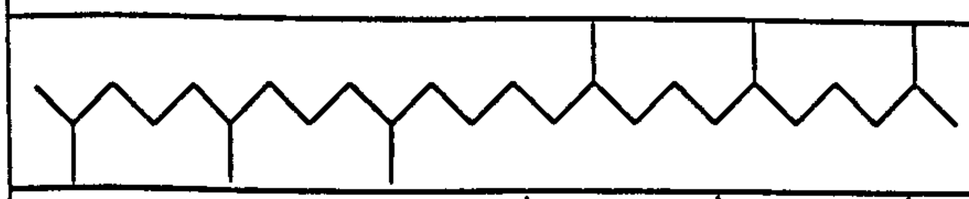	2,6,10,15,19,23-Hexamethyltetracosane	Squalane
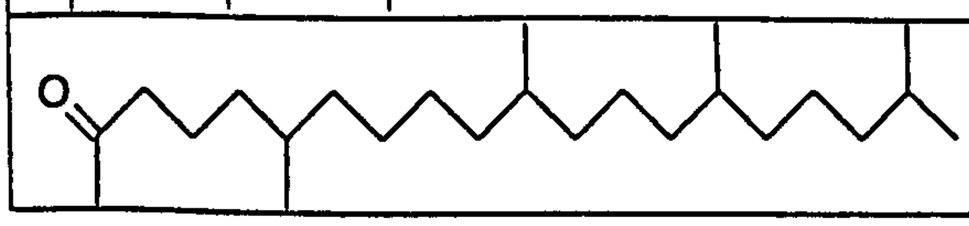	6,11,15,19-Tetramethyl-2-eicosanone	-

4.4. RESULTS

Amine101 (10.0 mmol dm^{-3} or 0.5 % w/w) in 5.0 cm^3 of squalane or Shell XHVI 8.2 was oxidised at temperatures between 180 °C to 210 °C in the flow intermediate reactor.

Figure 4.4 shows that the rate of Amine101 consumption increases with temperature.

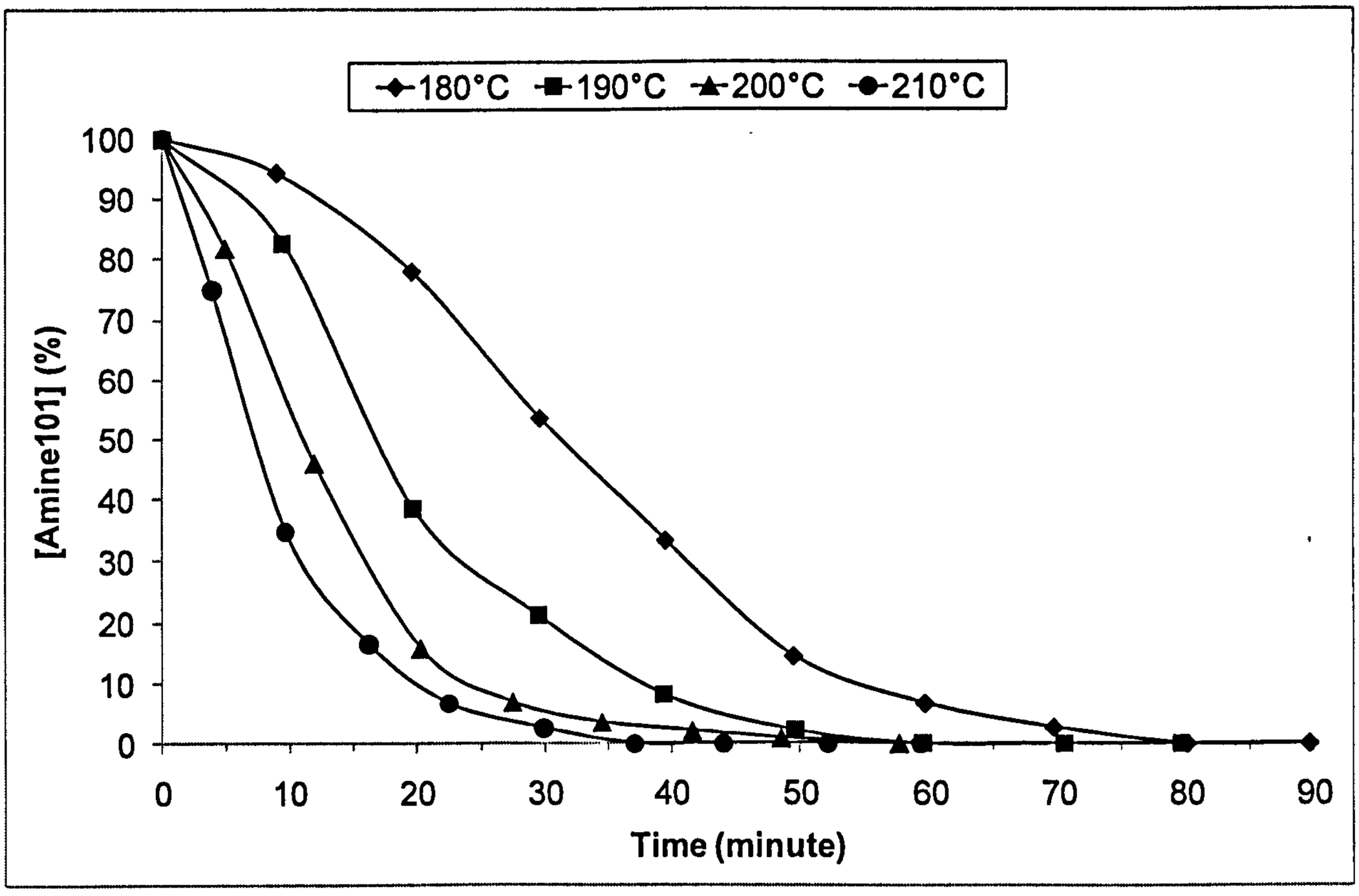

Figure 4.4: Amine101 concentration versus time and temperature in the oxidation of 10.0 mmol dm^{-3} Amine101 (by GC) in squalane between 180 °C to 210 °C in flow intermediate reactor

Figure 4.5 shows that oxygen was consumed in spite of the presence of large quantities of intact Amine101 antioxidant.

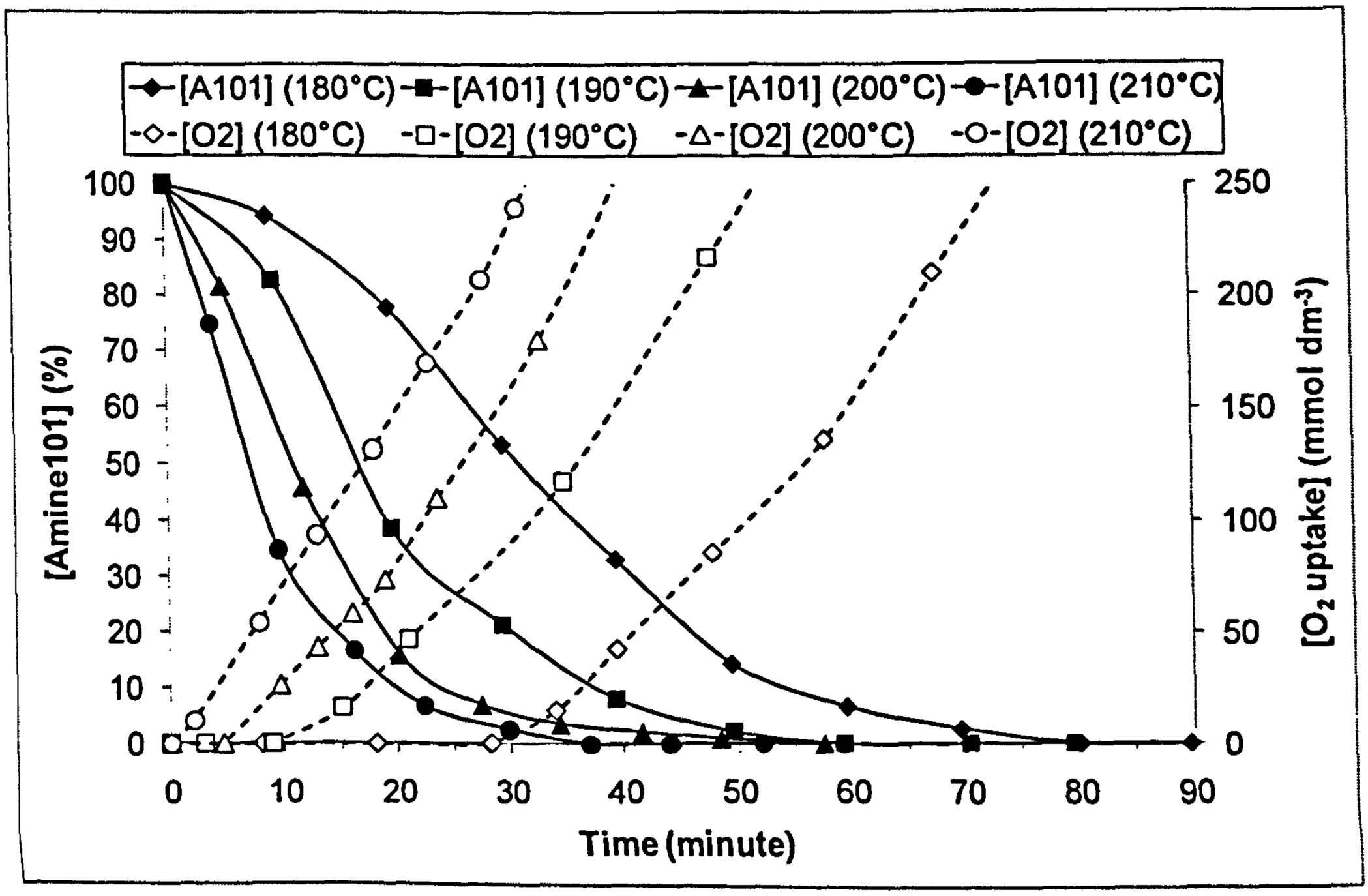

Figure 4.5: Oxygen uptake in the oxidation of 10.0 mmol dm^{-3} Amine101 (by GC) in squalane between 180 °C to 210 °C in flow intermediate reactor

Figure 4.6 shows that squalane degrades to carbonyl products in spite of the presence of large quantities of intact Amine101 antioxidant.

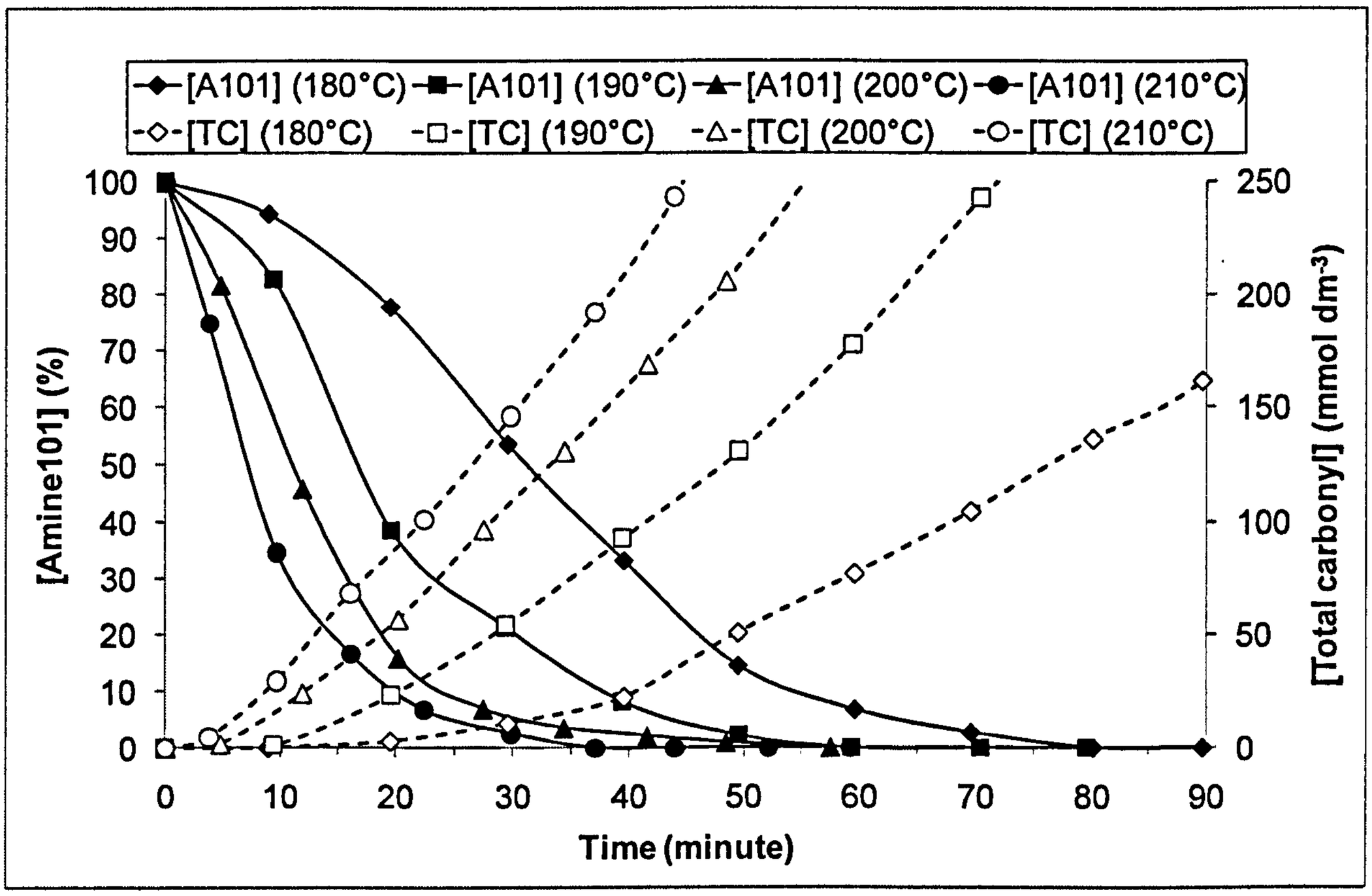

Figure 4.6: Total carbonyl formation (by FTIR) in the oxidation of 10.0 mmol dm^{-3} Amine101 (by GC) in squalane between 180 °C to 210 °C in flow intermediate reactor. TC: Total carbonyl

Figure 4.7 shows the formation of one of the ketones from squalane at the start of the reaction in spite of the presence of large quantities of intact Amine101 antioxidant. Ketone 6,11,15,19-tetramethyl-2-eicosanone was chosen as a representative oxidation product from squalane due to its low volatility.

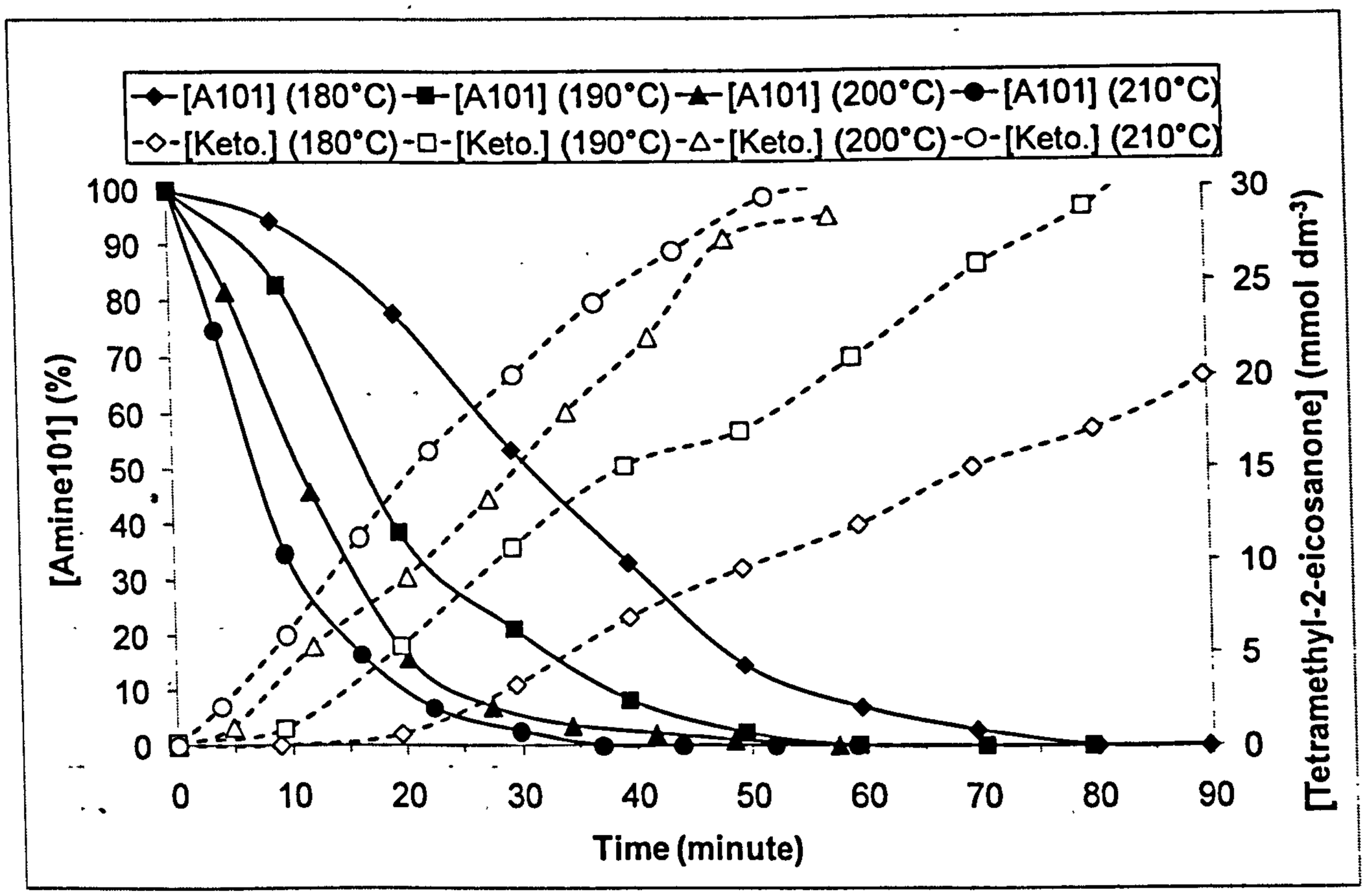

Figure 4.7: 6,11,15,19-tetramethyl-2-eicosanone (from squalane) formation (by GC) in the oxidation of 10.0 mmol dm^{-3} Amine101 (by GC) in squalane between 180 °C to 210 °C in flow intermediate reactor

Figure 4.8 and Figure 4.9 show that 0.5 % of Naugalube 438L is more effective in retarding carbonyl formation than 1.0 % of Naugalube 438L.

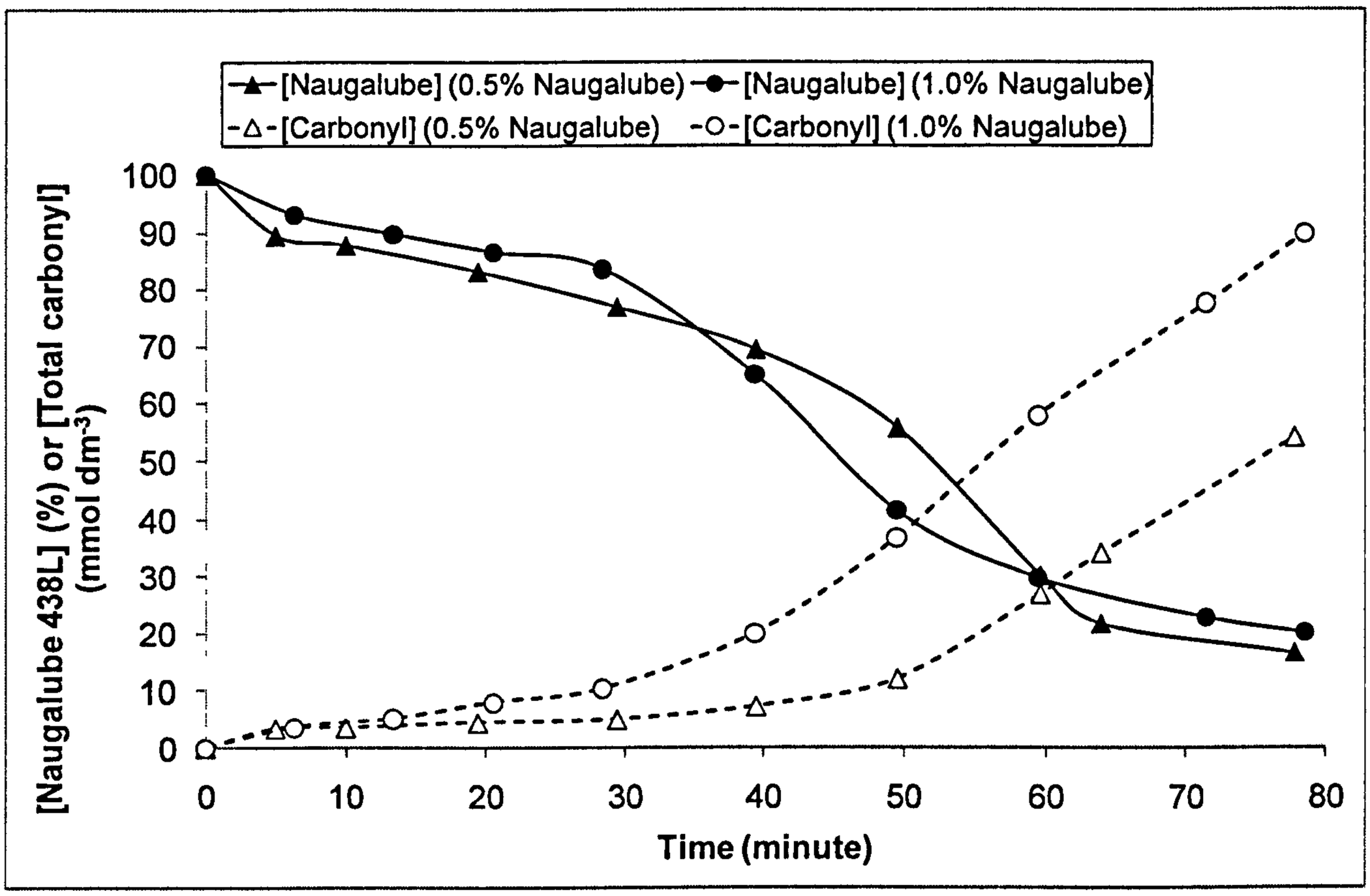

Figure 4.8: Relative decay of Naugalube 438L (by LC) in the oxidation of Shell XHVI 8.2 (+ succinimide dispersant & sulphonate detergent) at 200 °C in static large reactor

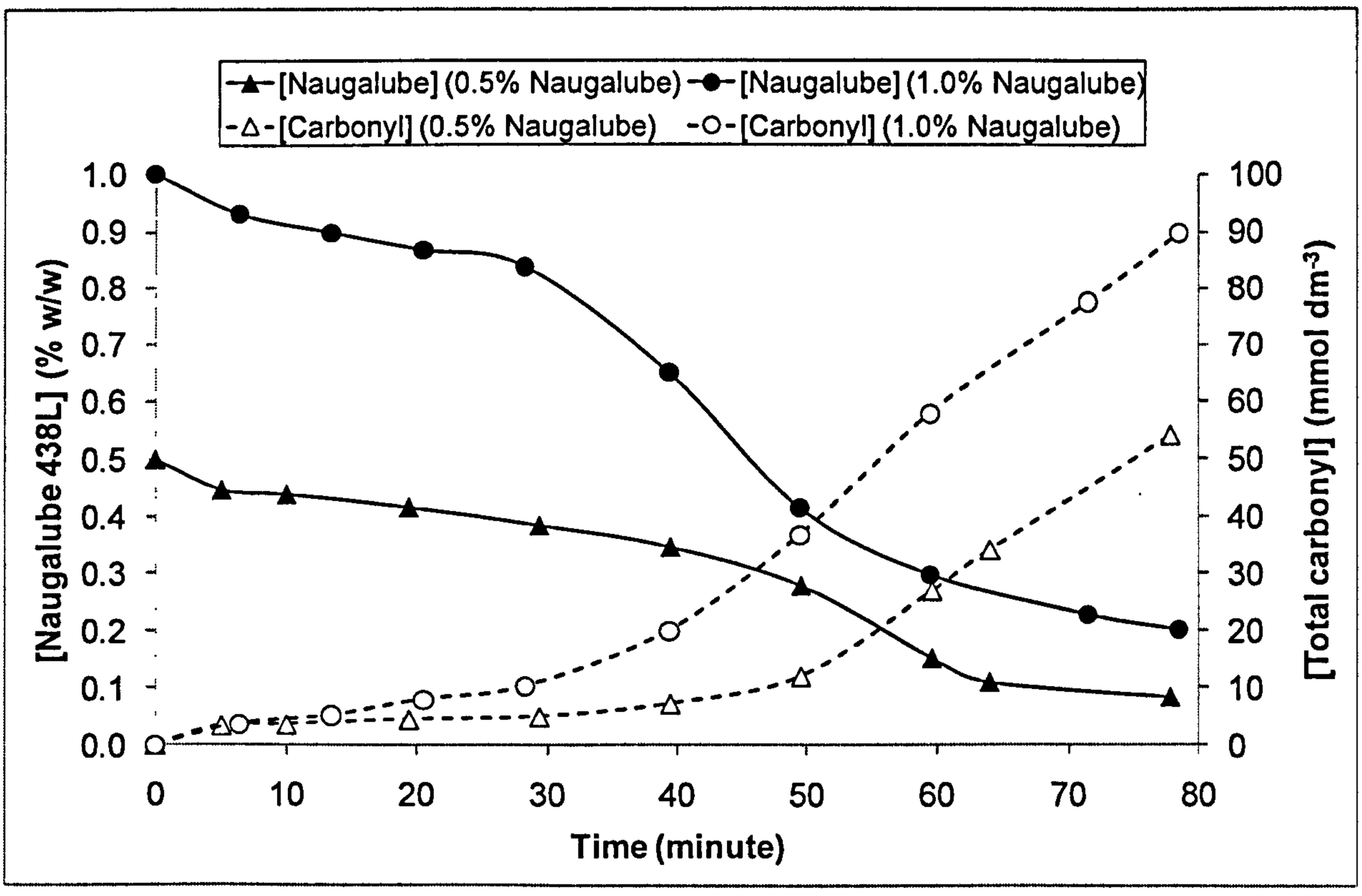

Figure 4.9: Absolute decay of Naugalube 438L (by LC) in the oxidation of Shell XHVI 8.2 (+ succinimide dispersant & sulphonate detergent) at 200 °C in static large reactor

4.5. DISCUSSION

4.5.1. Oxidation mechanism of Amine101

Squalane was partially protected from oxidation in the presence of Amine101, with the antioxidative protection level decreased as the reaction temperature increased (Figure 4.5, Figure 4.6, and Figure 4.7).

The poor performance of Amine101 at high temperatures can be attributed to the reaction between the aminyl radicals of Amine101 and the hydroperoxides, causing an increase in the level of peroxyl radicals (Varlamov and Denisov, 1987):

Am• (aminyl) + ROOH (hydroperoxide) ⇆ AmH (Amine101) + ROO• (peroxyl)

The enthalpy (ΔH) for the reaction between aminyl radicals and hydroperoxides is estimated to be ~3 kJ mol^{-1} (Varlamov and Denisov, 1987) [or modelled E = 16 kJ mol^{-1}, Denisov and Afanasev, 2005, p.505], which means that the reaction between aminyl radicals and hydroperoxides is reversible (i.e. unfavourable) (Varlamov and Denisov, 1987), and the reaction between aminic antioxidants and peroxyl radicals is favourable (Brownlie and Ingold, 1967).

The reaction between aminyl radicals and hydroperoxides becomes reversible (i.e. the reverse reaction becomes significant) above a critical (threshold) temperature, which will depend on to what extent the forward reaction is exothermic.

The reaction between the amine and peroxyl radicals (Brownlie and Ingold, 1967) is expected to be much more dominant than that with alkoxyl (MacFaul et al, 1996) and alkyl radicals (Burton et al, 1996) because peroxyl radicals have long life times (i.e. in the milliseconds range) and high rate of formation (Maillard et al, 1983) and consequently available on abundant quantities, whereas alkoxyl and alkyl radicals have short life times (i.e. in the microseconds range) and low rate of formation (Jensen et al, 1990 and Denisov and Denisova, 2000, p.52) and are expected to be present in low concentrations (Denisov and Afanasev, 2005, p.176; Ingold and MacFaul, 2000; and Wallington et al, 1997). Peroxyl radicals react preferentially with the hydrogen atom attached to the nitrogen atom due to the weaker N-H bond strength (Figure 4.10).

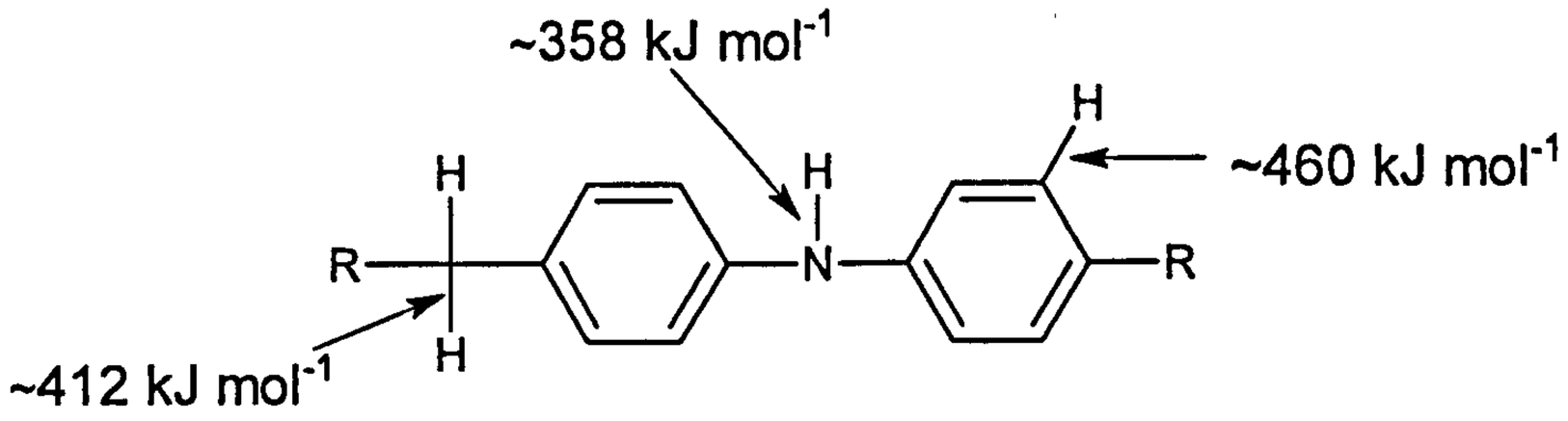

Figure 4.10: Bond strengths of a typical alkylated diaromatic amine (Denisov and Denisova, 2000)

The mechanism for the reaction Amine101 with peroxyl radicals is shown in Figure 4.12.

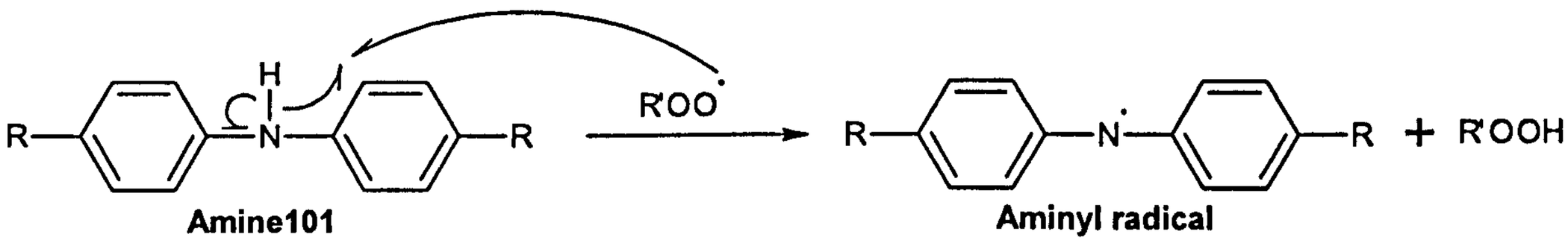

Figure 4.11: Reaction mechanism between a diaromatic amine and peroxyl radicals (Brownlie and Ingold, 1967)

Rate constants for the reaction of peroxyl radicals with Amine101 are not available and so data from other similar diaromatic amines (e.g. 4,4'-dimethyldiphenylamine and diphenylamine)[27] are given (Table 4.3).

Table 4.3: Rate constants for the reaction between diphenylamine and peroxyl radicals to give diphenylaminyl and hydroperoxides (references within table)

Peroxyl radical	Solvent	k ($M^{-1} s^{-1}$)	T. (°C)	Reference
Cyanoisopropylperoxyl	Chlorobenzene	3.4×10^5	75	Varlamov and Denisov, 1987
Cyclohexylperoxyl	Cyclohexanol	1.6×10^2	75	Howard, 1997
Styrylperoxyl	o-Dichlorobenzene	4×10^4	65	Brownlie and Ingold, 1967
Styrylperoxyl	Benzene	1.5×10^4	50	Lucarini et al, 1999

Critical evaluation of previous work

Thomas and Tolman (1962) and Jensen et al (1995) proposed that nitroxyl radicals react with alkyl radicals to give N-alkoxyldiaromatic amines. This reaction is expected to be negligible because alkyl radicals react rapidly with oxygen at the diffusion level (i.e. at a rate constant of $\approx 10^9$ M^{-1} s^{-1}; generally regardless of reaction temperature) (Maillard et al, 1983).

[27] The bond dissociation energy (N-H) of 4,4'-dimethyldiphenylamine and diphenylamine are 357.5 kJ mol^{-1} and 364.7 kJ mol^{-1}, respectively (Denisov and Denisova, 2000, p.91).

Jensen et al (1995) proposed that N-alkoxyldiaromatic amine decompose to give a hydroxylamine.[28] It seems that the authors missed two steps between N-alkoxyldiaromatic amine and hydroxylamine, i.e. the formation of a nitroxyl radical (Bolsman et al, 1978b) and the abstraction of a hydrogen atom by the nitroxyl radical (Howard, 1972, p.164). If that was the case, then the suggestion that hydroxylamines originated from N-alkoxyldiaromatic amines is not valid because the process of abstraction of a hydrogen atom by the nitroxyl radical to give a hydroxylamine is very endothermic, i.e. unfavourable (ΔH = BDE(R-H) – BDE(AmO-H) = 354.7[29] – 323[30] = 32 kJ mol^{-1}).

Jensen et al (1995) proposed that N-alkoxyldiaromatic amine decompose to give the original amine. If the amine is regenerated then one should expect the stoichiometric coefficient[31] of amines to be high; however, this was not the case (Table 4.4).

Table 4.4: Stoichiometric coefficients of diphenylamine (references within table)

Solvent	Temp. (°C)	Stoichiometric coefficient	Reference
Lithium grease	115	2.0	Ischuk and Butovets, 1991
Cumene	57	2.2	Thomas and Tolman, 1962
Benzene	63	2.8	Boozer et al, 1955
Paraffinic oil	130	41[32]	Bolsman et al, 1978b

Additional mechanistic clarifications

The reaction between aminyl radicals and peroxyl radicals is expected to occur mainly through the addition of peroxyl radicals to the para-position of the aminyl radical due to the high localised electron density at the para-position of the aminyl radical (Adamic and Ingold, 1969).

Nitroxyl radicals react with peroxyl radicals at k[diphenylnitroxyl+$PhC(Me)_2OO\bullet$] = 5.0×10^3 M^{-1} s^{-1} (68 °C) in $PhCMe_3$ (Denisov and Afanasev, 2005, p.512).

The reaction between aminyl radicals and oxygen is rapid (Maillard et al, 1983 and Musa et al, 1996) but expected to be insignificant as the oxygen molecule is expected to readily dissociate.

---

[28] No experimental results or references were used to backup this suggestion.
[29] The value is for ethylbenzene (Denisov and Denisova, 2000, p.23).
[30] The value is for $C_6H_5C(O)[(CH_3)_3C]NOH$ (Denisov and Denisova, 2000, p.93).
[31] Stoichiometric coefficient (n) = Rate of free radical formation ($[Antioxidant]_0$ / Reaction time).
[32] Calculation method not understood.

Detailed mechanisms in the oxidation of diaromatic amines can be found in Appendix C.

Amine101 oxidation mechanism for this work

The important steps in the oxidation of Amine101 for this work are highlighted in Figure 4.12.

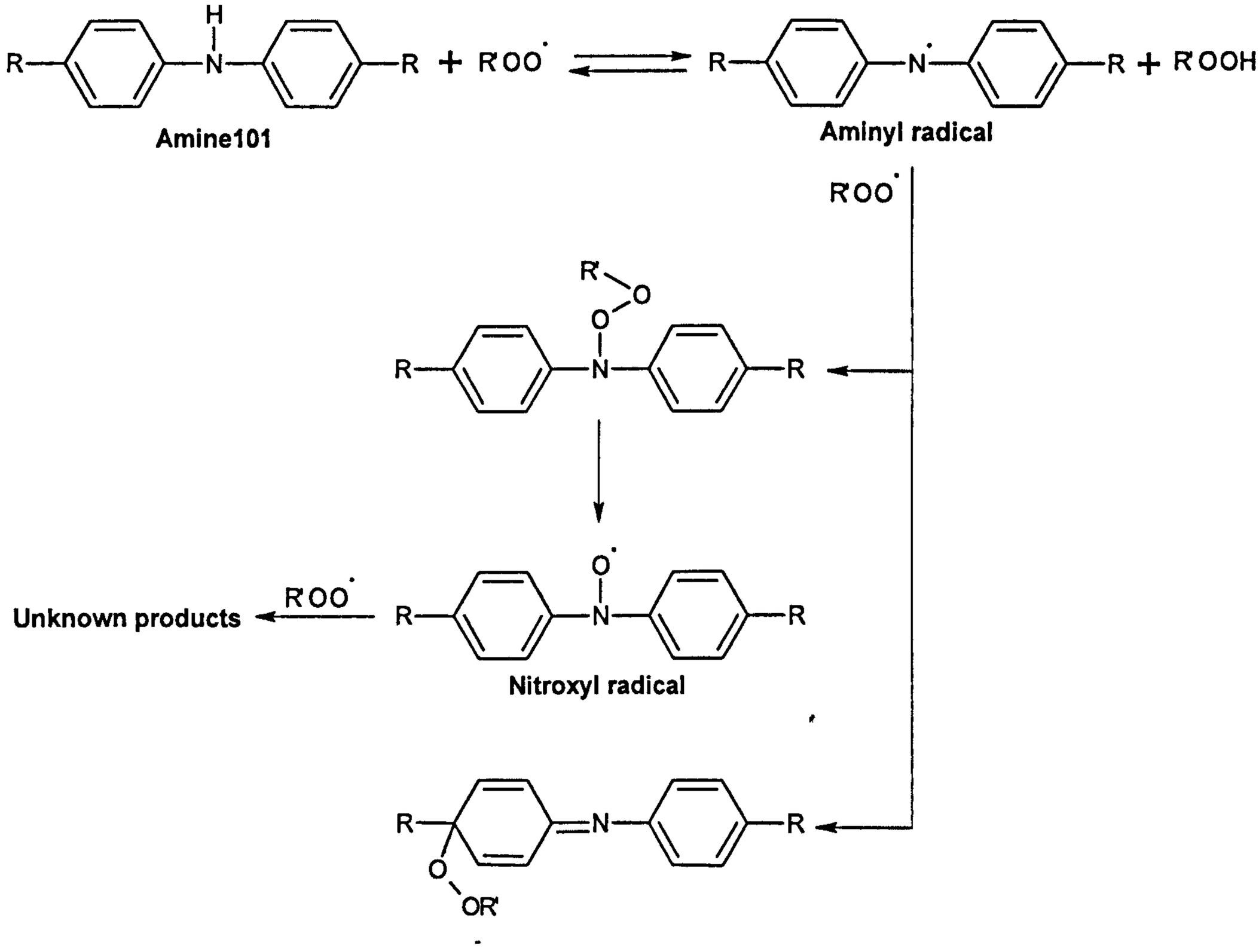

Figure 4.12: Scheme highlighting expected important steps in the oxidation of Amine101 for this work

4.5.2. Oxidation of Naugalube 438L antioxidant

Unexpected results came from the oxidation of Naugalube 438L; 1.0 % w/w of Naugalube 438L was found to be less efficient (in terms of total carbonyl formation) than 0.5 % w/w of Naugalube 438 in spite of the fact that both concentrations of Naugalube 438L degraded at similar rates (Figure 4.9). This was unexpected because one expects that increasing Naugalube 438L concentration would decrease the degradation rate of the base fluid as it has been demonstrated by a previous study.[33] The antioxidant concentrations used by the study (Jensen et al, 1979a) also diminishes any possible links between the critical antioxidant concentration phenomenon (see Chapter 5) and the above unexpected observation for Naugalube 438L in this study.

The possibility of the stock solutions being malformulated (i.e. incorrect antioxidant concentrations were used) is not valid because the concentrations of Naugalube 438L in the 0.5% blend and 1.0% blend stock solutions of Naugalube 438L were verified using liquid chromatography and Fourier transform infrared spectroscopy on at least two occasions. The possibility of a human error (i.e. mix up between labels or containers) is not valid too because the same results were obtained from a research engine (see Chapter 6) and pressurised differential scanning calorimetry technique (see Appendix D), which were operated by different persons than that carried out the bench-top reactions. The possibility of the succinimide dispersant or the sulphonate detergent playing a role is unlikely (see Chapter 7). No satisfactory explanation or suggestion can be offered at this stage for this unexpected observation for Naugalube 438L.

The above unexpected phenomenon requires the aid of additional techniques to shed some light on the origin of the carbonyl content and nature of the oxidation products of the amine.

---

[33] ~5-50 mmol dm^{-3} of Naugalube 438L in hexadecane and pentaerythrityl tetraheptanoate autoxidised at 180-220 °C (Jensen et al, 1979a).

4.6. SUMMARY

The behaviour of Amine101, at treat rate of 0.5 % w/w, has been studied in squalane in a bench-top reactor by oxidations at 180 °C to 210 °C and monitoring the concentrations of the starting materials, intermediates, oxygen uptake, and total carbonyl formation during the oxidations; to provide lubricant formulators with a good understanding of the mechanisms by which aminic antioxidants control lubricant deterioration.

Amine101 was chosen as a model for commercial aminics (e.g. Naugalube 438L), because it is made out of single structure and hence easier to analyse; in contrast, commercial aminics are made out of a combination of several structures. Previous work, mainly, investigated simplified model structures (e.g. diphenylamine) that have high volatility at high temperatures.

Amine101, at a treat rate of 0.5 % w/w, in squalane provided the inhibition times of 28, 9, 5, and 0 minutes at 180, 190, 200, and 210 °C, respectively. Amine101 was found to provide a partial antioxidative protection to squalane at temperatures below 210 °C and a negligible antioxidative protection above 210 °C. The poor performance of Amine101 at high temperatures was rationalised to be due to the temperature dependent reaction between aminyl radicals and hydroperoxides. The significance of the reaction between aminyl radicals and hydroperoxides in the oxidation of diaromatic amines at high temperatures was not described previously.

The most important steps in the inhibition mechanism of Amine101 are the abstraction of the easy-to-abstract hydrogen atom of the amine by peroxyl radicals and the addition of peroxyl radicals to the aminyl radical.

4.7. REFERENCES

Adamic, K. and Ingold, K. Formation of radicals in amine inhibited decomposition of t-butyl hydroperoxide. *Canadian Journal of Chemistry*, 1969, **47** (2): 295-299.

Adamic, K.; Dunn, M.; and Ingold, K. Formation of diphenyl nitroxide in diphenylamine inhibited autoxidations. *Canadian Journal of Chemistry*, 1969a, **47** (2): 287-294.

Adamic, K.; Dunn, M.; and Ingold, K. Formation of radicals in the amine inhibited decomposition of t-butyl hydroperoxide. *Canadian Journal of Chemistry*, 1969b, **47** (2): 295-309.

Becker, R. and Knorr, A. An evaluation of antioxidants for vegetable oils at elevated temperatures. *Lubrication Science*, 1996, **8** (2): 95-117.

Bolsman, T.; Blok, A.; and Frijns, J. Catalytic inhibition of hydrocarbon autoxidation by secondary amines and nitroxides. *Journal of the Royal Netherlands Chemical Society*, 1978a, **97** (12): 310-312.

Bolsman, T.; Blok, A.; and Frijns, J. Mechanism of the catalytic inhibition of hydrocarbon autoxidation by secondary amines and nitroxides. *Journal of the Royal Netherlands Chemical Society*, 1978b, **97** (12): 313-319.

Boozer, C.; Hammond, G.; Hamilton, C.; and Sen, J. Air oxidation of hydrocarbons II the stoichiometry and fate of inhibitors in benzene and chlorobenzene. *Journal of the American Chemical Society*, 1955, **77**: 3233-3237.

Brownlie, I. and Ingold, K. The inhibited autoxidation of styrene part VI the relative efficiencies and the kinetics for inhibition by N-aryl anilines and N-alkyl anilines. *Canadian Journal of Chemistry*, 1967, **45** (20): 2419-2425.

Burton, A.; Ingold, K.; and Walton, J. Absolute rate constants for the reactions of primary alkyl radicals with aromatic amines. *Journal of Organic Chemistry*, 1996, **61** (11): 3778-3782).

Denisov, E. and Afanasev, I. Oxidation and antioxidants in organic chemistry and biology. CRC Press of Taylor and Francis Group, Florida, 2005.

Denisov, E. and Denisova, T. Handbook of antioxidants bond dissociation energies rate constants activation energies and enthalpies of reactions (second edition). CRC Press LLC, Florida, 2000.

Dong, J.; Mulqueen, G.; Goode, M.; and Holt, A. Stabilizing compositions for lubricants. Chemtura Corporation, 2007, patent WO 2007/100726 A2.

Ekechukwu, A. and Simmons, R. Inhibition of the thin-film oxidation of n-dodecane by diphenylamine. *Journal of the Chemical Society Faraday Transactions* 1, 1988, **84** (6): 1871-1878.

Gatto, V. and Grina, M. Effects of base oil type oxidation test conditions and phenolic antioxidant structure on the detection and magnitude of hindered phenol/diphenylamine synergism. *Lubrication Engineering*, 1999, **55** (1): 11-20.

Gatto, V.; Moehle, W.; Cobb, T.; and Schneller, E. Oxidation fundamentals and its application to turbine oil testing. *Journal of ASTM International*, 2006, **3** (4): 1-20.

Hamblin, P. and Rohrbach, P. Piston deposit control using metal-free additives. *Lubrication Science*, 2001, **1** (14): 3-23.

Howard, J. Absolute rate constants for reactions of oxyl radicals. In: Williams, G. (editor). Advances in free-radical chemistry, volume 4. Logos Press Limited, London, 1972.

Howard, J. Radical reaction rates in liquids, In: Fischer (editor), H. Peroxyl and related radicals. Subvolume D2. Springer, London, 1997.

Ingold, K. and MacFaul, P. Distinguishing biomimetic oxidations from oxidations mediated by freely diffusing radicals. In: Meunier, B. (editor) Biomimetic oxidations catalyzed by transition metal complexes. Imperial College Press, London, 2000, page: 63.

Ischuk, Y. and Butovets, V. Estimation of grease oxidation stability under dynamic conditions and antioxidant testing. *NLGI Spokesman*, 1991, **55** (4): 133-138.

Jain, M.; Sawant, R.; Paulmer, R.; Ganguli, D.; and Vasuder, G. Evaluation of thermo-oxidative characteristics of gear oils by different techniques effect of antioxidant chemistry. *Thermochimica*, 2005, **435**: 172-175.

Jensen, R.; Korcek, S.; Mahoney, L.; Scheich, L.; and Zinbo, M. Kinetics and mechanism of 4,4'-dioctyldiphenylamine inhibited autoxidation at 160 to 220°C. In: Mahoney, L.; Korcek, S.; Willermet, P.; Hamilton, E.; Jensen, R.; Zinbo, M.; Kandah, S.; Norbeck, J.; and Scheich, L. Time-temperature studies of high temperature deterioration phenomena in lubricant systems synthetic ester lubricants. Internal Report of Ford Motor Company, 1979a, pages: 2-24.

Jensen, R.; Korcek, S.; Zinbo, M.; and Gerlock, J. Regeneration of amine in catalytic inhibition of oxidation. *Journal of Organic Chemistry*, 1995, **60** (17): 5396-5400.

Jensen, R.; Korcek, S.; Zinbo, M.; and Johnson, M. Initiation in hydrocarbon autoxidation at elevated temperatures. *International Journal of Chemical Kinetics*, 1990, **22**: 1095-1107.

Korcek, S.; Johnson, M.; Jensen, R.; and Zinbo, M. Determination of the high-temperature antioxidant capability of lubricants and lubricant compounds. *Industrial and Engineering Chemistry Product Research and Development*, 1986, **25** (4): 621-627.

Low, H. Antioxidants free radical chain terminators. *Industrial and Engineering Chemistry Product Research and Development*, 1966, **5** (1): 80-86.

Lucarini, M.; Pedrielli, P.; Pedulli, G.; Valgimigli, L.; Gigmes, D.; and Tordo, P. Bond dissociation energies of the N-H bond and rate constants for the reaction with alkyl alkoxyl and peroxyl radicals of phenothiazines and related compounds. *Journal of the American Chemical Society*, 1999, **121** (49): 11546-11553.

MacFaul, P.; Ingold, K.; and Lusztyk, J. Kinetic solvent effects on hydrogen atom abstraction from phenol, aniline, and diphenylamine the importance of hydrogen bonding on their radical-trapping (antioxidant) activities. *Journal of Organic Chemistry*, 1996, **61** (4): 1316-1321.

Maillard, B.; Ingold, K.; and Scaiano, J. Rate constants for the reactions of free radicals with oxygen in solution. *Journal of the American Chemical Society*, 1983, **105** (15): 5095-5099.

Mousavi, P.; Wang, D.; Grant, C.; Oxenham, W.; and Hauser, P. Effects of antioxidants on the thermal degradation of a polyol ester lubricant using GPC. *Industrial and Engineering Chemistry Research*, 2006, **45** (1): 15-22.

Muller, K.; Kristen, U.; and Hamblin, P. Effectiveness of ashless antioxidants in motor oils. From: Wirksamkeit von aschefreien antioxidantien in motorolen. *Schmiertechnik Tribologie*, 1982, **29** (3): 92-97.

Musa, O.; Horner, J.; Shahin, H.; and Newcomb, M. A kinetic scale for dialkylaminyl radical reactions. *Journal of the American Chemical Society*, 1996, **118** (16): 3862-3868.

Nishiyama, T.; Kagimasa, T.; and Yamada, F. Comparison of heteroatom-bridged analogues of methylenebisphenols for antioxidant activities. *Canadian Journal of Chemistry*, 1994, **72** (5): 1412-1414.

Psikha, B. and Kharitonov, V. Specific features of inhibition by some aromatic amines I the effect of inhibitors on the initiation properties of dicumyl peroxide. *Kinetic and Catalysis*, 1999, **40** (4): 459-466.

Rose, D. Analysis of antioxidant behaviour in lubricating oils. PhD thesis, University of Leeds, 1991.

Sharma, B.; Perez, J.; and Erhan, S. Soybean oil-based lubricants a search for synergistic antioxidants. *Energy and Fuels*, 2007, **21** (4): 2408-2414.

Sheikina, N.; Petrov, L.; Psikha, B.; Kharitonov, V.; Tyshchenko, V.; and Shabalina, T. Quantitative study of the inhibited oxidation of hydraulic oils. *Petroleum Chemistry*, 2005, **45** (4): 284-288.

Thomas, J. and Tolman, C. Oxidation inhibited by diphenylamine. *Journal of the American Chemical Society*, 1962, **84**: 2930-2935.

Varlamov, V. and Denisov, E. Kinetic spectrophotometric study of the kinetics of direct and reverse reactions of the peroxide radical with diphenylamine. *Russian Chemical Bulletin*, 1987, **36** (8): 1607-1612.

Wallington, T.; Nielsen, O.; and Sehested, J. Reactions of organic peroxy radicals in the gas phase. In: Alfassi, Z. (editor) Peroxyl radicals. John Wiley and Sons Limited, Chichester, 1997.

5. CRITICAL ANTIOXIDANT BEHAVIOUR AND STOICHIOMETRY COEFFICIENTS

5.1. INTRODUCTION

A good understanding of the Critical Antioxidant Concentration and Critical Temperature phenomena should enable lubricant formulators to choose the appropriate antioxidant concentration at a particular temperature. The critical antioxidant concentration was first described in 1958 by Semenov (Gugumus, 1998a) and can be generally defined as the threshold antioxidant concentration below which the rate of base fluid oxidation is only mildly decreased but above which the rate of base fluid oxidation is significantly reduced; whereas, the critical temperature can be generally defined as the oxidation temperature at which, for a given concentration of antioxidant, the antioxidant has no apparent inhibition effect.

The stoichiometry coefficient of an antioxidant is the number of free radicals trapped by the antioxidant. This coefficient can be used to assess the antioxidative efficiency of the antioxidant to enable lubricant formulators to choose the appropriate antioxidant type for a particular application.

There are no previous works, with experimental data, on the critical antioxidant concentration or the critical temperature phenomena. Previous work on the stoichiometry coefficients of antioxidants provided inconsistent and conflicting data (Table 5.1).

Table 5.1: Stoichiometry coefficients of AN2, BHT, and diphenylamine (references within table)

Antioxidant	Stoichiometry coefficient	Reference
AN2	2.2	Jensen et al, 1990
	10.0	Ischuk and Butovets, 1991
BHT	1.7	Ohkatsu and Nishiyama, 2000
	2.0	Boozer et al, 1955
	2.2	Ischuk and Butovets, 1991
	2.7	Yamada et al, 1989
Diphenylamine	2.0	Ischuk and Butovets, 1991
	2.2	Thomas and Tolman, 1962
	2.8	Boozer et al, 1955
	41	Bolsman et al, 1978b

The aims for this chapter are to investigate the critical antioxidant concentration and critical temperature phenomena, and the stoichiometry coefficients of phenolic and aminic antioxidants at 80 °C to 240 °C in bench-top reactors. Chemical structures of starting materials and oxidation products are listed in Table 5.2.

Table 5.2: Chemical structures and names of starting materials and oxidation products

Structure	CAS name	Abbreviation
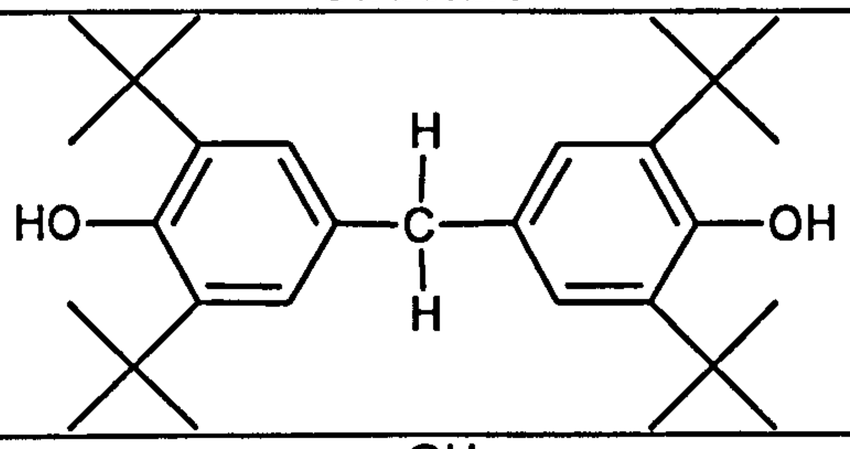	4,4'-Methylenebis[2,6-bis(1,1-dimethylethyl)]phenol	AN2
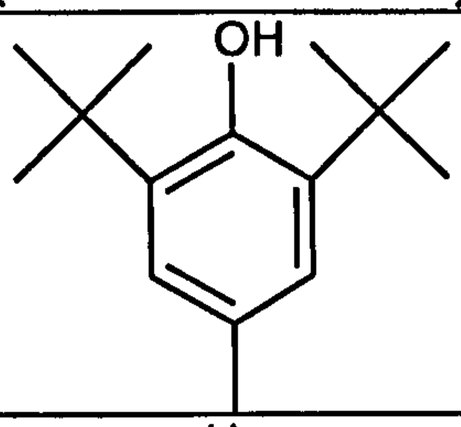	2,6-Bis(1,1-dimethylethyl)-4-methylphenol	BHT
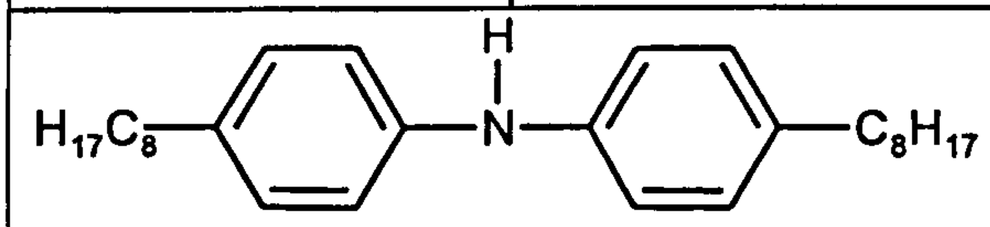	4-Octyl-N-(4-octylphenyl)benzenamine	Amine101
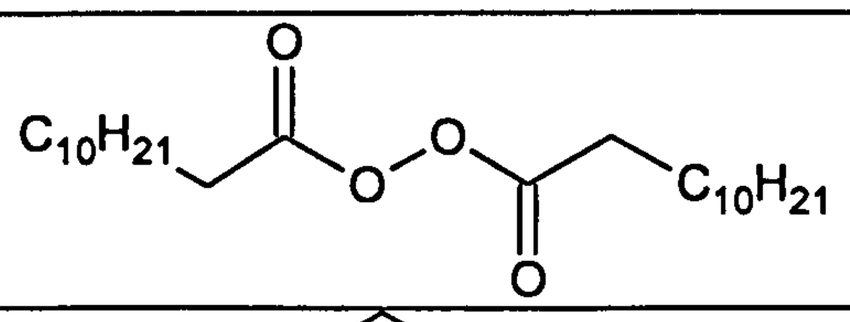	Bis(1-oxododecyl)peroxide	Lauroyl peroxide
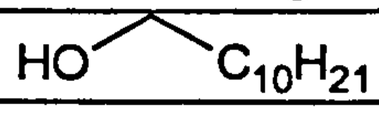	1-Undecanol	Undecanol
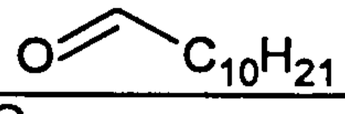	Undecanal	-
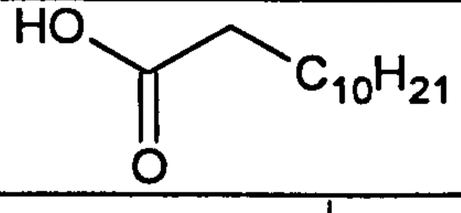	Dodecanoic acid	Lauric acid
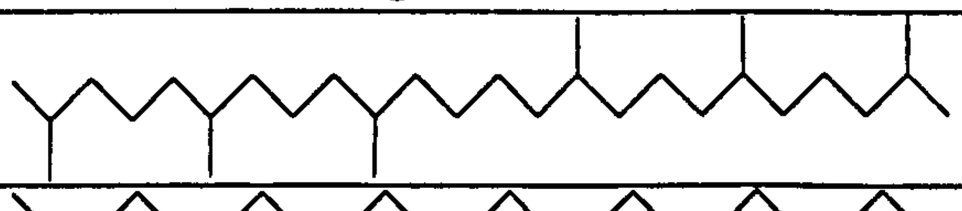	2,6,10,15,19,23-Hexamethyltetracosane	Squalane
	Hexadecane	-

5.2. RESULTS

5.2.1. Critical antioxidant concentration and critical temperature

AN2 in Shell XHVI 8.2 at 200-240 °C and Amine101 in squalane at 180-210 °C were oxidised in bench-top reactors to investigate the critical antioxidant concentration and critical temperature phenomena.

Figure 5.1 shows that beyond a threshold temperature, the reaction times become equal for the substrates with and without AN2 antioxidant.

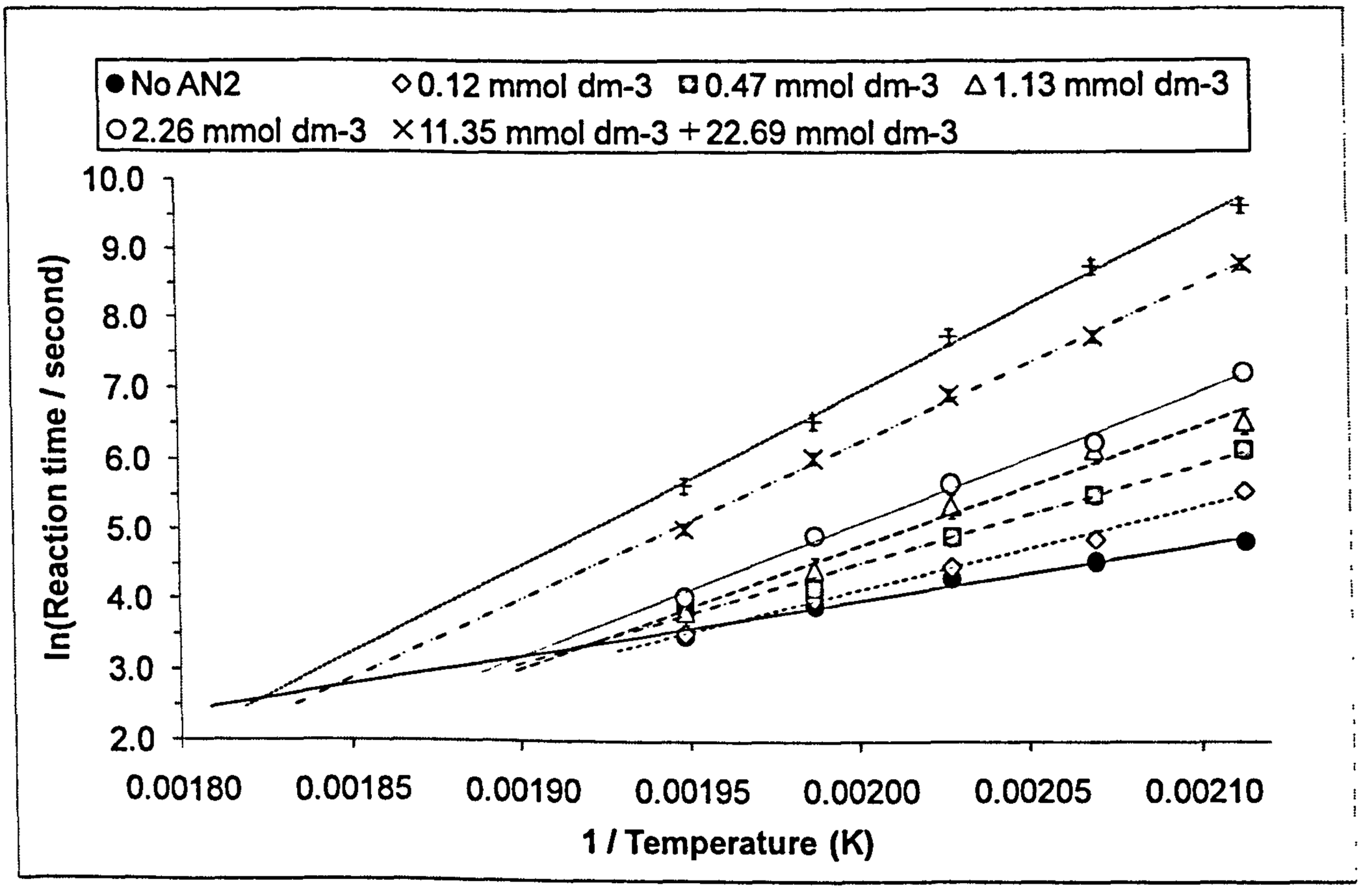

Figure 5.1: Oxidation of 0.00 mmol dm^{-3} to 22.69 mmol dm^{-3} AN2 in Shell XHVI 8.2 at 200 °C to 240 °C in static micro reactor

Figure 5.2 shows that oxygen was consumed in spite of the presence of large quantities of intact Amine101 antioxidant.

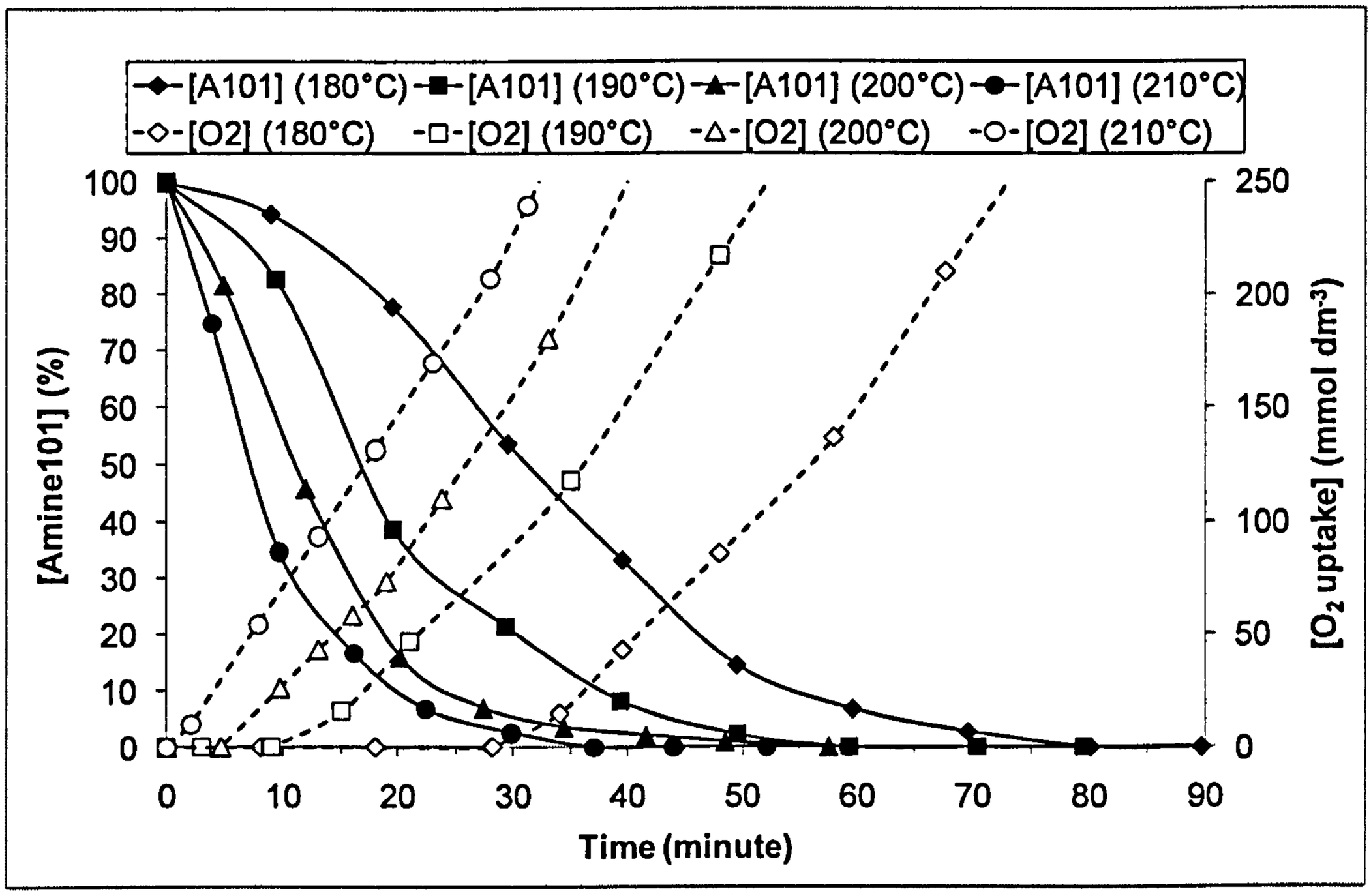

Figure 5.2: Oxidation of 0.5 % w/w (10.0 mmol dm^{-3}) Amine101 in 5.0 cm^3 squalane at 180 °C to 210 °C in flow intermediate reactor

5.2.2. Stoichiometry coefficients of antioxidants

Ten millimoles of BHT, AN2, and Amine101 were reacted with 20.0 mmol dm^{-1} of lauroyl peroxide in hexadecane at 80-120 °C in the flow intermediate reactor to determine the stoichiometry coefficients of antioxidants.

Figure 5.3 and Figure 5.4 show that the decomposition rate of lauroyl peroxide increases as the reaction temperature increases. In Figure 5.4, the line at 100 °C becomes concave after 1200 seconds, and so only the upper linear part will be used.

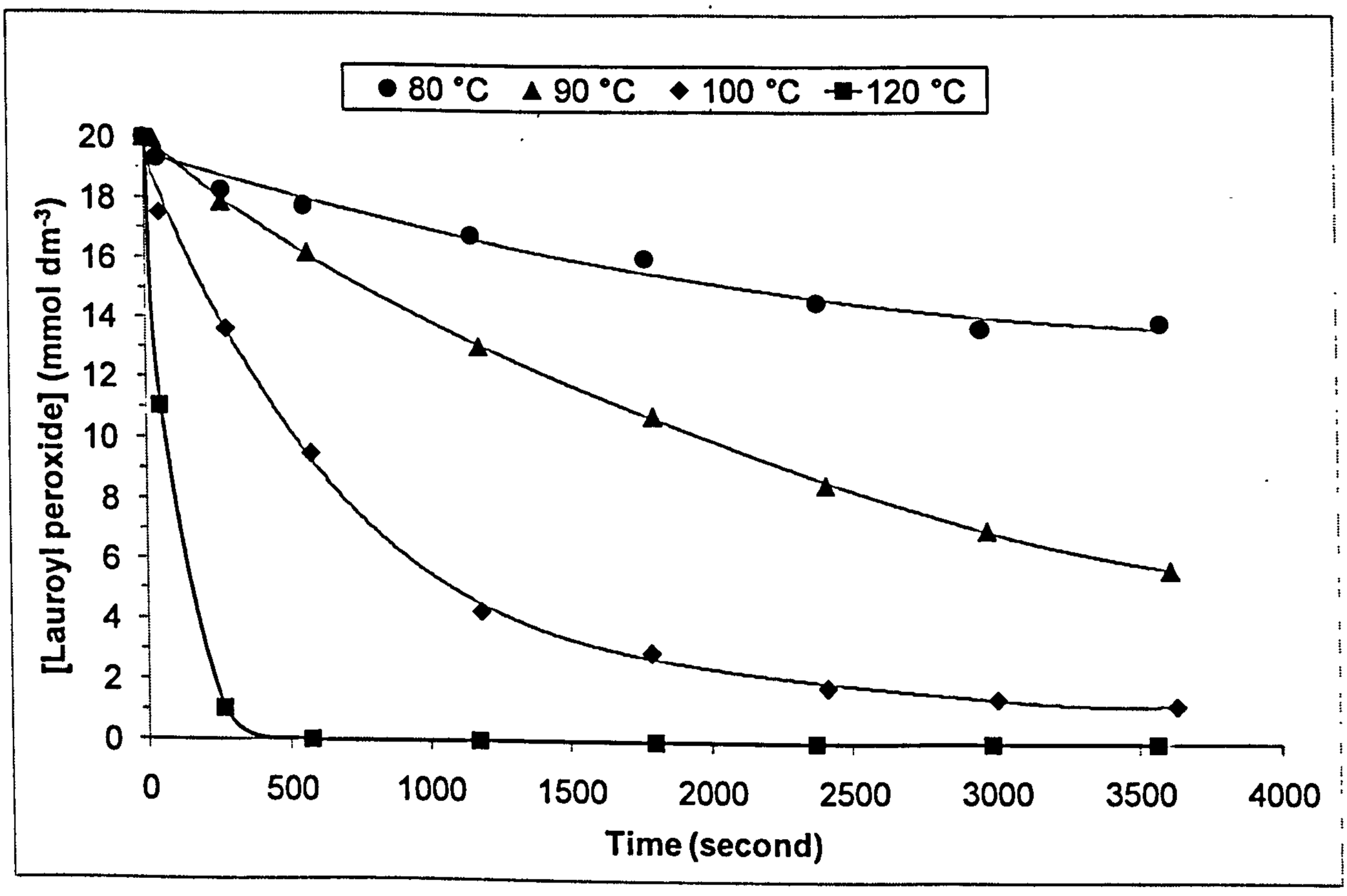

Figure 5.3: Decomposition of lauroyl peroxide (by FTIR) in the oxidation of 20.0 mmol dm^{-3} lauroyl peroxide plus 10.0 mmol dm^{-3} BHT in hexadecane at 80 °C to 120 °C in flow intermediate reactor

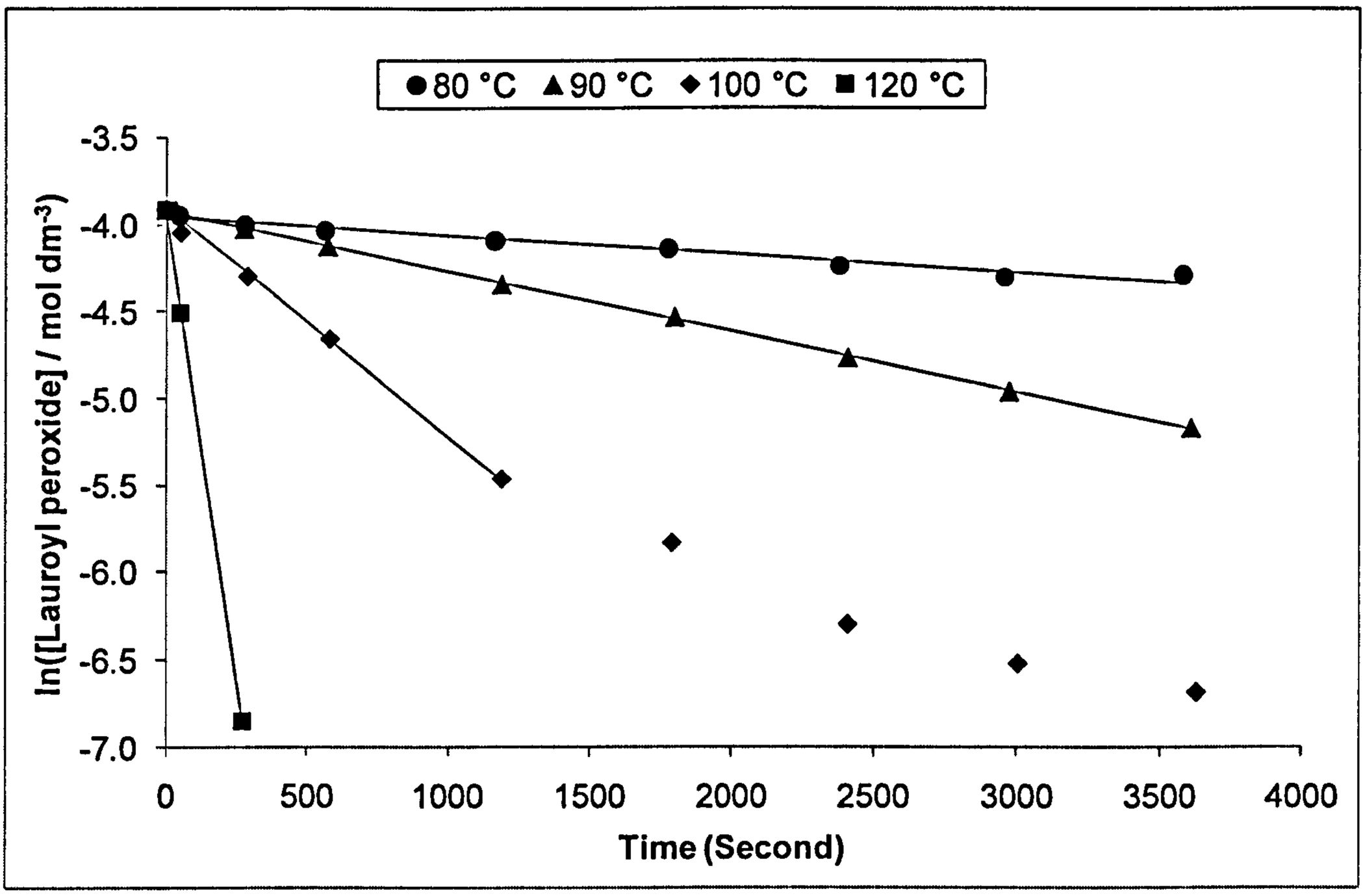

Figure 5.4: Logarithm plot of the decomposition of lauroyl peroxide (by FTIR) in the oxidation of 20.0 mmol dm^{-3} lauroyl peroxide plus 10.0 mmol dm^{-3} BHT in hexadecane at 80 °C to 120 °C in flow intermediate reactor

Figure 5.5 shows that the decomposition rate of lauroyl peroxide is slightly faster in the presence of antioxidants.

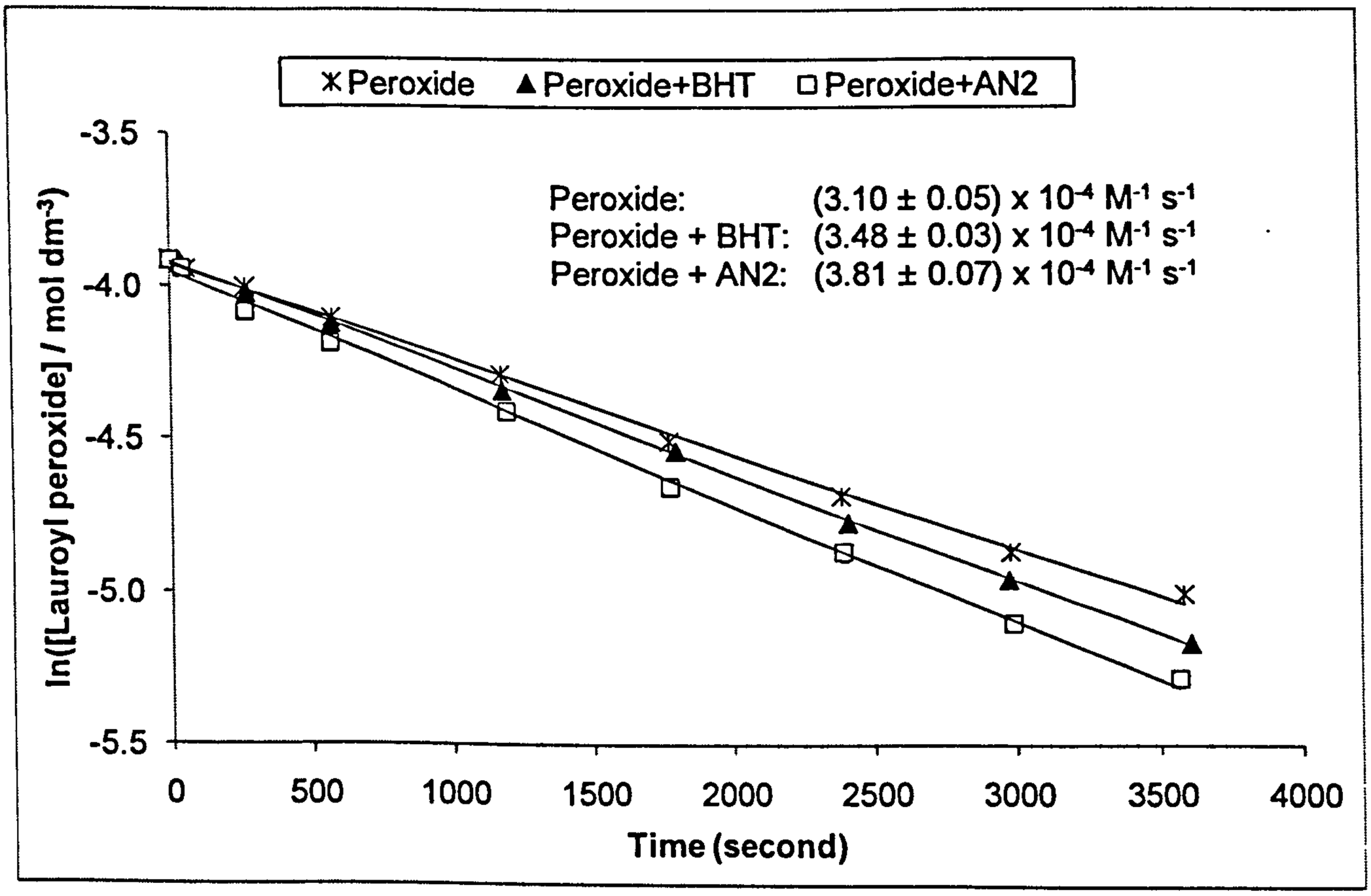

Figure 5.5: Decomposition of lauroyl peroxide (by FTIR) in the oxidation of 20.0 mmol dm^{-3} lauroyl peroxide plus 10.0 mmol dm^{-3} BHT or AN2 in hexadecane at 90 °C in flow intermediate reactor

Table 5.3 lists the first-order decomposition rates of lauroyl peroxide in hexadecane, which were obtained from Figure 5.4 and Figure 5.5.

Table 5.3: First-order decomposition rates of 20.0 mmol dm^{-3} lauroyl peroxide in hexadecane in flow intermediate reactor

Substrate	k (s^{-1})	Temp. (°C)
20 mmol dm^{-3} lauroyl peroxide (+10 mmol dm^{-3} BHT)	(1.05 ± 0.07) x 10^{-4}	80
20 mmol dm^{-3} lauroyl peroxide (+10 mmol dm^{-3} BHT)	(3.48 ± 0.03) x 10^{-4}	90
20 mmol dm^{-3} lauroyl peroxide (+10 mmol dm^{-3} BHT)	(1.28 ± 0.03) x 10^{-3}	100
20 mmol dm^{-3} lauroyl peroxide (+10 mmol dm^{-3} BHT)	(1.08 ± 0.03) x 10^{-2}	120
20 mmol dm^{-3} lauroyl peroxide	(3.10 ± 0.05) x 10^{-4}	90
20 mmol dm^{-3} lauroyl peroxide (+10 mmol dm^{-3} AN2)	(3.81 ± 0.07) x 10^{-4}	90

Figure 5.6 and Figure 5.7 show that the distribution of oxidation products from lauroyl peroxide is the same in the presence or absence of antioxidants.

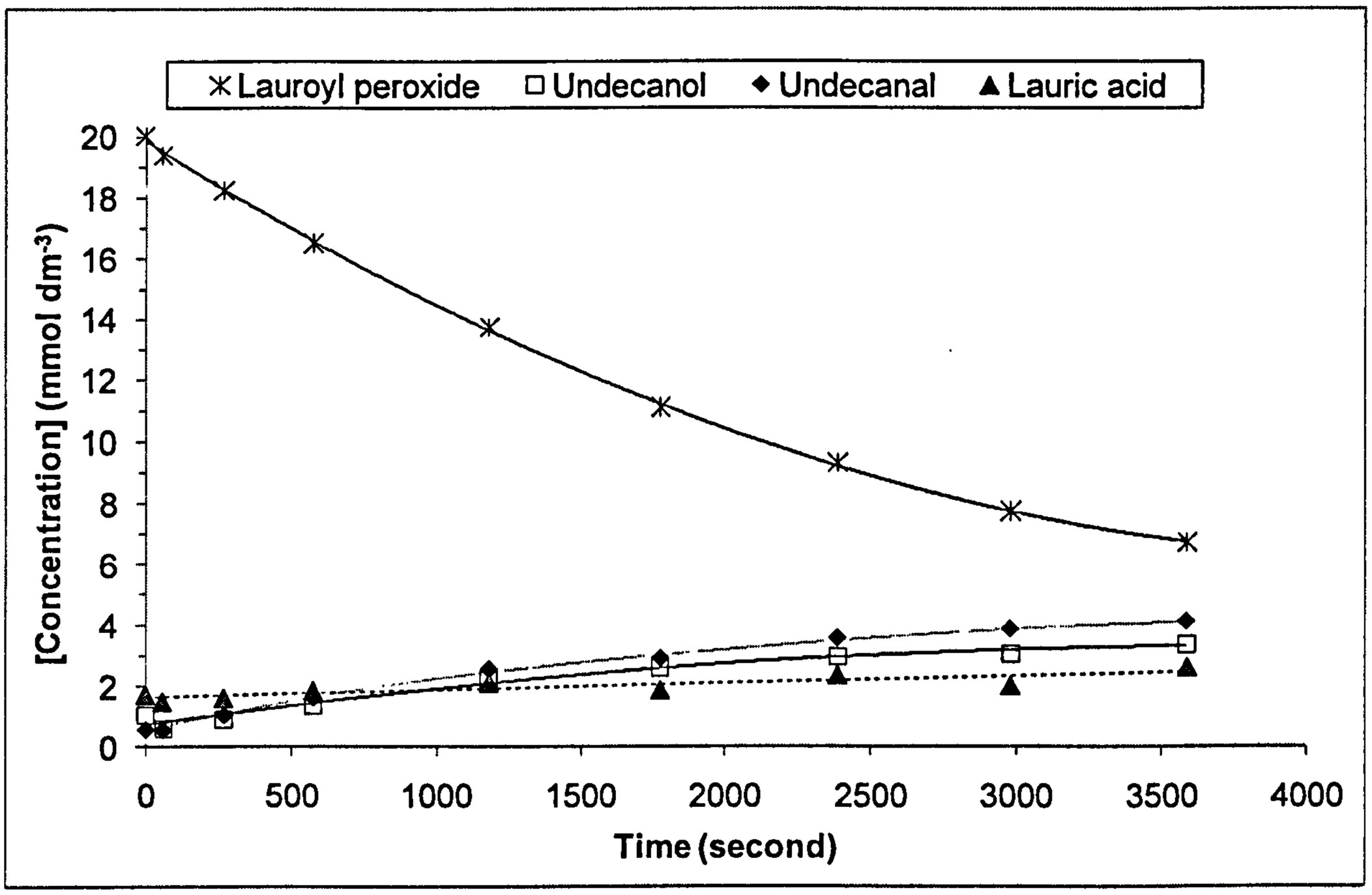

Figure 5.6: Oxidation products (by GC) of lauroyl peroxide in the oxidation of 20.0 mmol dm^{-3} lauroyl peroxide (by FTIR) in hexadecane at 90 °C in flow intermediate reactor

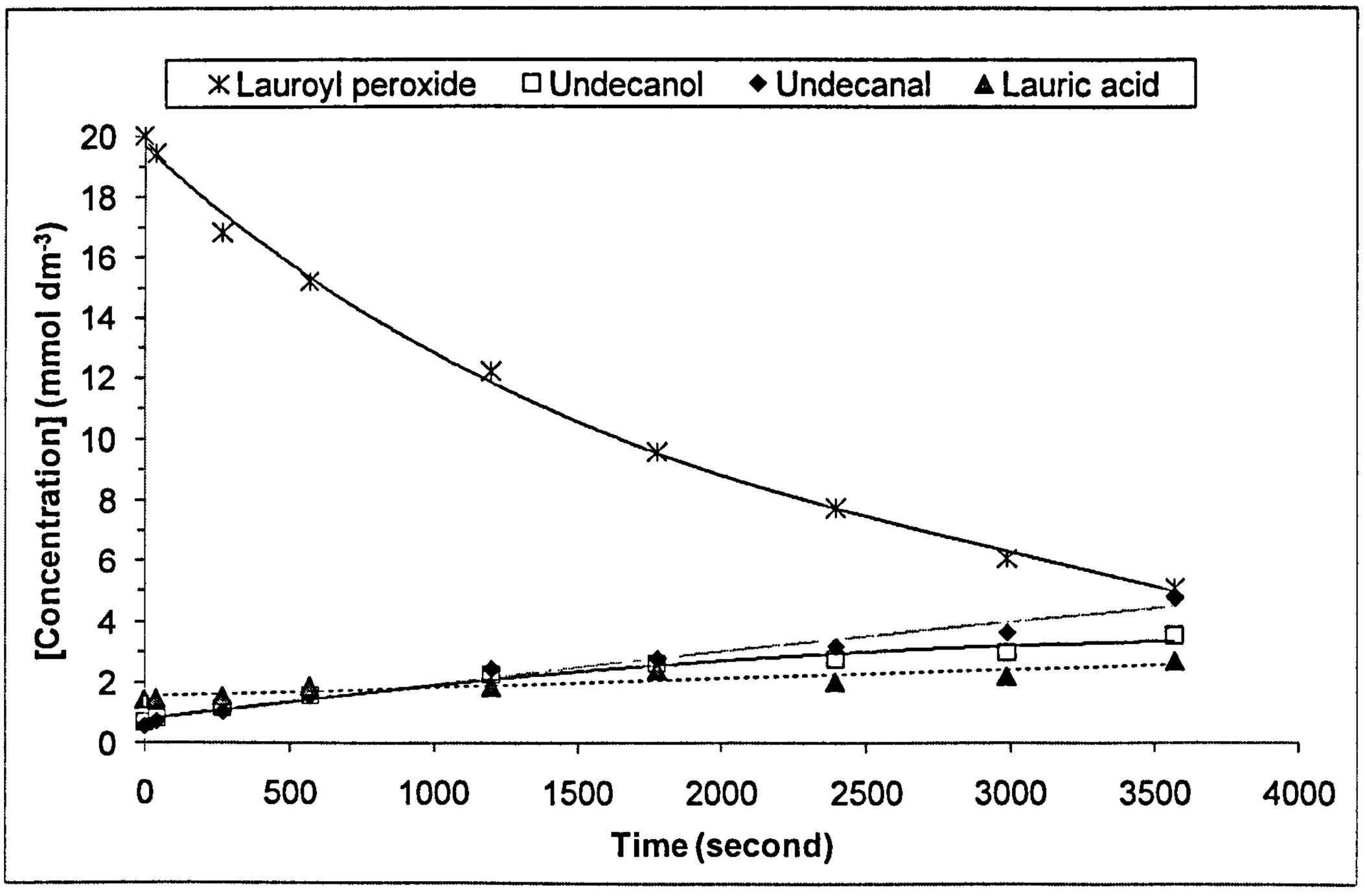

Figure 5.7: Oxidation products (by GC) of lauroyl peroxide in the oxidation of 20.0 mmol dm^{-3} lauroyl peroxide (by FTIR) plus 10.0 mmol dm^{-3} AN2 in hexadecane at 90 °C in flow intermediate reactor

Figure 5.8 and Figure 5.9 show the amount of antioxidant reacted against the amount of lauroyl peroxide reacted. By multiplying the gradient in Figure 5.9 by two (to account for radicals from peroxide), one can obtain the stoichiometry coefficient of the antioxidant. The trendlines in Figure 5.9 are forced through zero.

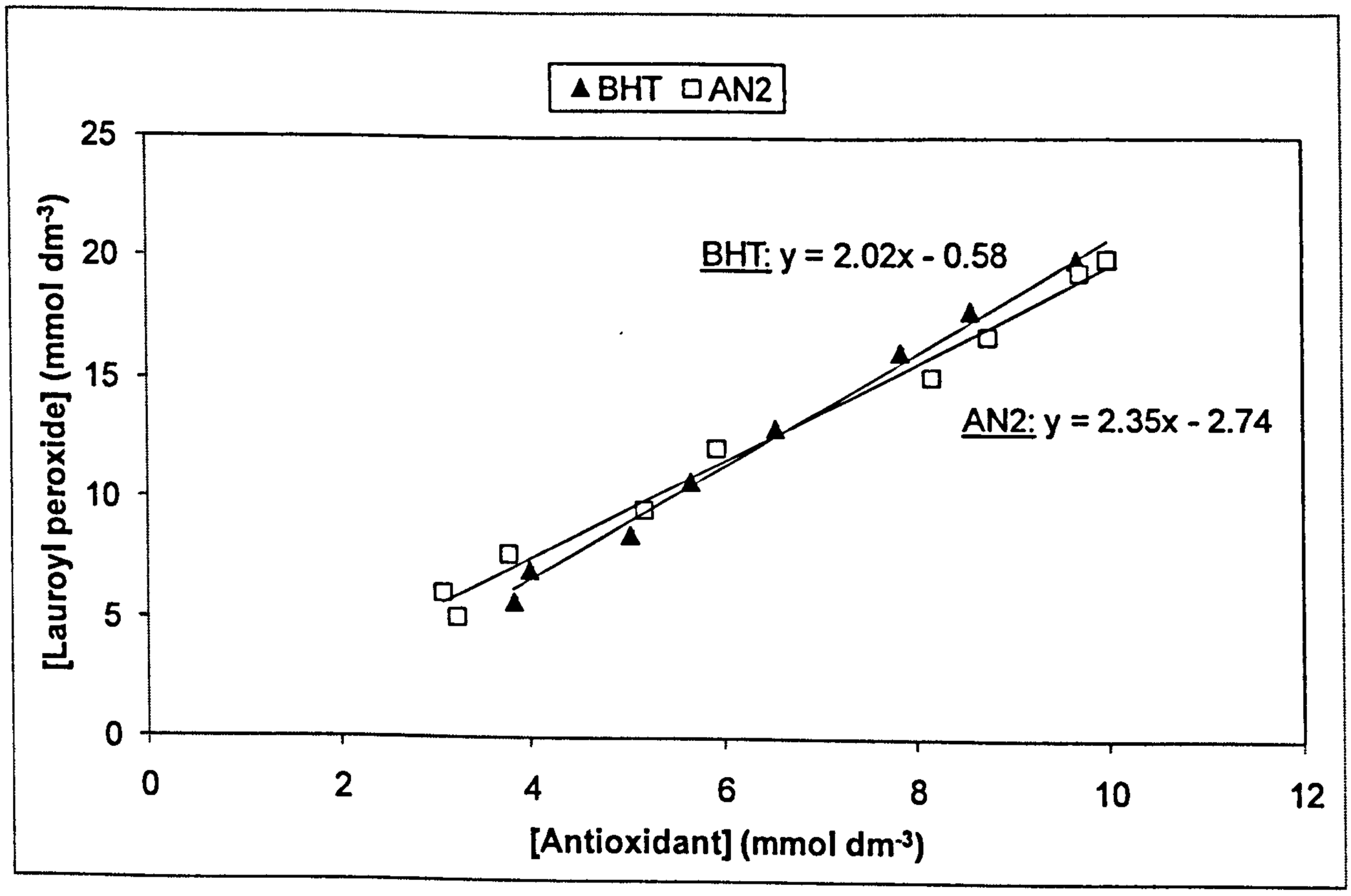

Figure 5.8: Decomposition of lauroyl peroxide (by FTIR) versus the decay of BHT (by GC) or AN2 (by GC) in the oxidation of 20.0 mmol dm^{-3} lauroyl peroxide plus 10.0 mmol dm^{-3} BHT or AN2 in hexadecane at 90 °C in flow intermediate reactor

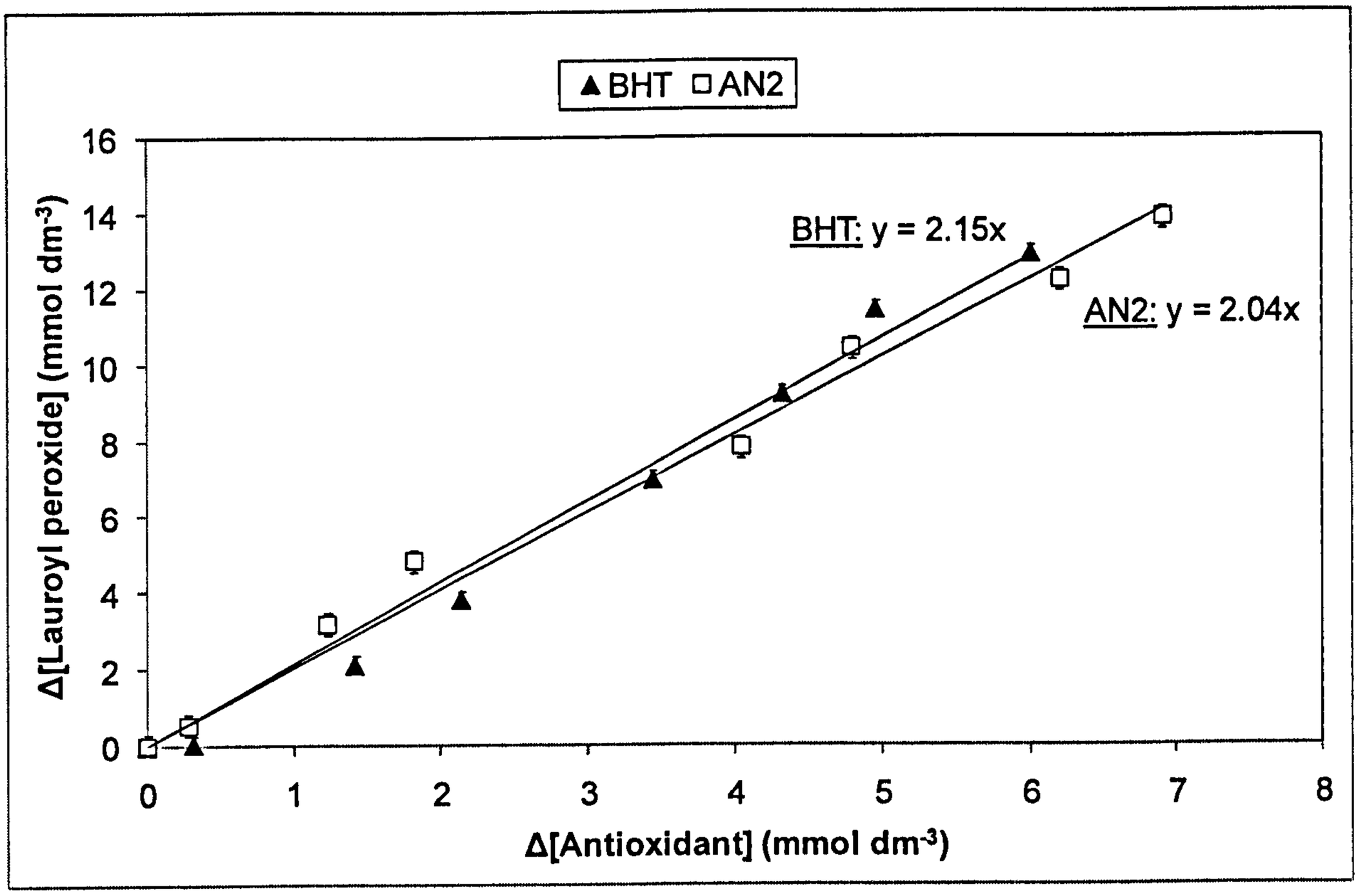

Figure 5.9: Decomposition of lauroyl peroxide (by FTIR) versus the decay of BHT (by GC) or AN2 (by GC) in the oxidation of 20.0 mmol dm^{-3} lauroyl peroxide plus 10.0 mmol dm^{-3} BHT or AN2 in hexadecane at 90 °C in flow intermediate reactor - error bars represent standard error

5.3. DISCUSSION

5.3.1. Critical antioxidant concentration and critical temperature

Critical antioxidant concentration of AN2

The definition of the critical antioxidant concentration is demonstrated in Figure 5.10. It has been argued (Gugumus, 1998b) that the observed critical antioxidant concentration does not arise from a chemical process but rather a mathematical distortion due to the usage of logarithms. This can be demonstrated to not be the case in this study as can be seen in Figure 5.11, where no logarithm of the reaction time was used but the phenomenon was still observable.

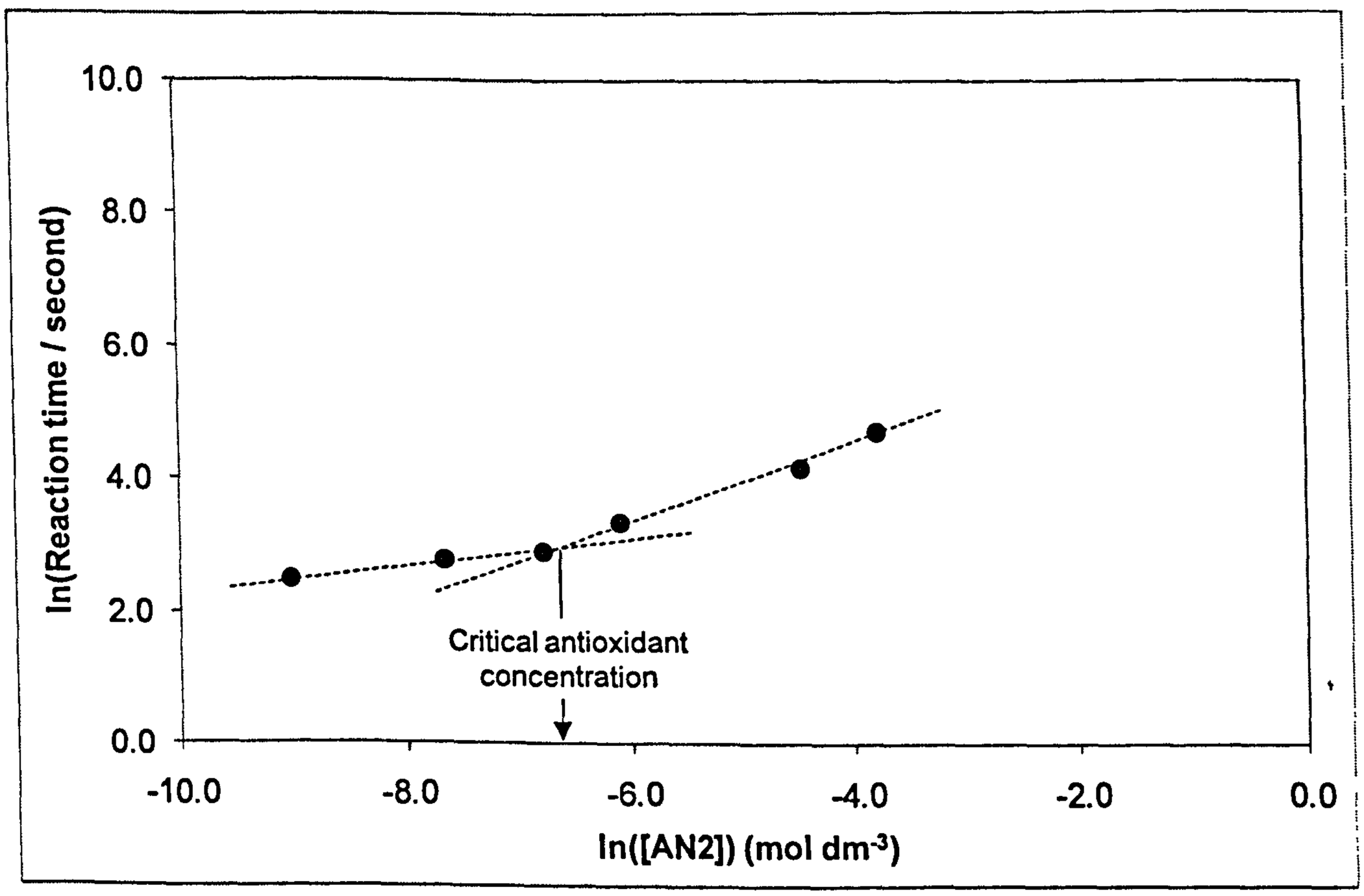

Figure 5.10: Plot of reaction time versus antioxidant concentration showing the critical antioxidant concentration of AN2 in XHVI 8.2 at 250 °C in static micro reactor – natural logarithm plot

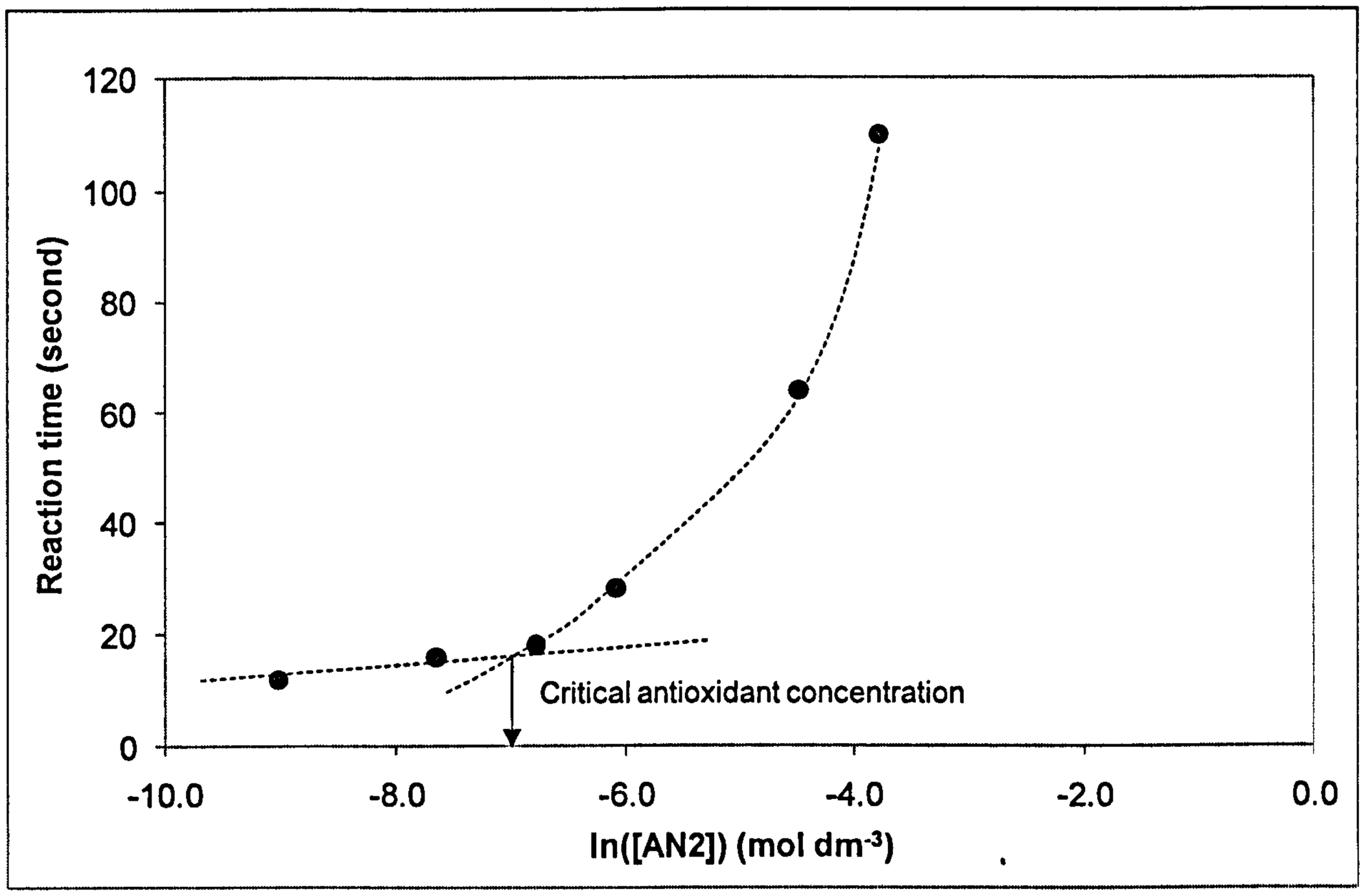

Figure 5.11: Plot of reaction time versus antioxidant concentration showing the critical antioxidant concentration of AN2 in XHVI 8.2 at 250 °C in static micro reactor

The critical antioxidant concentration can be envisaged as the competition between the base fluid (RH) and the antioxidant (InH) to react with peroxyl (ROO•) radicals (other radicals are ignored for simplicity):

$ROO\bullet + RH \rightarrow ROOH + R\bullet \ (k_1)$

$ROO\bullet + InH \rightarrow ROOH + In\bullet \ (k_2)$

$\Delta[\cancel{ROO\bullet}] / \Delta(Time) = k_1[\cancel{ROO\bullet}][RH] + k_2[\cancel{ROO\bullet}][InH]$

$k_1[RH] = k_2[InH]$, which can be rearranged to give: $[InH]_{Critical} = k_1[RH] / k_2$

The number of peroxyl radicals trapped by the antioxidant is represented by its stoichiometry coefficient (n). Incorporating the stoichiometry coefficient of the antioxidant with the above equation gives:

$[InH]_{Critical} = k_1[RH] / (k_2 \times n)$

Where, $k = A \times \exp(-E / RT)\ M^{-1}\ s^{-1}$; A: Pre-exponential factor; E: Activation energy in kJ mol^{-1}; R: Universal molar gas constant; and T: Absolute temperature.

The dependence of the critical antioxidant concentration (of AN2) on temperature (Figure 5.13) can be obtained from the point inflection in Figure 5.12.

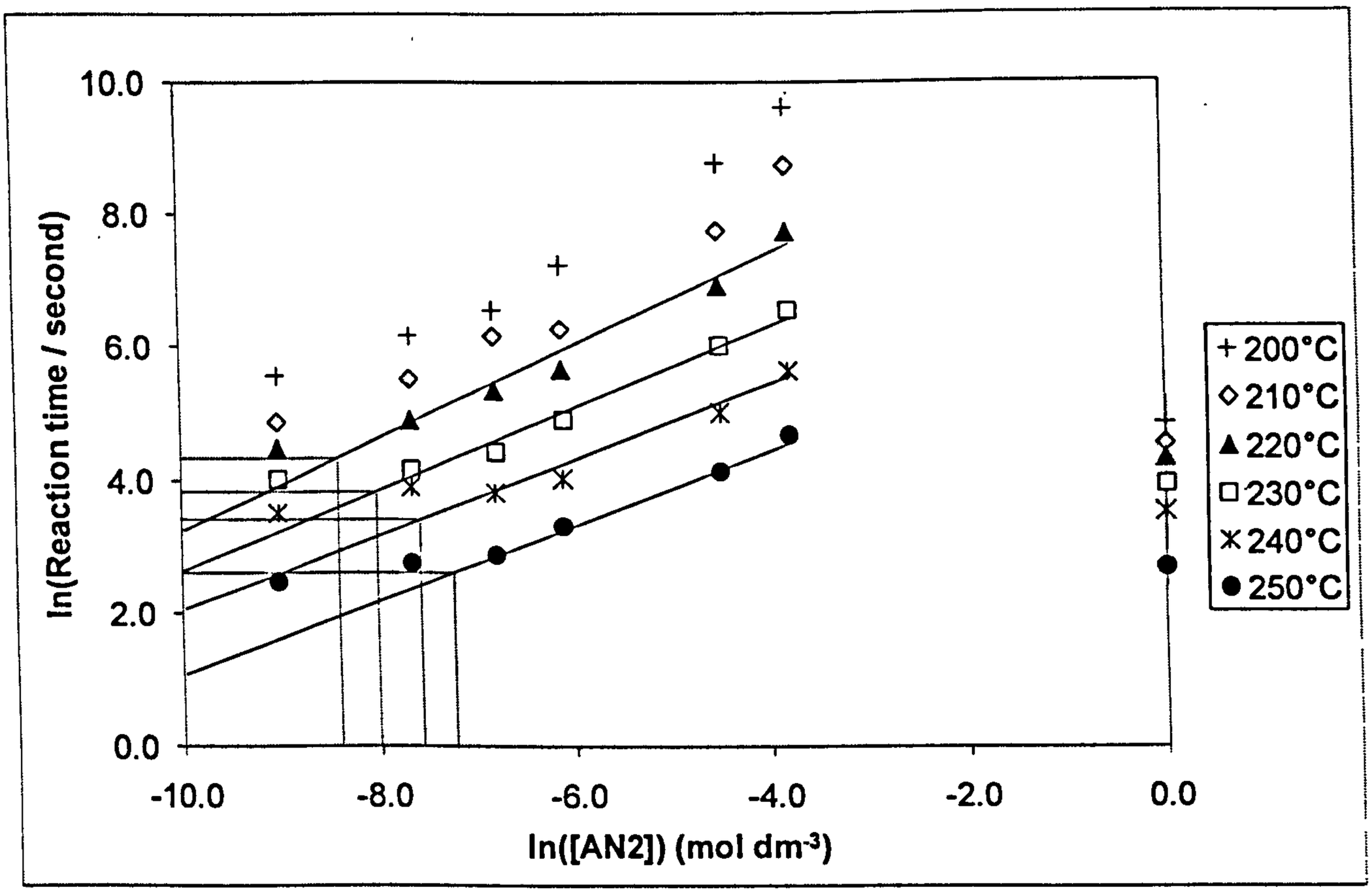

Figure 5.12: Dependence of critical antioxidant concentration of AN2 on temperature in XHVI 8.2 at 200 to 250 °C in static micro reactor (from Figure 5.1)

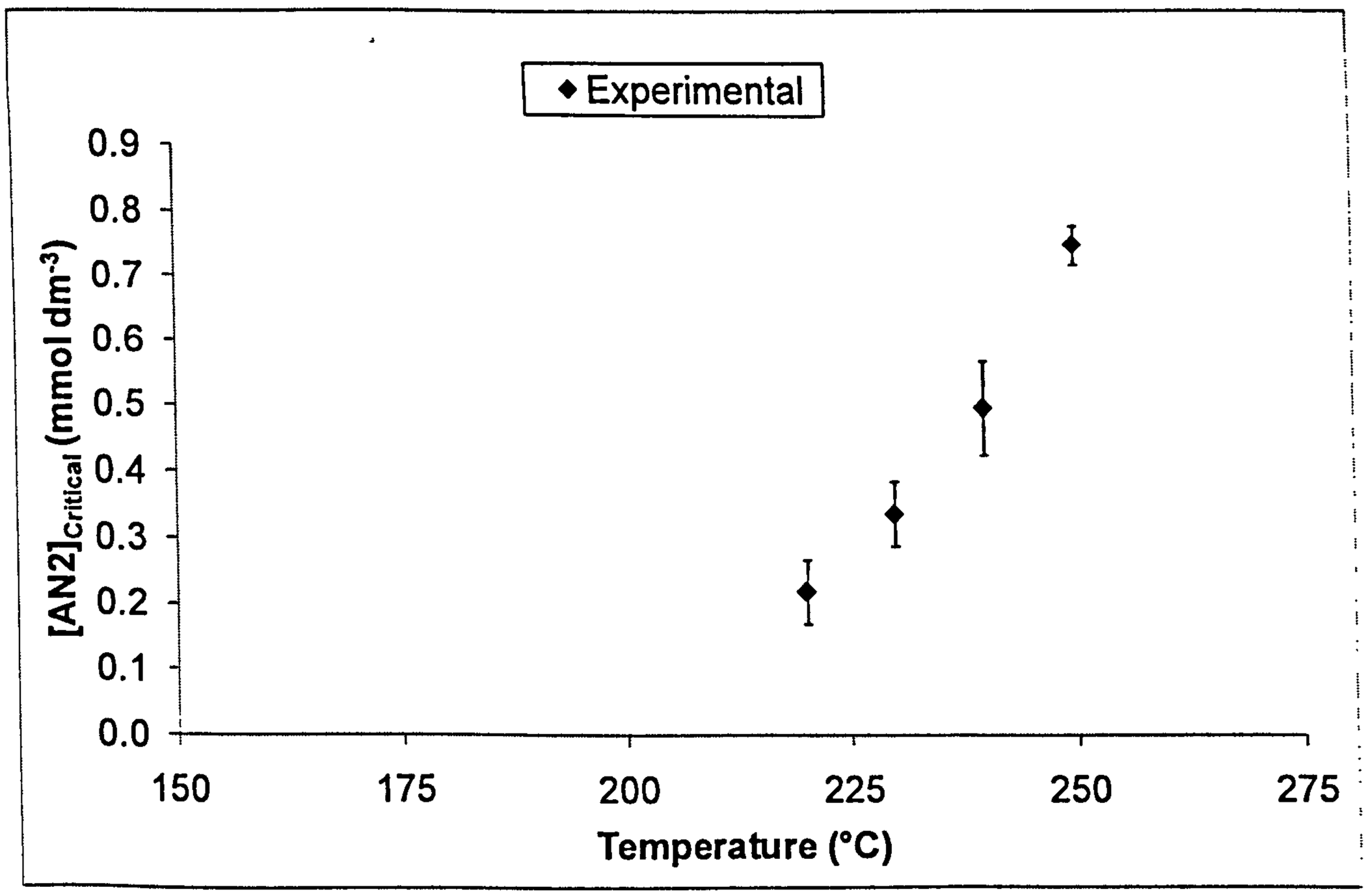

Figure 5.13: Dependence of critical antioxidant concentration of AN2 on temperature (from Figure 5.12)

The $[InH]_{Critical}$ equation can be used to see how the theory compares with the observed experimental results (Figure 5.13).

The base fluid was Shell XHVI 8.2 which has an average of 5.5 tertiary hydrogen atoms that make up 7.1 % of the total hydrogen atoms. Due to the weaker bond dissociation energy of tertiary hydrogen atoms (than secondary and primary hydrogen atoms) and simplicity, it is assumed that only the tertiary hydrogen atoms are abstracted by peroxyl radicals:

Moles of Shell XHVI 8.2	= 1.92 mol dm^{-3}
Number of tertiary hydrogen atoms	= 5.5 (average)
Percentage of tertiary hydrogen atoms	= 7.1 %
[RH] =(1.92 x 5.5) x (7.1 / 100)	= 0.75 mol dm^{-3}

Peroxyl radicals ($Me_3COO•$) abstract hydrogen atoms (from 3-methylpentane) at a pre-exponential factor of $3.2x10^9$ M^{-1} s^{-1} and an activation energy of 68.2 kJ mol^{-1} per hydrogen atom (Howard, 1997, p.291)

For AN2 antioxidant, there are no Arrhenius parameters for the reaction between peroxyl radicals and AN2 antioxidant. This necessitates the use of Arrhenius parameters of antioxidants that have similar structures to that of AN2. The pre-exponential factor of $7.9x10^7$ M^{-1} s^{-1} and the activation energy of 23.5 kJ mol^{-1} for the reaction between BHT and styrylperoxyl (Howard, 1972, p.131) will be used as the Arrhenius parameters for the reaction between peroxyl radicals and AN2 antioxidant.

For example, at 200 °C:

k_1	= $3.2x10^9$ x exp(-68200 / 8.3144x473)	= 94 M^{-1} s^{-1}
k_2	= $7.9x10^7$ x exp(-23500 / 8.3144x473)	= $2.0x10^5$ M^{-1} s^{-1}
[RH]	= 0.75 mol dm^{-3}	
n of AN2	= 4.0 (see Table 5.7)	
$[InH]_{Critical}$	= $k_1[RH] / (k_2 \times n)$	
$[InH]_{Critical}$	= $94x0.75 / (2x10^5 \times 4.0)$	
	= $8.8x10^{-5}$ mol dm^{-3} = 0.09 mmol dm^{-3}	

Figure 5.14 shows the experimental (Figure 5.13) and theoretical dependence of critical antioxidant concentration on temperature. There is a reasonable correlation between experimental and theoretical data at 220 °C; however, the correlation grows apart at temperatures over 220 °C. This can be explained by the supposition that at high temperatures, peroxyl radicals become less selective in the abstraction of hydrogen atoms from the base fluid and the antioxidant, which causes the stoichiometry coefficient of the antioxidant to decrease.

Adjusting[34] the stoichiometry coefficient of AN2 in a way that the theoretical line superimposes that of the experimental (Figure 5.15) suggests the stoichiometry coefficients in Table 5.4.

Table 5.4: Theoretical stoichiometry coefficients of AN2 at high temperatures

Temperature (°C)	150	160	170	180	190	200	210	220	230	240	250	260
n coefficient	4.0	4.0	3.8	3.5	3.2	2.9	2.6	2.3	2.0	1.7	1.4	1.1

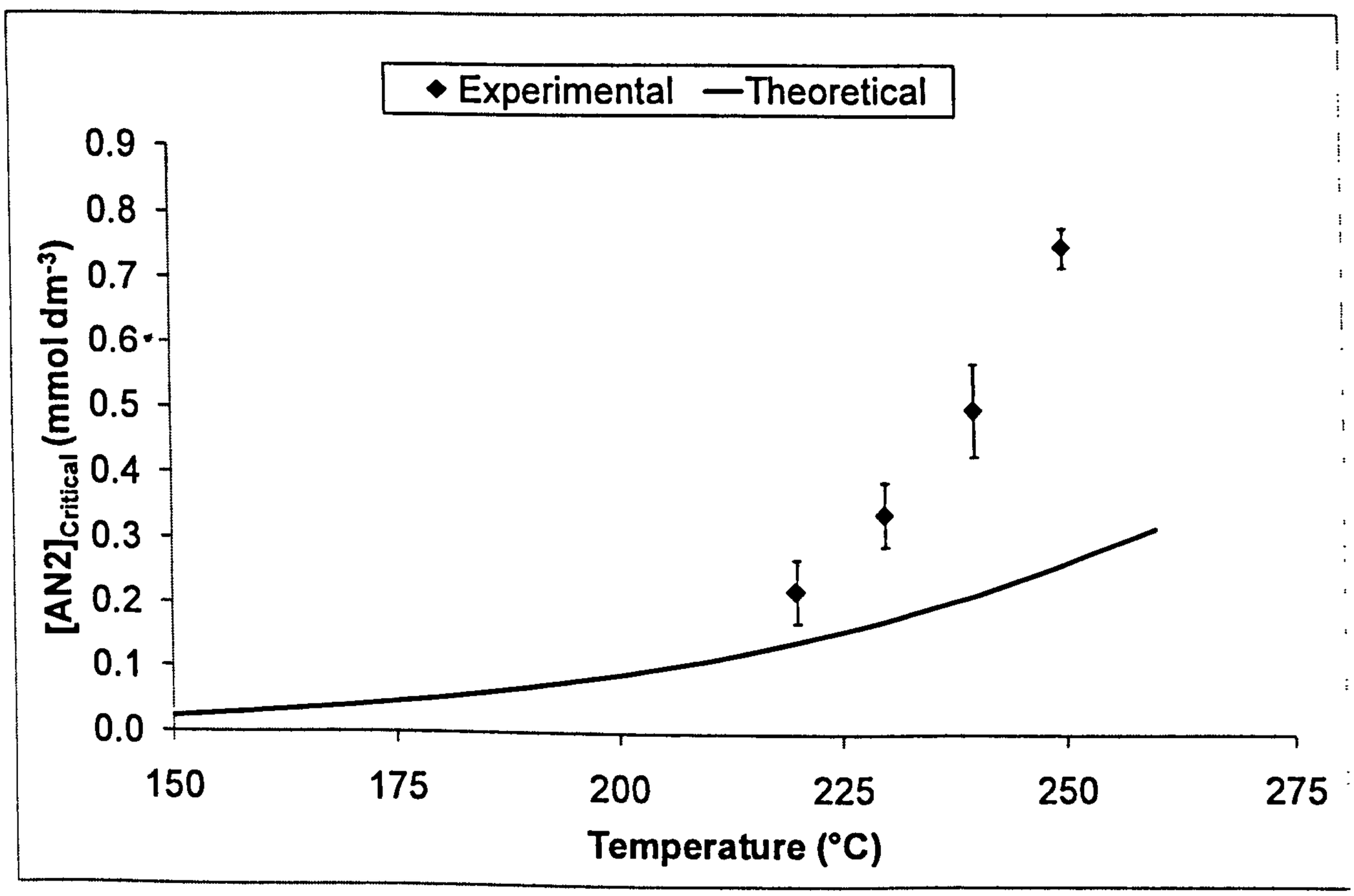

Figure 5.14: Comparison between experimental and theoretical dependence of critical antioxidant concentration of AN2 on temperature

[34] By manipulating the value of "n" in $[InH]_{Critical} = k1[RH] / (k_2 \times n)$.

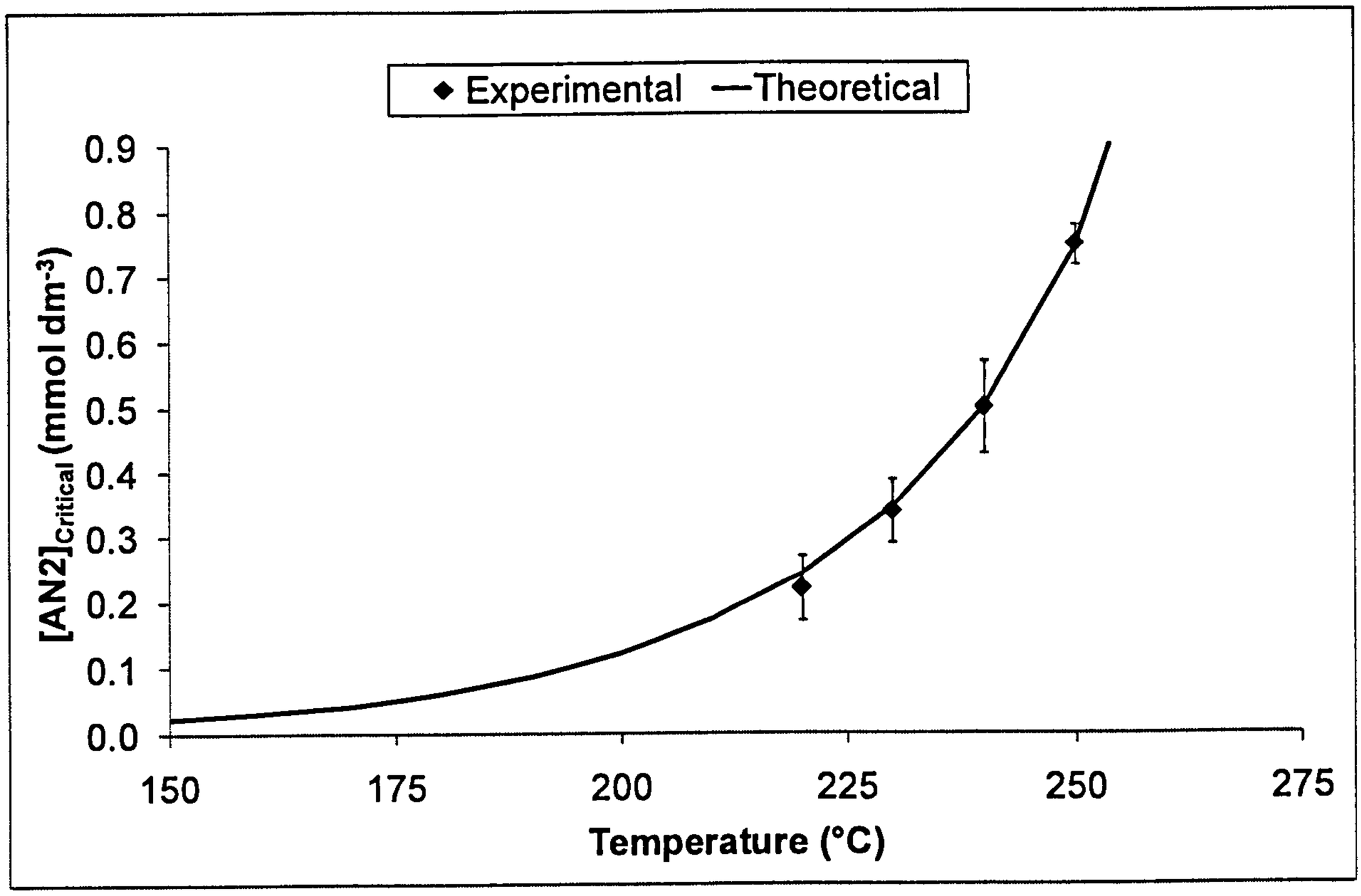

Figure 5.15: Adjusted stoichiometry coefficient of AN2 for the theoretical dependence of critical antioxidant concentration on temperature

The calculated decrease in the stoichiometry coefficient of AN2 as reaction temperature increases (Table 5.4) is expected to be due to the change in the reaction mechanism of AN2 as reaction temperature increases, where the phenoxyl radicals of AN2 disproportionate to give rise to galvinol and regenerate the AN2 molecule (Figure 5.16):

$$2 \times \text{AN2 phenoxyl} \rightarrow \text{Galvinol} + \text{AN2}$$

$$k = 2.7 \times 10^4\ M^{-1}\ s^{-1}\ (200\ °C)^{35}$$

ΔH = BDE(Ar_2C-H) – BDE(Ar_2O-H) in kJ mol^{-1}

= <<352[36] – 340.2[37] = exothermic [expected] (i.e. favourable)

[35] $k = 3.0 \times 10^6 \exp(-18.6\ kJ/mol\ /\ RT)\ M^{-1}\ s^{-1}$ in benzene (Roginskii, 1985).
[36] The BDE of the C-H bond of methylene bridge of AN2 is 352 ± 8 kJ mol^{-1} (McMillen and Golden, 1982) but the BDE of the C-H bond of the methylene bridge of the AN2 phenoxyl is expected to be much lower than 352 kJ mol^{-1} due to the destabilisation by the radical on the oxygen atom.
[37] Denisov and Denisova, 2000, p.89.

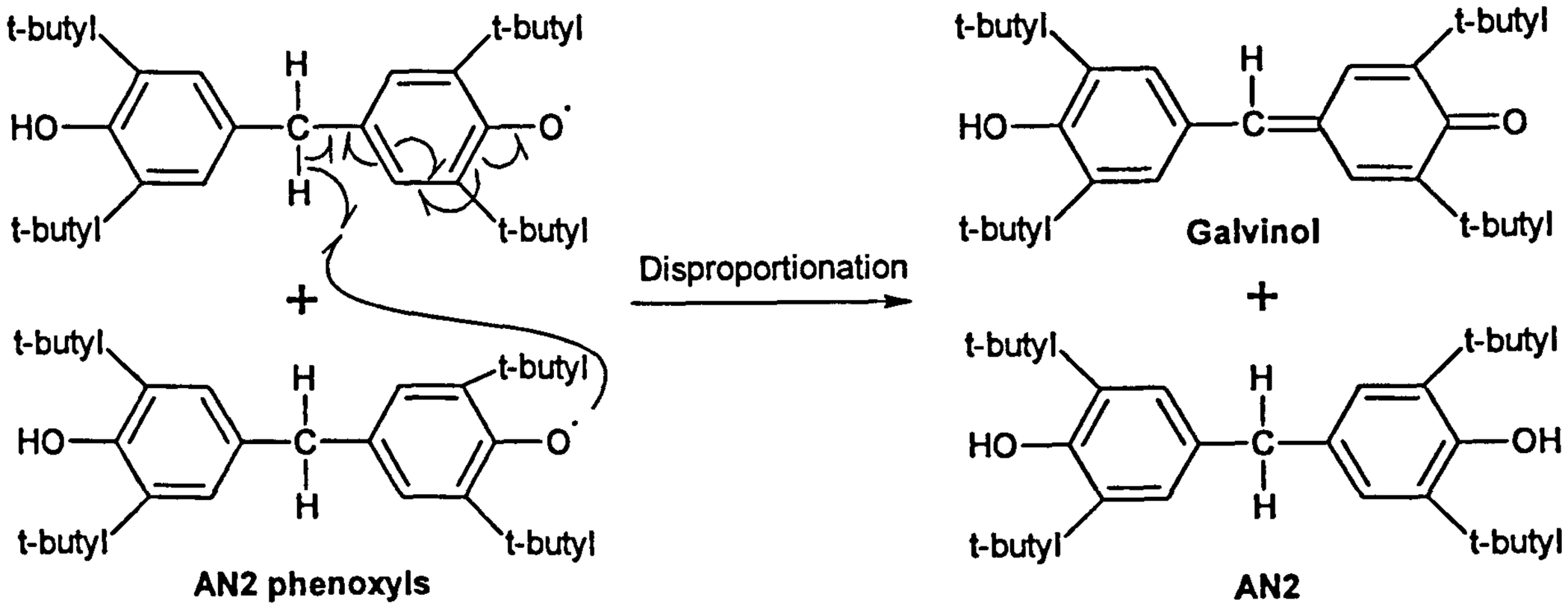

AN2 phenoxyls **AN2**

Figure 5.16: Proposed mechanism for the disproportionation of AN2 phenoxyl radicals (Roginskii, 1985)

Critical temperature of AN2

The definition of the critical antioxidant concentration is demonstrated in Figure 5.17, which shows that at 250 °C, the inhibited and the uninhibited base fluids have the same reaction time.

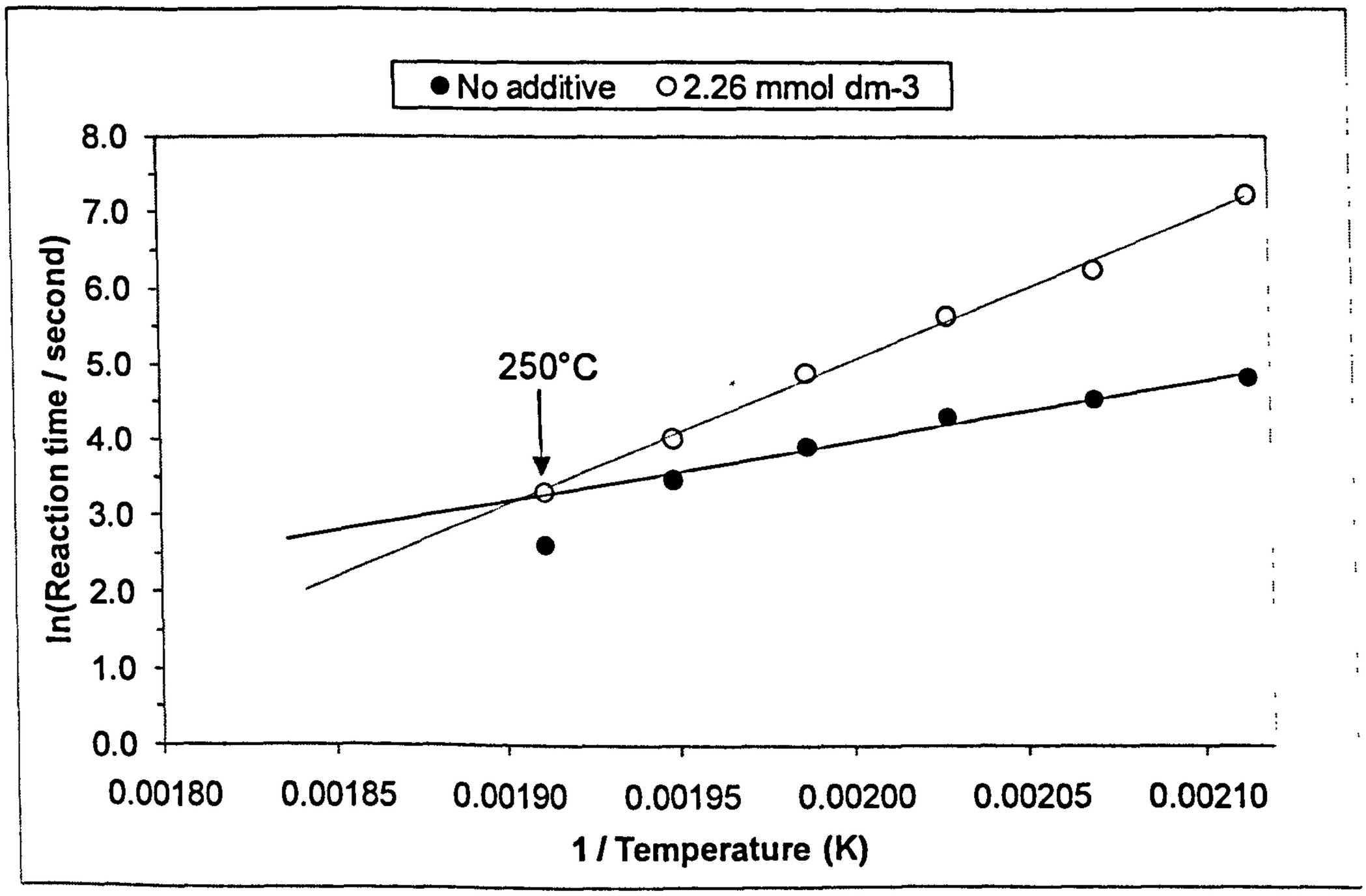

Figure 5.17: Critical temperature of 2.26 mmol dm^{-3} AN2 in XHVI 8.2 at 200 to 250 °C in static micro reactor

The critical temperature (of AN2) dependence on concentration (Figure 5.18) can be obtained from the projected lines in Figure 5.1.

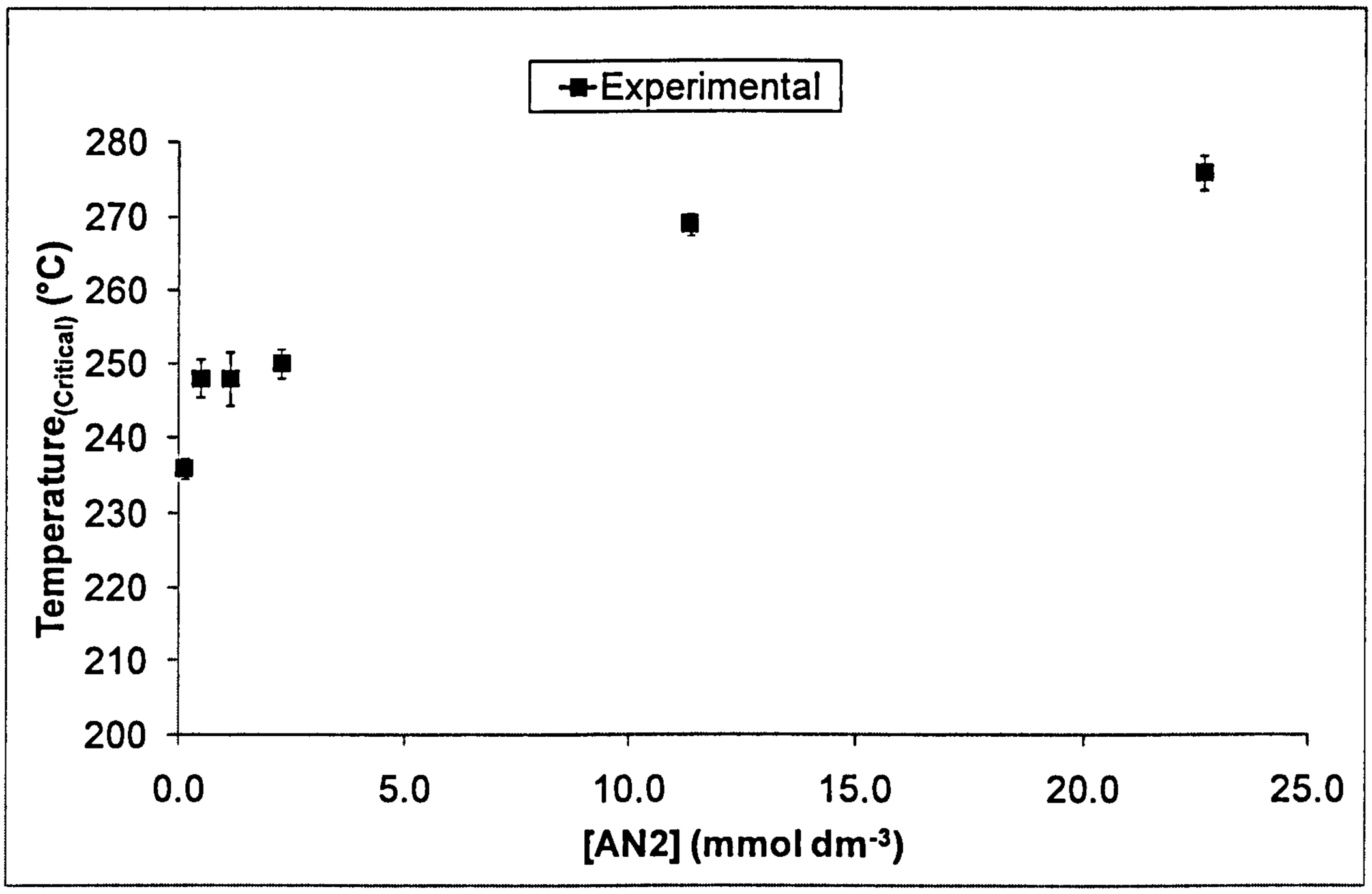

Figure 5.18: Dependence of the critical temperature on concentration (values obtained from the projected lines in Figure 5.1)

One of the ways to rationalise the critical temperature phenomenon is to contrast the temperature dependencies[38] of the reactions between peroxyl radicals with the base fluid and the antioxidant. It can be clearly seen in Table 5.5 that the temperature dependence of the reaction of peroxyl radicals with tertiary alkanes is approximately three times higher than that between peroxyl radicals with sterically-hindered phenols, which in turn means that as the temperature increases the difference between the rates of reaction between peroxyl radicals with the base fluid and the antioxidant shrinks.

Table 5.5: Activation energies of the reactions between peroxyl radicals (ROO•) with tertiary alkanes (tRH) and sterically-hindered phenols (Ar_2OH) (references within table)

Parameter	**tRH + ROO•**	**Ar_2OH + ROO•**
Activation energy (kJ mol^{-1})	68.2	23.5
Reference	Howard, 1997, p.291	Howard, 1972, p.131

[38] Temperature dependence = Activation energy / Universal molar gas constant.

Correlation between critical antioxidant concentration and critical temperature of AN2

Figure 5.19 shows the correlation between the dependence of the critical antioxidant concentration on temperature (Figure 5.13) and the dependence of the critical temperature on antioxidant concentration (Figure 5.18). There is a reasonable similarity between the two phenomena; in spite of the high uncertainty in determining the point inflections in Figure 5.12 and the intercept points from the projected lines in Figure 5.1.

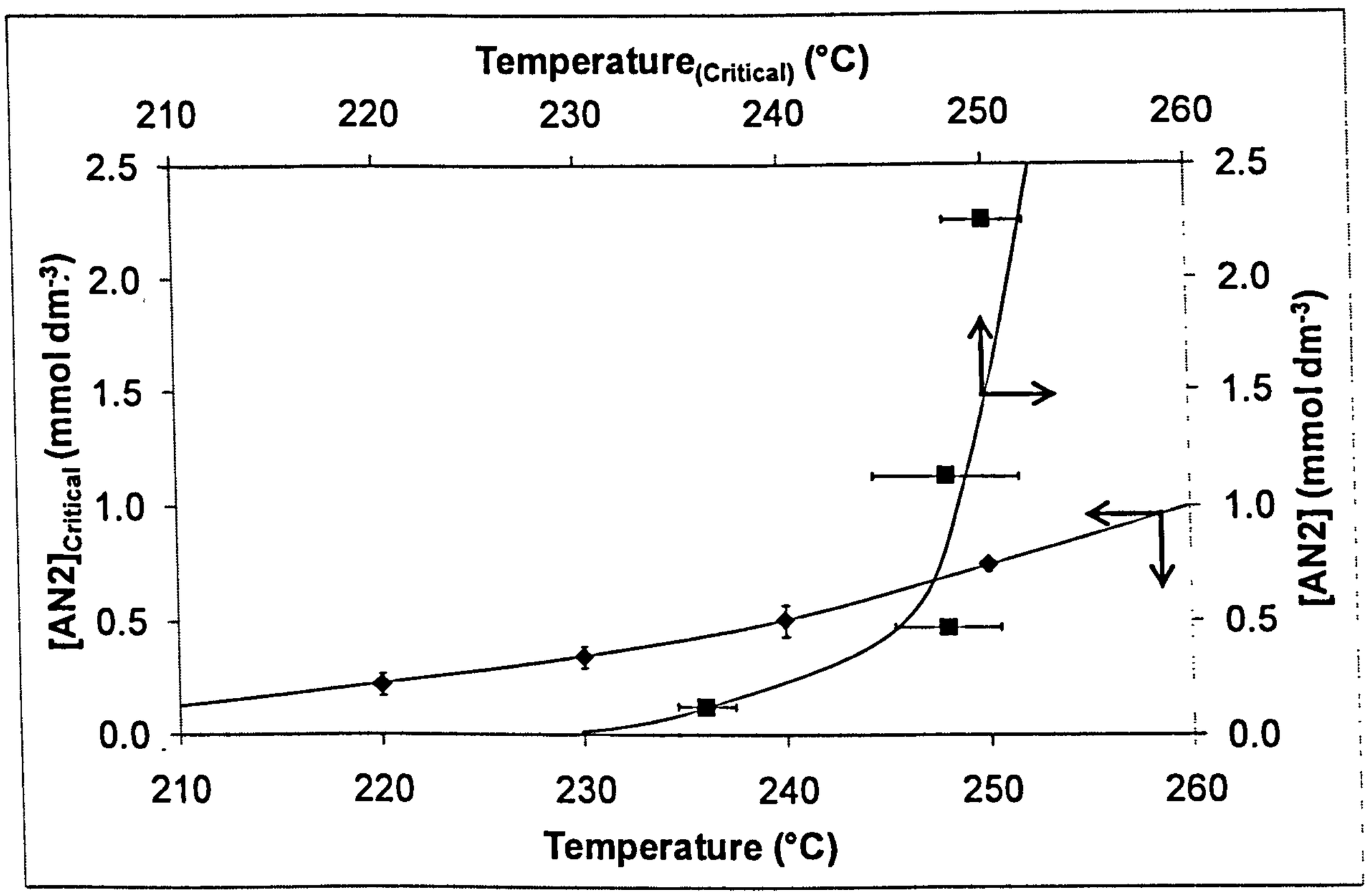

Figure 5.19: Correlation between the dependence of the critical antioxidant concentration on temperature (Figure 5.13) and the dependence of the critical temperature on antioxidant concentration (Figure 5.18)

Critical antioxidant concentration of Amine101

In the oxidations of Amine101 in squalane, at certain temperatures, and antioxidant concentrations, oxygen was prematurely consumed (due to the oxidation of squalane) even when substantial quantities of Amine101 were still present; and at 210 °C, oxygen was consumed without any restraint in the presence of 100 % (0.5 % w/w) of Amine101 (Figure 5.20). In contrast, in the oxidation of AN2, in Chapter 3, oxygen was only consumed when the antioxidant had run out.

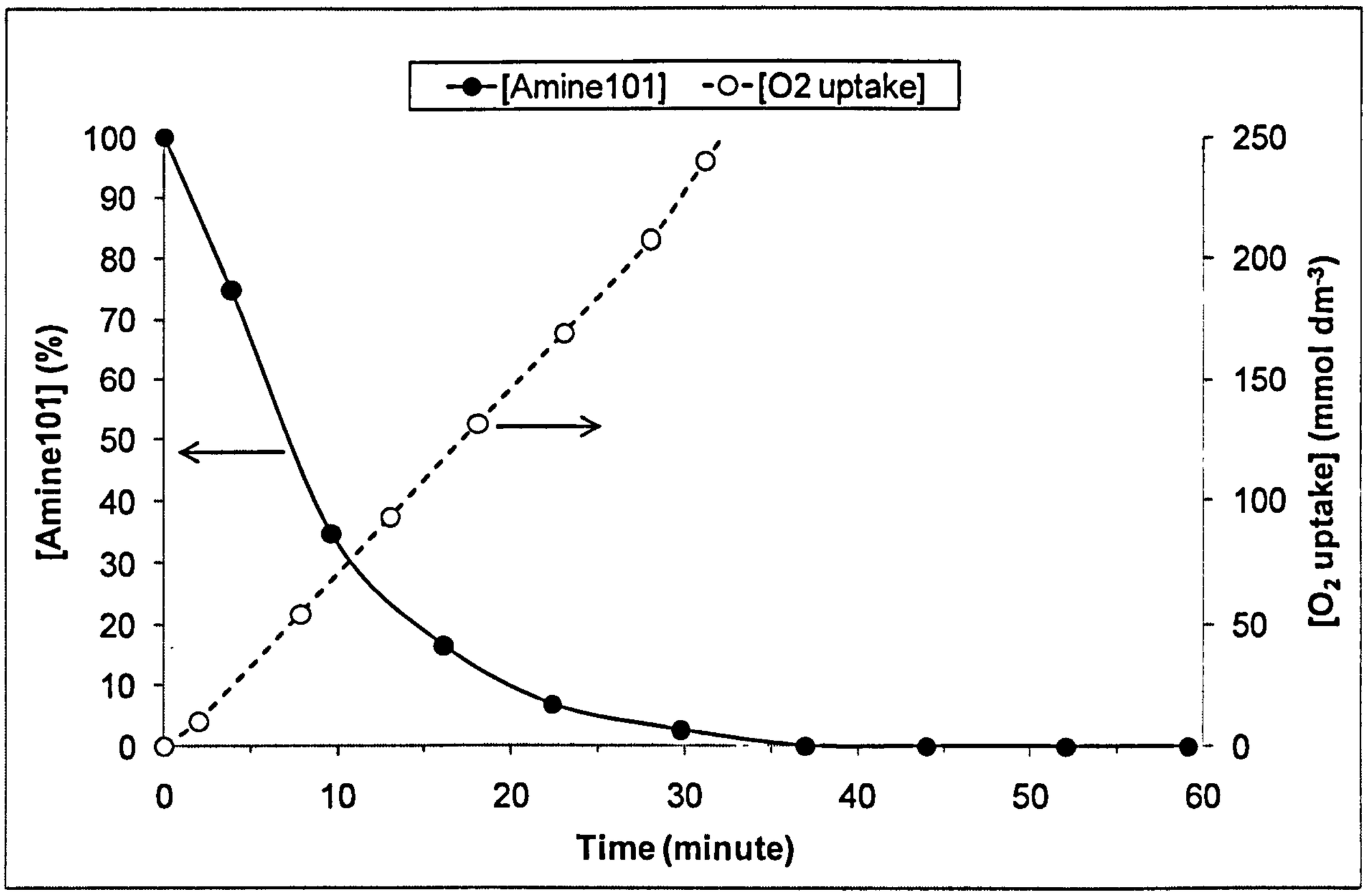

Figure 5.20: Oxidation of 0.5 % w/w (10.0 mmol dm^{-3}) Amine101 in 5.0 cm^3 squalane at 210 °C in flow intermediate reactor

This premature oxygen absorption in the oxidation of Amine101 makes the critical antioxidant concentration to be much higher (Figure 5.21) than that of AN2 (Figure 5.13).

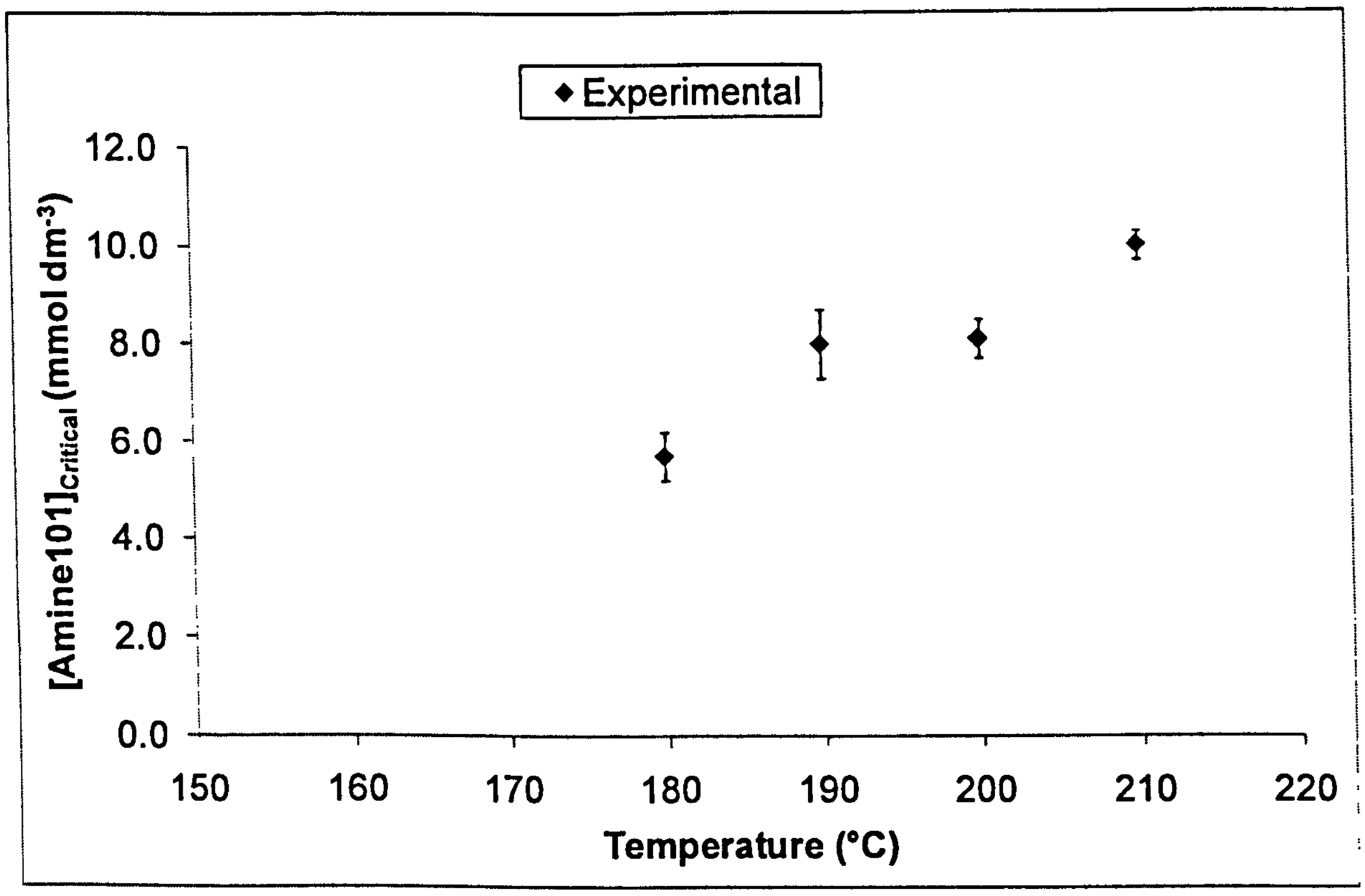

Figure 5.21: Dependence of critical antioxidant concentration of Amine101 on temperature in the oxidation of 0.5 % w/w (10.0 mmol dm^{-3}) Amine101 in 5.0 cm^3 squalane in flow intermediate reactor

The $[InH]_{Critical}$ equation can be used to see how the theory compares with the observed experimental results (Figure 5.21).

The base fluid was squalane which has six tertiary hydrogen atoms that make up 9.7 % of the total hydrogen atoms. Due to the weaker bond dissociation energy of tertiary hydrogen atoms (than secondary and primary hydrogen atoms) and simplicity, it is assumed that only the tertiary hydrogen atoms are abstracted by peroxyl radicals:

Moles of squalane	= 2.00 mol dm^{-3}
Number of tertiary hydrogen atoms	= 6
Percentage of tertiary hydrogen atoms	= 9.7 %
[RH] =(2.00 x 6) x (9.7 / 100)	= 1.16 mol dm^{-3}

Peroxyl radicals ($Me_3COO•$) abstract hydrogen atoms (from 3-methylpentane) at a pre-exponential factor of $3.2x10^9$ M^{-1} s^{-1} and an activation energy of 68.2 kJ mol^{-1} per hydrogen atom (Howard, 1997, p.291)

For Amine101 antioxidant, there are no Arrhenius parameters for the reaction between peroxyl radicals and Amine101 antioxidant or amines with similar structures to that of Amine101. This necessite the use of modelled Arrhenius parameters: 16.1 kJ mol^{-1} for the activation energy and $1.0x10^8$ M^{-1} s^{-1} for the pre-exponential factor for 4,4'-dimethyldiphenylamine (Denisov and Afanasev, 2005, p.507).

For example, at 200 °C:

k_1 = $3.2x10^9$ x exp(-68200 / 8.3144x473) = 94 M^{-1} s^{-1}

k_2 = $1.8x10^8$ x exp(-16100 / 8.3144x473) = $1.7x10^6$ M^{-1} s^{-1}

[RH] = 1.16 mol dm^{-3}

n of Am101 = 3.0 (see Chapter 4)

$[InH]_{Critical}$ = $k_1[RH] / (k_2 \times n)$

$[InH]_{Critical}$ = $94x1.16 / (1.7x10^6 \times 3.0)$

= $2.2x10^{-5}$ mol dm^{-3} = 0.02 mmol dm^{-3}

Figure 5.22 shows the experimental (Figure 5.21) and theoretical dependence of critical antioxidant concentration on temperature. There is no correlation between experimental and theoretical data. However, one can works backward and adjust the Arrhenius parameters in a way that the theoretical line superimposes that of the experimental (Figure 5.21). The theoretical line in Figure 5.23 is based on adjusted activation energy of 39.5 kJ mol^{-1}. This activation energy is based on the assumption that the pre-exponential factor is $1.0x10^8$ M^{-1} s^{-1} and a stoichiometry coefficient of 3.0, and so the activation energy should be decreased if the pre-exponential factor is higher than $1.0x10^8$ M^{-1} s^{-1} and visa versa.

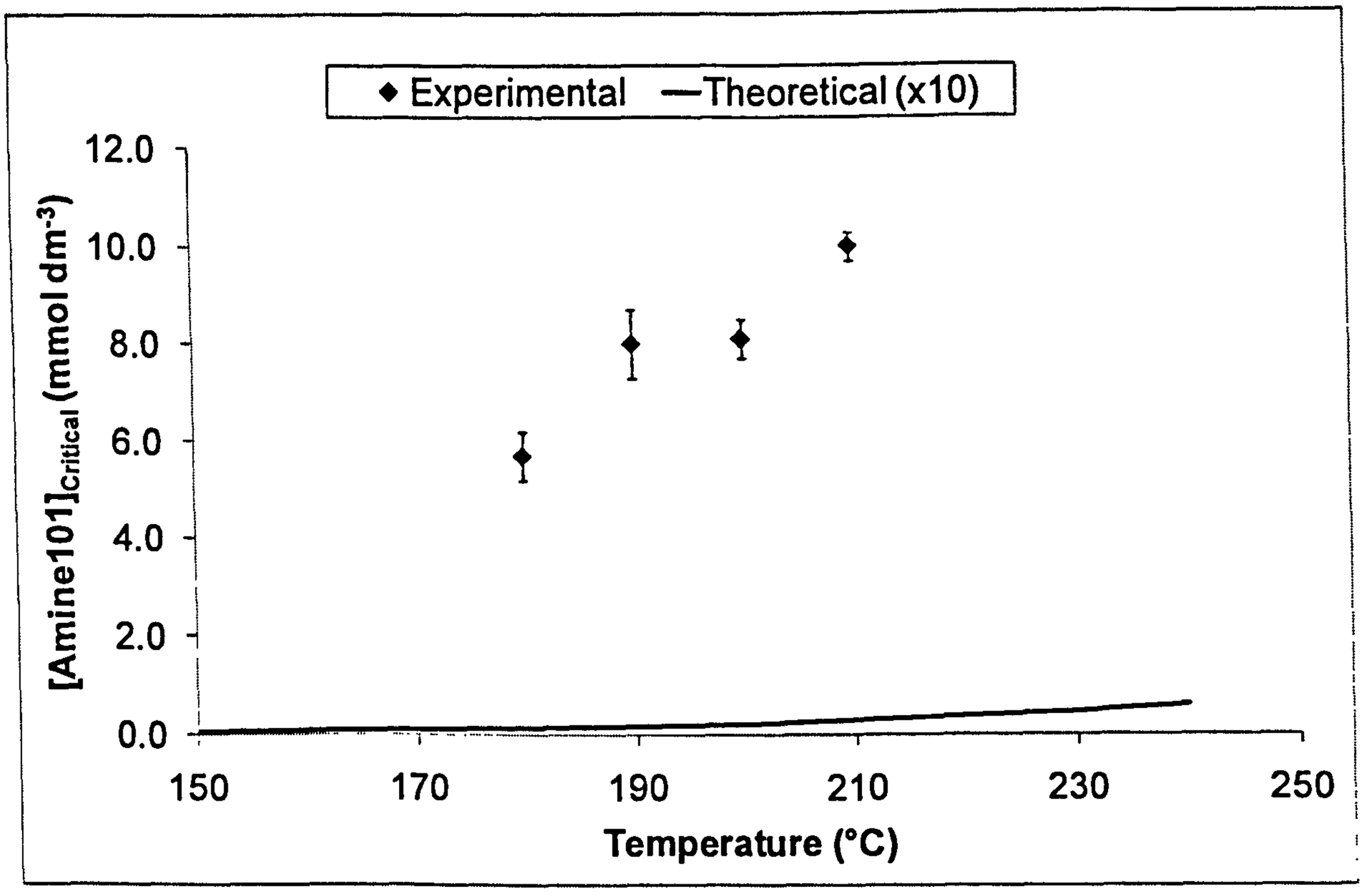

Figure 5.22: Comparison between experimental (Figure 5.21) and theoretical dependence of critical antioxidant concentration of Amine101 on temperature

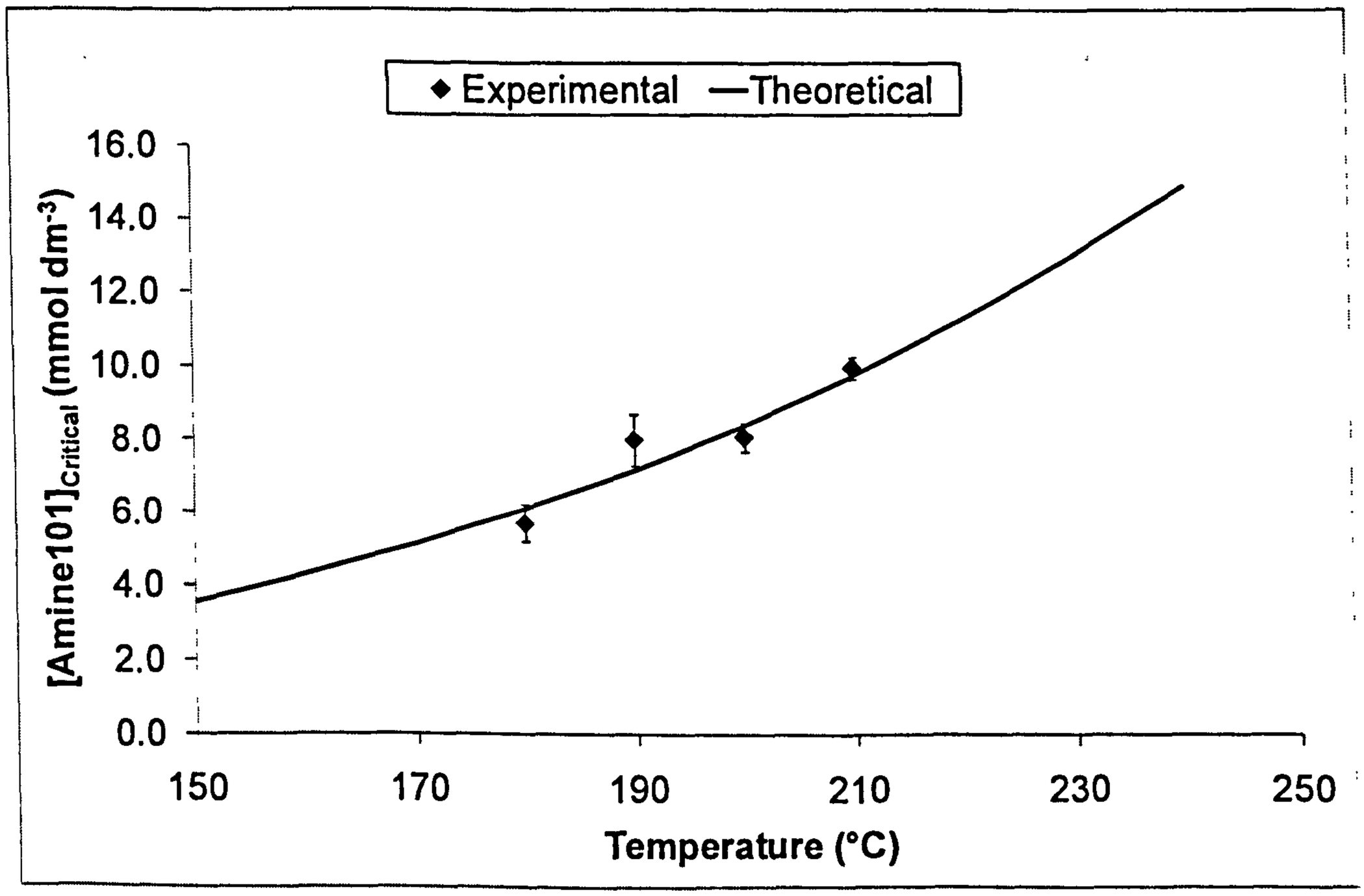

Figure 5.23: Adjusted Arrhenius parameters for the theoretical dependence of critical antioxidant concentration of Amine101 on temperature

5.3.2. Stoichiometry coefficients of antioxidants

Lauroyl peroxide was chosen as a source of radicals to study the stoichiometry coefficients of antioxidants because it has a low volatility at high temperatures, is commercially available, its decomposition mechanism is relatively simple (Figure 5.25), it can be quantified by infrared without ambiguity, and its decomposition products can be quantified by gas chromatography.

The decomposition of lauroyl peroxide has been studied in the past (Guillet and Gilmer, 1969) at temperatures up to 250 °C. However, the highest temperature lauroyl peroxide plus antioxidants was used in the intermediate reactor in this work was 120 °C; above this temperature the reaction becomes much faster than the manual sampling rate.

Reaction of lauroyl peroxide with sterically-hindered phenols

The natural logarithms of the decomposition rates of lauroyl peroxide were plotted against 1 / temperature (Figure 5.24) to obtain the temperature dependence from the gradient. The temperature dependence is related to the activation energy. By multiplying the temperature dependence by the universal molar gas constant, one can obtain the activation energy. Also, by dividing the intercept by 2.303, one can obtain the pre-exponential factor.

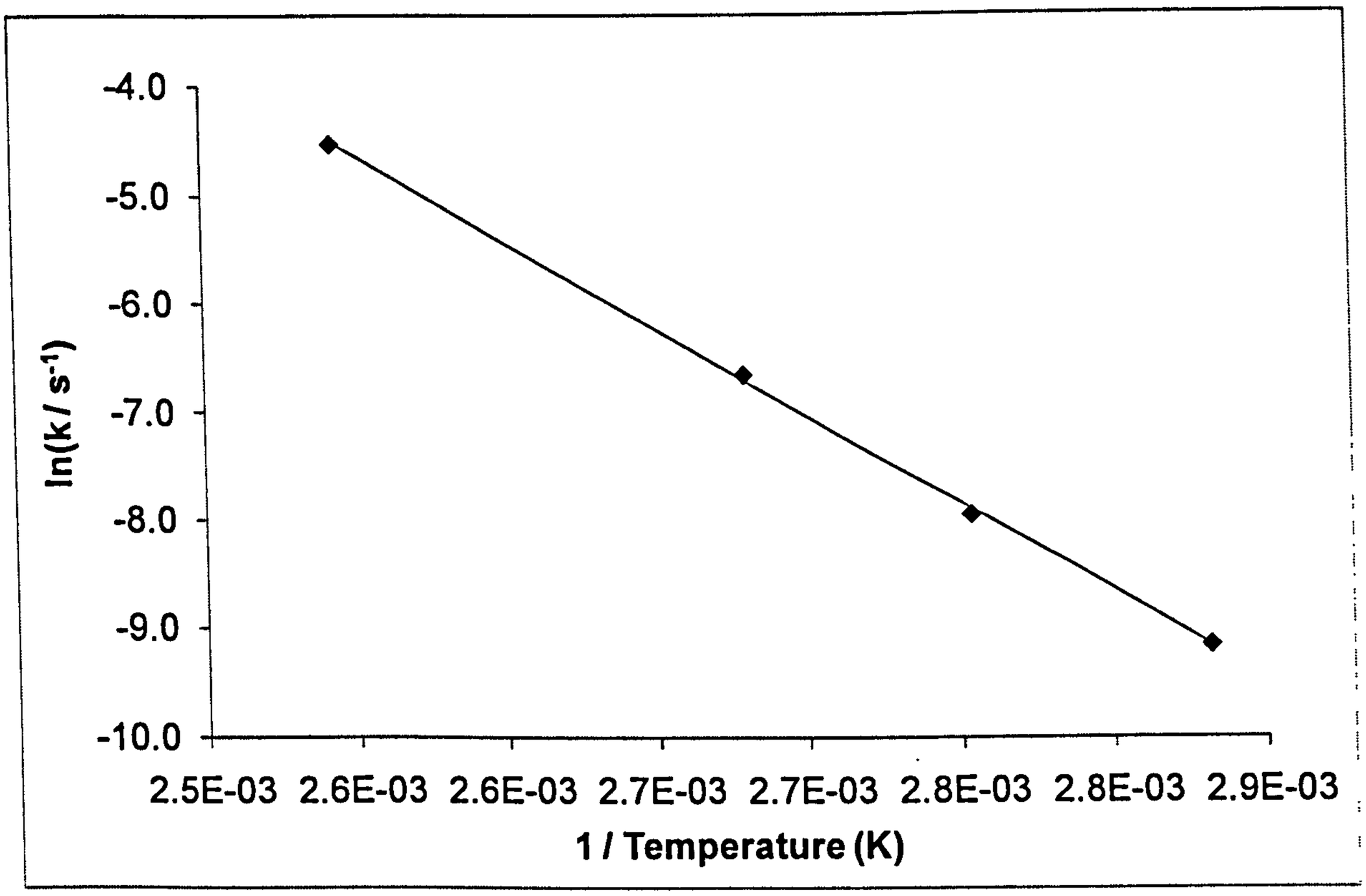

Figure 5.24: Arrhenius plot (natural logarithm) for the decomposition of lauroyl peroxide (by FTIR) in the oxidation of 20.0 mmol dm^{-3} lauroyl peroxide plus 10.0 mmol dm^{-3} BHT in hexadecane at 80 °C to 120 °C in flow intermediate reactor

The decomposition of lauroyl peroxide was initially studied in the absence of antioxidants to enable comparison with literature values (Table 5.6). The pre-exponential factor and activation energy for the decomposition of lauroyl peroxide were measured over a temperature range between 80 °C to 120 °C and are largely with the scope of the previous measurements (Table 5.6), but the measurements in this work are more precise.

Table 5.6: Arrhenius values for the autoxidation of diacyl peroxides (a: This work; b: Guillet and Gilmer, 1969; c: Ryzhkov, 1996; d: Antonovskii and Bezborodova, 1968; e: Pryor and Smith, 1970)

Diacyl peroxide	Solvent	$K_{decomposition}$ (s^{-1})	T. (°C)	Log(A) (s^{-1})	E (kJ mol^{-1})	Ref.
Lauroyl peroxide	Hexadecane	$(3.10 \pm 0.05) \times 10^{-4}$	90	15.9 ± 0.2	134.5 ± 2.2	a
Lauroyl peroxide	Mineral oil	3.21×10^{-4}	90	16.3 ± 2.5	137.8 ± 5.9	b
Lauroyl peroxide	Toluene-d_8	3.10×10^{-4}	89			c
Lauroyl peroxide	Hexadecane	9.97×10^{-5}	80	15.9 ± 0.2	134.5 ± 2.2	a
Lauroyl peroxide	Nonane	1.01×10^{-4}	80		126.0	d
Lauroyl peroxide	Mineral oil	8.80×10^{-5}	80	16.3 ± 2.5	137.8 ± 5.9	b
Octanoyl peroxide	Mineral oil	7.25×10^{-5}	80	16.0 ± 1.8	136.1 ± 5.0	b
Diacetyl peroxide	Octane	7.34×10^{-5}	80			e
Diacetyl peroxide	Hexadecane	5.39×10^{-5}	80			e

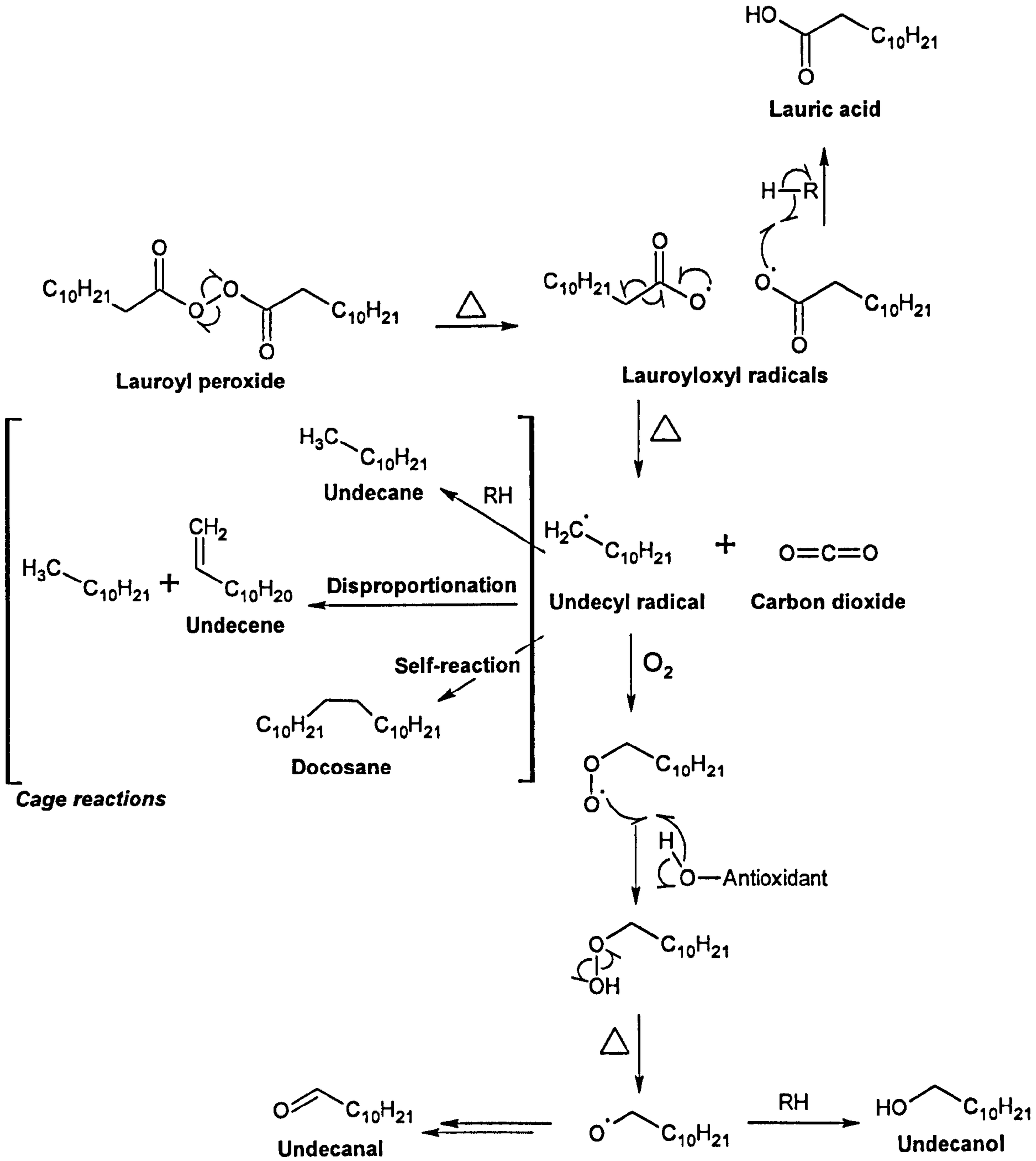

Figure 5.25: Provisional mechanism for homolysis of lauroyl peroxide proposed for this work

According to the mechanism in Figure 5.25, every molecule of lauroyl peroxide should give rise to two undecyl radicals. If these radicals escape the cage reactions, they will form two lauroyloxyl radicals. So, assuming a stoichiometry coefficient of two for BHT and four for AN2, every mole of lauroyl peroxide is expected to react with one mole of BHT or half a mole of AN2. The determined stoichiometry coefficients (n) for BHT and AN2 along with those from the literature are collected in Table 5.7. For this work, n = 2 x (Δ[peroxide] / Δ[antioxidant]); for all other works, n = rate of free radical formation ([antioxidant]$_0$ / reaction time).

Table 5.7: Stoichiometry coefficients of AN2 and BHT (references within table)

Antioxidant	Solvent	T. (°C)	Stoichiometry coefficient	Reference
AN2	Hexadecane	90	4.1 ± 0.2	This work
	Hexadecane	180	2.2	Jensen et al, 1990
	Lithium grease	115	10.0	Ischuk and Butovets, 1991
BHT	Hexadecane	90	4.3 ± 0.2	This work
	Styrene	50	1.7	Ohkatsu and Nishiyama, 2000
	Benzene	63	2.0	Boozer et al, 1955
	Lithium grease	115	2.2	Ischuk and Butovets, 1991
	Tetralin	60	2.7	Yamada et al, 1989

The stoichiometry coefficient of 4.1 ± 0.2 is comparable with the mechanisms discussed in Chapter 3. However, the stoichiometry coefficient of 4.3 ± 0.2 measured here for BHT was unexpected because it is generally thought that BHT traps two radicals (Table 5.7). It seems that the stoichiometry coefficient of BHT was underestimated in the past because the inhibitory effects of the oxidation products of BHT were not taken into account (Figure 5.26).

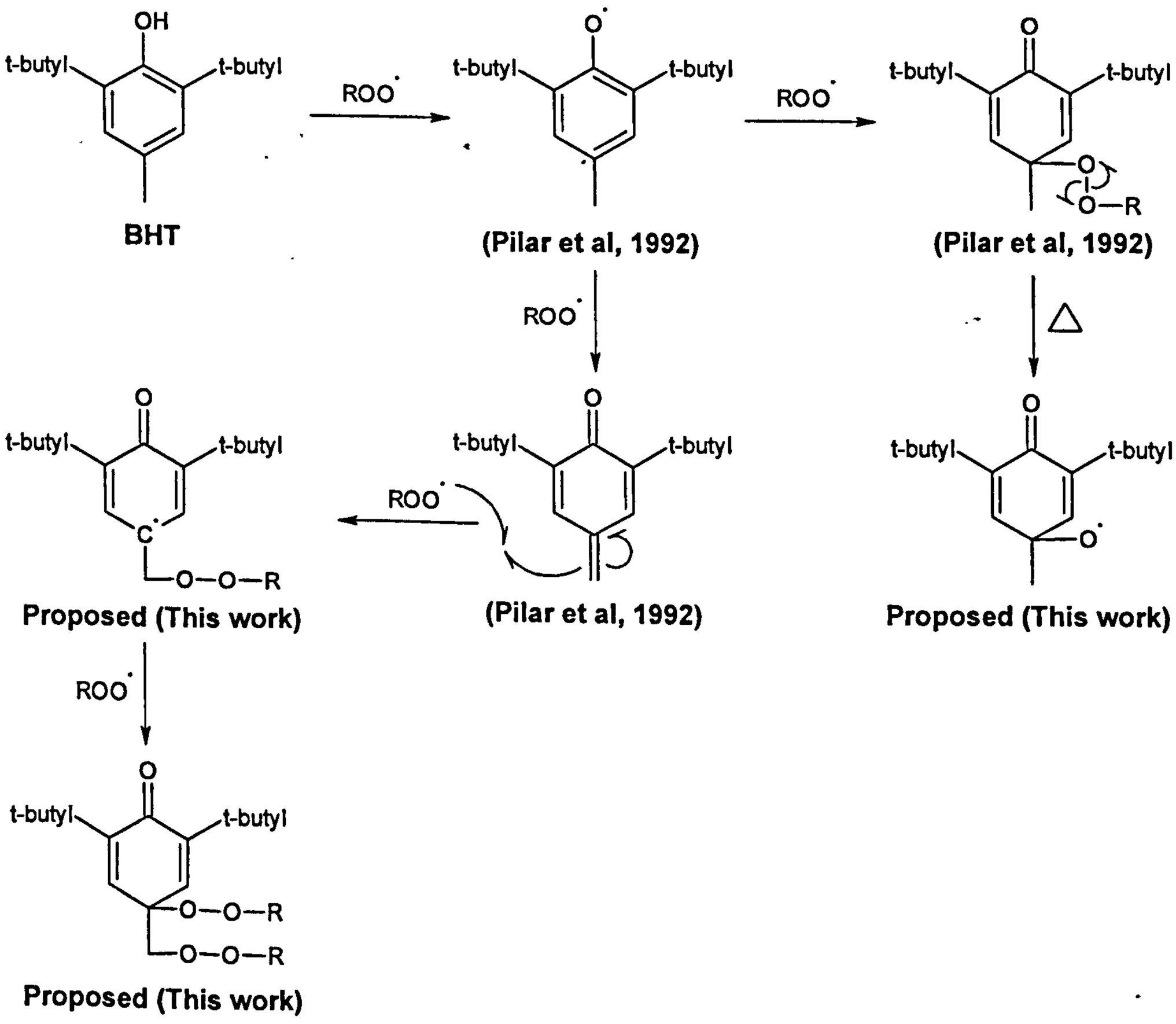

Figure 5.26: Provisional inhibition mechanism of BHT proposed for this work

Calculation of stoichiometry coefficient using rate of initiation

The rate of free radical formation or rate of initiation (R_i) has been used (Table 5.7) to calculate the stoichiometry coefficients ($n = R_i \times ([InH]_0 / IT)$)[39] of sterically-hindered phenols under steady-state conditions.

Free radicals are formed mainly through the decomposition of hydroperoxides (Jensen et al, 1990).[40] The alkoxyl and hydroxyl radicals formed from the decomposition of hydroperoxides, rapidly abstract hydrogen atoms from the solvent to give rise to alkyl radicals which also react rapidly with oxygen to give rise to peroxyl radicals. This suggests that the rate of peroxyl radical formation ($R_{ROO\bullet}$) is equal to the rate of free radical formation (Jensen et al, 1990):

$R_{ROO\bullet} = R_i = 2\ k[ROOH]$ (If oxygen pressure > 0.75 bar) (Jensen et al, 1990)

Evaluation of stoichiometry coefficient equations

The stoichiometry coefficients in Table 5.7 were obtained using two different equations. For this work, $n = 2 \times (\Delta[peroxide] / \Delta[antioxidant])$; for all other works, n = rate of free radical formation ($[antioxidant]_0$ / reaction time). The former equation is straightforward in a sense that it depends on the direct reaction between the antioxidant and the radicals from the decomposed peroxide; in contrast, the latter equation is exceedingly complex because it employs the rate of free radical formation parameter.

In order to measured the rate of free radical formation, one has to keep the concentration of hydroperoxides constant throughout the reaction because there is a direct relationship between the rate of hydroperoxide decomposition and the rate of free radical formation (Jensen et al, 1990).

Jensen et al (1990) assumed that in the oxidation of AN2, two molecules of hydroperoxides (through the abstraction of two hydroxyl hydrogen atoms) are formed per four peroxyl radicals trapped (two by hydrogen atom abstraction and two by addition to the para-positions) and four peroxyl radicals (originally from two

---

[39] IT is the reaction time and $[InH]_0$ is the starting concentration of the antioxidant.
[40] As soon as hydroperoxides are formed, the number of free radicals formed from the direct reaction of substrate with oxygen becomes insignificant (Jensen et al, 1990).

alkoxyl and two hydroxyl radicals) are formed from the decomposition of two hydroperoxide molecules, the overall outcome is unchanged in the hydroperoxide concentration during inhibition; thus, the rate of free radical formation should remain constant during inhibition. The argument by Jensen et al (1990) suggests that the equation only works with antioxidants that have stoichiometry coefficients of four.

The wide variations in the stoichiometry coefficients in Table 5.7 are likely to be caused by the differences in the physicochemical properties of the solvent and experimental conditions which are likely to alter the hydroperoxide concentration and consequently the stoichiometry coefficient of the antioxidant under investigation.

Reaction of lauroyl peroxide with Amine101

Attempts to determine the stoichiometry coefficients of diaromatic amines by reaction with lauroyl peroxide were unsuccessful because the reactants (i.e. lauroyl peroxide and Amine101) reacted at room temperature within minutes (91 % [18.2 mmol dm^{-3}] of peroxide and 78 % [7.8 mmol dm^{-3}] of Amine101) to give a dark orange solution. This phenomenon has been reported in the literature for the reaction between diphenylamine with benzoyl peroxide ($k = 1.8 \times 10^{-2}$ M^{-1} s^{-1} at 23 °C at $k = 8.51 \times 10^{7}$ exp(-55.53 kJ/mol / RT) with a proposed nucleophilic attack by the amine on the peroxide (Kashino et al, 1967). There are two likely sites for nucleophilic attack by amine on the peroxide: either on oxygen of the O-O bond or a carbonyl group. The former would give a lauric acid and the N-lauroyloxyl derivative of Amine101 and the latter would give a lauric acid amide and a lauric acid (John Lindsay Smith, 2008, private communication).

A large quantity of lauric acid (≈20 mmol dm^{-3}) was detected in comparison with that obtained from oxidation reactions without Amine101 (Figure 5.27). Lauric acid was found in small quantities in oxidation reactions without Amine101 probably because the lauroyloxyl radicals decompose to undecyl radicals and carbon dioxide before being able to abstract hydrogen atoms to give lauric acid.

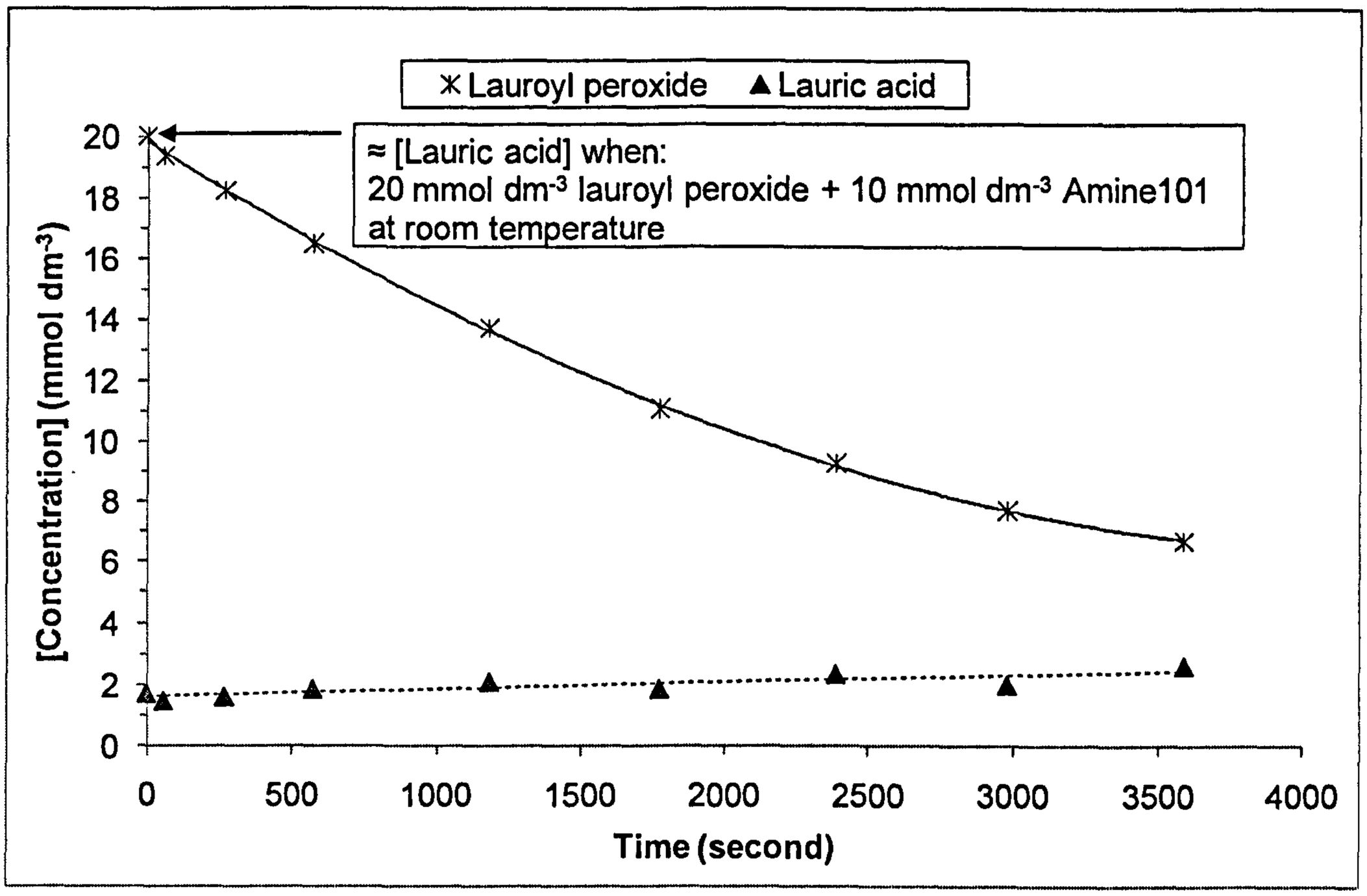

Figure 5.27: Lauric acid formation in the oxidation of 20.0 mmol dm^{-3} lauroyl peroxide in hexadecane at 90 °C in flow intermediate reactor

5.4. SUMMARY

The critical antioxidant concentration and critical temperature phenomena, and the stoichiometry coefficients of phenolic and aminic antioxidants have been investigated at 80 °C to 240 °C in bench-top reactors.

The critical antioxidant concentration of AN2 was found to be 0.22 ± 0.05 mmol dm^{-3} at 220 °C. Semi-empirical calculations suggest that the stoichiometry coefficient at AN2 decreases by ≈0.3 every 10 °C after 160 °C; that is to say, if the stoichiometry coefficient of AN2 is 4.0 at 160 °C, then it is going to shift down to 2.0 at 230 °C.

The critical antioxidant concentration of Amine101 was found to be 5.7 ± 0.5 mmol dm^{-3} at 180 °C. Semi-empirical calculations suggest that the activation energy for the reaction between Amine101 and peroxyl radicals is 40 kJ mol^{-1} (assuming the pre-exponential factor to be $1.0x10^{8}$ M^{-1} s^{-1} and the stoichiometry coefficient to be 3.0).

The stoichiometry coefficient of AN2 and BHT were found to be 4.1 ± 0.2 and 4.3 ± 0.2, respectively. These values conflicted with those in the literature. The unexpectedly high stoichiometry coefficient of BHT made it necessary to propose a new provisional inhibition mechanism for BHT.

5.5. REFERENCES

Antonovskii, V. and Bezborodova, L. Kinetics and stoichiometry of the reaction of lauroyl peroxide with α-naphthylamine. Translated from Russian by SciFinder Scholar from: *Zhurnal Fizicheskoi Khimii*, 1968, **42** (2): 351-354.

Bolsman, T.; Blok, A.; and Frijns, J. Mechanism of the catalytic inhibition of hydrocarbon autoxidation by secondary amines and nitroxides. *Journal of the Royal Netherlands Chemical Society*, 1978b, **97** (12): 313-319.

Boozer, C.; Hammond, G.; Hamilton, C.; and Sen, J. Air oxidation of hydrocarbons II the stoichiometry and fate of inhibitors in benzene and chlorobenzene. *Journal of the American Chemical Society*, 1955, **77**: 3233-3237.

Denisov, E. and Afanasev, I. Oxidation and antioxidants in organic chemistry and biology. CRC Press of Taylor and Francis Group, Florida, 2005.

Denisov, E. and Denisova, T. Handbook of antioxidants bond dissociation energies rate constants activation energies and enthalpies of reactions (second edition). CRC Press LLC, Florida, 2000.

Gugumus, F. Critical antioxidant concentrations in polymer oxidation – I fundamental aspects. *Polymer Degradation and Stability*, 1998a, **60**: 85-97.

Gugumus, F. Critical antioxidant concentrations in polymer oxidation – II experimental 'proofs'. *Polymer Degradation and Stability*, 1998b, **60**: 99-117.

Guillet, J. and Gilmer, J. Decomposition of lauroyl decanoyl and octanoyl peroxides in solution. *Canadian Journal of Chemistry*, 1969, **47** (23): 4405-4411.

Howard, J. Absolute rate constants for reactions of oxyl radicals. In: Williams, G. (editor). Advances in free-radical chemistry, volume 4. Logos Press Limited, London, 1972.

Howard, J. Radical reaction rates in liquids, In: Fischer (editor), H. Peroxyl and related radicals. Subvolume D2. Springer, London, 1997.

Ischuk, Y. and Butovets, V. Estimation of grease oxidation stability under dynamic conditions and antioxidant testing. *NLGI Spokesman*, 1991, **55** (4): 133-138.

Jensen, R.; Korcek, S.; Zinbo, M.; and Johnson, M. Initiation in hydrocarbon autoxidation at elevated temperatures. *International Journal of Chemical Kinetics*, 1990, **22**: 1095-1107.

Kashino, S.; Mugino, Y.; and Hasegawa, S. Studies of organic peroxides x the reaction of benzoyl peroxide with secondary amines. *Bulletin of the Chemical Society of Japan*, 1967, **40** (9): 2004-2008.

McMillen, D. and Golden, D. Hydrocarbon bond dissociation energies. *Annual Review of Physical Chemistry*, 1982, **33**: 493-532.

Ohkatsu, Y. and Nishiyama, T. Phenolic antioxidants-effect of ortho-substituents. *Polymer Degradation and Stability*, 2000, **67**: 313-318.

Pryor, W. and Smith, K. The viscosity dependence of bond homolysis a qualitative and semiquantitative test for cage return. *Journal of the American Chemical Society*, 1970, **92** (18): 5403-5412.

Roginskii, V. ESR spectra and kinetics of the disproportionation of substituted phenoxy radicals coomunication 2 radicals of 2,4,6-trialkyl-substituted mono-, p-bis-, p-tris-, and p-tetraphenols. *Bulletin of the Academy of Sciences of the USSR Division of Chemical Science*, 1985, **34** (9): 1833-1841, part 1.

Ryzhkov, L. Radical nature of pathways to alkene and ester from thermal decomposition of primary alkyl diacyl peroxide. *Journal of Organic Chemistry*, 1996, **61** (8): 2801-2808.

Thomas, J. and Tolman, C. Oxidation inhibited by diphenylamine. *Journal of the American Chemical Society*, 1962, **84**: 2930-2935.

Yamada, F.; Nishiyama, T.; Yamamoto, M.; and Tanaka, K. Substituted bisphenols as antioxidants for autoxidation of tetralin. *Bulletin of the Chemical Society of Japan*, 1989, **62** (11): 3603-3608.

6. BEHAVIOUR OF ANTIOXIDANTS IN GASOLINE ENGINES

6.1. INTRODUCTION

Antioxidants in automotive lubricants are thought to be chiefly degraded in the piston assembly (Mahoney et al, 1980). Hence, a good understanding of how and to what extent antioxidants decay in the piston assembly should enable lubricant formulators to choose the appropriate antioxidant type and concentration for lubricant formulations.

There is only a handful of published data on the behaviour of antioxidants under automotive engine conditions (Table 6.1).

Table 6.1: Previous works on the behaviour of antioxidants in automotive engines (references within table)

Engine	Lubricant formulation	Studied antioxidant	Reference
Diesel	Detergent	Aminic	Yasutomi et al, 1981
Diesel	Full	Phenolic and aminic	Muller et al, 1982
Gasoline	Full	Aminic	Bigarre and Legeron, 1987
Gasoline	Full	Phenolic and aminic	Inoue and Yamanaka, 1990
Gasoline and diesel	Full	Phenolic and aminic	Hamblin and Rohrbach, 2001

Studying antioxidants under engines conditions is a very expensive process; and so, antioxidants are normally evaluated in cost-effective bench-top reactors that produce results in some respects similar to those obtained from a research engine (Duchesne et al, 2000; Lashki and Vipper, 1979; and Kinker et al, private communication).

The major drawbacks in previous works (Table 6.1) are that no oil samples were collected from the piston assembly where the antioxidant decay and lubricant degradation are thought to occur (Mahoney et al, 1980), and many of them studied antioxidants in the presence of tens of other lubricant additives that could interact

with the antioxidant leading to a complication in the analysis and interpretation of results (Hsu and Lin, 1983).

The aim of this chapter is to study the behaviour of antioxidants in a research gasoline engine, by extraction of oil samples from the piston assembly and sump, to provide lubricant formulators with the understanding of how and to what extent antioxidants decay in the piston assembly. Chemical structures of starting materials and oxidation products are listed in Table 6.2.

Table 6.2: Chemical structures and names of starting materials and oxidation products

Structure	CAS name	Abbreviation
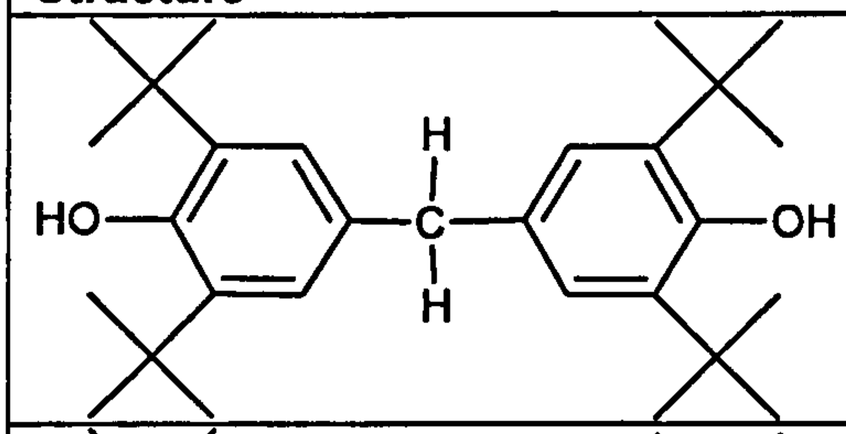	4,4'-Methylenebis[2,6-bis(1,1-dimethylethyl)]phenol	AN2
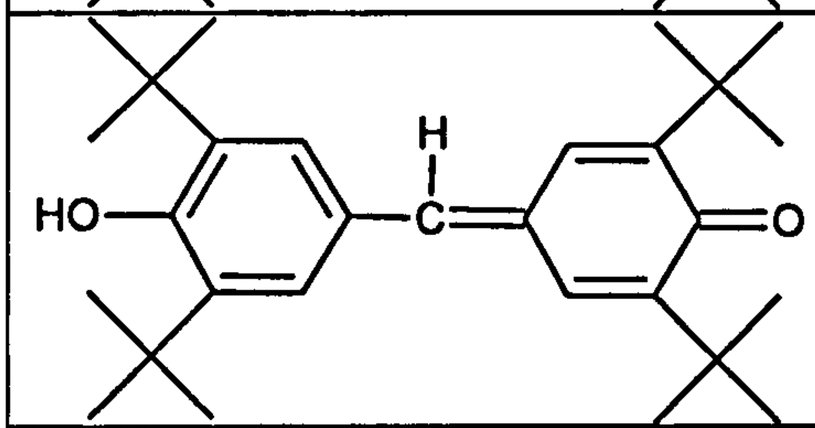	4-[[3,5-Bis(1,1-dimethylethyl)-4-hydroxyphenyl]methylene]-2,6-bis(1,1-dimethylethyl)- 2,5-cyclohexadien-1-one	Galvinol
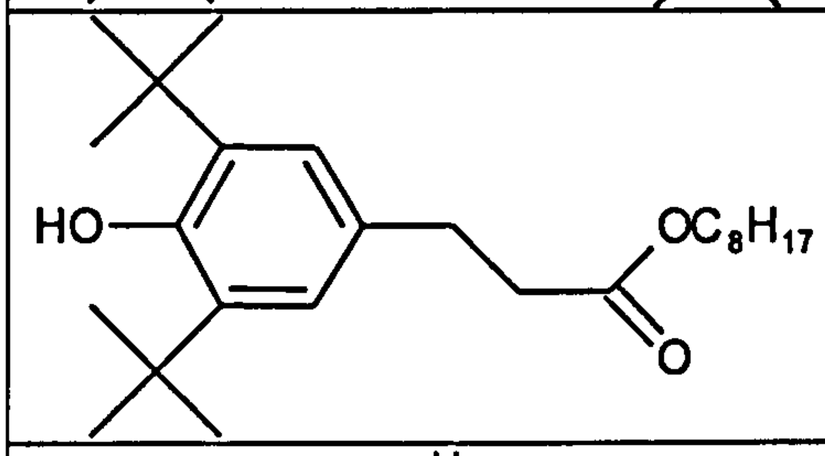	3,5-Di-tert-butyl-4-hydroxyhydrocinnamate	Irganox L135
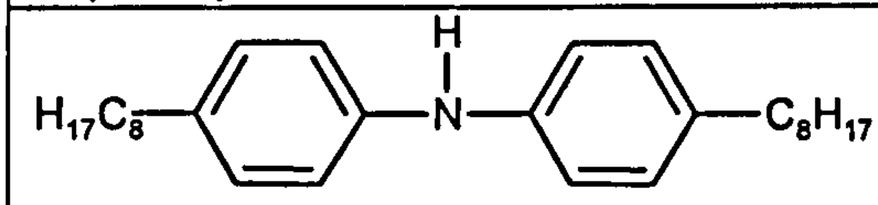	4-Octyl-N-(4-octylphenyl)benzenamine	Amine101
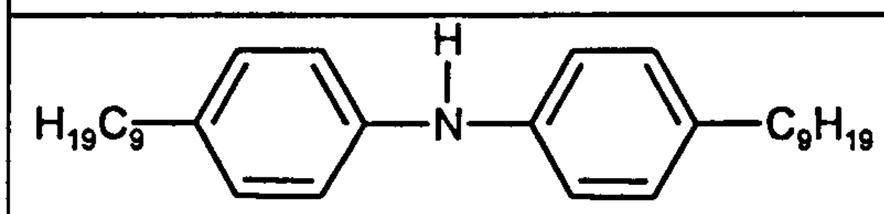	4-Nonyl-N-(4-nonylphenyl)benzenamine	Naugalube 438L
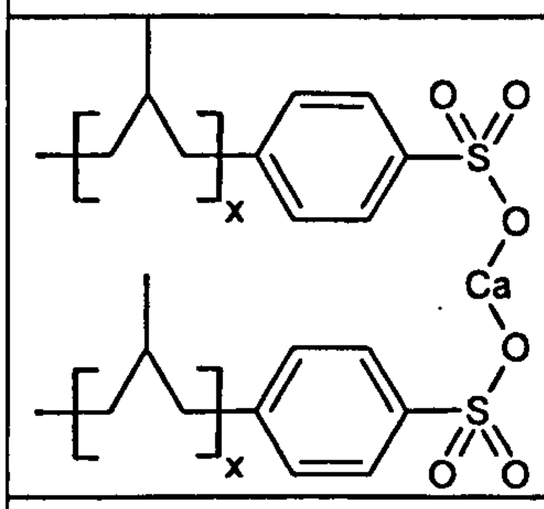	-	Sulphonate detergent
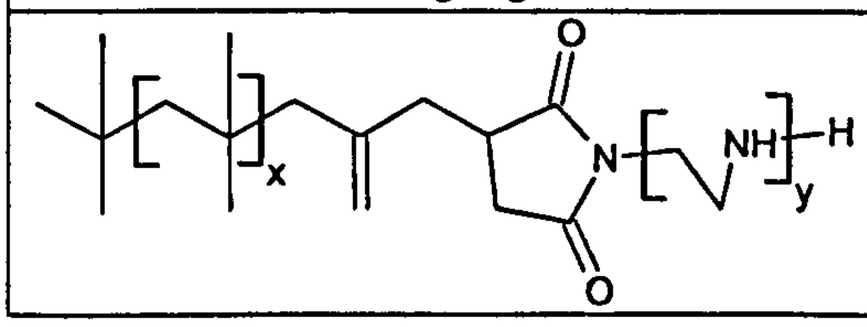	-	Succinimide dispersant

6.2. RESULTS

Semi-formulated base fluids are degraded in the engine to investigate the behaviour of antioxidants under engine conditions. The semi-formulated base fluids in Table 6.3 were degraded in the engine whilst the piston rings are unpinned (i.e. the rings are free to rotate), whereas formulations in Table 6.4 and Table 6.5 were degraded in the engine while the piston rings were pinned[41] (i.e. the rings are fixed in one position) to evaluate the piston rings rotation on the oil degradation process.

Table 6.3: Details of semi-formulated base fluids for June 2006 Hydra engine tests

Blend	Code	Oil blend formulation
Reference oil	LB368	Shell XHVI 8.2 + 2 % w/w neutral calcium alkyl sulphonate detergent (50 % / 50 % in a Group I diluent) + 2 % w/w succinimide dispersant (50 % / 50 % in a Group I diluent) + a few parts-per-million (unknown quantity) of a silicone anti-foaming agent
0.5% Irganox	LB6	LB368 + 0.5 % w/w (or 9.4 mmol dm^{-3}) Irganox L135
1.0% Irganox	LB10	LB368 + 1.0 % w/w Irganox L135
0.5% AN2	LB11	LB368 + 0.5 % w/w (nominal)[42] (or 9.4 mmol dm^{-3}) AN2
0.5% Naugalube	LB12	LB368 + 0.5 % w/w Naugalube 438L
1.0% Naugalube	LB13	LB368 + 1.0 % w/w Naugalube 438L
1.0% ZDDP	LB15	LB368 + 1.0 % w/w secondary (secondary-C4 [85 m %] & primary-C8 [15 m %] alcohols) ZDDP

Table 6.4: Details of semi-formulated base fluids for June 2007 Hydra engine tests

Blend	Oil blend formulation
XHVI 8.2	Shell XHVI 8.2
0.5% AN2 (June 07)	Shell XHVI 8.2 + 0.5 % w/w (or 9.4 mmol dm^{-3}) AN2

Table 6.5: Details of semi-formulated base fluids for August 2007 Hydra engine tests

Blend	Oil blend formulation
XHVI 8.2	Shell XHVI 8.2
0.5% Amine101	Shell XHVI 8.2 + 0.5 % w/w (or 10.1 mmol dm^{-3}) Amine101

Before each run, the engine was flushed twice with the reference oil and once with the sample oil for one hour.

The temperature of the sump was maintained, for this work, at ~80 °C to minimise antioxidant oxidation in the sump to a negligible level and hence eliminate potential oxidation interferences from the sump with oxidation data from the piston assembly. The conditions of the Ricardo Hydra engine are listed in Table 6.6.

---

[41] Top and second piston rings pinned at 180 degrees and top ring gap pinned at anti-thrust side.
[42] AN2 concentration of 0.5% AN2 blend has the same molar concentration as that of Irganox L135 of 0.5% Irganox blend.

Table 6.6: Conditions of Ricardo Hydra engine

Parameter	June 2006 tests	June 2007 tests	August 2007 tests
Load (%)	50	50	50
Speed (rpm)	1500	1500	1500
Piston rings pinning	No	Yes	Yes
Sump volume (litre)	3.0	3.0	3.0
Sump temperature (°C)	~80	~80	~80
Test duration (hour)	6.0	4.0	5.0
Fuel	Shell standard unleaded gasoline	Shell standard unleaded gasoline	Shell standard unleaded gasoline

Formation of carbonyls

Figure 6.1, Figure 6.2, Figure 6.3, Figure 6.4, and Figure 6.5 show the formation of total carbonyl in top ring zone and sump; with the concentrations of carbonyl in the top ring zone much higher than those in the sump.

The carbonyl concentrations were normalised to zero by using the reference oil as the background.

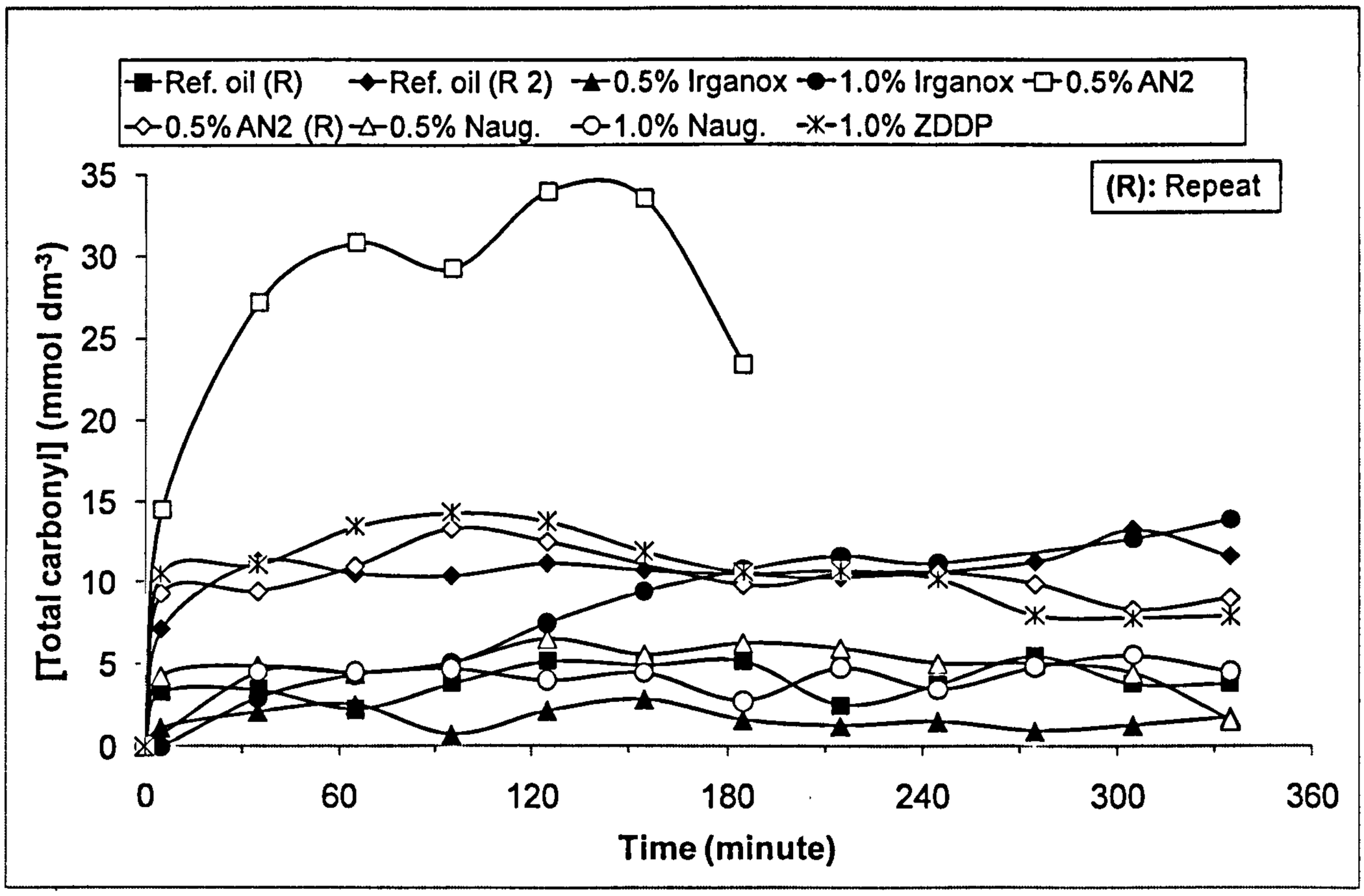

Figure 6.1: Total carbonyl (by FTIR) of oil samples from top ring zone (June 2006 tests)

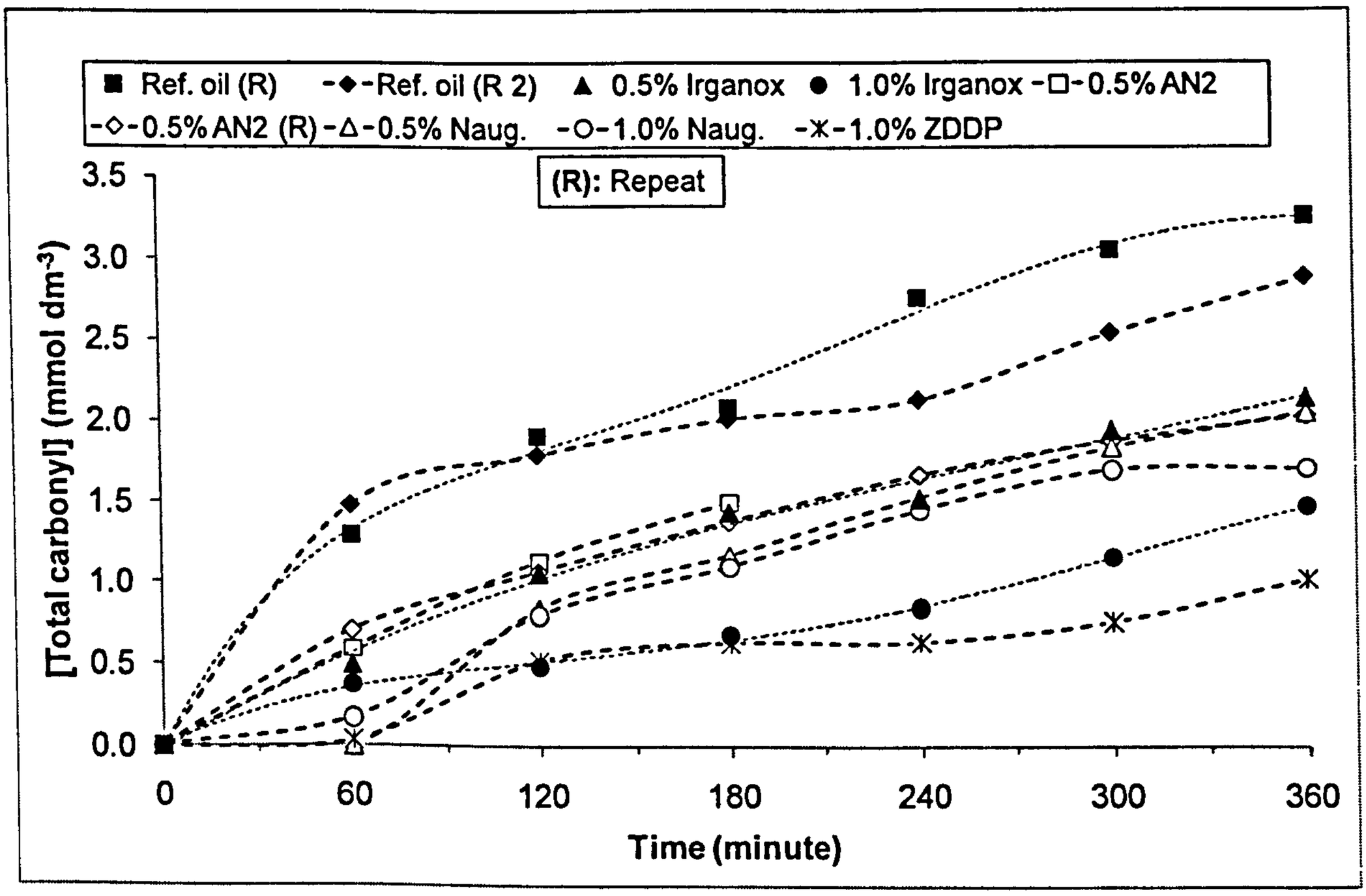

Figure 6.2: Total carbonyl (by FTIR) of oil samples from sump (June 2006 tests)

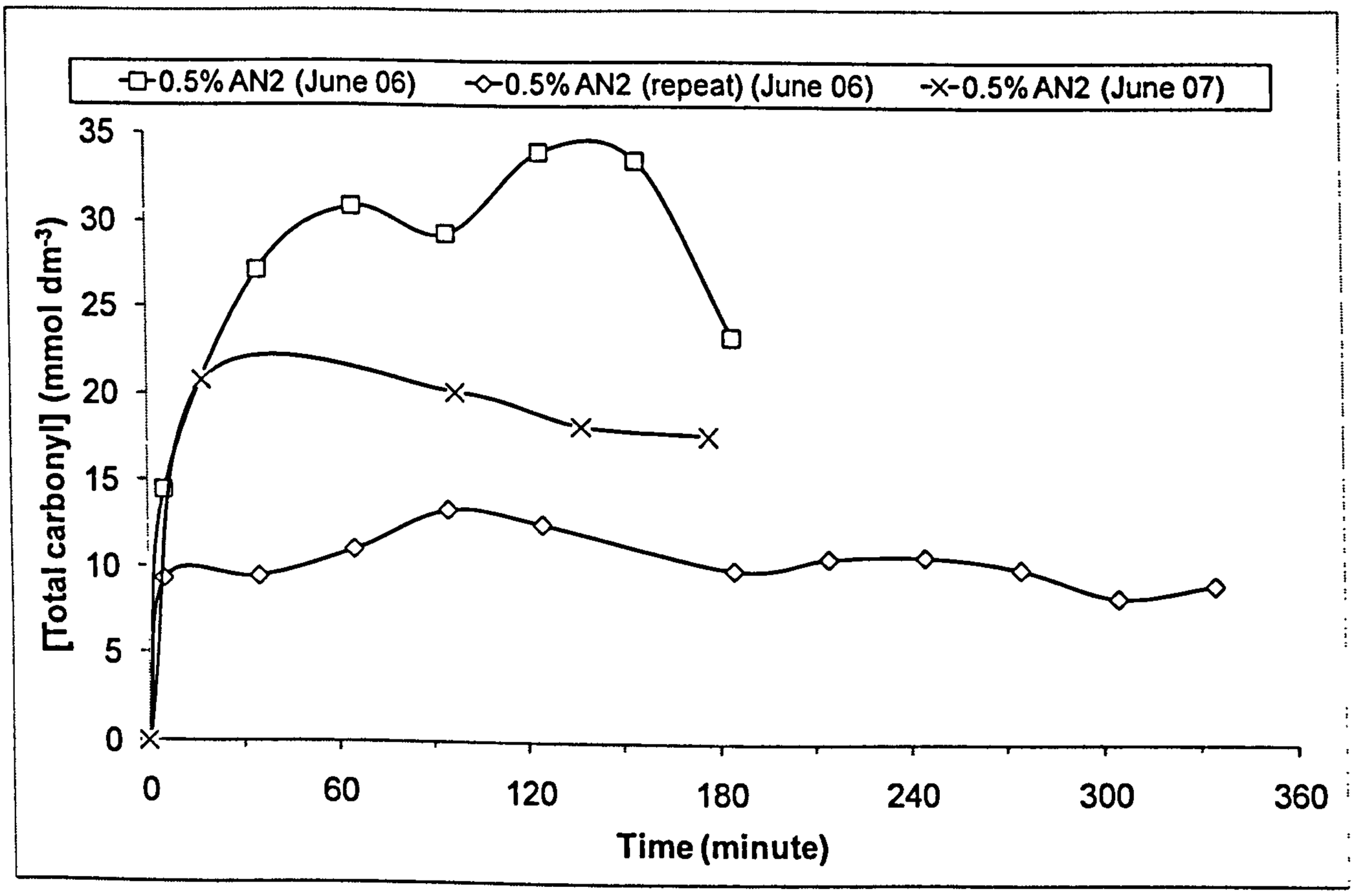

Figure 6.3: Total carbonyl (by FTIR) of oil samples from top ring zone (June 2006 and June 2007 tests)

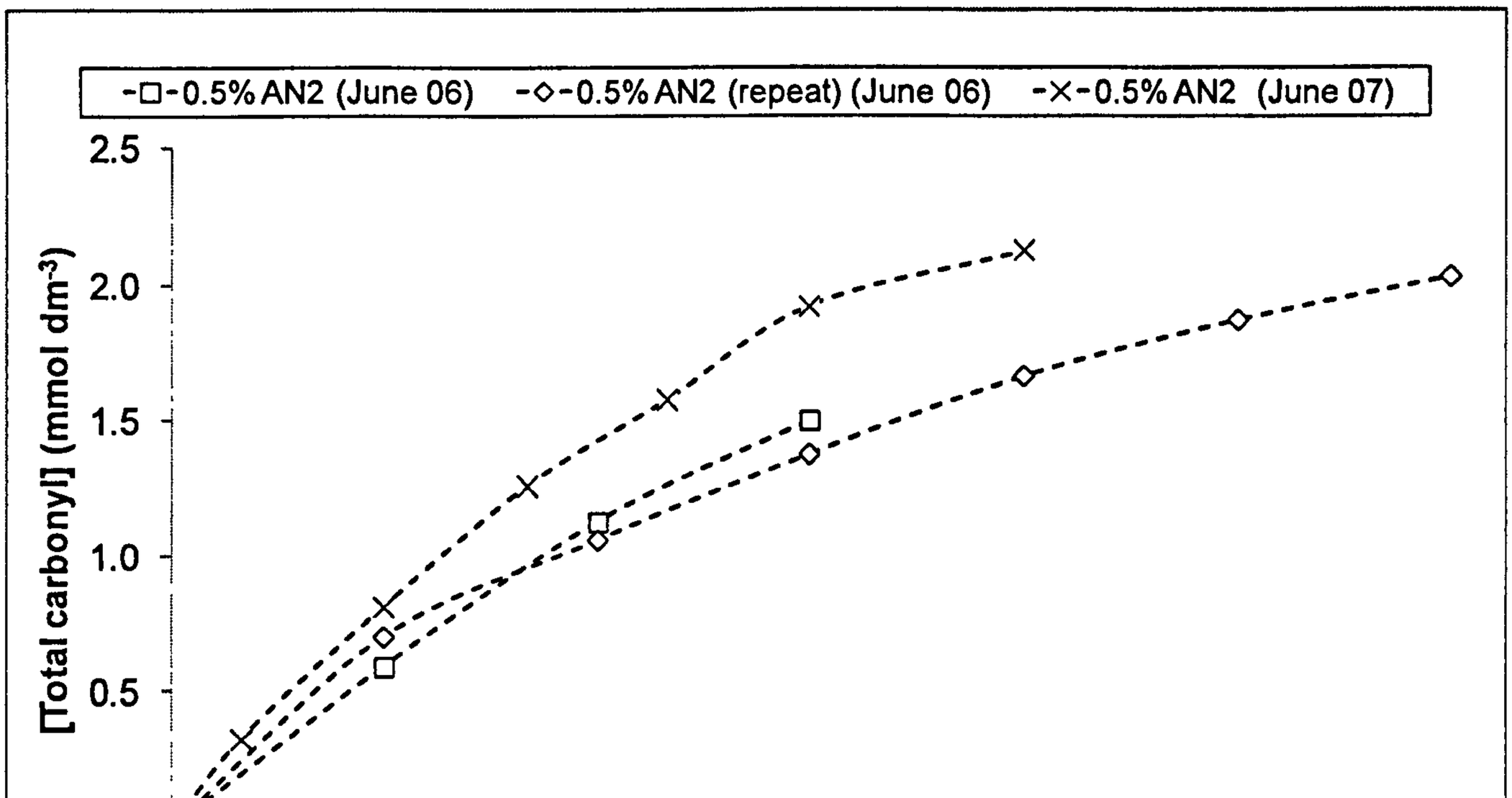

Figure 6.4: Total carbonyl (by FTIR) of oil samples from sump (June 2006 and June 2007 tests)

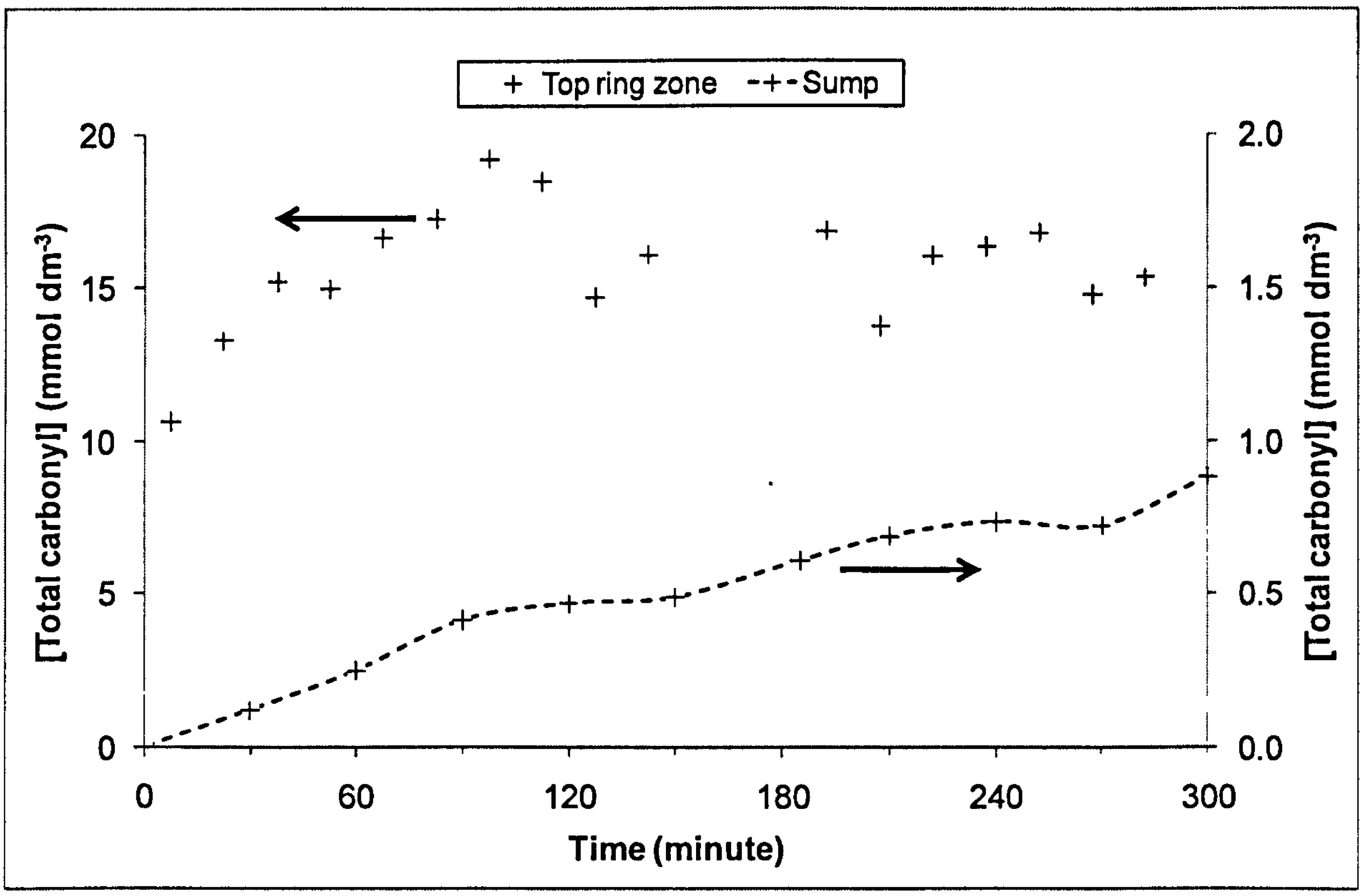

Figure 6.5: Total carbonyl (by FTIR) of oil samples from top ring zone and sump (0.5% Amine101 blend, August 2007)

Decay of antioxidants

Figure 6.6 and Figure 6.7 show the AN2 remaining in the top ring zone and sump, respectively; with the antioxidant level in the top ring zone much lower than that in the sump.

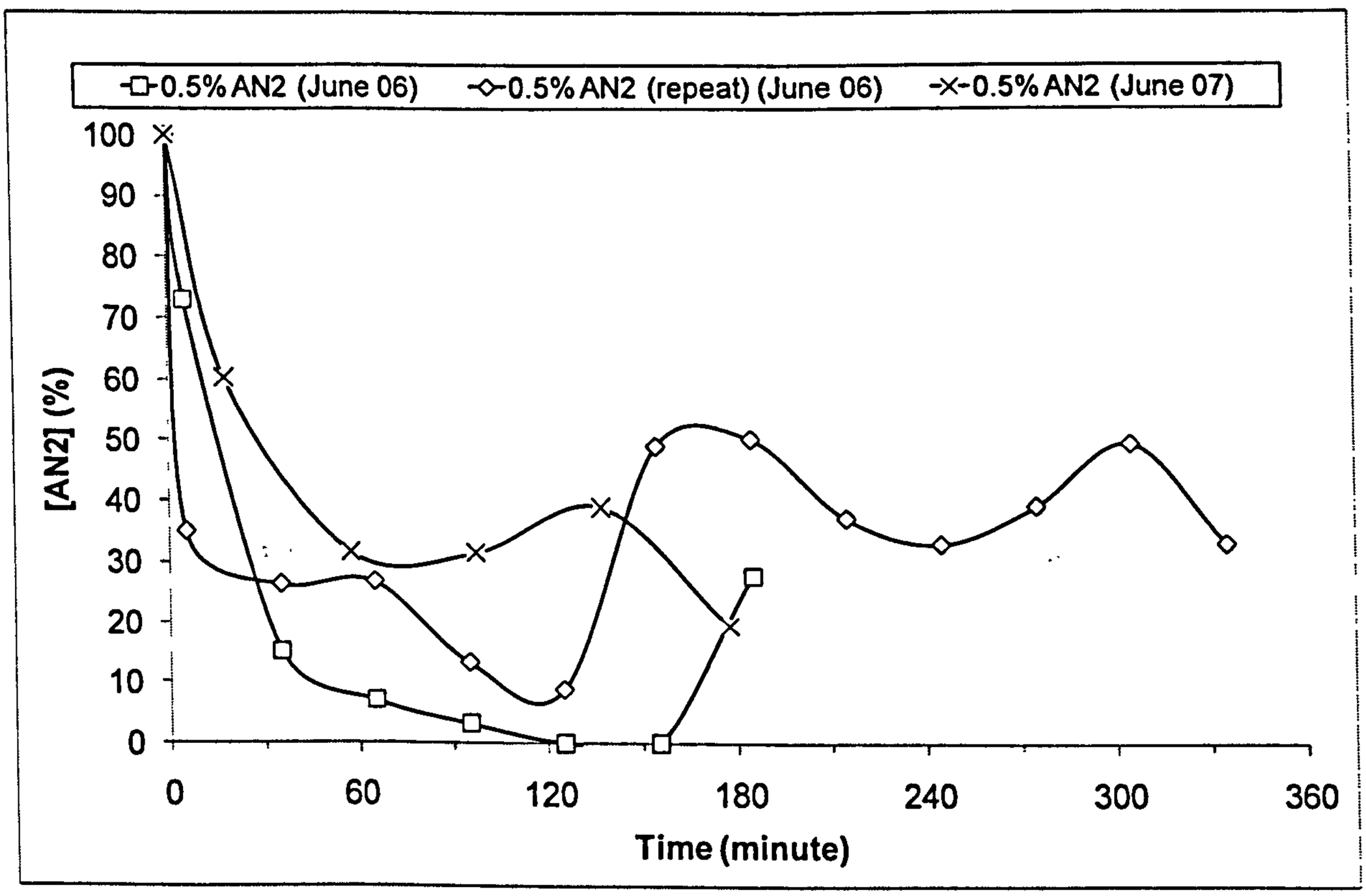

Figure 6.6: Decay of AN2 (by GC) in oils from top ring zone (June 2006 and June 2007 tests)

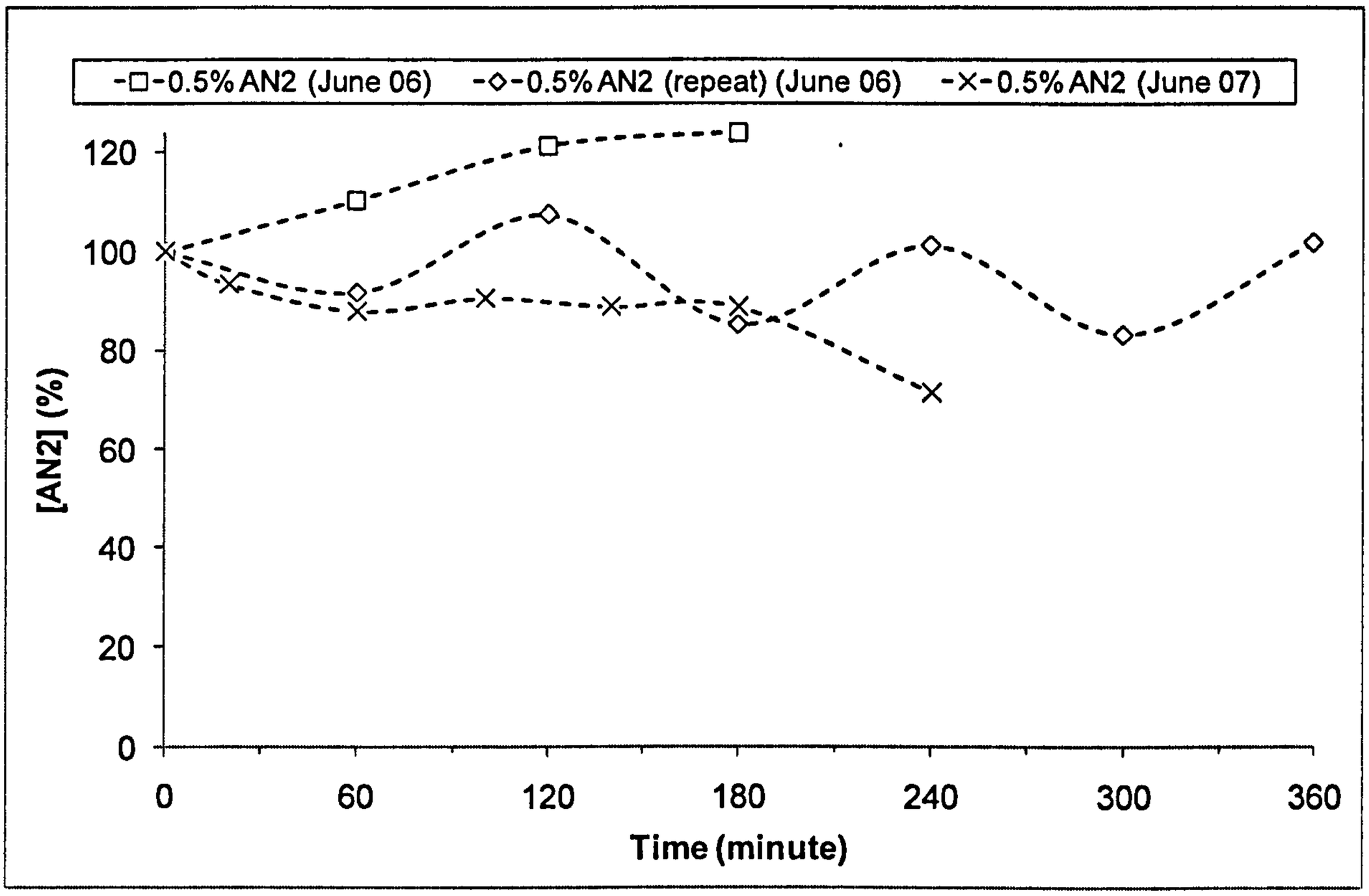

Figure 6.7: Decay of AN2 (by GC) in oils from sump (June 2006 and June 2007 tests)

Figure 6.8 shows the decay of Irganox L135 in the top ring zone and sump; with the antioxidant level in the top ring zone being sometimes lower than that in the sump. The results here seem to be heavily adulterated by, probably, interferences that have the same GC retention times as that of Irganox L135.

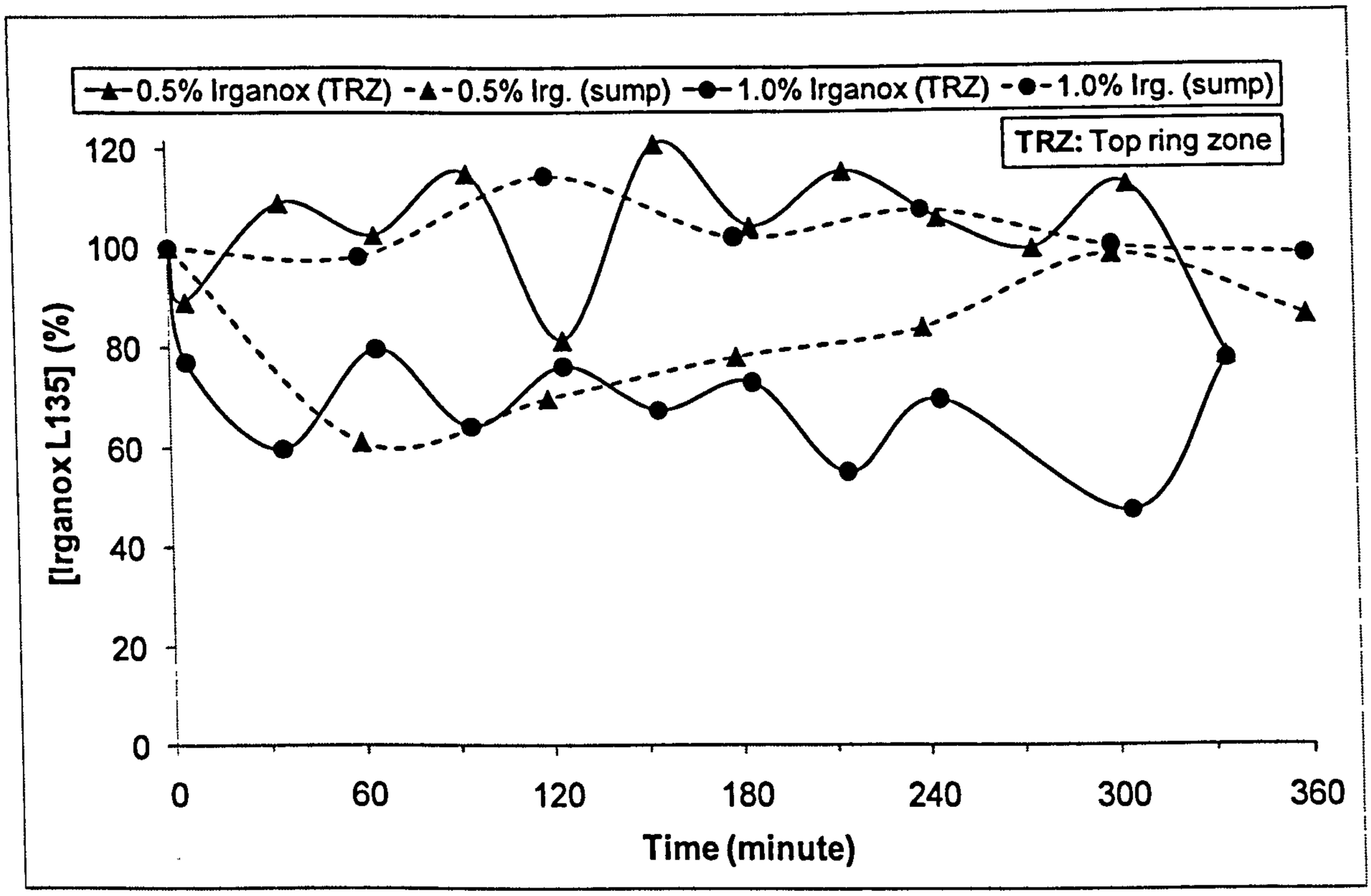

Figure 6.8: Decay of Irganox L135 (by GC) in oils from top ring zone and sump (June 2006 tests)

Figure 6.9 shows the decay of Amine101 in the top ring zone and sump; with the antioxidant level in the top ring zone lower than that in the sump. Also the results are greatly less erratic than those obtained from runs with unpinned piston rings.

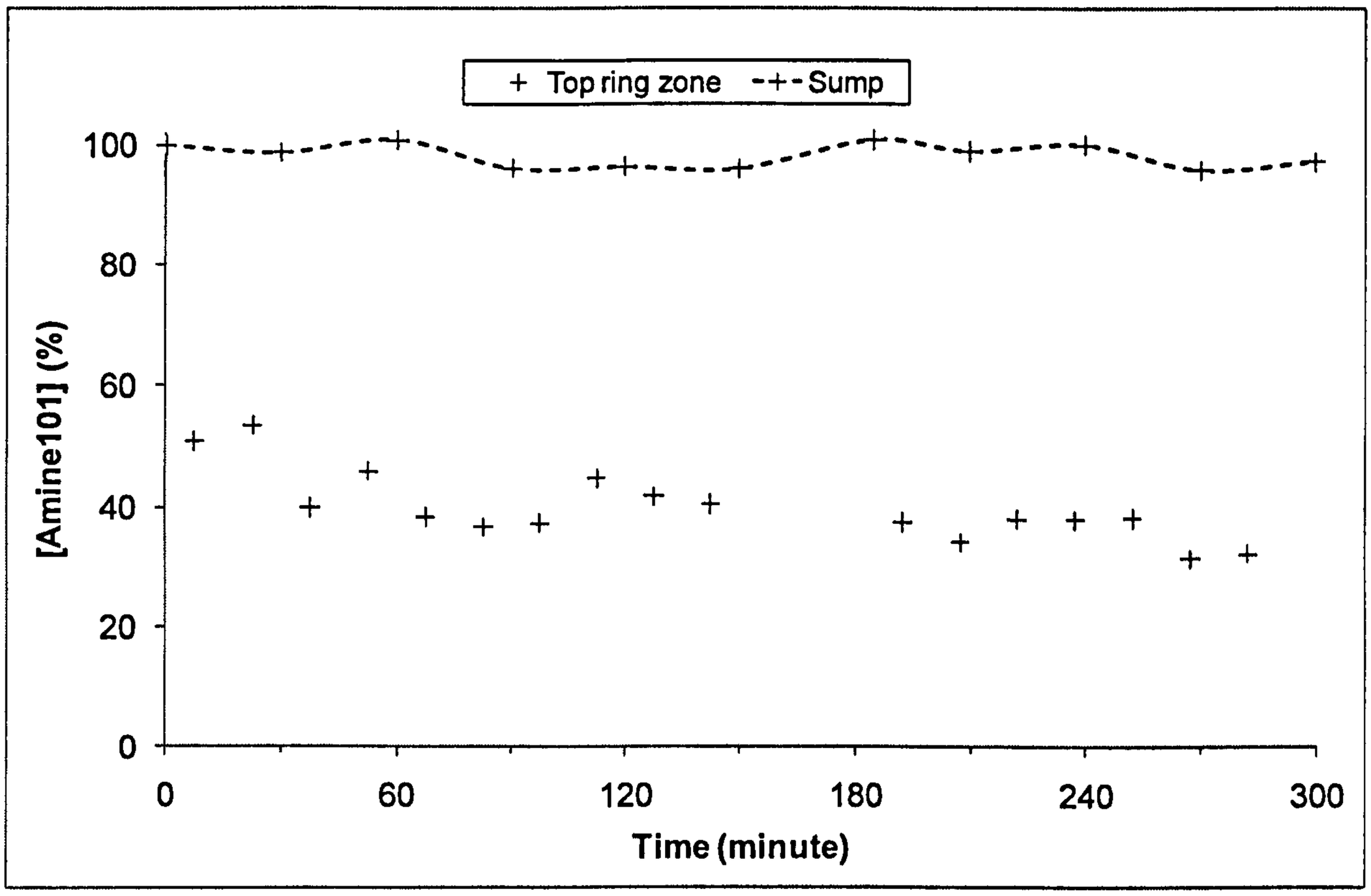

Figure 6.9: Decay of Amine101 (by GC) in oils from top ring zone and sump (0.5% Amine101 blend, August 2007)

Figure 6.10 shows the decay of Naugalube 438L in the top ring zone and sump; with the antioxidant level in the top ring zone lower than that in the sump.

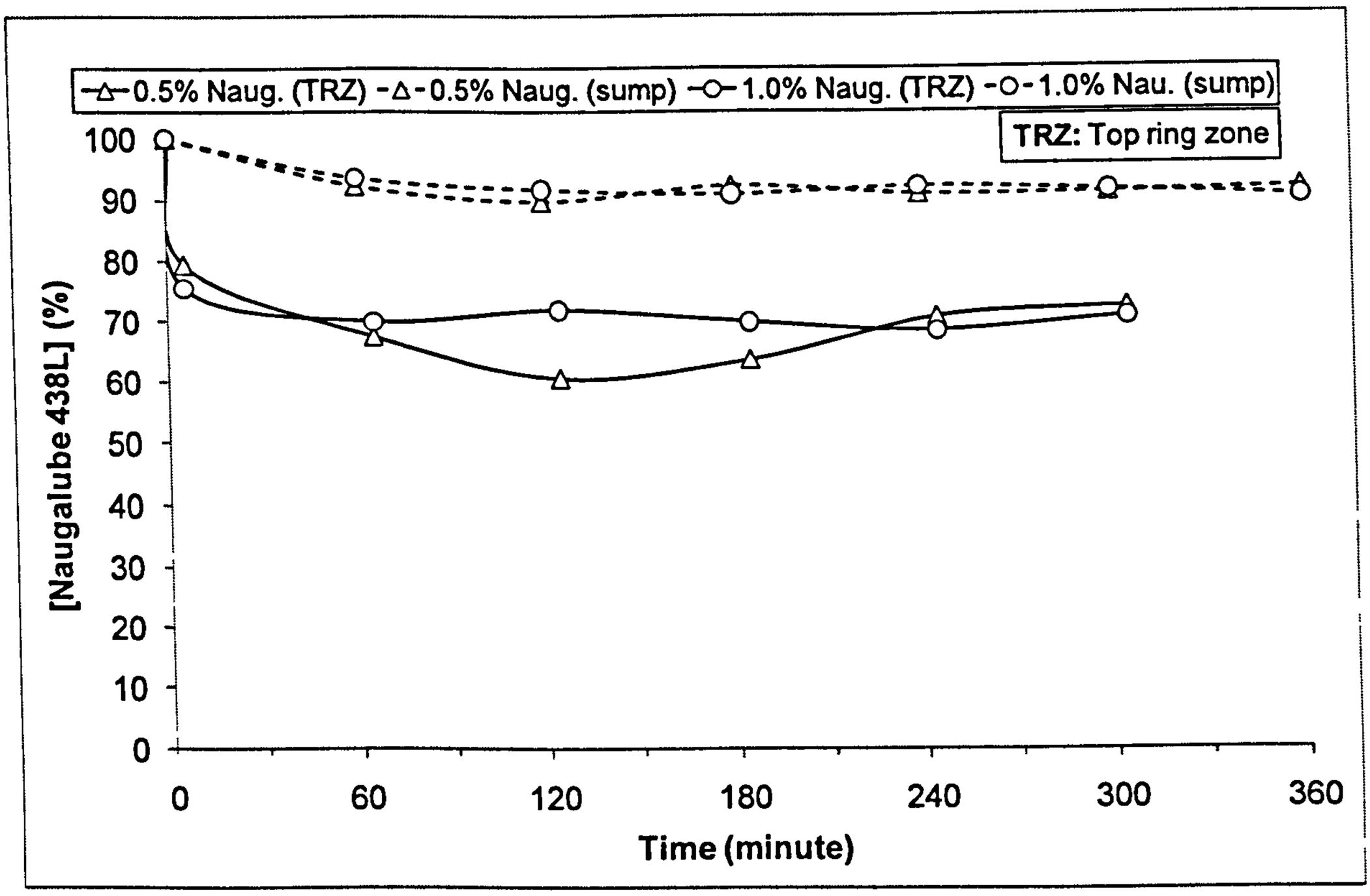

Figure 6.10: Decay of Naugalube 438L (by LC) in oils from top ring zone and sump (June 2006 tests)

Oxidation products of AN2

Figure 6.11 shows the formation of galvinol from AN2 in the top ring zone and sump, with the level of galvinol in the sump increasing with time.

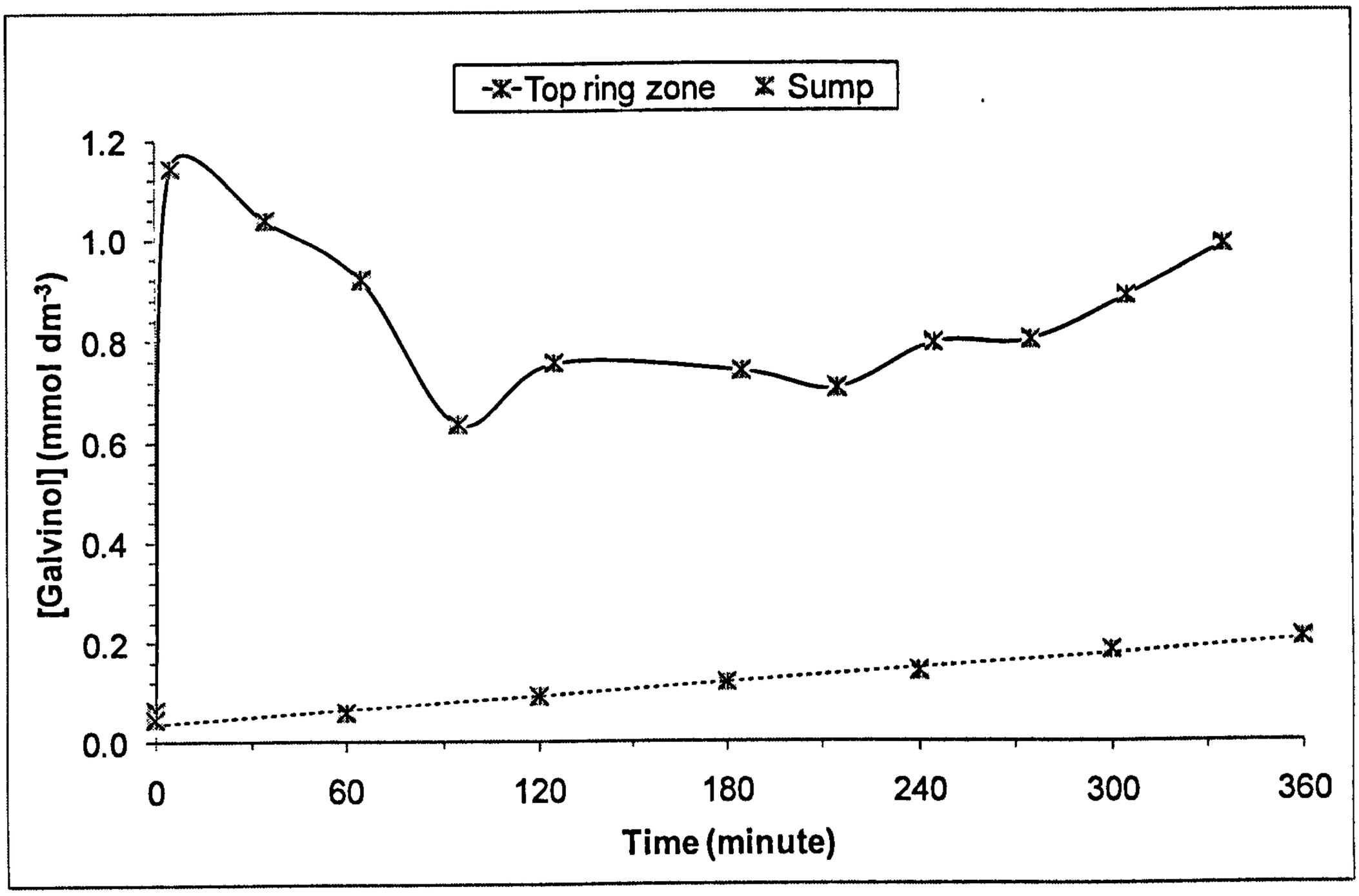

Figure 6.11: Galvinol formation (by LC) in top ring zone and sump in 0.5% AN2 (repeat) blend (June 2006 tests)

Figure 6.12 shows the formation of the oxidation products of AN2 in the top ring zone.

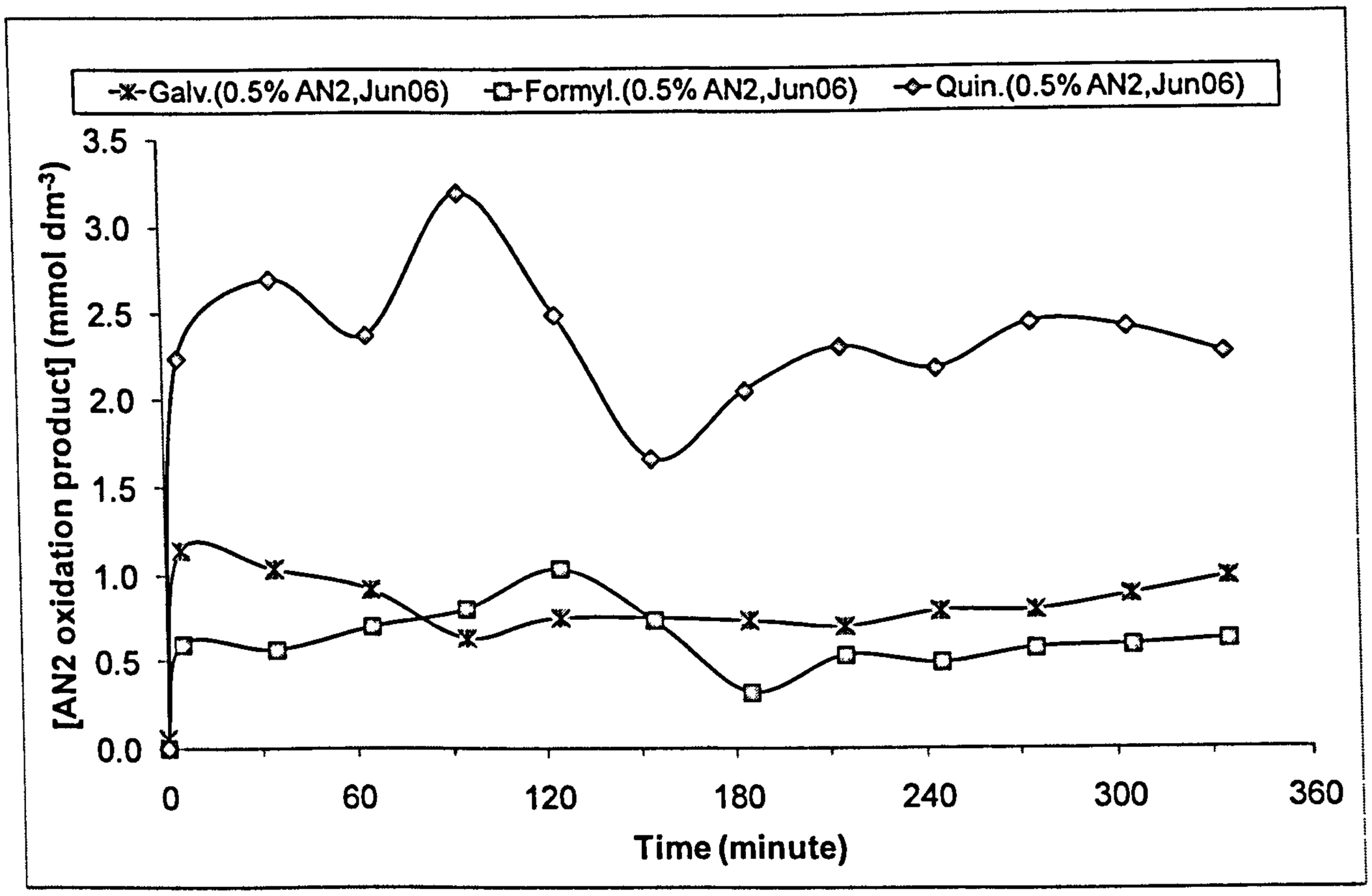

Figure 6.12: Formation of galvinol (by LC), formylphenol (by GC), and quinone (by GC) in top ring zone in 0.5% AN2 (repeat) blend (June 2006 tests)

Oil sample flow from top ring zone

The oil sample flow from the top ring zone is very erratic in runs with the piston rings unpinned (Figure 6.13 and Figure 6.14) or pinned (Figure 6.15). The irregularity of oil flow is further aggravated by interruptions by manual electron paramagnetic resonance sampling.

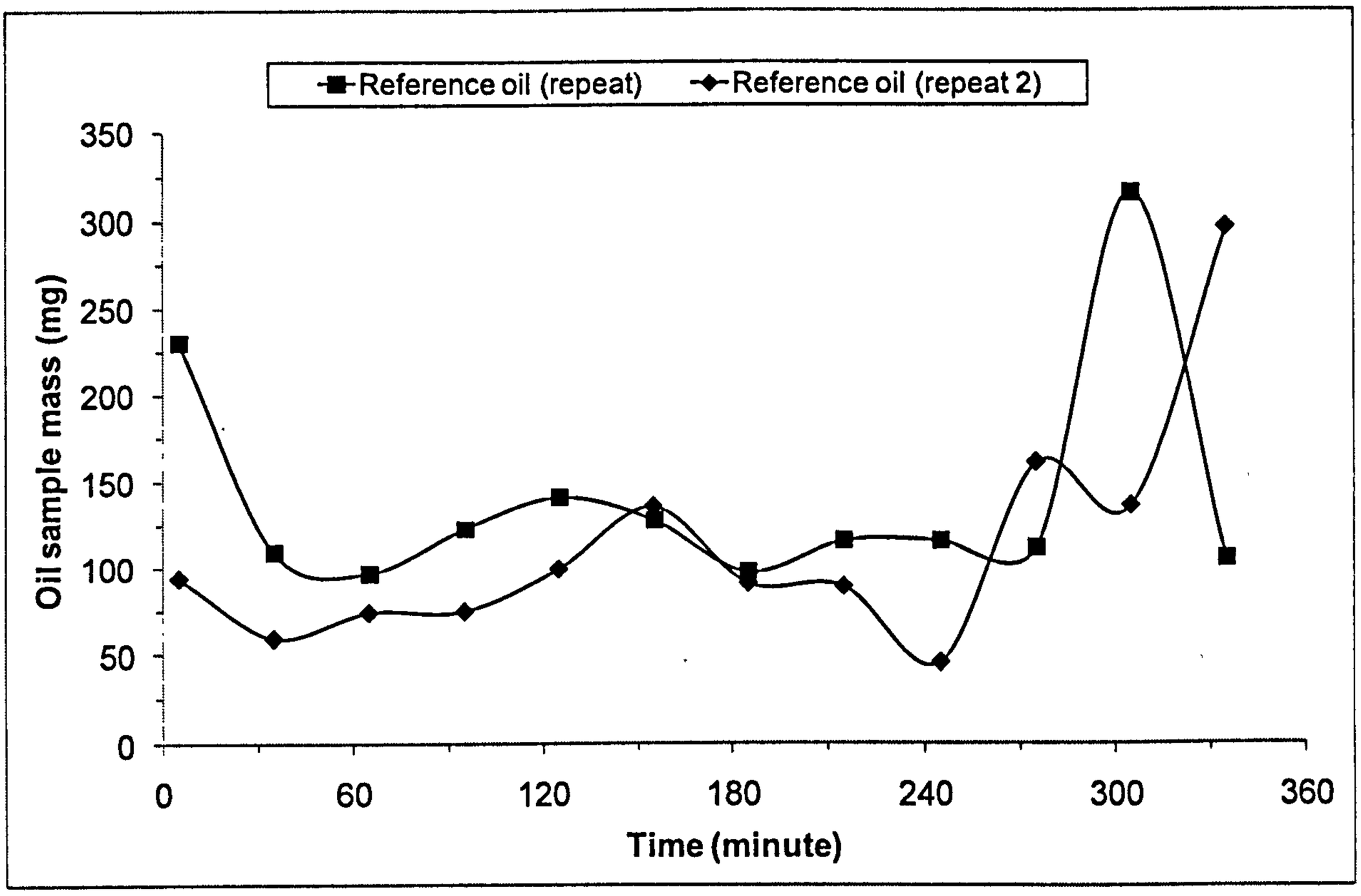

Figure 6.13: Oil sample flow for reference oil from top ring zone (June 2006 tests, unpinned rings)

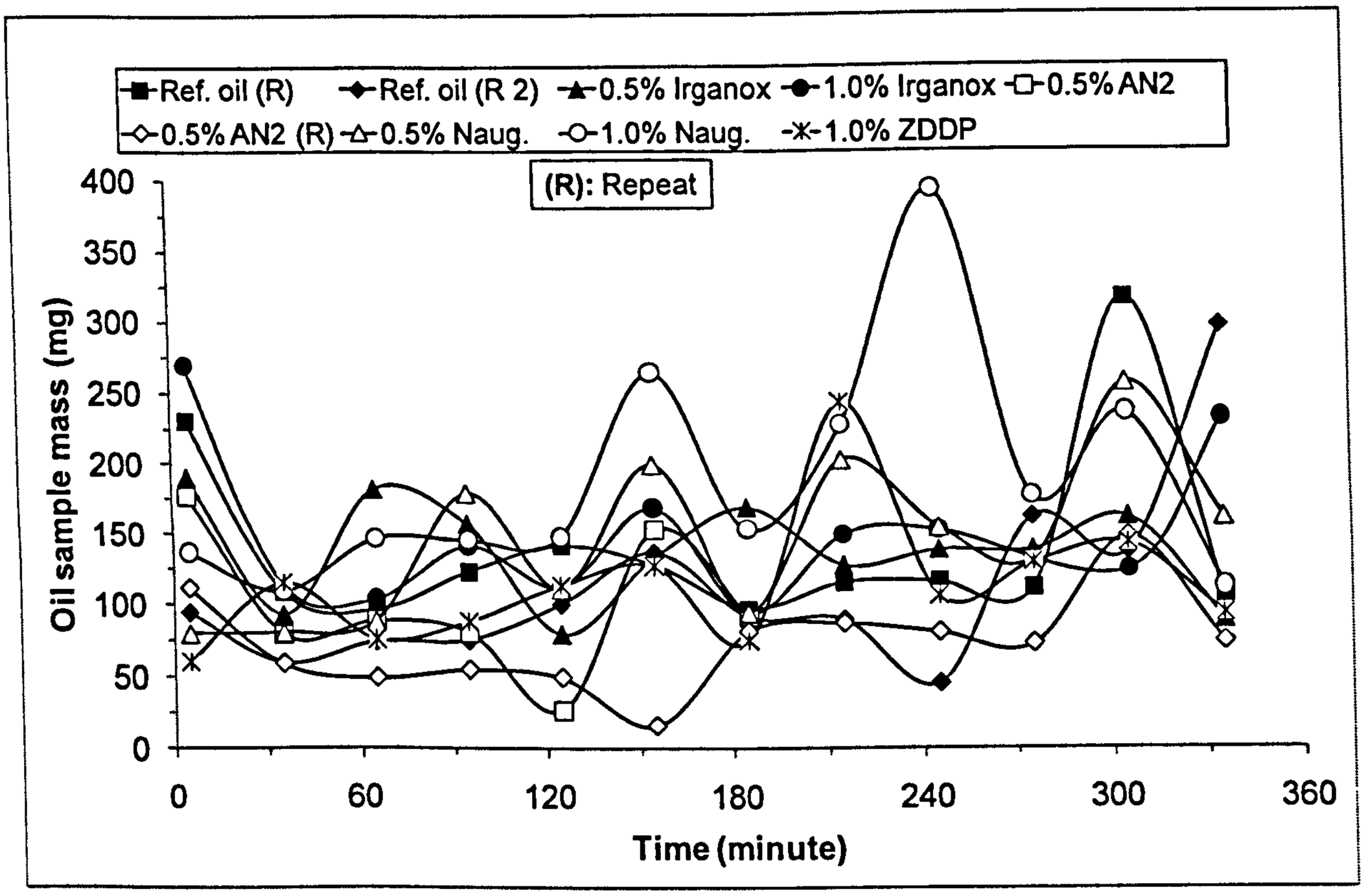

Figure 6.14: Oil sample flow from top ring zone (June 2006 tests, unpinned rings)

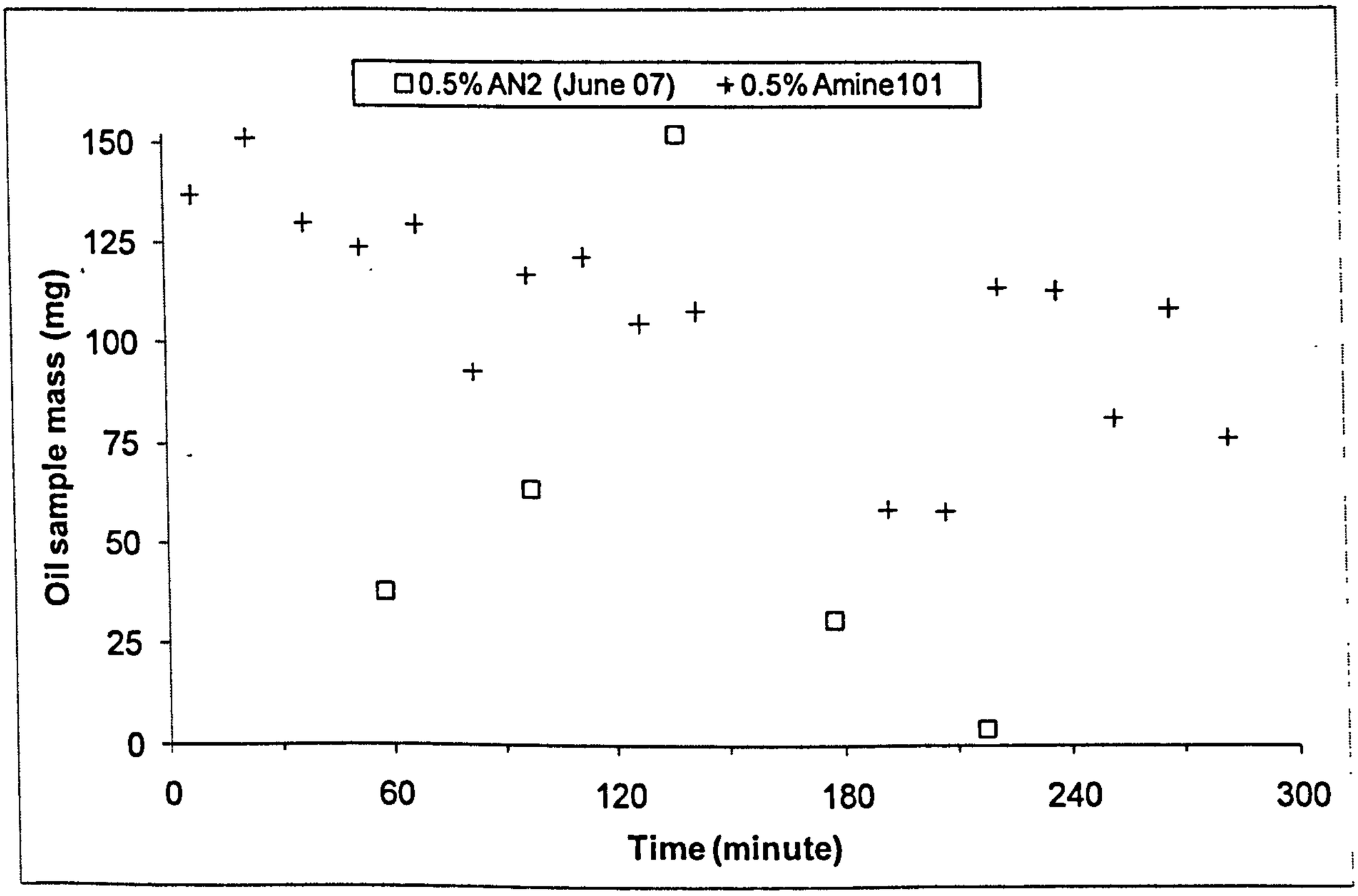

Figure 6.15: Oil sample flow from top ring zone (June and August 2007 tests, pinned rings)

6.3. DISCUSSION

Total carbonyl content

Figure 6.1 shows that the total carbonyl content for each oil formulation varied considerably. The reference oil had in some cases lower carbonyl content than oil formulations with antioxidants. It would have been expected that formulations with antioxidants should have better oxidative protection and hence end up with lower carbonyl contents than oil formulations without antioxidants. It seems very likely that these unexpected results were caused by the rotation of the top compression ring in the piston assembly. The piston rings rotate at a rate of ≈0.5 revolutions per minute at various speeds and loads (Schneider and Blossfeld, 1990 and Min et al, 1998), but the rate of rotation changes as a result of the changes in the shapes (from friction) of rings and piston grooves (Stecher, 1979) to sometimes causing the rings to be fixed in one place. For each engine run, after around 30 minutes when the engine warms up, the carbonyl content stabilises at one approximately constant level and remains so until the end of the run. This may imply that for each run, the piston rings are settled in one position throughout the run. Different top ring positions expose the oil to different temperatures and levels of reactive species from the combustion chamber and consequently degrade the lubricant at different levels. For example, the oil in 0.5% AN2 blend was severely degraded whereas the oil in 0.5% AN2 blend (repeat), which has the same formulation as that of 0.5% AN2 blend, was moderately degraded. To sum up, it is possible that the rotation of the top ring is the major factor in the observed variations in the carbonyl contents and accordingly it is not possible at this stage to differentiate between the ability of the different formulations to protect the base fluid of the investigated oil formulations.

Results from the piston assembly are periodical (Figure 6.1); however, the precision of results are enhanced by pinning the piston rings (Figure 6.5). In contrast, results from bench-top reactors are uniform because reactions are carried out under controlled conditions (see Chapter 3). The exposure of chemical reactions to periodical conditions is expected to alter reaction pathways.

Figure 6.2 shows that the carbonyl contents reasonably reflect the expected pattern for the investigated oil formulations. For instance, the reference oil had higher carbonyl contents than the rest of the oil formulations that contained antioxidants; 0.5% AN2 blend (original and repeat) have almost identical levels of carbonyl; and 1.0% w/w Irganox blend had half the level of carbonyl as that of 0.5% w/w Irganox blend.

It is generally accepted that small volumes of oil degrade in the hot piston and flow back to the warm sump (Yasutomi et al, 1981).[43] If this was the case, then it would have been expected that for the same carbonyl levels pattern observed from the piston to be reflected for the sump results with lower carbonyl concentrations (due to the dilution with fresh sump oil). However, in this work, the results from the sump (Figure 6.2) do not reflect those obtained from the piston assembly (Figure 6.1). The sump temperature was maintained at around 80 °C, and so, the possibility of oil degradation (with or without antioxidants) at 80 °C is not valid as it was experimentally demonstrated by others (Moray Stark and co-workers, private communication).

Sources of carbonyl

From bench-top oxidation studies, it is likely that as long as there is an effective antioxidant, say a sterically-hindered phenol (e.g. Irganox L135 or AN2), present in the base fluid, the base fluid does not degrade and hence no carbonyl-containing products are formed or oxygen consumed (see Section 3.4)

All the engine runs show that the total carbonyl content increase linearly with engine run time (Figure 6.2) in spite of the fact that the levels of antioxidants in the top ring zone varied from ~30 % to ~95 % and ~60 % when the piston rings are unpinned and pinned, respectively. This suggests that this carbonyl content is unlikely to be from the degradation of the base fluid due to the presence of antioxidants and so other contributors had to be the sources of the carbonyl. Figure 6.16 and Figure 6.17 show that in the presence of succinimide dispersant, carbonyl-containing species are formed during the induction period (i.e. prior to the

[43] Typical oil volumes are ~0.5 cm^3 (Stark et al, 2005) and ~4 litres for the piston ring pack and sump, respectively; and typical temperatures are ~200-300 °C (Kim et al, 1998) and ~90-130 °C (Kudynska and Buckmaster, 1997) for the piston ring pack and sump, respectively [Values vary with engine conditions and measured location].

onset of oxidation), which suggests that the carbonyl-containing species are unlikely to be from the oxidation of the base fluid.

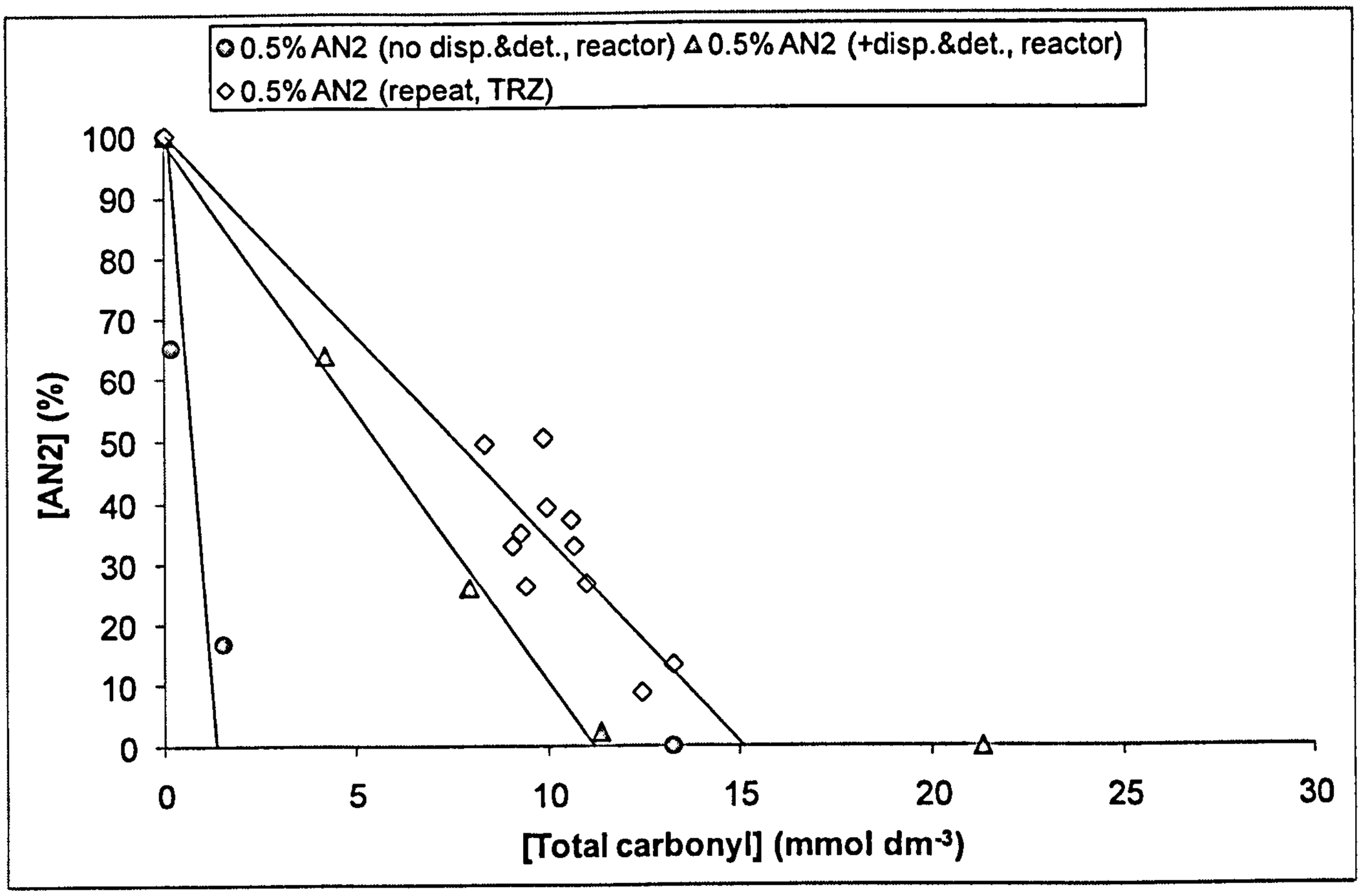

Figure 6.16: Correlation of AN2 level with total carbonyl from engine and reactor

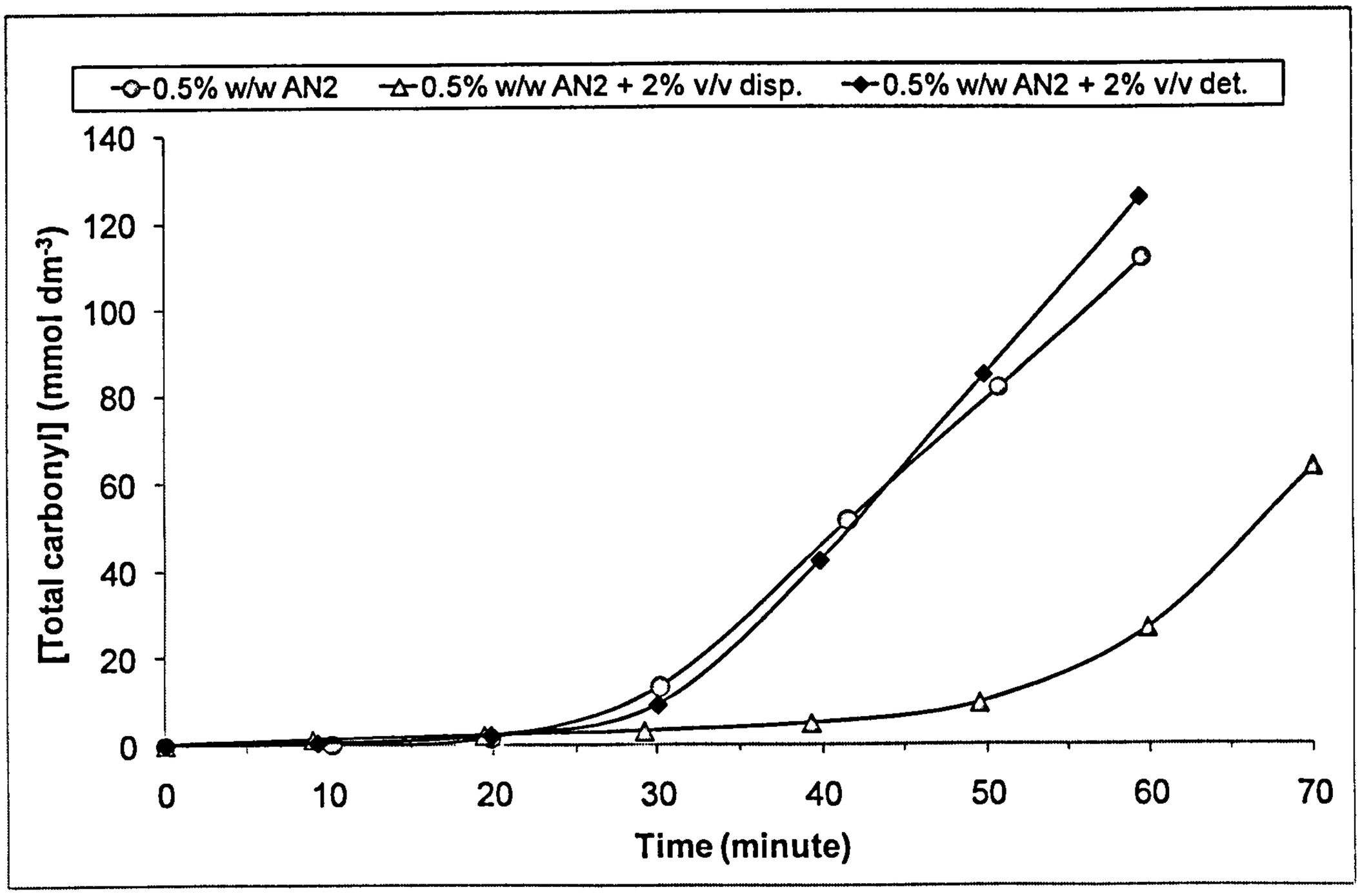

Figure 6.17: Total carbonyl formation (by FTIR) in the oxidation of AN2 with other additives in Shell XHVI 8.2 at 200 °C in flow intermediate reactor

It is possible that even in the absence of antioxidants, the base fluid may not degrade to give carbonyl species; this was demonstrated by an attempt to degrade squalane in the engine (Wilkinson, 2006). In 2004, Wilkinson (2006) degraded squalane (+ 2 % w/w calcium sulphonate detergent) in Ricardo Hydra engine (1500 rpm / half load) and compared degradation products of squalane from the top ring zone and a bench-top reactor. He tentatively identified only a single ketone from squalane in the top ring zone oil samples (Wilkinson, 2006, p.196-198). In 2007, the samples of squalane from the top ring zone were re-analysed (for this work) and the results were compared with data from a bench-top reactor (Figure 6.18). No oxidation products of squalane were found in the top ring zone samples. It can be demonstrated that the absence of the oxidation products (the biggest product is 352 g mol^{-1}) of squalane is unlikely to be due to the volatile loss of fragment oxidation products because much lighter oxidation products (220 g mol^{-1} for quinone and 234 g mol^{-1} for formylphenol) of AN2 were detected for this work (Figure 6.12). This observation would be consistent with the lubricant residence time being too short or the temperature of the top ring zone being not high enough, or the combination of both to sufficiently degrade the base fluid.

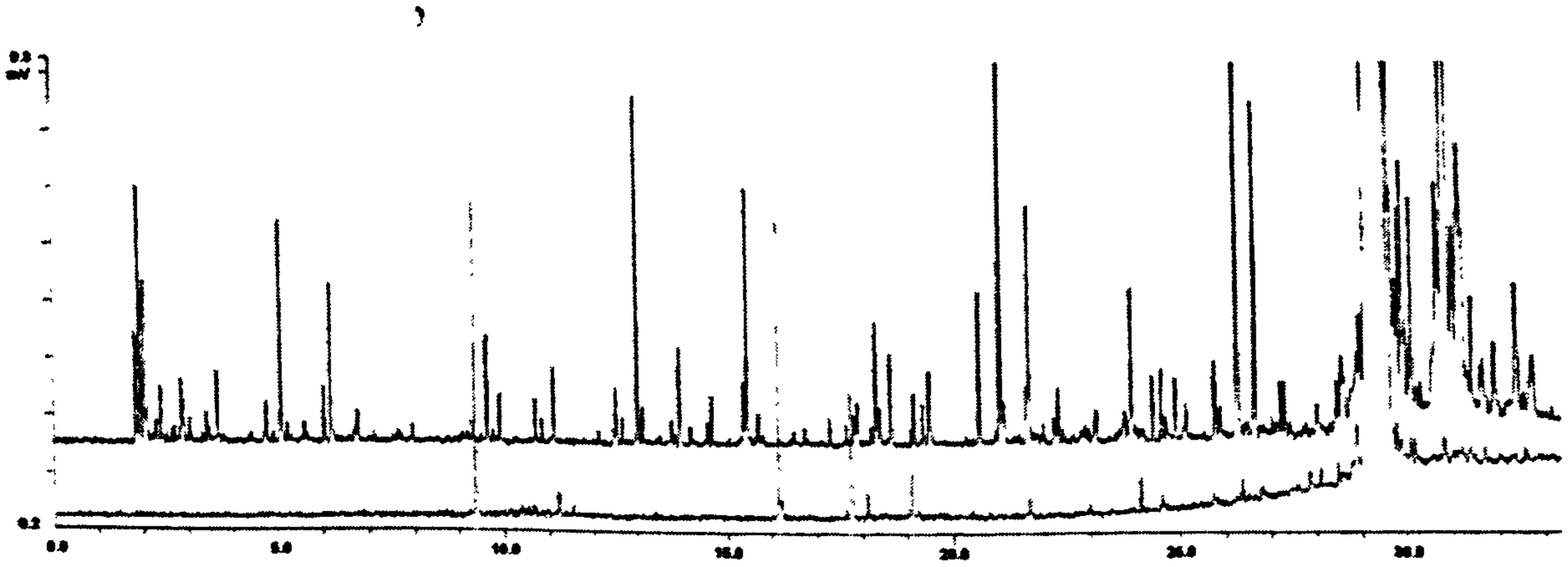

Figure 6.18: GC traces of degraded squalane (+ 2 % w/w calcium sulphonate detergent) in piston top ring zone for 2 hours[44] (bottom trace) and degraded squalane in flow intermediate reactor at 200 °C for 3 minutes (top trace)

Oil residence time in sump of Ricardo Hydra engine

The sump residence time has been defined as the time needed for all the oil in the engine to go through the piston ring pack once by Stark et al (2005). Using the sump and ring pack oil samples in Figure 6.11, the sump residence time for this engine run has been calculated (Stark et al, 2005) as:

[44] Sample belongs to Julian Wilkinson (see Wilkinson, 2006, p.196-198 for more details).

$$\text{Oil residence time in sump} = [\text{Galvinol}]_{\text{Ring pack}} / (\Delta[\text{Galvinol}]_{\text{Sump}} / \Delta(\text{time}))$$

Table 6.7: Oil flow in Ricardo Hydra engine (data from 0.5% AN2 blend, June 2006 tests). The error bar represents the standard error, which was obtained from Figure 6.11.

$[\text{Galvinol}]_{\text{Ring pack}}$ (mmol dm^{-3})	0.8
$\Delta[\text{Galvinol}]_{\text{Sump}}$ (mmol dm^{-3})	0.21
Δ(Time), time (hour)	6.0
Sump residence time (hour)	22.9
Sump volume (dm^{-3})	3.0
Normalised sump residence time (hour)	7.6 ± 1.0

The oil residence time in the sump of Ricardo Hydra at 1500 rpm and half load was previously found to be 46 ± 2 hours (Stark et al, 2005) and 7.6 ± 1.0 hours for this work (Table 6.7) using the same measurement method (Stark et al, 2005). The discrepancy in oil residence time between the two studies is probably due to the nature of marker species used in each study. The marker species were total carbonyl (i.e. 1760-1690 cm^{-1}) for the former study and galvinol (from AN2) for the latter study. The formulation used in the Stark et al (2005) study had no detergent or dispersant additives, which may have caused the carbonyl species to drop out of solution in the sump, and hence be underrepresented in the sump oils samples extracted from the engine; in contrast, galvinol is soluble due to the presence of a detergent and not precipitated in the sump unlike the ketones, also, galvinol was monitored by liquid chromatography at 400 nm (± 20 nm); where no other species absorb[45] (Figure 6.19).

[45] At 400 nm (± 20 nm), in Shell XHVI8.2 (+det.&disp.) no species interfere with the absorption of galvinol but in a fully-formulated oil other additives interfere with the absorption of galvinol.

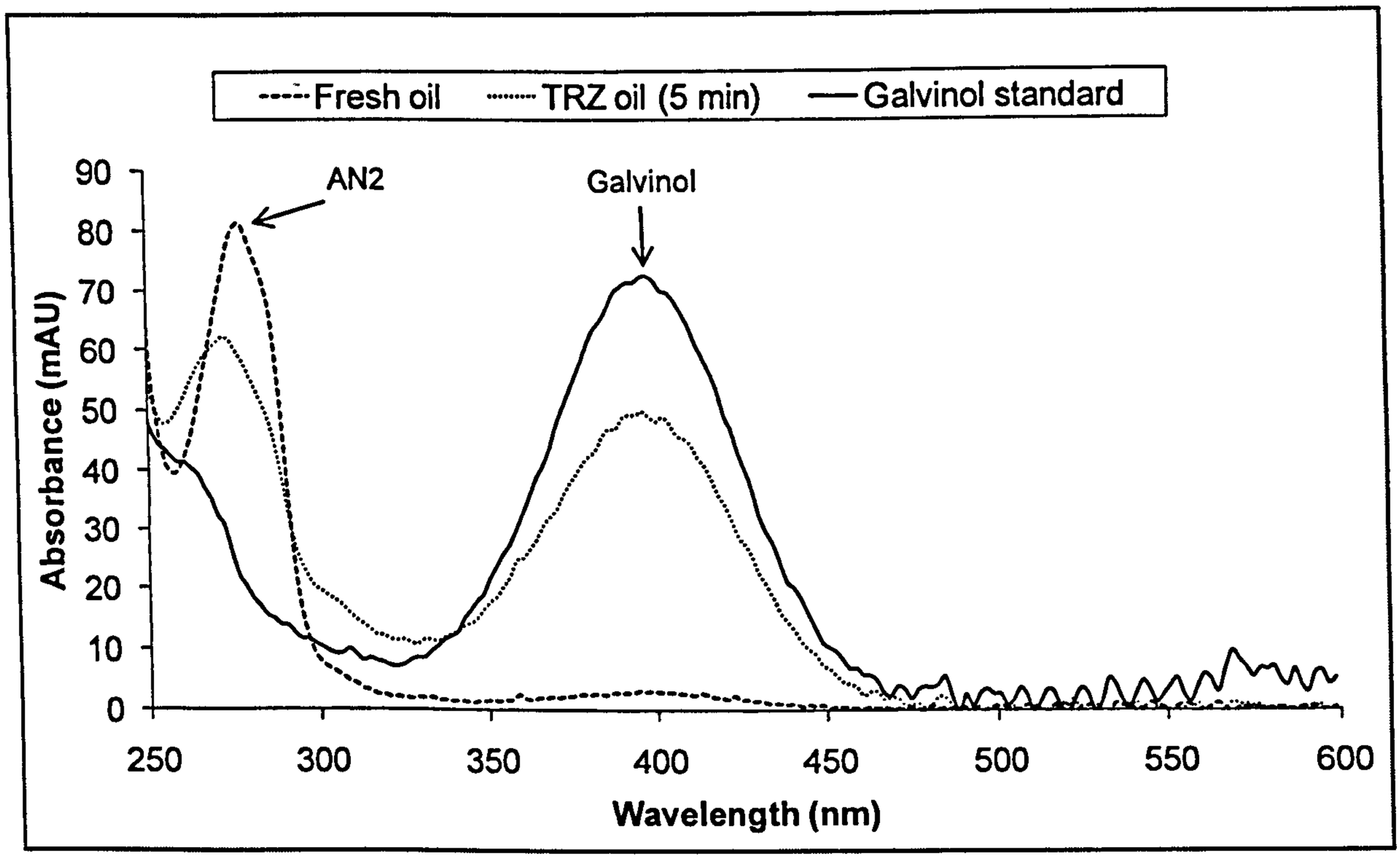

Figure 6.19: LC spectra of intact and degraded 0.5 % w/w AN2 in Shell XHVI 8.2 (+det.&disp.) from top ring zone of Ricardo Hydra engine compared with that of a galvinol standard

Estimation of top ring zone temperature by chemical analysis

Direct measurement of the temperature of the top ring zone of the piston assembly of the Ricardo Hydra engine has not yet been successful (Wilkinson, 2006, p.187); and so, the temperature was estimated by combining data from the chemical analysis of samples from the top ring zone of the Ricardo Hydra engine and from the flow intermediate bench-top reactor.

Engine results for AN2 and Amine101, show that, in the top ring zone, AN2 and Amine101 are consumed by 70 % (Figure 6.6) and 60 % (Figure 6.9), respectively. Using the previously measured ring pack residence time of 60 ± 15 seconds (Ricardo Hydra, 1500 rpm / half load; Stark et al, 2005), an estimate can be made using bench-top oxidation experiments of the temperature required to give 70 % and 60 % oxidation to AN2 (Figure 6.20) and Amine 101 (Figure 6.21), respectively. The 0.0 intercept was used to get the temperature because this intercept corresponds to one minute.

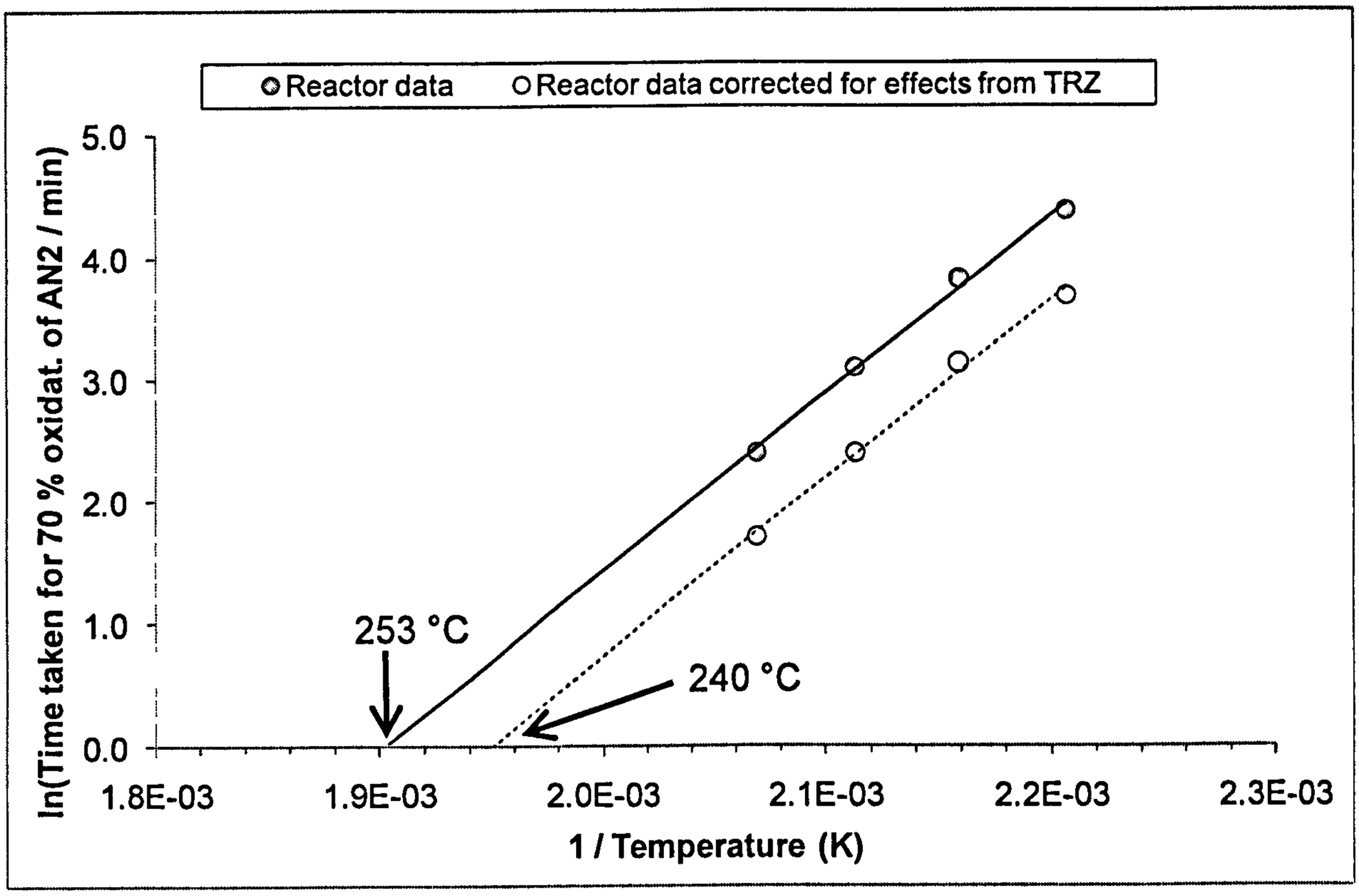

Figure 6.20: Time taken for 70 % of AN2 to be oxidised in the oxidation of 10.0 mmol dm^{-3} AN2 in squalane at 180-210 °C in flow intermediate reactor

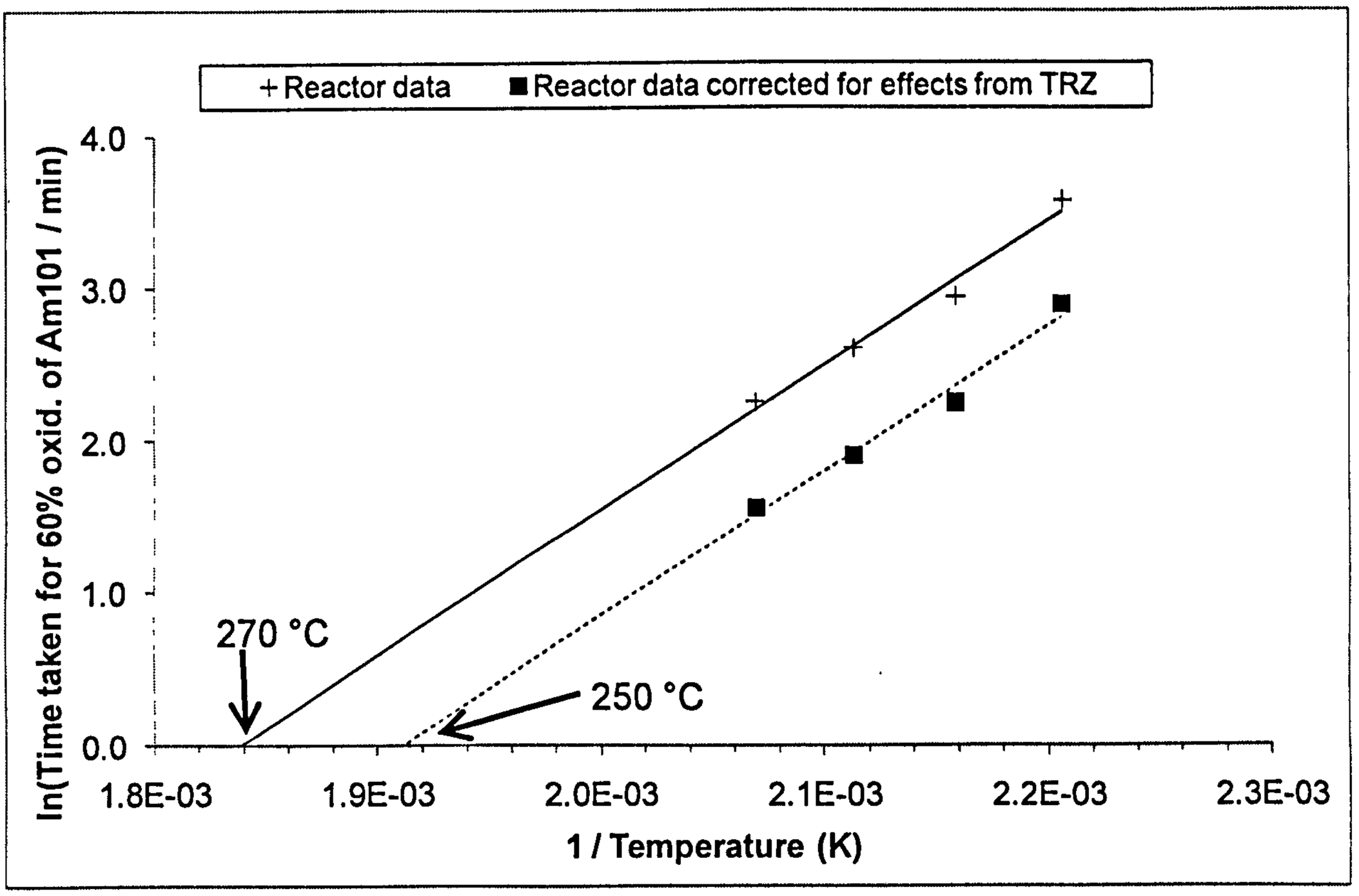

Figure 6.21: Time taken for 60 % of Amine101 to be oxidised in the oxidation of 10.0 mmol dm^{-3} Amine101 in squalane at 180-210 °C in flow intermediate reactor

However, the presence of other species such as nitrogen oxides, paramagnetic compounds,[46] and fuel affects the temperature estimation. The effect of the environment in the top ring zone on antioxidant oxidation was estimated by noting the difference in reaction times of oxidations of AN2 in squalane in bench-top reactor with blowby from top ring zone and pure oxygen (Figure 6.22).

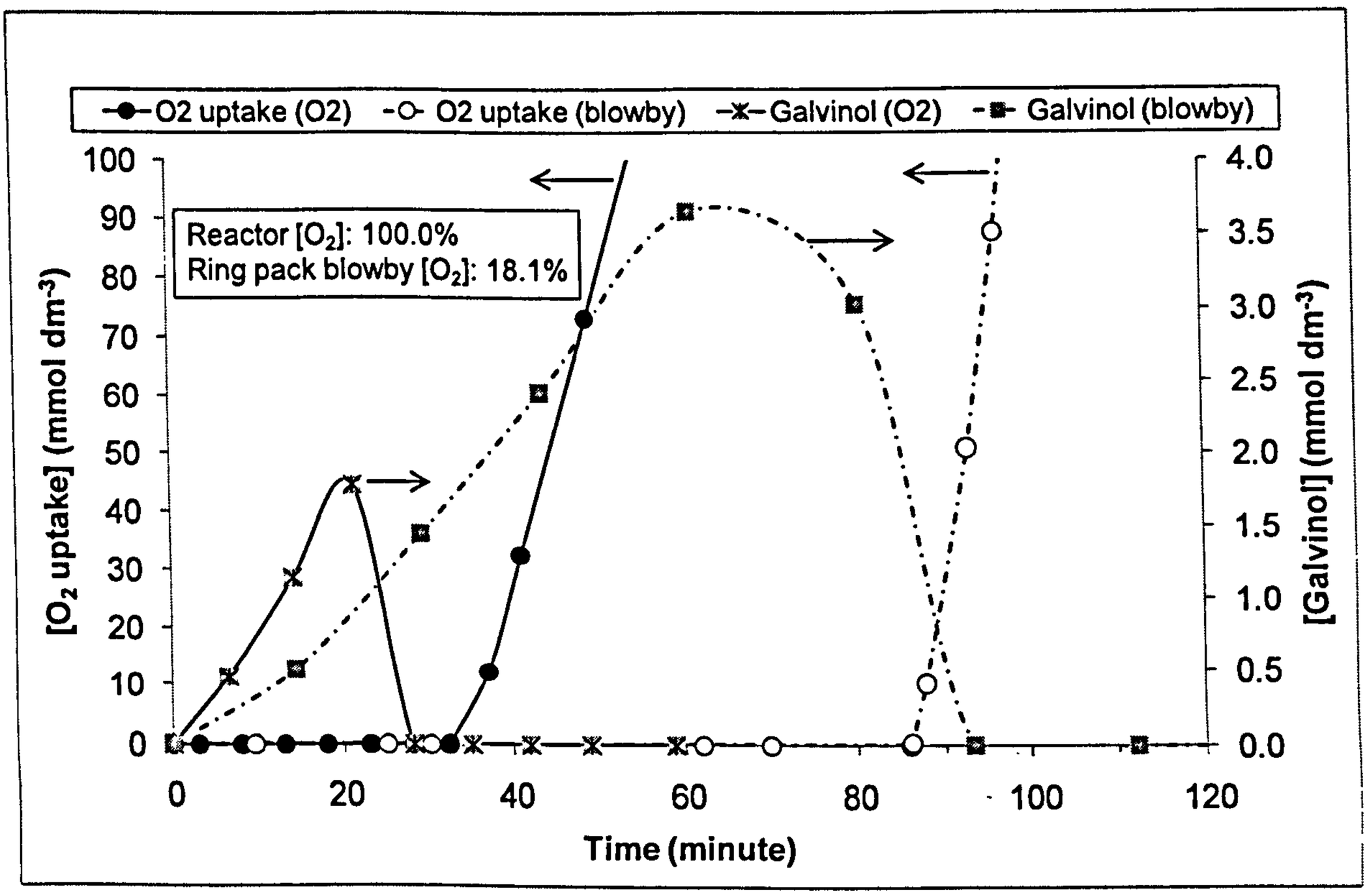

Figure 6.22: Oxidation of 10.0 mmol dm^{-3} (with O_2) or 9.4 mmol dm^{-3} (with TRZ blowby) AN2 in 5.0 cm^3 squalane at 200 °C in flow intermediate reactor

After taking the piston environment into account, the temperature of the top ring zone of Ricardo Hydra engine at 1500 rpm and half load is found to be roughly 240 °C for AN2 and 250 °C for Amine101, as upper limits.

The estimated temperature for the top ring zone of the piston assembly of the Ricardo Hydra engine is inline with experimental literature values (Table 6.8).

[46] These paramagnetic compounds are oxygenated because they form in the presence of oxygen but not in the presence of nitrogen. Their number is 0.9×10^{12} to 8.3×10^{13} in 1 mg of oil (Shimonaev and Zakharov, 1967).

Table 6.8: Piston temperatures of gasoline engines (references within table)

Fuel injection[47]	Measured location	Temp. (°C)	Measurement method	Conditions	Reference
Direct	Top land	297	Infrared telemetry	4500 rpm / full load	Opris et al, 1998
Unknown	Top land	242	Hardness-change technique	4600 rpm / full load	Li, 1982
Unknown	Second land	160	K-type thermocouple	3000 rpm / full load	Moritani and Nozawa, 2004
Unknown	Top ring groove	280	K-type thermocouple	≈4500 rpm / ? load	Kim et al, 1998
Unknown	Top ring groove	220	Thermocouple	3500 rpm / full load	Tada and Furuhama, 1964
Indirect	Top ring zone	< ~250	Chemical analysis	1500 rpm / half load	This work

Oil sample flow

The oil sampling used in this study was based on a well-established technique (Table 6.9).

Table 6.9: Studies used top ring zone sampling technique (references within table)

Engine	Type	Reference
Unknown	Unknown	Quillian et al, 1964
Diesel	Caterpillar	Saville et al, 1988
Diesel	Petter AA1	Bush et al, 1991
Diesel	Petter AA1	Singleton, 1993
Gasoline	Petter W1	Thomson, 1995
Gasoline	Petter W1	Fox et al, 1997
Diesel	Petter AA1 and Caterpillar	Fox et al, 1997a
Gasoline	Petter W1 and Mercedes Benz M111E	Pease, 2001
Gasoline and Diesel	Petter W1 and Petter AA1, respectively	Stow, 2001
Gasoline	Ricardo Hydra	Gamble, 2002
Gasoline	Ricardo Hydra	Hammond, 2003
Gasoline	Petter W1	Datoo and Fox, 2003
Gasoline	Unknown	Moritani and Nozawa, 2004
Gasoline	Ricardo Hydra	Stark et al, 2005
Gasoline	Ricardo Hydra	Lee, 2006
Gasoline	Petter W1	Aruna et al, 2006
Gasoline	Ricardo Hydra	Wilkinson, 2006
Gasoline	Ricardo Hydra	Smith, 2007

The oil sample flow from the top ring zone was periodical whether the piston rings were unpinned (Figure 6.13 and Figure 6.14) or pinned (Figure 6.15), which suggest that the rings rotation and the expected consequent occasional loss of oil through the combustion chamber (Lusted, 1994) is not responsible for the irregular flow of oil sample. The other factor that might have an effect is the 1/8" Teflon tube that carries the sample from the top ring zone to the sample vial. The oil mist from the top ring zone condenses in the tube to form droplets that then move along to

[47] Crown temperatures of direct fuel engines are ~~50 °C higher than those of indirect fuel injection engines (Opris et al, 1998).

the other side of the tube. Some of the mist goes straight to the vial and some condense on the tube to form droplets that grow in size as more mist passes through. When the droplets reach a critical size, they move down along the tube dragging with them small immature droplets. The process is repeated every a few seconds. The rate of formation and transfer of the oil sample droplets are expected to be responsible for the erratic flow of the oil samples.

6.4. SUMMARY

The behaviour of antioxidants in semi-formulated base fluids has been studied, to understand how antioxidants behave and decay under piston top ring zone conditions and to complement data from bench-top reactors, by degradation in a research gasoline engine.

The levels of antioxidants in the top ring zone varied from ~30 to ~95 % and ~60 % when the piston rings were unpinned and pinned, respectively. Pinning the piston rings greatly enhanced the precision of top ring zone data.

The XHVI 8.2 base fluid (assumed to be the same as the re-analysed squalane sample), with or without antioxidants, was not degraded by the engine at 1500 rpm and half load. This was rationalised by the oil residence time in the top ring zone being too short (i.e. a few seconds) and/or the temperature of the top ring zone was not high enough to sufficiently degrade the base fluid. Thus, the observed carbonyl formation is not from the degradation of the base fluid. One of the confirmed sources of carbonyl was found to be the succinimide dispersant

The oil residence time in the sump was found to be 7.6 ± 1.0 hours and the temperature of the top ring zone was estimated to be ~250 °C as an upper limit.

6.5. REFERENCES

Aruna, M.; Datoo, A.; and Fox, M. Differentiation between 'good', 'borderline', and 'poor' ASTM lubricant standards by ring zone sampling and multivariate data analysis. *Proceedings of the Institution of Mechanical Engineers Part D Journal of Automobile Engineering*, 2006, **220** (D2): 177-185.

Bigarre, I. and Legeron, J. Antioxidant kinetics in synthetic lubricants field testing. *Journal of Synthetic Lubrication*, 1987, **4** (3): 203-218.

Bush, G.; Fox, M.; Picken, D.; and Butcher, L. Composition of lubricating oil in the upper ring zone of an internal combustion engine. *Tribology International*, 1991, **24** (4): 231-233.

Datoo, A. and Fox, M. (Authors); Dowson, D.; Priest, M.; Dalmaz, G.; and Lubrecht, A. (editors) An initial investigation of lubricant condition in the automotive ring zone under cold start conditions. *Tribological Research and Design for Engineering Systems*, 2003: 517-522.

Duchesne, R.; Stunnenberg, F.; Tequi, P.; and Lecroq, S. Development of an engine test prediction model for the evaluation of engine lubricants based on multiple laboratory bench tests. *Society of Automotive Engineers Special Publication*, 2000, paper 2000-01-1814: 59-65.

Fox, M.; Jones, C.; Picken, D.; and Stow, C. The "limits of lubrication" concept applied to the piston ring zone lubrication of modern engines. *Journal Tribology Letters*, 1997a, **3** (1): 99-106.

Fox, M.; Picken, D.; Symons, M.; and Thomson, A. Paramagnetic species in I/C engine top ring zone lubricant samples. *Tribology International*, 1997, **30** (6): 417-422.

Gamble, R. Influence of lubricant degradation on piston assembly tribology. PhD Thesis, University of Leeds, 2002.

Hamblin, P. and Rohrbach, P. Piston deposit control using metal-free additives. *Lubrication Science*, 2001, **1** (14): 3-23.

Hammond, C. A mechanistic study of the autoxidation of ketones in the liquid phase, PhD thesis, University of York, 2003.

Hsu, S. and Lin, R. Interactions of additives and lubricating base oils. *SAE Technical Paper*, 1983, paper 831683: 61-69.

Inoue, K. and Yamanaka, Y. Change in performance of engine oils with degradation. *SAE Technical Paper*, 1990, paper 902122: 1-10.

Kim, J.; Min, B.; Lee, D.; Oh, D.; and Cho, J. The characteristics of carbon deposit formation in piston top ring groove of gasoline and diesel engine. *Society of Automotive Engineers Special Publication*, 1998, paper 980526: 147-154.

Kinker, B.; Romaszewski, R.; and Palmer, P. ROBO a bench procedure to replace sequence IIIGA engine test. RohMax Internal Report, private communication.

Kudynska, J. and Buckmaster, H. Oxidation of motor oils at crankcase temperatures further studies. *Fuel*, 1997, 76 (2): 195-198.

Lashki, V. and Vipper, A. Correlation between laboratory and single-cylinder engine tests on motor oils. *Chemistry and Technology of Fuels and Oils*, 1979, **15** (1): 55-57.

Lee, P. Lubricant degradation transport and the link to piston assembly tribology. PhD Thesis, University of Leeds, 2006.

Li, C. Piston thermal deformation and friction considerations. *SAE Technical Paper*, 1982, paper 820086: 1-15.

Lusted, R. Direct observation of oil consumption mechanisms techniques. Master of Science dissertation, Massachusetts Institute of Technology, 1994.

Mahoney, L.; Otto, K.; Korcek, S.; and Johnson, M. The effect of fuel combustion products on antioxidant consumption in a synthetic engine oil. *Industrial and Engineering Chemistry Product Research and Development*, 1980, **19** (1): 11-15.

Min, B.; Kim, J.; Oh, D.; and Choi, J. Dynamic characteristics of oil consumption relationship between the instantaneous oil consumption and the location of piston ring gap. *SAE Technical Paper*, 1998, paper 982442: 55-64.

Moritani, H. and Nozawa, Y. Oil degradation in second-land region of gasoline engine pistons. *R&D Review of Toyota CRDL*, 2004, **38** (3): 36-43.

Muller, K.; Kristen, U.; and Hamblin, P. Effectiveness of ashless antioxidants in motor oils. From: Wirksamkeit von aschefreien antioxidantien in motorolen. *Schmiertechnik Tribologie*, 1982, **29** (3): 92-97.

Opris, M.; Jason, R.; and Anderson, C. A comparison of time-averaged piston temperatures and surface heat flux between a direct-fuel injected and carburated two-stroke engine. *SAE Technical Paper*, 1998, paper 980763: 107-116.

Pease, N. Top ring zone oil sampling in gasoline engines. PhD thesis, De Montfort University, 2001.

Quillian, R.; Meckel, N.; and Moffitt, J. Cleaner crankcases with blowby diversion. *SAE Transactions*, 1964: 295-312.

Saville, S.; Gainey, F.; Cupples, S. Fox, M.; and Picken, D. A study of lubricant condition in the piston ring zone of single cylinder diesel engines under typical operating conditions. *SAE Technical Paper*, 1988, paper 881586.

Schneider, E. and Blossfeld, D. Method for measurement of piston ring rotation in an operating engine. *SAE Technical Paper*, 1990, paper 900224: 1-7.

Shimonaev, G. and Zakharov, G. Formation of stable paramagnetic compounds during the oxidation of motor oils. Translated from Russian by SciFinder Scholar from *Neftekhimiya*, 1967, **7** (4): 623-626.

Singleton, N. The chemical and physical analyses of new and degraded lubricating oils. PhD thesis, De Montfort University, 1993.

Smith, O. In-cylinder fuel and lubricant effects on gasoline engine friction. PhD thesis, University of Leeds, 2007.

Stark, M.; Gamble, R.; Hammond, C.; Gillespie, H.; Lindsay Smith, J.; Nagatomi, E.; Priest, M.; Taylor, C.; Taylor, R.; and Waddington, D. Measurement of lubricant flow in a gasoline engine. *Tribology Letters*, 2005, **19** (3): 163-168.

Stecher, F. Analysis of piston ring packs for combustion engines. *SAE Technical Paper*, 1979, paper 790863: 1-7.

Stow, C. Studies of lubricant degradation soot aggregation and soot morphology in the top ring zone of internal combustion engines. PhD thesis, De Montfort University, 2001.

Tada, T. and Furuhama, S. On the heat flow from the piston in a farm type gasoline engine. *Bulletin of JSME*, 1964, **7** (28): 784-791.

Thomson, A. An accelerated method to assess lubricant degradation in the piston ring zone of spark ignition engines. PhD thesis, De Montfort University, 1995.

Wilkinson, J. The autoxidation of branched hydrocarbons in the liquid phase as models for understanding lubricant degradation. PhD thesis, University of York, 2006.

Yasutomi, S.; Maeda, Y.; and Maeda, T. Kinetic approach to engine oil 2 antioxidant decay of lubricant in engine system. *Industrial and Engineering Chemistry Product Research and Development*, 1981, **20** (3): 536-540.

7. EFFECTS OF ADDITIVE INTERACTIONS ON LUBRICANT STABILITY

7.1. INTRODUCTION

A typical automotive engine lubricant consists of a base fluid (~75-95 % mass) and additives (~25-5 % mass) that enhance the quality of the lubricant (Taylor et al, 2005). Lubricant additives can interact with each other; the nature of interaction depends on the chemical nature of the reactants and the extent of interaction is concentration dependent (Hsu and Lin, 1983; and Pawlak, 2003).

In addition to additive-additive interactions, the behaviour of additives can be affected by sulphur compounds in the base fluid (Hsu et al, 1982), fuel from the combustion chamber (Cracknell and Head, 2005), blowby nitrogen oxides (Korcek and Johnson, 1993), and engine wear metals (Colclough, 1987).

The aim of this chapter is to investigate the interactions of antioxidants with other automotive lubricant additives, by degradation in bench-top reactors and a research gasoline engine, to provide lubricant formulators with a good understanding of the nature and extent of interactions between antioxidants and other lubricant additives (e.g. dispersants and detergents) so that they would formulate better lubricants. Chemical structures of starting materials and oxidation products are listed in Table 7.1.

Table 7.1: Chemical structures and names of starting materials and oxidation products

Structure	CAS name	Abbreviation
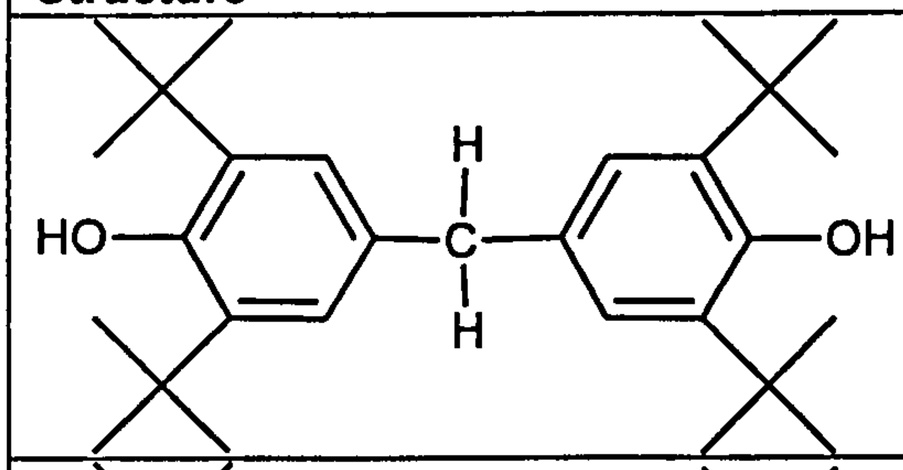	4,4'-Methylenebis[2,6-bis(1,1-dimethylethyl)]phenol	AN2
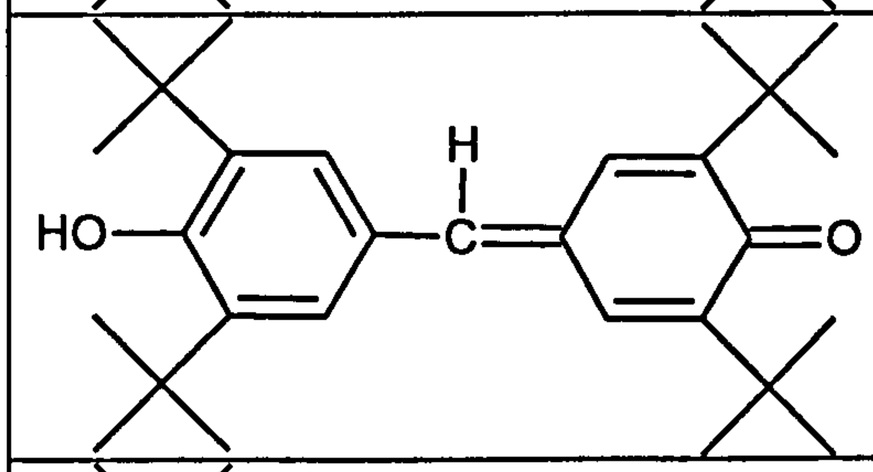	4-[[3,5-Bis(1,1-dimethylethyl)-4-hydroxyphenyl]methylene]-2,6-bis(1,1-dimethylethyl)- 2,5-cyclohexadien-1-one	Galvinol
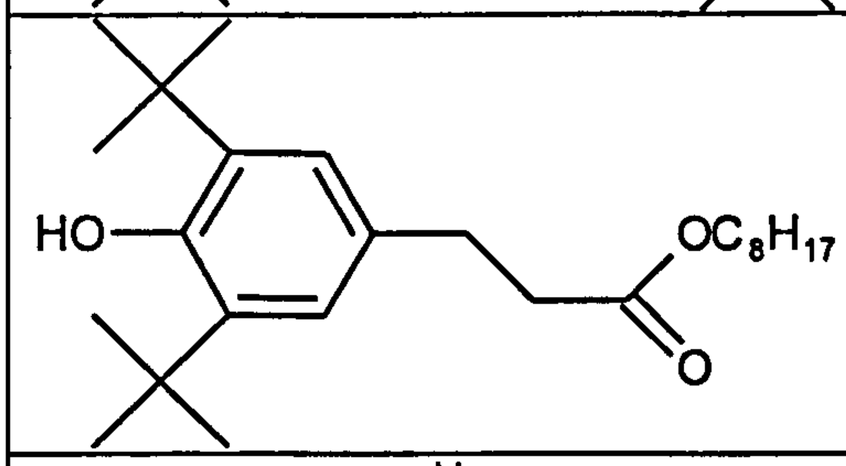	3,5-Di-tert-butyl-4-hydroxyhydrocinnamate	Irganox L135
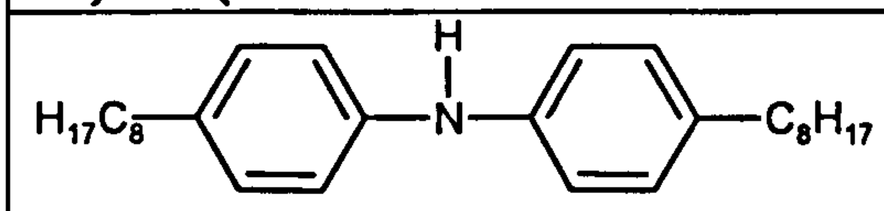	4-Octyl-N-(4-octylphenyl)benzenamine	Amine101
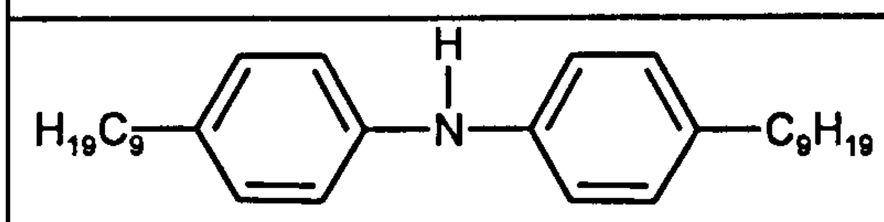	4-Nonyl-N-(4-nonylphenyl)benzenamine	Naugalube 438L
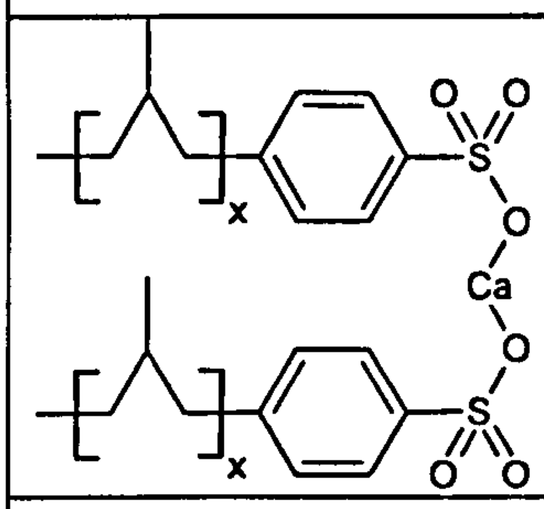	[Neutral calcium alkyl sulphonate detergent]	Sulphonate detergent
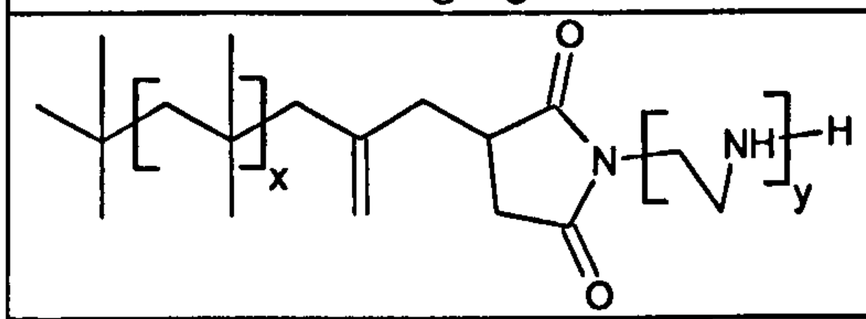	[Succinimide dispersant]	Succinimide dispersant
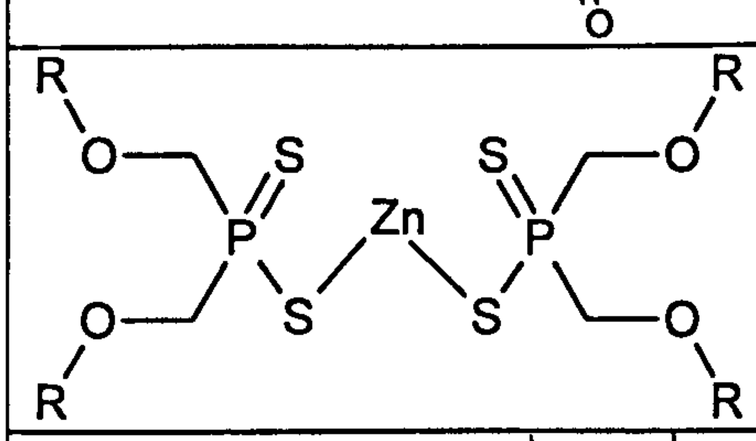	[Zinc dithiophosphate] {Secondary (secondary-C4 [85 m %] & primary-C8 [15 m %] alcohols) ZDDP}	ZDDP
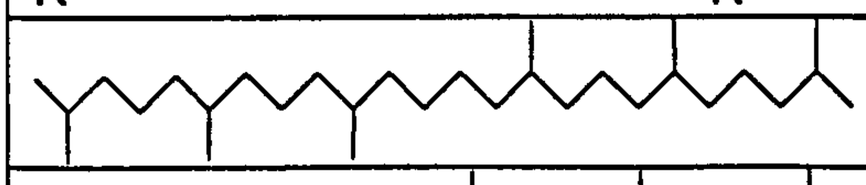	2,6,10,15,19,23-Hexamethyltetracosane	Squalane
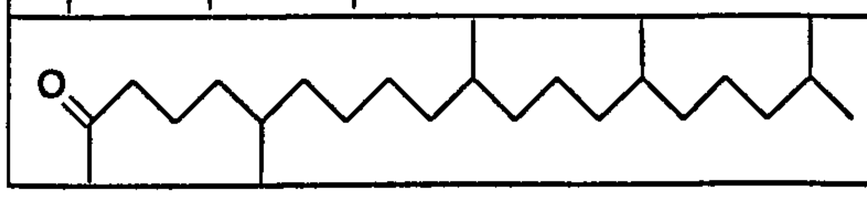	6,11,15,19-Tetramethyl-2-eicosanone	-

7.2. RESULTS

This section is divided in to four subsections:

7.2.1.: Interactions of additives in squalane in a bench-top reactor
7.2.2.: Interactions of additives in Shell XHVI 8.2 in a bench-top reactor
7.2.3.: Interactions of commercial additives in semi-formulated lubricants
7.2.4.: Interactions of additives in semi-formulated base fluids in a gasoline engine

7.2.1. Interactions of additives in squalane in a bench-top reactor

Antioxidants plus other additives were oxidised in squalane at 200 °C in the flow intermediate reactor to have a better understanding of the interactions between antioxidants and other lubricant additives.

Details of the examined blends are listed in Table 7.2.

Table 7.2: Details of blends in 5.0 cm^3 squalane

Blend	AN2	Amine101	Succinimide dispersant	Sulphonate detergent	ZDDP
	10.0 mmol dm^{-3} (or 0.5 % w/w)	10.0 mmol dm^{-3} (or 0.5 % w/w)	2.0% v/v	2.0% v/v	1.0% v/v
Squalane					
AN2	√				
Amine101		√			
AN2+Amine101	√	√			
AN2+Am101+disp.	√	√	√		
AN2+Am101+disp.+det.	√	√	√	√	
AN2+Am101+disp.+det.+Z.	√	√	√	√	√
AN2+Am101+ZDDP	√	√			√

Figure 7.1 shows the level of oxygen uptake in the presence of different blends; with AN2+Am101+disp.+det.+Z. and AN2+Am101+ZDDP blends being the most effective in retarding the oxygen uptake (it should be noted that the oxygen uptake for the above blends remain on axis at 180 minutes).

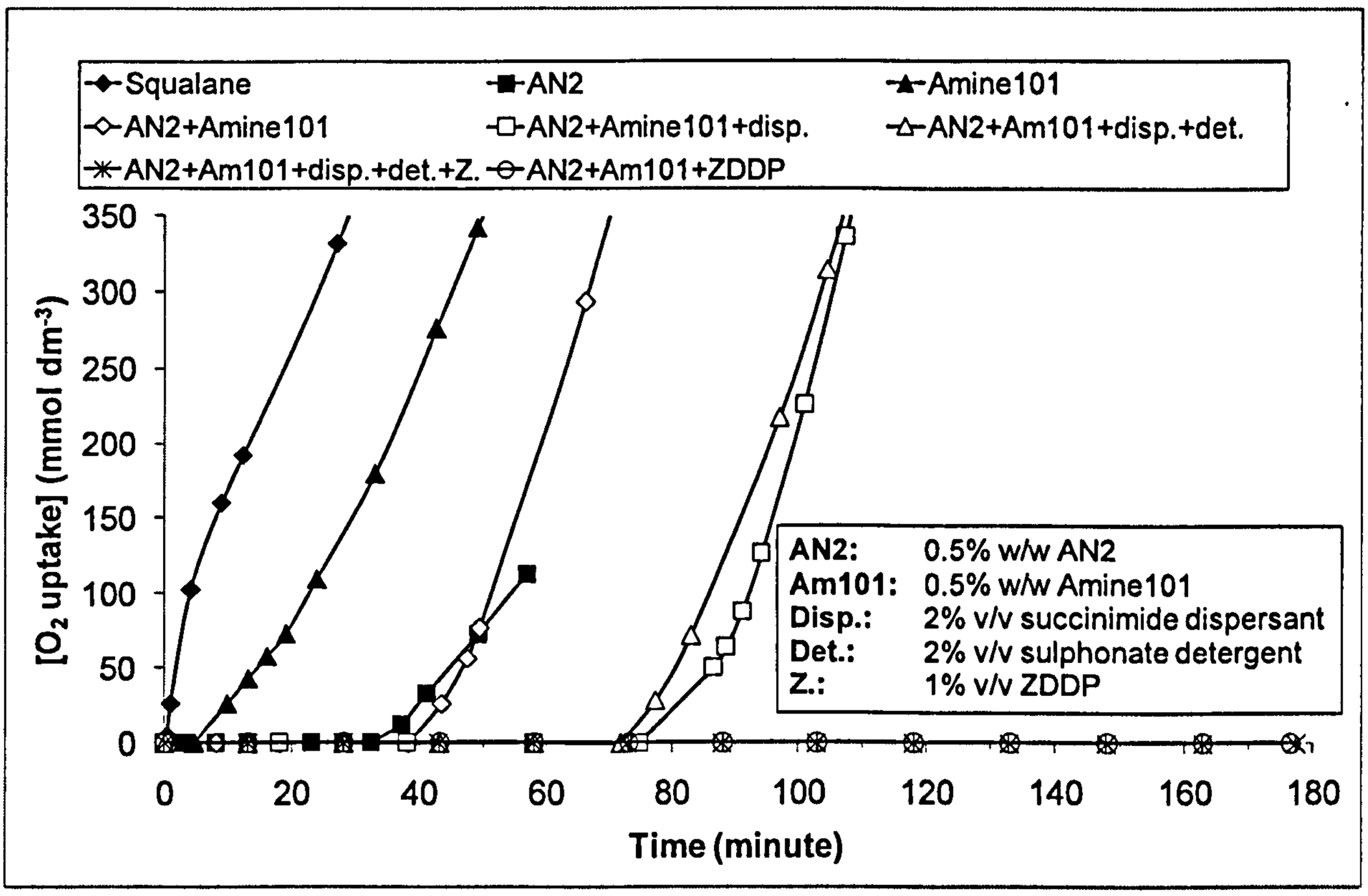

Figure 7.1: Oxygen uptake in the oxidation of additives in squalane at 200 °C in flow intermediate reactor

Figure 7.2 shows the formation of total hydroperoxide in the presence of different blends; with AN2+Am101+disp.+det.+Z. and AN2+Am101+ZDDP blends being the most effective in retarding hydroperoxide formation. The hydroperoxide level in some of the blends was not measured due to time restriction.

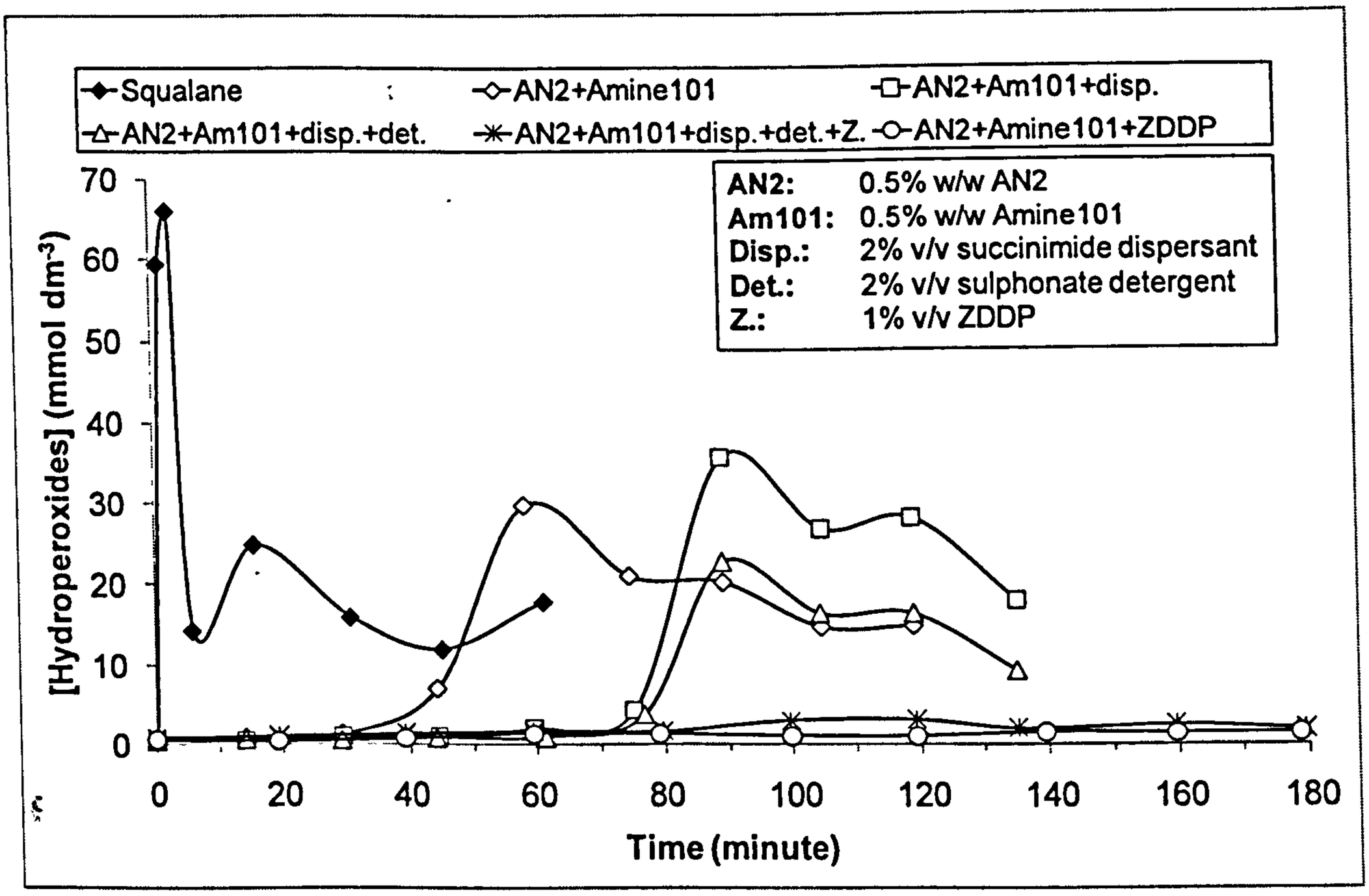

Figure 7.2: Hydroperoxides formation in the oxidation of additives in squalane at 200 °C in flow intermediate reactor

Figure 7.3 shows the formation of total carbonyl in the presence of different blends; with AN2+Am101+disp.+det.+Z. and AN2+Am101+ZDDP blends being the most effective in retarding carbonyl formation. The carbonyl level for squalane was not measured due to time restriction.

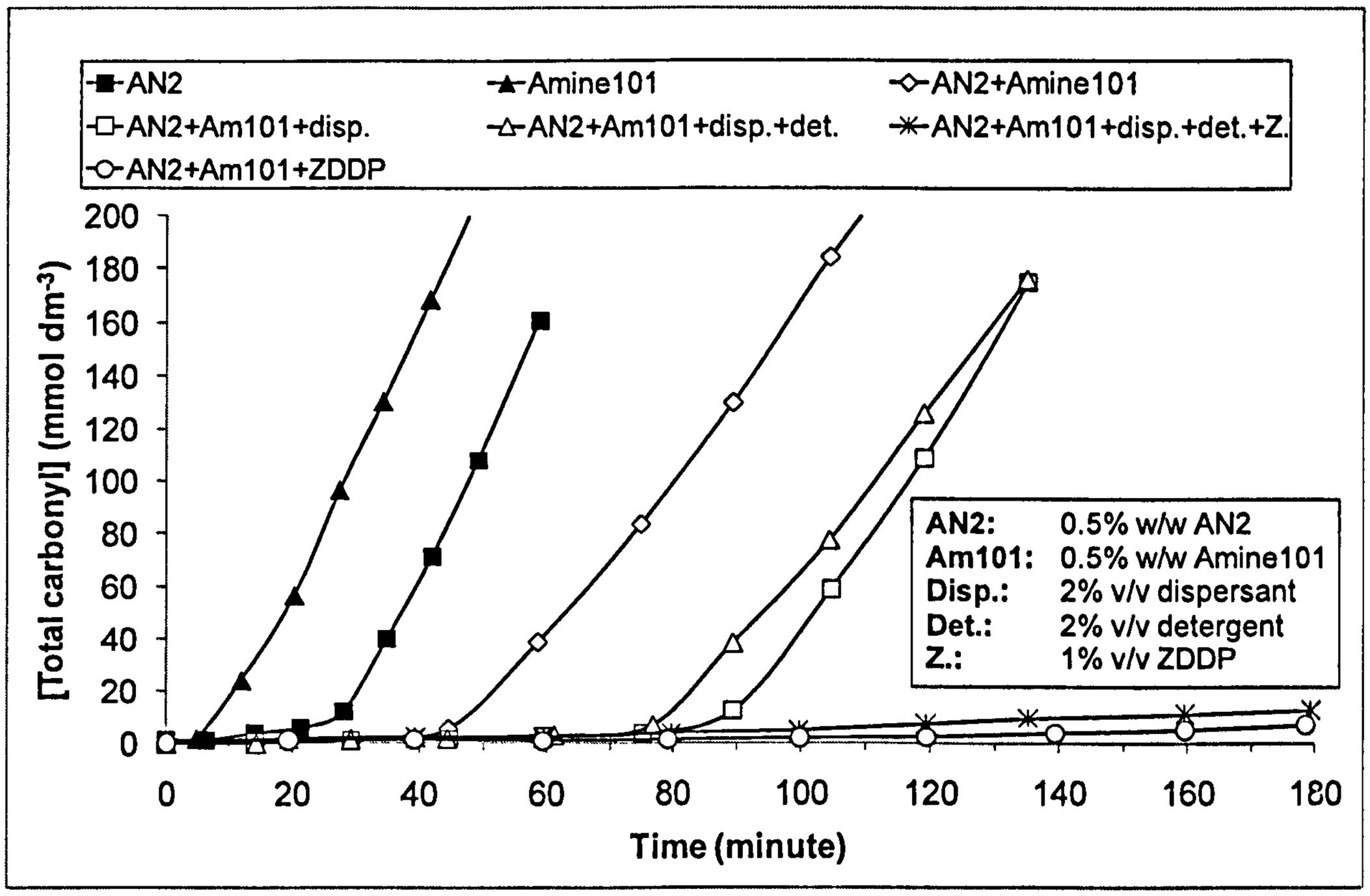

Figure 7.3: Total carbonyl formation (by FTIR) in the oxidation of additives in squalane at 200 °C in flow intermediate reactor

Figure 7.4 shows the formation of one of the ketones from squalane. Ketone 6,11,15,19-tetramethyl-2-eicosanone was chosen as a representative oxidation product from the model base fluid because it was the biggest observed ketone and hence its quantity was not affect by volatility at high reaction temperatures.

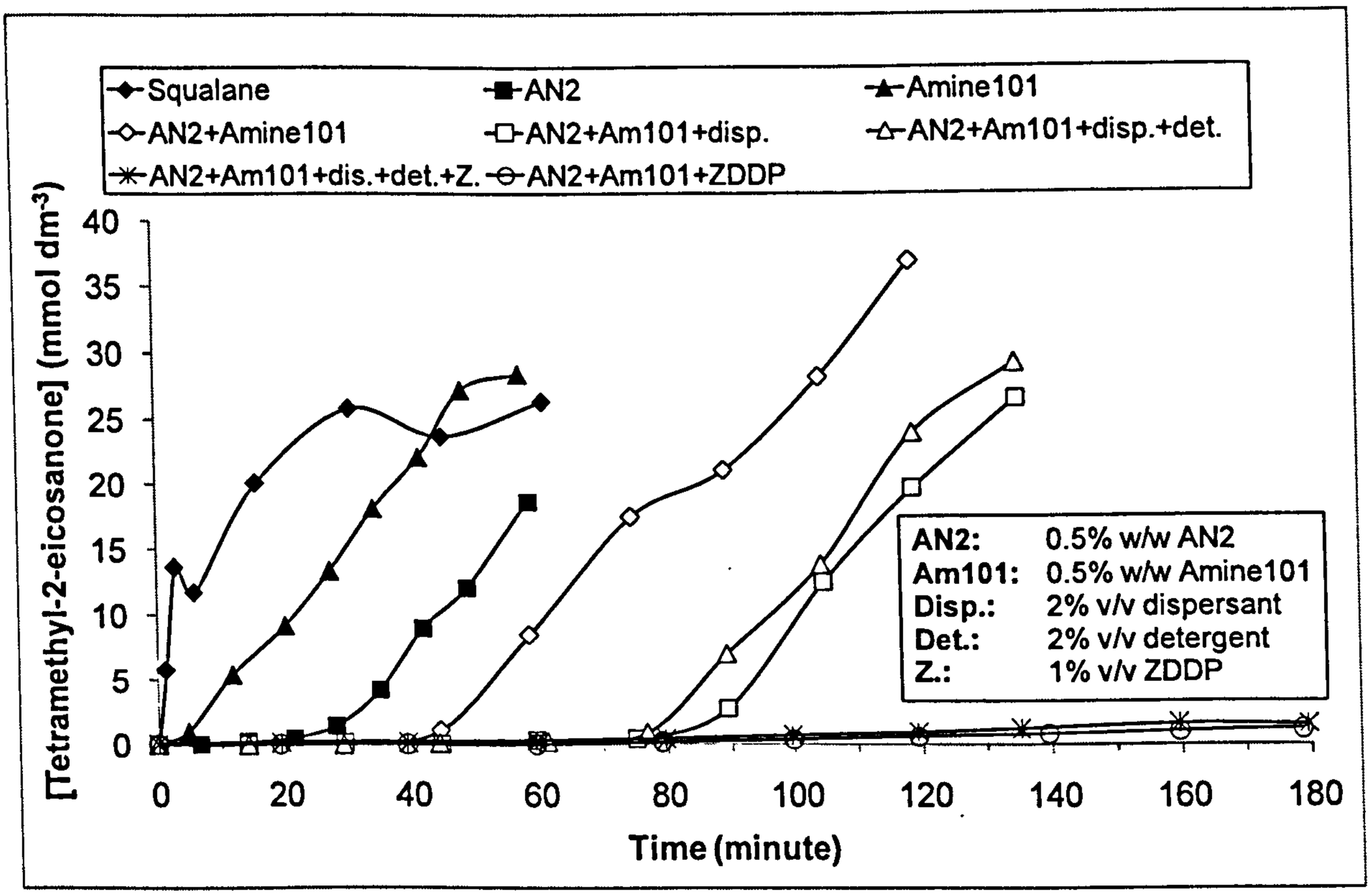

Figure 7.4: 6,11,15,19-tetramethyl-2-eicosanone (from squalane) formation (by GC) in the oxidation of additives in squalane at 200 °C in flow intermediate reactor

Figure 7.5 shows the decay of Amine101 in different blends. Amine101 lasts the longest in AN2+Am101+disp.+det.+Z. blend.

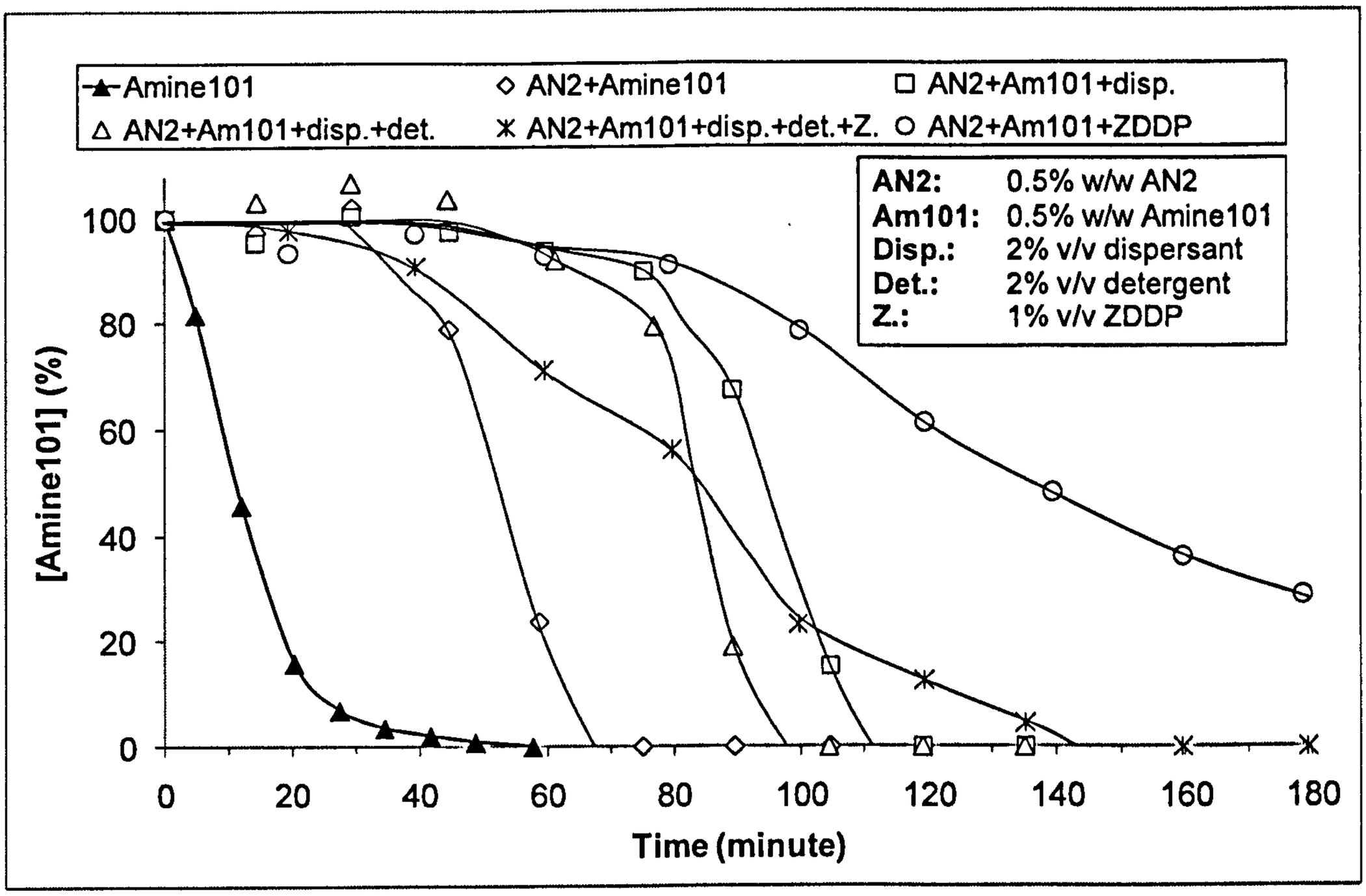

Figure 7.5: Decay of Amine101 (by GC) in the oxidation of additives in squalane at 200 °C in flow intermediate reactor

Figure 7.6 shows the decay of AN2 in different blends. AN2 lasts the longest in AN2+Am101+disp.+det.+Z. blend.

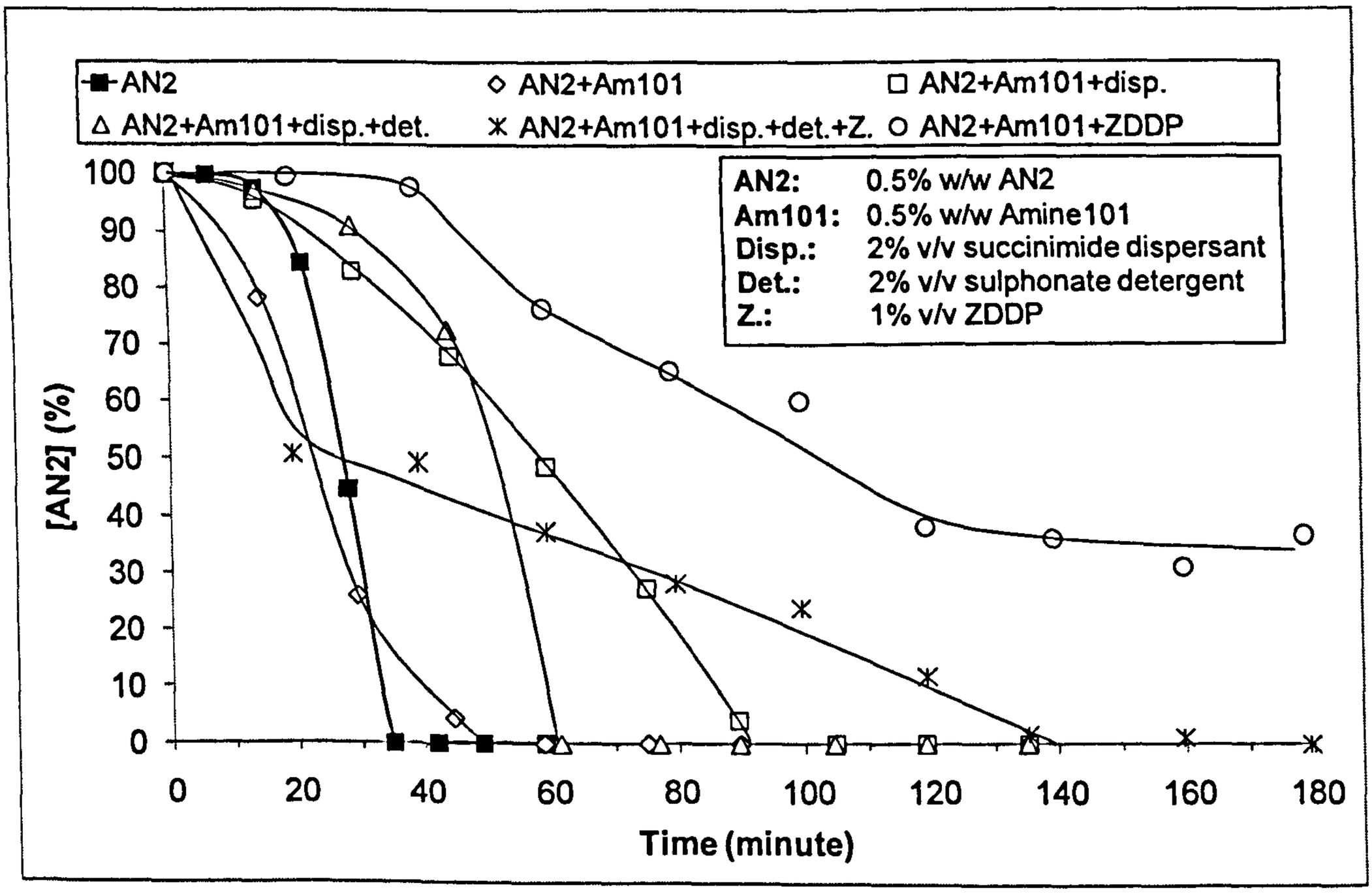

Figure 7.6: Decay of AN2 (by FTIR) in the oxidation of additives in squalane at 200 °C in flow intermediate reactor

Figure 7.7 shows the formation of galvinol (from AN2) in different blends. The concentrations of the other AN2 oxidation products (i.e. formylphenol and quinone) are available in Appendix D. The quantities of intermediates of AN2 formed in the presence of other additives aids the understanding of how intermediates interact with other additives.

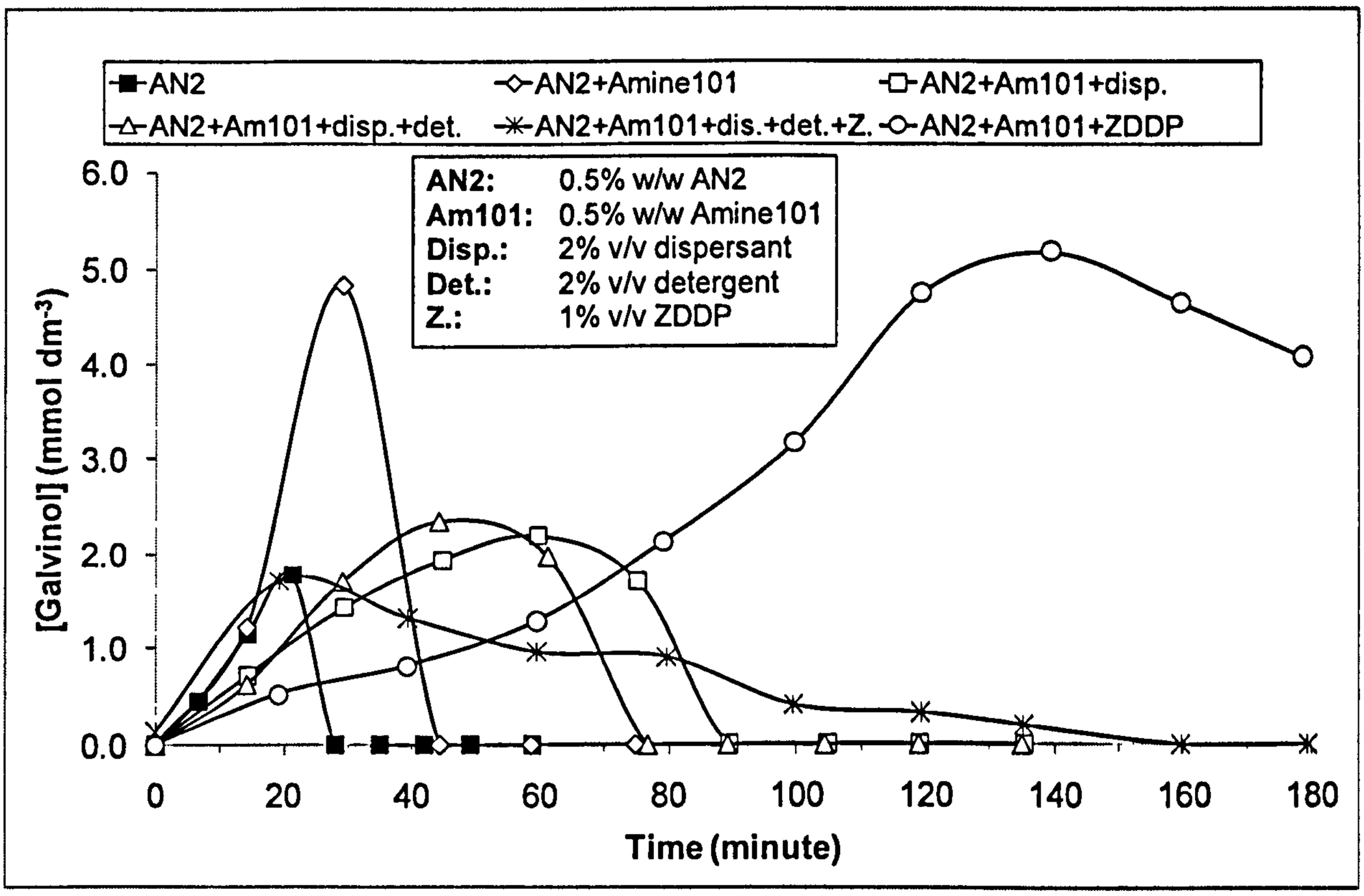

Figure 7.7: Formation of galvinol (by GC) from the decay of AN2 in the oxidation of additives in squalane at 200 °C in flow intermediate reactor

Figure 7.8 shows the decay of the succinimide dispersant in different blends. The –C-N- group of the succinimide dispersant was monitored by FTIR at 1238-1220 cm^{-1}. The succinimide dispersant lasts the longest in AN2+Am101+disp.+det.+Z. blend.

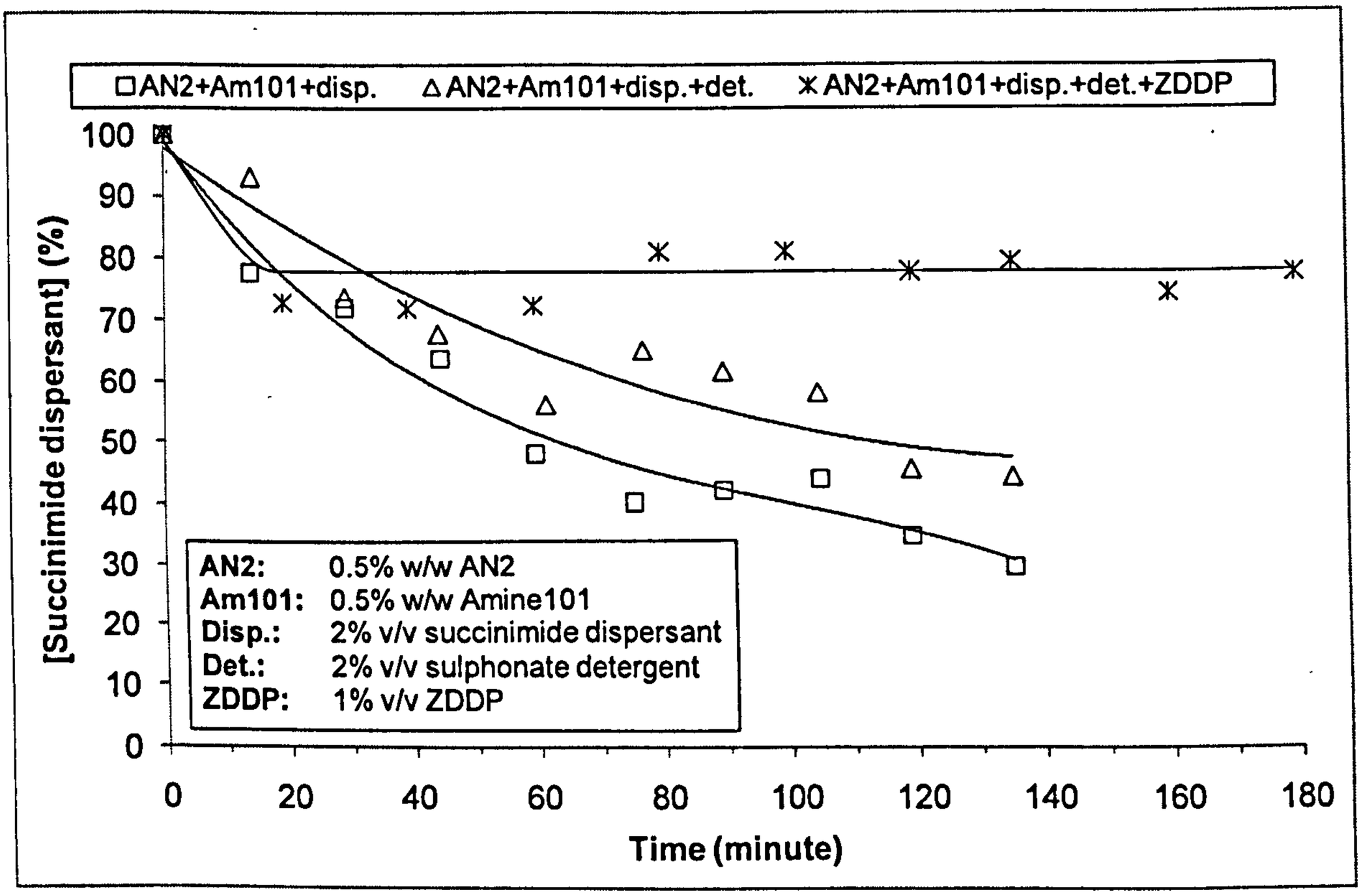

Figure 7.8: Decay of succinimide dispersant (by FTIR) in the oxidation of additives in squalane at 200 °C in flow intermediate reactor

7.2.2. Interactions of additives in Shell XHVI 8.2 in a bench-top reactor

AN2 plus other additives were oxidised in Shell XHVI 8.2 at 200 °C in the flow intermediate reactor to investigate if similar results were obtained using squalane or Shell XHVI 8.2 as a base fluid; and also to examine AN2+detergent on its own and AN2+dispersant on its own, and AN2+detergent+dispersant in the absence of aminic antioxidants.

Details of the examined blends are listed in Table 7.3.

Table 7.3: Details of blends in 5.0 cm^3 Shell XHVI 8.2

Blend	AN2	Succinimide dispersant	Sulphonate detergent
	10.0 mmol dm^{-3} (or 0.5 % w/w)	2.0% v/v	2.0% v/v
XHVI 8.2			
0.5% w/w AN2	√		
0.5% w/w AN2+2% v/v disp.	√	√	
0.5% w/w AN2+2% v/v det.	√		√
AN2+disp.+det.[48]	√	√	√

[48] 9.4 mmol dm^{-3} AN2 (or 0.5 % w/w) + 2 % w/w sulphonate detergent + 2 % w/w succinimide dispersant + parts-per-million (unknown quantity) of a silicone anti-foaming agent, in 10 cm^3 Shell XHVI 8.2.

Figure 7.9 shows oxygen uptake levels in the oxidation of different blends; with AN2+dispersant and AN2+detergent+dispersant blends being the most effective in retarding oxygen uptake.

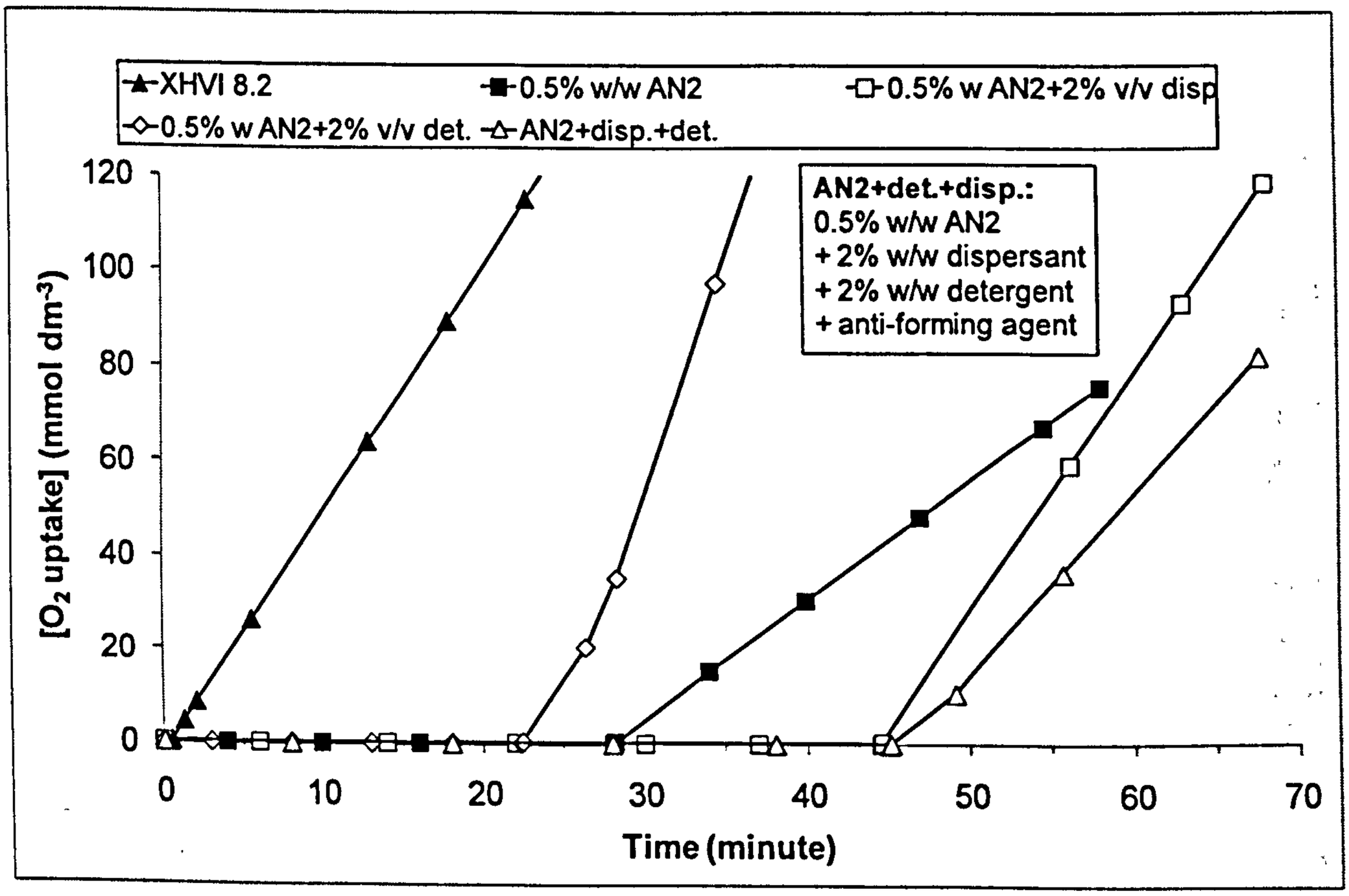

Figure 7.9: Oxygen uptake in the oxidation of AN2 with other additives in Shell XHVI 8.2 at 200 °C in flow intermediate reactor

Figure 6.17 shows the total carbonyl formation in the presence of different mixtures; with the AN2+dispersant blend being the most effective in retarding carbonyl formation. The total carbonyl contents for the other blends were not measured due to time restriction.

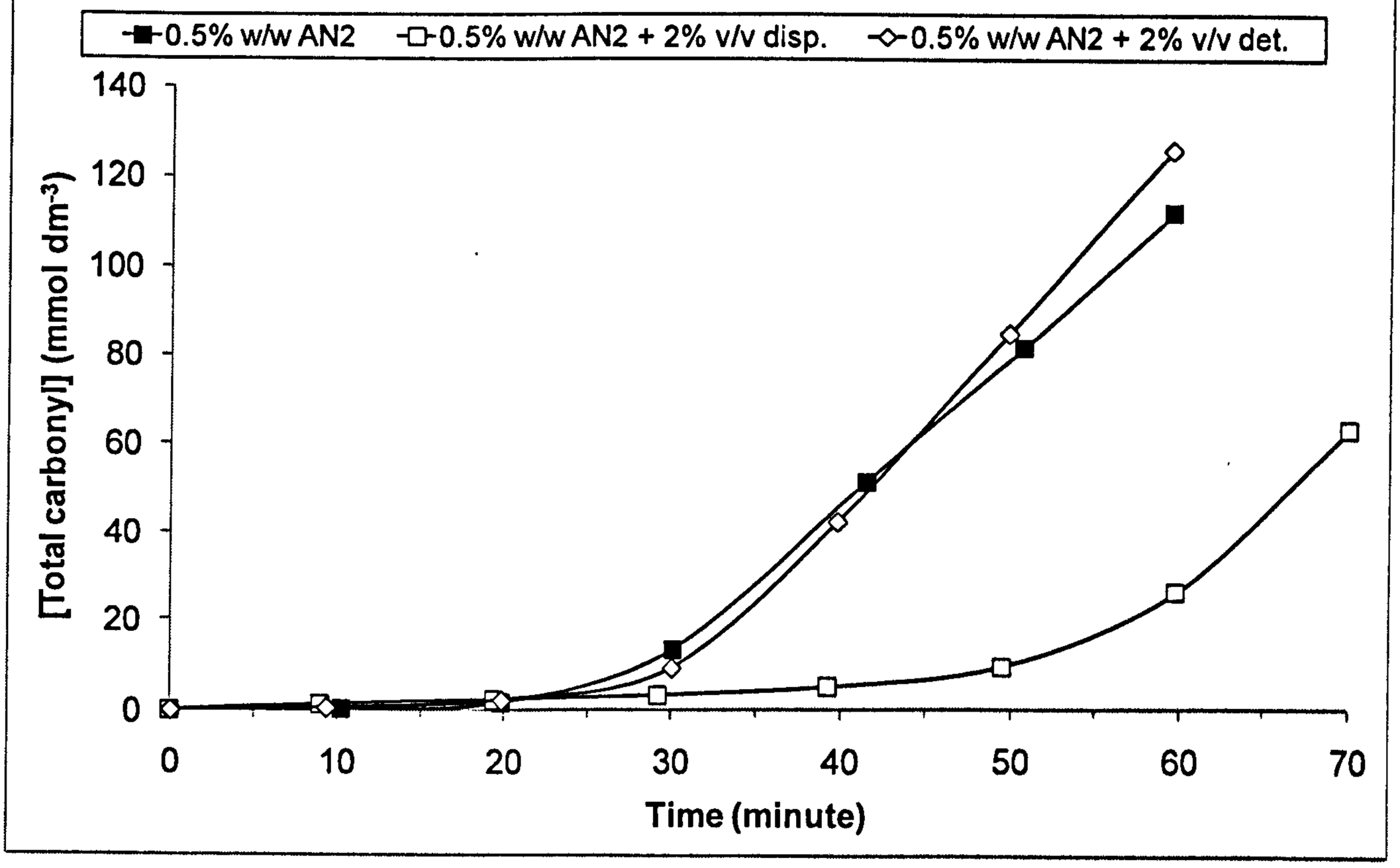

Figure 7.10: Total carbonyl formation (by FTIR) in the oxidation of AN2 with other additives in Shell XHVI 8.2 at 200 °C in flow intermediate reactor

Figure 7.11 and Figure 7.12 show the decay of AN2 in different blends. AN2 lasts the longest in AN2+dispersant blend. Figure 7.12 shows oxygen uptake would only take place when the AN2 is completely consumed.

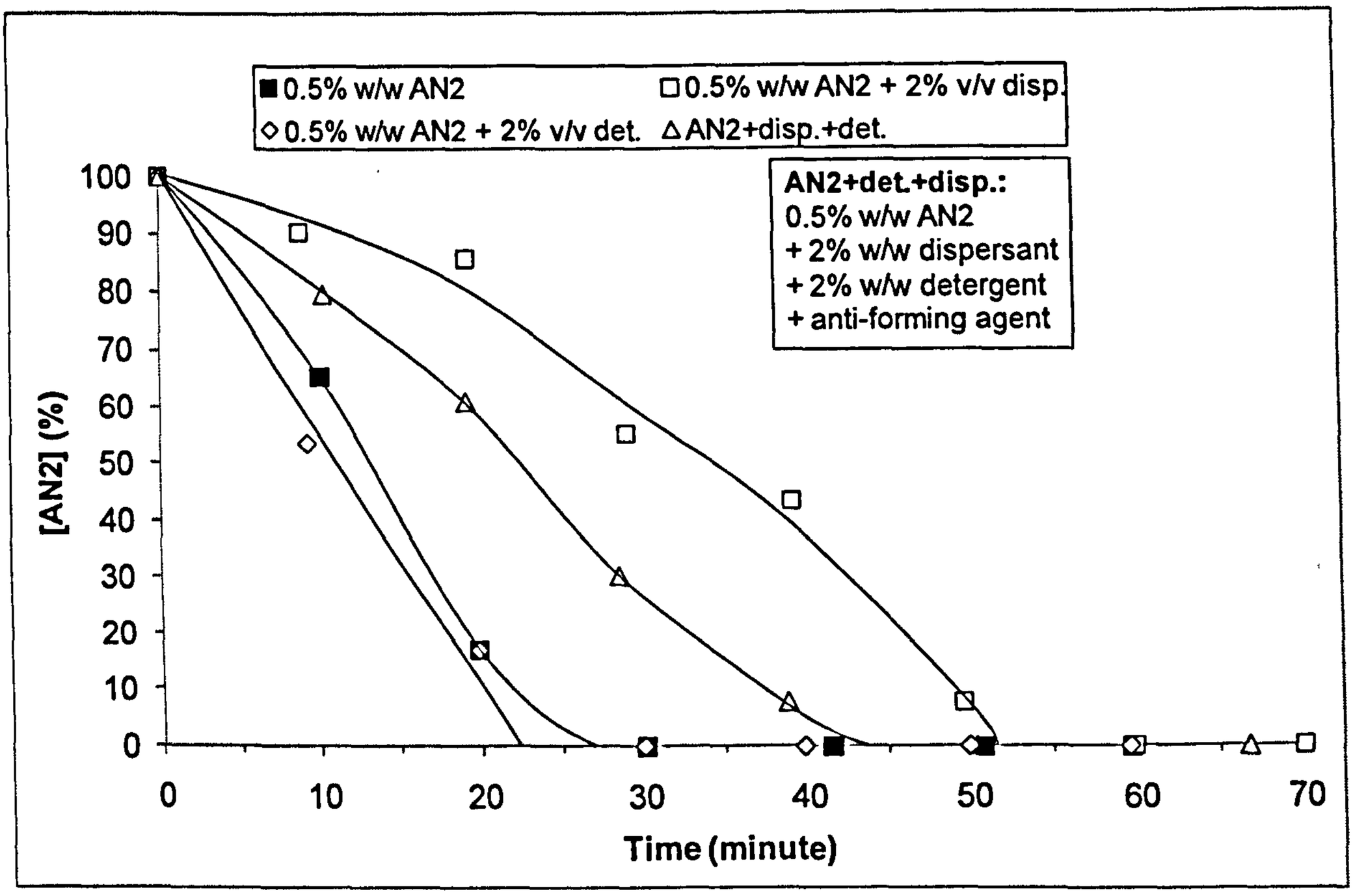

Figure 7.11: Decay of AN2 (by GC) in the oxidation of AN2 with other additives in Shell XHVI 8.2 at 200 °C in flow intermediate reactor

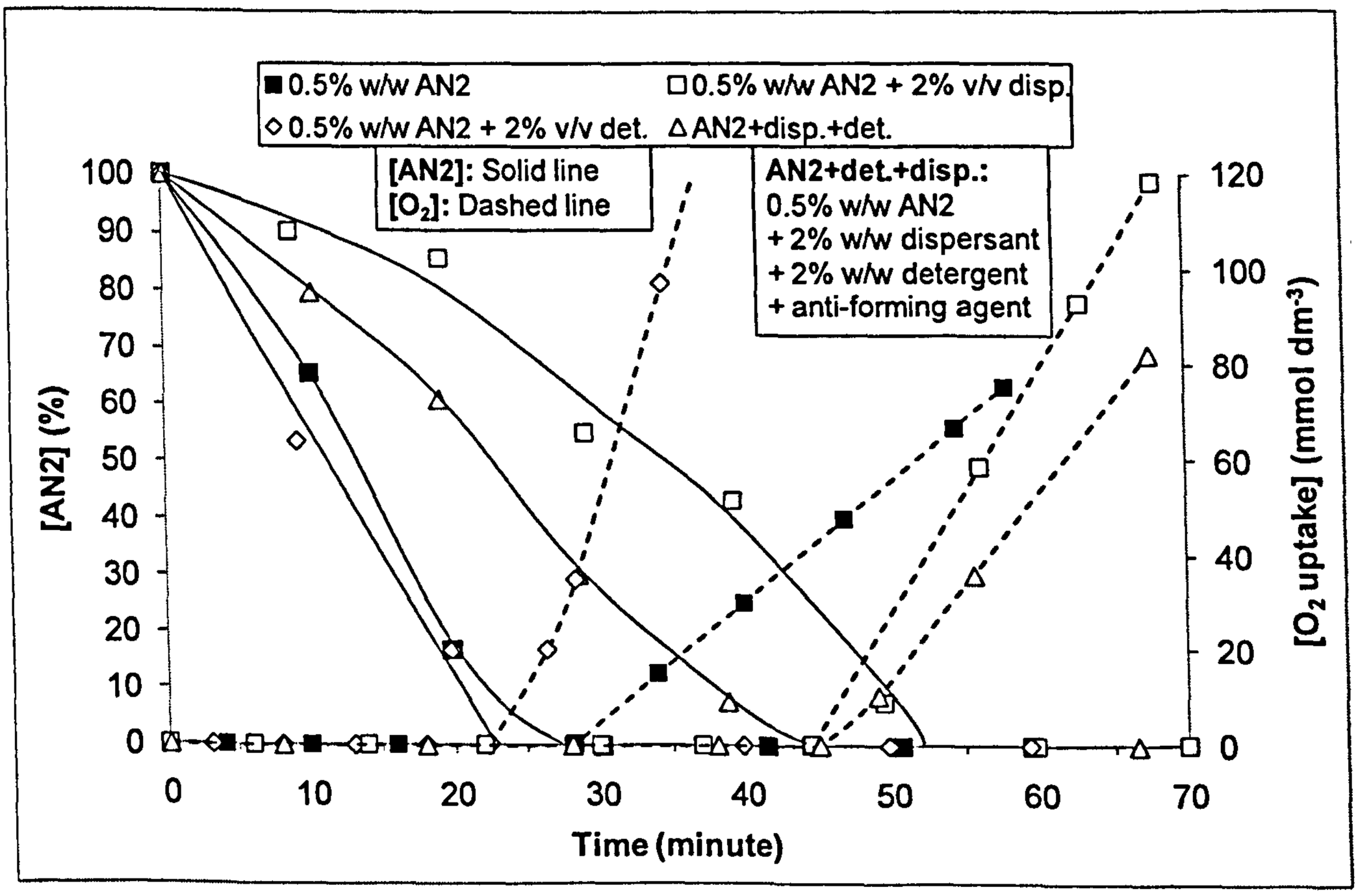

Figure 7.12: Overlaid data of the decay of AN2 (by GC) with that of oxygen uptake in the oxidation of AN2 with other additives in Shell XHVI 8.2 at 200 °C in flow intermediate reactor

Figure 7.13 shows the formation of galvinol (from AN2) in different blends. The concentrations of the other AN2 oxidation products (i.e. formylphenol and quinone) are available in Appendix D. The quantities of these products are similar to those obtained in squalane (Figure 7.7).

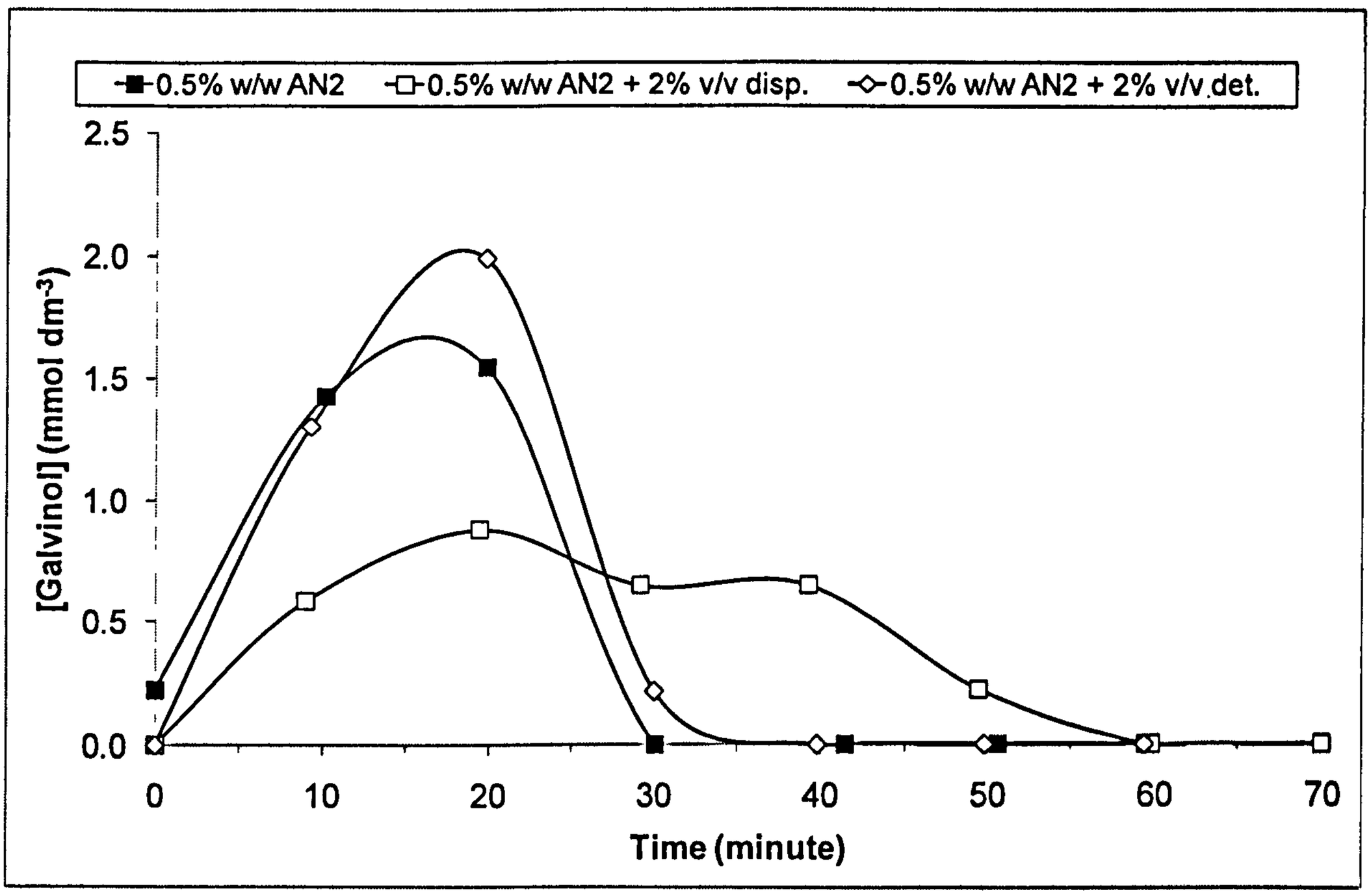

Figure 7.13: Formation of galvinol (by GC) from the decay of AN2 in the oxidation of AN2 with other additives in Shell XHVI 8.2 at 200 °C in flow intermediate reactor

7.2.3. Interactions of commercial additives in semi-formulated lubricants

Subsections 7.2.1 and 7.2.2 dealt with oxidations of model additives in model base fluids. In this subsection, the investigated additives and base fluid are used commercially, and hence the outcome should be more representative of what one would expects from commercial lubricants.

Details of the examined blends are listed in Table 7.4.

Table 7.4: Details of semi-formulated base fluids

Blend	Code	Oil blend formulation
Reference oil	LB368	Shell XHVI 8.2 + 2 % w/w neutral calcium alkyl sulphonate detergent (50 % / 50 % in a Group I diluent) + 2 % w/w succinimide dispersant (50 % / 50 % in a Group I diluent) + parts-per-million (unknown quantity) of a silicone anti-foaming agent
0.5% Irganox + 0.5% Naugalube	LB14	LB368 + 0.5 % w/w Irganox L135 + 0.5 % w/w Naugalube 438L
0.5% Irganox + 0.5% Naugalube + 1.0% ZDDP	LB16	LB368 + 0.5 % w/w Irganox L135 + 0.5 % w/w Naugalube 438L + 1.0 % w/w secondary ZDDP

Figure 7.14 shows the total carbonyl formation in the presence of combinations of different antioxidants; with 0.5% Irganox + 0.5% Naugalube + 1.0% ZDDP blend being more effective than 0.5% Irganox + 0.5% Naugalube blend in retarding carbonyl formation.

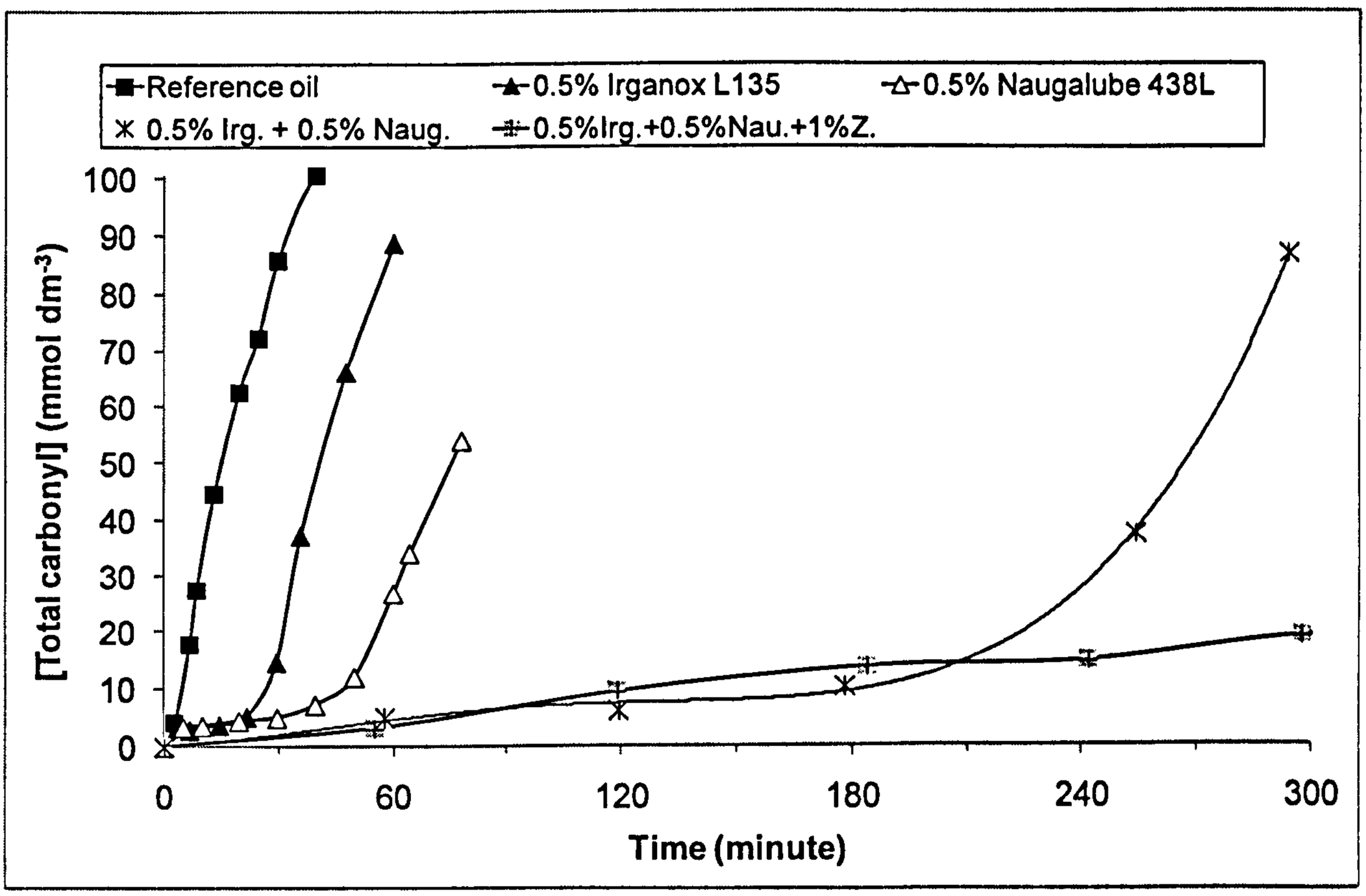

Figure 7.14: Total carbonyl formation (by FTIR) in the oxidation of 0.5% Irganox + 0.5% Naugalube and 0.5% Irganox + 0.5% Naugalube + 1.0% ZDDP semi-formulated base fluids at 200 °C in the static large reactor

Figure 7.15 shows the decay of Irganox L135 in the presence of combinations of different antioxidants. Irganox L135 lasts the longest in 0.5% Irganox + 0.5% Naugalube + 1.0% ZDDP blend.

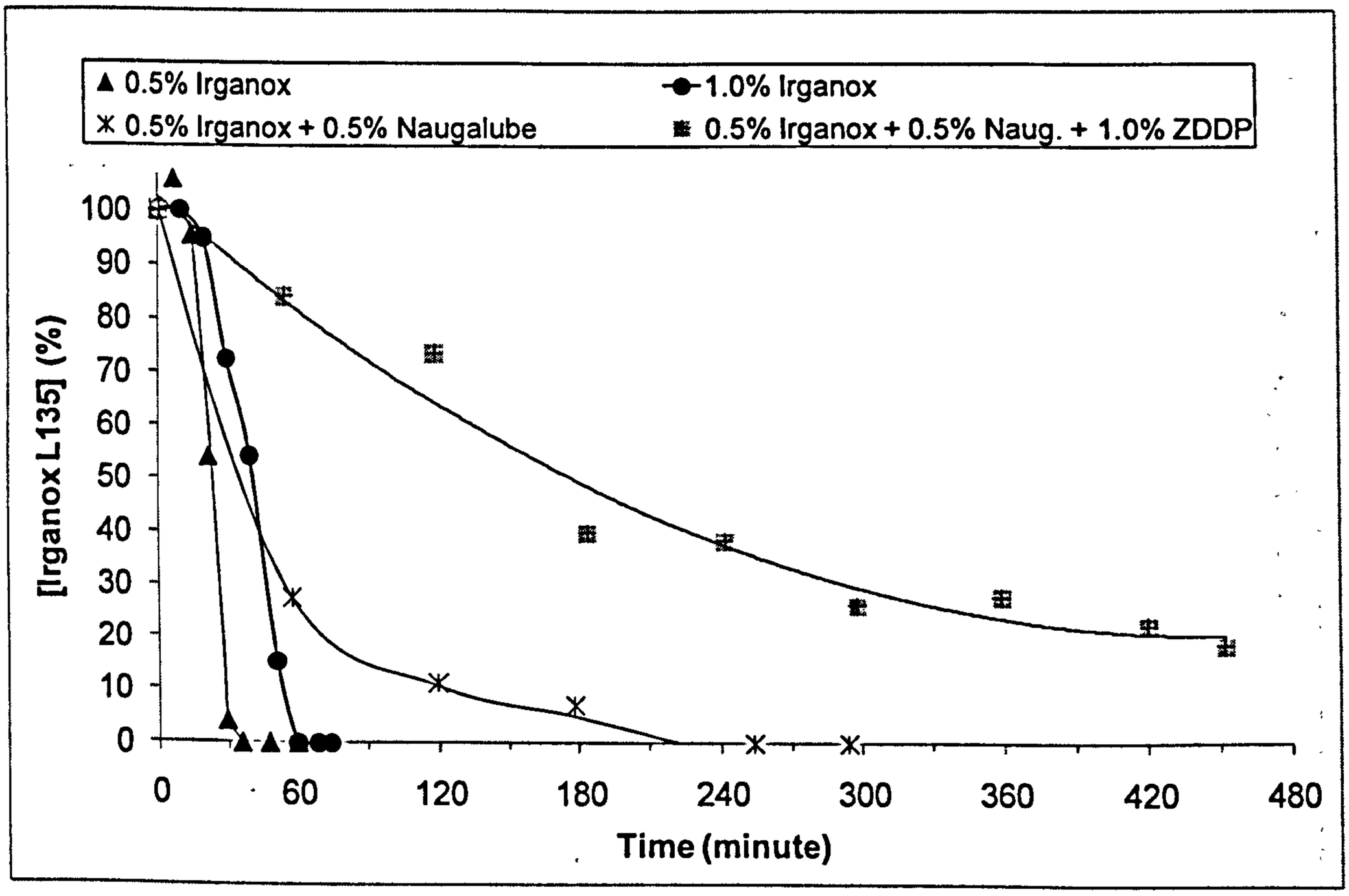

Figure 7.15: Decay of Irganox L135 (by GC) in the oxidation of 0.5% Irganox + 0.5% Naugalube and 0.5% Irganox + 0.5% Naugalube + 1.0% ZDDP semi-formulated base fluids at 200 °C in the static large reactor

Figure 7.16 shows the decay of Naugalube 438L in the presence of combinations of different antioxidants. Naugalube 438L lasts the longest in 0.5% Irganox + 0.5% Naugalube blend.

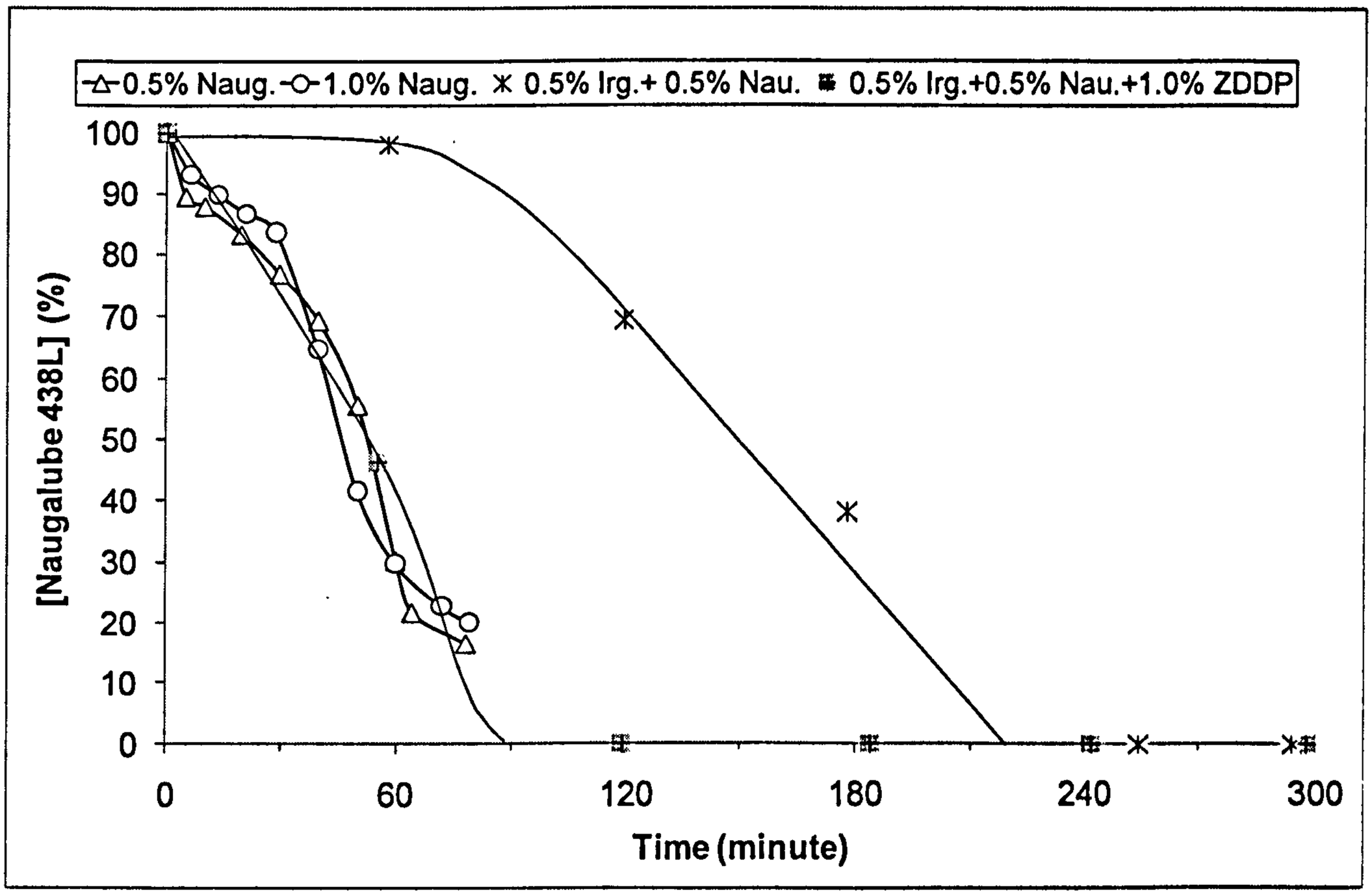

Figure 7.16: Decay of Naugalube 438L (by LC) in the oxidation of 0.5% Irganox + 0.5% Naugalube and 0.5% Irganox + 0.5% Naugalube + 1.0% ZDDP semi-formulated base fluids at 200 °C in the static large reactor

Figure 7.17 and Figure 7.18 show the decay of Irganox L135 and Naugalube 438L in combinations of mixtures.

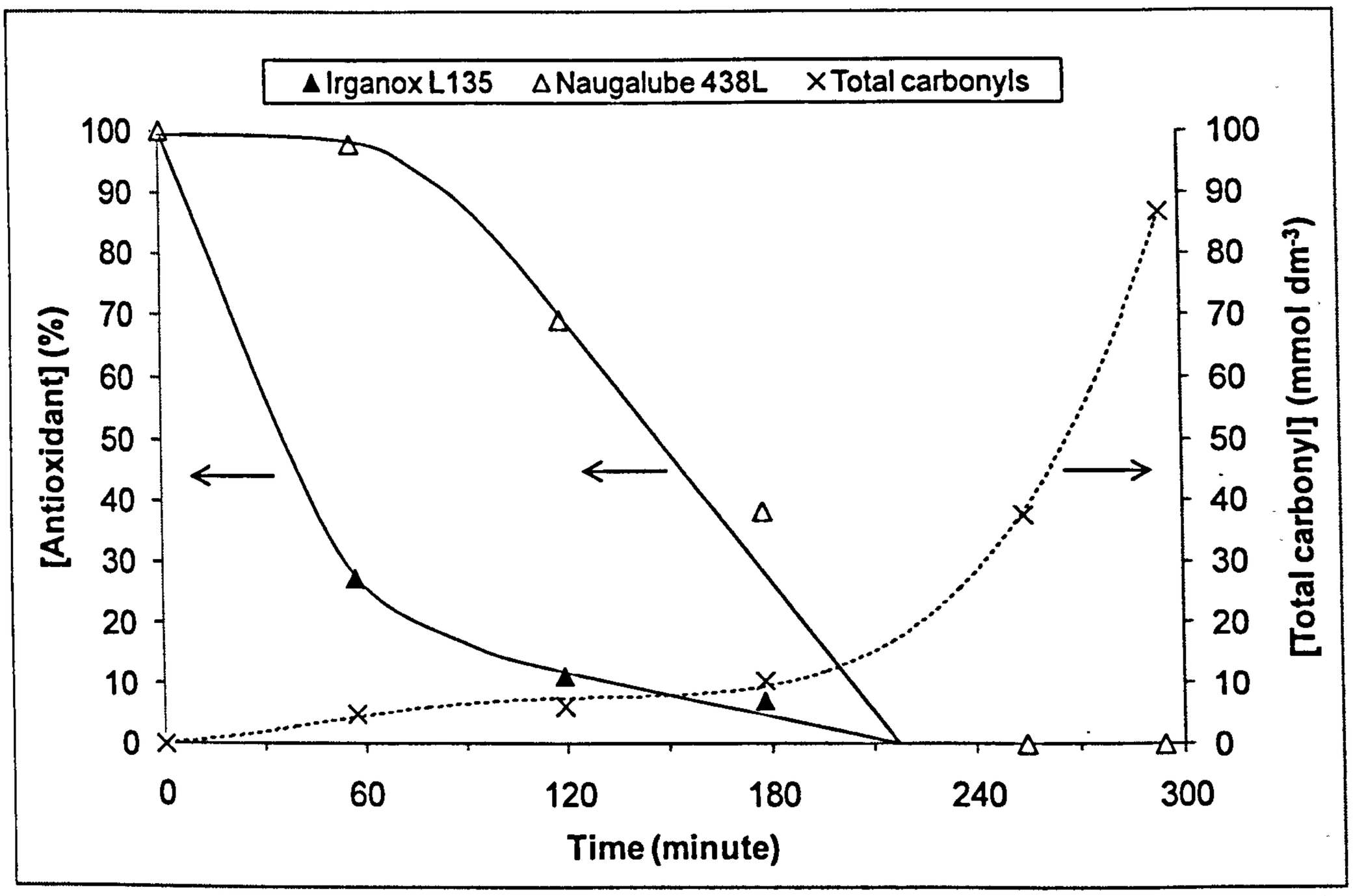

Figure 7.17: Decay of antioxidants in the oxidation of 0.5% Irganox + 0.5% Naugalube blend at 200 °C in the static large reactor

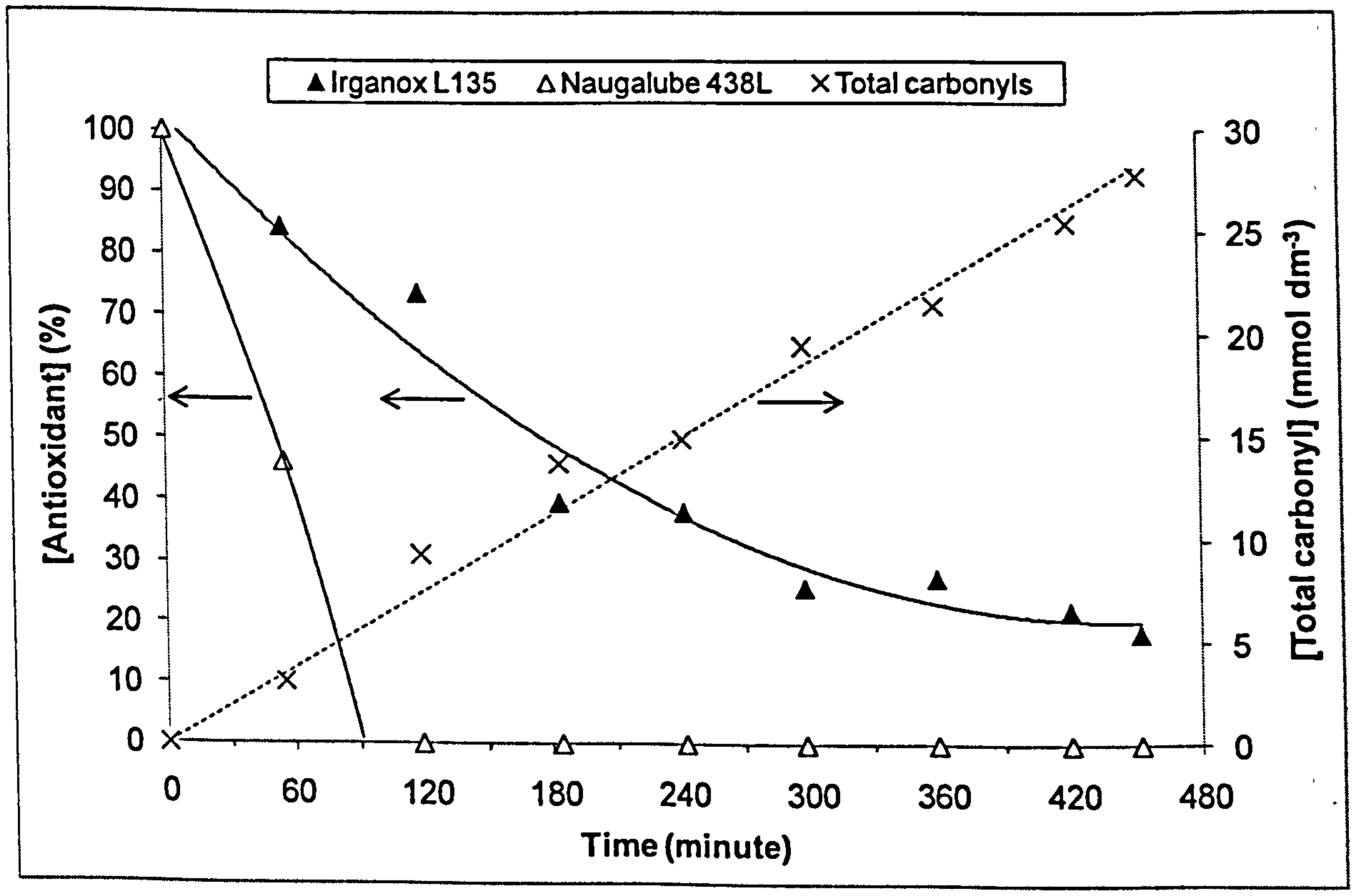

Figure 7.18: Decay of antioxidants in the oxidation of 0.5% Irganox + 0.5% Naugalube + 1.0% ZDDP blend at 200 °C in the static large reactor

7.2.4. Interactions of additives in semi-formulated base fluids in a gasoline engine

The semi-formulated base fluids in Table 7.5 are the same as those oxidised in the bench-top reactors under controlled conditions in Subsection 7.2.3. These formulations are degraded in the engine to investigate additives interactions under real engines conditions, and also, to compare and contrast results obtained from gasoline engines with those obtained from bench-top reactors.

Formulations described in Table 7.5 were degraded in the engine while the piston rings are unpinned (i.e. the rings are free to rotate), whereas the formulation in Table 7.6 was degraded in the engine while the piston rings are pinned (i.e. the rings a fixed in one position) to evaluate the piston rings rotation on the oil degradation process.

Table 7.5: Details of semi-formulated base fluids for June 2006 Hydra engine tests (piston rings unpinned)

Blend	Code	Oil blend formulation
Reference oil	LB368	Shell XHVI 8.2 + 2 % w/w neutral calcium alkyl sulphonate detergent (50 % / 50 % in a Group I diluent) + 2 % w/w succinimide dispersant (50 % / 50 % in a Group I diluent) + parts-per-million (unknown quantity) of a silicone anti-foaming agent
0.5% Irganox + 0.5% Naugalube	LB14	LB368 + 0.5 % w/w Irganox L135 + 0.5 % w/w Naugalube 438L
0.5% Irganox + 0.5% Naugalube + 1.0% ZDDP	LB16	LB368 + 0.5 % w/w Irganox L135 + 0.5 % w/w Naugalube 438L + 1.0 % w/w secondary ZDDP

Table 7.6: Details of semi-formulated base fluids for August 2007 Hydra engine tests (piston rings pinned)

Blend	Oil blend formulation
0.5% AN2 + 0.5% Amine101	Shell XHVI 8.2 + 0.5 % w/w (or 9.4 mmol dm^{-3}) AN2 + 0.5 % w/w Amine101

Before each run, the engine was flushed twice with the reference oil and once with the sample oil for one hour.

The temperature of the sump was maintained, for this work, at ~80 °C to minimise antioxidant oxidation in the sump to a negligible level and hence eliminate potential oxidation interferences from the sump with oxidation data from the piston assembly. The conditions of the Ricardo Hydra engine are listed in Table 7.7.

Table 7.7: Conditions of Ricardo Hydra engine

Parameter	June 2006 tests	June 2007 tests	August 2007 tests
Load (%)	50	50	50
Speed (rpm)	1500	1500	1500
Piston rings pinning	No	Yes	Yes
Sump volume (litre)	3.0	3.0	3.0
Sump temperature (°C)	~80	~80	~80
Test duration (hour)	6.0	4.0	5.0
Fuel	Shell standard unleaded gasoline	Shell standard unleaded gasoline	Shell standard unleaded gasoline

Formation of carbonyls

Figure 7.19 and Figure 7.20 show the formation of total carbonyl in top ring zone and sump, respectively; with the concentrations of carbonyl in the top ring zone higher than those in the sump.

It should be noted that the concentrations of carbonyl of starting materials were normalised to zero and those of the backgrounds were subtracted from all the results.

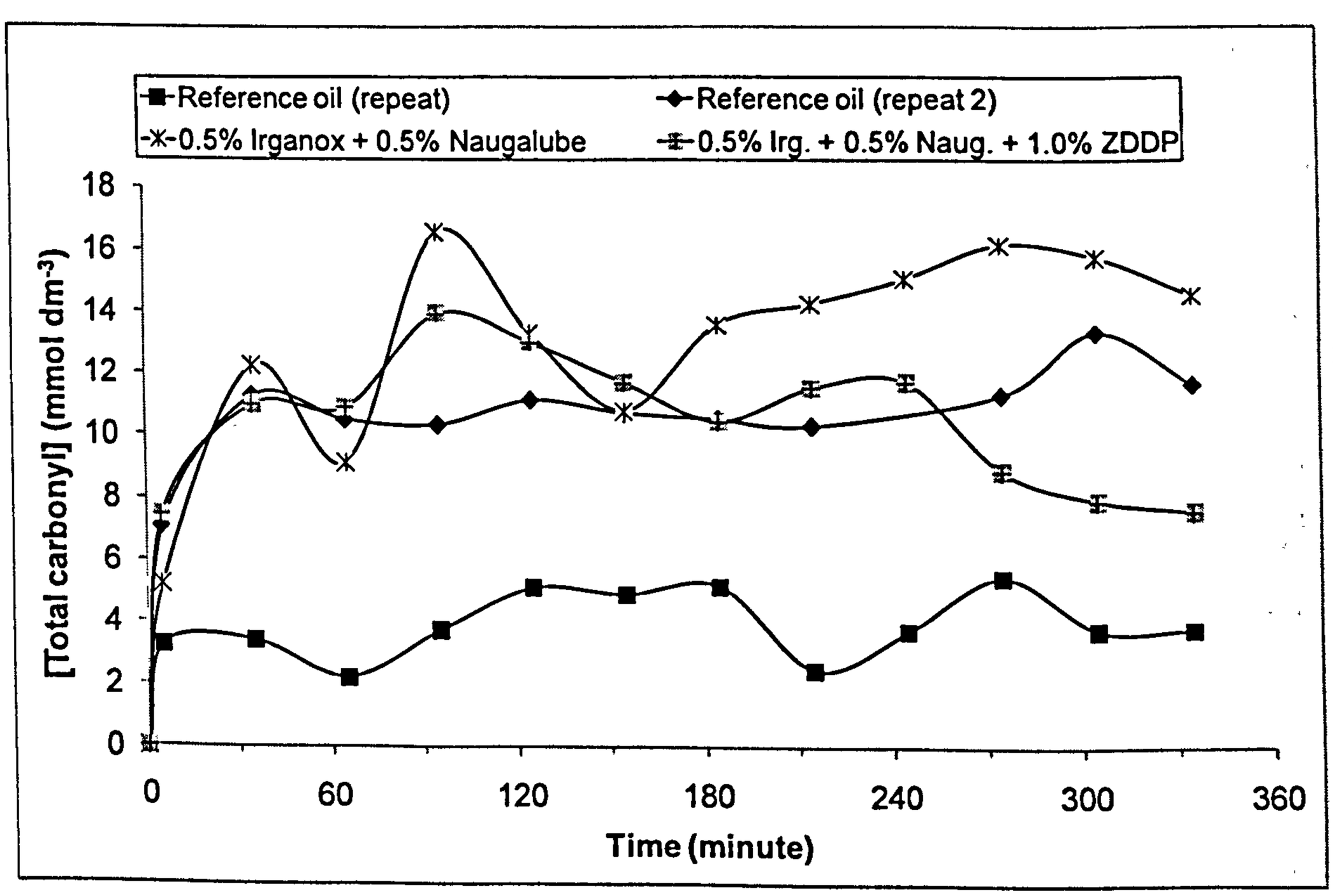

Figure 7.19: Total carbonyl (by FTIR) of oil samples from top ring zone (June 2006 tests)

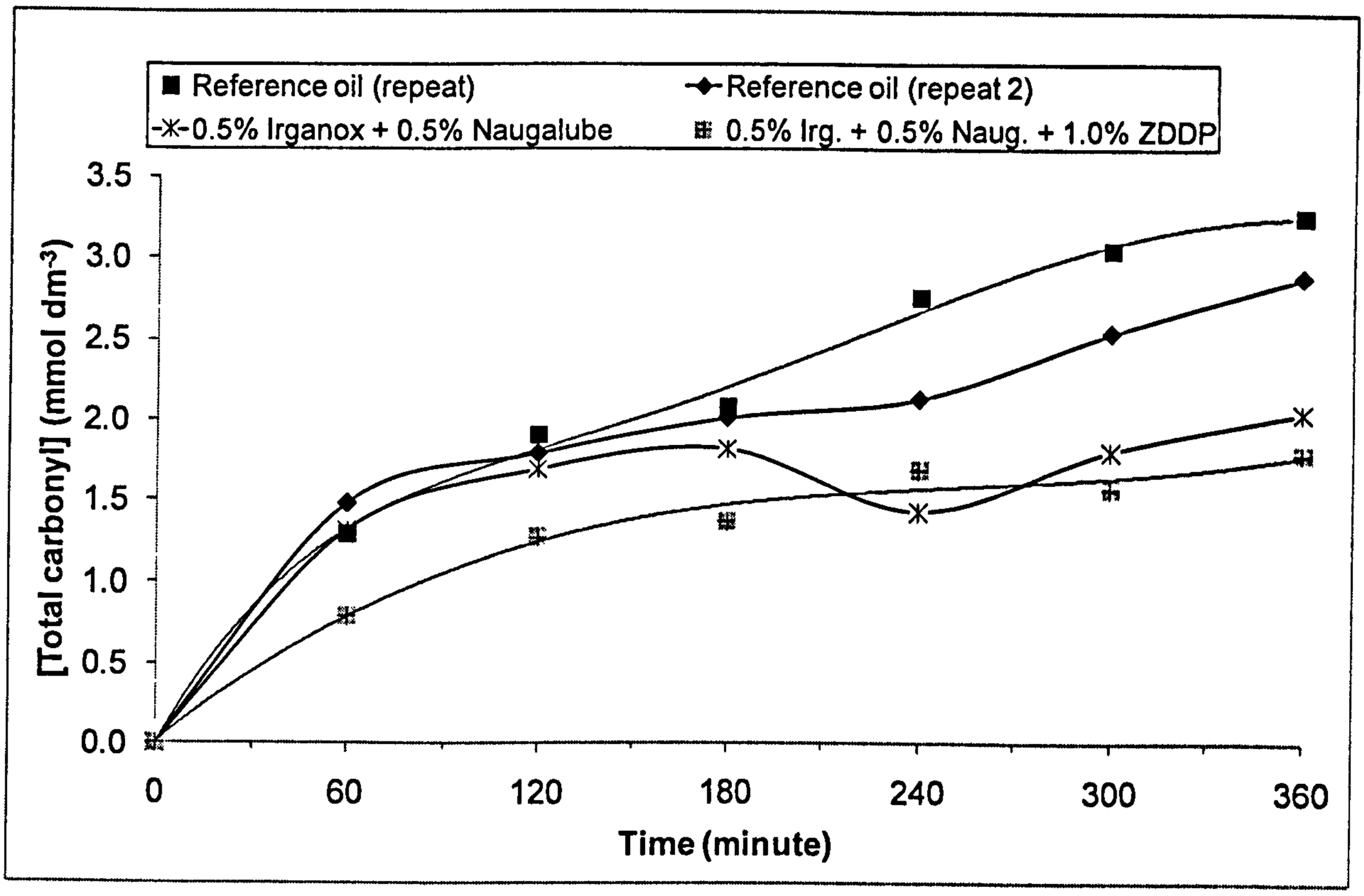

Figure 7.20: Total carbonyl (by FTIR) of oil samples from sump (June 2006 tests)

Figure 7.21 and Figure 7.22 show the formation of total carbonyl in top ring zone and sump, respectively; with the concentrations of carbonyl in the top ring zone higher than those in the sump and that the 0.5% AN2 + 0.5% Amine101 blend being the most effective in retarding carbonyl formation.

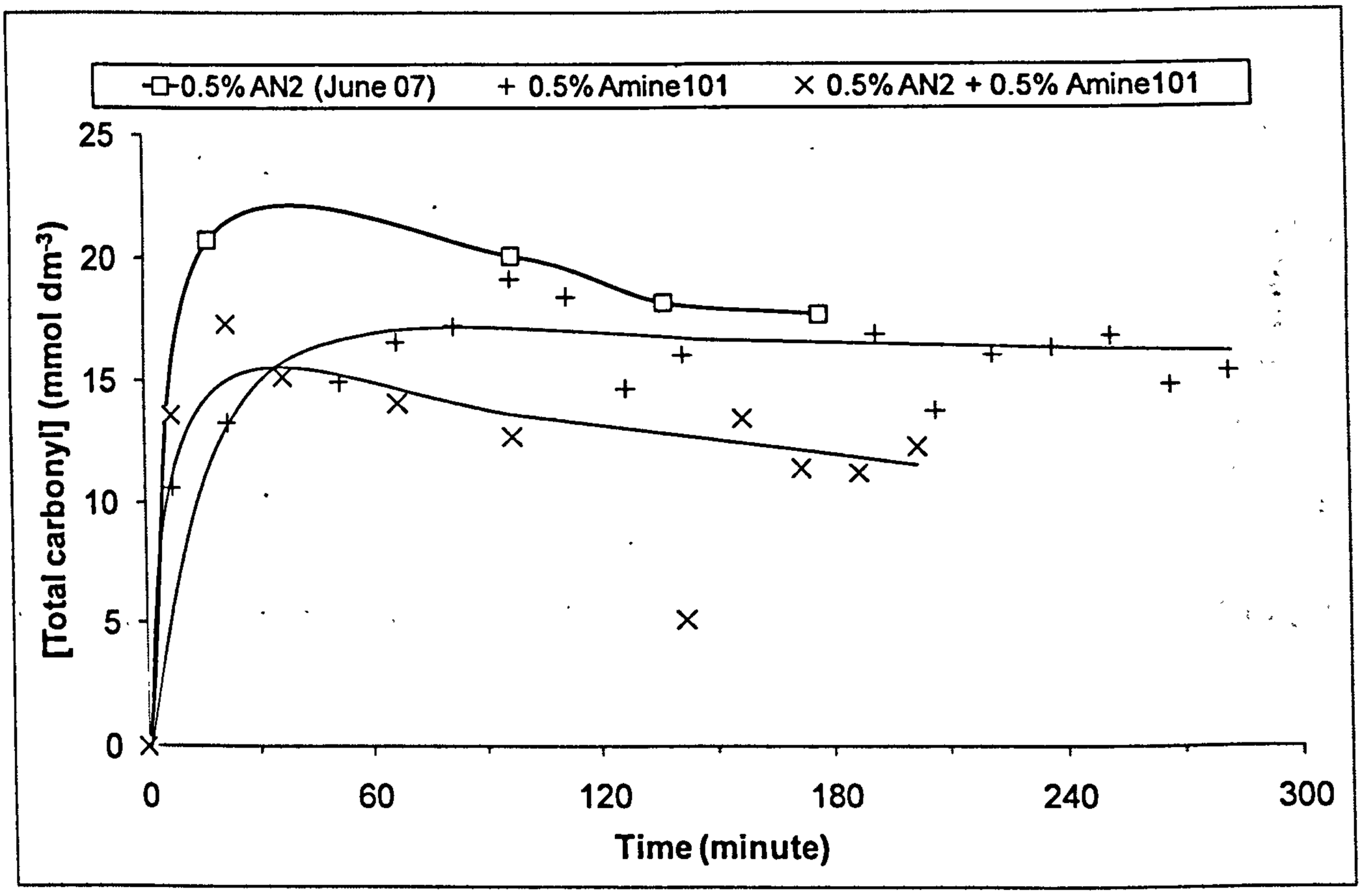

Figure 7.21: Total carbonyl formation (by FTIR) in 0.5% AN2 + 0.5% Amine101 blend (August 2007 test) from top ring zone

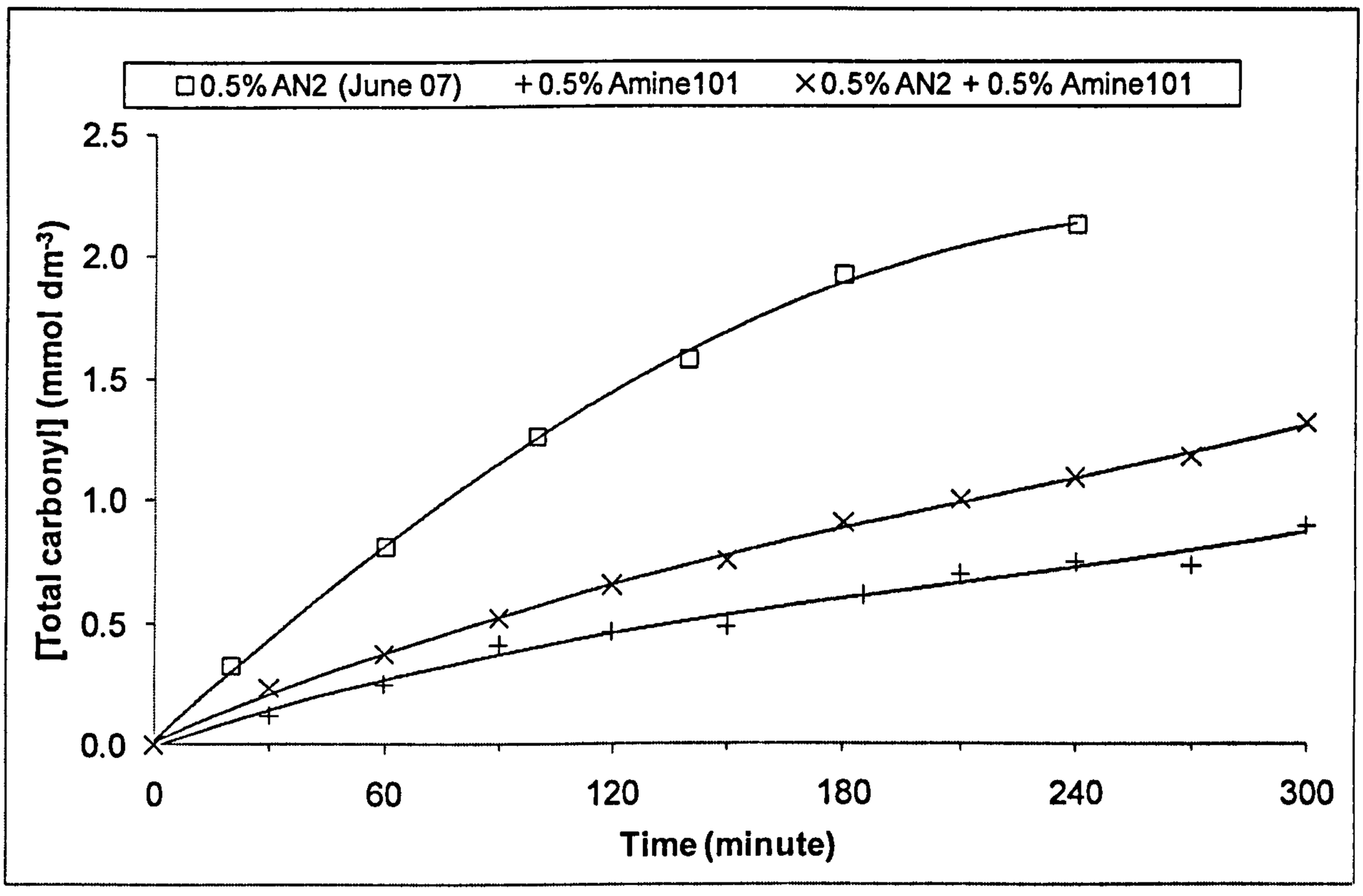

Figure 7.22: Total carbonyl formation (by FTIR) in 0.5% AN2 + 0.5% Amine101 blend (August 2007 test) from sump

Decay of antioxidants

Figure 7.23 shows the decay of Irganox L135 in the top ring zone and sump; with the antioxidant level in the top ring zone much lower than that in the sump.

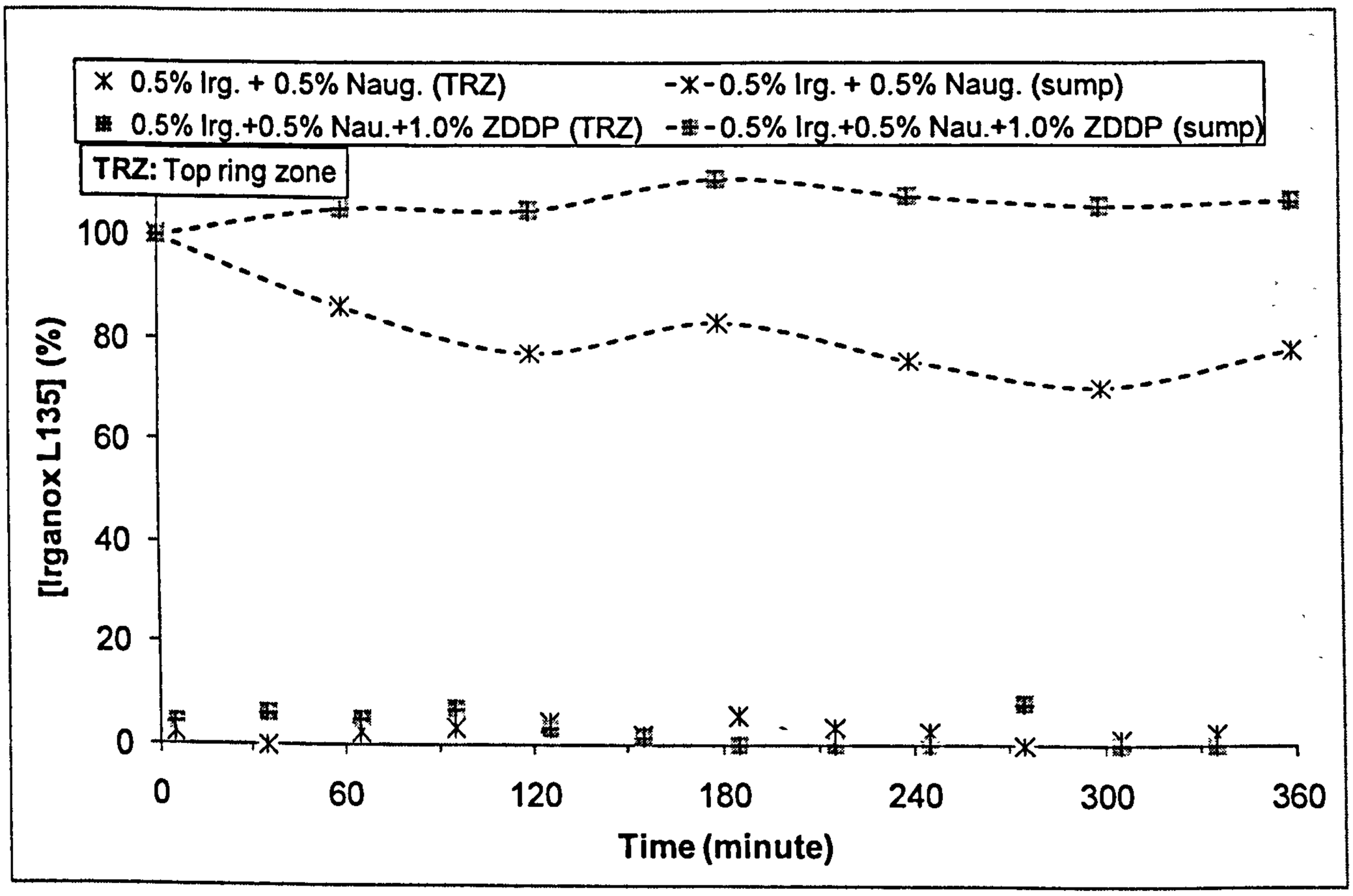

Figure 7.23: Decay of Irganox L135 (by GC) in oils from top ring zone and sump (June 2006 tests)

Figure 7.24 shows the decay of Naugalube 438L in the top ring zone and sump; with the antioxidant level in the top ring zone down by ~50 % and lower than that in the sump.

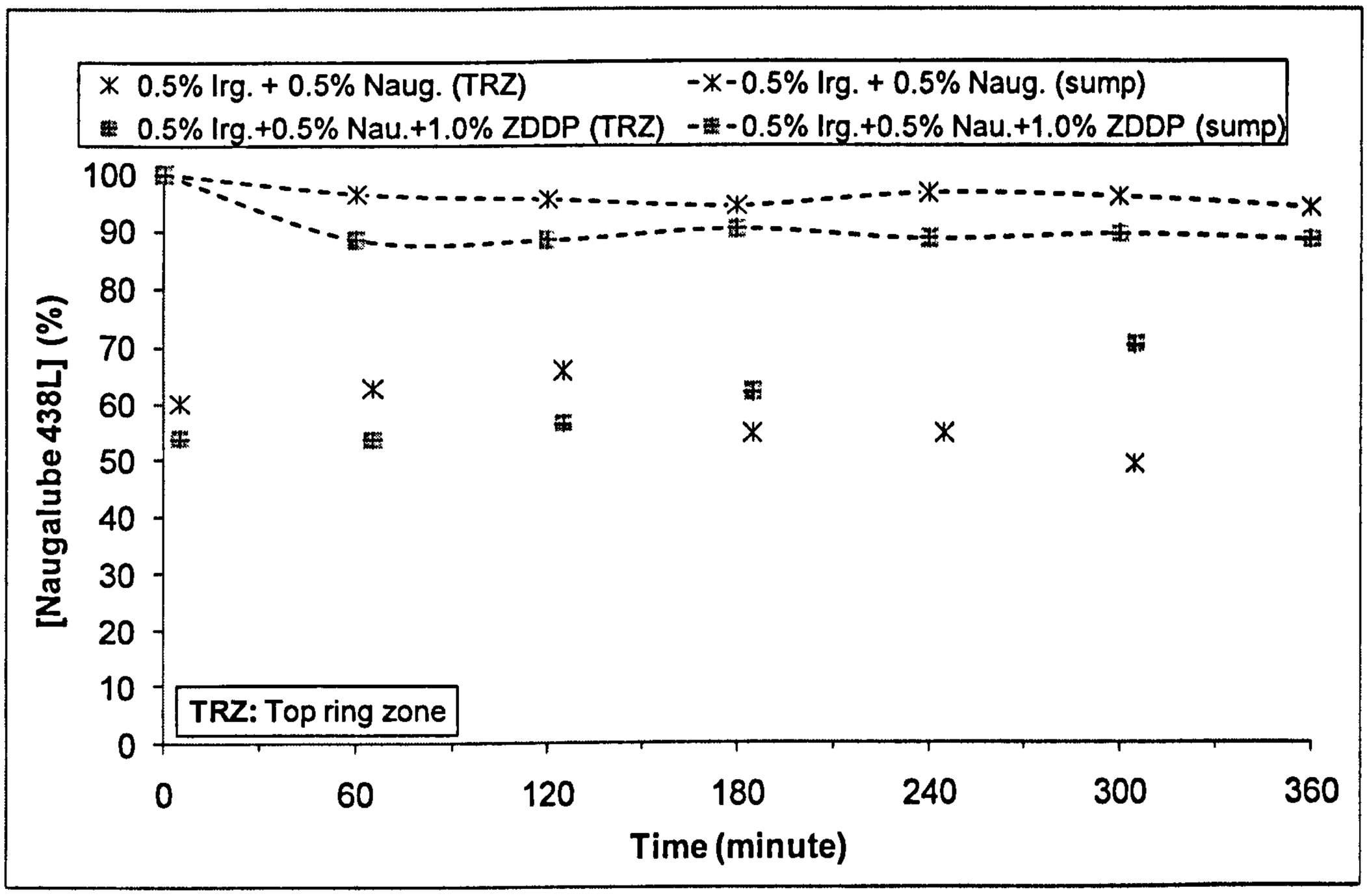

Figure 7.24: Decay of Naugalube 438L (by LC) in oils from top ring zone and sump (June 2006 tests)

Figure 7.25 and Figure 7.26 show the decay of Irganox L135 and Naugalube 438L in the presence of various antioxidants and additives. The results for the decay of antioxidants are fairly similar in 0.5% Irganox + 0.5% Naugalube and 0.5% Irganox + 0.5% Naugalube + 1.0% ZDDP blends.

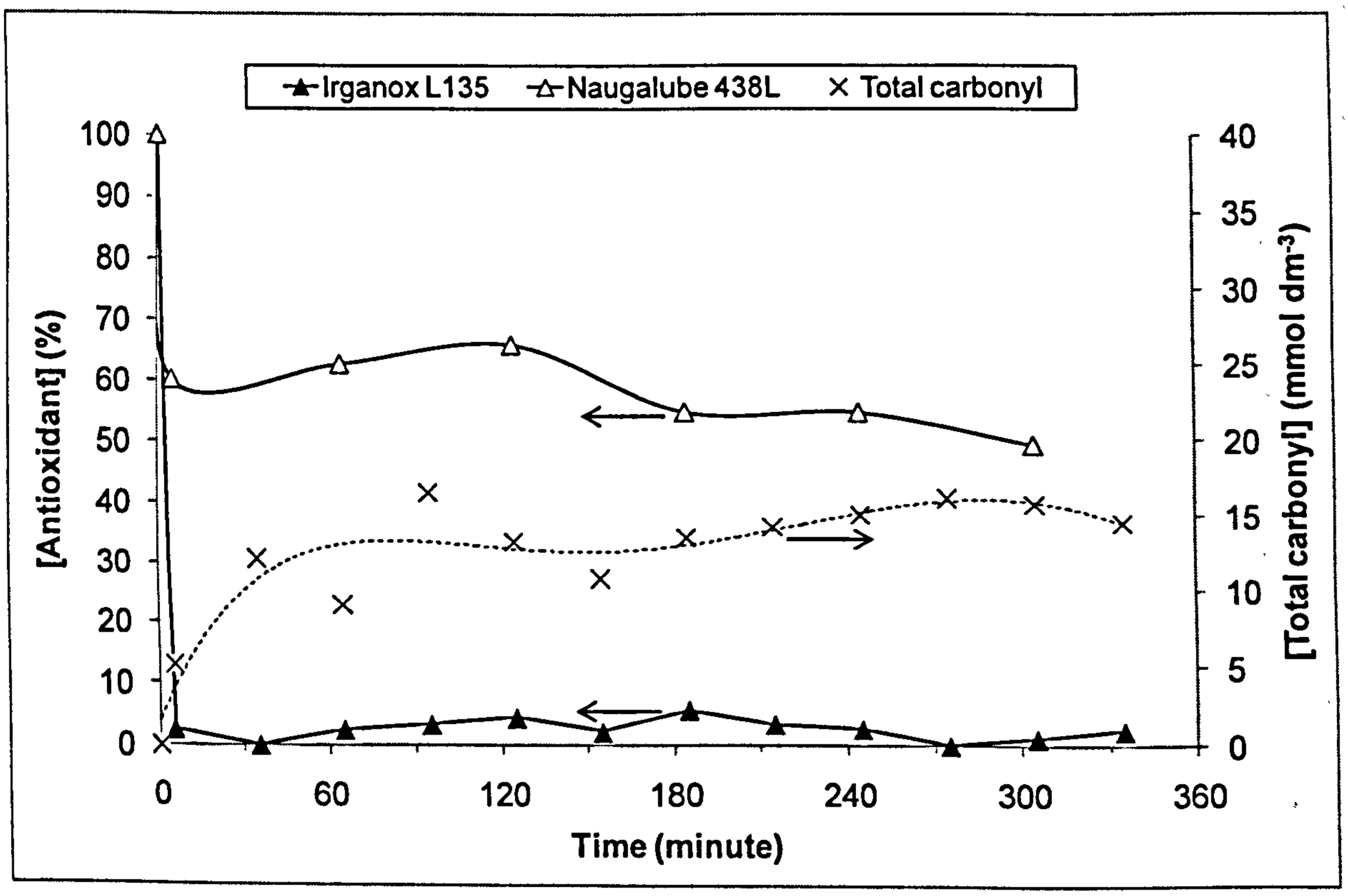

Figure 7.25: Decay of antioxidants in 0.5% Irganox + 0.5% Naugalube blend from top ring zone (June 2006 tests)

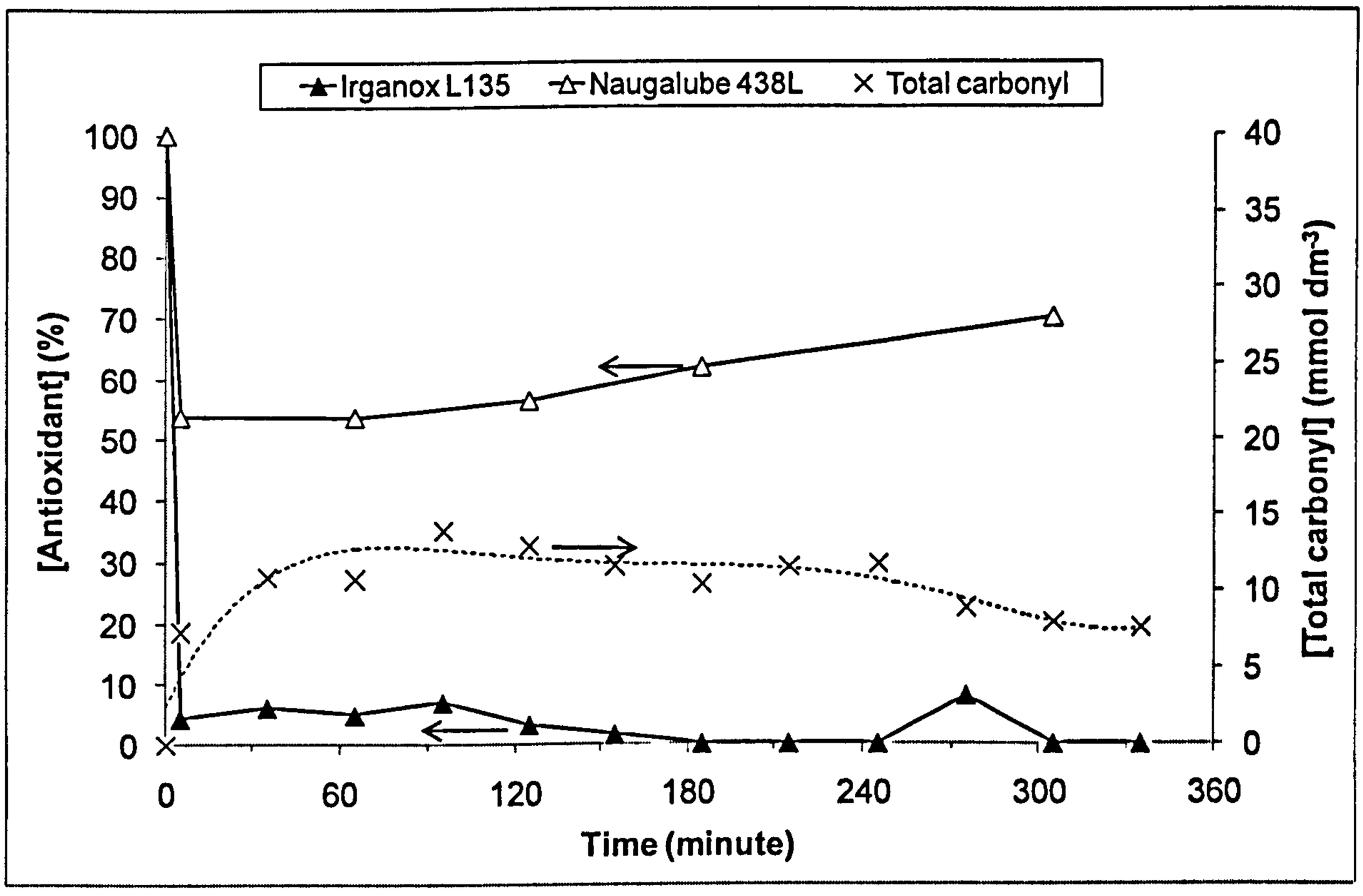

Figure 7.26: Decay of antioxidants in 0.5% Irganox + 0.5% Naugalube + 1.0% ZDDP blend from top ring zone (June 2006 tests)

Figure 7.27 and Figure 7.28 show that in the presence of AN2 and Amine101, Amine101 was better preserved and AN2 was completely consumed in the top ring zone.

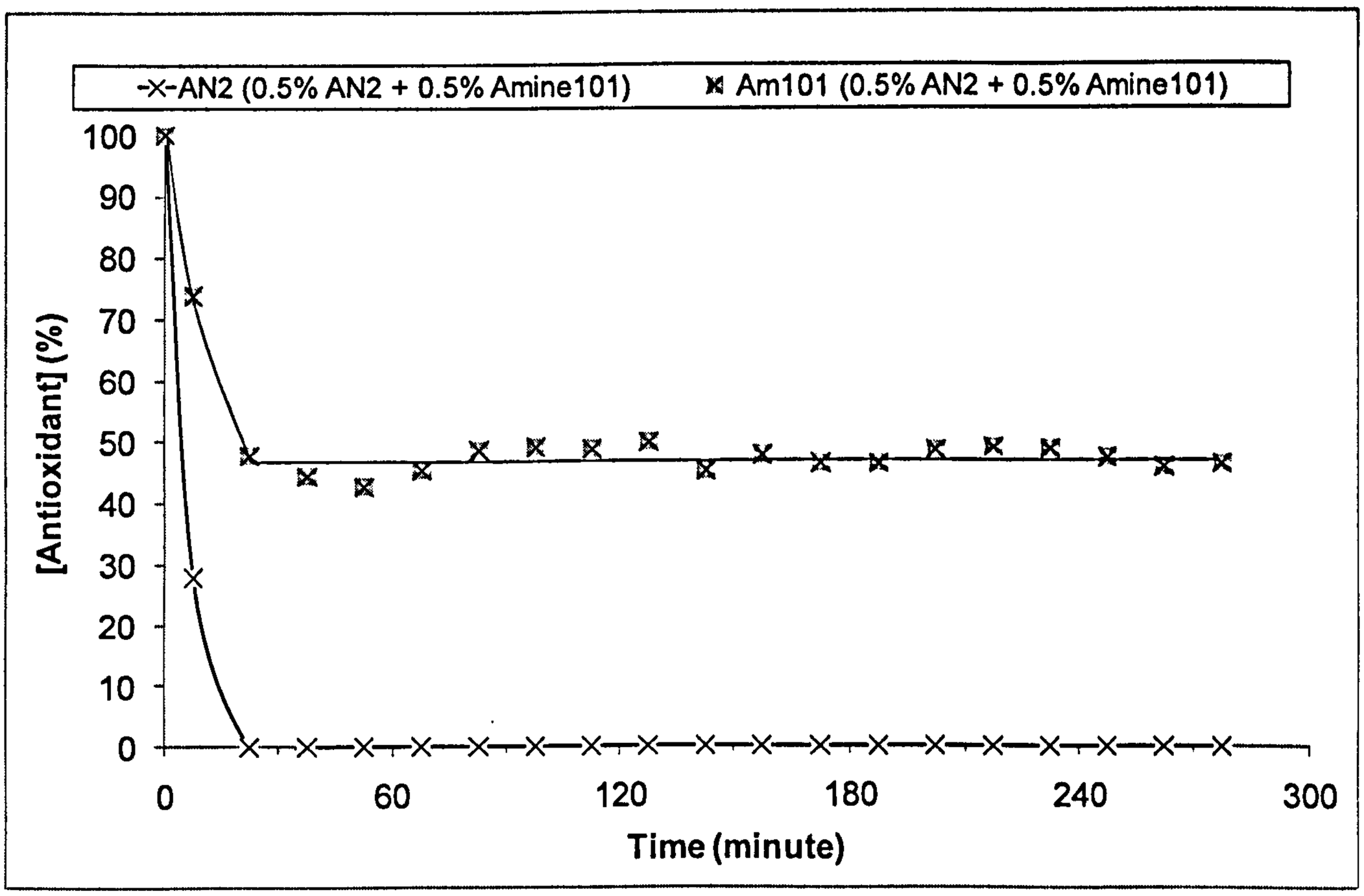

Figure 7.27: Decay of antioxidants (by GC) in 0.5% AN2 + 0.5% Amine101 blend (August 2007 test) from top ring zone

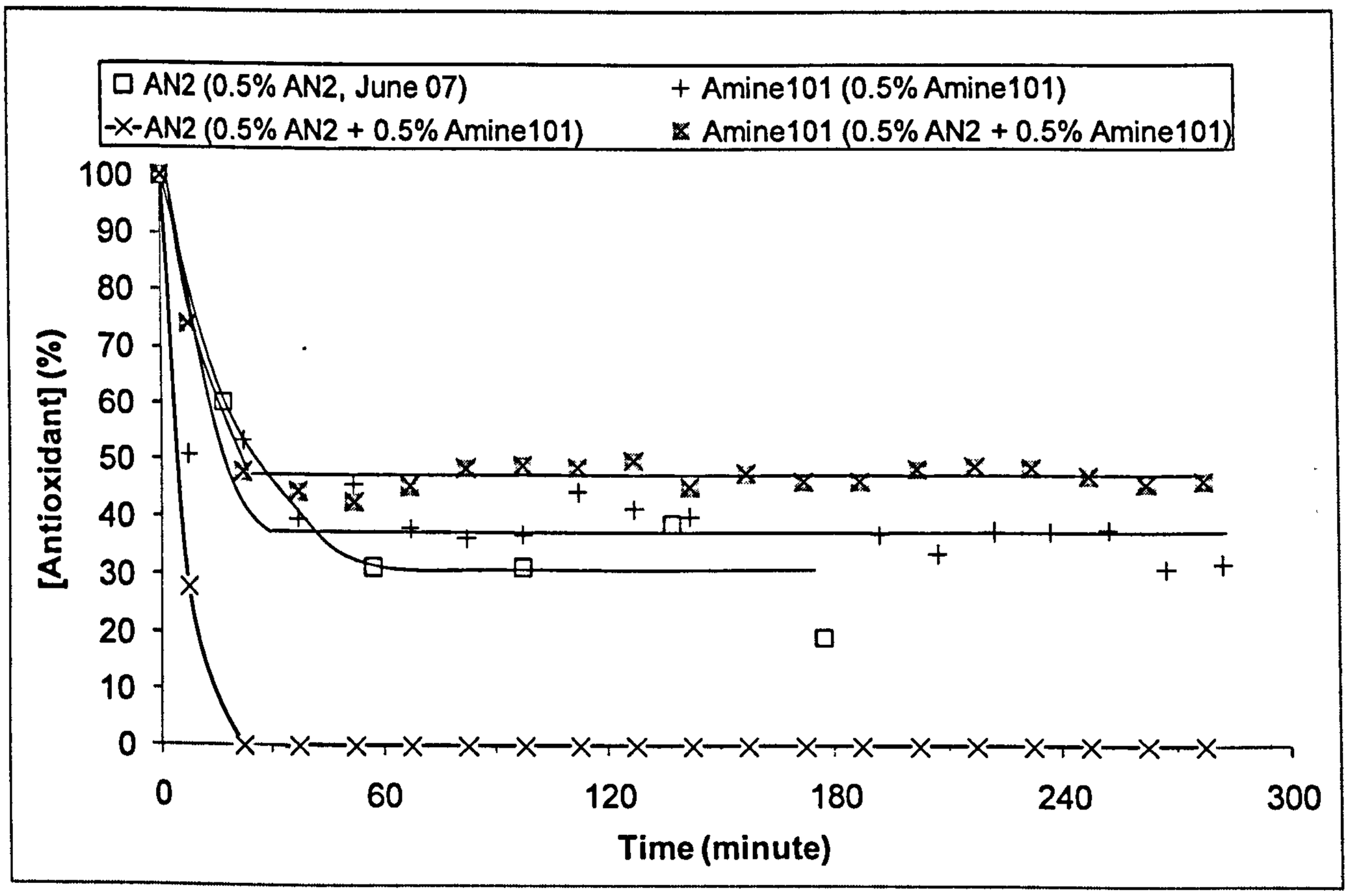

Figure 7.28: Decay of antioxidants (by GC) in 0.5% AN2 + 0.5% Amine101 blend (August 2007 test) from top ring zone

7.3. DISCUSSION

Sterically-hindered phenol and diaromatic amine interactions

Previous works have indicated that sterically-hindered phenols (phenolics) and diaromatic amines (aminics) work synergistically and additively (Table 7.8).

Table 7.8: Effect of sterically-hindered phenol and diaromatic amine interaction (references within table)

Mixture		Effect	Reference
AN2	+ diaromatic amine	Additively	Becker and Knorr, 1996
BHT	+ diaromatic amine	Synergistic	Bowman and Stachowiak, 1999
Sterically-hindered phenol	+ diaromatic aminic	Synergistic	Dong et al, 2007
Sterically-hindered phenol	+ diaromatic amine	Synergistic	Muller et al, 1982

Synergism can be defined as the co-operation between two or more species to create a total inhibitory effect greater than the sum of individual effects; whereas, additively can be defined as the total inhibitory effect is equal to the sum of individual effects.

The inhibitory effect of an antioxidant can be estimated using methods such as oxygen uptake, the pressure minimum as a measure of end of reaction, total carbonyl content, total acid number, and viscosity increase. The final inhibitory outcome can vary with each method. For instance, in the case of the reaction between AN2 and a diaromatic amine (Amine101), the extent of synergism varied considerably when using ketone (or carbonyl) formation (Figure 7.4) and oxygen uptake (Figure 7.1) methods:

$$\text{Extent of interaction} = \frac{\text{Reaction time of mixed antioxidants}}{\text{Sum of reaction times of individual antioxidants}}$$

Extent of interactions measured by ketone formation (Figure 7.4)

Reaction time of AN2 alone = 27 minutes

Reaction time of Amine101 alone = 5 minutes

Reaction time of AN2+Amine101 = 44 minutes

So, 44/(27+5) = 1.38; i.e. there is a 0.4 synergism

*Extent of interactions measured by oxygen uptake (*Figure 7.1*)*

Reaction time of AN2 alone = 20 minutes

Reaction time of Amine101 alone = 13 minutes

Reaction time of AN2+Amine101 = 38 minutes

So, 38/(20+13) = 1.15; i.e. there is a 0.2 synergism

Results obtained from the piston top ring zone oil samples show that phenolics survive (~30 %) in the top ring zone but completely disappear in the presence of aminics (Figure 7.28). The level of the aminic is little affected by the presence or absence of the phenolic (compare Figure 7.24 and Figure 6.10). Similarly, results from the bench-top reactors show that aminics degrade rapidly in the absence of phenolics and are preserved well in the presence of phenolics with the phenolics being consumed over time (Figure 7.17). These results can be explained by the well-established "Sacrificial" mechanism, where the aminyl radicals react with the phenolic to regenerate the amine (Denisov and Afanasev, 2005, p.604):

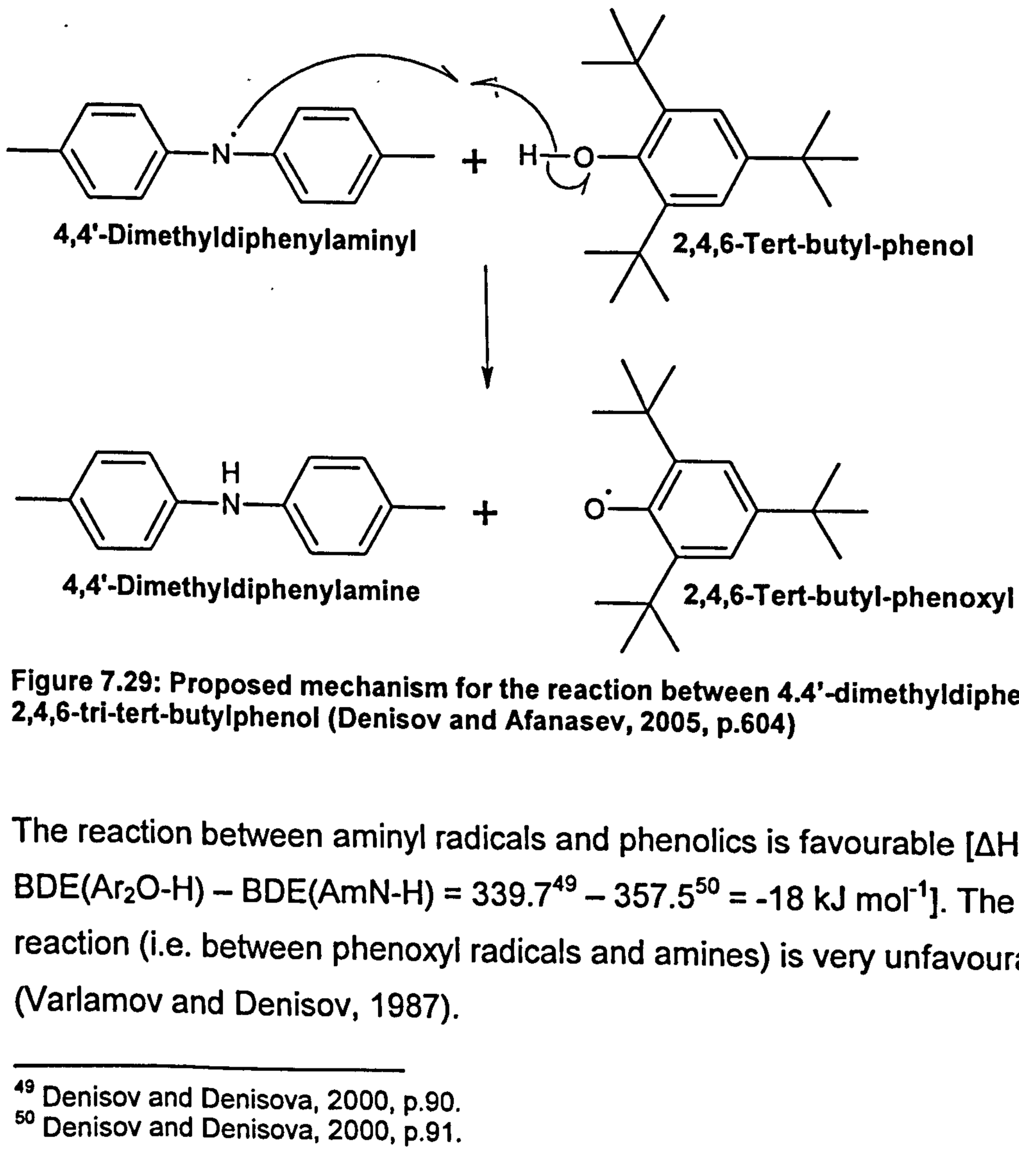

Figure 7.29: Proposed mechanism for the reaction between 4.4'-dimethyldiphenylaminyl and 2,4,6-tri-tert-butylphenol (Denisov and Afanasev, 2005, p.604)

The reaction between aminyl radicals and phenolics is favourable [ΔH = $BDE(Ar_2O\text{-}H) - BDE(AmN\text{-}H) = 339.7^{49} - 357.5^{50} = -18$ kJ mol^{-1}]. The reverse reaction (i.e. between phenoxyl radicals and amines) is very unfavourable (Varlamov and Denisov, 1987).

[49] Denisov and Denisova, 2000, p.90.
[50] Denisov and Denisova, 2000, p.91.

The complete disappearance of phenolics in the presence of aminics in the top ring zone (Figure 7.28) is probably due to the abundant quantities of free radicals in the top ring zone reacting with the phenolic and the aminic simultaneously, causing the levels of the phenolic and the aminic to be less than 50 %. The produced aminyls radicals react with the remainder phenolic causing the phenolic to completely disappear and the amine level to increase by regeneration.

Table 7.9 shows that the rate constant for the reaction between aminyl radicals and peroxyl radicals is higher than that for the reaction between aminyl radicals and phenolics. Although aminyl radicals react very rapidly with peroxyl radicals, this reaction is expected to be negligible because the concentration of peroxyl radicals is maintained at a low level by the amine. This leaves the reactive aminyl radicals more likely to react with oxygen and the phenol to regenerate the amine and to give rise to nitroxyl and phenoxyl radicals. The phenoxyl radicals are then expected to react with oxygen and peroxyl radicals. The reaction with oxygen is reversible and the rate constant of the dissociation of the oxygen molecule increases with temperature (Griva and Denisov, 1973). In turn, this leaves the reaction between phenoxyl and peroxyl radicals to be the dominant pathway.

Table 7.9: Absolute rate constants (in M^{-1} s^{-1}) of reacting species (references within table)

	Phenolic	Phenoxyl	Aminic	Aminyl	Nitroxyl
Phenoxyl	$3.2x10^4$ (200°C)[51]	$2.8x10^4$ (200°C)[52]	$7x10^3$ (75°C)[53]	-	-
Aminyl	$3.1x10^6$ (200°C)[54]	No data	$2.0x10^6$ (200°C)[55]	$2.3x10^6$ (25°C)[56]	-
Nitroxyl	$2.8x10^{-3}$ (200°C)[57]	No data	$1.3x10^3$ (200°C)[58]	No data	$2.4x10^4$ (200°C)[59]
Peroxide	$4.3x10^{-3}$ (200°C)[60]	$2.1x10^5$ (200°C)[61]	$8.8x10^{-5}$ (130°C)[62]	$4.5x10^4$ (20°C)[63]	6.3 (200°C)[64]
Peroxyl	$1.9x10^4$ (65°C)[65]	$3.8x10^7$ (200°C)[66]	$4x10^4$ (65°C)[67]	$6x10^8$ (25°C)[68]	$5.0x10^3$ (68°C)[69]
Oxygen	$8.1x10^{-4}$ (200°C)[70]	$1.2x10^8$ (M^{-2} s^{-1}) (200°C)[71]	$2.7x10^{-5}$ (200°C)[72]	$2x10^8$ (20°C)[73]	No data

[51] Modelled value, BHT + Phenoxyl (from BHT); $k = 1.0 \times 10^8 \exp(-31.6 \text{ kJ/mol} / RT)$ M^{-1} s^{-1} (Denisov and Denisova, 2000, p.159).
[52] 2 x Phenoxyl (from AN2); $k = 3.0 \times 10^6 \exp(-18.6 \text{ kJ/mol} / RT)$ M^{-1} s^{-1} in benzene (Roginskii, 1985).
[53] Diphenylamine + 2,4,6-Tri-tert-butylphenoxyl in CCl_4 (Varlamov and Denisov, 1987).
[54] 2,4,6-tri-tert-butylphenol + 4,4'-Dimethyldiphenylaminyl; $k = 3.9 \times 10^5 \exp(-(-8.1 \text{ kJ/mol} / RT)$ M^{-1} s^{-1} in decane (Denisov and Afanasev, 2005, p.604). Also, BHT + Diphenylaminyl; $k = 7.4 \times 10^5 \exp(-(-5.2 \text{ kJ/mol} / RT)$ M^{-1} s^{-1} in toluene (Varlamov et al, 1995). Note that the activation energy is negative; see Denisov and Afanasev, 2005, page 604 for explanation.
[55] Modelled value, Diphenylamine + Diphenylaminyl; $k = 1.0 \times 10^8 \exp(-15.3 \text{ kJ/mol} / RT)$ M^{-1} s^{-1} (Denisov and Denisova, 2000, p.166).
[56] 2 x 4,4'-Dimethyldiphenylaminyl (Denisov and Afanasev, 2005, p.520). Also, 2 x Diphenylaminyl; $k = 2.7 \times 10^7$ M^{-1} s^{-1} (25 °C) (Denisov and Afanasev, 2005, p.520).
[57] 2.6-Di-tert-butylphenol + Diphenylnitroxyl; $k = 4.8 \exp(-29.3 \text{ kJ/mol} / RT)$ M^{-1} s^{-1} in heptane (Howard, 1972, p.163).
[58] Modelled value, 4,4-Dimethoxydiphenylamine + TEMPO; $k = 7.9 \times 10^8 \exp(-52.4 \text{ kJ/mol} / RT)$ M^{-1} s^{-1} (Denisov and Afanasev, 2005, p.615).
[59] 2 x $Ph_2C{=}NO\bullet$; $k = 2.0 \times 10^5 \exp(-8.4 \text{ kJ/mol} / RT)$ M^{-1} s^{-1} in chlorobenzene (Denisov and Denisova, 2000, p.178).
[60] 2,4,6-Tri-tert-butylphenol + PhMe2COOH; $k = 4.0 \times 10^9 \exp(-108.4 \text{ kJ/mol} / RT)$ M^{-1} s^{-1} in decane (Denisov and Afanasev, 2005, p.120).
[61] Phenoxyl (from AN2) + Di-tert-butyl-peroxide; $k = 1.2 \times 10^7 \exp(-15.9 \text{ kJ/mol} / RT)$ M^{-1} s^{-1} (Prokofev et al, 1968).
[62] 4,4'-Dimethyldiphenylamine + Cumylhydroperoxide in decane/chlorobenzene (Denisov and Afanasev, 2005, p.536).
[63] Diphenylaminyl + Tert-butyl-hydroperoxide in cyclohexane (Varlamov and Denisov, 1986). Also, Diphenylaminyl + Cyanoisoproylperoxide; $k = 1.1 \times 10^5$ M^{-1} s^{-1} (20 °C) in cyclohexane (Varlamov and Denisov, 1987).
[64] Modelled value, TEMPO + 1,1-Dimethylethyl hydroperoxide, $k = 5.1 \times 10^7 \exp(-62.6 \text{ kJ/mol} / RT)$ M^{-1} s^{-1} (Denisov and Denisova, 2000, p.170).
[65] BHT + Styrylperoxyl; $k = 7.9 \times 10^7 \exp(-23.5 \text{ kJ/mol} / RT)$ M^{-1} s^{-1} (Howard, 1972, p.131).
[66] 2,4,6-Tri-tert-butylphenoxyl + Cyanoisopropylperoxyl; $k = 5.2 \times 10^7 \exp(-1.2 \text{ kJ/mol} / RT)$ M^{-1} s^{-1} (Rubtsov et al, 1979).
[67] Diphenylamine + Styrylperoxyl in o-dichlorobenzene (Brownlie and Ingold, 1967).
[68] Diphenylaminyl + Cyclohexylperoxyl in cyclohexane (Denisov and Afanasev, 2005, p.511).
[69] Diphenylnitroxyl + $PhCH(Me)_2OO\bullet$ (Denisov and Afanasev, 2005, p.512).
[70] Modelled value, 2,4,6-Tri-tert-butylphenol + O_2; $k = 1.1 \times 10^{10} \exp(-119.0 \text{ kJ/mol} / RT)$ M^{-1} s^{-1} in (Denisov and Afanasev, 2005, p.531).
[71] 2,4,6-Tri-tert-butylphenoxyl + O_2; $k = 3.2 \times 10^{-5} \exp(114 \text{ kJ/mol} / RT)$ M^{-2} s^{-1} (Denisov and Afanasev, 2005, p.527).
[72] 4,4'-Dimethyldiphenylamine + O_2; $k = 4.2 \times 10^{10} \exp(-137.5 \text{ kJ/mol} / RT)$ M^{-1} s^{-1} in (Denisov and Afanasev, 2005, p.531).
[73] Dialkylaminyl + O_2 (Musa et al, 1996).

Additive-succinimide dispersant interactions

Succinimide dispersants (Figure 7.30) are also reported to work synergistically in inhibition with AN2 (Vipper and Tarasov, 1971), react negatively with calcium salicylate detergents (Baladincz et al, 1998), and interact with calcium sulphonate detergents[74] (Figure 7.31) (Vuk et al, 1997).

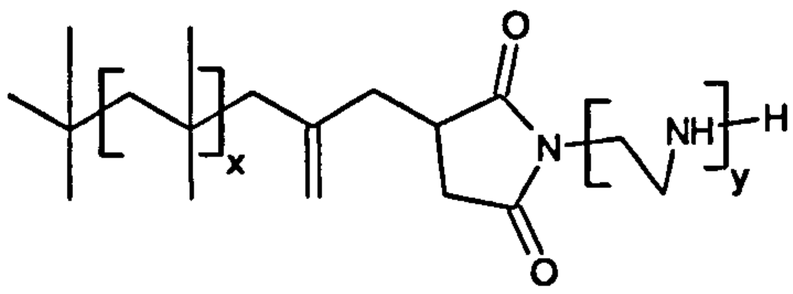

Figure 7.30: Mono-succinimide dispersant

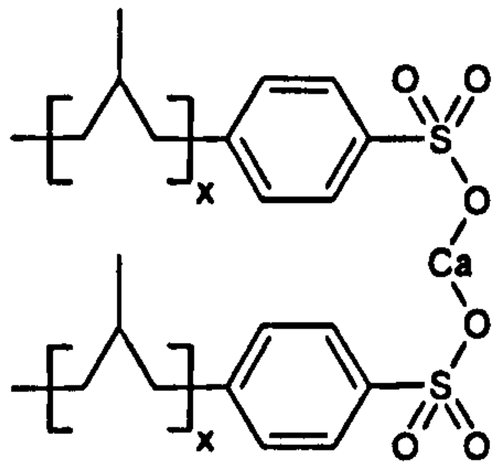

Figure 7.31: Calcium sulphonate detergent

The reaction between AN2 and succinimide dispersant (a mixture of mono-, bi-, tris-succinimide) resulted in a synergism between the two additives, using oxygen uptake as a measure of the reaction time. Oxidations of 10.0 mmol dm^{-3} AN2 and 2.0 % v/v succinimide dispersant in Shell XHVI 8.2 at 200 °C resulted in the following reaction times:

Reaction time of AN2 alone = 28 minutes (Figure 7.9)
Reaction time of dispersant alone = 2 minutes (Figure 7.32)
Reaction time of AN2+dispersant = 45 minutes (Figure 7.9)
So, 45/(28+2) = 1.50; i.e. there is a 0.5 synergism

[74] The interaction increases in the order: Ca-salycilate > Ca-phenate > Ca-sulphonate (Vuk et al, 1997).

The succinimide dispersant does have some antioxidant properties (Figure 7.32).

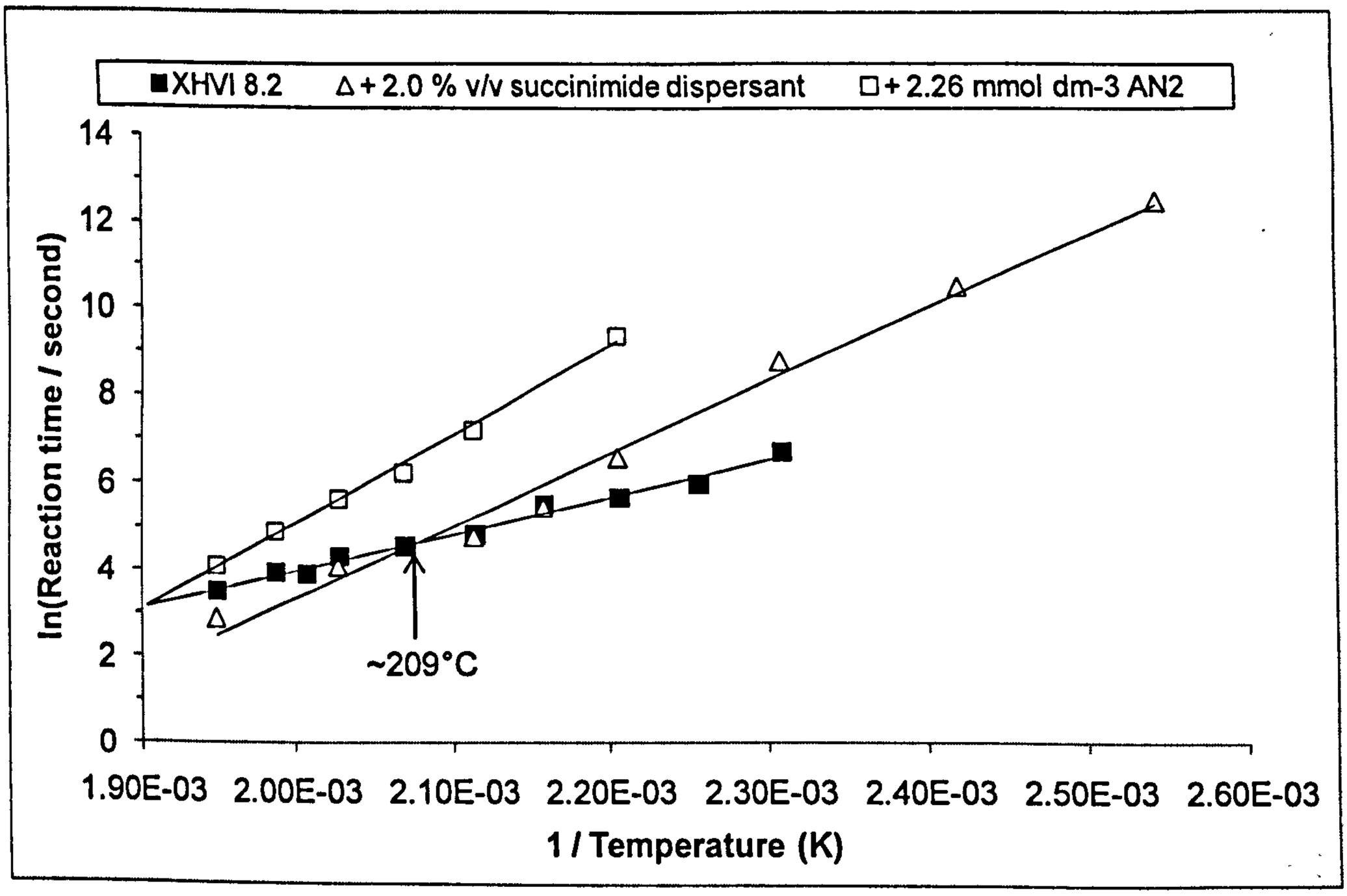

Figure 7.32: Oxidation of 2.0 % v/v succinimide dispersant in 1.0 cm^3 Shell XHVI 8.2 in static micro reactor

The possibility of the dispersant acting as an aminic antioxidant (i.e. the hydrogen atom of aliphatic amine group being regenerated by AN2) is not valid because, if this was the case, then one expects the concentration of AN2 to be low in the presence of Amine101 and lower in the presence of Amine101 plus the dispersant - this was not the case (Figure 7.33).

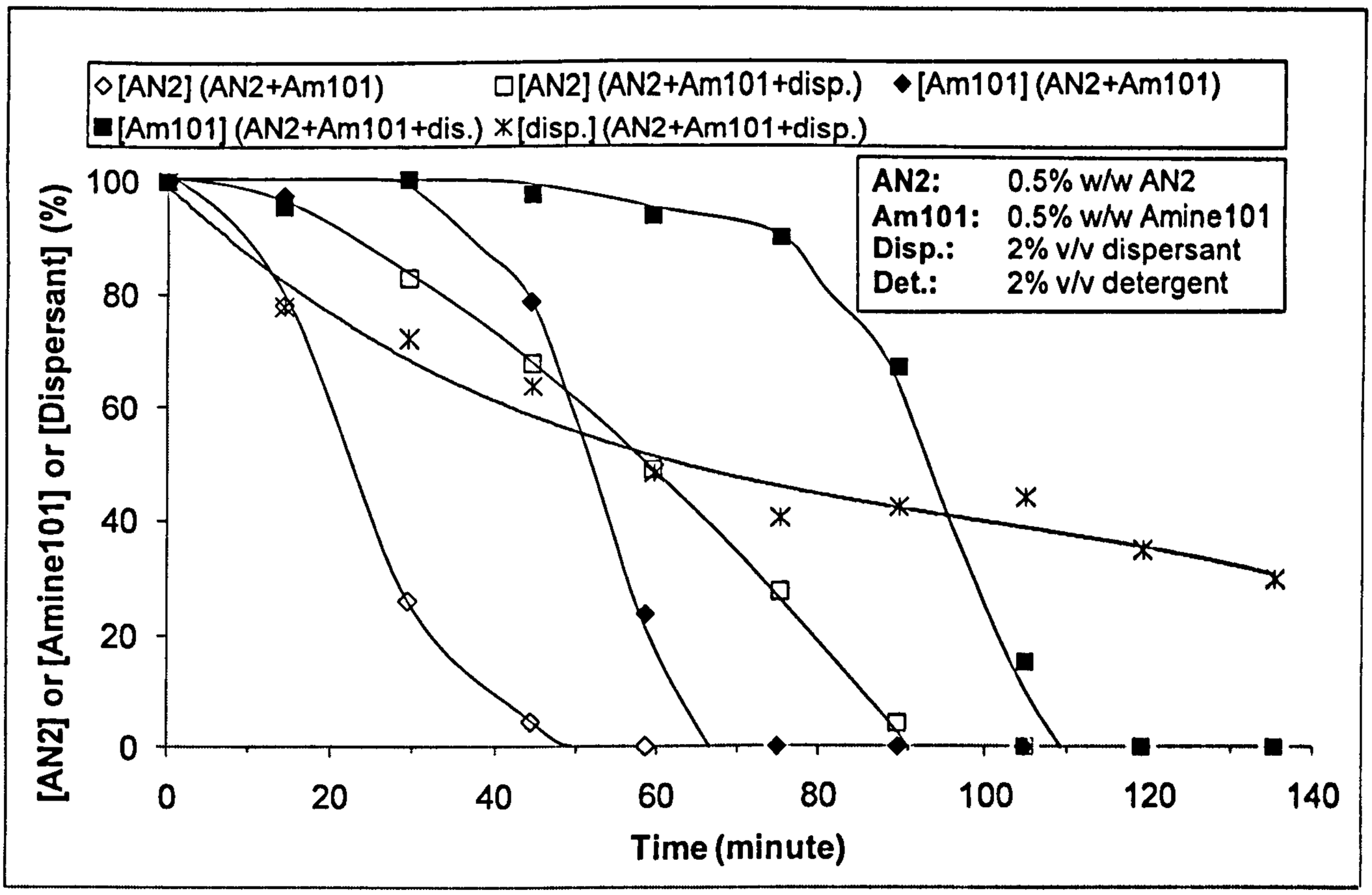

Figure 7.33: Decay of 10.0 mmol dm^{-3} AN2 (by FTIR), 10.0 mmol dm^{-3} Amine101 (by GC), and 2.0 % v/v succinimide dispersant (by FTIR) in the oxidation of additives in squalane at 200 °C in flow intermediate reactor

The only available explanation in the literature (Vipper and Tarasov, 1971) for this synergism is that the succinimide dispersant disperse the AN2 antioxidant into the solvent and hence providing extra antioxidative protection against free radicals (Vipper and Tarasov, 1971). This explanation seems very plausible.

Additive-sulphonate detergent interactions

The reaction between the calcium sulphonate detergent and ZDDP seems to give rise to oxidation products that react strongly with Amine101 (Figure 7.5) and AN2 (Figure 7.6); although succinimide dispersant was present, it did not react with ZDDP because the level of the dispersant remained almost unchanged throughout the reaction (Figure 7.8).

Additive-ZDDP interactions

The high efficiency of ZDDP in inhibition oxidation reactions (Figure 7.14) arises from the ability of ZDDP (and/or its oxidation products) in reacting with peroxyl radicals (Denisov and Afanasev, 2005, p.591) and hydroperoxides (Denisov and Afanasev, 2005, p.589). ZDDP (and/or its oxidation products) also interacts synergistically with AN2 (Becker and Knorr, 1996) and diaromatic amines (Chao et al, 1984).

Additive-nitrogen oxides interactions

The main nitrogen oxides in piston blowby are the free radicals of nitric oxide (NO•) and nitrogen dioxide (NO_2•) (Korcek and Johnson, 1993). Typical concentrations of blowby nitrogen oxides are listed in Table 7.10.

Table 7.10: Typical concentrations of blowby nitrogen oxides (Chatterjee, 1993)

Nitrogen oxides	Concentration (ppm)
NO•	8-500
NO_2•	0.3-155

Nitric oxide and nitrogen dioxide exist in a temperature dependent equilibrium. Nitric oxide dominates at high temperatures and nitrogen dioxide dominates at low temperatures (Korcek and Johnson, 1993) because nitrogen dioxide decays at high temperatures in the gas phase by the reaction: $2\ NO_2\bullet \rightarrow 2\ NO\bullet + O_2$ (Denisov and Afanasev, 2005, p.111). NO_2• is a stable radical with an unpaired electron and forms the dimer N_2O_4 in the equilibrium reaction: $2\ NO_2\bullet \leftrightarrows N_2O_4$ (Denisov and Afanasev, 2005, p.111).

Nitrogen dioxide reacts with phenolic antioxidants (Korcek and Johnson, 1993). For example, reacting AN2 with NO_2• (150 ppm) in cyclohexane at 25 °C gives rise to a dienone (Figure 7.34) (Chatterjee, 1993, p.263). However, such reactions are unfavourable:

ΔH = BDE(Ar_2O-H) – BDE(ONO-H) in kJ mol^{-1}

= $340.2^{75} - 330.7^{76}$ = 10 kJ mol^{-1} (endothermic, i.e. reversible)

[75] Denisov and Denisova, 2000, p.89.
[76] Luo, 2007, p.260.

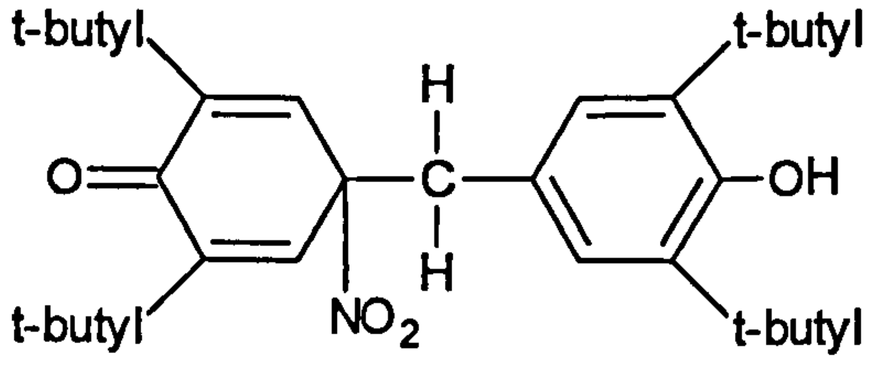

Figure 7.34: Dienone of AN2 (Chatterjee, 1993, p.263)

The reaction was found to be first order in AN2 and second order in NO_2•: -d[AN2] / dt = k$[NO_2]^2$x[AN2] (Chatterjee, 1993):

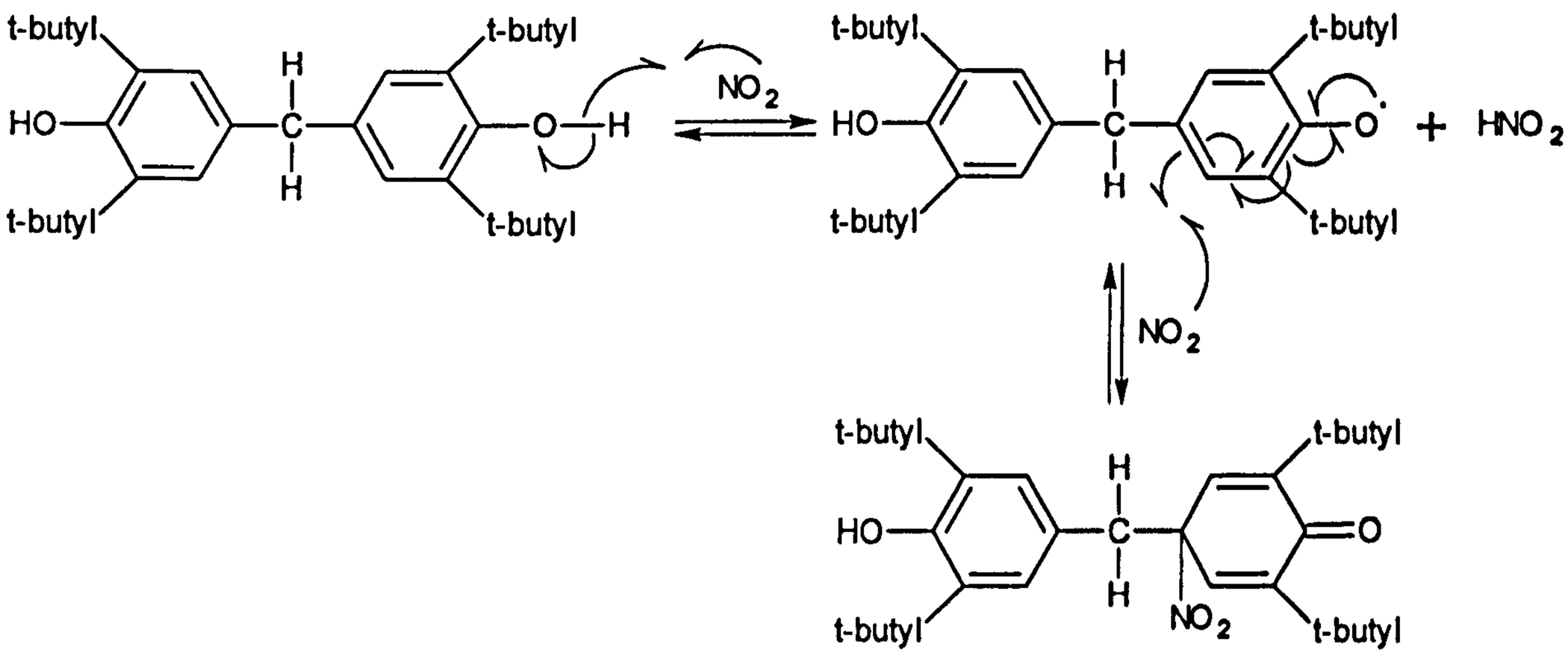

Figure 7.35: Proposed mechanism for the reaction between AN2 and NO_2• at 25 °C in the presence of oxygen (Chatterjee, 1993, p. 286)

In this work, the dienone either was in very low concentrations or does not have a "distinctive" UV absorption between 240 nm to 300 nm (Figure 7.36) and so it is not possible at this stage to confirm or deny the existence of dienone in top ring zone oil samples (Figure 7.37).

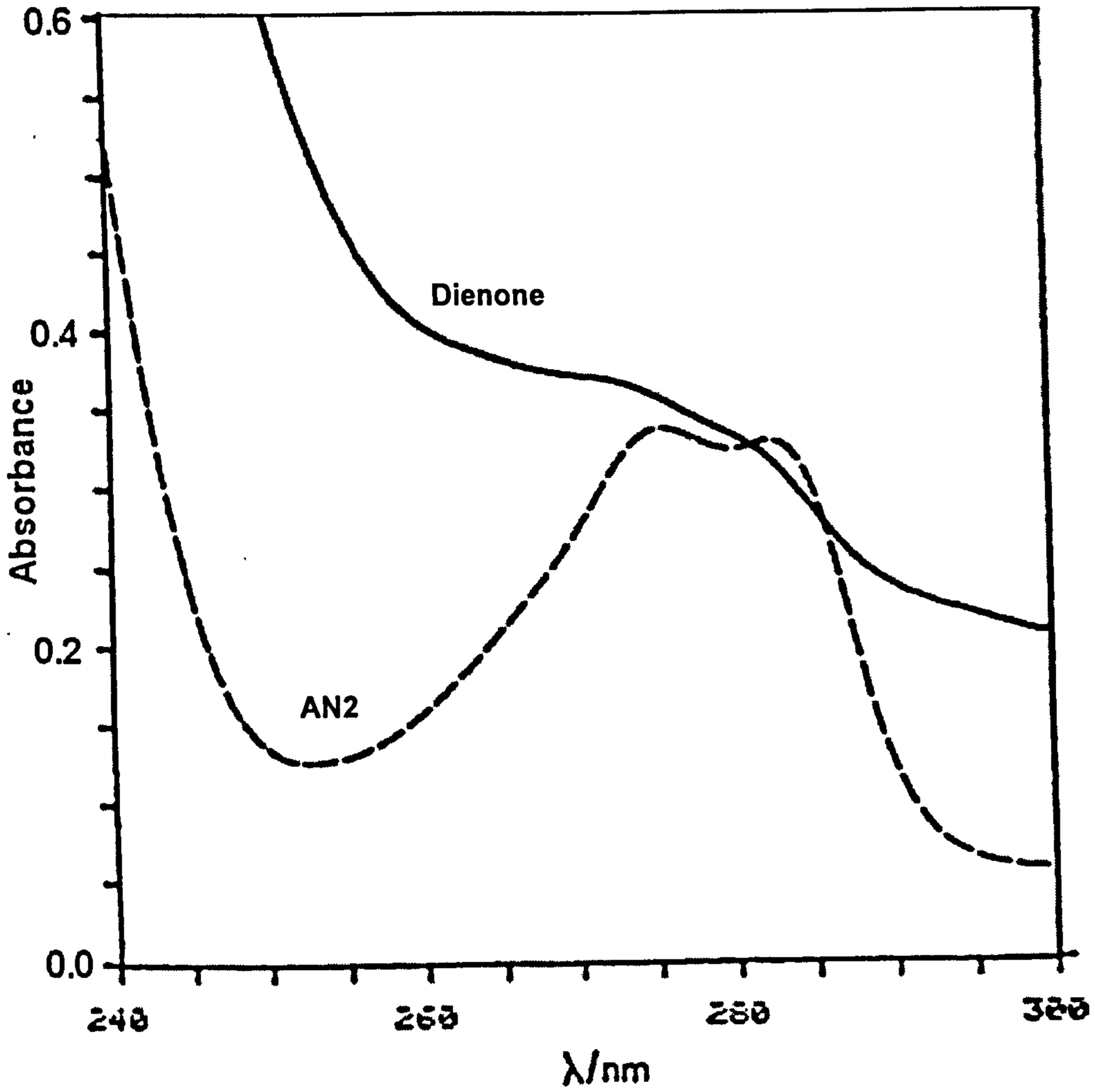

Figure 7.36: UV spectra of AN2 (0.064 mmol dm^{-3}) and dienone (0.064 mmol dm^{-3}) in cyclohexane (Chatterjee, 1993)

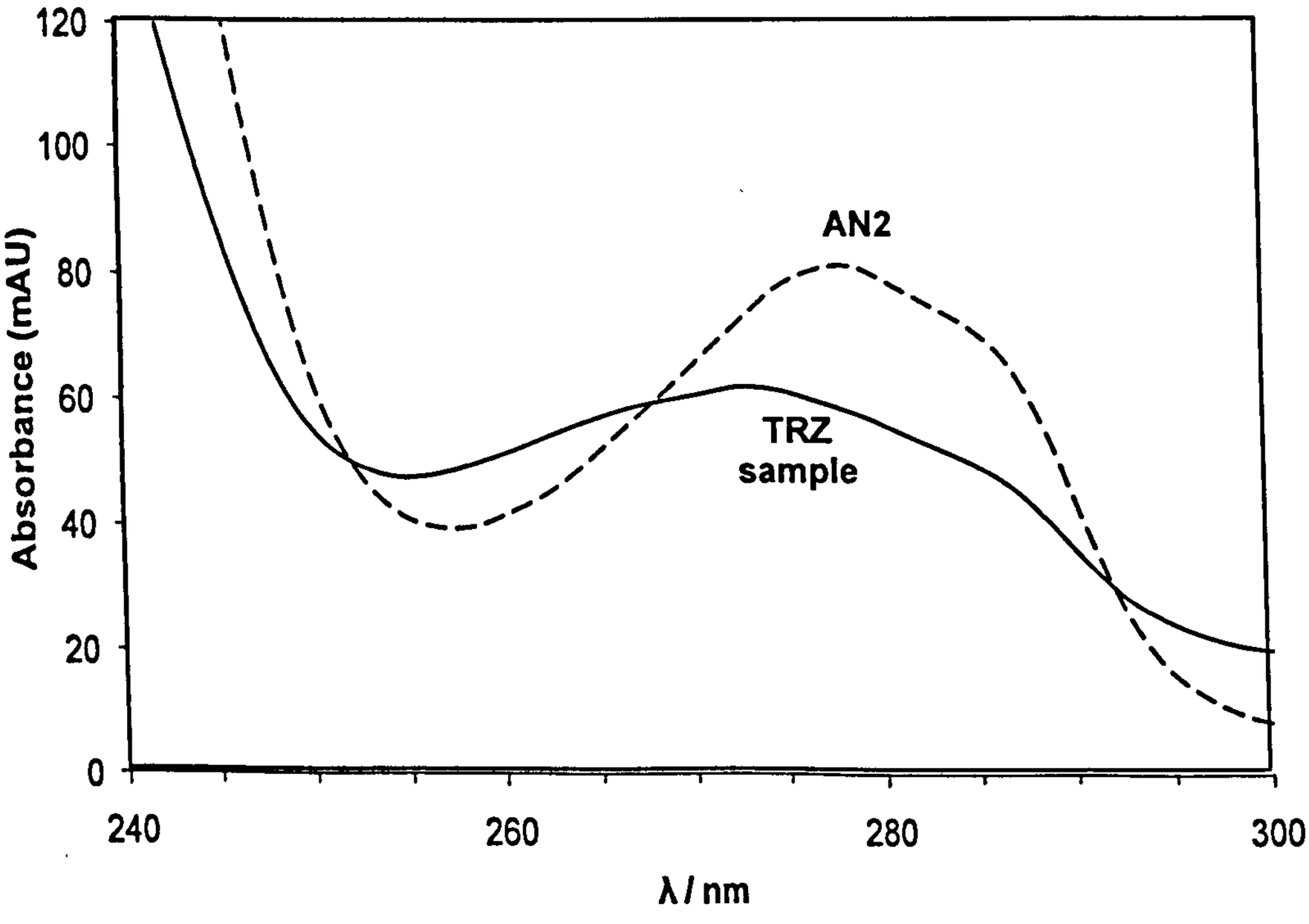

Figure 7.37: Diode array-LC spectra of fresh and top ring zone (TRZ) degraded (1500 rpm / half load) AN2 (9.4 mmol dm^{-3}) (+det.&disp.) in Shell XHVI 8.2

Metals content

The concentrations of iron, copper, manganese, and chromium in an oil sample (XHVI 8.2 with AN2, succinimide, and sulphonate) obtained from the top ring zone of the piston assembly of the Ricardo Hydra engine were below the detection limit of 0.003, 0.0005, 0.003, and 0.001 ppm for iron, copper, manganese, and chromium, using atomic absorption spectroscopy. The very low metal concentrations were unexpected because in the absence of a tribofilm (no ZDDP was present), the engine parts would rub each other directly and thus were expected to produce large amounts of metals. However, low metal contents were found, most likely, due to the very short engine operation (that is to say, six hours).

7.4. SUMMARY

The interactions of antioxidants with other automotive lubricant additives were investigated, by degradation in bench-top reactors at top ring zone temperatures and a research gasoline engine, to provide lubricant formulators with a good understanding of the nature and extent of interactions between antioxidants and other lubricant additives.

Sterically-hindered phenols and diaromatic amines were found to interact strongly with each other. In the bench-top reactor, the degree of synergism was found to be ≈0.3. In the top ring zone, ≈10 % of the aminic was regenerated at the expense of 50 % of the phenolic. The synergistic interaction between a phenolic and an aminics was attributed to the phenolic providing easy-to-abstract hydrogen atoms to the aminyl radicals of the amine to regenerate the amine. It is worth mentioning that although hydrogen atoms from phenolics are much easier to abstract than those from aminics, peroxyl radicals preferentially react with aminics due to the faster rate constant (Table 7.9).

AN2 was found to interact strongly with the succinimide dispersant. The degree of synergism was found to be 0.5. The synergistic interaction between AN2 and the succinimide dispersant was attributed to the succinimide dispersant dispersing the AN2 antioxidant into the solvent and hence providing extra antioxidative protection against free radicals.

The reaction between the calcium sulphonate detergent and ZDDP seems to give rise to oxidation products that react strongly, in a negative manner, with Amine101 and AN2.

7.5. REFERENCES

Baladincz, J.; Vuk, T.; Auer, J.; Kis, G.; and Bartha, L. Interactions of additives in lubricating oil compositions. *Hungarian Journal of Industrial Chemistry*, 1998, **26**: 155-159.

Becker, R. and Knorr, A. An evaluation of antioxidants for vegetable oils at elevated temperatures. *Lubrication Science*, 1996, **8** (2): 95-117.

Bowman, W. and Stachowiak, G. Application of sealed capsule differential scanning calorimetry part II assessing the performance of antioxidants and base oils. *Lubrication Engineering*, 1999, **55** (5): 22-29.

Brownlie, I. and Ingold, K. The inhibited autoxidation of styrene part VI the relative efficiencies and the kinetics for inhibition by N-aryl anilines and N-alkyl anilines. *Canadian Journal of Chemistry*, 1967, **45** (20): 2419-2425.

Chao, T.; Hutchison, D.; and Kjonaas, M. Some synergistic antioxidants for synthetic lubricants. *Industrial and Engineering Chemistry Product Research and Development*, 1984, **23** (1): 21-27.

Chatterjee, J. The mechanisms of some reactions of nitrogen dioxide with alkenes and aromatic compounds. PhD thesis, City University London, 1993.

Colclough, T. Role of additives and transition metals in lubricating oil oxidation. *Industrial and Engineering Chemistry Research*, 1987, **26** (9): 1888-1985.

Cracknell, R. and Head, R. Influence of fuel properties on lubricant oxidative stability part 1 engine tests. *SAE Technical Paper*, 2005, paper 2005-01-3839.

Denisov, E. and Afanasev, I. Oxidation and antioxidants in organic chemistry and biology. CRC Press of Taylor and Francis Group, Florida, 2005.

Denisov, E. and Denisova, T. Handbook of antioxidants bond dissociation energies rate constants activation energies and enthalpies of reactions (second edition). CRC Press LLC, Florida, 2000.

Dong, J.; Mulqueen, G.; Goode, M.; and Holt, A. Stabilizing compositions for lubricants. Chemtura Corporation, 2007, patent WO 2007/100726 A2.

Griva, A. and Denisov, E. Kinetics of the reactions of 2,4,6-tri-t-butylphenoxyl with cumene hydroperoxides cumylperoxyl radicals and molecular oxygen. *International Journal of Chemical Kinetics*, 1973, **5** (5): 869-877.

Howard, J. Absolute rate constants for reactions of oxyl radicals. In: Williams, G. (editor). Advances in free-radical chemistry, volume 4. Logos Press Limited, London, 1972.

Hsu, S. and Lin, R. Interactions of additives and lubricating base oils. *SAE Technical Paper*, 1983, paper 831683: 61-69.

Hsu, S.; Ku, C.; and Lin, R. Relationship between lubricating basestock composition and the effects of additives on oxidation stability. *Society of Automotive Engineers, Special Publication S26*, 1982, paper 821237: 29-56.

Korcek, S. and Johnson, M. Effects of NOx on liquid phase oxidation and inhibition of elevated temperatures. In: Bartz, W. (editor). Engine oils and automotive lubrication. Marcel Dekker Incorporation, New York, 1993.

Luo, Y. Comprehensive handbook of chemical bond energies. CRC Press Incorporation, Florida, 2007.

Muller, K.; Kristen, U.; and Hamblin, P. Effectiveness of ashless antioxidants in motor oils. From: Wirksamkeit von aschefreien antioxidantien in motorolen. *Schmiertechnik Tribologie*, 1982, **29** (3): 92-97.

Musa, O.; Horner, J.; Shahin, H.; and Newcomb, M. A kinetic scale for dialkylaminyl radical reactions. *Journal of the American Chemical Society*, 1996, **118** (16): 3862-3868.

Pawlak, Z. Tribochemistry of lubricating oils. Elsevier, London; Amsterdam, 2003. Chapter 2.

Prokofev, A.; Solodovnikov, S.; and Nikiforov, G. Interaction of coppinger radicals with di-tert-butyl peroxide. Translated from Russian by SciFinder Scholar from *Teoreticheskaya I ekspermentalnaya khimiya*, 1968, **4** (5): 700-704.

Roginskii, V. ESR spectra and kinetics of the disproportionation of substituted phenoxy radicals coomunication 2 radicals of 2,4,6-trialkyl-substituted mono-, p-bis-, p-tris-, and p-tetraphenols. *Bulletin of the Academy of Sciences of the USSR Division of Chemical Science*, 1985, **34** (9): 1833-1841, part 1.

Rubtsov, V.; Roginskii, V.; Dubinskii, V.; and Miller, V. Rate constants for phenoxy radical reactions in hydrocarbon oxidations inhibited by 2,4,6-tri-tert-butylphenol. 1979: 921-925.

Taylor, R.; Mainwaring, R.; and Mortier, R. Engine lubricant trends since 1990. *Proceedings of the Institution of Mechanical Engineers-part J-Journal of Engineering Tribology*, **219**: 1-16, 2005.

Varlamov, V. and Denisov, E. Kinetics of reactions in the thermal decomposition of tetraphenylhydrazine in the presence of a mixture of sterically hindered phenol and hydroperoxides. *Russian Chemical Bulletin*, 1986, **35** (11): 2211-2215.

Varlamov, V. and Densiov, E. Kinetic spectrophotometric study of the kinetics of direct and reverse reactions of the peroxide radical with diphenylamine. *Russian Chemical Bulletin*, 1987, **36** (8): 1607-1612.

Varlamov, V.; Denisov, N.; and Nadtochenko, V. Negative activation energies and compensation effects for the reactions of diarylaminyl radicals with phenols. *Russian Chemical Bulletin*, 1995, **44** (12): 2282-2286.

Vipper, A. and Tarasov, V. Synergistic effect of succinimide and bisphenol additives. Translated from Russian by Marilyn Olaechea on 7-August-1972 from: *Neftepererabotka i Neftekhimiya*, 1971, (3): 25-27.

Vuk, T.; Baladincz, J.; Bartha, L.; and Auer, J. Succinimide type additive containing engine oil composition. Additives in Petroleum Refinery and Petroleum Product Formulation Practice Proceedings, Sopron, Hungary, May 1997, pages: 67-73.

8. CONCLUSIONS AND RECOMMENDATIONS FOR FUTURE WORK

8.1. CONCLUSIONS

8.1.1. Antioxidative protection by antioxidants

The behaviours of the bis-phenolic antioxidant AN2, at a treat rate of 0.5 % w/w, and the diaromatic aminic antioxidant Amine101, at a treat rate of 0.5 % w/w, have been studied in squalane at 180 °C to 210 °C in the flow intermediate rector. AN2 was found to provide a full antioxidative protection to squalane, and squalane would only oxidise when AN2 is totally consumed. The high antioxidative efficiency of AN2 was attributed to its ability to provide ready-to-abstract hydrogen atoms to peroxyl radicals. In contrast, Amine101 was found to provide partial antioxidative protection to squalane at temperatures below 210 °C and a negligible antioxidative protection above 210 °C.

The poor performance of Amine101 at high temperatures was attributed to the temperature dependent reaction between aminyl radicals and hydroperoxides; that is to say, the reaction between peroxyl radicals and the amine is reversible at high temperatures:

Am• (aminyl) + ROOH (hydroperoxide) ⇆ AmH (Amine101) + ROO• (peroxyl)

This finding contradicts with the wide belief in the literature that aminics are better antioxidants than phenolics at high temperatures (Reyes-Gavilan and Odorisio, 2001). This contradiction could be due to the use of different techniques (by researchers), which generate results that may be interpreted differently (e.g. results from total carbonyl and oxygen uptake methods). In this work, it was possible to observe the above finding when three different techniques were used simultaneously to monitor various reactions parameters online.

This finding is significant because it enables lubricant formulators to choose the appropriate antioxidant type for lubricant formulations that are required to function at the typical appliance temperatures (e.g. engine and gear lubricants).

8.1.2. Critical antioxidant behaviour

The critical antioxidant concentration and critical temperature phenomena of AN2 and Amine101 antioxidants have been investigated at 180 °C to 240 °C in bench-top reactors.

The critical antioxidant concentration of AN2 was found to be 0.22 ± 0.05 mmol dm^{-3} at 220 °C, and that of Amine101 was found to be 5.7 ± 0.5 mmol dm^{-3} at 180 °C.

Such data aid lubricant formulators to add the correct concentration of an antioxidant to the lubricant formulation.

8.1.3. Stoichiometry coefficients of antioxidants

The stoichiometry coefficients of phenolic antioxidants AN2 and BHT have been investigated in hexadecane at 80 °C to 120 °C in bench-top reactors.

The stoichiometry coefficients of AN2 and BHT at 90 °C were found to be 4.1 ± 0.2 and 4.3 ± 0.2, respectively. These values conflicted with those in the literature. The conflict between the values obtained in this work and those in the literature was attributed to the methods used to measure the stoichiometry coefficients.

The finding that BHT reacts with four peroxyl radicals should be taken as provisional because the cage effects on the production of peroxyl radicals is so far unknown (see Section 8.2.1). However, what is striking in this finding is that BHT and AN2 have almost the same stoichiometry coefficient; in spite of the fact that BHT is a mono-phenol and AN2 is a bis-phenol.

BHT is a well-known antioxidant used in gear lubricants, polymers, and textiles. Hence, this finding is significant because it shows that BHT is much more effective than previously measured (Boozer et al, 1955).

8.1.4. Behaviour of antioxidants under engine conditions

The behaviour of antioxidants in semi-formulated base fluids has been studied, to understand how antioxidants behave and decay under piston top ring zone conditions, by degradation in a research gasoline engine.

The levels of antioxidants in the top ring zone varied from ~30 to ~95 % and ~60 % when the piston rings were unpinned and pinned, respectively. Pinning the piston rings greatly enhanced the precision of top ring zone data.

The oil residence time in the sump was found to be 7.6 ± 1.0 hours and the temperature of the top ring zone was estimated to be ~250 °C as an upper limit. Such data aid lubricant formulators to add the correct concentration of an antioxidant to the lubricant formulation.

8.1.5. Additive-additive interactions

The interactions of antioxidants with other automotive lubricant additives were investigated, by degradations in bench-top reactors at top ring zone temperatures and a research gasoline engine, to provide lubricant formulators with a good understanding of the nature and extent of interactions between antioxidants and other lubricant additives.

The phenolic-aminic synergism was already known to occur in the laboratory using bench-top reactors and differential scanning calorimetry (Reyes-Gavilan and Odorisio, 2001). Phenolic-aminic synergism mechanism was demonstrated for the first time in the piston assembly. Sterically-hindered phenols and diaromatic amines were found to interact strongly with each other. In the bench-top reactor, the degree of synergism was found to be ≈0.3. In the top ring zone, ≈10 % of the aminic was regenerated at the expense of 50 % of the phenolic. The synergistic

interaction between a phenolic and an aminics was attributed to the phenolic providing easy-to-abstract hydrogen atoms to the aminyl radicals of the amine to regenerate the amine.

AN2 was found to interact strongly with the succinimide dispersant. The degree of synergism was found to be 0.5. The synergistic interaction between AN2 and the succinimide dispersant was attributed to the succinimide dispersant dispersing the AN2 antioxidant into the solvent and hence providing extra antioxidative protection against free radicals.

The reaction between the calcium sulphonate detergent and ZDDP seemed to give rise to oxidation products that react strongly, in a negative manner, with Amine101 and AN2.

These findings are significant because they provide lubricant formulators with the understanding that the lubricant is much better oxidiatively protected when using a combination of phenolic and aminic antioxidants than individual antioxidants; and also, the presence of other additives (e.g. calcium sulphonate detergent plus ZDDP) affect the performance of phenolic and aminic antioxidants.

8.2. RECOMMENDATIONS FOR FUTURE WORK

8.2.1. Stoichiometry coefficients of antioxidants at high temperatures

The stoichiometry coefficients of antioxidants were obtained at 90 °C. The reaction temperatures could be extended to 200 °C to evaluate the temperature effect on the stoichiometry coefficients of antioxidants. At temperatures over 120 °C, lauroyl peroxide decomposes at rates faster than the sample extraction rate from the reactor; and hence at high temperatures, a new reactor has to be designed (see reactor design of Guillet and Gilmer, 1969).

Lauroyl peroxide decomposes into two undecyl radicals that are trapped in cage reactions and/or react with oxygen to give peroxyl radicals. The extent of cage reactions can be evaluated by varying the viscosity of the solvent (the reactivity of the reaction varies with the nature of the solvent, e.g. linear and branched alkane).

8.2.2. Engine tests

Squalane was not degraded in the top ring zone at 1500 rpm and half load (Wilkinson, 2006); future work is needed to confirm this result. Also, future work is needed to understand why the oil viscosity increases while there are large quantities of intact antioxidants (Figure 8.1).

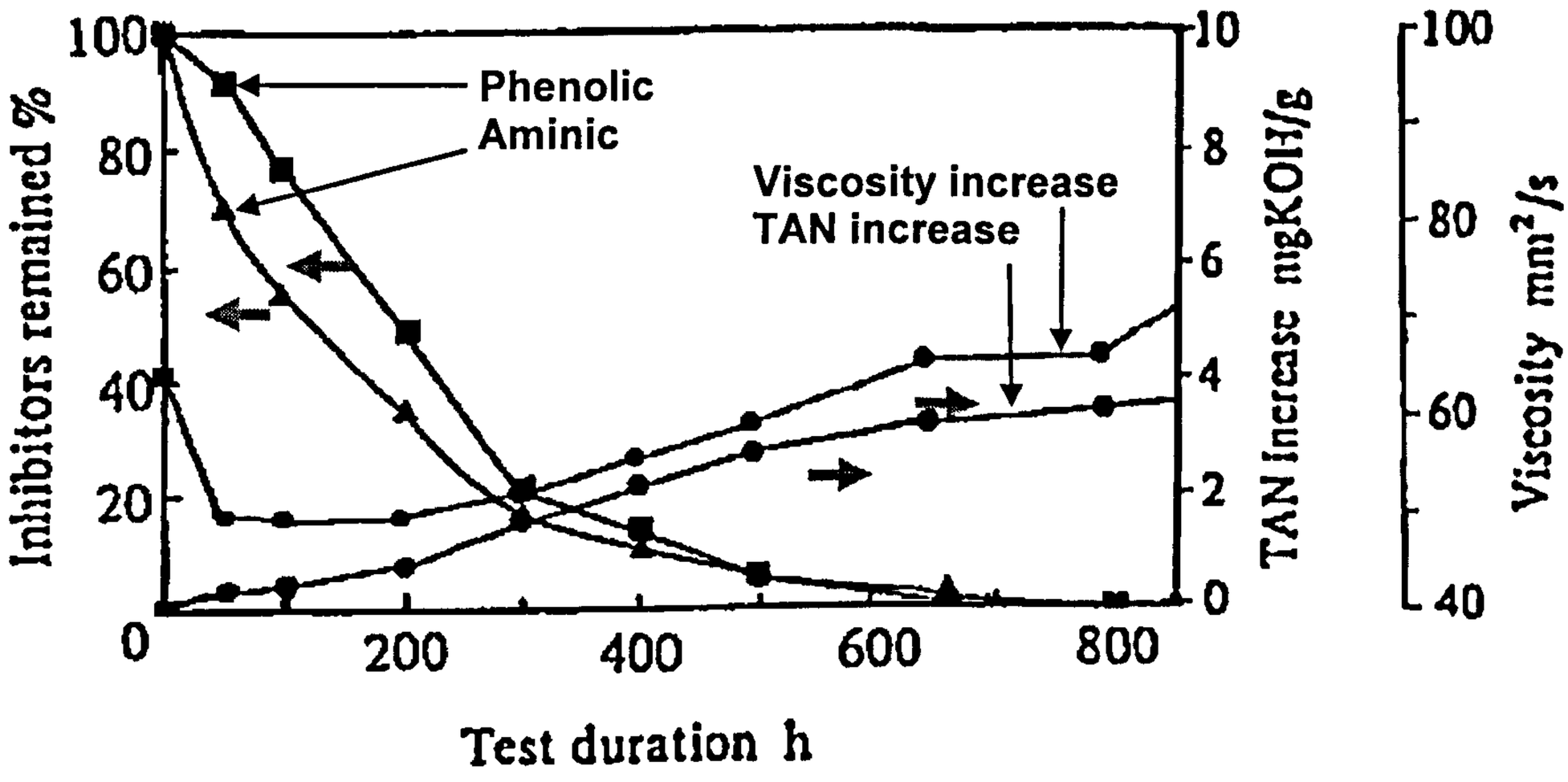

Figure 8.1: Decay of antioxidants in a fully-formulated automotive lubricant in sump of 1500 cc Toyota gasoline engine at ~2300 rpm and ~75 % load (constructed figure from data in Inoue and Yamanaka, 1990). TAN: Total acid number

8.2.3. Bench-top reactor as a model engine

The engine temperatures can be generally divided into the low sump temperature and the high piston top ring zone temperature. The intermediate bench-top reactor, which was used to simulate the conditions in the engine, can only be operated at one particular temperature at a time. The design of the intermediate bench-top reactor (see Chapter 2) has to improve to reflect genuine engine temperatures.

A new bench-top reactor (Figure 8.2) with two independent heating jackets could be used to simulate the conditions of the sump and the piston top ring zone. The speed of the stirrer regulates the volume of oil contacting hot surfaces and the degree angle of the hinge regulates the residence time of the oil before being collected via a tube.

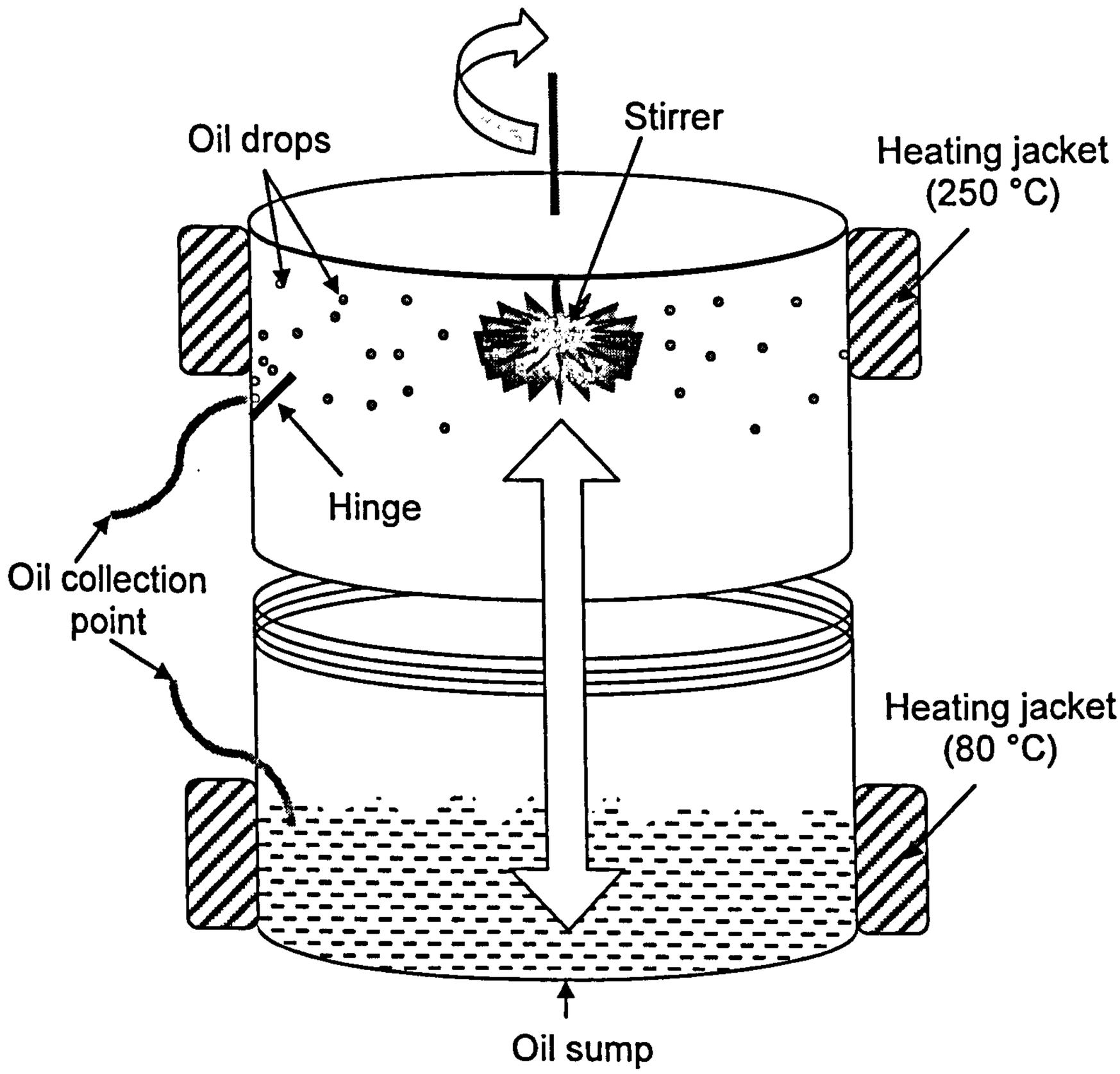

Figure 8.2: Proposed bench-top reactor

It would also be, sometimes, better to use a real blowby instead of oxygen or air because real blowby contains nitrogen oxides and persistent radicals that are expected to have significant effects on antioxidant behaviour. Easy sources of blowby are from a lawn mower and a small scooter.

8.3. REFERENCES

Boozer, C.; Hammond, G.; Hamilton, C.; and Sen, J. Air oxidation of hydrocarbons II the stoichiometry and fate of inhibitors in benzene and chlorobenzene. *Journal of the American Chemical Society*, 1955, **77**: 3233-3237.

Guillet, J. and Gilmer, J. Decomposition of lauroyl decanoyl and octanoyl peroxides in solution. *Canadian Journal of Chemistry*, 1969, **47** (23): 4405-4411.

Inoue, K. and Yamanaka, Y. Change in performance of engine oils with degradation. SAE Technical Paper, 1990, paper 902122: 1-10.

Reyes-Gavilan, J. and Odorisio, P. A review of the mechanisms of action of antioxidants metal deactivators and corrosion inhibitors. *NLGI Spokesman*, **64** (11): 22-33.

Wilkinson, J. The autoxidation of branched hydrocarbons in the liquid phase as models for understanding lubricant degradation. PhD thesis, University of York, 2006.

APPENDICES

A. APPENDIX A: EXPERIMENTAL

Temperature stability of reactors

The temperature stabilities of the micro and large reactors are ± 0.1 °C (standard deviation) (Figure A.1) and ± 0.3 °C (standard deviation) (Figure A.2 and Figure A.3), respectively. The temperature regulation of the temperature of the micro reactor[77] is better than that of the large reactor[78] because the stirring of the micro reactor (5000 rpm) is five times faster than that of the large reactor (1000 rpm); hence, the heat generated from the reaction moves faster from the centre to the wall of the reactor, where the thermocouple of the heater band is located.

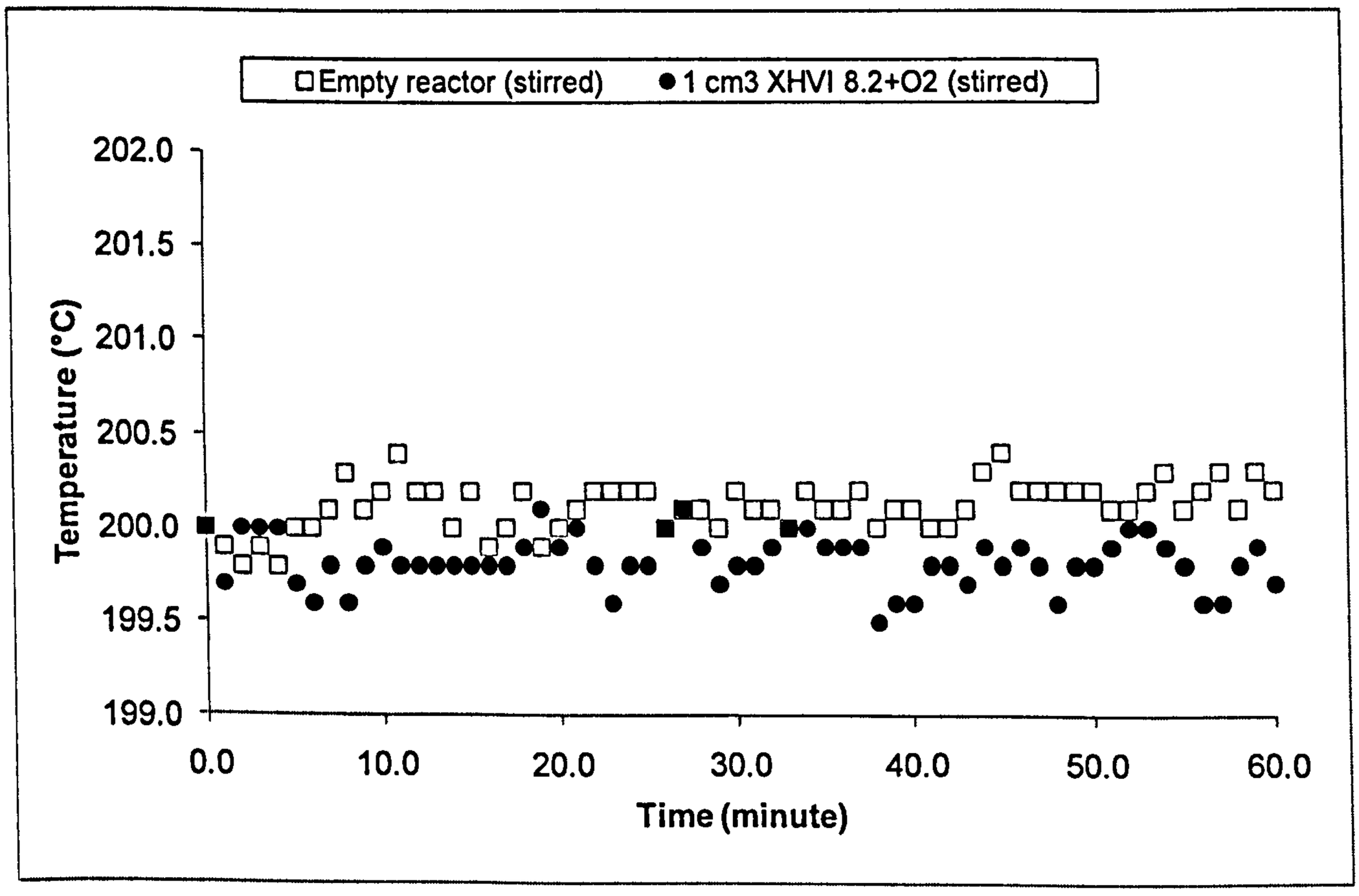

Figure A.1: Temperature stability of static micro reactor at 200.0 °C

[77] Temperature of micro reactor is that of lid (which is the same as that of liquid).
[78] Temperature of large reactor is that of liquid.

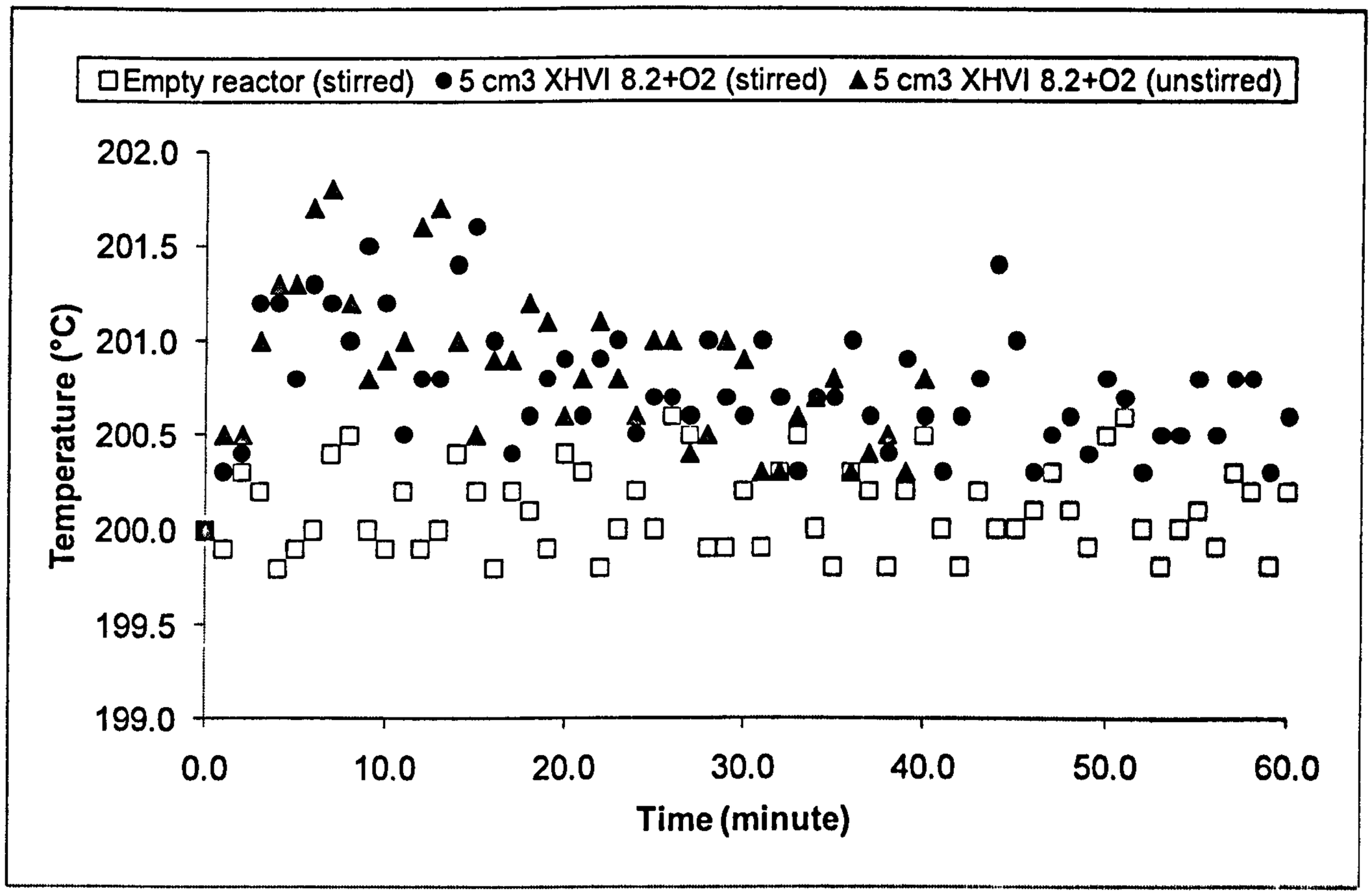

Figure A.2: Temperature stability of static large reactor at 200.0 °C

Figure A.3 shows that in the presence of oxygen the average temperature increases due to reaction; whereas, in the presence of the non-reactive nitrogen the average temperature does not change much.

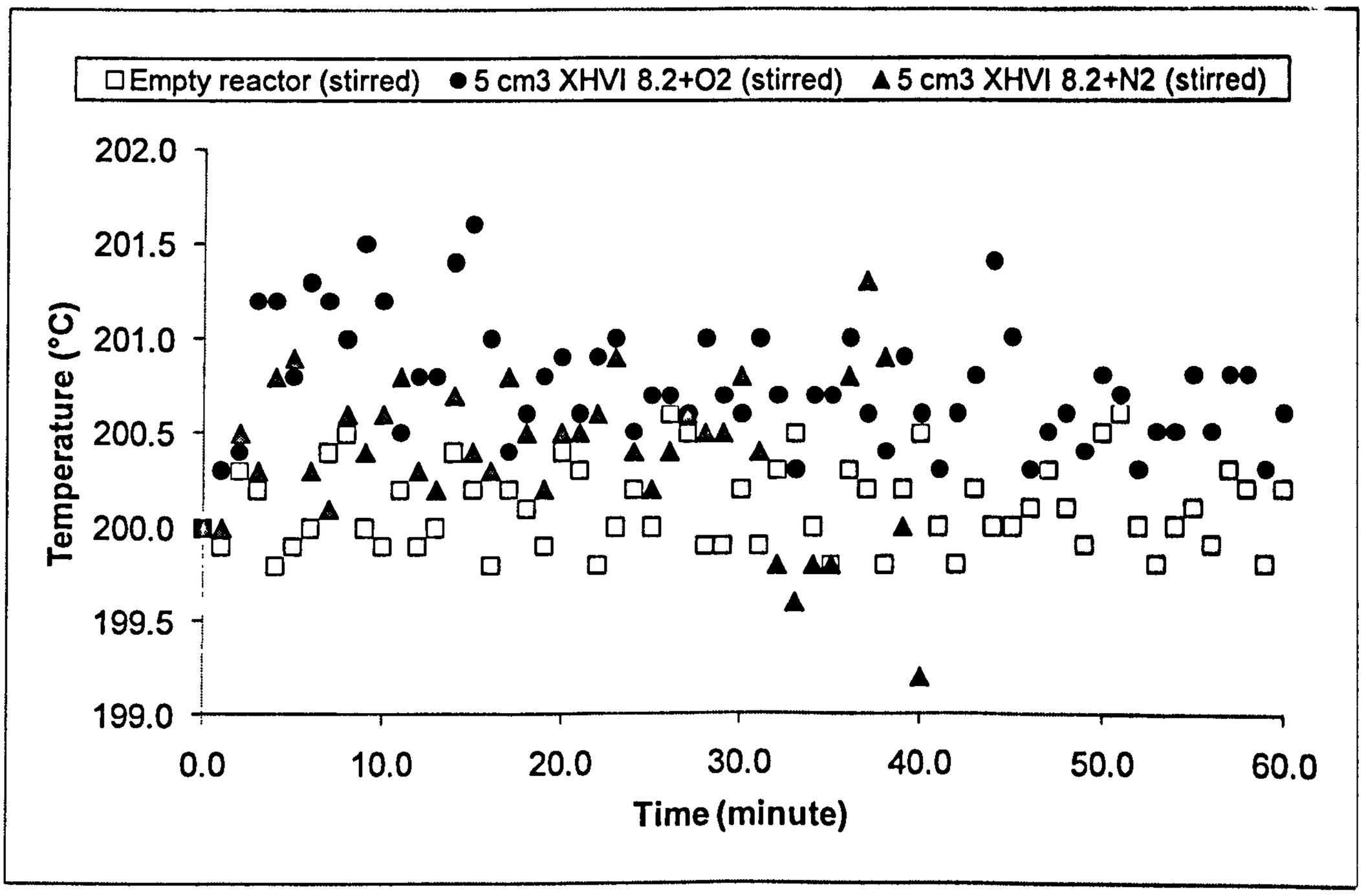

Figure A.3: Temperature stability of static large reactor in the presence of oxygen and nitrogen at 200.0 °C

Reaction time estimation

The reaction time was obtained by measuring the time taken for the pressure to reach its lowest point (Figure A.4).[79] When the magnetic stirrer was turned on, oxygen dissolved into the substrate causing the pressure to drop by ~20 mbar. Once oxygen is dissolved into the substrate, a typical autoxidation reaction starts but the pressure level remains more or less constant as long as an efficient antioxidant is present in the substrate. Once the phenolic antioxidant is fully consumed, the substrate starts to oxidise causing the pressure to drop and oxidation products to form. The reduction in pressure never reaches zero because oxidation products such as water, carbon dioxide, and light hydrocarbons have high vapour pressures and hence remain in the gas phase at 200 °C. Once the reactor has been cooled, volatile oxidation products condense to the liquid phase causing the pressure to drop sharply. The water content in a reaction can be calculated from the pressure trace (see Appendix A). It should be noted that the slight reduction in pressure after the pressure minimum in Figure A.4 is due to the condensation of volatiles in the upper pipes of the reactor.

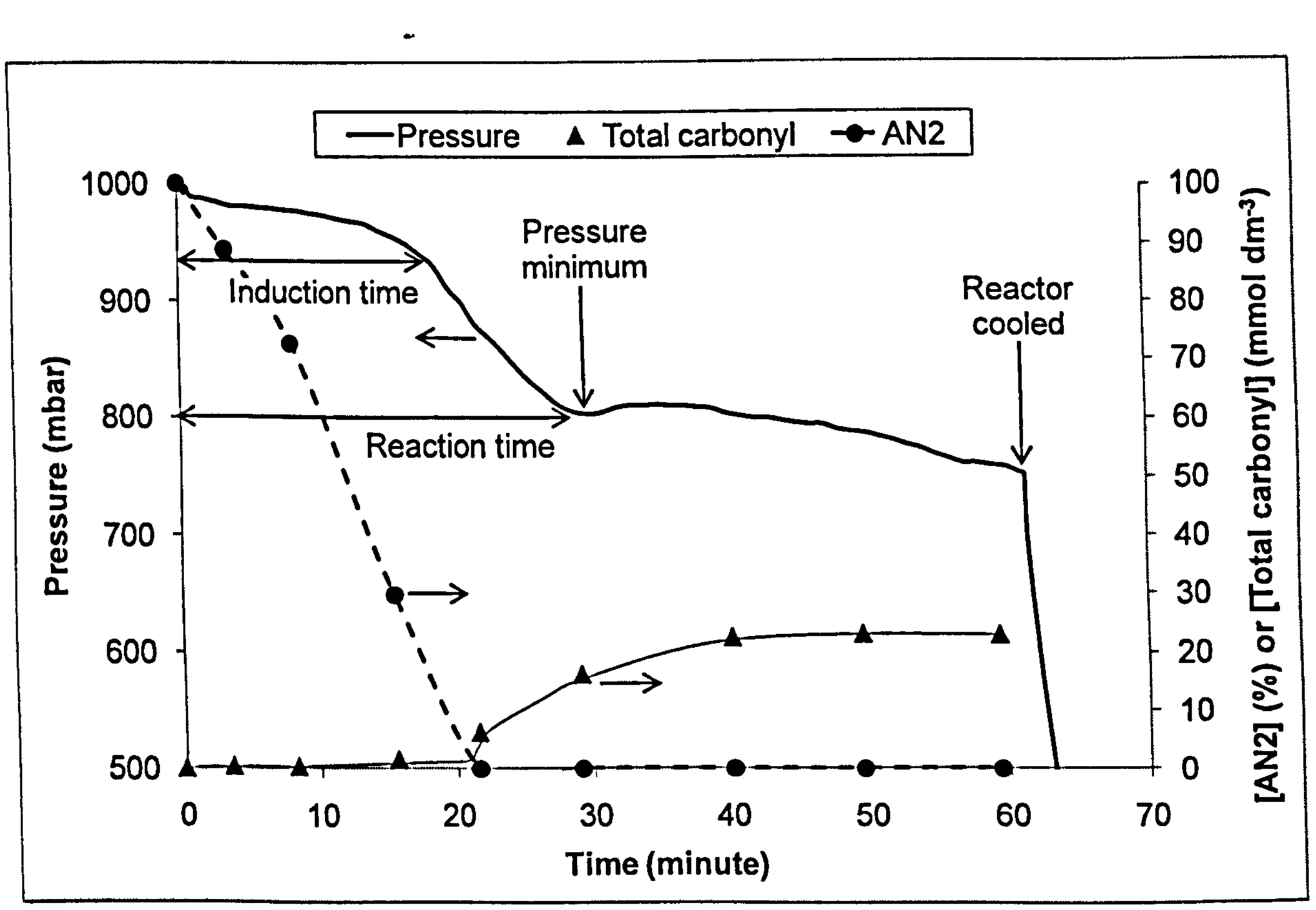

Figure A.4: Pressure trace for the oxidation of 10.0 mmol dm^{-3} AN2 in squalane at 200 °C in static intermediate reactor

[79] The figure is for squalane, which is expected to be fairly similar to the semi-formulated base fluids.

Effective carbon number (ECN) method

The effective carbon number method (Scanlon and Willis, 1985) was used when authentic compounds were unavailable:

ECN = (GC response / Carbon constant) x (1 / Compound carbon atoms)

The carbon constant can be obtained by dividing the calibration slope by the number of combustible carbon atoms of known compound (i.e. galvinol, formylphenol, and quinone) (Table A.1).

Table A.1: Carbon constants of known compounds (average carbon constant ≈ 450)

Compound	Calibration factor or Slope	Combustible carbons	Carbon constant
Galvinol	12346	29	426
Formylphenol	6072	14	434
Quinone	6759	14	483
Average	-	-	≈ 450

Figure A.5 shows that there is a good similarity between the concentrations obtained from authentic calibrations and effect carbon number method.

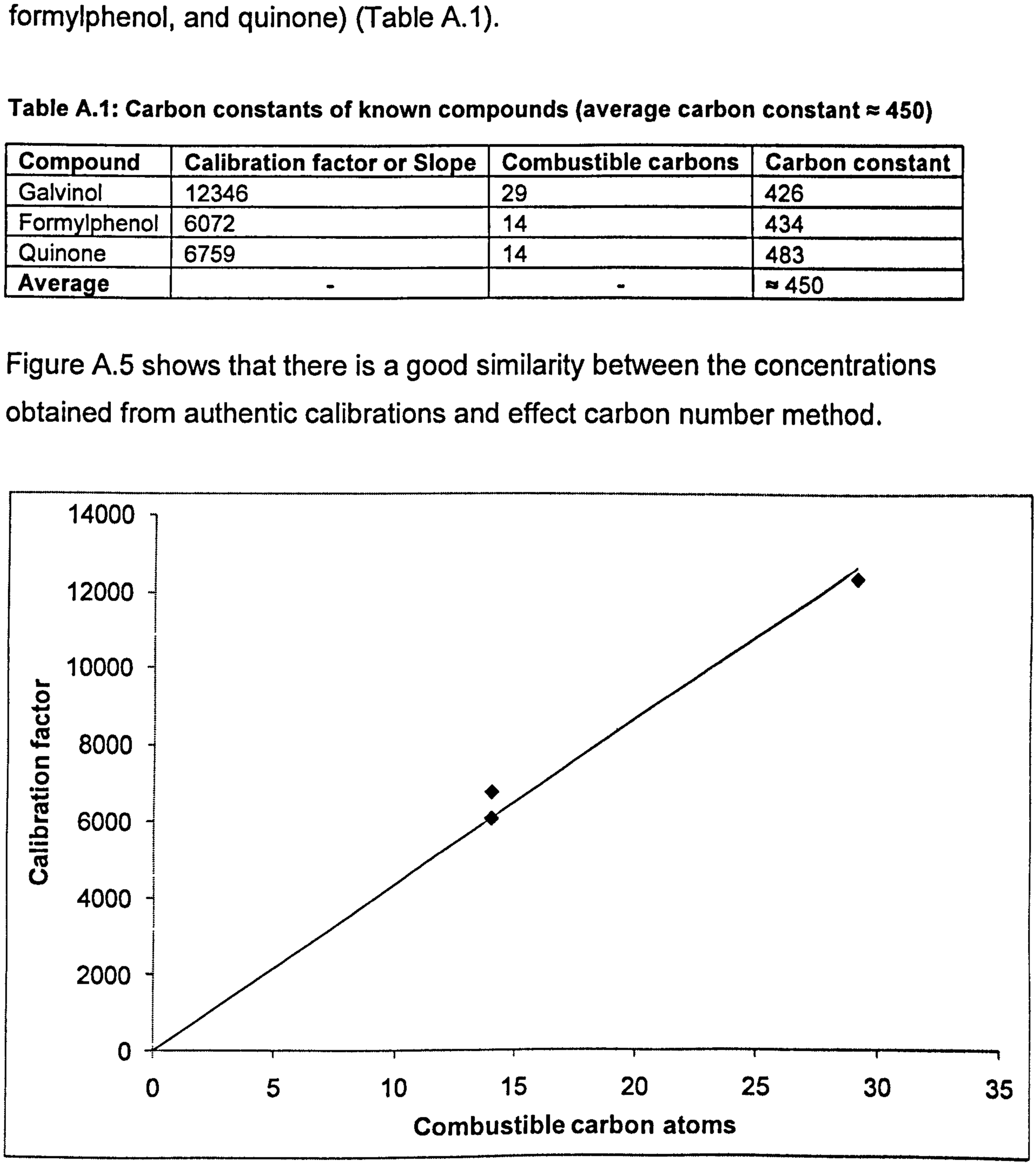

Figure A.5: Correlation between GC calibration factors and the number of combustible carbon atoms of various compounds

Oxygen uptake calculations

$[O_2]$ (mol dm^{-3})	= sum (mol) / substrate volume (dm^{-3})
Sum (mol)	= latter sum cell + adjacent integral cell
Integral (mol min^{-1})	= O_2 uptake (mol min^{-1}) x time difference (min)
Time difference (min)	= latter time cell - former time cell
O_2 uptake (mol min^{-1})	= (pressure in mbar x 100) x (O_2 uptake in dm^{-3} min^{-1}/1000) / (molar gas constant x absolute temperature)
O_2 uptake (dm^{-3} min^{-1})	= O_2 actual uptake (%) x O_2 flow rate (dm^{-3} min^{-1}) / 100
Corrected time	= oxidation time - O_2 detector response time

Table A.2: Oxygen uptake calculations in the oxidation of 10.0 mmol dm^{-3} AN2 in 5 cm^3 of squalane at 200 °C in flow intermediate reactor

Time (min)	Corrected time (min)	O_2 uptake (%)		O_2 flow rate (litres min^{-1})	O_2 uptake (litres min^{-1})	Pressure (mbar)	O_2 uptake (mol min^{-1})	Δ Time (min)	Integral (mol min^{-1})	Sum (mol)	$[O_2]$ in 5 cm^3 (mol dm^{-3})
		Recorded	Actual								
		100 0								0 00E+00	
0 0	0 0	100 0	0 0	0.1	0.00E+00	1033	0.00E+00	0.0	0.00E+00	0 00E+00	0.000
5.0	3.0	100.0	0 0	0.1	0 00E+00	1033	0.00E+00	3 0	0 00E+00	0.00E+00	0.000
10 0	8 0	100 0	0.0	0.1	0 00E+00	1033	0 00E+00	5.0	0.00E+00	0 00E+00	0.000
15 0	13 0	100 0	0.0	0.1	0.00E+00	1033	0 00E+00	5 0	0 00E+00	0 00E+00	0 000
20 0	18 0	100 0	0.0	0.1	0 00E+00	1033	0.00E+00	5 0	0 00E+00	0.00E+00	0.000
25.0	23 0	100 0	0.0	0.1	0.00E+00	1033	0 00E+00	5 0	0 00E+00	0.00E+00	0 000
30 0	28 0	100.0	0 0	0.1	0.00E+00	1033	0.00E+00	5 0	0 00E+00	0.00E+00	0.000
34.2	32 2	100 0	0 0	0.1	0.00E+00	1033	0.00E+00	4.2	0.00E+00	0.00E+00	0.000
34 3	32.3	99.7	0.3	0.1	3.00E-04	1033	1.27E-05	0.1	1.27E-06	1.27E-06	0.000
39 0	37.0	99.7	0.3	0.1	3.00E-04	1033	1.27E-05	4.7	5 98E-05	6.11E-05	0.012
43.0	41.0	99 4	0 6	0.1	6 00E-04	1033	2.54E-05	4.0	1.02E-04	1.63E-04	0.033
51 0	49.0	99 4	0 6	0.1	6 00E-04	1033	2.54E-05	8.0	2 04E-04	3 66E-04	0.073
58 8	56.8	99.4	0.6	0.1	6 00E-04	1033	2.54E-05	7.8	1.98E-04	5.65E-04	0.113

Arrhenius parameters from graphs

Table A.3: Arrhenius parameters in graphs (where, C: Concentration; sec: Second; k: Rate constant; T: Absolute temperature; T_0: Temperature dependence; E: Activation energy; R: Universal molar gas constant; and A: Pre-exponential factor)

Y axis	X axis	Slope	Comment
ln([C]) (mol)	Time (sec)	-k (s^{-1})	First-order rate
1 / [C] (mol)	Time (sec)	k (dm^3 mol^{-1} s^{-1})	Second-order rate
ln(k)	1 / T (K)	T_0 (K)	$E = T_0 \times R$ and A = Intercept / 2.303[80]
ln(Time) (sec)	1 / T (K)	T_0 (K)	

[80] The intercept is divided by 2.303 to compensate for the difference between natural and base logarithms.

Water content in reactions

Table A.4: Amount of water in the reaction of 5 cm^3 of squalane at 200 °C for one hour In static intermediate reactor

Parameter	Temperature		Pressure		Amount		
	(°C)	(K)	(mbar)	(Pa)	(mol)	(mol dm^{-3})	(mmol dm^{-3})
Before cooling	200.4	473.6	601	6.01E+04	6.41E-04	1.53E-02	15.3
After cooling	50.0	323.2	290	2.90E+04	4.53E-04	1.08E-02	10.8
Pressure due to fixed gases	50.0	323.2	425	4.25E+04	6.64E-04	1.58E-02	15.8
Pressure due to water	50.0	323.2	176	1.76E+04	2.75E-04	6.55E-03	6.6

where,

Pressure due to fixed gases = pressure after cooling x (temperature before cooling / temperature after cooling)

Pressure due to water = pressure before cooling - pressure due to fixed gases

Water (mol) = (pressure in Pa x reactor volume in m^3) / (molar gas constant x absolute temperature)

Water (mol dm^{-3}) = amount of water in mol / reactor volume in litre

Available reactor volume (42 cm^3)= absolute reactor volume (54 cm^3) - (substrate volume (5 cm^3) + flea volume (7 cm^3))

Vapour pressures at high temperatures

Although were not used in the thesis, the vapour pressures of compounds can be calculated (Table A.5) by using Clausius-Clapeyron equation:

$$P_2 = \exp((-\text{enthalpy of vaporisation} / \text{molar gas constant}) \times (1 / T_2 - 1 / T_1)) \times P_1$$

where,

T_1: 298.15 K (25 °C)

T_2: Desired temperature (e.g. 150 °C, 200 °C, or 250 °C)

P_1: Vapour pressure at 25 °C (obtained from SciFinder Scholar)

P_2: Vapour pressure at desired temperature

Table A.5: Calculated vapour pressure of compounds using Clausius-Clapeyron equation

Compound	RMM (g)	Density (g cm^{-3})	Amount (mol)	Enthalpy of vap. (J mol^{-1})	25 °C	150 °C	200 °C	250 °C
					Vapour pressure (bar)			
BHT	220.35	1.048	4.76E-03	52170	8.3E-06	4.2E-03	2.0E-02	7.1E-02
AN2	424.66	0.981	2.31E-03	75760	6.1E-12	5.1E-08	5.0E-07	3.1E-06
Hexadecane	226.45	0.773	3.41E-03	50460	6.0E-06	2.5E-03	1.1E-02	3.8E-02
Squalane	422.82	0.810	1.92E-03	70480	1.9E-11	8.6E-08	7.1E-07	4.0E-06

The number of moles of compounds in liquid and gas phases were calculated (Table A.6) using the following equations:

$$\text{Gas (mol)} = (P_2 \times 3.056\times10^{-6}) / (\text{universal molar gas constant} \times T_2)$$

$$\text{Liquid (mol)} = \text{liquid (mol) at } T_1 - \text{gas (mol) at } T_2$$

Table A.6: Calculated number of moles of compounds in liquid and gas phases

Compound	25 °C		150 °C		200 °C		250 °C	
	Liquid	Gas	Liquid	Gas	Liquid	Gas	Liquid	Gas
BHT	4.8E-03	1.0E-14	4.8E-03	3.6E-12	4.8E-03	1.6E-11	4.8E-03	5.0E-11
AN2	2.3E-03	7.6E-21	2.3E-03	4.4E-17	2.3E-03	3.9E-16	2.3E-03	2.2E-15
Hexadecane	3.4E-03	7.4E-15	3.4E-03	2.1E-12	3.4E-03	8.7E-12	3.4E-03	2.7E-11
Squalane	1.9E-03	2.4E-20	1.9E-03	7.5E-17	1.9E-03	5.5E-16	1.9E-03	2.8E-15

B. APPENDIX B: GC TRACES AND MASS SPECTRA

GC traces of starting materials and oxidation products

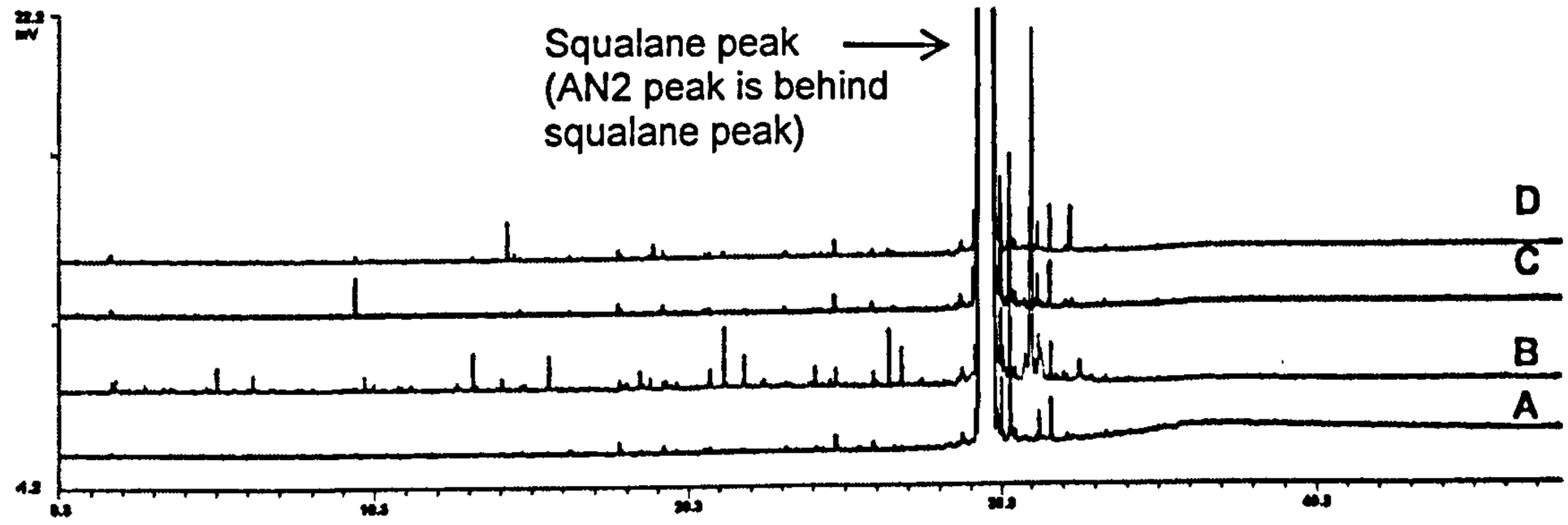

Figure B.1: GC traces of unoxidised (trace A) and oxidised (trace B) squalane at 200 °C for 9 minutes in static intermediate reactor; and unoxidised (trace C) and oxidised (trace D) 10.0 mmol dm^{-3} AN2 in squalane at 200 °C for 21 minutes in flow intermediate reactor

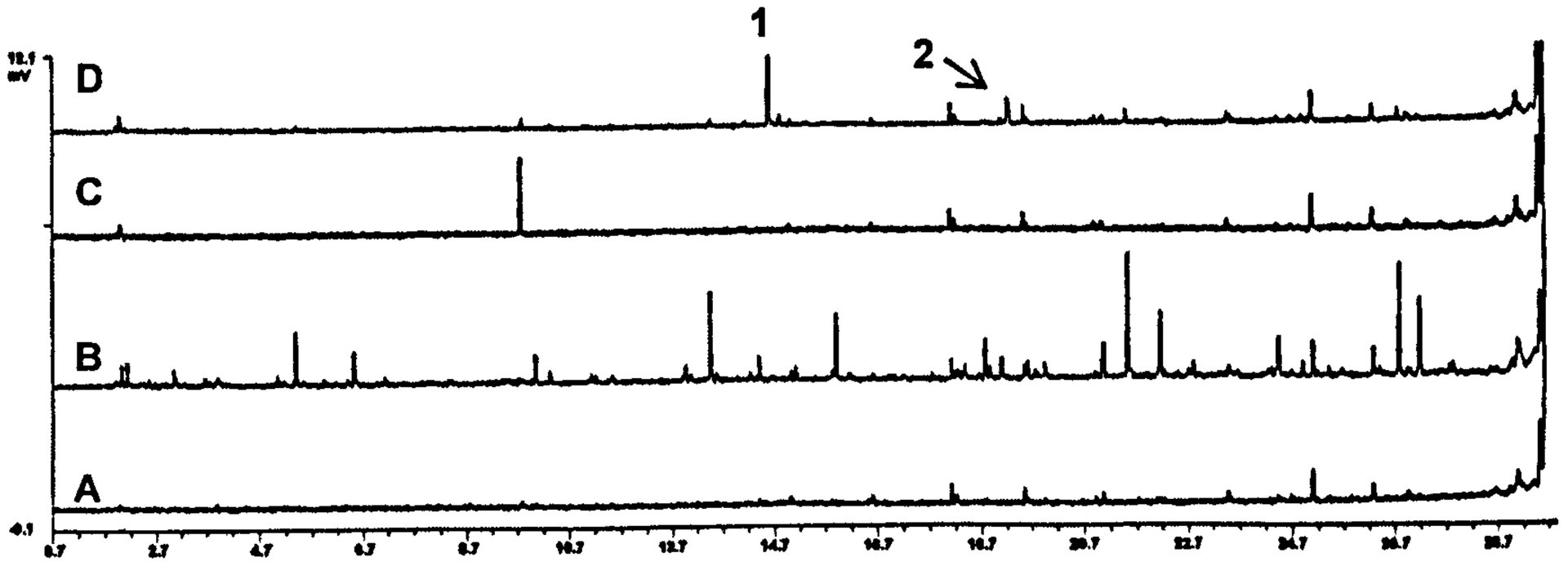

Figure B.2: GC traces of unoxidised (trace A) and oxidised (trace B) squalane at 200 °C for 9 minutes in static intermediate reactor; and unoxidised (trace C) and oxidised (trace D) 10.0 mmol dm^{-3} AN2 in squalane at 200 °C for 21 minutes in flow intermediate reactor – part 1 (1 to 29 minutes). Peaks 1: Quinone; and 2: Formylphenol

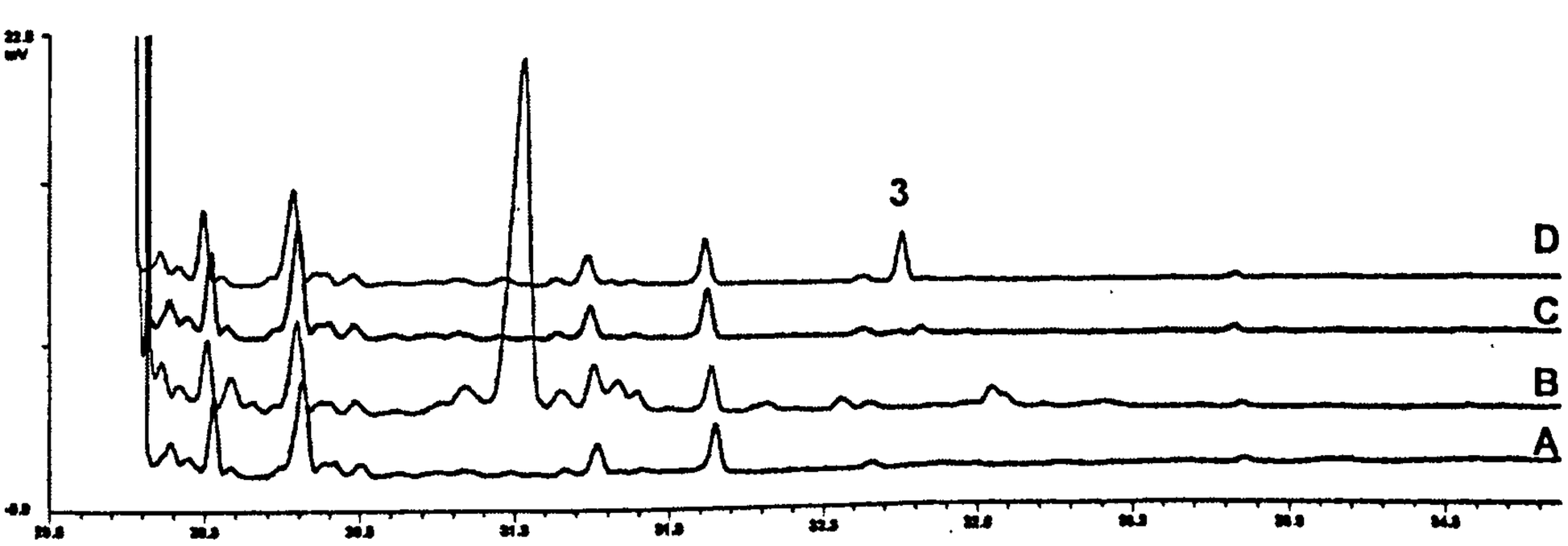

Figure B.3: GC traces of unoxidised (trace A) and oxidised (trace B) squalane at 200 °C for 9 minutes in static intermediate reactor; and unoxidised (trace C) and oxidised (trace D) 10.0 mmol dm^{-3} AN2 in squalane at 200 °C for 21 minutes in flow intermediate reactor – part 2 (29 to 35 minutes). Peak 3: Galvinol

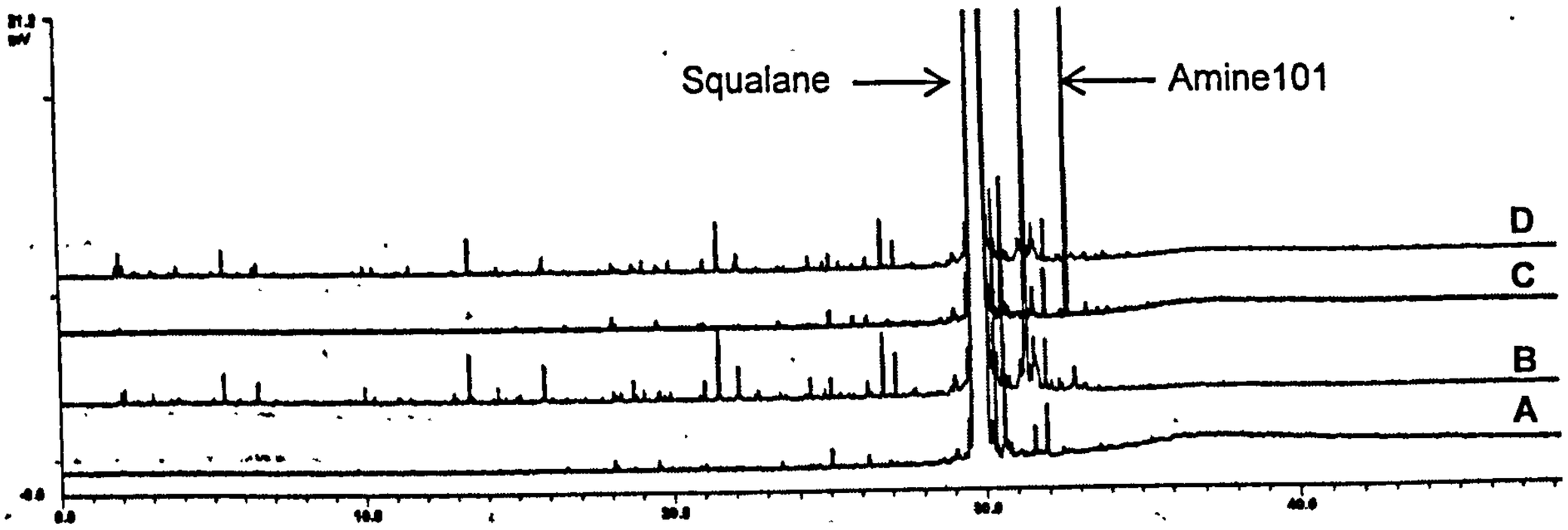

Figure B.4: GC traces of unoxidised (trace A) and oxidised (trace B) squalane at 200 °C for 9 minutes in static intermediate reactor; and unoxidised (trace C) and oxidised (trace D) 10.0 mmol dm^{-3} Amine101 in squalane at 200 °C for 20 minutes in flow intermediate reactor

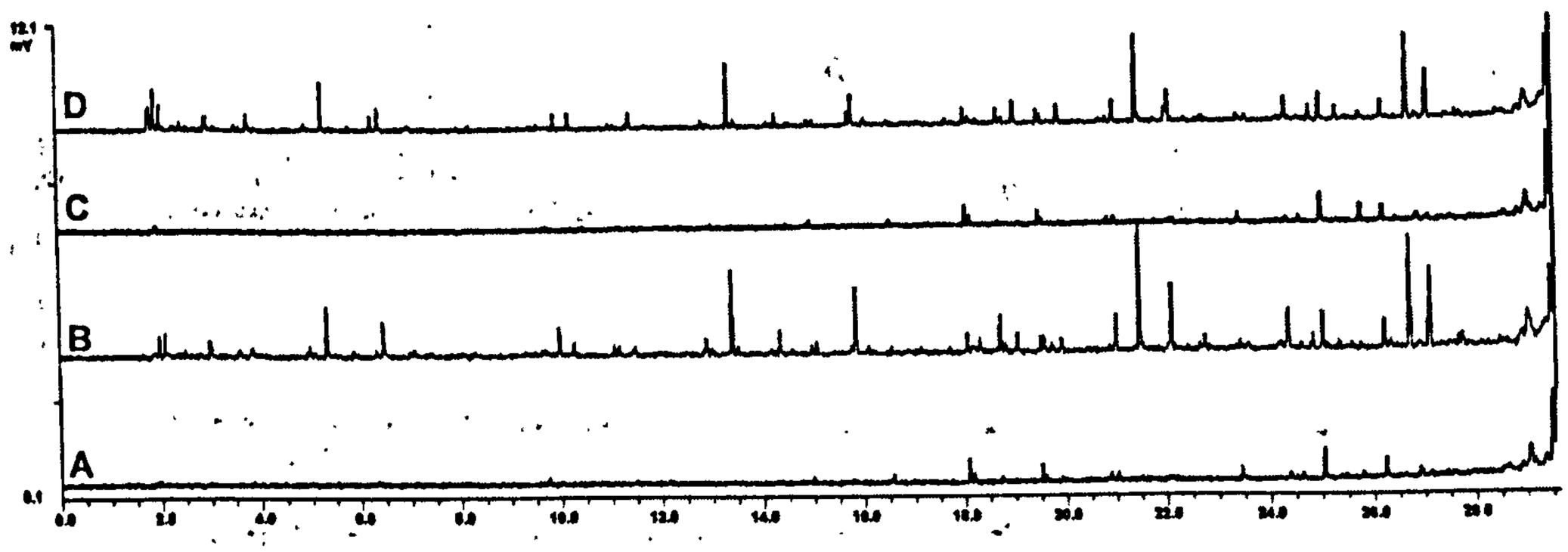

Figure B.5: GC traces of unoxidised (trace A) and oxidised (trace B) squalane at 200 °C for 9 minutes in static intermediate reactor; and unoxidised (trace C) and oxidised (trace D) 10.0 mmol dm^{-3} Amine101 in squalane at 200 °C for 20 minutes in flow intermediate reactor – part 1 (0 to 30 minutes)

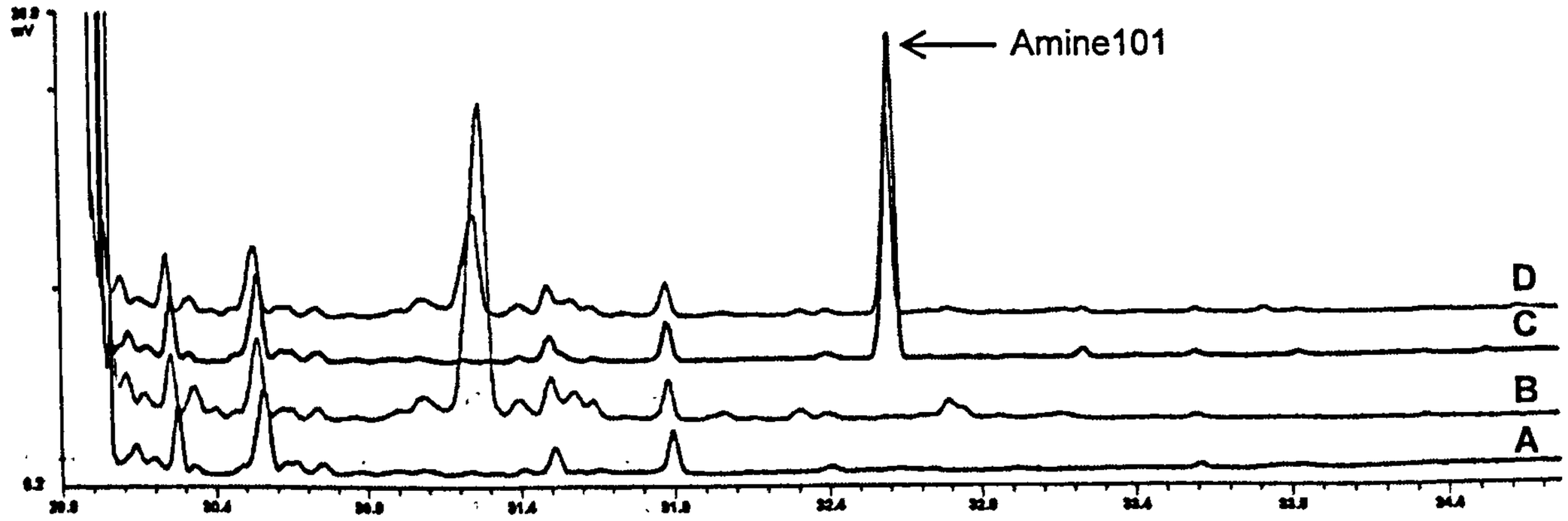

Figure B.6: GC traces of unoxidised (trace A) and oxidised (trace B) squalane at 200 °C for 9 minutes in static intermediate reactor; and unoxidised (trace C) and oxidised (trace D) 10.0 mmol dm^{-3} Amine101 in squalane at 200 °C for 20 minutes in flow intermediate reactor – part 2 (30 to 35 minutes)

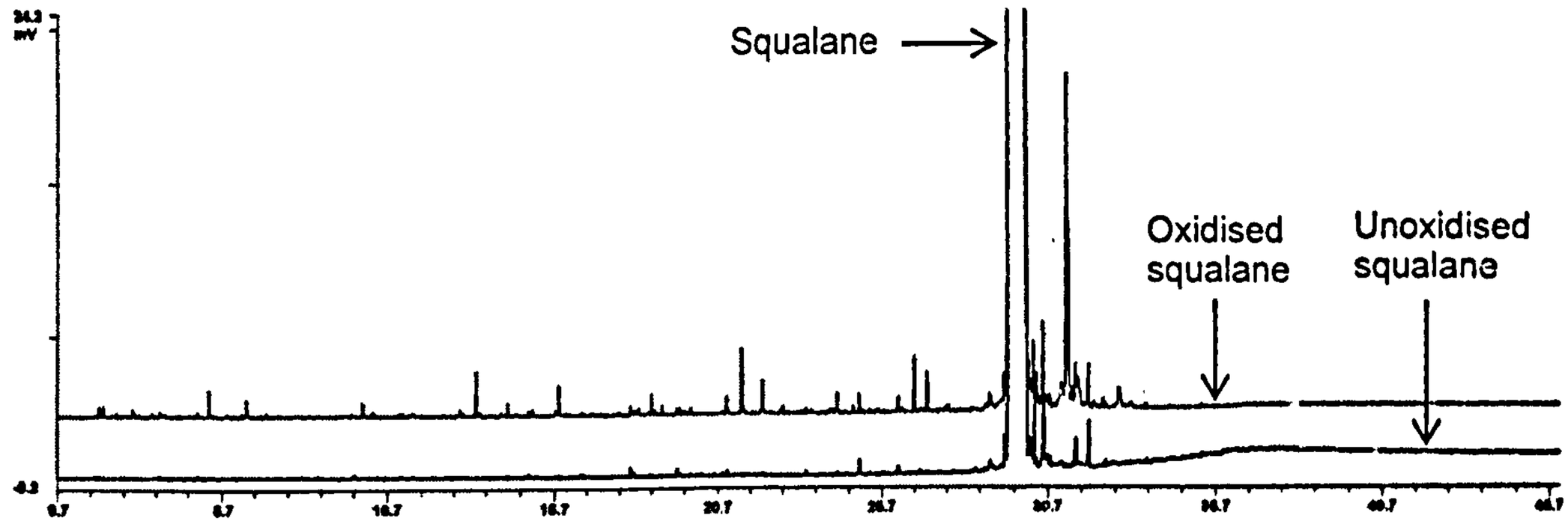

Figure B.7: GC traces of unoxidised (bottom trace) and oxidised (top trace) squalane at 200 °C for 9 minutes in static intermediate reactor

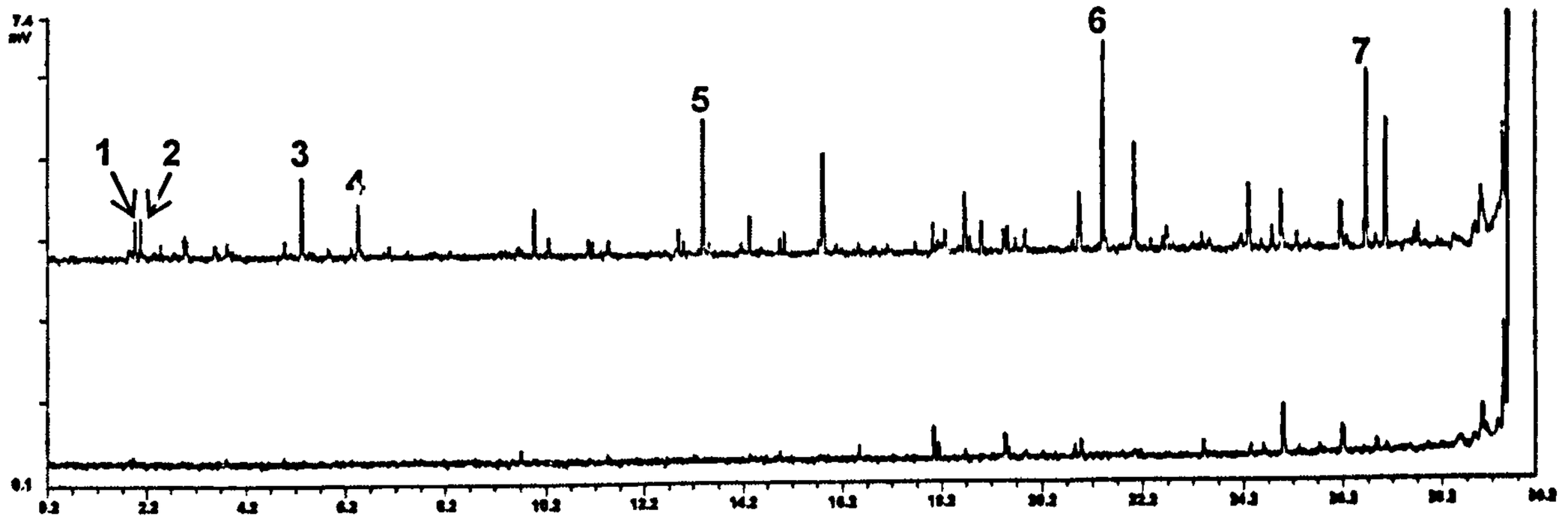

Figure B.8: GC traces of unoxidised (bottom trace) and oxidised (top trace) squalane at 200 °C for 9 minutes in static intermediate reactor – part 1 (0 to 30 minutes). Peaks 1: propanone; 2: 2-methylpentane; 3: 6-methyl-2-heptanone; 4: 2,6-dimethylnonane; 5: 6,10-dimethyl-2-undecanone; 6: 7,11,15-trimethyl-2-hexadecanone; and 7: 6,11,15,19-tetramethyl-2-eicosanone

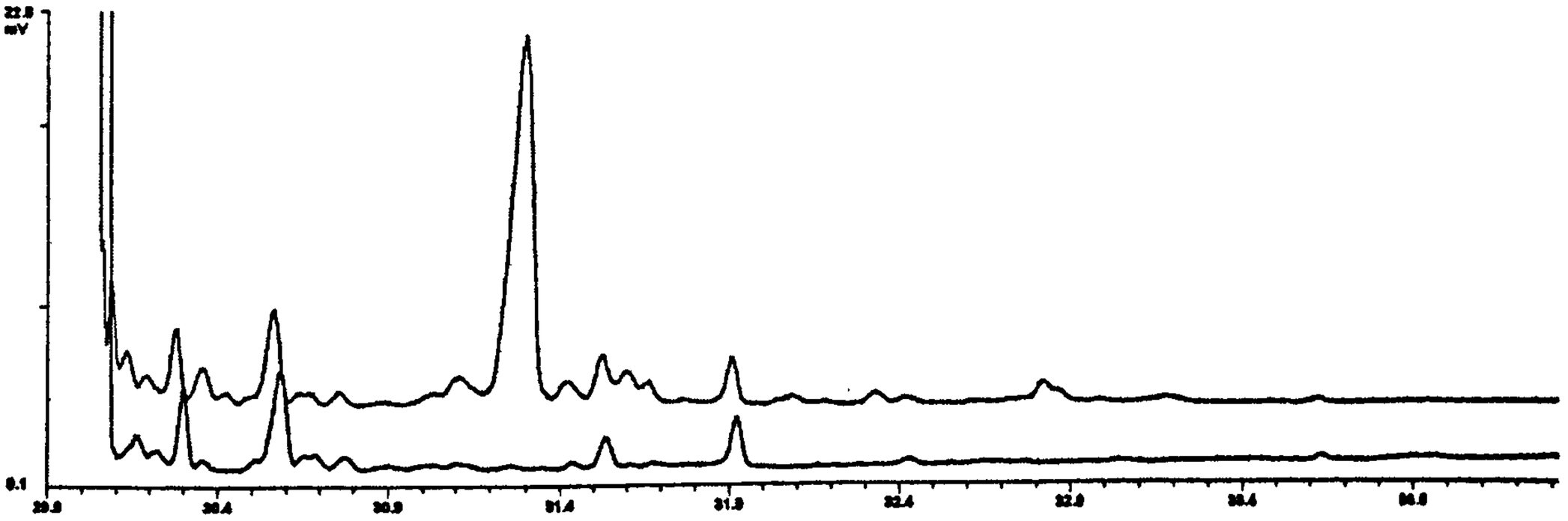

Figure B.9: GC traces of unoxidised (bottom trace) and oxidised (top trace) squalane at 200 °C for 9 minutes in static intermediate reactor – part 2 (30 to 34 minutes)

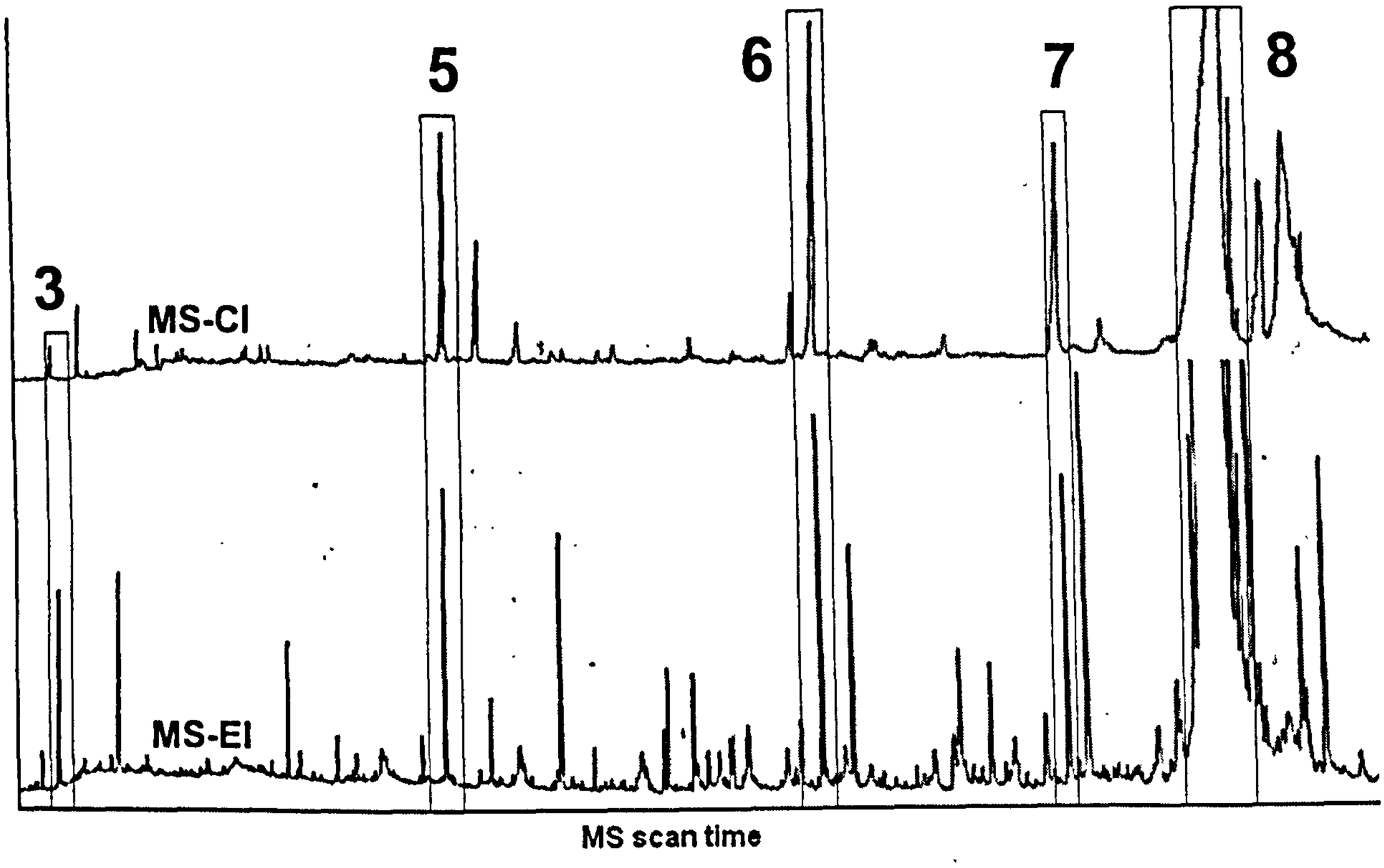

Figure B.10: Chemical ionization (top trace) and electron impact (bottom trace) mass spectra of the oxidation of squalane at 200 °C in flow intermediate reactor [note that MS scan time is not shown because MS-CI and MS-EI have different scan times]. Peaks 3: 6-methyl-2-heptanone; 5: 6,10-dimethyl-2-undecanone; 6: 7,11,15-trimethyl-2-hexadecanone; 7: 6,11,15,19-tetramethyl-2-eicosanone; and 8: squalane

Mass spectra of starting materials and oxidation products

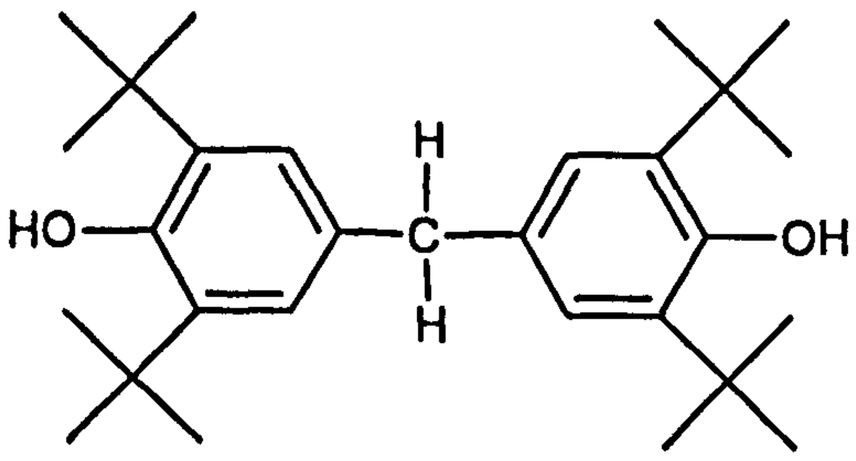

Name: 4,4'-Methylenebis[2,6-bis(1,1-dimethylethyl)]phenol (AN2)

RMM[81]: 424.66 g mol^{-1}

GC-MS-Electron impact, mass-to-charge ratio (relative intensity):

Authentic: 41 (16), 57 (34), 197 (12), 219 (21), 367 (26), 409 (100), 424 (80).

LC-MS-APCI[82], mass-to-charge ratio (relative intensity):

Authentic: 421.5 (16), 422.4 (33), 423.4 (100), 424.4 (30).

[81] Relative molecular mass.
[82] Atmospheric pressure chemical ionisation.

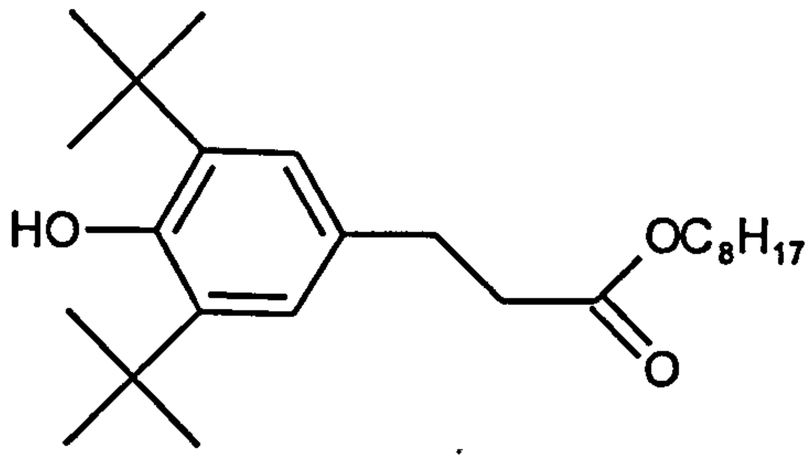

Name: 3,5-Di-tert-butyl-4-hydroxyhydrocinnamate (Irganox L135)

RMM: 390 g mol^{-1}

GC-MS-Electron impact, mass-to-charge ratio (relative intensity):

Authentic: 43 (45), 57 (85), 71 (27), 91 (6), 147 (13), 161 (8), 189 (6), 203 (19), 219 (60), 323 (7), 263 (8), 277 (7), 375 (100), 390 (80).

LC-MS-APCI, mass-to-charge ratio (relative intensity):

Authentic: 387.8 (14), 389.2 (100), 390.2 (23), 403.2 (9).

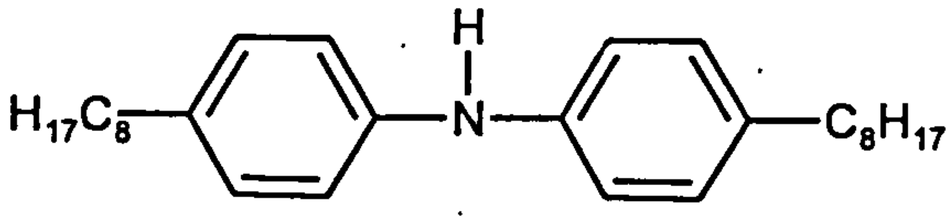

Name: 4-Octyl-N-(4-octylphenyl)benzenamine (Amine101)

RMM: 393.65 g mol^{-1}

GC-MS-Electron impact, mass-to-charge ratio (relative intensity):

Authentic: 41 (6), 57 (8), 250 (15), 322 (100), 393 (12).

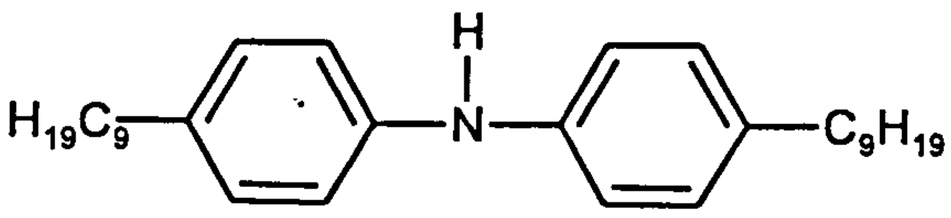

Name: 4-Nonyl-N-(4-nonylphenyl)benzenamine (Naugalube 438L)

RMM: 421 g mol^{-1}

LC-MS-APCI, mass-to-charge ratio (relative intensity):

Authentic: 420.5 (100), 421.5 (33), 434.5 (13), 436.4 (8), 546.5 (46), 547.5 (18).

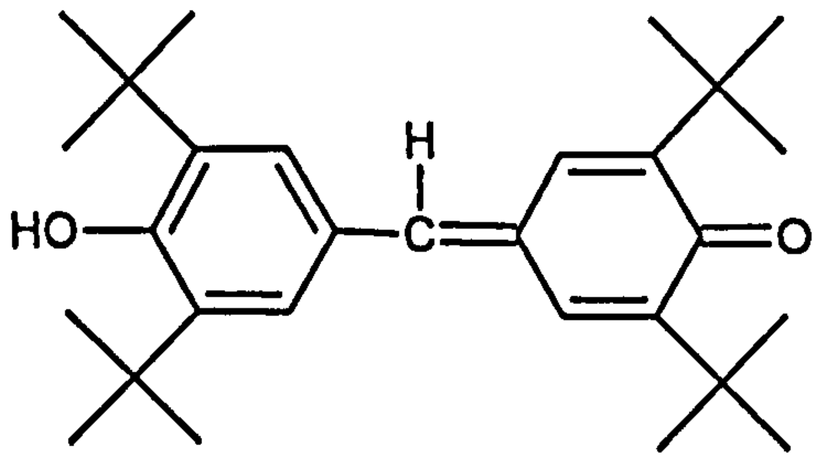

Name: 4-[[3,5-Bis(1,1-dimethylethyl)-4-hydroxyphenyl]methylene]-2,6-bis(1,1-dimethylethyl)- 2,5-cyclohexadien-1-one (Galvinol)

RMM: 422 g mol^{-1}

GC-MS-Electron impact, mass-to-charge ratio (relative intensity):

Reaction: 41 (37), 57 (66), 69 (17), 123 (27), 216 (19), 365 (95), 379 (16), 391 (6), 407 (100), 422 (42).

Authentic: 41 (21), 57 (33), 216 (5), 365 (71), 379 (11), 391 (5), 407 (100), 422 (35).

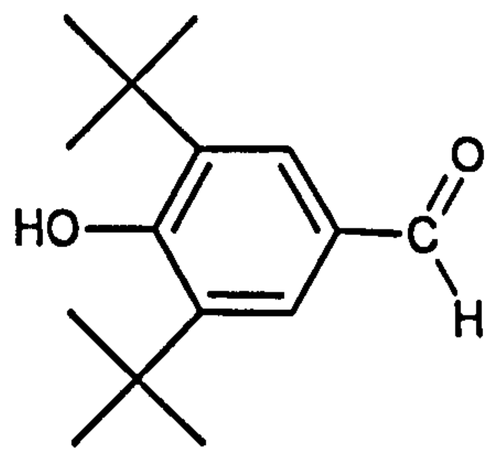

Name: 3,5-Bis(1,1-dimethylethyl)-4-hydroxy-benzaldehyde (Formylphenol)

RMM: 234 g mol^{-1}

GC-MS-Electron impact, mass-to-charge ratio (relative intensity):

Reaction: 41 (26), 57 (39), 91 (14), 115 (8), 159 (6), 175 (11), 191 (17), 203 (10), 219 (100), 234 (22).

Authentic: 41 (19), 57 (21), 91 (10), 115 (7), 159 (6), 191 (15), 219 (100), 234 (20).

SDBS[83]: 41 (10), 57 (23), 91 (6), 175 (5), 191 (18), 219 (100), 234 (24).

NIST[84]: 41 (14), 57 (20), 91 (11), 175 (8), 191 (32), 219 (100), 234 (28).

[83] Online database of Spectral Database for Organic Compounds; National Institute of Advanced Industrial Science & Technology (Japan).
[84] Online database of the National Institute of Standards & Technology (United States).

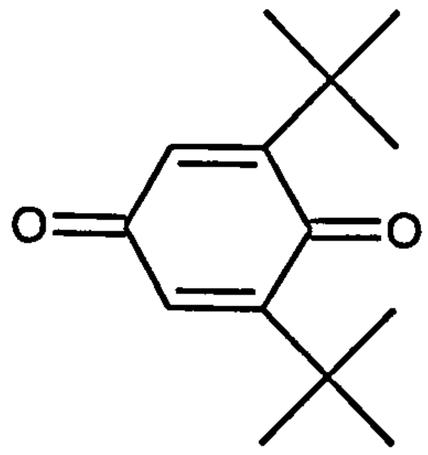

Name: 2,6-Bis(1,1-dimethylethyl)-2,5-cyclohexadiene-1,4-dione (Quinone)

RMM: 220 g mol^{-1}

GC-MS-Electron impact, mass-to-charge ratio (relative intensity):

Reaction: 41 (62), 57 (35), 67 (35), 121 (16), 135 (39), 149 (35), 163 (26), 177 (100), 192 (10), 205 (24), 220 (52).

Authentic: 41 (53), 57 (28), 67 (37), 121 (13), 135 (35), 149 (33), 163 (20), 177 (100), 192 (10), 205 (27), 220 (52).

SDBS: 41 (51), 57 (37), 67 (33), 135 (36), 149 (30), 163 (25), 177 (100), 205 (30), 220 (66).

NIST: 41 (62), 57 (33), 67 (37), 135 (34), 149 (30), 163 (24), 177 (100), 205 (28), 220 (73).

Name: 2-Methyl-pentane

RMM: 86 g mol^{-1}

GC-MS-Electron impact, mass-to-charge ratio (relative intensity):

Reaction: 41 (31), 42 (42), 43 (100), 57 (10), 71 (32), 86 (18).

SDBS: 41 (30), 42 (53), 43 (100), 57 (17), 71 (40), 86 (6).

NIST: 41 (29), 42 (54), 43 (100), 57 (10), 71 (27), 86 (3).

POP[85]: 43 (100), 57 (11), 71 (32), 86 (2).

[85] POP: Pristane oxidation product (Wilkinson, 2006)

Name: 2,6-Dimethyl-nonane

RMM: 156 g mol^{-1}

GC-MS-Electron impact, mass-to-charge ratio (relative intensity):

Reaction: 41 (33), 43 (100), 57 (88), 71 (96), 85 (8), 113 (15), 133 (13), 141 (12), 156 (10).

SciFinder[86]: 41 (26), 43 (100), 57 (78), 71 (74), 85 (9), 113 (7), 141 (1), 156 (1).

POP: 43 (100), 57 (79), 71 (90), 85 (11), 113 (13), 141 (1), 156 (0.7).

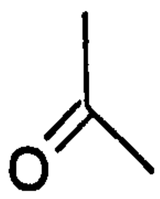

Name: Propanone

RMM: 58 g mol^{-1}

GC-MS-Electron impact, mass-to-charge ratio (relative intensity):

Reaction: 43 (100), 58 (35)

SDBS: 43 (100), 58 (64)

NIST: 43 (100), 58 (64)

POP: 43 (100), 58 (40)

Name: 6-Methyl-2-Heptanone

RMM: 128 g mol^{-1}

GC-MS-Electron impact, mass-to-charge ratio (relative intensity):

Reaction: 43 (100), 58 (66), 71 (66), 85 (18), 95 (43), 110 (36), 128 (6).

SDBS: 43 (100), 58 (67), 71 (13), 85 (6), 95 (8), 110 (6), 128 (2).

NIST: 43 (100), 58 (67), 71 (13), 85 (6), 95 (8), 110 (6), 128 (2).

POP: 43 (100), 58 (72), 71 (13), 85 (6), 95 (9), 110 (7), 128 (2).

GC-MS-Chemical ionisation, mass-to-charge ratio (relative intensity):

Reaction: 58 (78), 71 (25), 85 (32), 95 (40), 110 (100), 128 (15), 129 (25), 134 (7), 146 (89).

[86] SciFinder Scholar of the American Chemical Society.

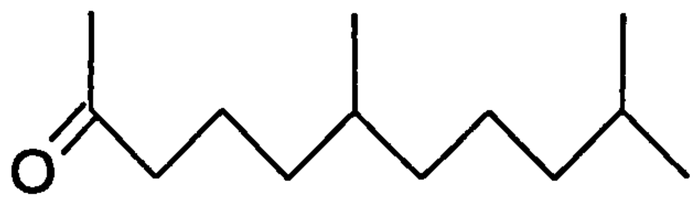

Name: 6,10-Dimethyl-2-undecanone

RMM: 198 g mol^{-1}

GC-MS-Electron impact, mass-to-charge ratio (relative intensity):

Reaction: 43 (99), 58 (100), 71 (39), 85 (20), 95 (10), 109 (11), 123 (21), 140 (34), 180 (40), 198 (4).

NIST: 43 (99), 58 (100), 71 (31), 85 (17), 95 (10), 109 (11), 140 (6), 180 (8), 198 (1).

POP: 43 (100), 58 (93), 71 (34), 85 (82), 95 (51), 109 (11), 123 (4), 140 (5), 180 (6), 198 (1).

GC-MS-Chemical ionisation, mass-to-charge ratio (relative intensity):

Reaction: 58 (32), 69 (14), 85 (24), 95 (22), 109 (30), 140 (11), 180 (41), 198 (8), 199 (13), 216 (100).

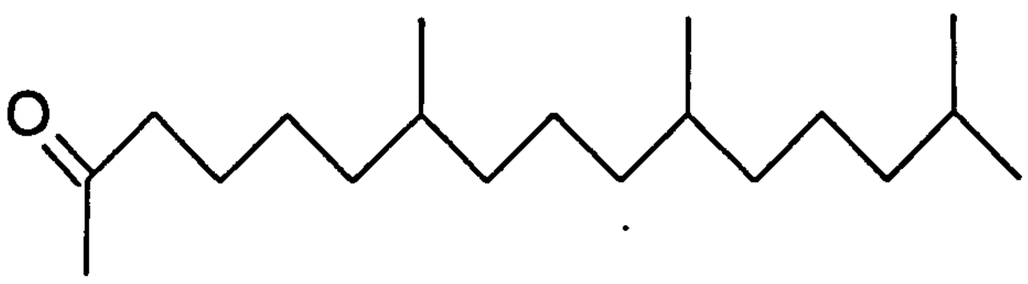

Name: 7,11,15-Trimethyl-2-hexadecanone

RMM: 282 g mol^{-1}

GC-MS-Electron impact, mass-to-charge ratio (relative intensity):

Reaction: 43 (100), 58 (68), 71 (40), 109 (17), 137 (40), 151 (13), 179 (24), 193 (6), 222 (44), 249 (7), 264 (58), 282 (10).

GC-MS-Chemical ionisation, mass-to-charge ratio (relative intensity):

Reaction: 58 (23), 82 (15), 95 (17), 109 (30), 123 (10), 137 (16), 151 (5), 179 (6), 222 (25), 264 (14), 282 (8), 300 (100).

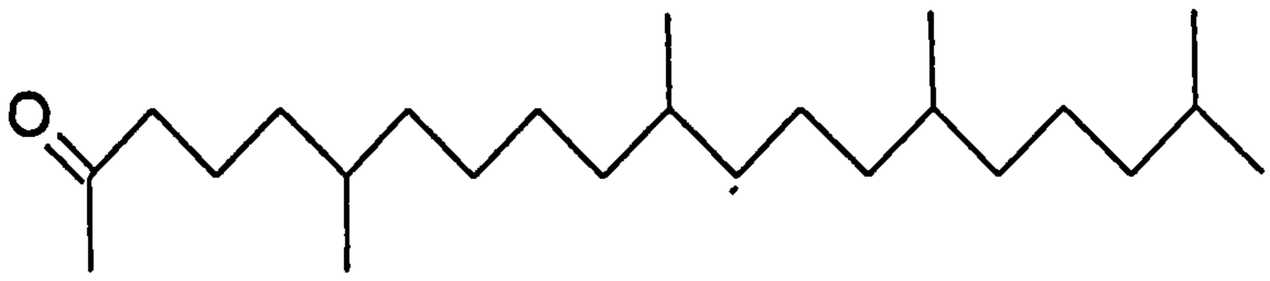

Name: 6,11,15,19-Tetramethyl-2-eicosanone

RMM: 352 g mol^{-1}

GC-MS-Electron impact, mass-to-charge ratio (relative intensity):

Reaction: 43 (100), 58 (62), 71 (47), 85 (23), 95 (17), 109 (20), 138 (41), 151 (20), 179 (14), 222 (14), 309 (4), 334 (42), 351 (10), 352 (10).

GC-MS-Chemical ionisation, mass-to-charge ratio (relative intensity):

Reaction: 58 (20), 71 (11), 85 (16), 95 (19), 109 (25), 123 (10), 138 (14), 222 (6), 334 (34), 351 (10), 352 (10), 370 (100).

Fragment assignment for unknown products

Two ketones (7,11,15-trimethyl-2-hexadecanone and 6,11,15,19-tetramethyl-2-eicosanone) tentatively identified here from the oxidation of squalane have no library data for comparison and so chemical structures for the fragments from each ketone were suggested.

The ketones have four common fragments:

m/z 43 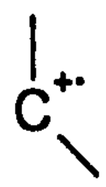

m/z 58 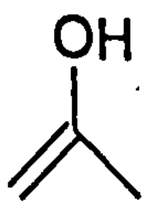 (see Figure B.11)

m/z 71 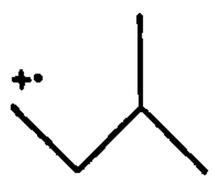

m/z 85 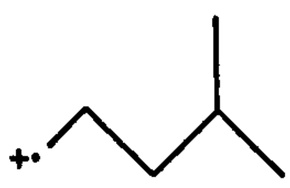

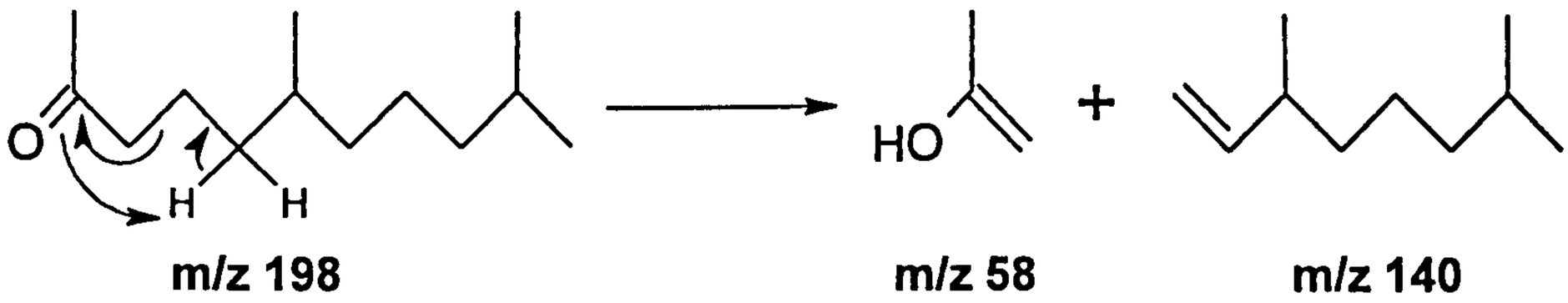

Figure B.11: McLafferty's rearrangement in 6,10-dimethyl-2-undecanone

One of the ketones (6,10-dimethyl-2-undecanone) that has a library spectrum has three common fragments (m/z 95, 109, and 180 or 179 when cation) with the two tentatively identified ketones (7,11,15-trimethyl-2-hexadecanone and 6,11,15,19-tetramethyl-2-eicosanone). The structures of these fragments remain unknown. The mass ions by both EI and CI ionisation of the two unknown ketones correspond well to the proposed structures.

C. APPENDIX C: LITERATURE REVIEW

Origin of oxidation products based on a literature review

Absolute rate constants in the liquid phase will be given where applicable. However, in the absence of experimental data, modelled data will be given. The data modelling is by the method of Evgeny Denisov using the Intersecting Parabolas Model[87] (Denisov and Afanasev, 2005, p.214-215).

Oxidation mechanism of squalane

The suggested (based on a literature review) oxidation mechanism of squalane is presented in Figure C.1.

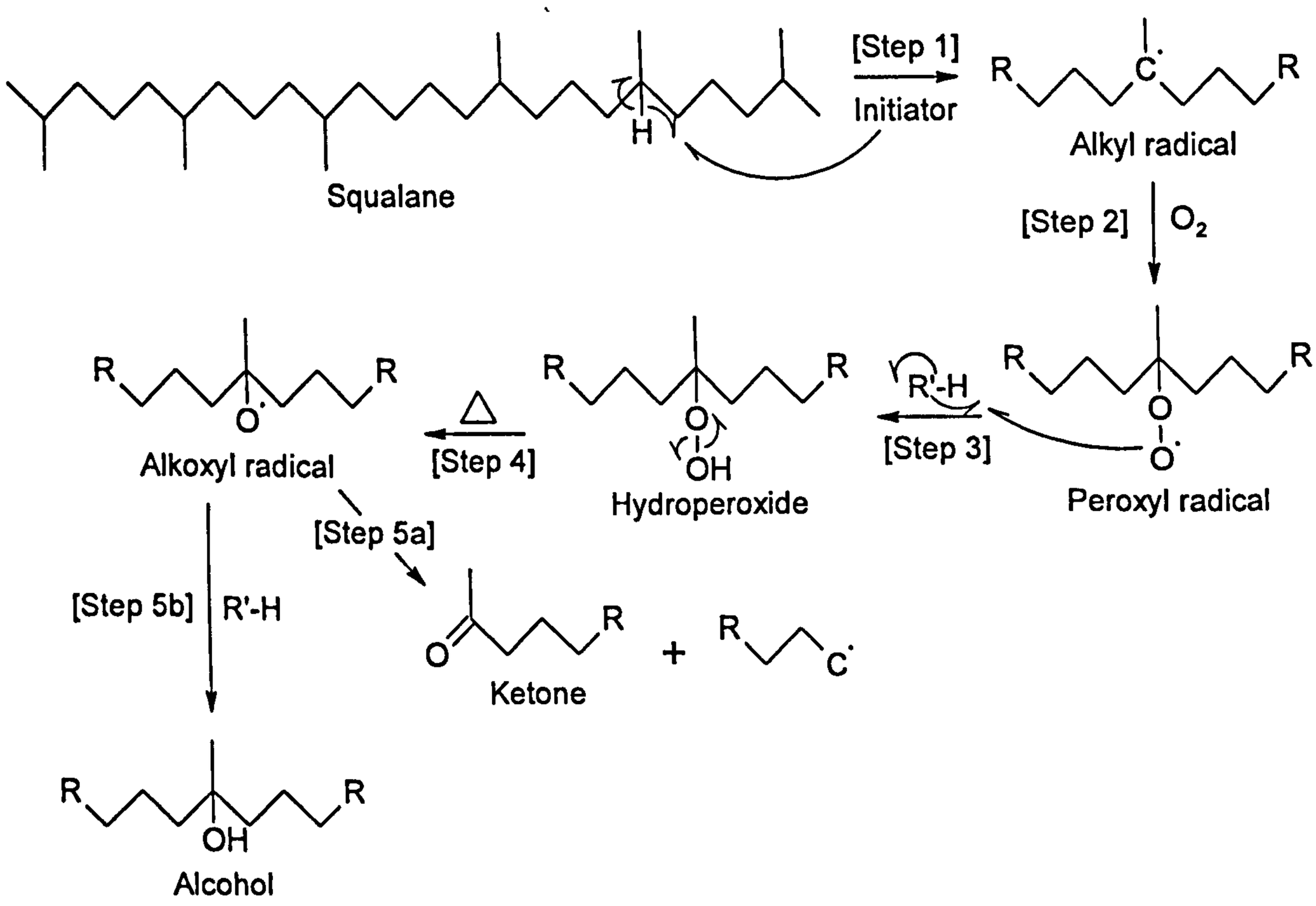

Figure C.1: Constructed oxidation mechanism of branched alkanes from a literature review (see text for references)

[87] The Intersecting Parabolas Model assumes that the hydrogen atom transfer is the resultant intersection of two potential curves. The potential curves describe the potential energies of the vibrations of the hydrogen atom along the dissociating bond in the initial molecule (e.g. R-H) and the forming bond in the reaction product (e.g. ROO-H).

Step 1: Initiation

Oxygen autoxidises the hydrocarbon (RH), either tertiary (tRH) or secondary (sRH) (primary hydrocarbon is ignored due to its high stability), to give rise to a carbon-centred alkyl radical (R•) and a hydroperoxyl radical (HOO•):

$(Me)_2CHCH_2Me$ (tRH) + O_2 → tR• + HOO•

$k = 4.1 \times 10^{-6}\ M^{-1}\ s^{-1}$ (200 °C)[88]

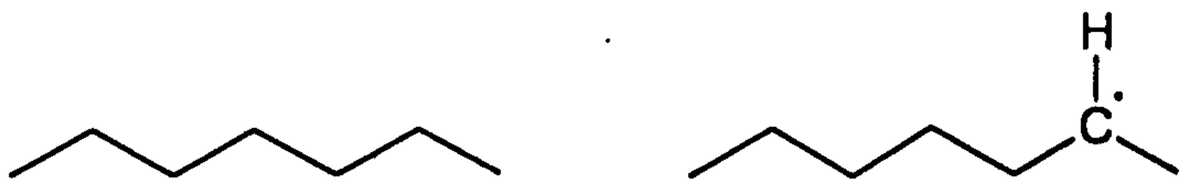

$Me(CH_2)_5Me$ (sRH) + O_2 → sR• + HOO•

$k = 3.3 \times 10^{-6}\ M^{-1}\ s^{-1}$ (200 °C)[89]

Steps 2: Oxygen addition to alkyl radicals

Alkyl radicals react very rapidly with oxygen to give rise to peroxyl radicals (ROO•) (Maillard et al, 1983):

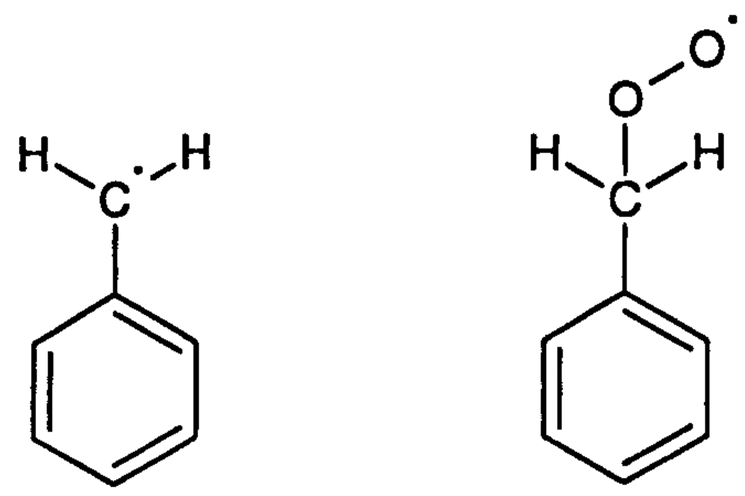

$PhCH_2• + O_2$ → ROO•

$k = 1.04 \times 10^{9}\ M^{-1}\ s^{-1}$ (27 °C) in hexadecane (Maillard et al, 1983)

[88] $k = 1.5 \times 10^{12} \exp(-159.0\ kJ/mol\ /\ RT)\ M^{-1}\ s^{-1}$ in benzene (Denisov and Denisova, 2000, p.52).
[89] $k = 3.2 \times 10^{14} \exp(-181.0\ kJ/mol\ /\ RT)\ M^{-1}\ s^{-1}$ in benzene (Denisov and Denisova, 2000, p.52).

Step 3: Reaction of peroxyl radicals with hydrocarbon

Peroxyl radicals react with the hydrocarbon to give rise to further alkyl radicals and hydroperoxide (ROOH):

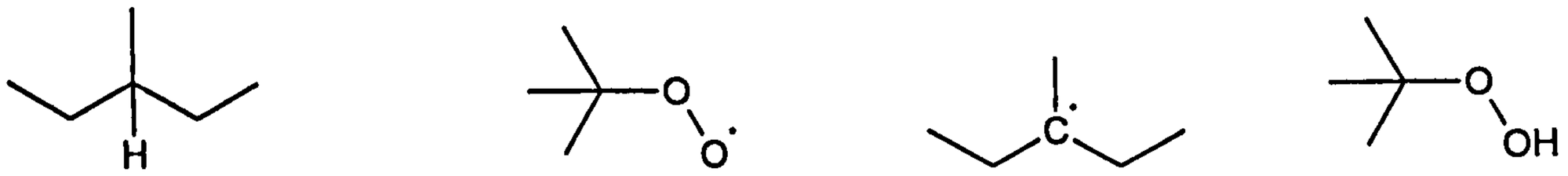

3-Methylpentane (3 ° H) + $Me_3COO\bullet$ → R• + ROOH

$k = 93\ M^{-1}\ s^{-1}$ (200 °C)[90]

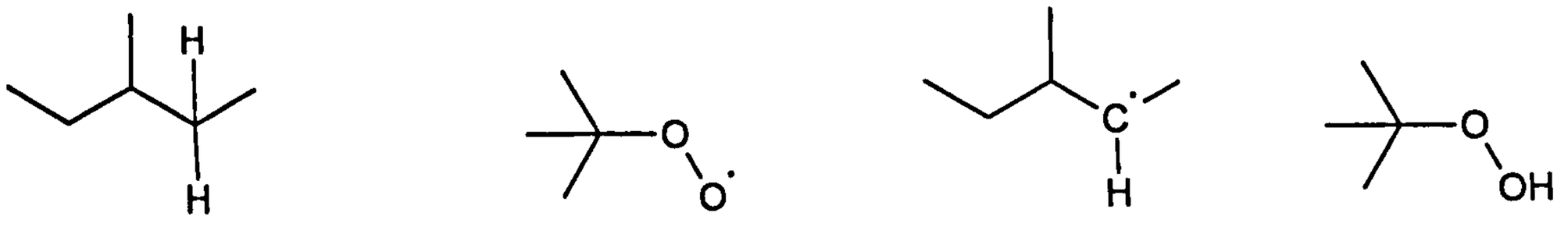

3-Methylpentane (2 ° H) + $Me_3COO\bullet$ → R• + ROOH

$k = 6.4\ M^{-1}\ s^{-1}$ (200 °C)[91]

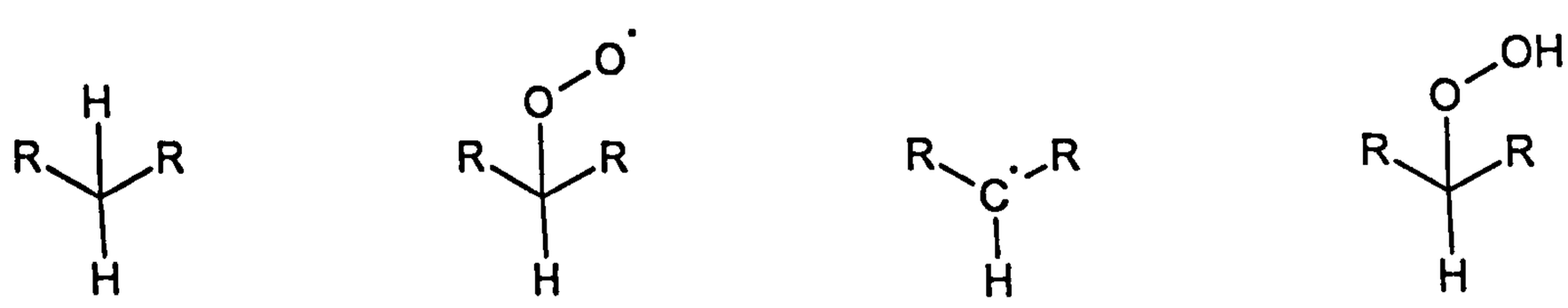

Hexadecane + Hexadecylperoxyl → R• + ROOH

$k = 16\ M^{-1}\ s^{-1}$ (200 °C)[92]

[90] $k = 3.2 \times 10^9 \exp(-68.2\ kJ/mol\ /\ RT)\ M^{-1}\ s^{-1}$ per hydrogen atom (Howard, 1997, p.291).
[91] $k = 7.9 \times 10^8 \exp(-73.3\ kJ/mol\ /\ RT)\ M^{-1}\ s^{-1}$ per hydrogen atom (Howard, 1997, p.291).
[92] $k = 4.0 \times 10^8 \exp(-67.0\ kJ/mol\ /\ RT)\ M^{-1}\ s^{-1}$ per hydrogen atom in hexadecane (Jensen et al, 1994).

Step 4: Decomposition of hydroperoxide

Hydroperoxides decompose unimolecularly to give rise to alkoxyl (RO•) and hydroxyl (HO•) radicals; or decompose bimolecularly to give rise to peroxyl radicals, water, and alkoxyl radicals:

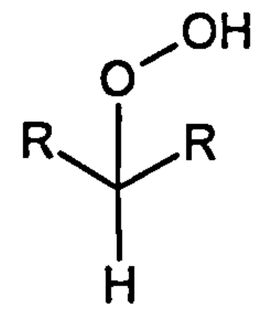

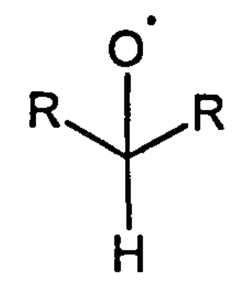

Hexadecylperoxide → RO• + HO•

$k = 3.1 \times 10^{-4}\ s^{-1}$ (200 °C)[93]

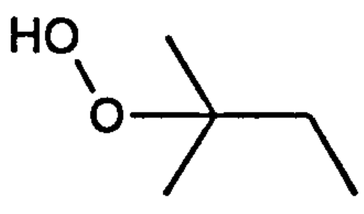

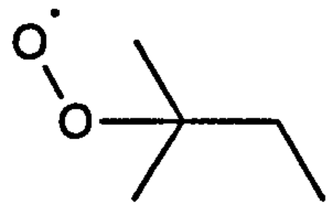

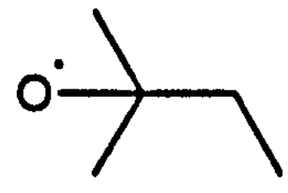

2 x $Me_2C(OOH)Et$ → ROO• + H_2O + RO•

$k = 5.7 \times 10^{-4}\ M^{-1}\ s^{-1}$ (200 °C)[94]

Step 5a: Formation of ketones from alkoxyl radicals

Tertiary alkoxyl radicals fragment to give rise to ketones:

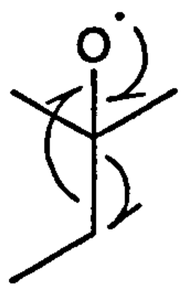

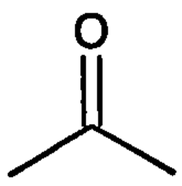

$H_3C—CH_2^{\bullet}$

$EtMe_2CO^{\bullet}$ → $R_1R_2C(O)$ + R•

$k = 3.5 \times 10^{7}\ s^{-1}$ (200 °C)[95]

[93] $k = 3.2 \times 10^{8} \exp(-108.8\ kJ/mol\ /\ RT)\ s^{-1}$ in hexadecane (Jensen et al, 1990).
[94] $k = 6.31 \times 10^{7} \exp(-100.0\ kJ/mol\ /\ RT)\ M^{-1}\ s^{-1}$ in 2-methylbutane (Denisov and Afanasev, 2005, p.155).
[95] $k = 6.31 \times 10^{11} \exp(-38.5\ kJ/mol\ /\ RT)\ s^{-1}$ in Cl_2=CHCl (Denisov and Afanasev, 2005, p.74).

Step 5b: Reaction of alkoxyl radicals with hydrocarbon

Alkoxyl radicals abstract hydrogen atoms to give rise to alcohols:

$Me_2CHCHMe_2$ + Me_3CO• → R• + ROH

$k = 4.6 \times 10^5\ M^{-1}\ s^{-1}$ (45 °C) in benzene (Denisov and Afanasev, 2005, p.73).

Oxidation mechanism of AN2

The suggested (based on a literature review) inhibition mechanism of AN2 is divided into three parts: part 1 is about the formation of AN2 phenoxyl radical (Figure C.2), part 2 is about the reactions of AN2 phenoxyl radical (Figure C.3), and part 3 is about the reactions of AN2 oxidation products (Figure C.4).

In the absence of data on reactions of AN2 with other species, data from similar sterically-hindered phenols (e.g, BHT, 2,4,6-tri-tert-butylphenol, and 2,6-di-tert-butylphenol) are given.

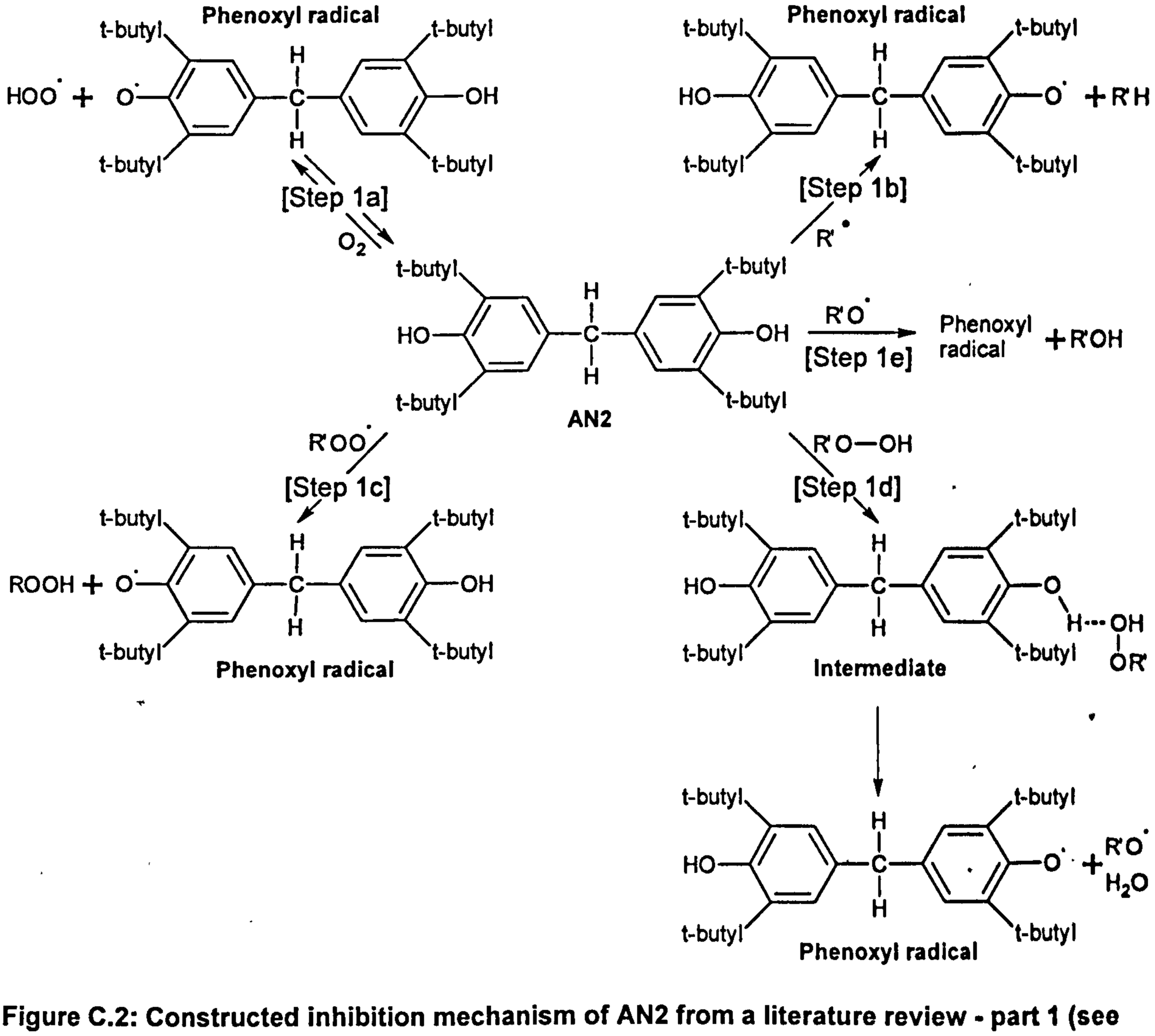

Figure C.2: Constructed inhibition mechanism of AN2 from a literature review - part 1 (see text for references)

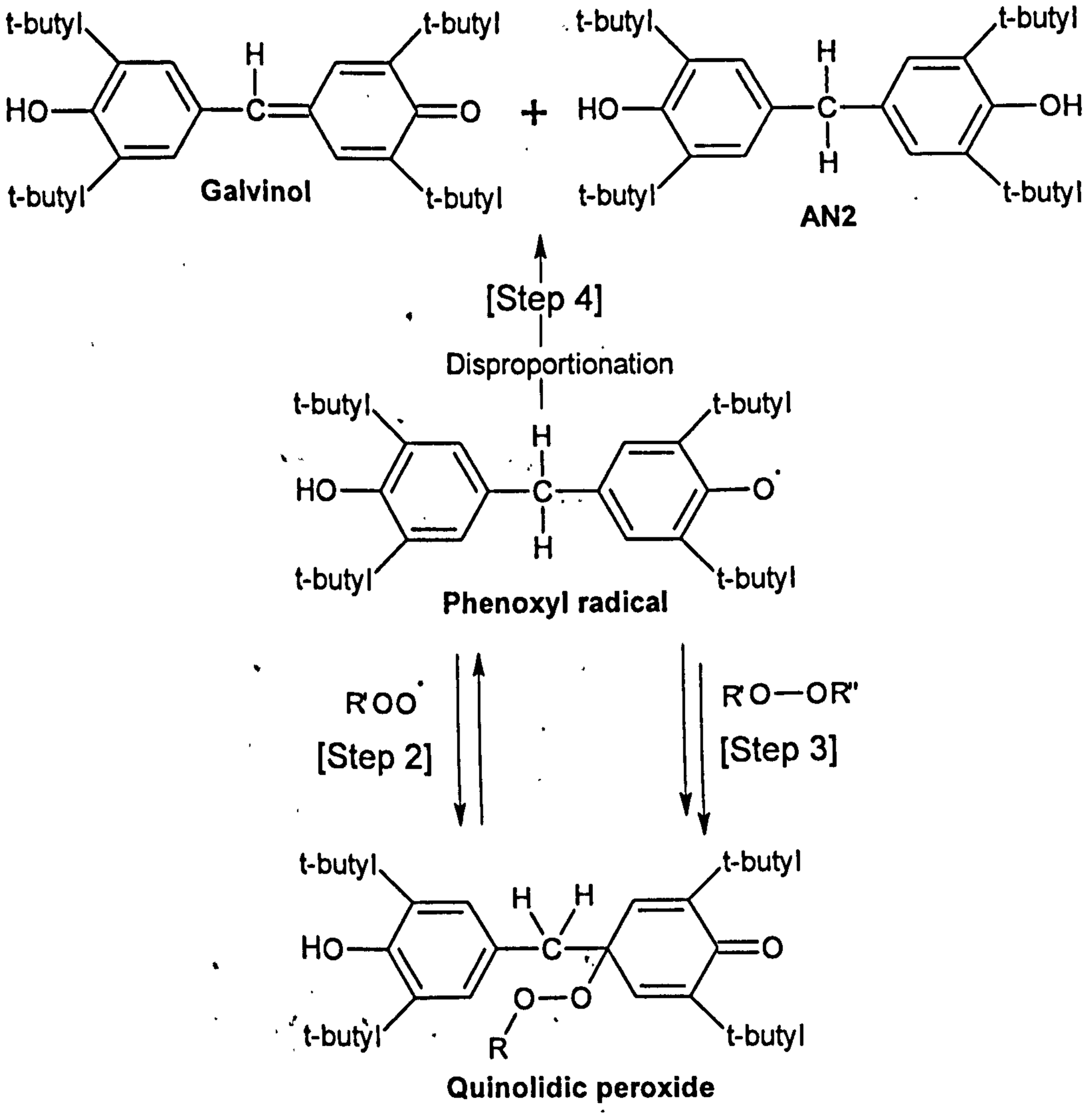

Figure C.3: Constructed inhibition mechanism of AN2 from a literature review - part 2 (see text for references)

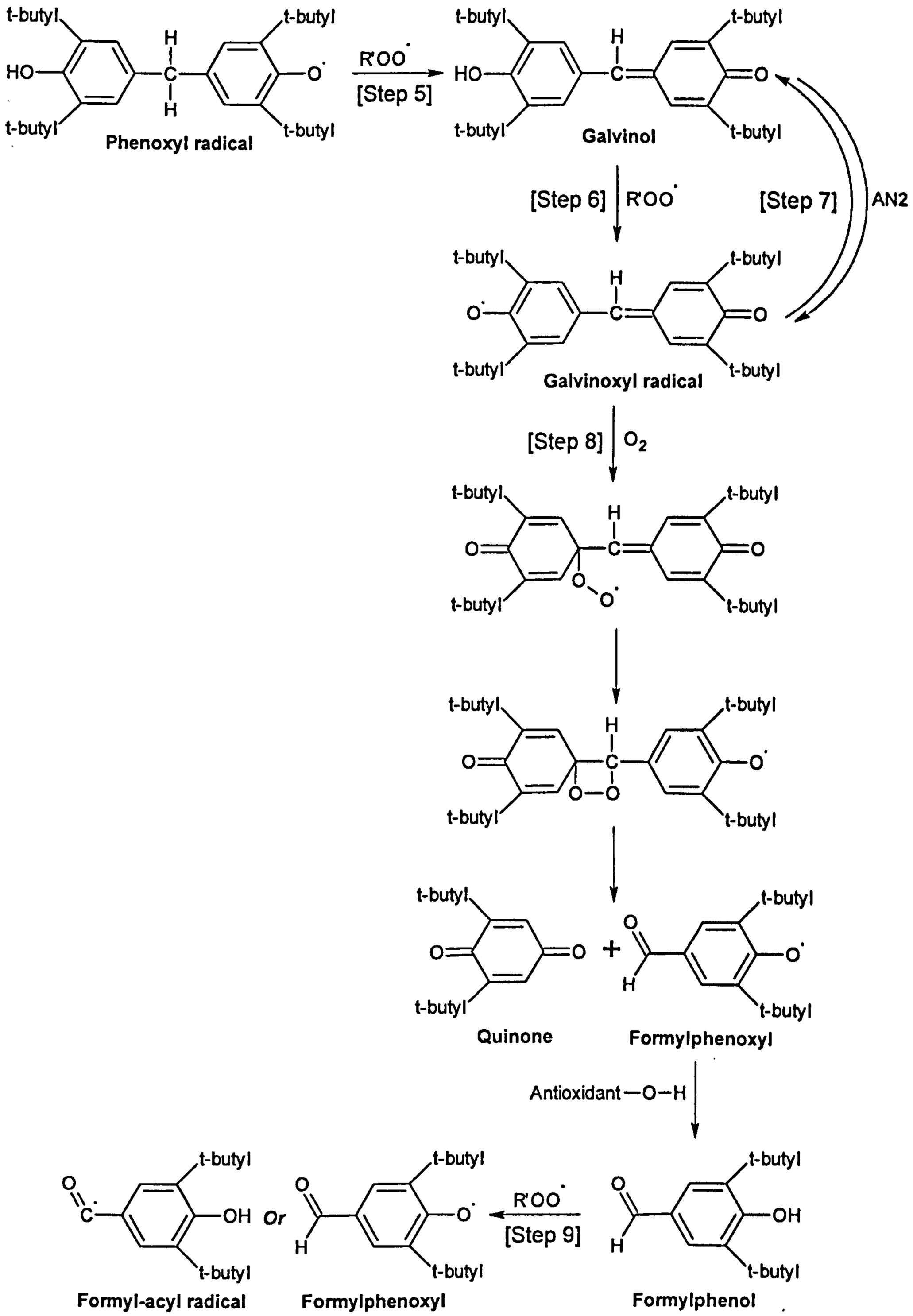

Figure C.4: Constructed inhibition mechanism of AN2 from a literature review- part 3 (see text for references)

Step 1a: Reaction of AN2 with oxygen

Sterically-hindered phenols (Ar_2OH) react with oxygen to give rise to a phenoxyl radical ($Ar_2O•$) and a hydroperoxyl radical (Denisov and Afanasev, 2005, p.531):

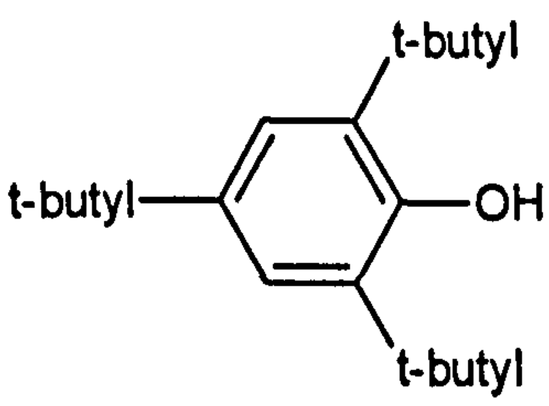

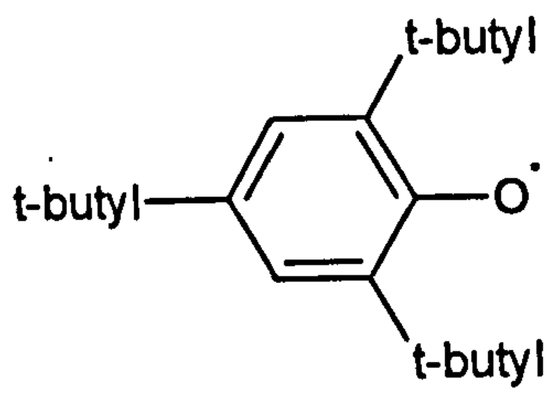

2,4,6-Tri-tert-butylphenol + O_2 ⇆ $Ar_2O•$ + HOO•

$k = 8.1 \times 10^{-4}\ M^{-1}\ s^{-1}$ (200 °C) (modelled)[96]

ΔH = BDE(Ar_2O-H) – BDE(H-OO•) in kJ mol^{-1}

= 339.7[97] – 220[98] = 120 kJ mol^{-1} (endothermic, i.e. reversible)

Step 1b: Reaction of AN2 with alkyl radicals

Ar_2OH reacts with alkyl radicals to give rise to a phenoxyl radical and a hydrocarbon:

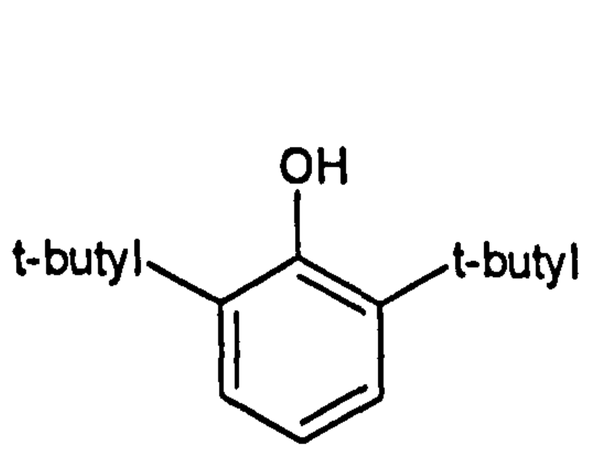

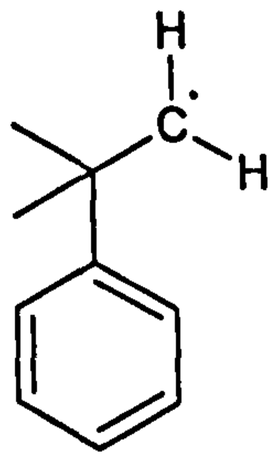

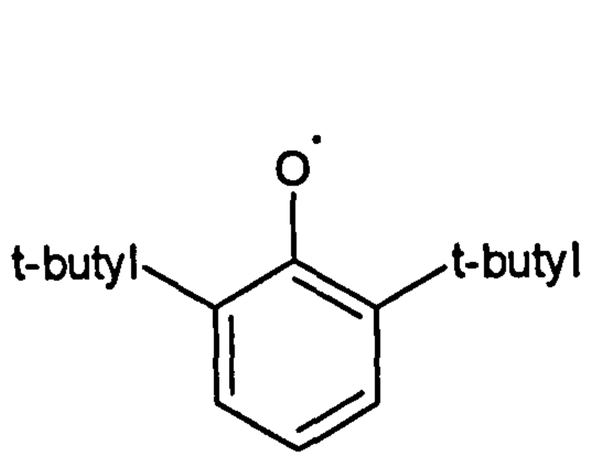

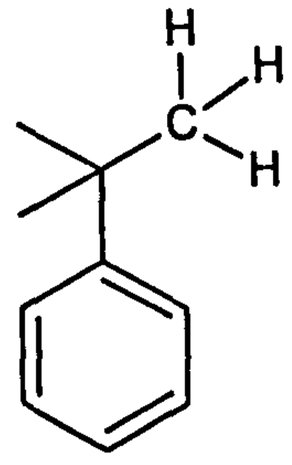

2,6-Di-tert-butylphenol + Neophyl (R•) → $Ar_2O•$ + RH

$k = 2.4 \times 10^{4}\ M^{-1}\ s^{-1}$ (200 °C)[99]

ΔH = BDE(Ar_2O-H) – BDE(R-H) in kJ mol^{-1}

= 346.4[100] – 420[101] = -74 kJ mol^{-1} (exothermic, i.e. favourable)

---

[96] $k = 1.1 \times 10^{10} \exp(-119.0\ kJ/mol / RT)\ M^{-1}\ s^{-1}$ in (Denisov and Afanasev, 2005, p.531).
[97] Denisov and Denisova, 2000, p.90.
[98] Denisov and Afanasev, 2005, p.528.
[99] $k = 1.1 \times 10^{6} \exp(-15.2\ kJ/mol / RT)\ M^{-1}\ s^{-1}$ in benzene (Franchi et al, 1999).
[100] Denisov and Denisova, 2000, p.89.
[101] Denisov and Denisova, 2000.

Step 1c: Reaction of AN2 with peroxyl radicals

Peroxyl radicals react with AN2 to give rise to hydroperoxides and phenoxyl radicals:

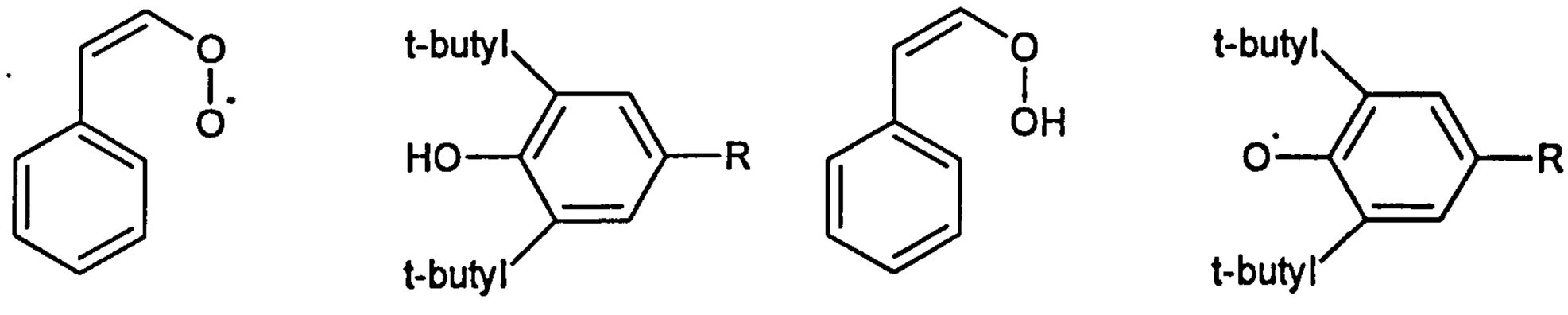

Styrylperoxyl[102] + AN2 → ROOH + Ar_2O•

$k = 7.70 \times 10^3\ M^{-1}\ s^{-1}$ (30 °C) in chlorobenzene (Amorati et al, 2003)

ΔH = BDE(Ar_2O-H) – BDE(ROO-H) in kJ mol^{-1}

= 340.2[103] – 366[104] = -26 kJ mol^{-1} (exothermic, i.e. favourable)

Step 1d: Reaction of AN2 with hydroperoxides

Ar_2OH reacts with hydroperoxides to give rise to a phenoxyl radical, alkoxyl radical, and water. The reaction proceeds via an intermediate (Denisov and Afanasev, 2005, p.532) (Figure C.5):

2,4,6-Tri-tert-butylphenol + $PhMe_2COOH \rightarrow Ar_2O\bullet + RO\bullet + H_2O$

$k = 4.3 \times 10^{-3}\ M^{-1}\ s^{-1}$ (200 °C)[105]

ΔH = -18 kJ mol^{-1} (modelled)[106] (exothermic, i.e. favourable)

---

[102] CAS name and number are 2-phenyl-ethenyldioxyl and 25032-94-4, respectively.
[103] Denisov and Denisova, 2000, p.89.
[104] Denisov and Afanasev, 2005, p.41.
[105] $k = 4.0 \times 10^9 \exp(-108.4\ kJ/mol / RT)\ M^{-1}\ s^{-1}$ in decane (Denisov and Denisova, 2000, p.120).
[106] Denisov and Denisova, 2000, p.117.

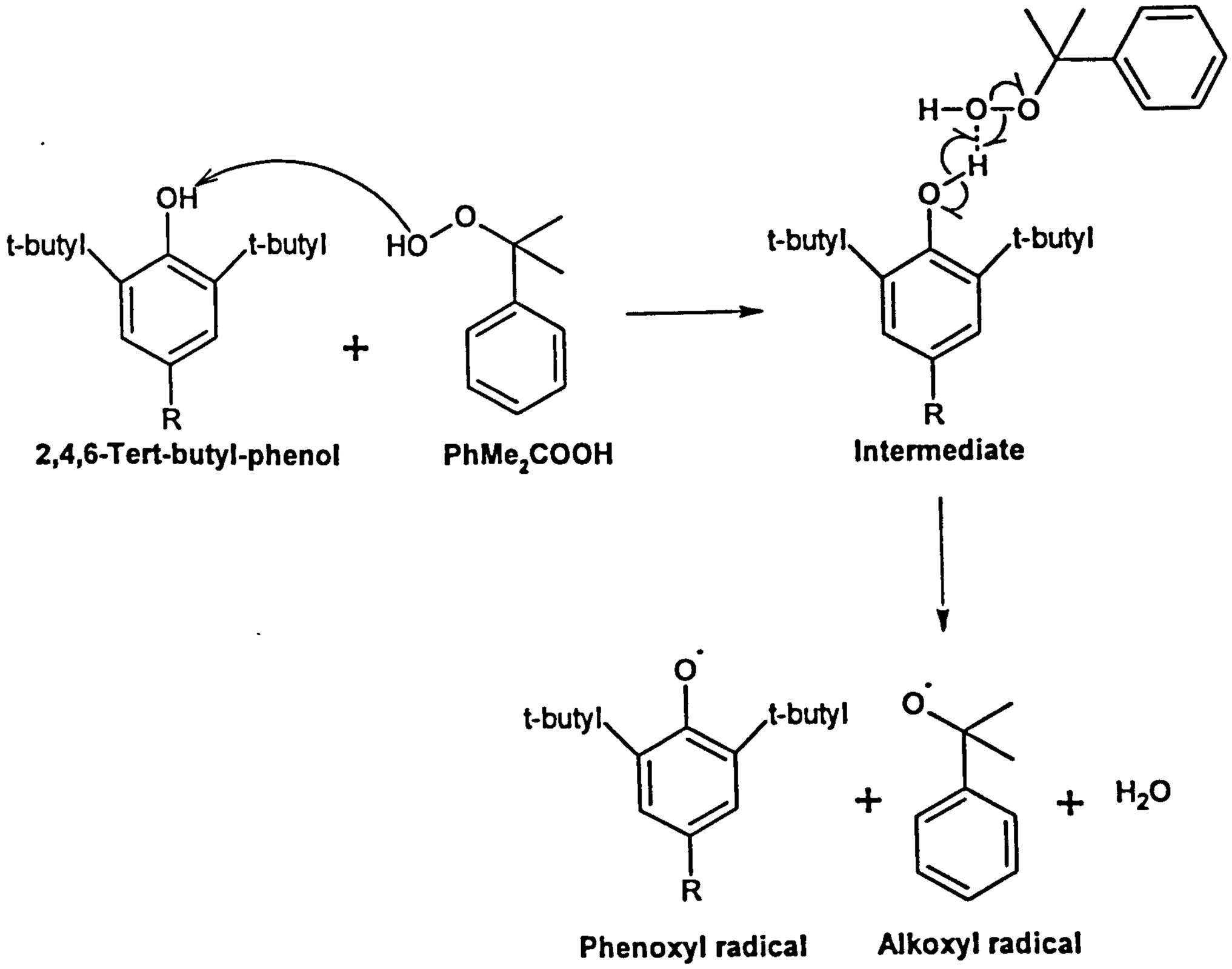

Figure C.5: Proposed mechanism for the reaction between 2,4,6-tri-tert-butylphenol and $PhMe_2COOH$

Step 1e: Reaction of AN2 with alkoxyl radicals

Ar_2OH reacts with alkoxyl radicals to give rise to a phenoxyl radical and an alcohol:

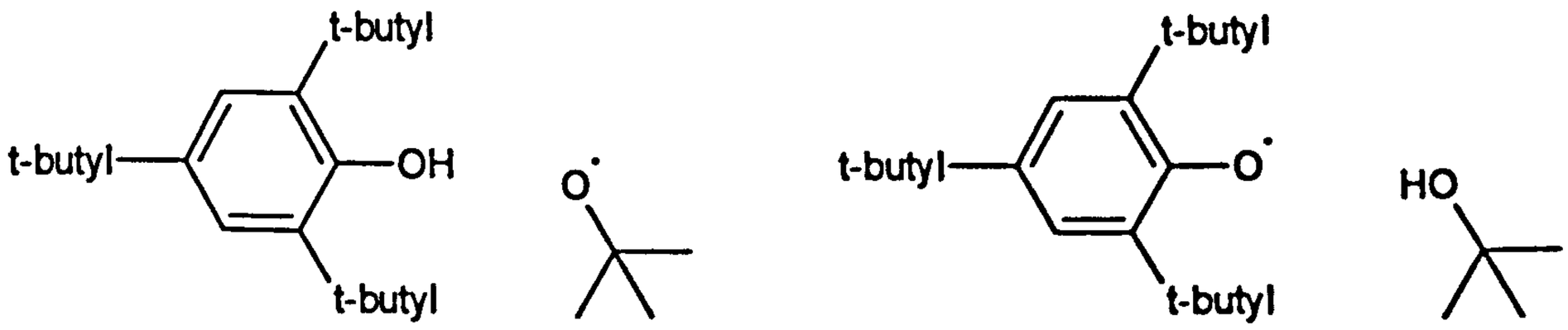

2,4,6-Tri-tert-butylphenol + $(Me)_3CO\bullet \rightarrow$ $Ar_2O\bullet$ + $(Me)_3COH$

$k = 2.10 \times 10^9\ M^{-1}\ s^{-1}$ (23 °C) in pentane (Snelgrove et al, 2001)

ΔH = BDE(Ar_2O-H) – BDE(RO-H) in kJ mol^{-1}

= 339.7[107] – 441.4[108] = -102 kJ mol^{-1} (exothermic, i.e. favourable)

---

[107] Denisov and Denisova, 2000, p.90.
[108] Luo, 2003, p.164.

Step 2: Reaction of AN2 phenoxyl with peroxyl radicals

Peroxyl radicals preferentially react with the para-position of the phenoxyl radicals (Denisov and Afanasev, 2005, p.510) to give rise to quinolidic peroxide (Figure C.6):

2,4,6-Tert-butylphenoxyl + Cyanoisopropylperoxyl ⇆ Quinolidic peroxide

$k = 3.8 \times 10^7\ M^{-1}\ s^{-1}$ (200 °C)[109]

The reaction is reversible because the peroxide readily decomposes at temperatures above 77 °C (Denisov and Afanasev, 2005, p.510).

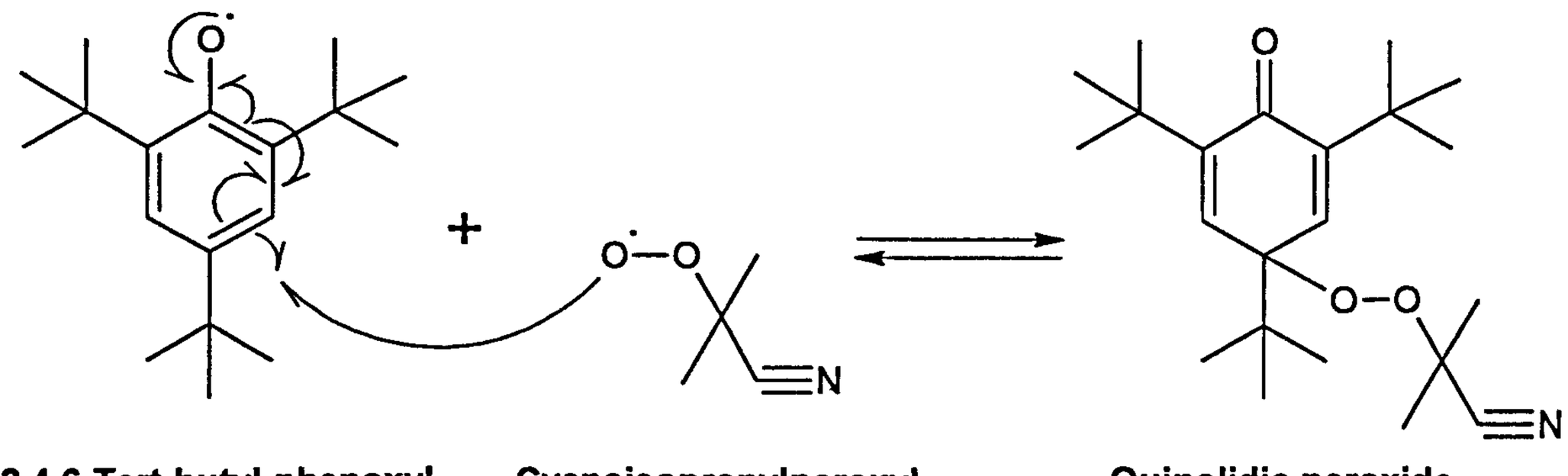

2,4,6-Tert-butyl-phenoxyl **Cyanoisopropylperoxyl** **Quinolidic peroxide**

Figure C.6: Proposed mechanism for the reaction between 2,4,6-tert-butylphenoxyl and cyanoisopropylperoxyl

Step 3: Reaction of AN2 phenoxyl with organic peroxides

$Ar_2O\bullet$ reacts with organic peroxides to give rise to quinolidic peroxide (Figure C.7):

AN2 phenoxyl + Di-tert-butylperoxide ⇉ Quinolidic peroxide

$k = 2.1 \times 10^5\ M^{-1}\ s^{-1}$ (200 °C)[110]

[109] $k = 5.2 \times 10^7 \exp(-1.2\ kJ/mol\ /\ RT)\ M^{-1}\ s^{-1}$ (Rubtsov et al, 1979).
[110] $k = 1.2 \times 10^7 \exp(-15.9\ kJ/mol\ /\ RT)\ M^{-1}\ s^{-1}$ (Prokofev et al, 1968).

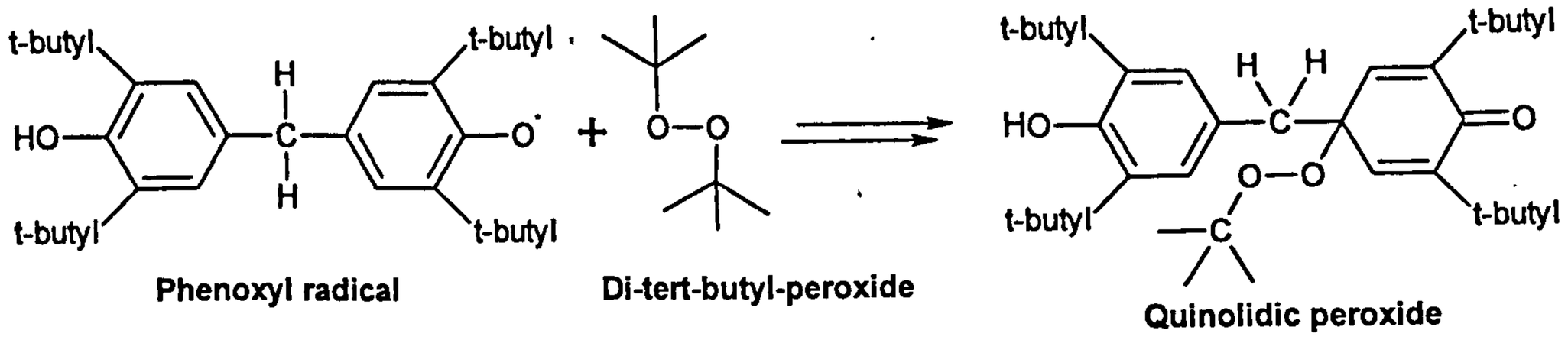

Figure C.7: Reaction between AN2 phenoxyl and di-tert-butylperoxide (Prokofev et al, 1968) [the multi-steps are unknown]

Step 4: Disproportionation of AN2 phenoxyl radicals

AN2 phenoxyl radicals disproportionate to give rise to galvinol and regenerate the AN2 molecule (Figure 5.16):

$$2 \times \text{AN2 phenoxyl} \rightarrow \text{Galvinol} + \text{AN2}$$

$$k = 2.7 \times 10^4\ M^{-1}\ s^{-1}\ (200\ °C)^{111}$$

ΔH = $BDE(Ar_2C\text{-}H) - BDE(Ar_2O\text{-}H)$ in kJ mol^{-1}

= <<352[112] – 340.2[113] = exothermic [expected] (i.e. favourable)

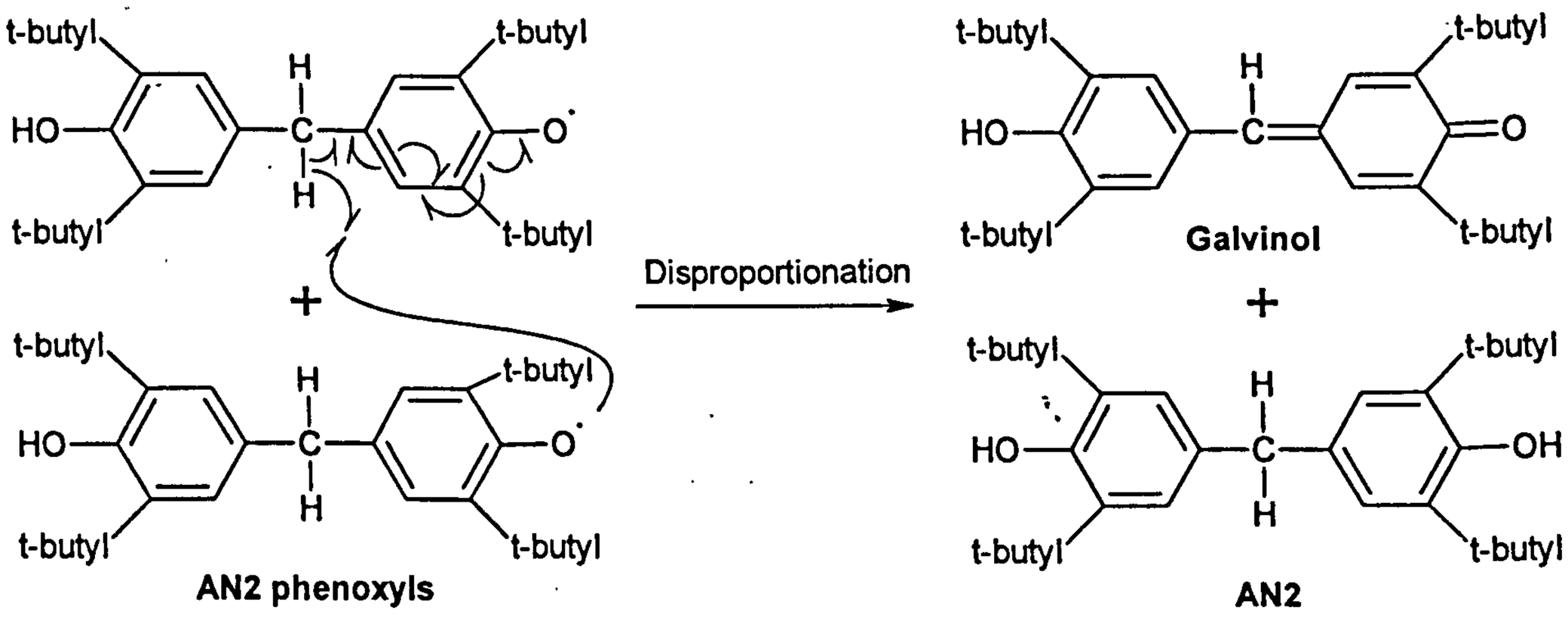

Figure C.8: Proposed mechanism for the disproportionation of AN2 phenoxyl radicals (Roginskii, 1985)

---

[111] $k = 3.0 \times 10^6 \exp(-18.6\ kJ/mol\ /\ RT)\ M^{-1}\ s^{-1}$ in benzene (Roginskii, 1985).

[112] The BDE of the C-H bond of methylene bridge of AN2 is 352 ± 8 kJ mol^{-1} (McMillen and Golden, 1982) but the BDE of the C-H bond of the methylene bridge of the AN2 phenoxyl is expected to be much lower than 352 kJ mol^{-1} due to the destabilisation by the radical on the oxygen atom.

[113] Denisov and Denisova, 2000, p.89.

Step 5: Reaction of AN2 phenoxyl with peroxyl radicals

Peroxyl radicals would be expected to abstract hydrogen atoms in the same way as phenoxyl radicals to give rise to galvinol (Figure C.9):

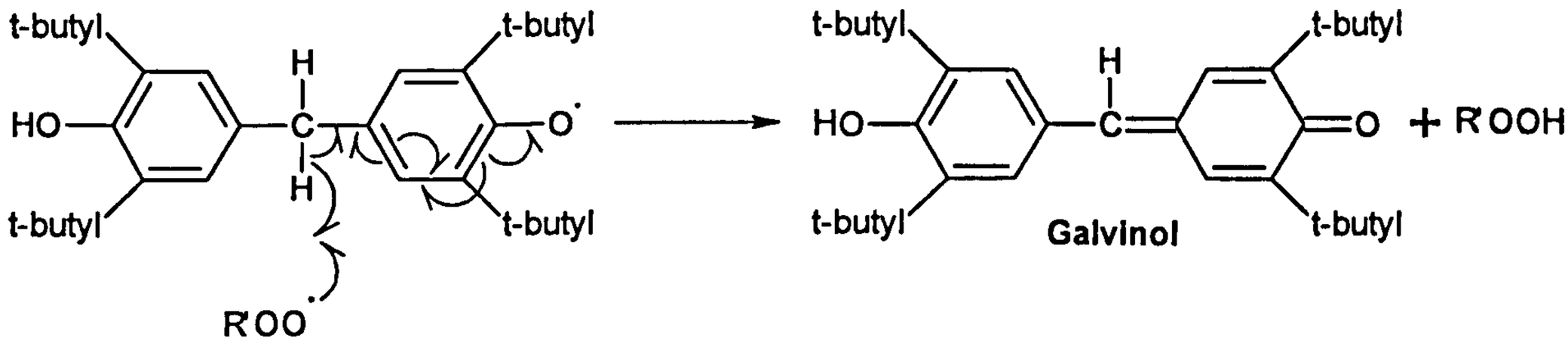

Figure C.9: Proposed mechanism for the reaction between AN2 phenoxyl radicals and peroxyl radicals

Step 6: Reaction of galvinol with peroxyl radicals

One of the pathways for the formation of galvinoxyl radical is via the reaction between galvinol and peroxyl radicals (Figure C.10):

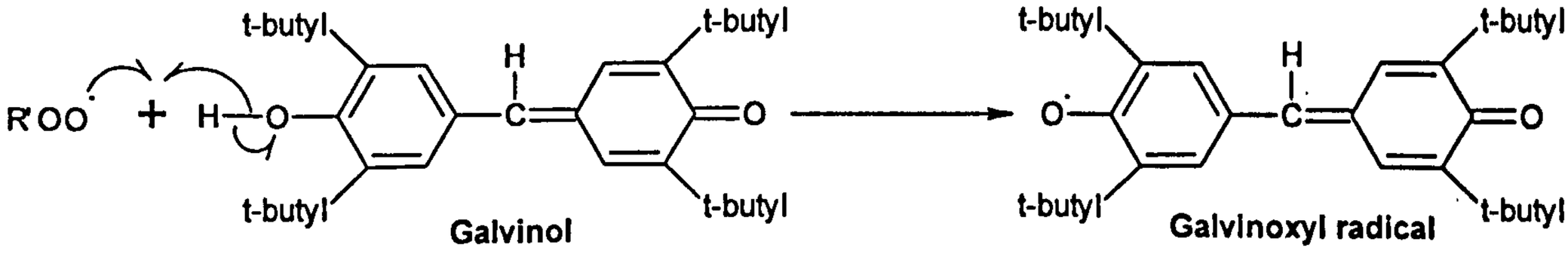

Figure C.10: Proposed mechanism for the reaction between galvinol and peroxyl radicals

ΔH = BDE(Ar_2O-H) – BDE(ROO-H) in kJ mol^{-1}

= 329.1[114] – 359[115] = -30 kJ mol^{-1} (exothermic, i.e. favourable)

[114] Denisov and Denisova, 2000, p.89.
[115] Denisov and Afanasev, 2005, p.41.

Step 7: Reaction of galvinoxyl radicals with AN2

Galvinoxyl radicals react with AN2 to give rise to galvinol and phenoxyl radicals (Figure C.11):

Galvinoxyl + AN2 ⇆ Galvinol + Phenoxyl radical

$k = 1.1 \times 10^3\ M^{-1}\ s^{-1}$ (200 °C)[116]

ΔH = BDE(Ar_2O-H) – BDE(Ar_2O-H) in kJ mol^{-1}

= 340.2[117] – 329.1[118] = 11 kJ mol^{-1} (endothermic, i.e. reversible)

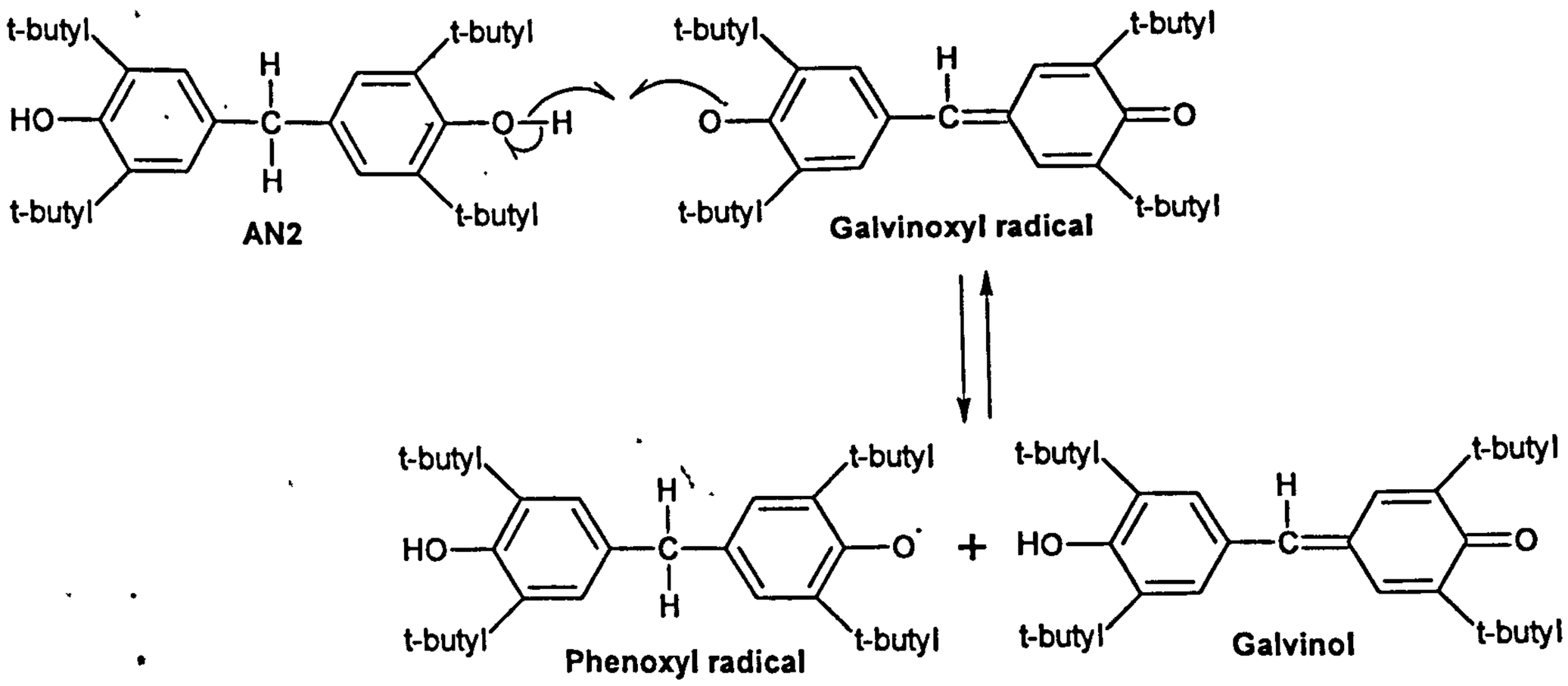

Figure C.11: Proposed mechanism for the reaction between galvinoxyl radicals with AN2

[116] $k = 7.2 \times 10^6 \exp(-34.6\ kJ/mol\ /\ RT)\ M^{-1}\ s^{-1}$ [Arrhenius parameters were derived from rate constants that were mentioned in the reference] in cyclohexane (Adam and Chin, 1971).
[117] Denisov and Denisova, 2000, p.89.
[118] Denisov and Denisova, 2000, p.89.

Step 8: Formation of formylphenol[119] and quinone[120]

Formylphenol and quinone are formed from galvinoxyl radical (Greene and Adam, 1963 and Colegate and Hewgill, 1980) (Figure C.12).

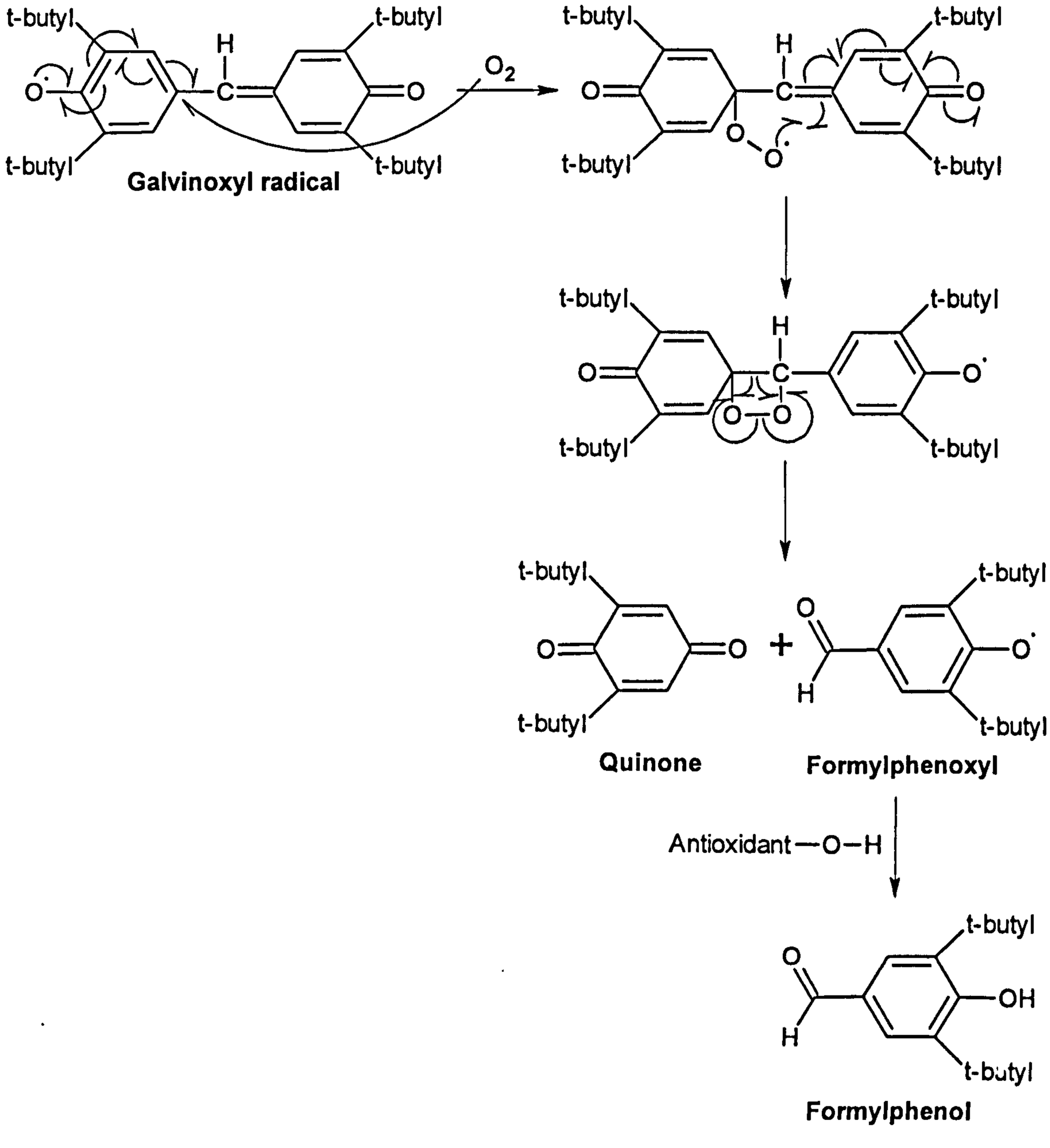

Figure C.12: Proposed mechanism for the formation of formylphenol and quinone from galvinoxyl radical (Colegate and Hewgill, 1980)

[119] 3,5-Bis(1,1-dimethylethyl)-4-hydroxy-benzaldehyde.
[120] 2,6-Bis(1,1-dimethylethyl)-2,5-cyclohexadiene-1,4-dione.

Step 9: Reaction of formylphenol with peroxyl radicals

Formylphenol is expected to react with peroxyl radicals (Khursan et al, 1989); however, the site of reaction was not identified:

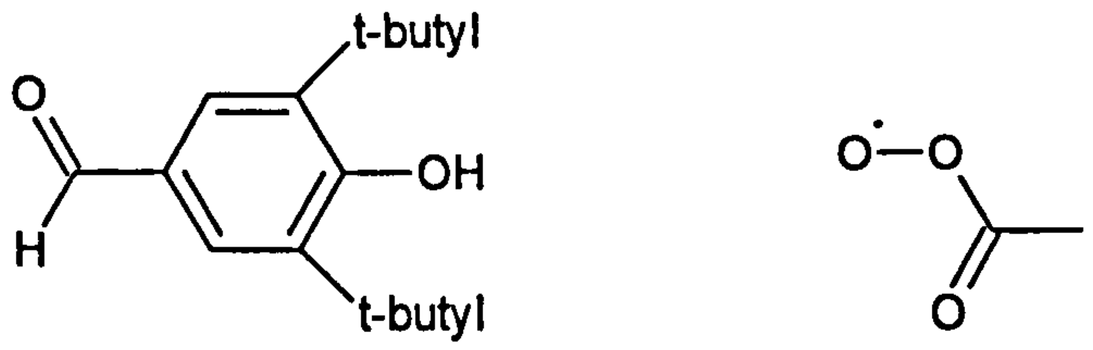

Formylphenol + Acetylperoxyl

Oxidation mechanism of aromatic amines

The suggested (based on a literature review) oxidation mechanism of Amine101 is divided into three parts: part 1 is about the formation of aminyl radical (Figure C.13), part 2 is about the reactions of aminyl radical (Figure C.14), and part 3 is about the reactions of nitroxyl radical (Figure C.15).

In the absence of data on reactions of Amine101 with other species, data from similar diaromatic amines (e.g. diphenylamine) are given.

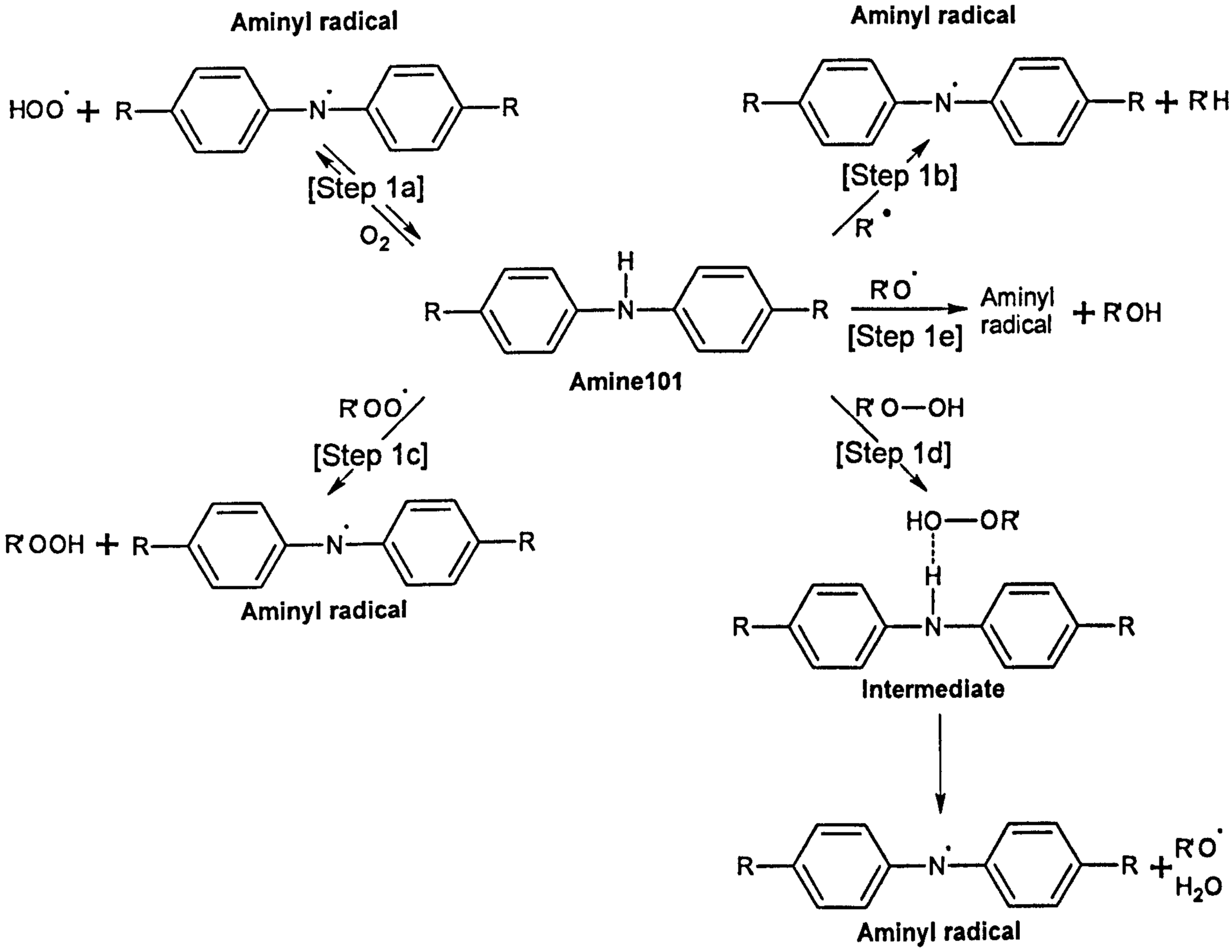

Figure C.13: Constructed inhibition mechanism of Amine101 from a literature review- part 1 (see text for references)

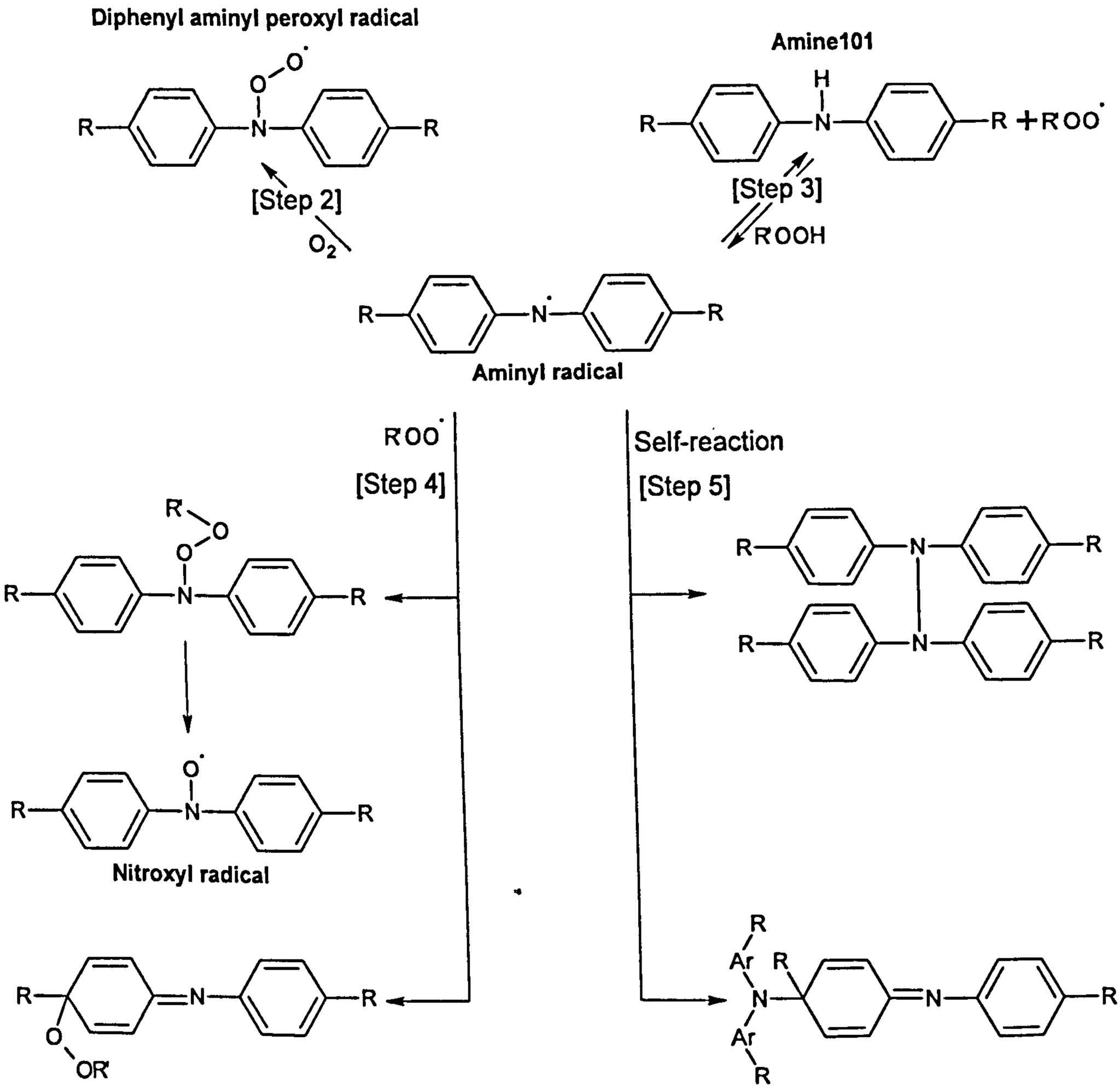

Figure C.14: Constructed inhibition mechanism of Amine101 from a literature review - part 2 (see text for references)

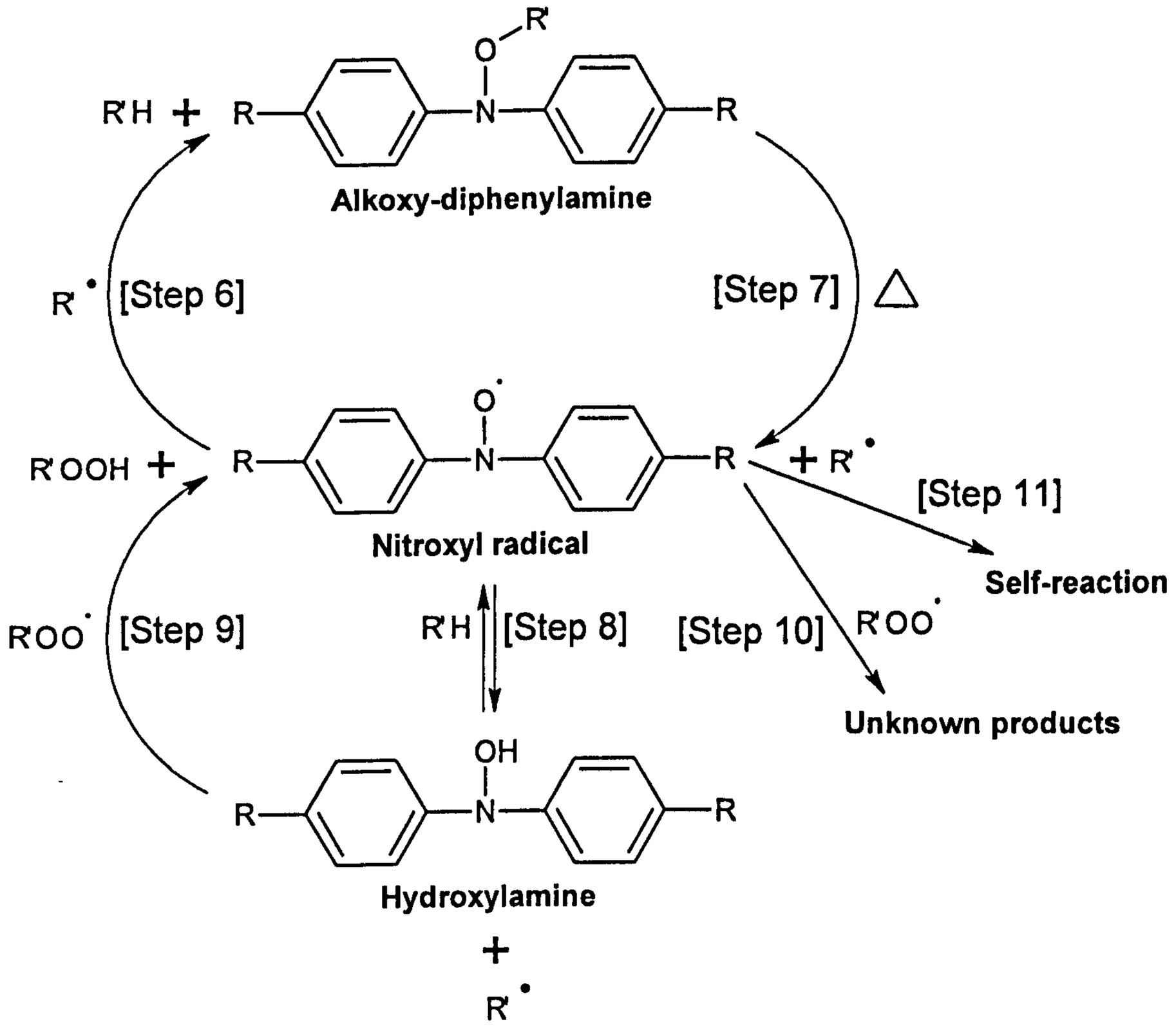

Figure C.15: Constructed inhibition mechanism of Amine101 from a literature review- part 3 (see text for references)

Step 1a: Reaction of Amine101 with oxygen

Diaromatic amines (AmH) react with oxygen to give rise to aminyl radicals (Am•) and hydroperoxyl radicals:

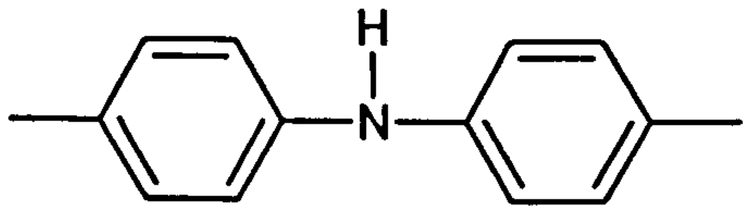

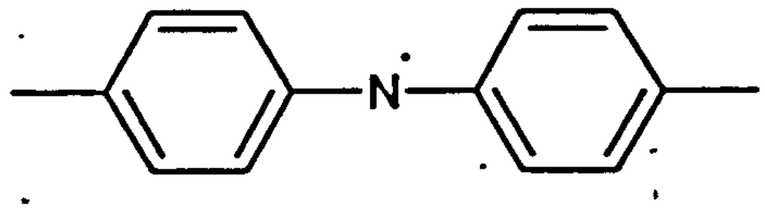

4,4'-Dimethyldiphenylamine + O_2 ⇆ Aminyl radical + HOO•

$k = 2.7 \times 10^{-5}\ M^{-1}\ s^{-1}$ (200 °C) (modelled)[121]

ΔH = BDE(AmN-H) – BDE(H-OO•) in kJ mol^{-1}

= 357.5[122] – 220[123] = 138 kJ mol^{-1} (endothermic, i.e. reversible)

Step 1b: Reaction of Amine101 with alkyl radicals

AmH reacts with alkyl radicals to give rise to an aminyl radical and a hydrocarbon:

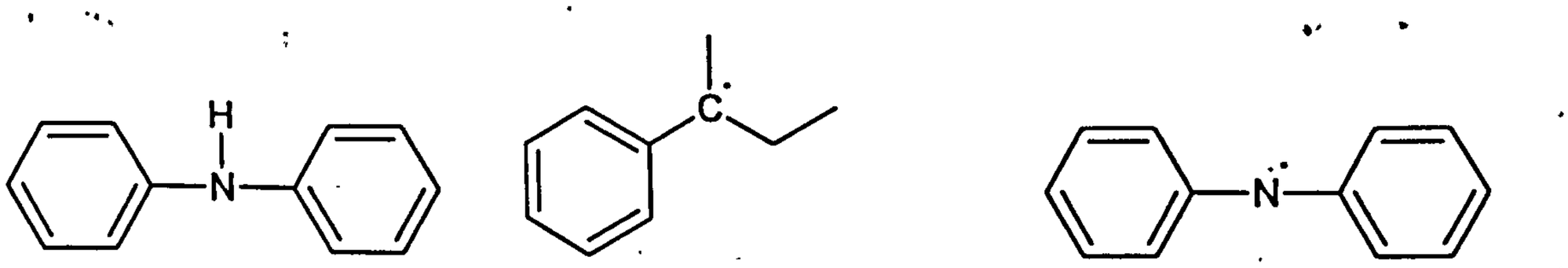

Diphenylamine + 2-Methyl-2-phenylpropyl ⇆ Am• + RH

$k = 1.3 \times 10^{6}\ M^{-1}\ s^{-1}$ (100 °C) in dodecane (Burton et al, 1996)

ΔH = BDE(AmN-H) – BDE(R-H) in kJ mol^{-1}

= 364.7[124] – 354.7[125] = 10 kJ mol^{-1} (endothermic, i.e. reversible)

---

[121] $k = 4.2 \times 10^{10} \exp(-137.5\ kJ/mol\ /\ RT)\ M^{-1}\ s^{-1}$ in (Denisov and Afanasev, 2005, p.531).
[122] Denisov and Denisova, 2000, p.91.
[123] Denisov and Afanasev, 2005, p.528.
[124] Denisov and Denisova, 2000, p.91.
[125] Denisov and Denisova, 2000, p.23.

Step 1c: Reaction of Amine101 with peroxyl radicals

AmH reacts with peroxyl radicals to give rise to aminyl radicals and hydroperoxides:

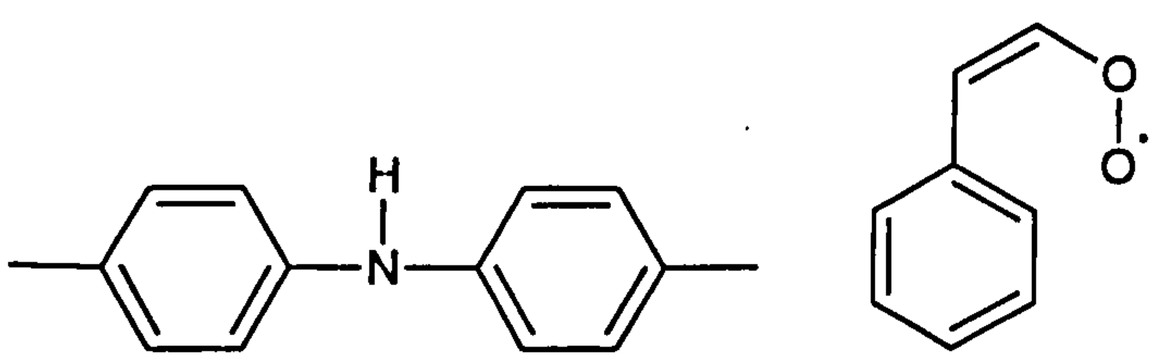

4,4'-Dimethyldiphenylamine + Styrylperoxyl → Am• + ROOH

$k = 1 \times 10^5\ M^{-1}\ s^{-1}$ (65 °C) in o-dichlorobenzene (Brownlie and Ingold, 1967)

ΔH = BDE(AmN-H) – BDE(ROO-H) in kJ mol^{-1}

= 357.5[126] – 366[127] = -8 kJ mol^{-1} (exothermic, i.e. favourable)

Step 1d: Reaction of Amine101 with hydroperoxides

AmH reacts with hydroperoxides to give rise to an aminyl radical, alkoxyl radical, and water (Denisov and Afanasev, 2005, p.536). The reaction is likely to proceed via an intermediate (Figure C.16). The pathway is expected to be similar to that for the reaction between sterically-hindered phenols and hydroperoxides:

4,4'-Dimethyldiphenylamine + Cumylhydroperoxide → Am• + RO• + H_2O

$k = 8.8 \times 10^{-5}\ M^{-1}\ s^{-1}$ (130 °C) in decane/chlorobenzene (Denisov and Afanasev, 2005, p.536)

ΔH = -36 kJ mol^{-1} (modelled)[128] (exothermic, i.e. favourable)

[126] Denisov and Denisova, 2000, p.91.
[127] Denisov and Afanasev, 2005, p.41.
[128] Denisov and Denisova, 2000, p.118.

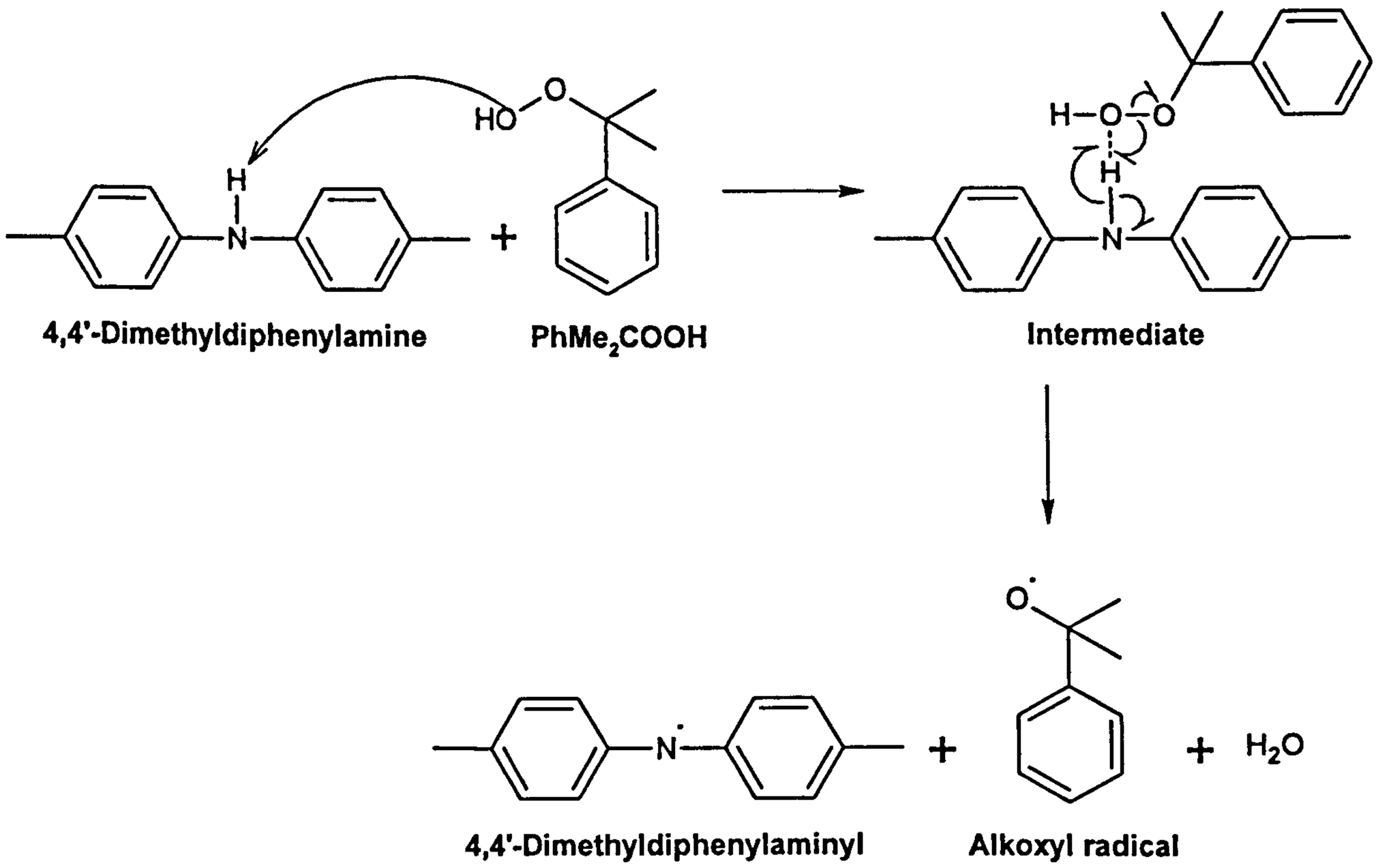

4,4'-Dimethyldiphenylamine **$PhMe_2COOH$** **Intermediate**

4,4'-Dimethyldiphenylaminyl **Alkoxyl radical**

Figure C.16: Proposed mechanism for the reaction between 4,4'-dimethyldiphenylamine and cumylhydroperoxide

Step 1e: Reaction of Amine101 with alkoxyl radicals

AmH reacts with alkoxyl radicals to give rise to an aminyl radical and alcohol:

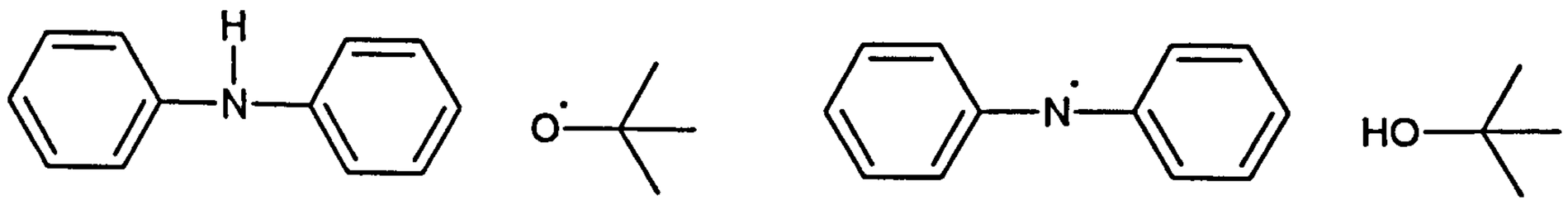

Diphenylamine + Tert-butoxyl → Am• + ROH

$k = 9.9 \times 10^8\ M^{-1}\ s^{-1}$ (22 °C) in chlorobenzene (MacFaul et al, 1996)

ΔH = BDE(AmN-H) – BDE(RO-H) in kJ mol^{-1}

= 364.7[129] – 441.4[130] = -76 kJ mol^{-1} (exothermic, i.e. favourable)

[129] Denisov and Denisova, 2000, p.91.
[130] Luo, 2003, p.164.

Step 2: Reaction of aminyl radicals with oxygen

Aminyl radicals react with oxygen (Maillard et al, 1983) to give rise to aminyl peroxyls:

Diaromatic aminyl + O_2 → Diaromatic aminyl peroxyl

Step 3: Reaction of aminyl radicals with hydroperoxide

Aminyl radicals react with hydroperoxides to give rise to diaromatic amine and peroxyl radicals:

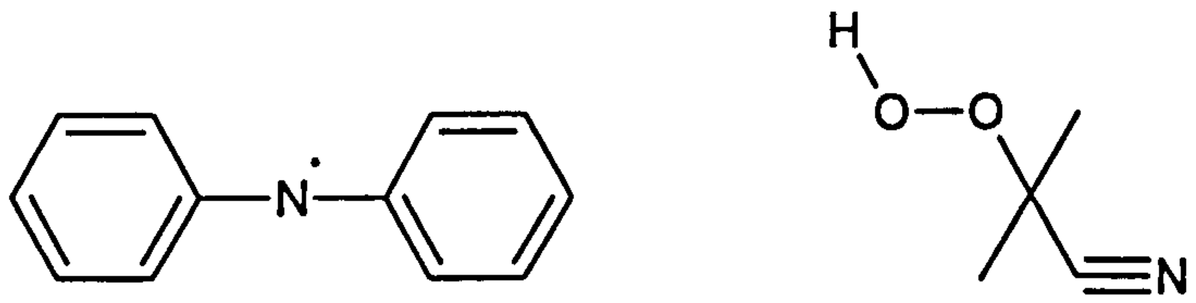

Diphenylaminyl + Cyanoisopropylperoxide ⇆ Diphenylamine + ROO•

$k = 1.1 \times 10^5\ M^{-1}\ s^{-1}$ (20 °C) in cyclohexane (Varlamov and Denisov, 1987)

ΔH = BDE(ROO-H) – BDE(AmN-H) in kJ mol^{-1}

= $364.7^{131} - 359^{132}$ = 6 kJ mol^{-1} (endothermic, i.e. reversible)

[131] Denisov and Denisova, 2000, p.91.
[132] Denisov and Afanasev, 2005, p.41.

Step 4: Reaction of aminyl radicals with peroxyl radicals

Peroxyl radicals are thought to react at the nitrogen atom of the aminyl radical to give rise to a nitroxyl radical (AmO•) and to attack the para-position of the aromatic ring of the aminyl radical (Adamic and Ingold, 1969) (Figure C.17):

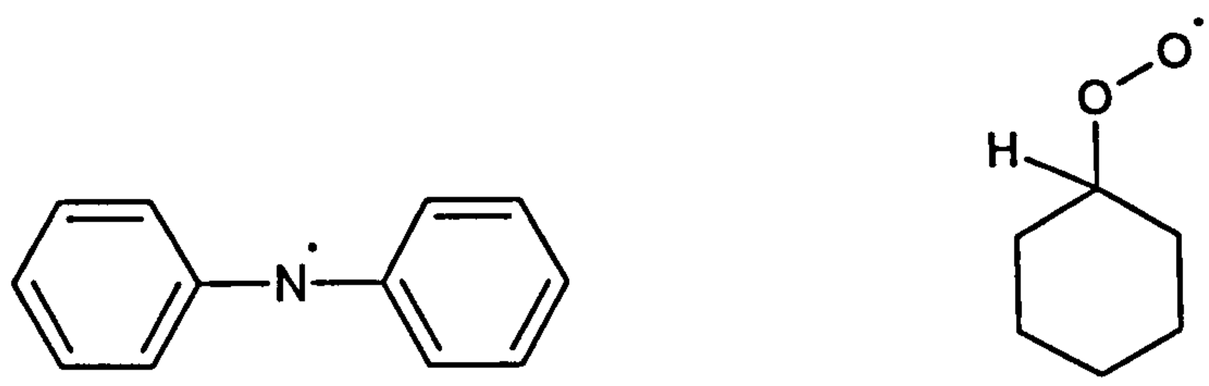

Diphenylaminyl + Cyclohexylperoxyl

$k = 6 \times 10^8\ M^{-1}\ s^{-1}$ (25 °C) in cyclohexane (Denisov and Afanasev, 2005, p.511)

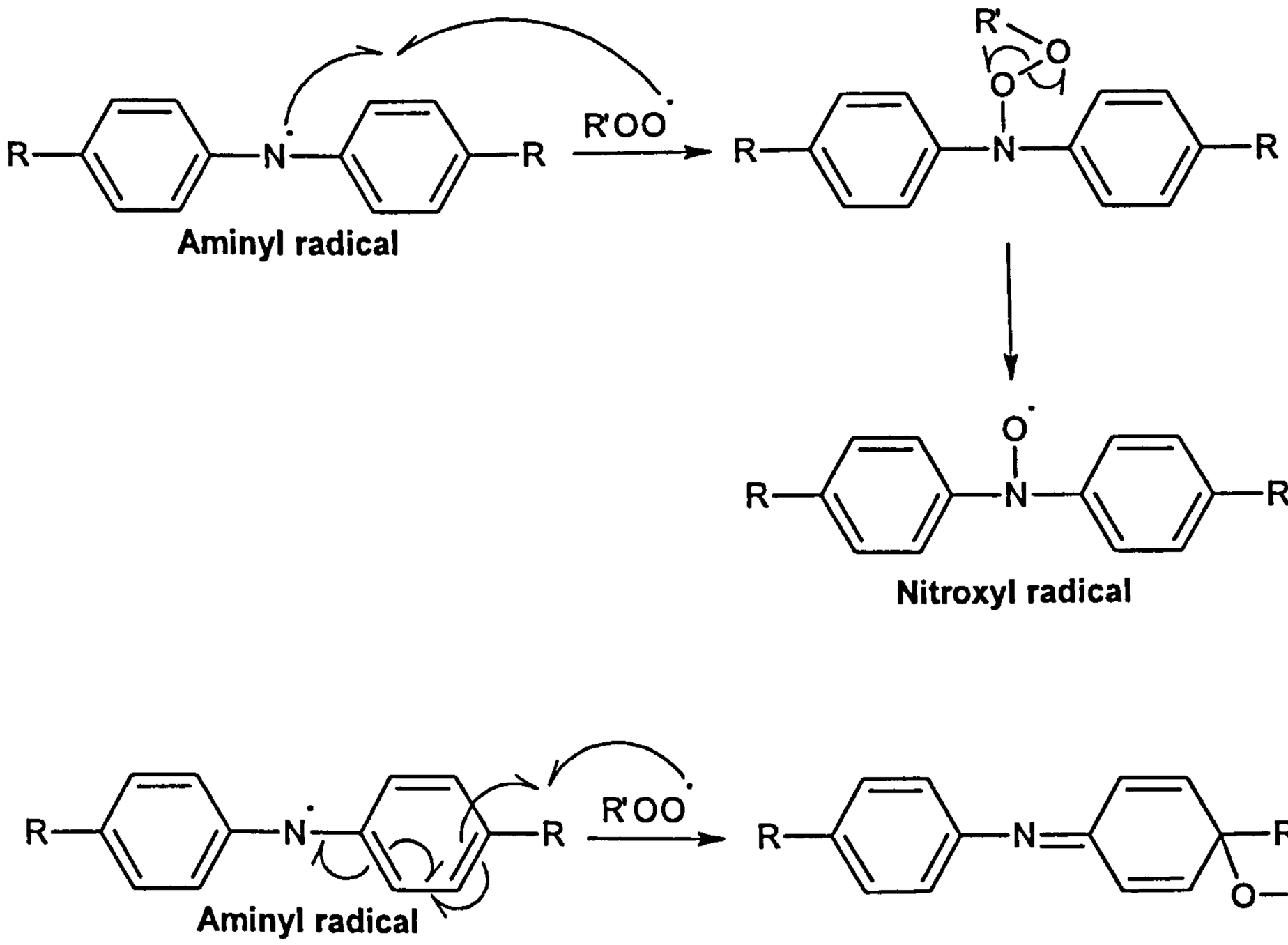

Figure C.17: Proposed mechanisms for the reaction between aminyl radicals and peroxyl radicals (Adamic and Ingold, 1969)

Step 5: Self-reaction of aminyl radicals

The aminyl radicals self-react at the nitrogen atoms and the para-position of the aromatic ring at a relative ratio of 1 : 0.15, respectively (Figure C.18) (Denisov and Afanasev, 2005, p.518):

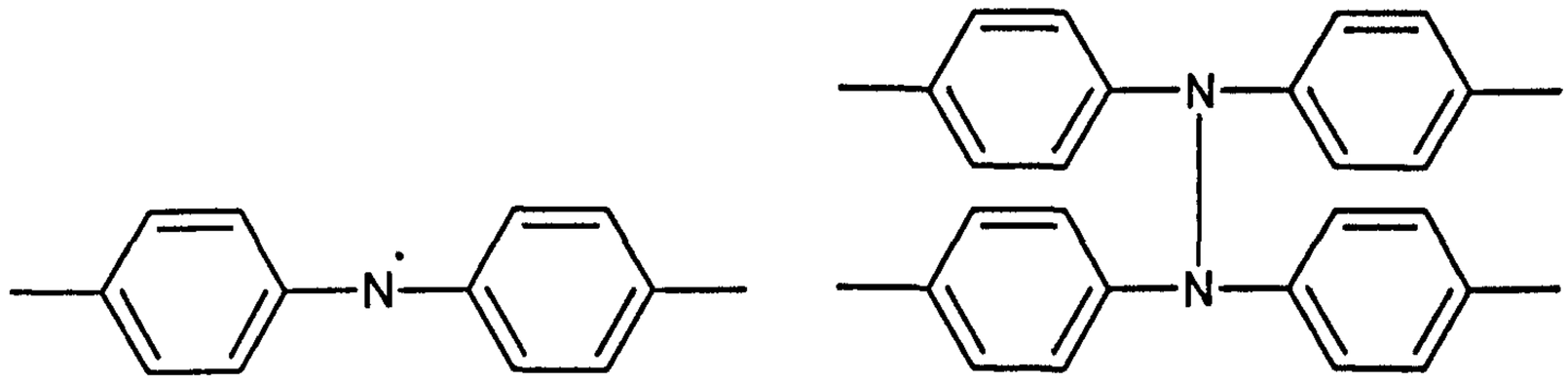

2 x 4,4'-Dimethyldiphenylaminyl → $(R\text{-}Ar)_2N\text{-}N(Ar\text{-}R)_2$

$k = 2.3 \times 10^6\ M^{-1}\ s^{-1}$ (25 °C) (Denisov and Afanasev, 2005, p.520)

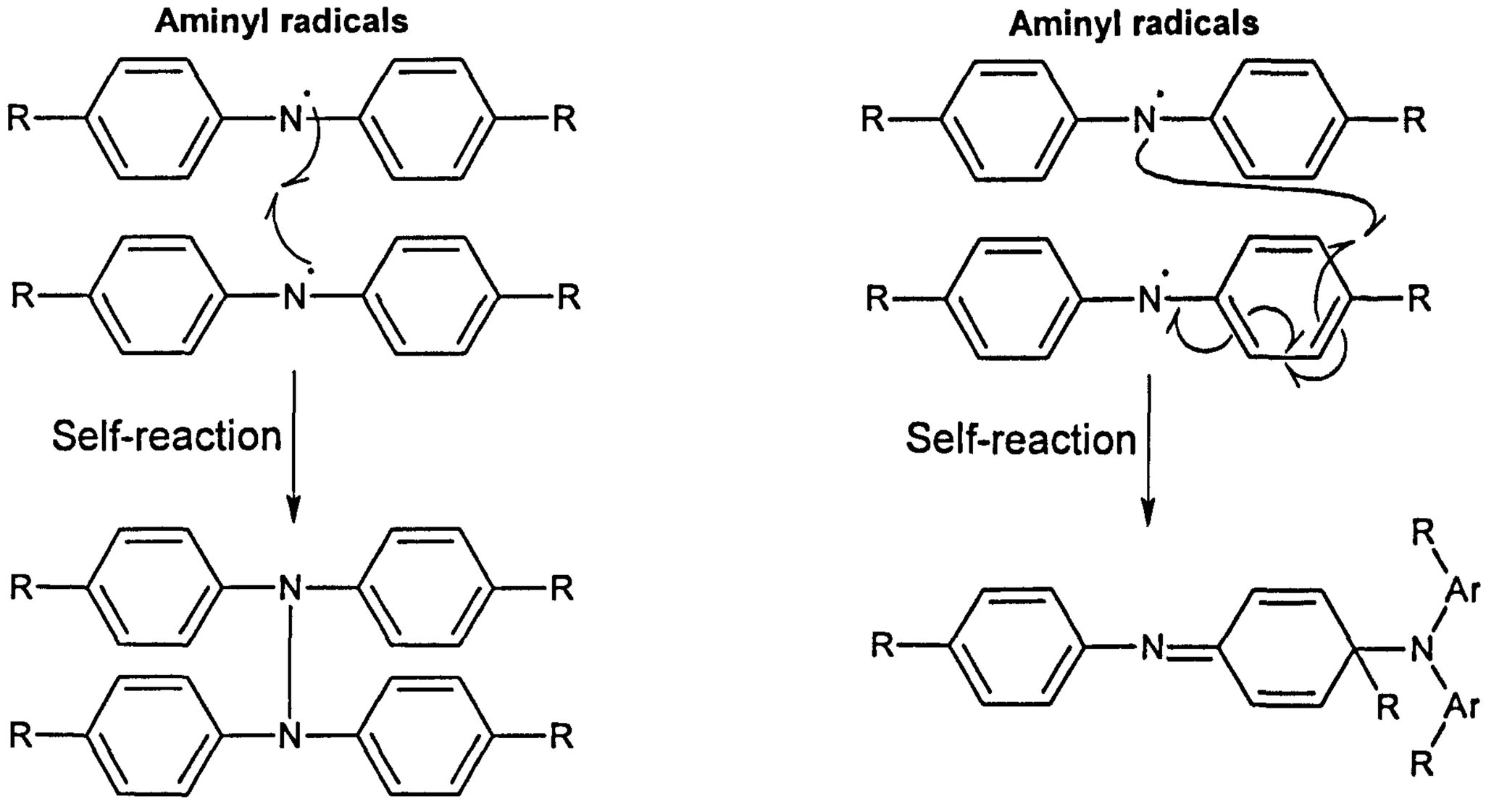

Figure C.18: Proposed mechanism for the self-reaction of aminyl radicals

Step 6: Reaction of nitroxyl radicals with alkyl radicals

Nitroxyl radicals are thought to react with alkyl radicals to give rise to an N-alkoxydiphenylamine (Figure C.19) (Thomas and Tolman, 1962).

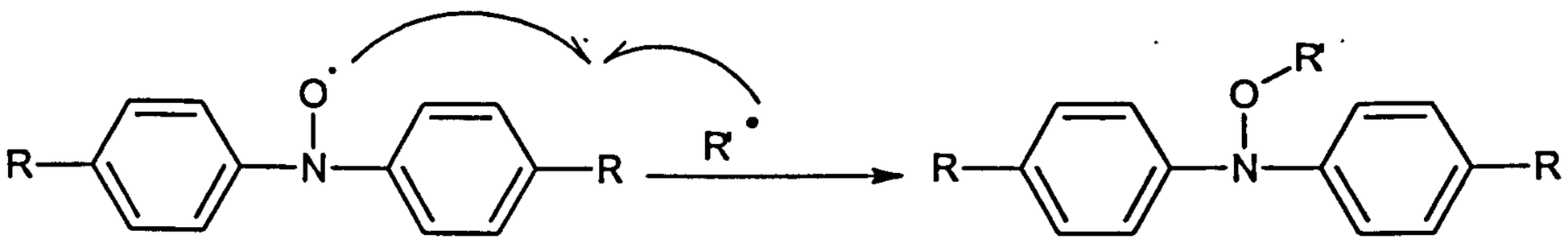

Nitroxyl radical **N-Alkoxydiphenylamine**

Figure C.19: Proposed mechanism for the reaction between nitroxyl and alkyl radicals (Thomas and Tolman, 1962)

Step 7: Thermal decomposition of N-alkoxydiphenylamines

N-alkoxydiphenylamines are thought to thermally decompose to a nitroxyl radical and an alkyl radical (Figure C.20) (Bolsman et al, 1978b).

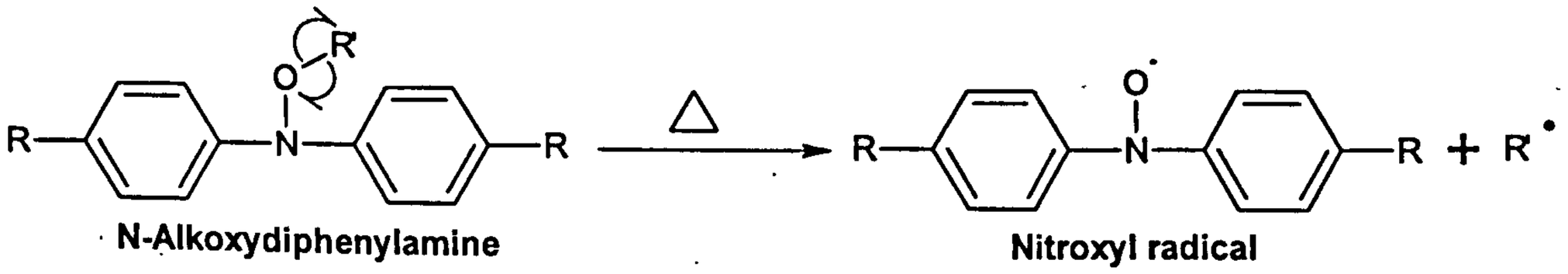

N-Alkoxydiphenylamine **Nitroxyl radical**

Figure C.20: Proposed mechanism for the thermal decomposition of alkoxyl-diphenylamines (Bolsman et al, 1978b)

Step 8: Reaction of nitroxyl radicals with hydrocarbons

Nitroxyl radicals react with hydrocarbons to give rise to a hydroxylamine (AmOH) and an alkyl radical (Figure C.21):

Diphenylnitroxyl + Ethylbenzene ⇆ Hydroxylamine + R•

$k = 1.1 \times 10^3\ M^{-1}\ s^{-1}$ (200 °C)[133]

ΔH = BDE(R-H) – BDE(AmO-H) in kJ mol^{-1}

= 354.7[134] – 323[135] = 32 kJ mol^{-1} (endothermic, i.e. reversible)

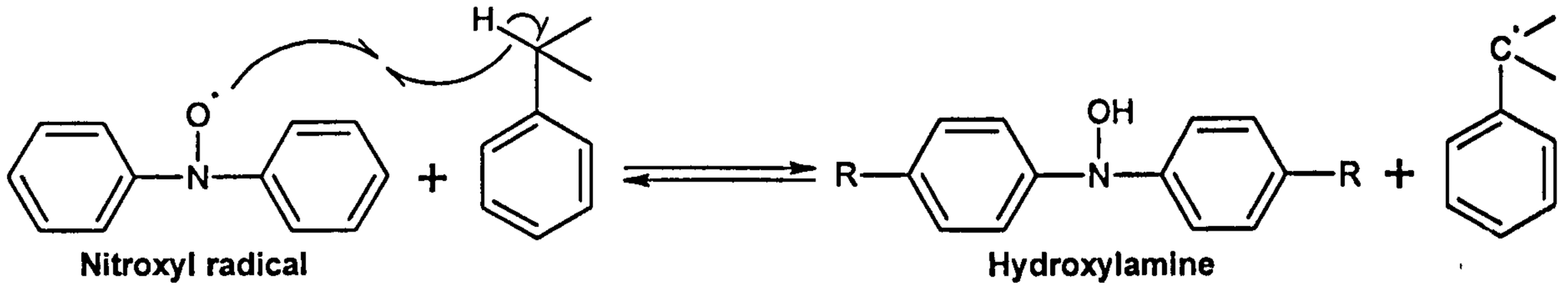

Figure C.21: Proposed mechanism for the reaction between diphenylnitroxyl and ethylbenzene

Step 9: Reaction of hydroxylamines with peroxyl radicals

Hydroxylamines are thought to react with peroxyl radicals (Figure C.22) (Bolsman et al, 1978b).

ΔH = BDE(AmO-H) – BDE(ROO-H) in kJ mol^{-1}

= 323[136] - 366[137] = -43 kJ mol^{-1} (exothermic, i.e. favourable)

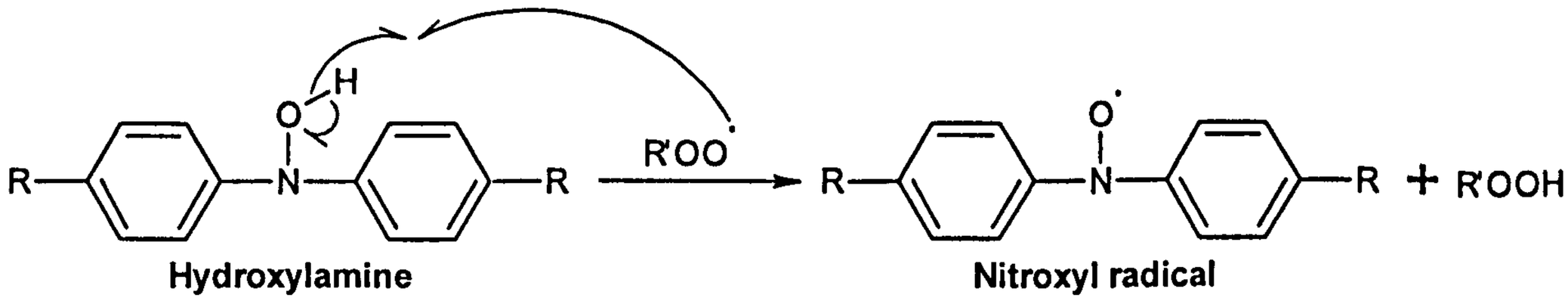

Figure C.22: Proposed mechanism for the reaction between hydroxylamine and peroxyl radicals

---

[133] $k = 7.8 \times 10^5 \exp(-80.0\ kJ/mol / RT)\ M^{-1}\ s^{-1}$ (Howard, 1972, p.164).
[134] Denisov and Denisova, 2000, p.23.
[135] The value is for $C_6H_5C(O)[(CH_3)_3C]NOH$ (Denisov and Denisova, 2000, p.93).
[136] The value is for $C_6H_5C(O)[(CH_3)_3C]NOH$ (Denisov and Denisova, 2000, p.93).
[137] Denisov and Afanasev, 2005, p.41.

Step 10: Reaction of nitroxyl radicals with peroxyl radicals

Nitroxyl radicals react with peroxyl radicals (Denisov and Afanasev, 2005, p.512) (the mechanism for this reaction is unknown):

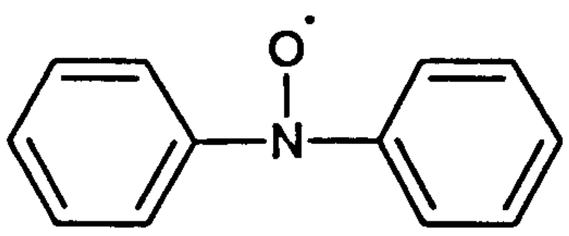

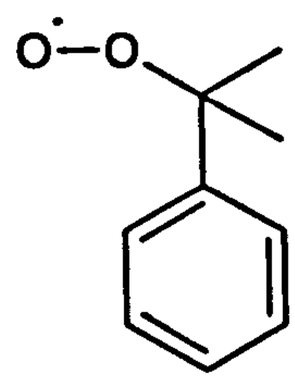

Diphenylnitroxyl + $PhC(Me)_2OO\bullet$

$k = 5.0 \times 10^3\ M^{-1}\ s^{-1}$ (68 °C) in $PhCMe_3$ (Denisov and Afanasev, 2005, p.512)

Step 11: Self-reaction of nitroxyl radicals

Nitroxyl radicals self-react (Denisov and Denisova, 2000, p.178):

2 x Diphenylnitroxyl → Self-reaction (unknown products)

$k = 2.4 \times 10^4$ (200 °C)[138]

[138] 2 x $Ph_2C{=}NO\bullet$; $k = 2.0 \times 10^5 \exp(-8.4\ kJ/mol\ /\ RT)\ M^{-1}\ s^{-1}$ in chlorobenzene (Denisov and Denisova, 2000, p.178).

D. APPENDIX D: SURPLUS RESULTS

Evaluation of reactor and pressurised differential scanning calorimetry (PDSC) results

The semi-formulated base fluids were also oxidised in static micro and intermediate reactors to:

- Evaluate the repeatability of reaction times in static reactors (Figure D.1)
- Compare results between micro and large reactors (Figure D.3)
- Compare and contrast reactor and DSC results (Figure D.4)

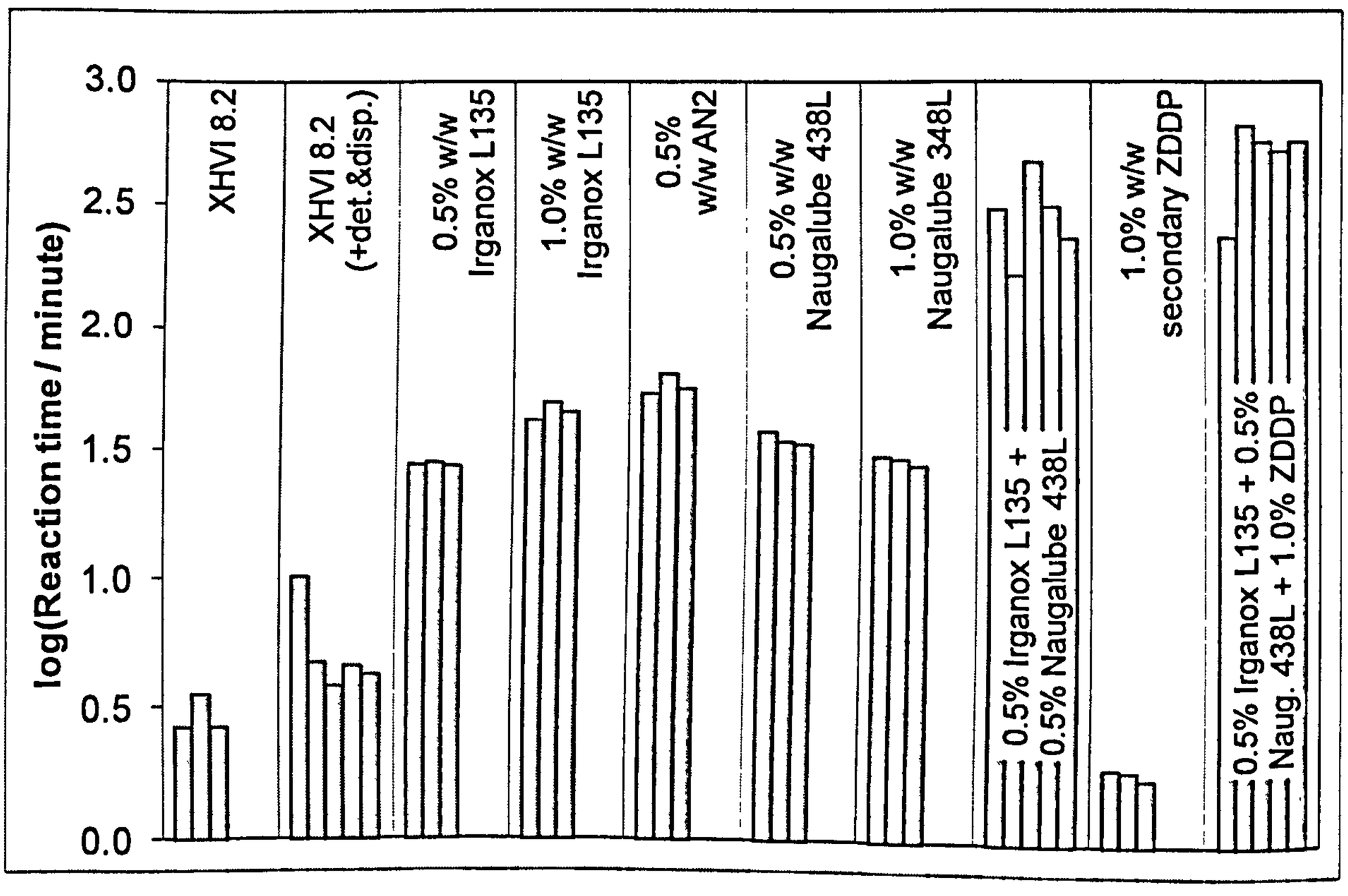

Figure D.1: Repeated oxidations of 0.5% Irganox + 0.5% Naugalube and 0.5% Irganox + 0.5% Naugalube + 1.0% ZDDP semi-formulated base fluids at 200 °C in the static micro reactor

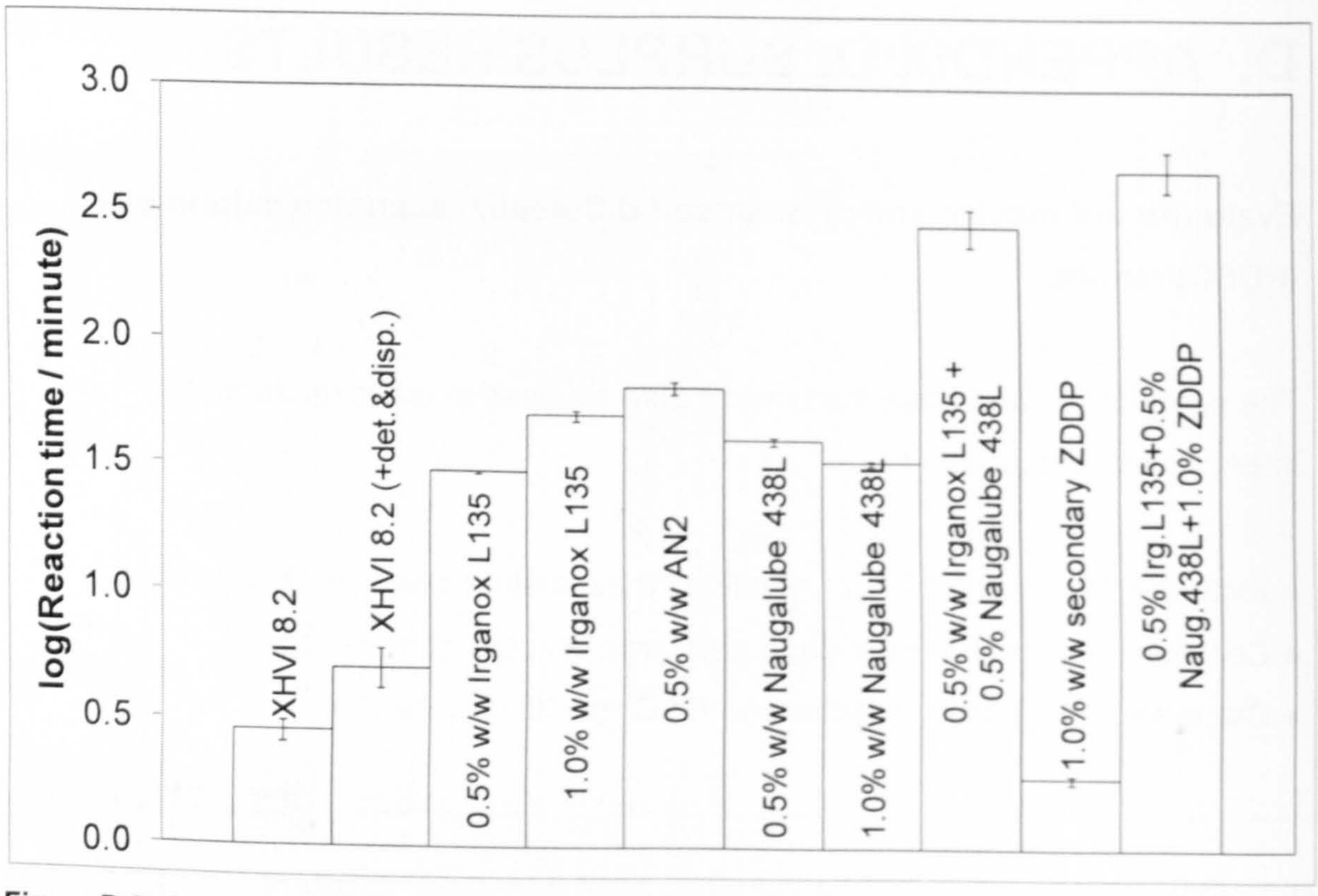

Figure D.2: Averaged reaction times of the repeated oxidations (Figure D.1) of 0.5% Irganox + 0.5% Naugalube and 0.5% Irganox + 0.5% Naugalube + 1.0% ZDDP semi-formulated base fluids at 200 °C in the static micro reactor – error bars represent standard error

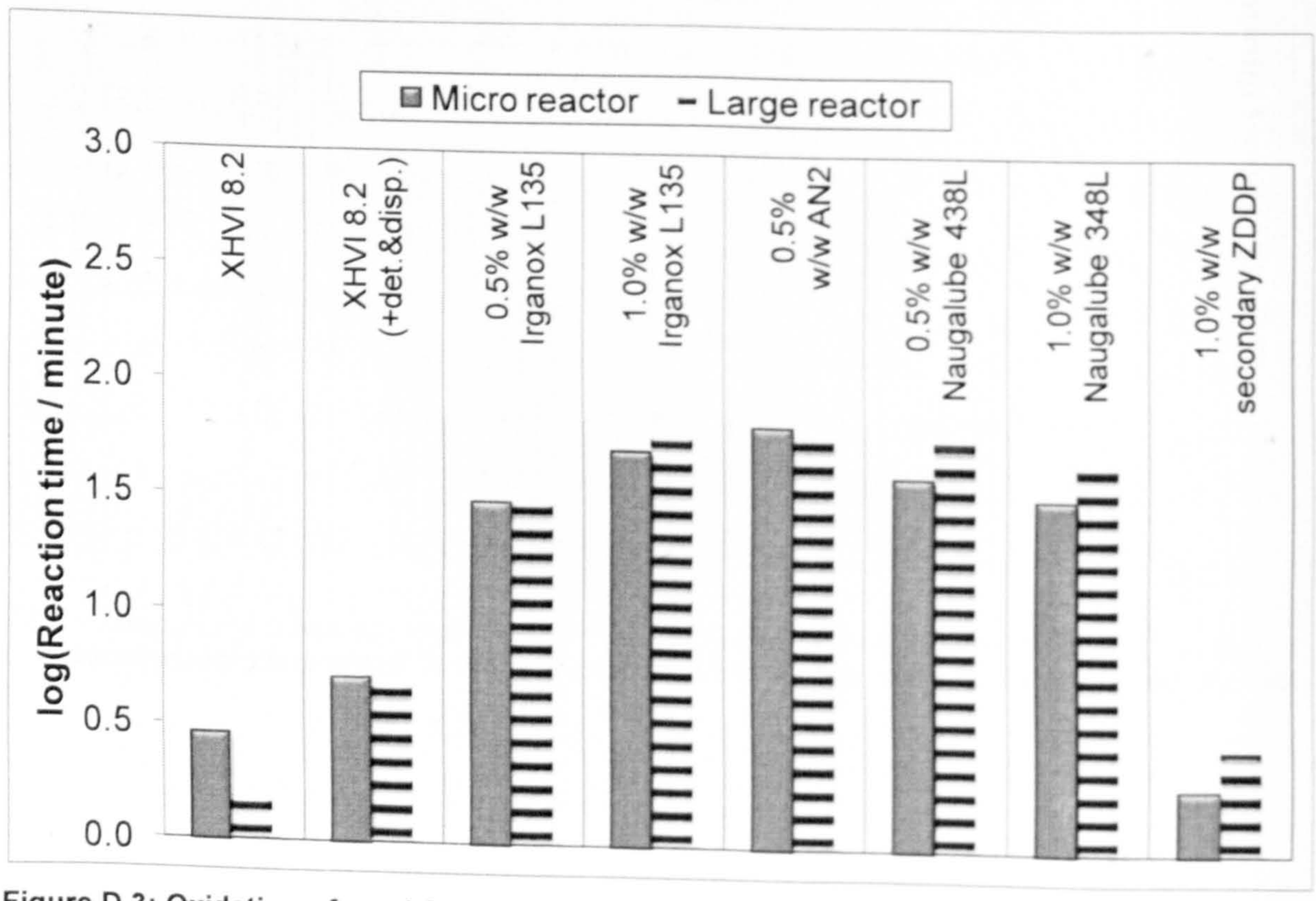

Figure D.3: Oxidation of semi-formulated base fluids at 200 °C in static micro (averaged reaction times) and large reactors

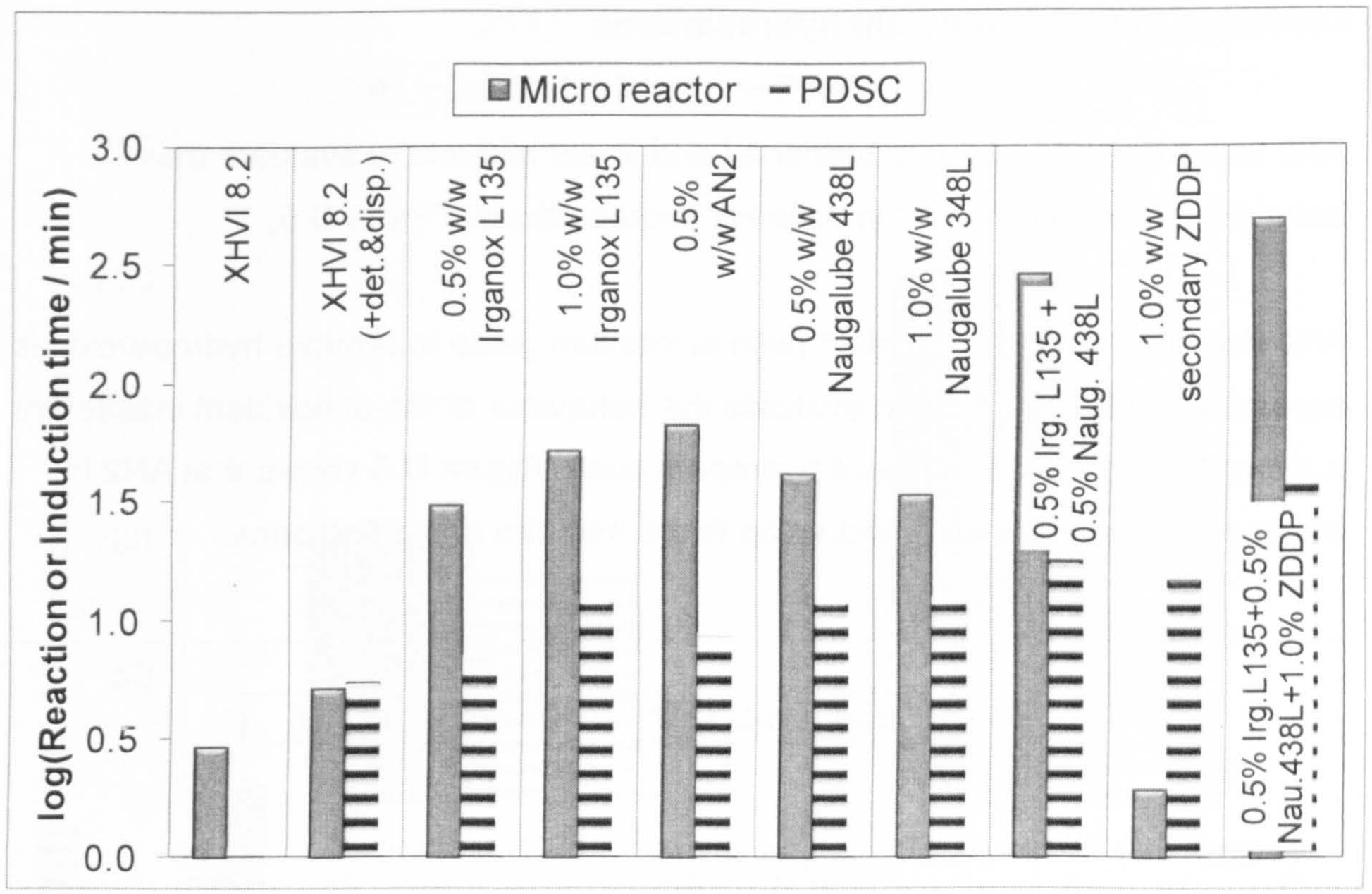

Figure D.4: Oxidation of 0.5% Irganox + 0.5% Naugalube and 0.5% Irganox + 0.5% Naugalube + 1.0% ZDDP semi-formulated base fluids at 200 °C in the static micro reactor (averaged reaction times) (this work) and pressurised differential scanning calorimetry (Wang, 2007)

Repeatability of reaction times in static reactors (Figure D.1) and the similarity between the results obtained from the micro and large reactors (Figure D.3) are reasonably good. By comparing data from the micro reactor and PDSC (Figure D.4), one notices that the reference oil has almost the same reaction time using both techniques. However, in the presence of antioxidants, the reaction times obtained by PDSC are much shorter than those obtained by the micro reactor; and the overall trend of the effectiveness of blends is poorly distinguished by PDSC in comparison with the data obtained using the micro reactor. The differences in the data obtained by PDSC and the micro reactor are probably due to the differences in the techniques used. For instance, the sample in PDSC is static and constantly well mixed by stirring in the micro reactor, the differences in the distribution of oxygen and antioxidants in the samples probably had effects on the overall chemistries of the blends, which were manifested on the reaction times. The micro reactor is not suitable for studying the 1.0 % ZDDP blend because in the presence of ZDDP, excessive volumes of gas were produced causing the pressure to rise to move than 1.15 bar. This increase in pressure made it difficult to accurately distinguish the actual reaction pressure minimum. Thus, the datum for the 1.0 % ZDDP blend from PDSC is more reliable than that obtained from the micro reactor.

Oxidation of AN2 in different hydrocarbons

AN2 was oxidised in various branched and linear alkanes to evaluate the behaviour of the antioxidant in different hydrocarbons (Figure D.5).

AN2 was also reacted in purified (with aluminium oxide to remove hydroperoxides) squalane and hexadecane to evaluate the behaviour of the antioxidant in different hydrocarbons in the absence of hydroperoxides. Figure D.6 shows that AN2 in purified alkanes have lower induction times than the unpurified ones.

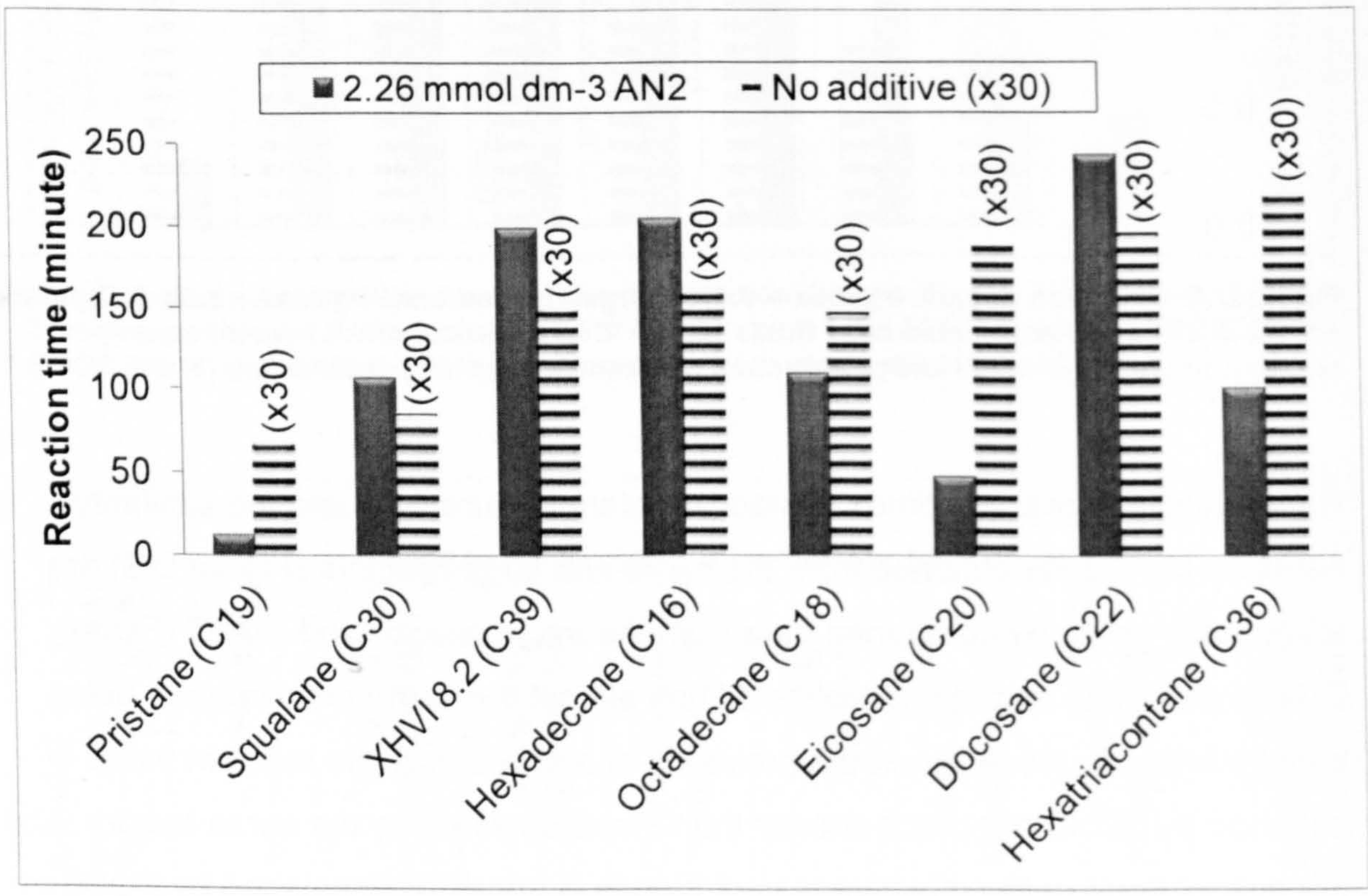

Figure D.5: Oxidation of hydrocarbons without and with 2.26 mmol dm^{-3} AN2 at 180 °C in static micro reactor

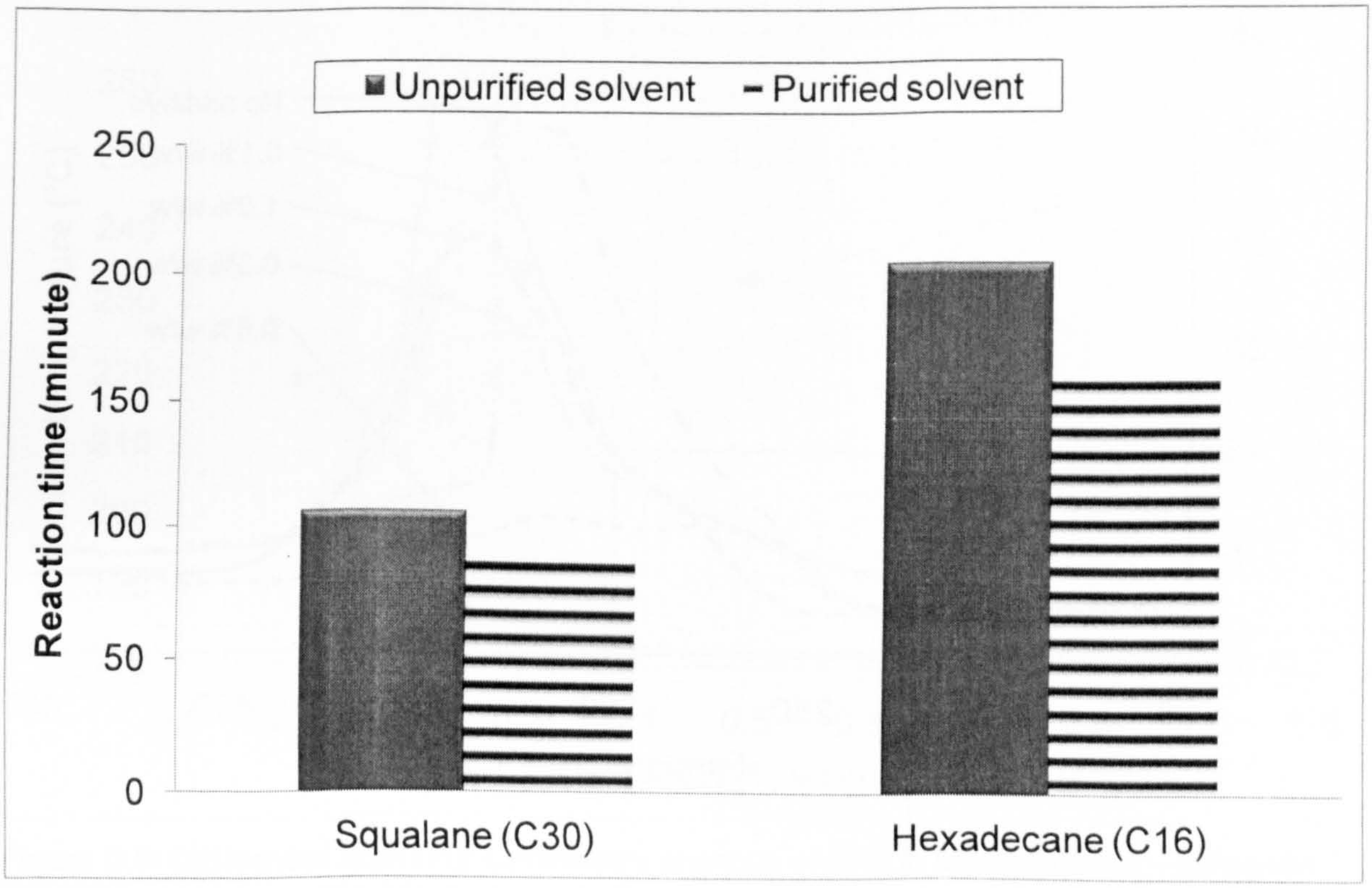

Figure D.6: Oxidation of in unpurified and purified hydrocarbons with 2.26 mmol dm^{-3} AN2 at 180 °C in static micro reactor

Differential scanning calorimetry (DSC) analysis of AN2

Heavy antioxidants (e.g. Naugalube 438L) are not volatile in gas chromatography and difficult to analyse by liquid chromatography. So DSC was tested, with AN2, to be used as a potential tool to determine antioxidant concentration by DSC induction temperature (Figure D.7). Figure D.8 shows that there is a correlation between antioxidant concentration and DSC induction temperature.

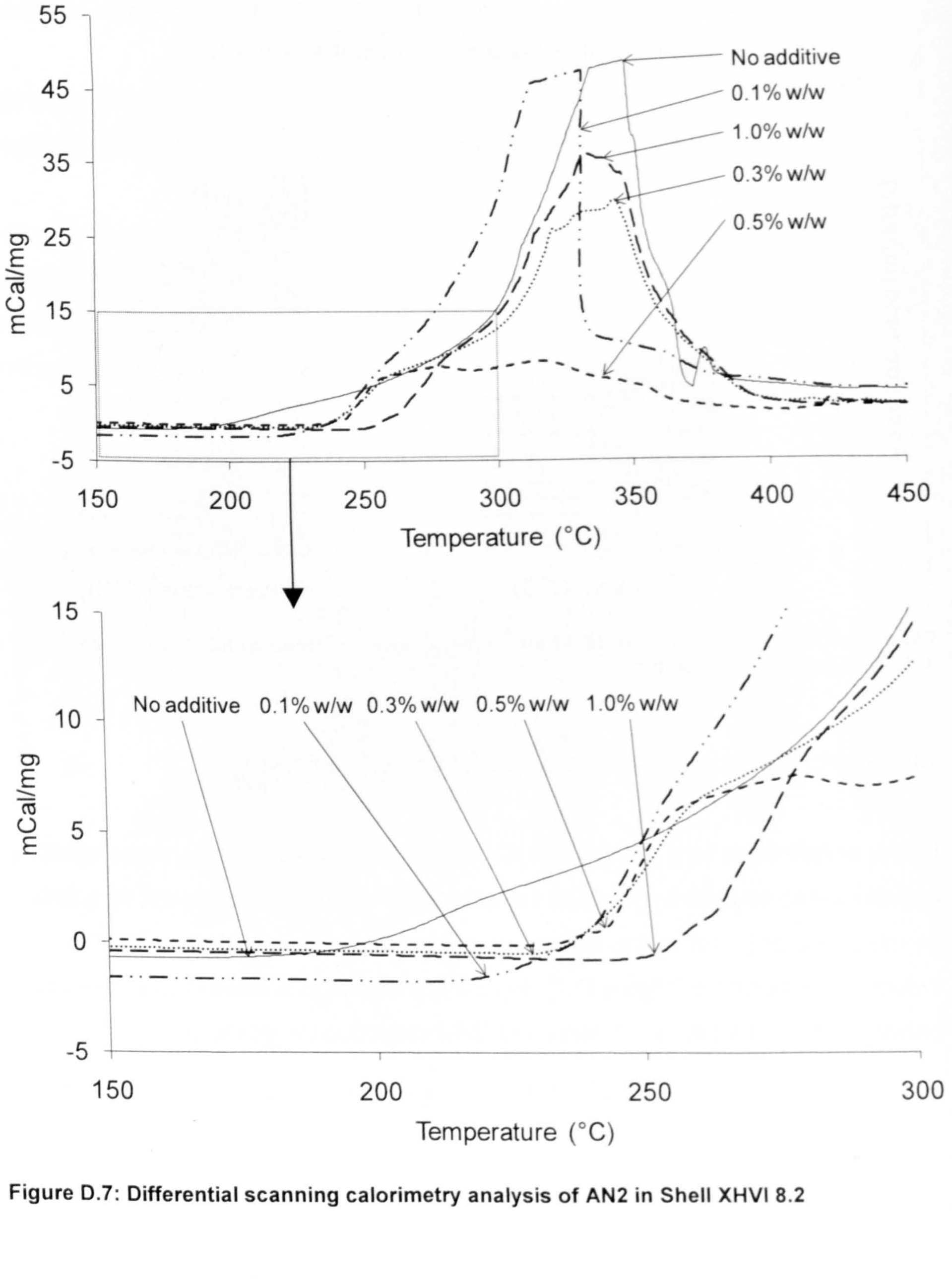

Figure D.7: Differential scanning calorimetry analysis of AN2 in Shell XHVI 8.2

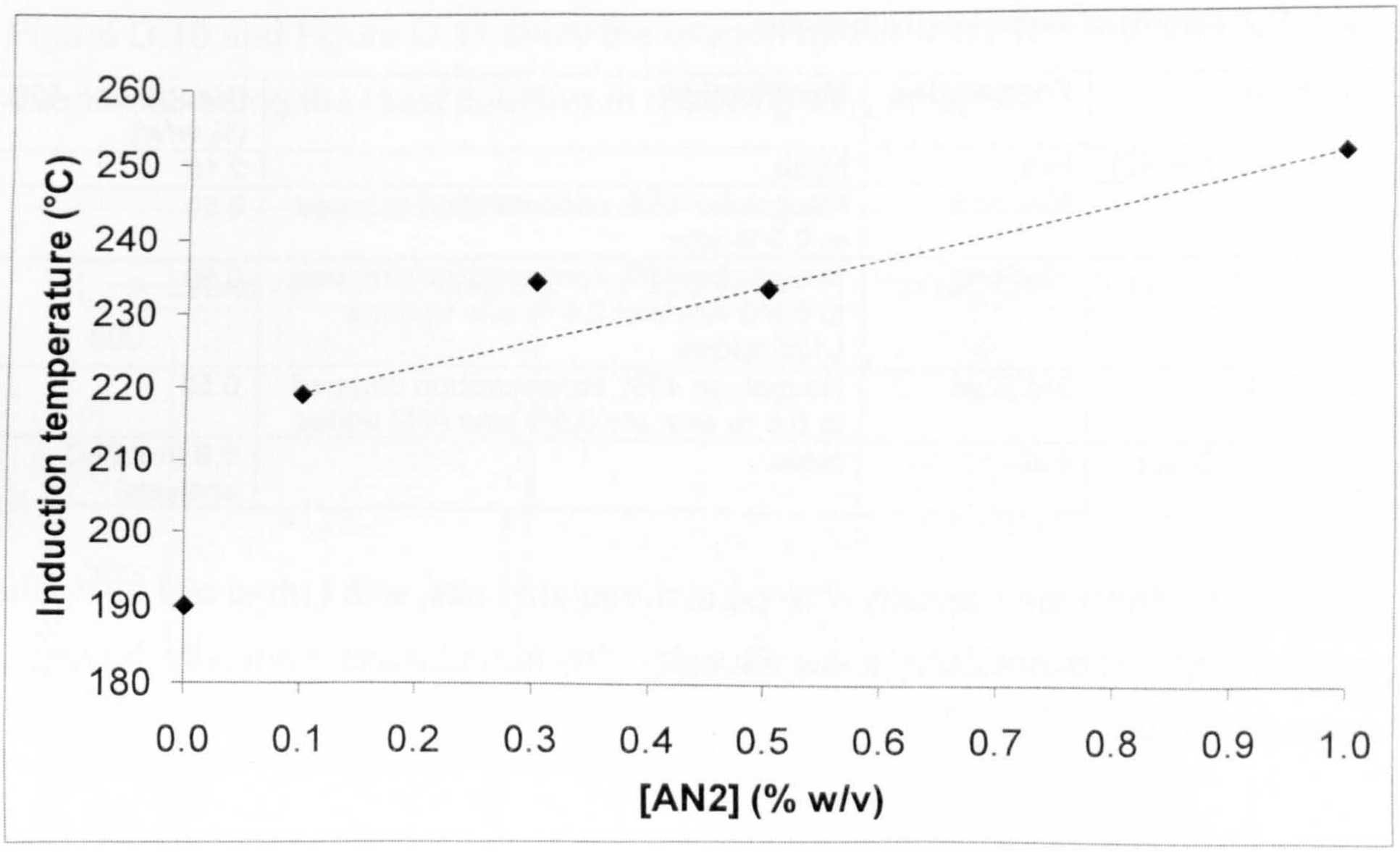

Figure D.8: Differential scanning calorimetry analysis of AN2 in Shell XHVI 8.2 – Induction temperature versus antioxidant concentration

Oxidations of antioxidants in fully-formulated lubricants in flow intermediate reactor

Different concentrations of antioxidant and combinations in fully-formulated lubricants were evaluated by viscosity change and the level of oxygen uptake.

Lubad oil1 is Lubad 1322 (Table D.1) and Lubad oil2-4 are the modified oils of Lubad 1322 (Table D.2).

Table D.1: Chemical composition of Lubad 1322

General name	Mass %
High total base number high soap salicylate	2.10
High total base number low soap salicylate	0.96
Cl cat high molecular weight lightly B dispersant	3.20
Thermal base high molecular weight non-B dispersant	2.50
85 %-secondary ZDDP	1.21
Naugalube 438L	2.10
Diluent oil	1.83
Base oil	10.00
Base oil	14.30
Base oil	39.30
Shell Vis51 viscosity modifier	22.00
Pour point depressant	0.50
Total	**100.00**

Table D.2: Details of formulated lubricants

Lubricant	Formulation	Modification	[Naugalube 438L] (% w/w)
Lubad oil1 (5W-40)	Full	None	2.10
Lubad oil2	Modified	Naugalube 438L concentration dropped to 0.5 % w/w	0.50
Lubad oil3	Modified	Naugalube 438L concentration dropped to 0.5% w/w and 0.5 % w/w Irganox L135 added	0.50
Lubad oil4	Modified	Naugalube 438L concentration dropped to 0.5 % w/w and 0.5% w/w AN2 added	0.50
Shell Helix Super (15W-40)	Full	None	0.3 (from LC analysis)

Figure D.9 shows the viscosity change in formulated oils; with Lubad oil3 being the most effective in maintaining a low viscosity. The formulations, generally, have a crescent shape.

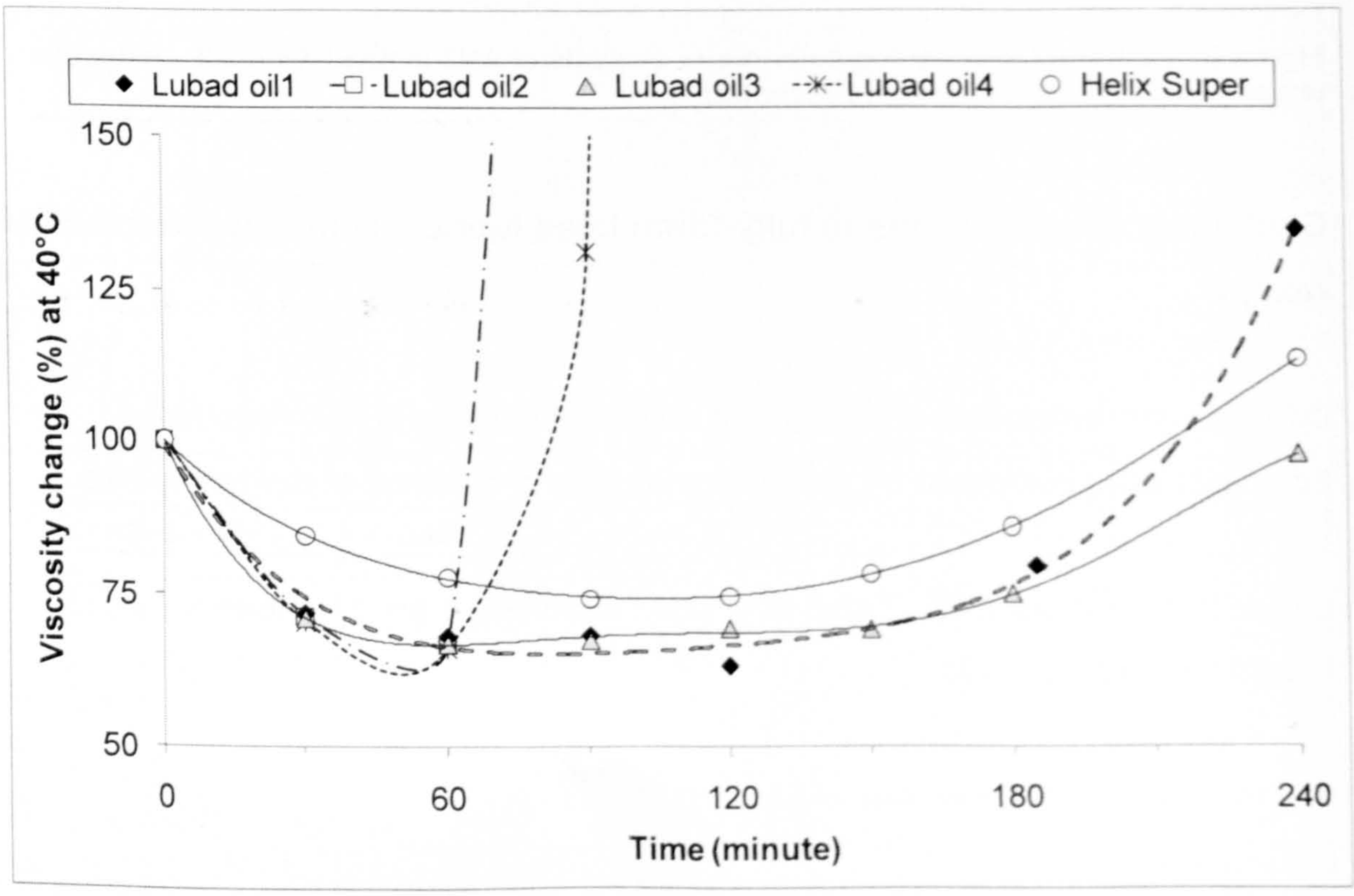

Figure D.9: Viscosity change in the oxidation of 10.0 cm^3 formulated base fluids at 220 °C in flow intermediate reactor

Figure D.10 and Figure D.11 show the oxygen uptake level in formulated oils; with Lubad oil3 being the most effective in retarding oxygen uptake.

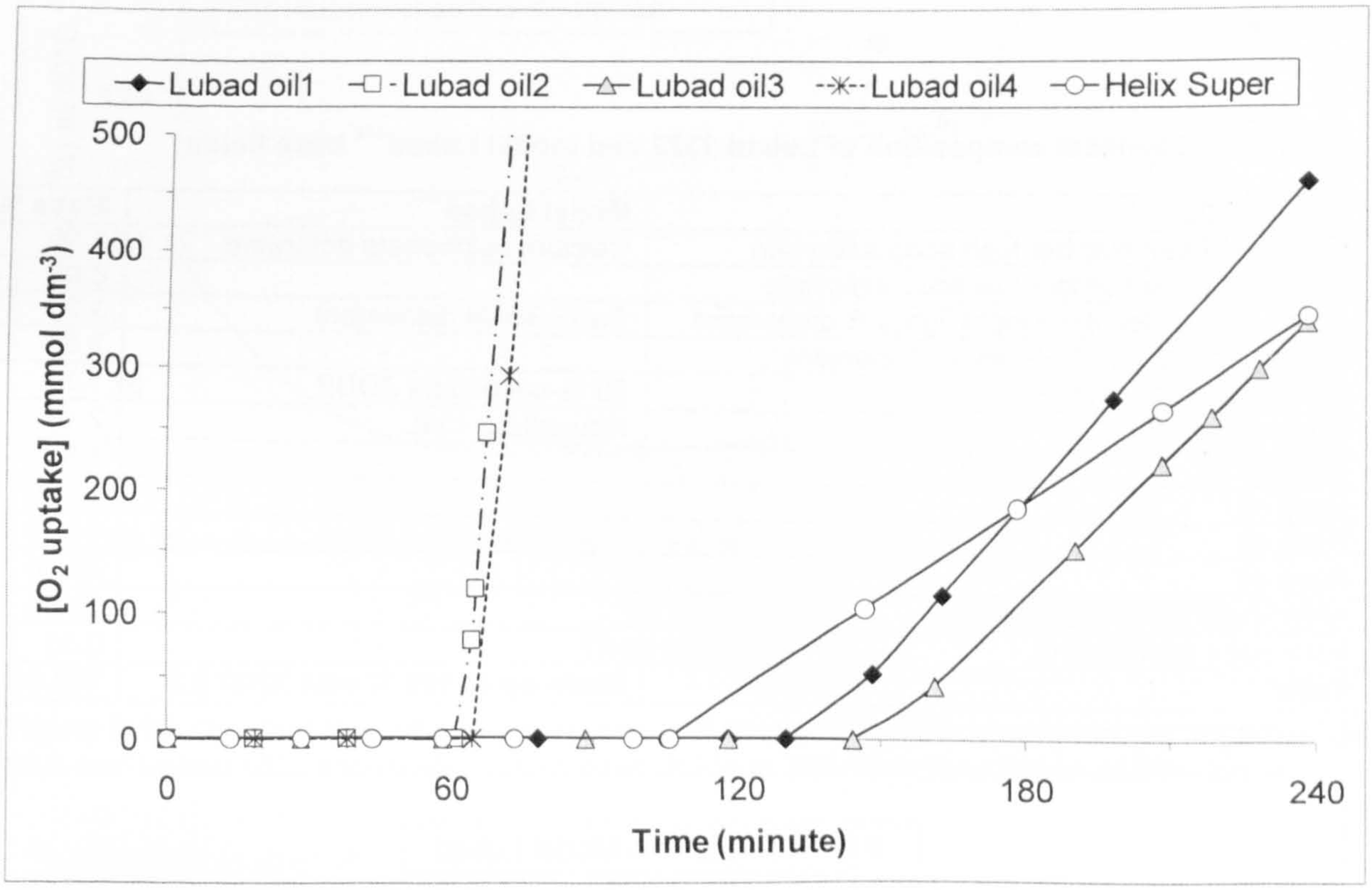

Figure D.10: Oxygen uptake in the oxidation of 10.0 cm^3 formulated base fluids at 220 °C in flow intermediate reactor

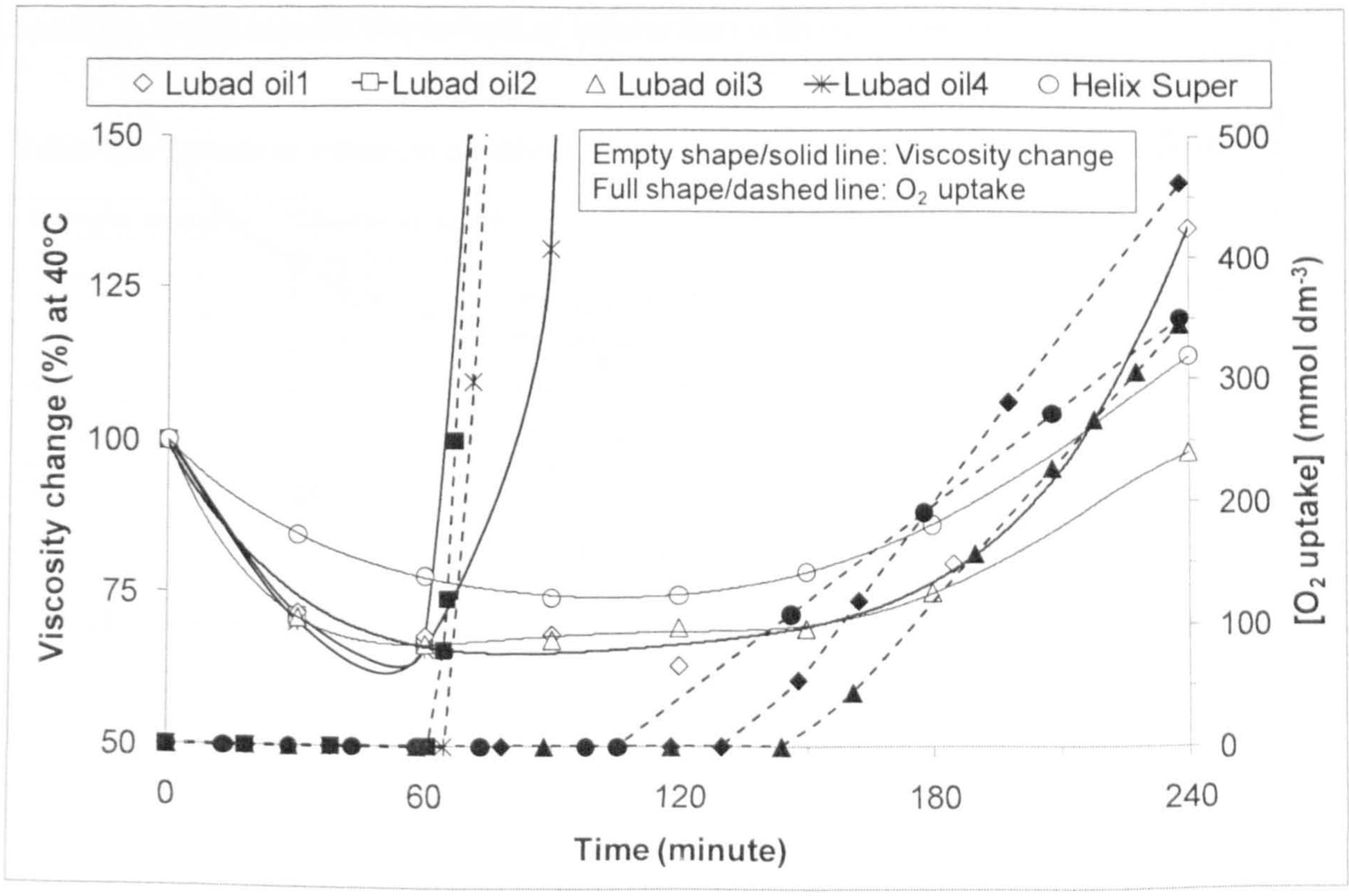

Figure D.11: Overlaid data of oxygen uptake with that of viscosity change in the oxidation of 10.0 cm^3 formulated base fluids at 220 °C in flow intermediate reactor

The "Crescent Effect"[139] was expected to be as a result of the degradation of the viscosity modifier and subsequent aggregation of oxidation products. So an approximate model of Lubad (Table D.3) was made to exclude the viscosity modifier.

Table D.3: Chemical composition of Lubad 1322 and model Lubad[140] base fluids

Lubad 1322	**Model Lubad**	**Mass %**
High total base number high soap salicylate	Calcium sulphonate detergent	2.10
High total base number low soap salicylate	-	0.96
Cl cat high molecular weight lightly B dispersant	Succinimide dispersant	3.20
Thermal base high MW non-B dispersant	-	2.50
85 %-secondary ZDDP	85 %-secondary ZDDP	1.21
Naugalube 438L	Naugalube 438L	2.10
Diluent oil	-	1.83
Base oil	-	10.00
Base oil	-	14.30
Base oil	-	39.30
Shell Vis51 viscosity modifier	-	22.00
Pour point depressant	-	0.50
Total	**Made up to 100 % with XHVI 8.2**	**100.00**

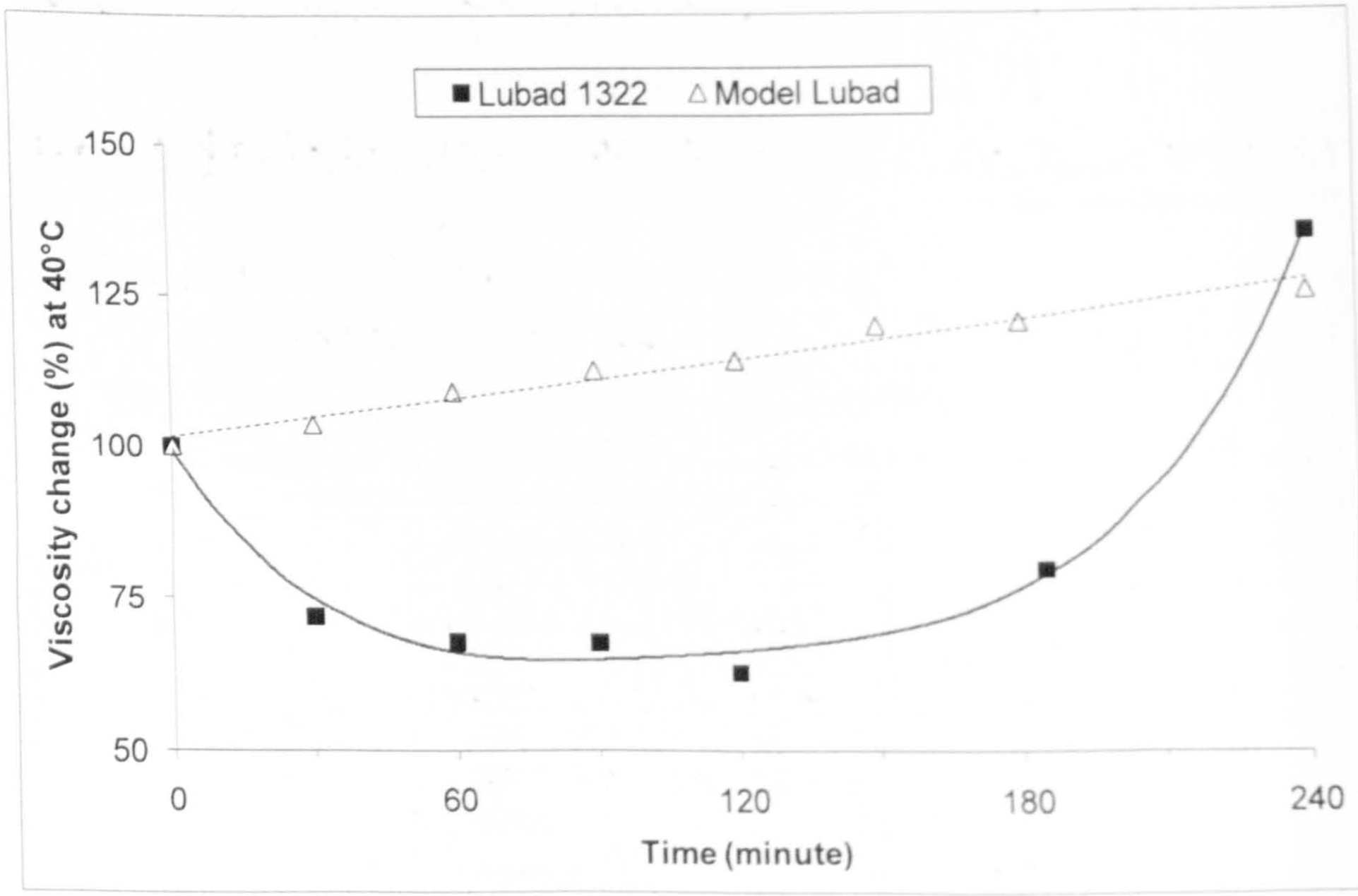

Figure D.12: Viscosity change in the oxidation of 10.0 cm^3 Lubad 1322 and model Lubad base fluids at 220 °C in flow intermediate reactor

[139] Applied to viscosities that decrease then increase to give a distinctive crescent shape.
[140] The additives and base oil used in model Lubad are different from those used in Lubad 1322.

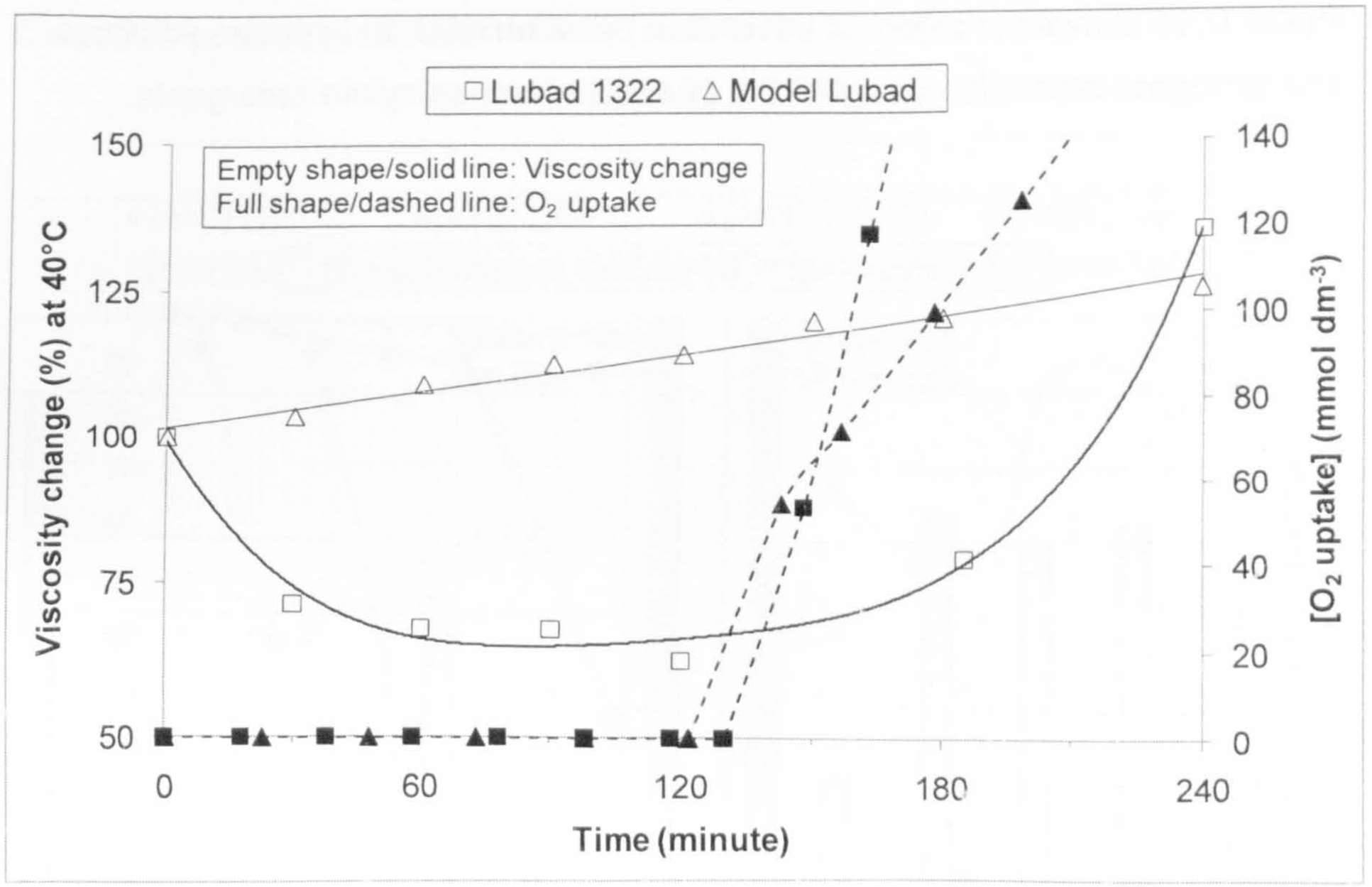

Figure D.13: Overlaid data of oxygen uptake with that of viscosity change in the oxidation of 10.0 cm^3 Lubad 1322 and model Lubad base fluids at 220 °C in flow intermediate reactor

Interactions of AN2 with Infineum lubricant additives in static micro reactor

AN2 was reacted with various engine oil additives (Table D.4) to rapidly (using reaction time) screen the extent of interaction with each additive.

Table D.4: Details of Infineum additives

Sample number	Chemical name
1	Shell XHVI 8.2
2	3.5 % Succinimide dispersant 1
3	3.5 % Succinimide dispersant 2
4	2.0 % High TBN Calcium sulphonate detergent
5	2.4 % Low TBN Calcium phenlate detergent
6	2.0 % Low TBN Calcium salicylate detergent
7	2.2 % Low TBN Calcium sulphonate detergent
8	0.2 % Organic ester friction modifier
9	0.2 % Moly trimer friction modifier
10	10 % Polymer 1 viscosity modifier
11	6.8 % Polymer 2 viscosity modifier
12	6.0 % Polymer 3 viscosity modifier

Figure D.14 shows the extent of interaction between AN2 and various additives. The strongest interaction was with the phenolate and salicylate detergents.

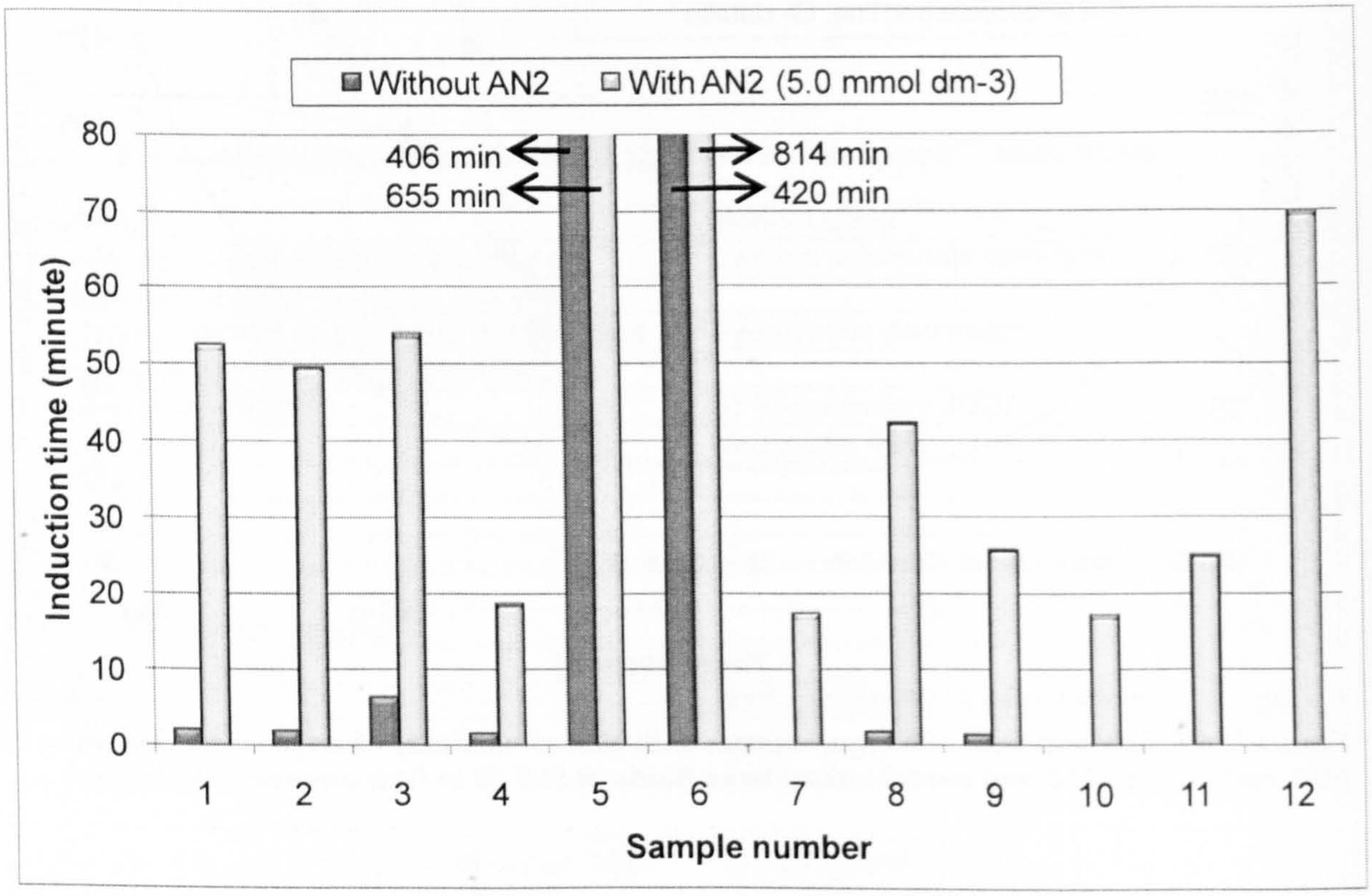

Figure D.14: Oxidation of lubricant additives without and with 5.0 mmol dm^{-3} AN2 in Shell XHVI 8.2 at 200 °C in static micro reactor

Oxidation products of AN2

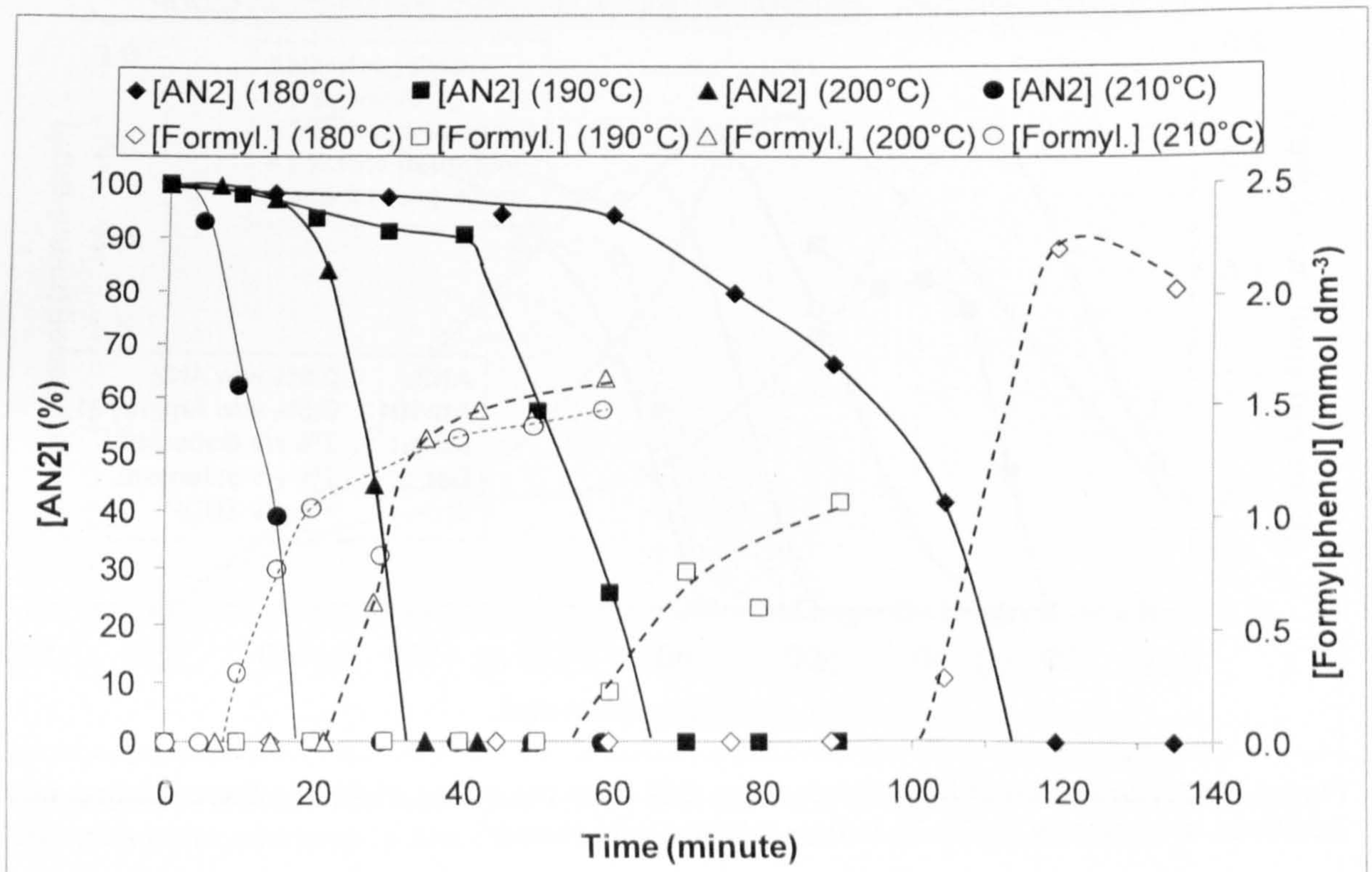

Figure D.15: Distribution of formylphenol (by GC) in the oxidation of 10.0 mmol dm^{-3} AN2 (by FTIR) in squalane between 180 °C to 210 °C in flow intermediate reactor

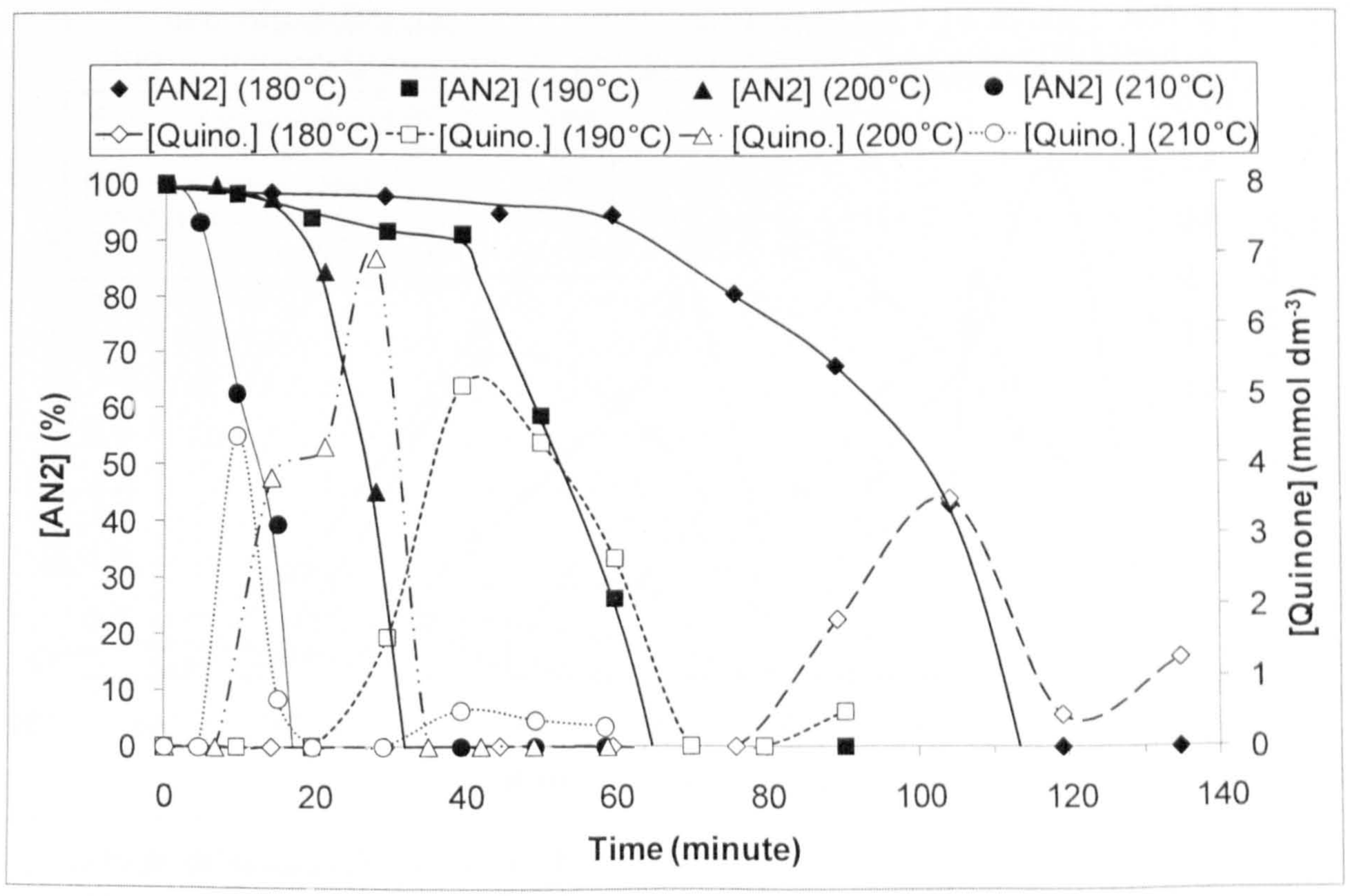

Figure D.16: Distribution of quinone (by GC) in the oxidation of 10.0 mmol dm^{-3} AN2 (by FTIR) in squalane between 180 °C to 210 °C in flow intermediate reactor

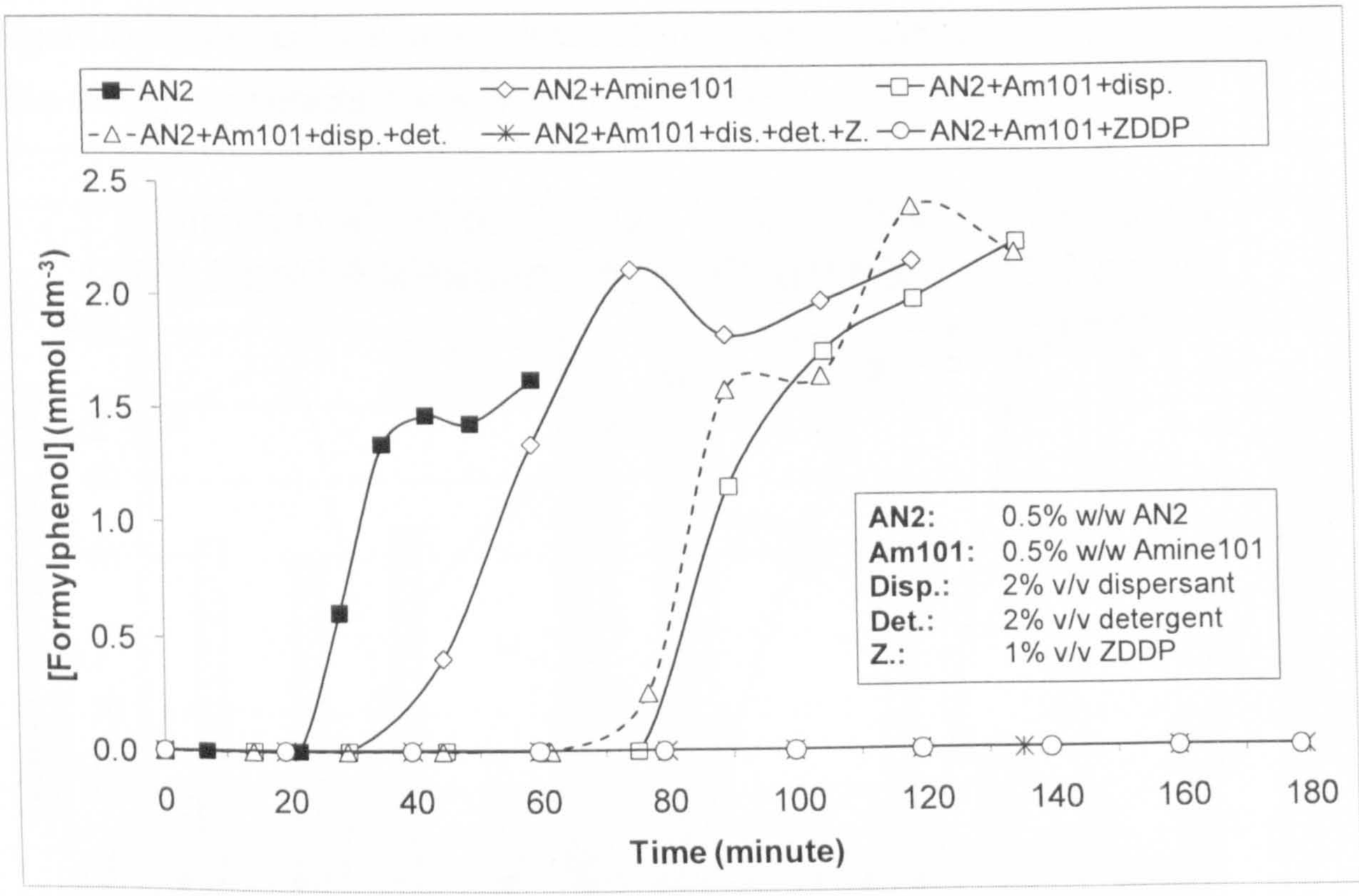

Figure D.17: Formation of formylphenol (by GC) from the decay of AN2 in the oxidation of additives in squalane at 200 °C in flow intermediate reactor

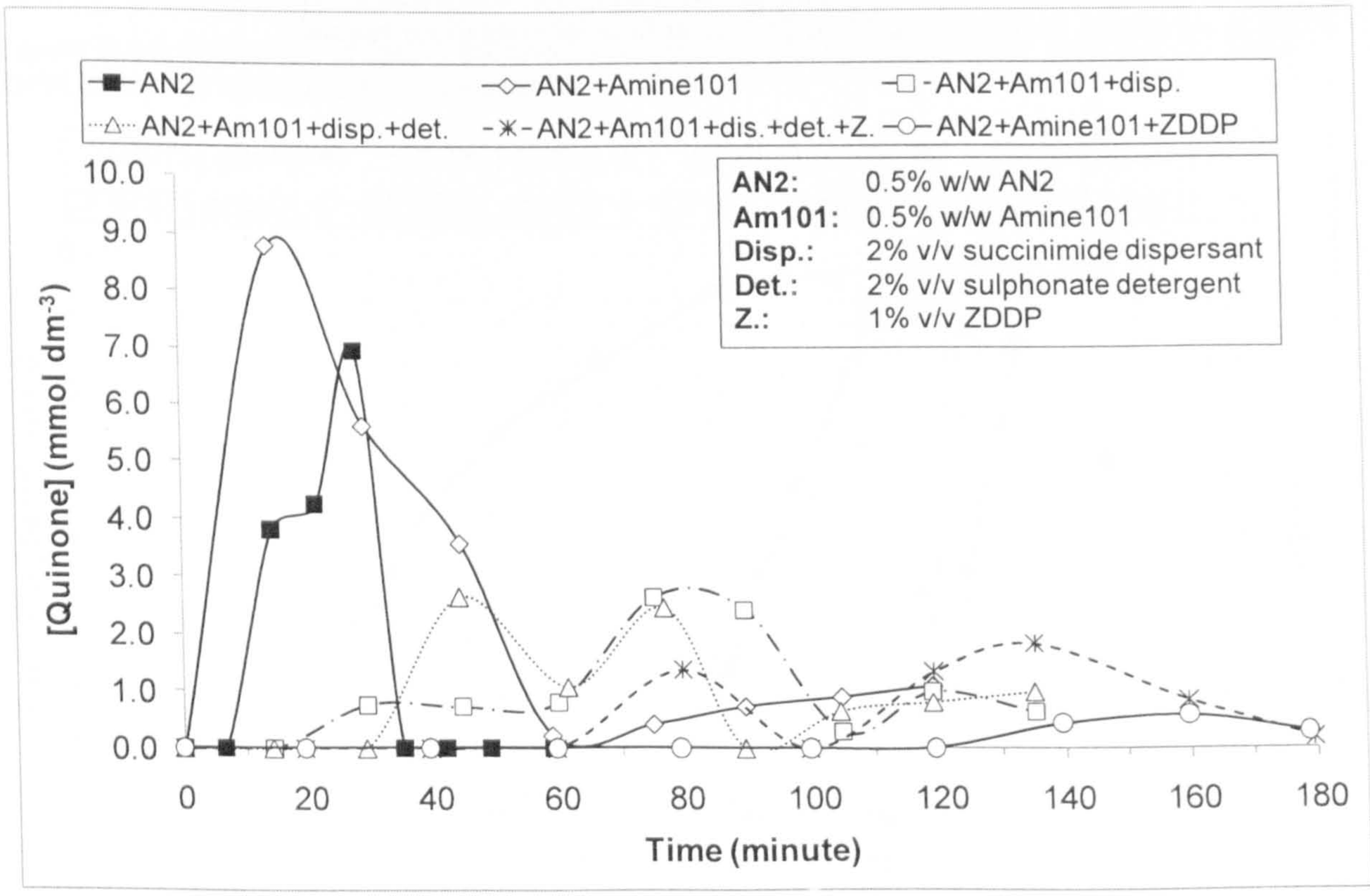

Figure D.18: Formation of quinone (by GC) from the decay of AN2 in the oxidation of additives in squalane at 200 °C in flow intermediate reactor

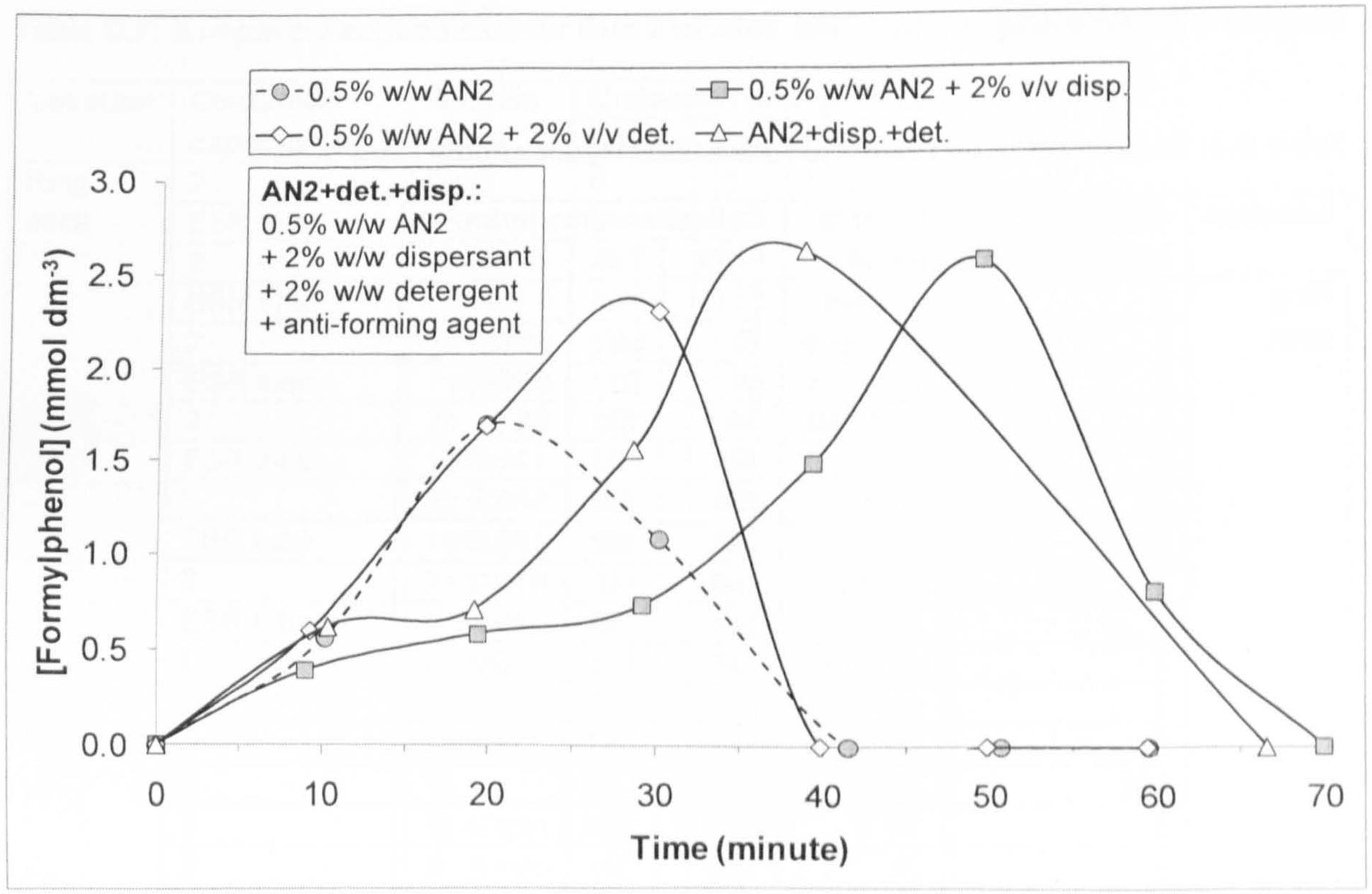

Figure D.19: Formation of formylphenol (by GC) from the decay of AN2 in the oxidation of AN2 with other additives in Shell XHVI 8.2 at 200 °C in flow intermediate reactor

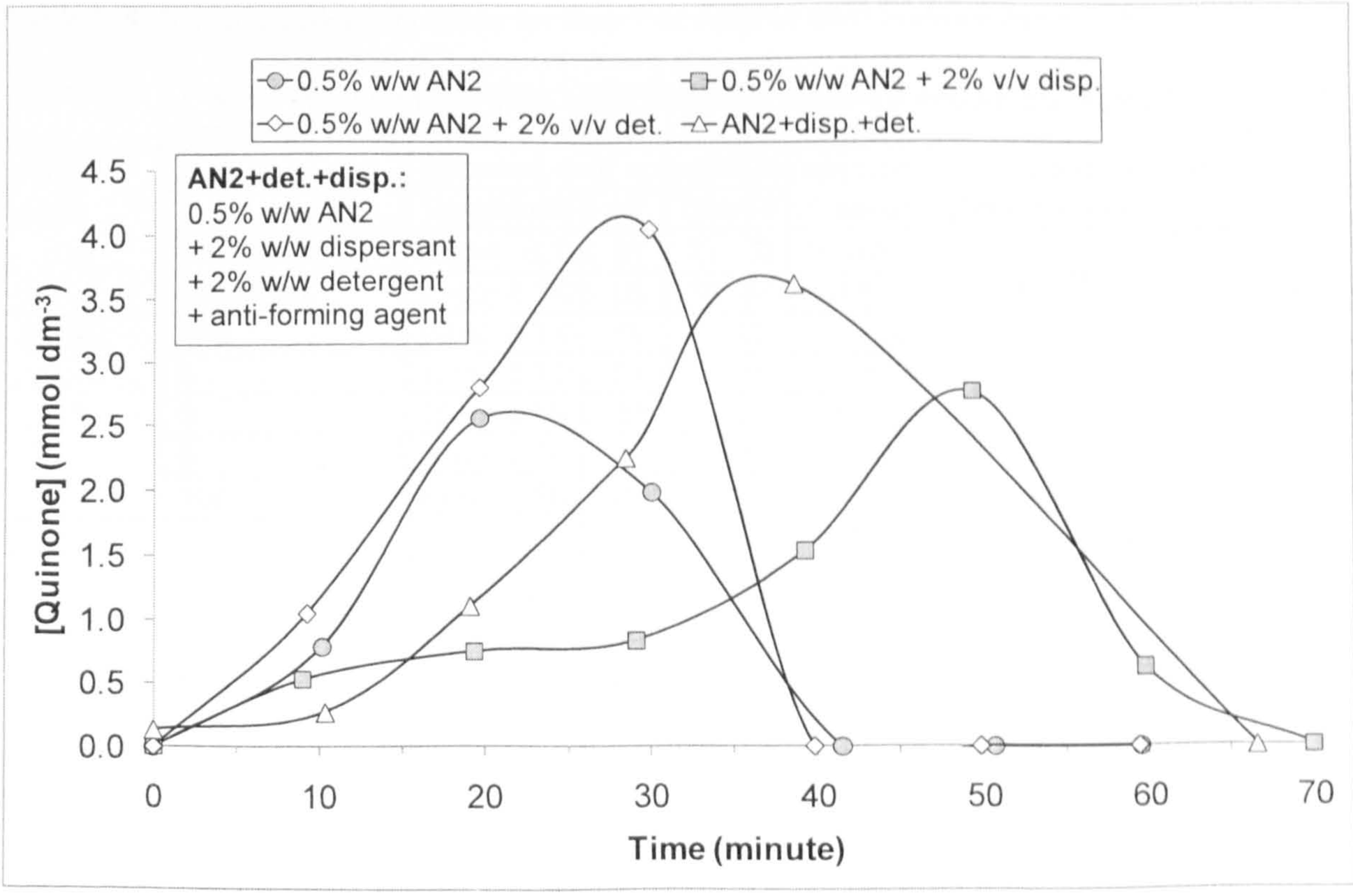

Figure D.20: Formation of quinone (by GC) from the decay of AN2 in the oxidation of AN2 with other additives in Shell XHVI 8.2 at 200 °C in flow intermediate reactor

Engine oil sampling

Table D.5: Sample collection times for June 2006 Hydra engine tests

Location	Container capacity (cm^3)	Sample name	Collection time (minute)		
			From	To	Average
Ring pack	2	0h 0min	0	10	5.0
	2	0h 10min	10	60	35.0
	2	1h	60	70	65.0
	2	1h 10min	70	120	95.0
	2	2h	120	130	125.0
	2	2h 10min	130	180	155.0
	2	3h	180	190	185.0
	2	3h 10min	190	240	215.0
	2	4h	240	250	245.0
	2	4h 10min	250	300	275.0
	2	5h	300	310	305.0
	2	5h 10min	310	360	335.0
Sump	100	Initial[141]	0	-	-
	5	1h	60	-	-
	5	2h	120	-	-
	5	3h	180	-	-
	5	4h	240	-	-
	5	5h	300	-	-
	5	6h	360	-	-
	100	Final	365	-	-

Table D.6: Sample collection times for Run 1 of June 2007 Hydra engine tests

Location	Container capacity (cm^3)	Sample name	Collection time (minute)		
			From	To	Average
Ring pack	2	0min	0	15	7.5
	ESR[142] tube	15min	15	20	17.5
	2	20min	20	35	27.5
	ESR tube	35min	35	40	37.5
	2	40min	40	55	47.5
	ESR tube	55min	55	60	57.5
	ESR tube	60min	60	65	62.5
Sump	100	0min	0	-	-
	5	20min	20	-	-
	5	35min	35	-	-
	5	50min	50	-	-
	100	1h 5min	65	-	-

[141] Collected prior to starting firing engine.
[142] Electron spin resonance.

Table D.7: Sample collection times for Run 2 of June 2007 Hydra engine tests

Location	Container capacity (cm^3)	Sample name	Collection time (minute)		
			From	To	Average
Ring pack	2	0min	0	35	17.5
	ESR tube	35min	35	40	37.5
	2	40min	40	75	57.5
	ESR tube	75min	75	80	77.5
	2	1h 20min	80	115	97.5
	ESR tube	115min	115	120	117.5
	2	2h	120	155	137.5
	ESR tube	155min	155	160	157.5
	2	2h 40min	160	195	177.5
	ESR tube	195min	195	200	197.5
	2	3h 20min	200	235	217.5
	ESR tube	235min	235	240	237.5
	ESR tube	240min	240	245	242.5
Sump	100	0min	0	-	-
	5	20min	20	-	-
	5	1h	60	-	-
	5	1h 40min	100	-	-
	5	2h 20min	140	-	-
	5	3h	180	-	-
	5	3h 40min	220	-	-
	100	4h	240	-	-

Table D.8: Sample collection times for Run 1 of August 2007 Hydra engine tests

Location	Container capacity (cm^3)	Sample name	Collection time (minute)		
			From	To	Average
Ring pack	2	0min	0	10	5.0
	2	10min	10	20	15.0
	ESR tube	20min	20	25	22.5
	ESR tube	25min	25	30	27.5
Sump	100	Initial	0	-	-
	5	10min	10	-	-
	5	20min	20	-	-
	5	30min	30	-	-
	100	Final	31	-	-

Table D.9: Sample collection times for Run 2 of August 2007 Hydra engine tests

Location	Container capacity (cm^3)	Sample name	Collection time (minute)		
			From	To	Average
Ring pack	2	0min	0	15	7.5
	2	15min	15	30	22.5
	2	30min	30	45	37.5
	2	45min	45	60	52.5
	2	1h	60	75	67.5
	2	1h 15min	75	90	82.5
	2	1h 30min	90	105	97.5
	2	1h 45min	105	120	112.5
	2	2h	120	135	127.5
	2	2h 15min	135	150	142.5
	ESR tube	2h 43min	163	185	174.0
	2	3h 5min	185	200	192.5
	2	3h 20min	200	215	207.5
	2	3h 35min	215	230	222.5
	2	3h 50min	230	245	237.5
	2	4h 5min	245	260	252.5
	2	4h 20min	260	275	267.5
	2	4h 35min	275	290	282.5
	ESR tube	4h 50min	290	295	292.5
Sump	100	Initial	0	-	-
	5	30min	30	-	-
	5	1h	60	-	-
	5	1h 30min	90	-	-
	5	2h	120	-	-
	5	2h 30min	150	-	-
	5	3h 5min	185	-	-
	5	3h 30min	210	-	-
	5	4h	240	-	-
	5	4h 30min	270	-	-
	5	5h	300	-	-
	100	Final	301	-	-

Table D.10: Sample collection times for Run 3 of August 2007 Hydra engine tests

Location	Container capacity (cm^3)	Sample name	Collection time (minute)		
			From	To	Average
Ring pack	2	0min	0	15	7.5
	2	15min	15	30	22.5
	2	30min	30	45	37.5
	2	45min	45	60	52.5
	2	1h	60	75	67.5
	2	1h 15min	75	90	82.5
	2	1h 30min	90	105	97.5
	2	1h 45min	105	120	112.5
	2	2h	120	135	127.5
	2	2h 15min	135	150	142.5
	2	2h 30min	150	165	157.5
	2	2h 45min	165	180	172.5
	2	3h	180	195	187.5
	2	3h 15min	195	210	202.5
	2	3h 30min	210	225	217.5
	2	3h 45min	225	240	232.5
	2	4h	240	255	247.5
	2	4h 15min	255	270	262.5
	2	4h 30min	270	285	277.5
	ESR tube	4h 45min	285	295	290.0
Sump	100	Initial	0	-	-
	5	30min	30	-	-
	5	1h	60	-	-
	5	1h 30min	90	-	-
	5	2h	120	-	-
	5	2h 30min	150	-	-
	5	3h	180	-	-
	5	3h 30min	210	-	-
	5	4h	240	-	-
	5	4h 30min	270	-	-
	5	5h	300	-	-
	100	Final	301	-	-

References

Adam, W. and Chiu, W. The mechanism of a rate-controlled cross-disproportionation between phenoxyl radicals. *Journal of the American Chemical Society*, 1971, **13** (15): 3687-3693.

Adamic, K. and Ingold, K. Formation of radicals in amine inhibited decomposition of t-butyl hydroperoxide. *Canadian Journal of Chemistry*, 1969, **47** (2): 295-299.

Amorati, R.; Lucarini, M.; Mugnaini, V.; and Pedulli, G. Antioxidant activity of o-bisphenols the role of intramolecular hydrogen bonding. *Journal of Organic Chemistry*, 2003, **68** (13): 5198-5204.

Bolsman, T.; Blok, A.; and Frijns, J. Mechanism of the catalytic inhibition of hydrocarbon autoxidation by secondary amines and nitroxides. *Journal of the Royal Netherlands Chemical Society*, 1978b, **97** (12): 313-319.

Brownlie, I. and Ingold, K. The inhibited autoxidation of styrene part VI the relative efficiencies and the kinetics for inhibition by N-aryl anilines and N-alkyl anilines. *Canadian Journal of Chemistry*, 1967, **45** (20): 2419-2425.

Burton, A.; Ingold, K.; and Walton, J. Absolute rate constants for the reactions of primary alkyl radicals with aromatic amines. *Journal of Organic Chemistry*, 1996, **61** (11): 3778-3782).

Colegate, S. and Hewgill, R. Oxidation of bisphenols II some compounds related to galvinoxyl. *Australian Journal of Chemistry*, 1980, **33**: 351-369.

Denisov, E. and Afanasev, I. Oxidation and antioxidants in organic chemistry and biology. CRC Press of Taylor and Francis Group, Florida, 2005.

Denisov, E. and Denisova, T. Handbook of antioxidants bond dissociation energies rate constants activation energies and enthalpies of reactions (second edition). CRC Press LLC, Florida, 2000.

Franchi, P.; Lucarini, M.; Pedulli, G.; Valgimigli, L.; and Lunelli, B. Reactivity of substituted phenols toward alkyl radicals. *Journal of the American Chemical Society*, 1999, **121** (3): 507-514.

Greene, F. and Adam, W. Autoxidation of galvinoxyl. *Journal of Organic Chemistry*, 1963, **28** (12): 3550-3551.

Howard, J. Absolute rate constants for reactions of oxyl radicals. In: Williams, G. (editor). Advances in free-radical chemistry, volume 4. Logos Press Limited, London, 1972.

Howard, J. Radical reaction rates in liquids, In: Fischer (editor), H. Peroxyl and related radicals. Subvolume D2. Springer, London, 1997.

Jensen, R.; Korcek, S.; and Zinbo, M. Liquid-phase autoxidation of organic compounds at elevated temperatures absolute rate constant for intermolecular hydrogen abstraction in hexadecane autoxidation at 120-190 °C. *International Journal of Chemical Kinetics*, 1994, **26**: 673-680.

Jensen, R.; Korcek, S.; Zinbo, M.; and Johnson, M. Initiation in hydrocarbon autoxidation at elevated temperatures. *International Journal of Chemical Kinetics*, 1990, **22**: 1095-1107.

Khursan, S.; Gerchikov, A.; Nazarov, A.; Maslennikov, S.; Martemyanov, V. and Komissarov, V. Rate constants for the reactions of butyl acetate peroxyl radicals with sterically hindered phenols. Translated from Russian by SciFinder Scholar from: *Khimicheskaya Fizkia*,1989, **8** (7): 942-948.

Luo, Y. Handbook of bond dissociation energies in organic compounds. CRC Press, Florida, 2003.

MacFaul, P.; Ingold, K.; and Lusztyk, J. Kinetic solvent effects on hydrogen atom abstraction from phenol, aniline, and diphenylamine the importance of hydrogen bonding on their radical-trapping (antioxidant) activities. *Journal of Organic Chemistry*, 1996, **61** (4): 1316-1321.

Maillard, B.; Ingold, K.; and Scaiano, J. Rate constants for the reactions of free radicals with oxygen in solution. *Journal of the American Chemical Society*, 1983, **105** (15): 5095-5099.

McMillen, D. and Golden, D. Hydrocarbon bond dissociation energies. *Annual Review of Physical Chemistry*, 1982, **33**: 493-532.

Prokofev, A.; Solodovnikov, S.; and Nikiforov, G. Interaction of coppinger radicals with di-tert-butyl peroxide. Translated from Russian by SciFinder Scholar from *Teoreticheskaya i Ekspermentalnaya Khimiya*, 1968, **4** (5): 700-704.

Roginskii, V. ESR spectra and kinetics of the disproportionation of substituted phenoxy radicals coomunication 2 radicals of 2,4,6-trialkyl-substituted mono-, p-bis-, p-tris-, and p-tetraphenols. *Bulletin of the Academy of Sciences of the USSR Division of Chemical Science*, 1985, **34** (9): 1833-1841, part 1.

Rubtsov, V.; Roginskii, V.; Dubinskii, V.; and Miller, V. Rate constants for phenoxy radical reactions in hydrocarbon oxidations inhibited by 2,4,6-tri-tert-butylphenol. ?, 1979, **?** (?): 921-925.

Scanlon, J. and Willis, D. Calculation of flame ionization detector relative response factors using the effective carbon number concept. *Journal of Chromatographic Science*, 1985, **23**: 333-340.

Snelgrove, D.; Lusztyk, J.; Banks, J.; Mulder, P.; and Ingold, K. Kinetic solvent effects on hydrogen-atom abstractions reliable quantitative predictions via a single empirical equation. *Journal of the American Chemical Society*, 2001, **123** (3): 469-477.

Thomas, J. and Tolman, C. Oxidation inhibited by diphenylamine. *Journal of the American Chemical Society*, 1962, **84**: 2930-2935.

Varlamov, V. and Densiov, E. Kinetic spectrophotometric study of the kinetics of direct and reverse reactions of the peroxide radical with diphenylamine. *Russian Chemical Bulletin*, 1987, **36** (8): 1607-1612.

Wang. A. PDSC analysis of test oil formulation used in Ricardo Hydra engine testing. Infineum Internal Document. 2007.

Wilkinson, J. The autoxidation of branched hydrocarbons in the liquid phase as models for understanding lubricant degradation. PhD thesis, University of York, 2006.